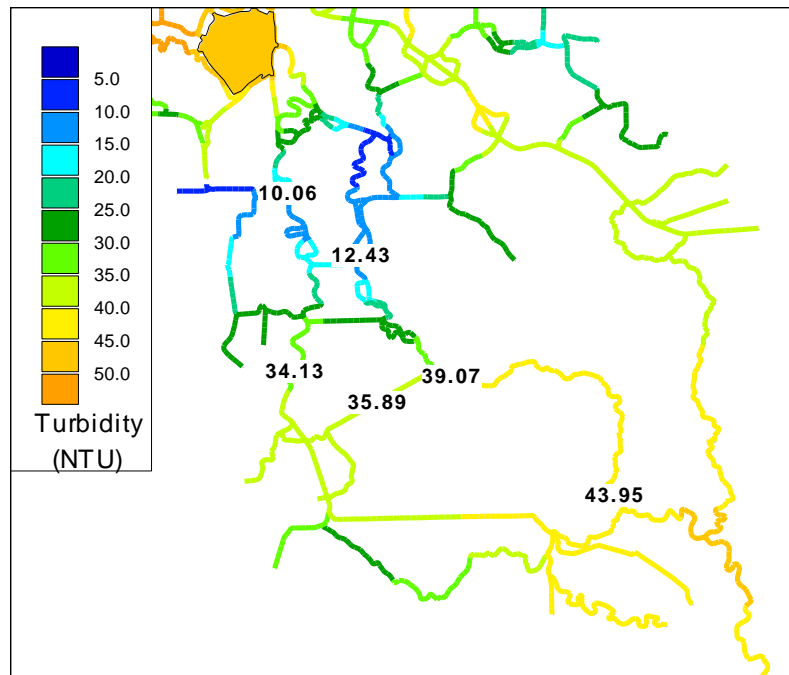


## Turbidity Modeling with DSM2-QUAL:

# 2013 QUAL Recalibration, Updated Historical Model and Analysis of the Potential for Turbidity Bridge Formation



*February 1998 Historical Model: Turbidity Bridge Formation Primarily Due to High San Joaquin Inflow and Turbidity*

**Prepared For:**

Metropolitan Water District of Southern California  
October 2013

**Contact:**

Dr. Paul Hutton  
Authorized Technical Representative  
916 – 650 – 2620

**Prepared By:**

Resource Management Associates  
4171 Suisun Valley Road, Suite J  
Fairfield, CA 94534

**Contact:**

Dr. Marianne Guerin  
707 – 864 – 2950

## Table of Contents

1	Executive Summary .....	1
2	Introduction.....	4
2.1	Objectives.....	4
2.2	Background .....	4
2.3	Challenges in modeling turbidity .....	5
3	Turbidity Model Calibration - Background and Methodology.....	5
3.1	Definition of calibration .....	5
3.2	QUAL turbidity calibration background and data.....	6
3.3	Methodology for turbidity calibration.....	10
3.4	Residual analysis .....	14
3.5	Linear regression analysis .....	15
3.6	Documentation of statistics .....	15
3.7	Model output and calibration calculations .....	15
4	Model set-up .....	19
4.1	High flow period Historical simulations: WY2010, WY2011, WY2013.....	19
4.2	Long term (1975 – 2011) Historical Simulations.....	19
5	Calibration Results.....	54
5.1	Calibration priorities .....	54
5.2	Calibration metrics .....	54
5.2.1	Model Skill: Two Delta-wide calibration metrics .....	54
5.3	Calibration results for WY2010 and WY2011, comparing revised and original DMS calibration simulations .....	55
6	Evaluation of the Calaveras Boundary Condition and Its Role in Turbidity Bridge Formation.....	60
6.1	Background .....	60
6.2	Calaveras Turbidity Boundary .....	60
6.3	Turbidity Bridge Formation .....	61
6.4	Summary Discussion.....	62
7	Results of the Long Term QUAL Historical Turbidity Simulation – Water Years 1975 - 2011.....	90

7.1	EMP data .....	90
7.2	Changes to the Mixed-WARMF-SSC Boundary Conditions .....	90
7.3	Simulation results – Model residuals and regressions comparing long-term simulations with EMP data.....	91
7.4	Conditions Potentially Leading to “Turbidity Bridges”.....	96
7.4.1	Analysis methodology .....	96
7.4.2	Results.....	96
7.4.3	Summary of Analysis.....	97
8	Summary and Conclusions .....	126
9	References.....	129
10	Appendix I .....	131
10.1	Model Skill .....	131
10.1.1	Background.....	131
10.1.2	Decisions on model skill assessment for this report .....	132
11	Appendix II – Updated QUAL Turbidity calibration statistics .....	132
11.1	Daily-averaged CDEC data and model output – WY2013.....	132
11.2	Daily-averaged CDEC data and model output – WY2011.....	135
11.3	Daily-averaged CDEC data and model output – WY2010.....	164
12	Appendix III – Updated QUAL Turbidity calibration statistics, 15-min.....	189
12.1	Fifteen Minute CDEC data and model output – WY2013 .....	189
12.2	Fifteen Minute CDEC data and model output – WY2011 .....	191
12.3	Fifteen minute CDEC data and model output – WY2010.....	220
13	Appendix IV– Figures and Statistics Documenting DSM2 QUAL Historical 1975 – 2011Turbidity Model Application with Mixed SSC-WARMF Boundary Conditions.....	244
13.1	Early years: 1975 -1990.....	244
13.4	Recent years: 1991 – 2011.....	271

## Figures

Figure 3-1 CDEC turbidity measurement locations.....	8
Figure 3-2 Location of the three turbidity compliance locations.....	9
Figure 3-3 The colored lines define the DSM2 grid channels – the segments that are blue define channels where the $K_3$ parameter was set to the indicated value. These figures show the lowest two values used for the settling parameter.....	11
Figure 3-4 The colored lines define the DSM2 grid channels – the segments that are blue define channels where the $K_3$ parameter was set to the indicated value. These figures show two middle values used for the settling parameter.....	12
Figure 3-5 The colored lines define the DSM2 grid channels – the segments that are blue define channels where the $K_3$ parameter was set to the indicated value. This figure shows the highest two values used for the settling parameter.....	13
Figure 3-6An illustration of the output prepared for each data location including calibration statistics for each Water Year. This location is the compliance site at Prisoner’s Point and the year is WY2011. ....	16
Figure 3-7An illustration of the output prepared for each data location including calibration statistics for each Water Year. This location is the compliance site at Prisoner’s Point and the year is WY2011. Peaks in the data (upper plot) not captured in the model in February are due to wind/rain events. ....	17
Figure 3-8An illustration of the output prepared for each data location including calibration statistics for each Water Year. This location is the compliance site at Prisoner’s Point and the year is WY2013. The peak in the data (upper plot) not captured in the model in mid-to-late-January is due to resuspension of sediments due to wind.....	18
Figure 4-1 WY2010 flow BCs at Freeport and the Yolo Bypass. ....	23
Figure 4-2 WY2010 flow BCs at Vernalis and on the Calaveras River. ....	24
Figure 4-3 WY2010 flow BCs on the Mokelumne and Cosumnes Rivers. ....	25
Figure 4-4 WY2010 Turbidity BCs at Freeport and Vernalis. ....	26
Figure 4-5 WY2010 Turbidity BCs for the Yolo Bypass (upper) and the Calaveras River (lower). ....	27
Figure 4-6 WY2010 Turbidity BCs for the Cosumnes and Mokelumne Rivers (upper, sourced from a previous WARMF model) and at Martinez (lower). ....	28
Figure 4-7 WY2010 export BCs at the SWP and CVP locations. ....	29
Figure 4-8 WY2010 export BCs at the CCWD Contra Costa Canal and Old River locations. ....	30
Figure 4-9 WY2010 export BCs at the North Bay Aqueduct and at the CCWD Victoria Canal location.....	31
Figure 4-10 WY2011 flow BCs at the Freeport and Yolo Bypass locations.....	32
Figure 4-11 WY2011flow BCs at the Vernalis and Calaveras River locations.....	33
Figure 4-12 WY2011 flow BCs at the Mokelumne and Cosumnes River locations. ....	34
Figure 4-13 WY2011 Turbidity BCs at Freeport and Vernalis. ....	35

Figure 4-14 WY2011 Turbidity BCs for the Yolo Bypass (upper) and the Calaveras River (lower).....	36
Figure 4-15 WY2011 Turbidity BCs at the Cosumnes and Mokelumne Rivers (upper, sourced from previous WARMF output) and at Martinez (lower). ....	37
Figure 4-16 WY2011 export BCs at the SWP and CVP locations. ....	38
Figure 4-17 WY2011 export BCs at the CCWD Contra Costa Canal and Old River locations...	39
Figure 4-18 WY2011 export BCs at the North Bay Aqueduct and CCWD Victoria Canal locations. ....	40
Figure 4-19 WY2013 flow BCs at Freeport and Yolo Bypass locations.....	41
Figure 4-20 WY2013 flow BCs at the Vernalis and Calaveras River locations.....	42
Figure 4-21 WY2013 flow BCs at the Mokelumne and Cosumnes River locations. ....	43
Figure 4-22 WY2013 turbidity BCs at Freeport and Vernalis.....	44
Figure 4-23 Turbidity BCs for the Yolo Bypass (upper) and the Calaveras River (lower).....	45
Figure 4-24 WY2013 turbidity BCs for the Mokelumne and Cosumnes Rivers (upper plot) and Martinez (lower plot). ....	46
Figure 4-25 WY2013 export BCs at the SWP and CVP locations. ....	47
Figure 4-26 WY2013 export BCs at the CCWD Contra Costa Canal and Old River locations...	48
Figure 4-27 WY2013 export BCs at the North Bay Aqueduct and CCWD Victoria Canal locations. ....	49
Figure 4-28 Model output and EMP grab-sample data at the IEP “C3” location at Hood for the early period historical model. ....	50
Figure 4-29 Model output and EMP grab-sample data at the IEP “C7” location at Mossdale and the “C10” location at SJR-McCune for the early period historical model. ....	51
Figure 4-30 Model output and EMP grab-sample data at the IEP “C3” location at Hood for the later period historical model. ....	52
Figure 4-31 Model output and EMP grab-sample data at the IEP “C7” location at Mossdale and the “C10” location at SJR-McCune for the later period historical model. ....	53
Figure 6-1 WY2013 turbidity data and book-end model output along with volumetric plots at Rough-N-Ready. ....	66
Figure 6-2 WY2013 turbidity data and book-end model output along with volumetric plots at Holland Cut.....	67
Figure 6-3 WY2013 turbidity data and book-end model output along with volumetric plots at Prisoner’s Point.....	68
Figure 6-4 WY2013 turbidity data and book-end model output along with volumetric plots at Victoria-Canal-at-Byron. ....	69
Figure 6-5 WY2013 turbidity data and book-end model output along with volumetric plots at Turner-Cut-Holt. ....	70
Figure 6-6 WY2013 turbidity data and book-end model output along with volumetric plots at Middle-R-Holt.....	71

Figure 6-7 WY2013 turbidity data and book-end model output along with volumetric plots at Middle-at-Middle.....	72
Figure 6-8 WY2011 turbidity data and book-end model output along with volumetric plots at Rough-N-Ready.....	73
Figure 6-9 WY2011 turbidity data and book-end model output along with volumetric plots at Holland-Cut.....	74
Figure 6-10 WY2011 turbidity data and book-end model output along with volumetric plots at Prisoner’s Point.....	75
Figure 6-11 WY2011 turbidity data and book-end model output along with volumetric plots at Victoria-Canal-Byron.....	76
Figure 6-12 WY2011 turbidity data and book-end model output along with volumetric plots at Turner-Cut-Holt.....	77
Figure 6-13 WY2011 turbidity data and book-end model output along with volumetric plots at Middle-at-Middle.....	78
Figure 6-14 WY2011 turbidity data and book-end model output along with volumetric plots at Middle-R-Holt.....	79
Figure 6-15 WY2010 turbidity data and book-end model output at Rough-N-Ready.....	80
Figure 6-16 WY2010 turbidity data and book-end model output at Holland-Cut (upper) and Prisoner’s Point (lower).....	81
Figure 6-17 WY2010 turbidity data and book-end model output at Victoria-Canal-Byron (upper) and Turner-Cut-Holt (lower).....	82
Figure 6-18 WY2010 turbidity data and book-end model output at Middle-R-Holt (upper) and Middle-at-Middle (lower).....	83
Figure 6-19 WY2010 contour plot showing the modeled distribution of turbidity in February 14, 2010. Values shown are near the compliance locations.....	84
Figure 6-20 Combined flows – inflow from the northern Delta and export flows from the south Delta (upper plot) and OMR flow (lower lot) during February, WY2010.....	85
Figure 6-21 WY2011 contour plot showing the modeled distribution of turbidity on March 29, 2011. Values shown are near the compliance locations.....	86
Figure 6-22 Combined flows – inflow from the northern Delta and export flows from the south Delta (upper plot) and OMR flow (lower lot) during March, WY2011.....	87
Figure 6-23 WY2013 contour plot showing the modeled distribution of turbidity on Dec. 16, 2012. Values shown are near the compliance locations.....	88
Figure 6-24 Combined flows – inflow from the northern Delta and export flows from the south Delta (upper plot) and OMR flow (lower lot) during December, WY2013.....	89
Figure 7-1 Mixed-SSC-WARMF results at D26 in the recent years time frame.....	92
Figure 7-2 Mixed-SSC-WARMF results at D26 in the early years time frame.....	93
Figure 7-3 Locations used to investigate the formation of a turbidity bridge in the south Delta illustrated in the DSM2 grid.....	100

Figure 7-4 Plots show the modeled turbidity output at the three compliance locations along with the 12 NTU compliance value for WYs 1991 – 1994. ....	101
Figure 7-5 Plots show the modeled turbidity output at the three compliance locations along with the 12 NTU compliance value for WYs 1995 – 1998. ....	102
Figure 7-6 Plots show the modeled turbidity output at the three compliance locations along with the 12 NTU compliance value for WYs 1999 – 2000. ....	103
Figure 7-7 Turbidity time series at six key “bridge” locations (upper), and Sacramento, Yolo Bypass and San Joaquin inflow (lower) in WY 1991.....	104
Figure 7-8 March 16, 1991 contour plot showing values at the six key locations. Turbidity is travelling south down Old River, and then east into Middle River. ....	105
Figure 7-9 March 17 (upper) and 21 (lower) 1991 contour plots showing values at the six key locations and the predominant progression of the turbidity pulse southwards down Old River into Middle River, and also intruding into the south Delta and northwards from San Joaquin flow. ....	106
Figure 7-10 Turbidity time series at six key “bridge” locations (upper), and Sacramento, Yolo Bypass and San Joaquin inflow (lower) in WY 1992.....	107
Figure 7-11 February (upper) and 25 (lower) 1992 contour plots showing values at the six key locations and the progression of the predominant turbidity pulse along Old and Middle Rivers from the south (upper), and then is joined in the central Delta by turbidity traveling south from both San Joaquin sources from the East and Sacramento sources from the north.....	108
Figure 7-12 Turbidity time series at six key “bridge” locations (upper), and Sacramento, Yolo Bypass and San Joaquin inflow (lower) in WY 1993.....	109
Figure 7-13 January 12, 1993 contour plot showing values at the six key locations. Turbidity is predominantly travelling south down Old River, and additionally traveling northwards from the south into Old and Middle Rivers.....	110
Figure 7-14 Turbidity time series at six key “bridge” locations (upper), and Sacramento, Yolo Bypass and San Joaquin inflow (lower) in WY 1994.....	111
Figure 7-15 February 22, 1994 contour plot showing values at the six key locations. A turbidity bridge did not form. ....	112
Figure 7-16 Turbidity time series at six key “bridge” locations (upper), and Sacramento, Yolo Bypass and San Joaquin inflow (lower) in WY 1995.....	113
Figure 7-17 January 12, 1995 contour plot showing values at the six key locations. This is the progression predominantly from the north down Old River for the first turbidity pulse this wet season. The San Joaquin pulse also contributes to the bridge from the south. ....	114
Figure 7-18 March 12 (upper) and 14 (lower) contour plots showing values at the six key locations for the second turbidity pulse of this season - the progression of the predominant turbidity pulse is northward along Old and Middle Rivers from the south (upper). ....	115
Figure 7-19 Turbidity time series at six key “bridge” locations (upper), and Sacramento, Yolo Bypass and San Joaquin inflow (lower) in WY 1996.....	116
Figure 7-20 January 13, 1996 contour plot showing values at the six key locations. This is the progression equally from the north and south along Old and Middle Rivers. ....	117

Figure 7-21 Turbidity time series at six key “bridge” locations (upper), and Sacramento, Yolo Bypass and San Joaquin inflow (lower) in WY 1997.....	118
Figure 7-22 December 19, 1996 contour plot showing values at the six key locations. This is the progression primarily from the south and east from the high San Joaquin River inflow. ....	119
Figure 7-23 Turbidity time series at six key “bridge” locations (upper), and Sacramento, Yolo Bypass and San Joaquin inflow (lower) in WY 1998.....	120
Figure 7-24 January 21 (upper) and February 3 (lower) 1998 contour plots showing values at the six key locations for the two turbidity pulses of this season - the progression of the predominant turbidity pulse is northward along Old and Middle Rivers from the south due to the high San Joaquin River inflow.....	121
Figure 7-25 Turbidity time series at six key “bridge” locations (upper), and Sacramento, Yolo Bypass and San Joaquin inflow (lower) in WY 1999.....	122
Figure 7-26 February 18, 1999 contour plot showing values at the six key locations. A turbidity bridge just barely formed this year, and this may simply be considered an artifact of the bias toward high turbidity values. ....	123
Figure 7-27 Turbidity time series at six key “bridge” locations (upper), and Sacramento, Yolo Bypass and San Joaquin inflow (lower) in WY 2000.....	124
Figure 7-28 February 5 (upper) and 19 (lower) 200 contour plots showing values at the six key locations for the two turbidity pulses of this season - the progression of the predominant turbidity pulse is initially southward along Old and Middle Rivers, and later from the south due to the increased San Joaquin River inflow.....	125
Figure 11-1 WY2013 new RMA calibration results at Antioch. ....	133
Figure 11-2 WY2013 new RMA calibration results at Cache-Ryer. ....	134
Figure 11-3 WY2011 revised calibration results at Antioch. ....	135
Figure 11-4 WY2011 revised calibration results at Cache-Ryer. ....	136
Figure 11-5 WY2011 revised calibration results at Decker Island. ....	137
Figure 11-6 WY2011 revised calibration results at False River. ....	138
Figure 11-7 WY2011 revised calibration results at Freeport.....	139
Figure 11-8 WY2011 revised calibration results at Georgiana-Below-Sac.....	140
Figure 11-9 WY2011 revised calibration results at Georgiana-at-Sac. ....	141
Figure 11-10 WY2011 revised calibration results at Grant Line.....	142
Figure 11-11 WY2011 revised calibration results at Grant-Line Tracy. ....	143
Figure 11-12 WY2011 revised calibration results at Holland Cut. ....	144
Figure 11-13 WY2011 revised calibration results at Hood. ....	145
Figure 11-14 WY2011 revised calibration results at Little Potato Slough-at-Terminous. ....	146
Figure 11-15 WY2011 revised calibration results at Mallard Slough. ....	147
Figure 11-16 WY2011 revised calibration results at Middle River-at-Howard Rd.....	148
Figure 11-17 WY2011 revised calibration results at Middle River-at-Holt. ....	149
Figure 11-18 WY2011 revised calibration results at Miner Slough. ....	150
Figure 11-19 WY2011 revised calibration results at Mokelumne-at-San Joaquin.....	151

Figure 11-20 WY2011 revised calibration results at Mossdale.....	152
Figure 11-21 WY2011 revised calibration results at North Mokelumne. ....	153
Figure 11-22 WY2011 revised calibration results at Prisoner Point. ....	154
Figure 11-23 WY2011 revised calibration results at Prisoner Point-at-Terminus. ....	155
Figure 11-24 WY2011 revised calibration results at Rio Vista.....	156
Figure 11-25 WY2011 revised calibration results at Rough-N-Ready Island.....	157
Figure 11-26 WY2011 revised calibration results at San Joaquin-at-Garwood. ....	158
Figure 11-27 WY2011 revised calibration results at San Joaquin-at-McCune (Vernalis). ....	159
Figure 11-28 WY2011 revised calibration results at South Mokelumne. ....	160
Figure 11-29 WY2011 revised calibration results at Threemile-Slough-at-San Joaquin. ....	161
Figure 11-30 WY2011 revised calibration results at Turner Cut-at-Holt.....	162
Figure 11-31 WY2011 revised calibration results at Victoria Canal-at-Byron. ....	163
Figure 11-32 WY2010 revised calibration results at Antioch. ....	164
Figure 11-33 WY2010 revised calibration results at Cache-at-Ryer Island. ....	165
Figure 11-34 WY2010 revised calibration results at Decker Island.....	166
Figure 11-35 WY2010 revised calibration results at False River.....	167
Figure 11-36 WY2010 revised calibration results at Freeport.....	168
Figure 11-37 WY2010 revised calibration results at Georgiana-Below-Sac.....	169
Figure 11-38 WY2010 revised calibration results at Georgiana-Sac. ....	170
Figure 11-39 WY2010 revised calibration results at Grant Line.....	171
Figure 11-40 WY2010 revised calibration results at Holland Cut. ....	172
Figure 11-41 WY2010 revised calibration results at Hood. ....	173
Figure 11-42 WY2010 revised calibration results at Little Potato Slough-at-Terminus. ....	174
Figure 11-43 WY2010 revised calibration results at Mallard Slough. ....	175
Figure 11-44 WY2010 revised calibration results at Middle River-at-Holt. ....	176
Figure 11-45 WY2010 revised calibration results at Miner Slough. ....	177
Figure 11-46 WY2010 revised calibration results at Mokelumne-at-San Joaquin.....	178
Figure 11-47 WY2010 revised calibration results at Mossdale.....	179
Figure 11-48 WY2010 revised calibration results at Prisoner Point. ....	180
Figure 11-49 WY2010 revised calibration results at Prisoner Point-at-Terminus. ....	181
Figure 11-50 WY2010 revised calibration results at Rio Vista.....	182
Figure 11-51 WY2010 revised calibration results at Rough-N-Ready Island.....	183
Figure 11-52 WY2010 revised calibration results at San Joaquin-at-Garwood. ....	184
Figure 11-53 WY2010 revised calibration results at San Joaquin-at-McCune (Vernalis). ....	185
Figure 11-54 WY2010 revised calibration results at Threemile-Slough-at-San Joaquin. ....	186
Figure 11-55 WY2010 revised calibration results at Turner Cut-at-Holt.....	187
Figure 11-56 WY2010 revised calibration results at Victoria Canal-at-Byron. ....	188
Figure 12-1 WY2013 15-min RMA new calibration results at Antioch. ....	190
Figure 12-2 WY2011 15-min revised calibration results at Antioch.....	192
Figure 12-3 WY2011 15-min revised calibration results at Cache-Ryer. ....	193

Figure 12-4 WY2011 15-min revised calibration results at Decker Island. ....	194
Figure 12-5 WY2011 15-min revised calibration results at False River. ....	195
Figure 12-6 WY2011 15-min revised calibration results at Freeport. ....	196
Figure 12-7 WY2011 15-min revised calibration results at Georgiana-Below-Sac. ....	197
Figure 12-8 WY2011 15-min revised calibration results at Georgiana-at-Sac. ....	198
Figure 12-9 WY2011 15-min revised calibration results at Grant Line. ....	199
Figure 12-10 WY2011 15-min revised calibration results at Grant-Line Tracy. ....	200
Figure 12-11 WY2011 15-min revised calibration results at Holland Cut. ....	201
Figure 12-12 WY2011 15-min revised calibration results at Hood. ....	202
Figure 12-13 WY2011 15-min revised calibration results at Little Potato Slough-at-Terminus. .....	203
Figure 12-14 WY2011 15-min revised calibration results at Mallard Slough. ....	204
Figure 12-15 WY2011 15-min revised calibration results at Middle River-at-Howard Rd. ....	205
Figure 12-16 WY2011 15-min revised calibration results at Middle River-at-Holt. ....	206
Figure 12-17 WY2011 15-min revised calibration results at Miner Slough. ....	207
Figure 12-18 WY2011 15-min revised calibration results at Mokelumne-at-San Joaquin. ....	208
Figure 12-19 WY2011 15-min revised calibration results at Mossdale. ....	209
Figure 12-20 WY2011 15-min revised calibration results at North Mokelumne. ....	210
Figure 12-21 WY2011 15-min revised calibration results at Prisoner Point. ....	211
Figure 12-22 WY2011 15-min revised calibration results at Prisoner Point-at-Terminus. ....	212
Figure 12-23 WY2011 15-min revised calibration results at Rio Vista. ....	213
Figure 12-24 WY2011 15-min revised calibration results at Rough-N-Ready Island. ....	214
Figure 12-25 WY2011 15-min revised calibration results at San Joaquin-at-Garwood. ....	215
Figure 12-26 WY2011 15-min revised calibration results at San Joaquin-at-McCune (Vernalis). .....	216
Figure 12-27 WY2011 15-min revised calibration results at South Mokelumne. ....	217
Figure 12-28 WY2011 15-min revised calibration results at Threemile-Slough-at-San Joaquin. .....	218
Figure 12-29 WY2011 15-min revised calibration results at Turner Cut-at-Holt. ....	219
Figure 12-30 WY2011 15-min revised calibration results at Victoria Canal-at-Byron. ....	219
Figure 12-31 WY2010 15-min revised calibration results at Antioch. ....	220
Figure 12-32 WY2010 15-min revised calibration results at Cache-at-Ryer Island. ....	221
Figure 12-33 WY2010 15-min revised calibration results at Decker Island. ....	222
Figure 12-34 WY2010 15-min revised calibration results at False River. ....	223
Figure 12-35 WY2010 15-min revised calibration results at Freeport. ....	224
Figure 12-36 WY2010 15-min revised calibration results at Georgiana-Below-Sac. ....	225
Figure 12-37 WY2010 15-min revised calibration results at Grant Line. ....	226
Figure 12-38 WY2010 15-min revised calibration results at Holland Cut. ....	227
Figure 12-39 WY2010 15-min revised calibration results at Hood. ....	228

Figure 12-40 WY2010 15-min revised calibration results at Little Potato Slough-at-Terminus.	229
Figure 12-41 WY2010 15-min revised calibration results at Mallard Slough.....	230
Figure 12-42 WY2010 15-min revised calibration results at Middle River-at-Holt. ....	231
Figure 12-43 WY2010 15-min revised calibration results at Miner Slough. ....	232
Figure 12-44 WY2010 15-min revised calibration results at Mokelumne-at-San Joaquin. ....	233
Figure 12-45 WY2010 15-min revised calibration results at Mossdale. ....	234
Figure 12-46 WY2010 15-min revised calibration results at Prisoner Point.....	235
Figure 12-47 WY2010 15-min revised calibration results at Prisoner Point-at-Terminus. ....	236
Figure 12-48 WY2010 15-min revised calibration results at Rio Vista. ....	237
Figure 12-49 WY2010 15-min revised calibration results at Rough-N-Ready Island. ....	238
Figure 12-50 WY2010 15-min revised calibration results at San Joaquin-at-Garwood.....	239
Figure 12-51 WY2010 15-min revised calibration results at San Joaquin-at-McCune (Vernalis).	240
Figure 12-52 WY2010 15-min revised calibration results at Threemile-Slough-at-San Joaquin.	241
Figure 12-53 WY2010 15-min revised calibration results at Turner Cut-at-Holt. ....	242
Figure 12-54 WY2010 15-min revised calibration results at Victoria Canal-at-Byron.....	243
Figure 13-1 DSM2 daily-averaged turbidity model results using USGS-SSC at Freeport and Vernalis, and WARMF turbidity at other inflow boundaries compared to EMP grab-sample data, early years– location is EMP C3.....	245
Figure 13-2 DSM2 daily-averaged turbidity model results using USGS-SSC at Freeport and Vernalis, and WARMF turbidity at other inflow boundaries compared to EMP grab-sample data, early years– location is EMP C7.....	246
Figure 13-3 DSM2 daily-averaged turbidity model results using USGS-SSC at Freeport and Vernalis, and WARMF turbidity at other inflow boundaries compared to EMP grab-sample data, early years– location is EMP C9.....	247
Figure 13-4 DSM2 daily-averaged turbidity model results using USGS-SSC at Freeport and Vernalis, and WARMF turbidity at other inflow boundaries compared to EMP grab-sample data, early years– location is EMP C10.....	248
Figure 13-5 DSM2 daily-averaged turbidity model results using USGS-SSC at Freeport and Vernalis, and WARMF turbidity at other inflow boundaries compared to EMP grab-sample data, early years– location is EMP D4. ....	249
Figure 13-6 DSM2 daily-averaged turbidity model results using USGS-SSC at Freeport and Vernalis, and WARMF turbidity at other inflow boundaries compared to EMP grab-sample data, early years– location is EMP D6. ....	250
Figure 13-7 DSM2 daily-averaged turbidity model results using USGS-SSC at Freeport and Vernalis, and WARMF turbidity at other inflow boundaries compared to EMP grab-sample data, early years– location is EMP D7. ....	251

Figure 13-8 DSM2 daily-averaged turbidity model results using USGS-SSC at Freeport and Vernalis, and WARMF turbidity at other inflow boundaries compared to EMP grab-sample data, early years– location is EMP D8. ....	252
Figure 13-9 DSM2 daily-averaged turbidity model results using USGS-SSC at Freeport and Vernalis, and WARMF turbidity at other inflow boundaries compared to EMP grab-sample data, early years– location is EMP D9. ....	253
Figure 13-10 DSM2 daily-averaged turbidity model results using USGS-SSC at Freeport and Vernalis, and WARMF turbidity at other inflow boundaries compared to EMP grab-sample data, early years– location is EMP D10. ....	254
Figure 13-11 DSM2 daily-averaged turbidity model results using USGS-SSC at Freeport and Vernalis, and WARMF turbidity at other inflow boundaries compared to EMP grab-sample data, early years– location is EMP D11. ....	255
Figure 13-12 DSM2 daily-averaged turbidity model results using USGS-SSC at Freeport and Vernalis, and WARMF turbidity at other inflow boundaries compared to EMP grab-sample data, early years– location is EMP D12. ....	256
Figure 13-13 DSM2 daily-averaged turbidity model results using USGS-SSC at Freeport and Vernalis, and WARMF turbidity at other inflow boundaries compared to EMP grab-sample data, early years– location is EMP D14A.....	257
Figure 13-14 DSM2 daily-averaged turbidity model results using USGS-SSC at Freeport and Vernalis, and WARMF turbidity at other inflow boundaries compared to EMP grab-sample data, early years– location is EMP D15. ....	258
Figure 13-15 DSM2 daily-averaged turbidity model results using USGS-SSC at Freeport and Vernalis, and WARMF turbidity at other inflow boundaries compared to EMP grab-sample data, early years– location is EMP D16. ....	259
Figure 13-16 DSM2 daily-averaged turbidity model results using USGS-SSC at Freeport and Vernalis, and WARMF turbidity at other inflow boundaries compared to EMP grab-sample data, early years– location is EMP D19. ....	260
Figure 13-17 DSM2 daily-averaged turbidity model results using USGS-SSC at Freeport and Vernalis, and WARMF turbidity at other inflow boundaries compared to EMP grab-sample data, early years– location is EMP D22. ....	261
Figure 13-18 DSM2 daily-averaged turbidity model results using USGS-SSC at Freeport and Vernalis, and WARMF turbidity at other inflow boundaries compared to EMP grab-sample data, early years– location is EMP D24. ....	262
Figure 13-19 DSM2 daily-averaged turbidity model results using USGS-SSC at Freeport and Vernalis, and WARMF turbidity at other inflow boundaries compared to EMP grab-sample data, early years– location is EMP D26. ....	263
Figure 13-20 DSM2 daily-averaged turbidity model results using USGS-SSC at Freeport and Vernalis, and WARMF turbidity at other inflow boundaries compared to EMP grab-sample data, early years– location is EMP D28A.....	264

Figure 13-21 DSM2 daily-averaged turbidity model results using USGS-SSC at Freeport and Vernalis, and WARMF turbidity at other inflow boundaries compared to EMP grab-sample data, early years– location is EMP MD7A. ....	265
Figure 13-22 DSM2 daily-averaged turbidity model results using USGS-SSC at Freeport and Vernalis, and WARMF turbidity at other inflow boundaries compared to EMP grab-sample data, early years– location is EMP MD10. ....	266
Figure 13-23 DSM2 daily-averaged turbidity model results using USGS-SSC at Freeport and Vernalis, and WARMF turbidity at other inflow boundaries compared to EMP grab-sample data, early years– location is EMP P8. ....	267
Figure 13-24 DSM2 daily-averaged turbidity model results using USGS-SSC at Freeport and Vernalis, and WARMF turbidity at other inflow boundaries compared to EMP grab-sample data, early years– location is EMP P10A. ....	268
Figure 13-25 DSM2 daily-averaged turbidity model results using USGS-SSC at Freeport and Vernalis, and WARMF turbidity at other inflow boundaries compared to EMP grab-sample data, early years– location is EMP P12. ....	269
Figure 13-26 DSM2 daily-averaged turbidity model results using USGS-SSC at Freeport and Vernalis, and WARMF turbidity at other inflow boundaries compared to EMP grab-sample data, early years– location is EMP S42. ....	270
Figure 13-27 DSM2 daily-averaged turbidity model results using USGS-SSC at Freeport and Vernalis, and WARMF turbidity at other inflow boundaries compared to EMP grab-sample data, recent years– location is EMP C3. ....	272
Figure 13-28 DSM2 daily-averaged turbidity model results using USGS-SSC at Freeport and Vernalis, and WARMF turbidity at other inflow boundaries compared to EMP grab-sample data, recent years– location is EMP C7. ....	273
Figure 13-29 DSM2 daily-averaged turbidity model results using USGS-SSC at Freeport and Vernalis, and WARMF turbidity at other inflow boundaries compared to EMP grab-sample data, recent years– location is EMP C9. ....	274
Figure 13-30 DSM2 daily-averaged turbidity model results using USGS-SSC at Freeport and Vernalis, and WARMF turbidity at other inflow boundaries compared to EMP grab-sample data, recent years– location is EMP C10. ....	275
Figure 13-31 DSM2 daily-averaged turbidity model results using USGS-SSC at Freeport and Vernalis, and WARMF turbidity at other inflow boundaries compared to EMP grab-sample data, recent years– location is EMP D4. ....	276
Figure 13-32 DSM2 daily-averaged turbidity model results using USGS-SSC at Freeport and Vernalis, and WARMF turbidity at other inflow boundaries compared to EMP grab-sample data, recent years– location is EMP D6. ....	277
Figure 13-33 DSM2 daily-averaged turbidity model results using USGS-SSC at Freeport and Vernalis, and WARMF turbidity at other inflow boundaries compared to EMP grab-sample data, recent years– location is EMP D7. ....	278

Figure 13-34 DSM2 daily-averaged turbidity model results using USGS-SSC at Freeport and Vernalis, and WARMF turbidity at other inflow boundaries compared to EMP grab-sample data, recent years– location is EMP D8.....	279
Figure 13-35 DSM2 daily-averaged turbidity model results using USGS-SSC at Freeport and Vernalis, and WARMF turbidity at other inflow boundaries compared to EMP grab-sample data, recent years– location is EMP D9.....	280
Figure 13-36 DSM2 daily-averaged turbidity model results using USGS-SSC at Freeport and Vernalis, and WARMF turbidity at other inflow boundaries compared to EMP grab-sample data, recent years– location is EMP D10.....	281
Figure 13-37 DSM2 daily-averaged turbidity model results using USGS-SSC at Freeport and Vernalis, and WARMF turbidity at other inflow boundaries compared to EMP grab-sample data, recent years– location is EMP D11.....	282
Figure 13-38 DSM2 daily-averaged turbidity model results using USGS-SSC at Freeport and Vernalis, and WARMF turbidity at other inflow boundaries compared to EMP grab-sample data, recent years– location is EMP D12.....	283
Figure 13-39 DSM2 daily-averaged turbidity model results using USGS-SSC at Freeport and Vernalis, and WARMF turbidity at other inflow boundaries compared to EMP grab-sample data, recent years– location is EMP D14A.....	284
Figure 13-40 DSM2 daily-averaged turbidity model results using USGS-SSC at Freeport and Vernalis, and WARMF turbidity at other inflow boundaries compared to EMP grab-sample data, recent years– location is EMP D15.....	285
Figure 13-41 DSM2 daily-averaged turbidity model results using USGS-SSC at Freeport and Vernalis, and WARMF turbidity at other inflow boundaries compared to EMP grab-sample data, recent years– location is EMP D16.....	286
Figure 13-42 DSM2 daily-averaged turbidity model results using USGS-SSC at Freeport and Vernalis, and WARMF turbidity at other inflow boundaries compared to EMP grab-sample data, recent years– location is EMP D22.....	287
Figure 13-43 DSM2 daily-averaged turbidity model results using USGS-SSC at Freeport and Vernalis, and WARMF turbidity at other inflow boundaries compared to EMP grab-sample data, recent years– location is EMP D24.....	288
Figure 13-44 DSM2 daily-averaged turbidity model results using USGS-SSC at Freeport and Vernalis, and WARMF turbidity at other inflow boundaries compared to EMP grab-sample data, recent years– location is EMP D26.....	289
Figure 13-45 DSM2 daily-averaged turbidity model results using USGS-SSC at Freeport and Vernalis, and WARMF turbidity at other inflow boundaries compared to EMP grab-sample data, recent years– location is EMP D28A.....	290
Figure 13-46 DSM2 daily-averaged turbidity model results using USGS-SSC at Freeport and Vernalis, and WARMF turbidity at other inflow boundaries compared to EMP grab-sample data, recent years– location is EMP MD7A.....	291

Figure 13-47 DSM2 daily-averaged turbidity model results using USGS-SSC at Freeport and Vernalis, and WARMF turbidity at other inflow boundaries compared to EMP grab-sample data, recent years– location is EMP MD10. .... 292

Figure 13-48 DSM2 daily-averaged turbidity model results using USGS-SSC at Freeport and Vernalis, and WARMF turbidity at other inflow boundaries compared to EMP grab-sample data, recent years– location is EMP P8. .... 293

Figure 13-49 DSM2 daily-averaged turbidity model results using USGS-SSC at Freeport and Vernalis, and WARMF turbidity at other inflow boundaries compared to EMP grab-sample data, recent years– location is EMP P10A. .... 294

Figure 13-50 DSM2 daily-averaged turbidity model results using USGS-SSC at Freeport and Vernalis, and WARMF turbidity at other inflow boundaries compared to EMP grab-sample data, recent years– location is EMP P12. .... 295

## Tables

Table 1 Inflow and stage boundary conditions - data sources and shifts in timing. ....	21
Table 2 Turbidity BC - sources and alterations in timing and magnitude. ....	22
Table 3 WY2010 calibration statistics for QUAL turbidity – comparison of New calibration run and Original RMA calibration. Bold font in the name indicates compliance locations; blue font in the statistic denotes a better result at the compliance location. ....	56
Table 4 WY2011 calibration statistics for QUAL turbidity – comparison of New calibration run and Original RMA calibration. Bold font in the name indicates compliance locations; blue font in the statistic denotes a better result at the compliance location. ....	57
Table 5 WY2013 calibration statistics for QUAL turbidity – comparison of New calibration run and Original RMA calibration. Bold font in the name indicates compliance locations; blue font in the statistic denotes a better result in the calibration comparison. ....	58
Table 6 Overall calibration metrics for the New calibration run and the Original RMA calibration run. Blue, bold font indicates a superior calibration result. Black, bold font indicates equivalent results. ....	59
Table 6-1 Flow and turbidity values for the month in which the three compliance locations exceeded 12 NTU in each Water Year modeled in the recalibration effort. ....	64
Table 6-2 Comparison of calibration statistics in WY2010 for the lower and higher Calaveras turbidity boundary condition (CDEC Rough-N-Ready)*10) that was used as the final setting. Bold font indicates a compliance location while blue font indicates a better result in comparison with the other simulation. ....	65
Table 6-3 Overall calibration metrics for the WY2010 calibration run and with low and high Calaveras turbidity boundary. Blue, bold font indicates a superior calibration result. Black, bold font indicates equivalent results. ....	65
Table 7-1 Statistics for the simulation in early years (1975 – 1990) for the Mixed-SSC-WARMF simulation. ....	94
Table 7-2 Statistics for the simulation in recent years (1991 – 2011) for the Mixed-SSC-WARMF simulation. ....	95
Table 7-3 Turbidity bridge decision variables, 1991 – 1994. Bold font indicates primary driver(s) for turbidity, shaded column indicates no bridge formed. ....	98
Table 7-4 Turbidity bridge decision variables, 1995 – 1997. Bold font indicates primary driver(s) for turbidity. ....	98
Table 7-5 Turbidity bridge decision variables, 1998 – 2000. Bold font indicates primary driver(s) for turbidity, shaded columns indicate no bridge formed. ....	99

## 1 Executive Summary

This report documents the extension of the calibration period of DSM2-QUAL's turbidity model to the wet season in Water Year 2013 (WY2013), building on previous documentation by Resource Management Associates (RMA) for QUAL calibration based on the wet seasons of WY2010 and WY2011 (RMA 2013). The current work is preceded by projects funded by the Metropolitan Water District of Southern California (MWD) for RMA to develop a turbidity transport model in RMA two-dimensional models of the Sacramento San Joaquin Delta (RMA 2008, 2009a, 2009b, 2010a, 2010b, 2011, 2012a, 2012b). The current work, and previous work, is part of an ongoing effort to model the hydrodynamic transport of turbidity as a proxy for the transport of suspended sediment. The reader is referred to previous documents for the motivation behind development of turbidity modeling in RMA models.

The work covered in the current document is based on the implementation of a turbidity model in the one-dimensional QUAL transport model by the Delta Modeling Section (DMS) of the Department of Water Resources (DWR), as discussed in (DWR 2011). For the work discussed in this report, RMA used the previous (RMA 2013) calibration of QUAL's turbidity model as background for the three main project objectives:

1. Refine RMA's previous QUAL turbidity model calibration (RMA 2013) using WYs 2010, 2011 and 2013.
2. Use the refined calibration to recalculate and refine the historical simulation, 1975–2011, of turbidity in QUAL to support calibration of the Turbidity ANN (Artificial Neural Network), and to update and refine Historical calibration statistics using EMP (Environmental Monitoring Program) data.
3. Refine and extend the documentation of the analysis of conditions leading to turbidity bridge formation (RMA, 2013).

As in previous documentation (RMA 2013), statistical measures were employed to quantify the success of the modeling recalibration effort. Metrics were used to quantify the success of the modeling effort at individual data locations and as a whole for each modeled wet season in WYs 2010, 2011 and 2013. The intent of these metrics was to supply information to aid in appropriate model application with a focus on decision support.

When RMA's previously calibrated model was used in WY2013 to model wet season turbidity, the model did a poor job of reproducing turbidity measurements so a decision was made to see if the calibration could be improved in WY2013 and in general by including WY2013 in the calibration effort. As has been mentioned in previous documentation (RMA 2010b, 2011, 2012b, 2013), the compromise of using a turbidity model instead of a physically-based suspended sediment model means that the accuracy of model results can vary widely from year-to-year as variations in the character of the suspended sediment at inflow locations and the effects of wind resuspension, for example, are not captured in a turbidity model.

Work refining the QUAL turbidity calibration, covered in Objective One, focused on improving QUAL's accuracy in modeling turbidity in the winter of WY2013 and on improving calibration in WY2010 and WY2011 if possible. If trade-offs between calibration quality in WY2013 and previous years proved necessary, the objective was to compromise the quality of the calibration in WYs 2010 and 2011 as little as possible. As in the previous calibration effort (RMA 2013), a series of calibration statistics were calculated for the wet seasons of WY2010, WY2011 and WY2013 quantifying the results of the recalibration effort, and comparing them to the previous calibration completed and documented in (RMA 2013). Although the wet season of WY2012 was modeled, it was not included in the calibration assessment and the results are not included in this report, as inflow and turbidity concentrations were too low and outside of the conditions needed for successful application of the QUAL turbidity model.

The calibration statistics document that the recalibration substantially improved the representation of Delta turbidity in WY2013 and WY2011 and mixed results in WY2010 at the three turbidity measurement compliance locations in the central and south Delta – Holland Cut, Prisoner Point and Victoria Canal at Byron. In WY2010 there was a loss in the results for the model bias (PBIAS) statistic particularly along Old River and at the Holland Cut compliance location. Conversely, results were markedly better along Old River and at the Holland Cut compliance location in WY2011 and WY2013. These particular results clearly indicate the difficulty in this calibration work, as there was a clear trade-off in model performance between these modeled years. The Model Skill assessment indicate that the overall model skill was improved by the recalibration effort in WY2011 and WY2013, with a mix of loss and improvements in WY2010.

As part of the current recalibration work, significant effort was taken to prepare the best possible boundary conditions for both HYDRO and for the QUAL turbidity model. In HYDRO, flow and stage boundary conditions were carefully screened to eliminate spurious data and time shifts were implemented in boundary time series to ensure the best possible match with both timing and magnitude of stage and flow data. Turbidity boundary conditions were subject to the same intense level of scrutiny both before and during the recalibration process for each WY.

As the work progressed, particular focus was placed on the setting of the Calaveras River turbidity boundary condition. The CDEC data location at Rough-N-Ready Island on the San Joaquin River was used to set the boundary as it is the closest location to the Calaveras inflow. For WY2013 and WY2010, setting the Calaveras turbidity as (CDEC Rough-N-Ready)\*10 and shifted by 12 hours was found to give a reasonable result at downstream locations. In WY2011, a high flow year on the Calaveras, the CDEC data was applied directly (i.e., without a scaling factor), but also shifted by 12 hours. Subsequent volumetric analysis showed that the volume of Calaveras water at several central and south Delta locations had a substantial influence on the modeled turbidity result in WY2011, but not in the lower Calaveras flow years WY2010 and WY2013. However, the source of the associated suspended sediment – Calaveras R. and/or San Joaquin R. – is an open question.

Objective Two focused on refining the previous long-term (1975-2011) Historical turbidity model, which supports the Turbidity ANN. Documentation on the previous development of the QUAL Historical turbidity model is available in (RMA 2013). In addition to refining the Historical turbidity model, the

statistical approach for calibration using the EMP grab-sample turbidity data was modified to include only data for a standard “wet season” from December to March in each modeled period.

The Mixed-SSC-WARMF set of turbidity boundary condition for the San Joaquin and Sacramento Rivers were reviewed, and although the San Joaquin boundary was found to retain a good match with EMP data, the Sacramento boundary conditions was revised. The QUAL turbidity boundary conditions at Freeport, which are based on USGS suspended sediment data, were tested by increasing and decreasing the scale factor applied to the USGS SSC data for the early years and the recent years separately to improve the results. Importantly, it was noted IEP grab-sample data is very low (< 100 NTU) in comparison with the range of CDEC 15-minute turbidity data at Hood (~50 – 350 NTU, or higher). Therefore, the Freeport boundary condition was revised to produce a range of modeled values at Hood that are comparable to the range of CDEC turbidity data values seen at Hood during periods of high inflow, as well as to improve calibration results. The statistical results for the new long-term Historical model calibration are thus biased to overestimating the IEP data.

The newly calibrated model was applied in the wet seasons of WY2010, WY2011 and WY2013 and the Mixed-SSC-WARMF simulation high flow/high turbidity periods of Water Years 1991 – 2000 to investigate the formation of “turbidity bridges” of 12 NTU (or greater) between the central and south Delta. The conditions under which a turbidity bridge might form were slightly different for the two cases – for WYs 2010, 2011 and 2013, a turbidity bridge was deemed to have formed when the 12 NTU value was exceeded in the daily-averaged CDEC data at the compliance locations. For the Mixed-SSC-WARMF simulation the conditions were more stringent as the results are less reliable, since the boundary conditions were either obtained from WARMF model output or synthesized from USGS-SSC data and the EMP data available for calibration was clearly low in many Delta locations.

In general, the analysis shows that there is more than one mode under which a turbidity bridge is likely to form which depends on the magnitude of the primary drivers (Sacramento or San Joaquin River inflow, export flows) and their timing. The long term Historical model results are based on synthetic boundary conditions not wholly supported by the IEP data, so results should be interpreted with caution. The results from the WY2010, 2011 and 2013 simulations are therefore a better indicator of the “bridge” conditions, although clearly limited in scope. In addition, in these recent wet season simulations, it was seen that high Calaveras River flows can be important driver in establishing a turbidity bridge. For the longer term simulation, it was found that the change in the calibration parameters changed the results somewhat from the previous turbidity bridge analysis in (RMA 2013), but the general trends were similar.

The model set-up and calibration results indicate the importance of setting sensible boundary conditions, as the example with the Calaveras River in WY2011 clearly shows. It would be helpful to have an additional CDEC turbidity location on the Calaveras River for turbidity model applications. Finally, as suggested in previous RMA documentation (RMA 2010b, 2011, 2012b, 2013), development of a suspended sediment model should be considered. The capability in a suspended sediment model to include wind-driven re-suspension of sediments, tidally-influenced suspension of sediments, variations in the character of suspended sediment composition at model boundaries, and other factors that are

not considered in these turbidity model calculations, have the potential to improve the quality and reliability of model results.

## 2 Introduction

### 2.1 Objectives

In this report, RMA utilized DWR-DMS's early turbidity modeling effort in DSM2-QUAL in support of two main project objectives, to:

1. Refine the previous DMS QUAL turbidity model calibration
2. Refine the historical model of turbidity in QUAL covering the period 1975 – 2011 as well as the statistical measures of the calibration from step 1 using EMP data.
3. Investigate conditions leading to the formation of a turbidity bridge in the central Delta.

The work refining QUAL turbidity calibration, covered in Objective One, focused on improving QUAL's accuracy in modeling turbidity in the winters of WY2010, 2011 and 2013 when high tributary inflows substantially increased turbidity in the Delta. Work on the second objective focused on refining the use USGS daily suspended sediment measurements as boundary conditions for the Sacramento and San Joaquin Rivers in the revised calibration of the turbidity model. Work on the third objective included investigating conditions for both of the simulations in step 1 (WY2010, 2011 and 2013) and step 2 (long Historical simulation).

### 2.2 Background

Turbidity has long been associated with the movement and habitat preferences of delta smelt (RMA 2008, 2009a, 2009b, 2010a, 2010b). Although the exact nature of the links between delta smelt and turbidity are subject to differing interpretations, common hypotheses include: facilitating feeding through visual contrast of delta smelt prey against the background; as a form of cover from predators; and, as a cue for winter migration upstream to fresher waters to spawn. Increases in Delta turbidity have also been associated with increases in entrainment in south Delta export locations, particularly when export pumping increases central Delta turbidity by forming a "turbidity bridge" linking the south Delta with high inflow pulses of turbidity from Delta tributaries, primarily the Sacramento River and the San Joaquin River.

Given the establishment of three turbidity measurement compliance locations – at Holland Cut, Prisoner Point and Victoria Canal at Byron – and the importance of delta smelt to current Delta operations, the QUAL turbidity model calibration discussed herein placed a high priority on calibration at these locations. These three turbidity compliance locations are used by the Delta Smelt Working Group for recommending constraints on Delta operations if it is suspected delta smelt may follow turbidity cues to the central Delta and potentially be subject to harm at the export pumps.

This document presents: calibration results along with a comparison with the previous calibration metrics; the update of the long-term simulation of Historical turbidity in the Delta and the refinement of

statistical measures calculated during this period; and, investigations conditions leading to the formation of a “turbidity bridge” (of 12 NTU or more) linking the central and south Delta

### **2.3 Challenges in modeling turbidity**

As discussed in previous documentation (RMA 2008, 2009a, 2009b, 2010a, 2010b, 2011, 2012b), there are conceptual challenges to modeling turbidity in a transport model such as DSM2-QUAL, or RMA11 (King 1995), as turbidity is an optical property of water not a physical property. The more appropriate quantity to model is suspended sediment concentration (SSC), as the transport of sediment has a known physical interpretation. That said, there is frequently a linear relationship between measured turbidity and SSC, and reasonable success has been obtained by using simple one parameter decay rates in the RMA11 transport model or settling rates for a non-conservative constituent in the QUAL model.

A turbidity model based on settling coefficients or decay rates is not capable of capturing all of the processes in sediment transport, so some mismatch between the model and turbidity data is not unexpected as turbidity measurements are used as a proxy for suspended sediment concentration. The model calibration results presented herein illustrate the difficulties in several aspects of the turbidity/suspended sediment relationship: the relationship can vary by location, by the characteristics of upstream suspended sediment load, by the characteristics of the underlying sediment, and by effects driven by local meteorology such as wind, rain and run-off. As a consequence, it can be expected that any turbidity model calibration will work better in some years than others, and since coefficients are not related to changes in the bed or in other sediment characteristics that change in time, the model will perform better at some locations and times than at others.

An additional challenge is setting turbidity boundary conditions at inflow locations. At Freeport and Vernalis, there are good turbidity sensors to use. For the Yolo Bypass and the Cosumnes and Mokelumne River, there are locations downstream of the inflow that can be used in many instances to set the inflow turbidity, perhaps with a shift in the time. The Calaveras River turbidity boundary condition is more problematic as there is not a good CDEC sensor to use just near the inflow location in the model domain. This challenge is discussed later in this document (Section 6).

## **3 Turbidity Model Calibration - Background and Methodology**

### **3.1 Definition of calibration**

In this document we assume the simple definition that calibration is the process of adjusting a set of model parameters so that model agreement with respect to a set of experimental data is maximized (Trucano et al., 2006). Similarly, validation is the quantification of the predictive ability of the model through comparison with a set of experimental data (Trucano et al., 2006). For the purposes of this project, the general calibration methodology discussed in Moriasi (2007) was modified for the turbidity model assessment and for the selection of criteria for assessing the goodness-of-fit of the model to the data. A validation step was not performed using a separate dataset.

### 3.2 QUAL turbidity calibration background and data

As discussed in (DWR 2011), the QUAL nutrient model equation for CBOD was used to simulate the transport of turbidity in the DSM2 model domain. Water temperature and the other nutrients in the QUAL nutrient model were not simulated.

The CBOD function in QUAL is expressed as:

$$\frac{dL}{dt} = -K_1L - K_3L$$

where:

L = concentration of CBOD (mg/L)

$K_1$  = deoxygenation rate coefficient ( $\text{day}^{-1}$ )

$K_3$  = settling rate of CBOD ( $\text{day}^{-1}$ ).

For our purpose,  $K_1$  was set to zero, as were all other coefficient in the QUAL nutrient model except  $K_3$  which was used to represent the settling of sediment as an approximation to the transport of turbidity.

Turbidity data needed for the calibration and to set Freeport and Vernalis boundary conditions was downloaded from the CDEC database – locations used in the calibration process are shown in Figure 3-1. Turbidity compliance locations are shown in Figure 3-2. Statistics were calculated for all available data of sufficient quality – the turbidity data was “cleaned”, i.e., questionable values were deleted using professional judgment based on familiarity with the data. For example, significant increases in turbidity are generally reflected in downstream locations, so when downstream locations did not reflect upstream changes, local increases could frequently be ascribed to instrument fouling or to short term trends in magnitude. However, increases in turbidity due to wind and rain events were not screened out, nor were changes in turbidity that were deemed reasonable. For example, changes in magnitude that did not appear to be due to instrument fouling or wind but were not necessarily reflected downstream (i.e., that might be due to localized events) were not screened out of the data set. Missing or deleted data values were filled using linear interpolation in HEC DSSVue software.

Calibration of the settling rate coefficient ( $K_3$ ) to turbidity data was accomplished using the wet season data of three Water Years - 2010, 2011 and 2013. These years were chosen as they have the best (least noisy) data and most numerous turbidity measurement stations, as well as the having data available for setting boundary conditions. Boundary locations without data were set using WARMF model output.

Turbidity data was also obtained from Environmental Monitoring Program data base<sup>1</sup>. These are discrete water samples (aka “grab samples”) generally collected from land-based collection locations or from DWR or USBR research vessels. Field methods are available at the following website:

---

<sup>1</sup><http://www.water.ca.gov/bdma/meta/index.cfm>

<http://www.water.ca.gov/bdma/meta/discrete.cfm>

These data were used in comparison with QUAL long term turbidity simulation output, 1975 – 2011, to assess the performance of this Historical model run. Figures showing the locations used and the results are discussed in Section 7.

DRAFT

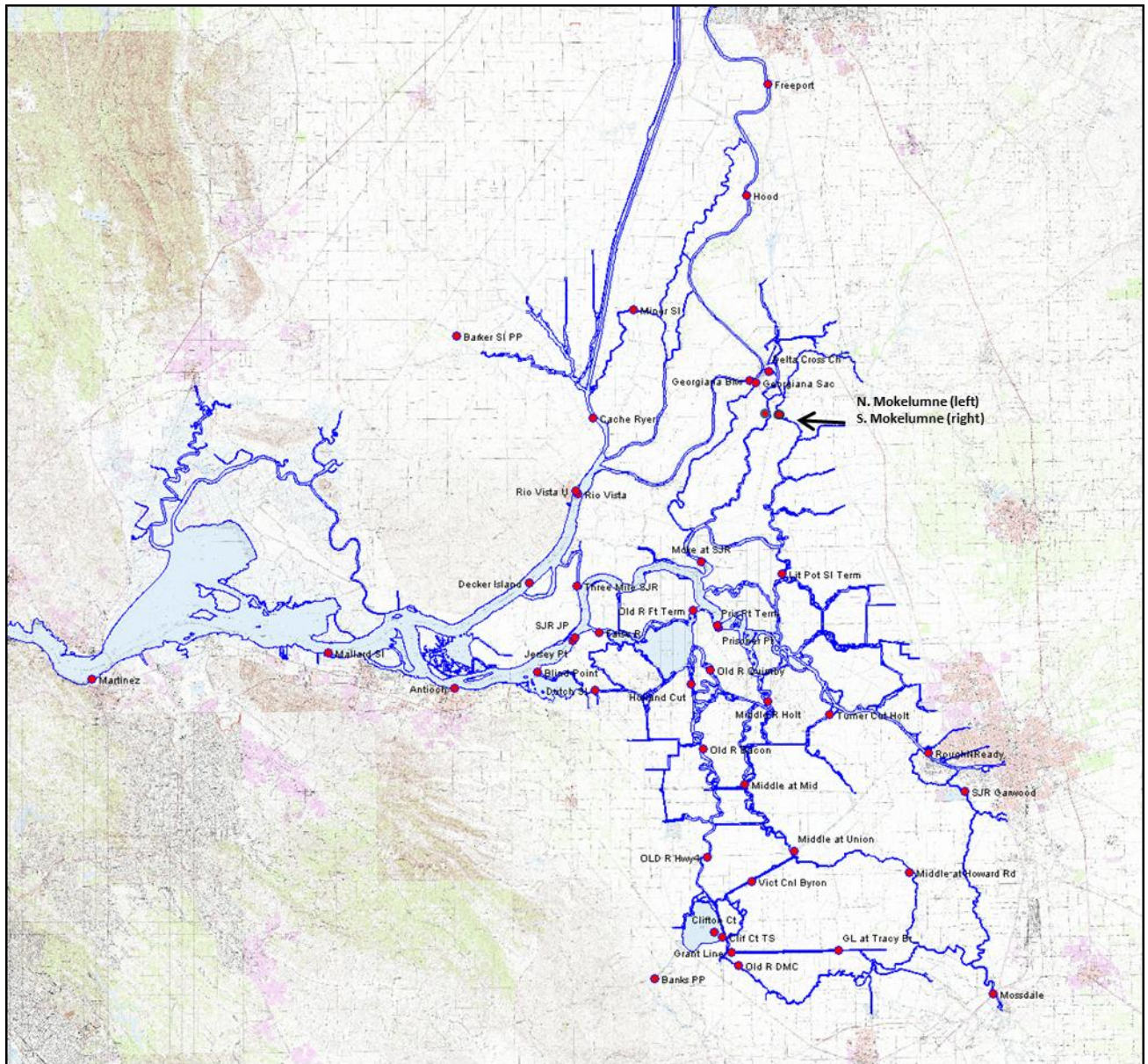


Figure 3-1 CDEC turbidity measurement locations.

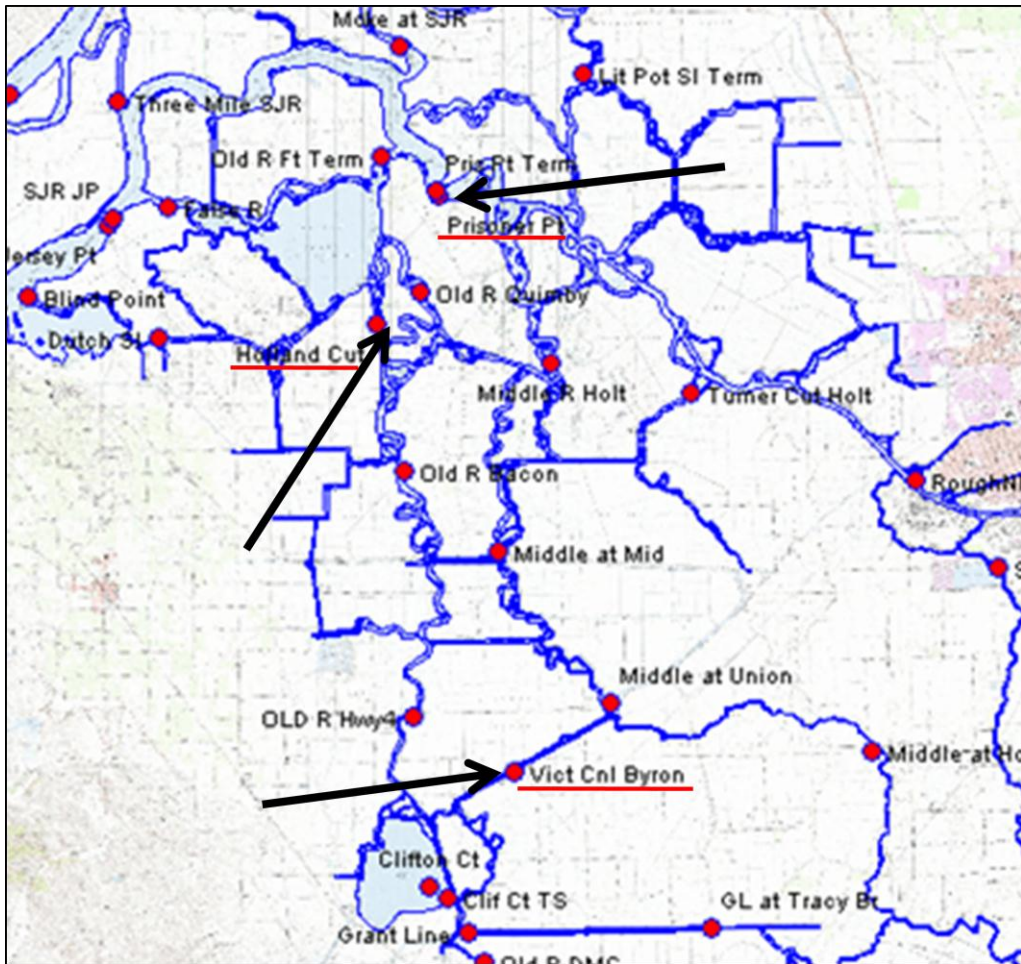


Figure 3-2 Location of the three turbidity compliance locations.

### 3.3 Methodology for turbidity calibration

The majority of the statistics used to assess model calibration at each Delta data location were calculated from model residuals. A residual is defined herein as the difference between a data value and the corresponding calculated model value (*i.e.*, data - model). Residuals were calculated at each location with available data.

One widely used residual statistic was used to assess the goodness-of-fit of the model to the data using the residuals, the Percent Bias (PBIAS). In addition, linear regressions were calculated at each available data location and the R<sup>2</sup> goodness of fit statistic between the data and the calibrated model was the second statistics used to assess the quality of the calibration.

Both daily-averaged and 15-minute CDEC data and model output were used in calculation of the statistics, but the daily-averaged data were used to assess the quality of the calibration<sup>2</sup>. After daily averaging the model output and data, model residual statistics and linear regression statistics were calculated and recorded at each available data location. In addition to presenting statistics at each measurement location, several metrics were selected to assess the overall quality of the calibration in each Water Year – *i.e.*, a “model skill” assessment.

Model calibration began with WY2013 and proceeded until the final set of rate constants represented a condition in which the calibration statistics for WY2013 were no longer improving. This set of rate constants was then applied to WY2010 and WY2011 and minor adjustments were made until each year did not improve significantly or degrade at the compliance locations in comparison with the previous simulations. Finally, revisions were made to the Calaveras River boundary condition until downstream locations no longer improved in statistical fit. In what follows, calibration metrics are presented in comparison with the previous QUAL turbidity calibration undertaken by RMA in WY2012 (RMA 2013).

The final set of values for the K<sub>3</sub> parameter are documented in Figure 3-3 through Figure 3-5. An ancillary objective for the calibration was to keep the number of regions and parameter values to a minimum, so only six parameter values were used.

Statistics were also calculated to assess the new set of calibration parameters with respect to the Historical simulations. In this case, Environmental Monitoring Program (EMP) grab sample data was compared with daily-averaged model output on the collection day in each Water Year from December through the following March. The calibration output information is documented fully in Appendix IV (Section 13), and discussed in Section 7.

---

<sup>2</sup> Statistical results using the 15-minute data and model output are presented in the Appendices.



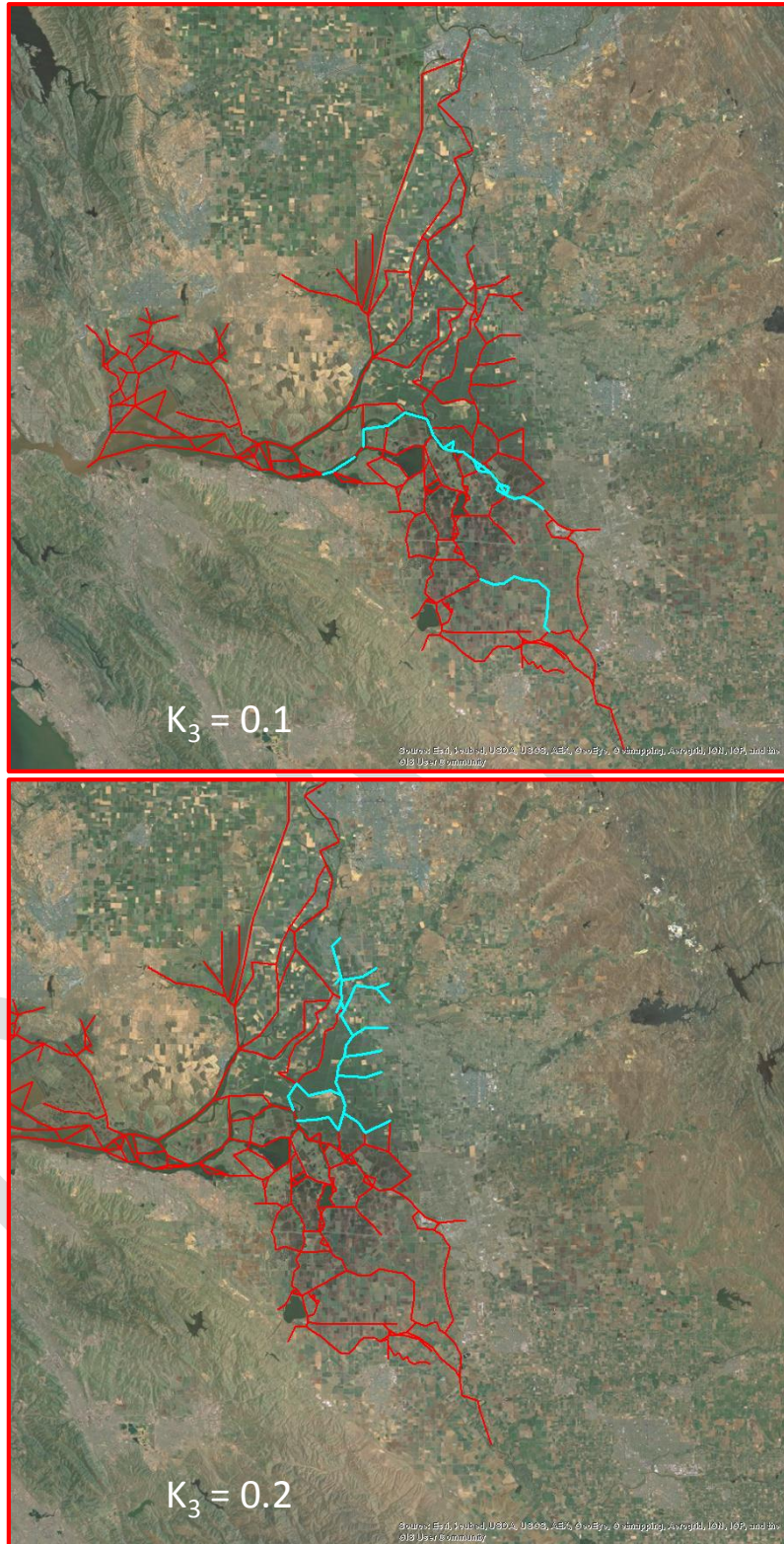


**Figure 3-4** The colored lines define the DSM2 grid channels – the segments that are blue define channels where the  $K_3$  parameter was set to the indicated value. These figures show two middle values used for the settling parameter.

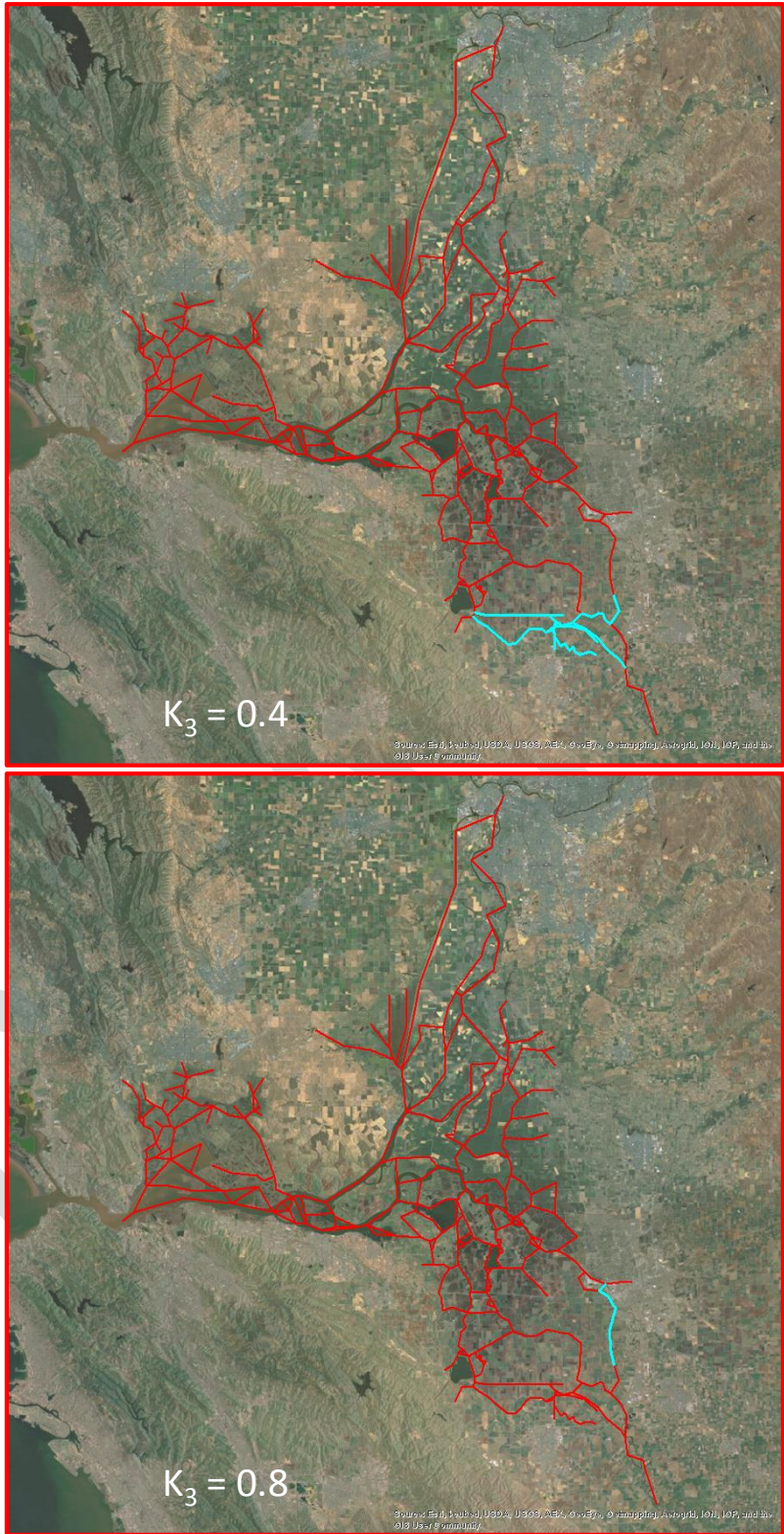


**Figure 3-5** The colored lines define the DSM2 grid channels – the segments that are blue define channels where the  $K_3$  parameter was set to the indicated value. This figure shows the highest two values used for the settling parameter.

### 3.4 Residual analysis

Residuals are defined as the difference (data – model) between the measured data and the modeled result. The following definitions (Moriassi et al., 2007) were used for calculating residual statistics:

**Mean Residual** – The mean of the residual values gives an indication of the magnitude of model under-prediction (positive residuals) or over-prediction in a region. The optimal value is zero, which occurs in the unlikely situation that the model is a perfect fit for the data.

**Standard Deviation of Residual** – The standard deviation of the residual values gives an indication of the variability in model under-prediction and over-prediction in a region.

**Residual Histogram** – The histogram documents the shape of the residual distribution. Along with the mean and standard deviation, this gives a first-order view of the goodness of model fit. The ideal histogram would have an approximately normal shape centered at zero with a small spread. Histograms were prepared using daily averaged calculations at each data location.

**MSE** – The Mean Squared Error is a standard statistic that measures the quality of the prediction. The optimal value is zero:

$$MSE = \left[ \frac{\sum_{i=1}^n (Y_i^{Obs} - Y_i^{Sim})^2}{n} \right] \quad (A3)$$

**RMSE** – The Root Mean Squared Error is a standard statistic used to indicate the accuracy of the simulation. It is the square root of the MSE. The optimal value is zero.

**NSE** – The Nash-Sutcliffe Efficiency is a normalized statistic that measures the relative magnitude of the residual variance compared to the data variance. NSE indicates how well the measured vs. modeled data fit the 1:1 line (Moriassi et al., 2007). A value of 1 is optimal, values between 0 and 1 are acceptable, and negative values indicate that the data mean is a better predictor of the data than the model:

$$NSE = 1 - \left[ \frac{\sum_{i=1}^n (Y_i^{Obs} - Y_i^{Sim})^2}{\sum_{i=1}^n (Y_i^{Obs} - Y_i^{Mean})^2} \right] \quad (A4)$$

**PBIAS** – Percent bias measures the average tendency of the simulated data to be larger or smaller than the measured data. A value of 0 is optimal – a positive value indicates underestimation bias and a negative value indicates overestimation bias:

$$PBIAS = \left[ \frac{\sum_{i=1}^n (Y_i^{Obs} - Y_i^{Sim}) * 100}{\sum_{i=1}^n (Y_i^{Obs})} \right] \quad (A5)$$

**RSR**– The RMSE-observation standard deviation ratio is a statistic that normalizes the RMSE using the standard deviation of the observations. Because it is normalized, it can be used to compare errors among various constituents (Moriassi et al., 2007). A value of 0 is optimal:

$$RSR = \frac{\left[ \sqrt{\sum_{i=1}^n (Y_i^{Obs} - Y_i^{Sim})^2} \right]}{\left[ \sqrt{\sum_{i=1}^n (Y_i^{Obs} - Y_i^{Mean})^2} \right]} \quad (A6)$$

### 3.5 Linear regression analysis

Linear regressions were calculated and recorded in plots, along with the  $R^2$  goodness of fit statistic and the regression equation, comparing the data to the model output at each available location for the newly calibrated model and for the original QUAL turbidity model developed by the DMS. Note that the intercept was NOT forced through zero in the linear regressions. For many locations, the NSE statistic and the  $R^2$  values are the same within two decimal places – this indicates that the linear regression nearly fits the 1-1 line (*i.e.*, with an intercept at zero).

### 3.6 Documentation of statistics

Documentation of the statistical analyses is accomplished using tabular information and figure plots. The tables in Section 5 document the two selected statistics as well as the overall statistics used to assess the skill of the model in each Water Year in comparison with the previous calibration. Figures (for example, Figure 3-6 through Figure 3-8) show a comparison between the data and model output, the residual plot, a linear regression analysis with associated statistics (slope, intercept and  $R^2$ ), and a histogram of the residual along with the numerical values of all the regression statistics.

### 3.7 Model output and calibration calculations

At each data location and for each Water Year 2010, 2011 and 2013, daily-averaged data and model output and residuals were plotted, linear regressions were calculated and plotted, and residual statistics were calculated and plotted along with a residual histogram. Figure 3-6 through Figure 3-8 illustrate of the output provided at each location – Prisoner’s Point in WY2010, WY2011 and WY2013 are shown for the new RMA turbidity calibration. Appendix II, Section 11 presents the complete set of these figures. For comparison, Section 12, Appendix III, presents figures and associated statistics using 15-minute data and model output. However, these results were not used in the final analyses as daily-averaged data is used in the calculation of compliance location turbidity values.

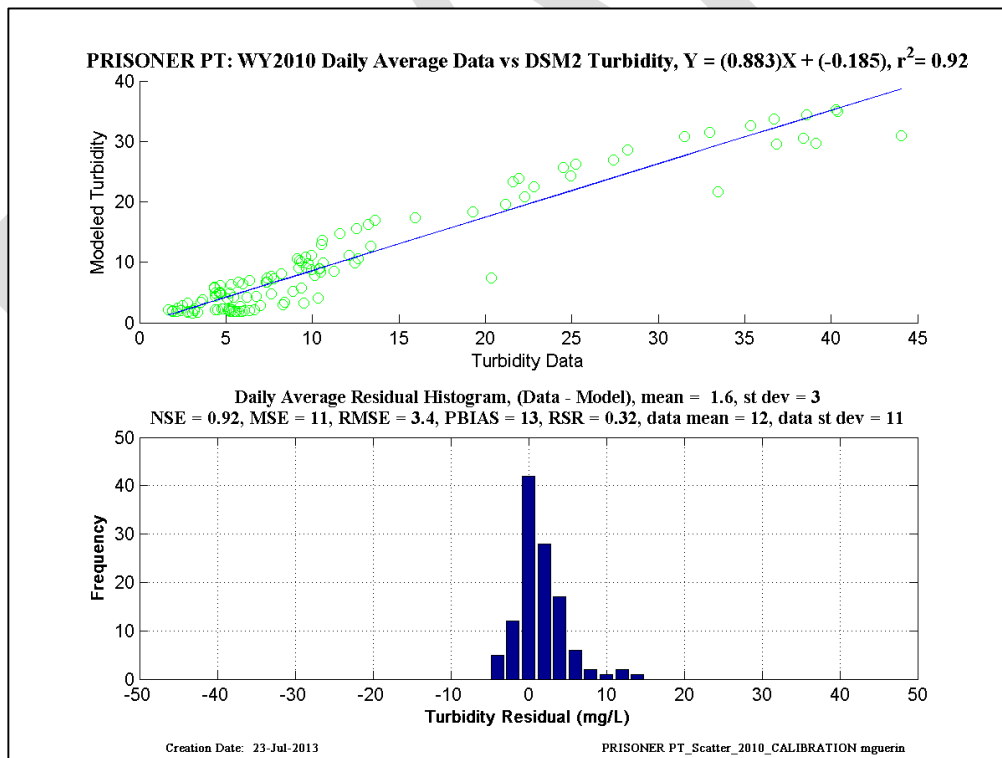
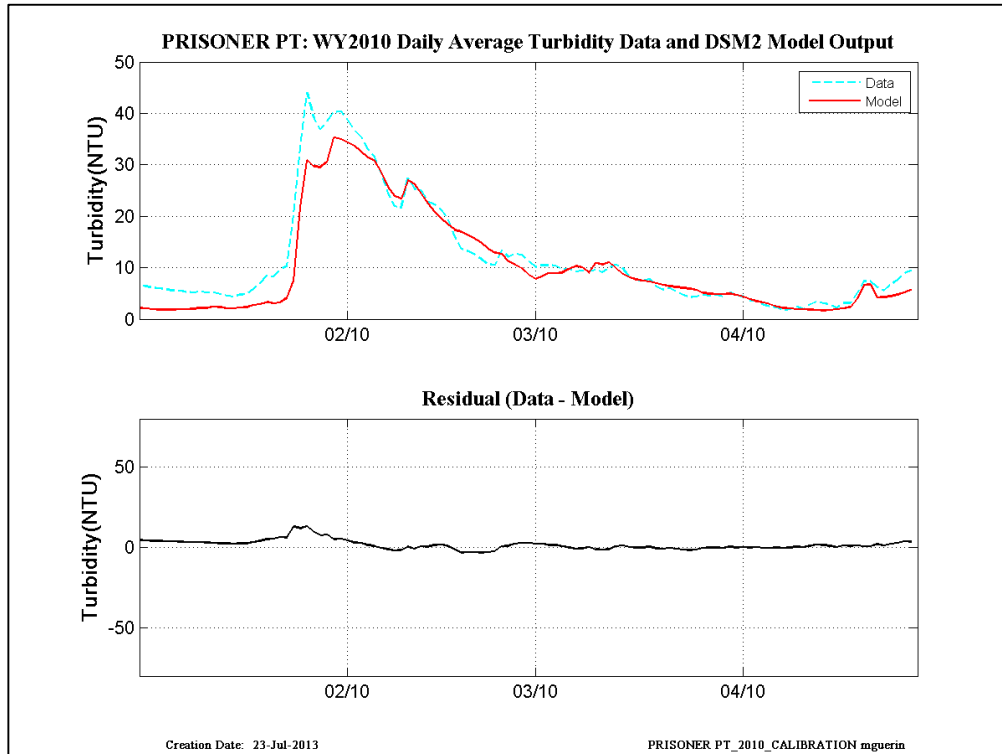


Figure 3-6An illustration of the output prepared for each data location including calibration statistics for each Water Year. This location is the compliance site at Prisoner’s Point and the year is WY2011.

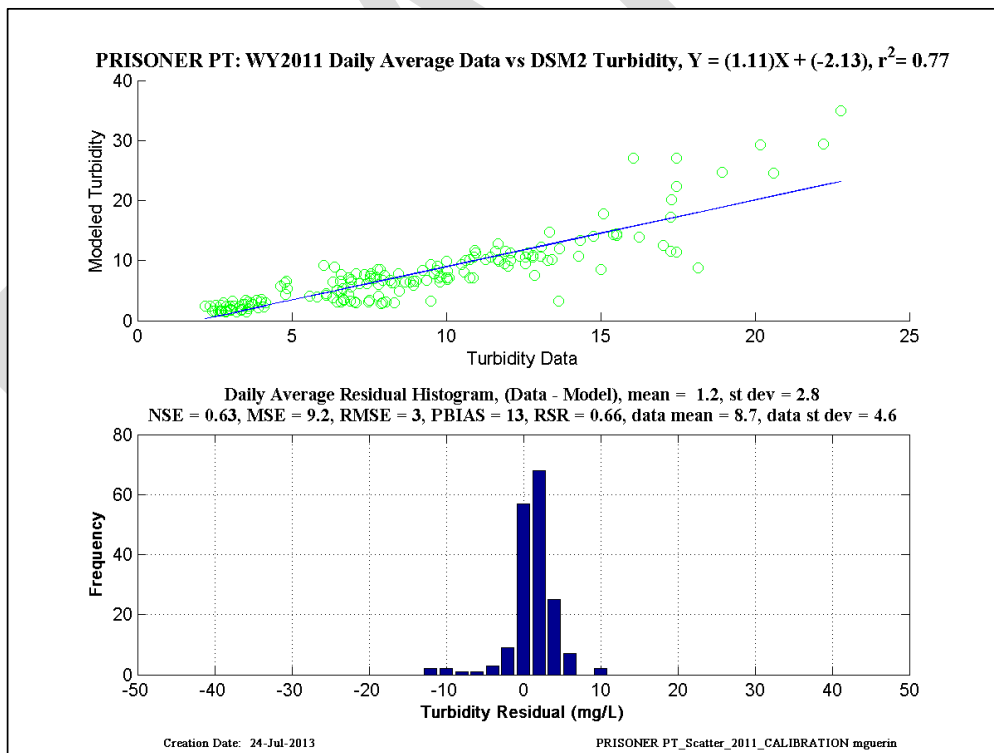
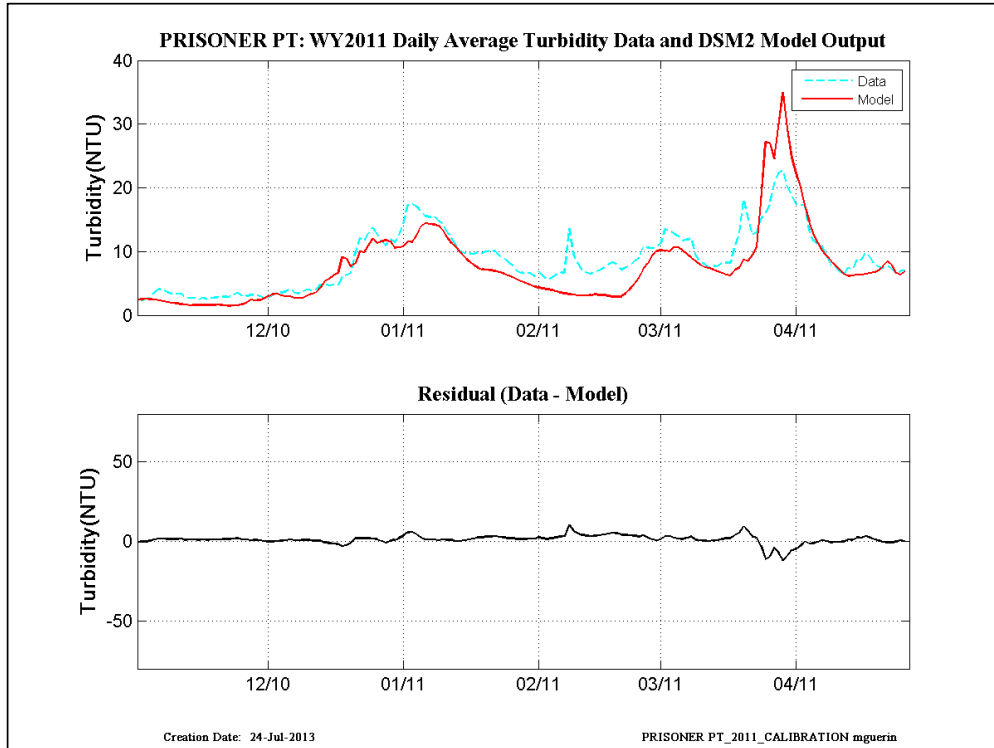


Figure 3-7 An illustration of the output prepared for each data location including calibration statistics for each Water Year. This location is the compliance site at Prisoner’s Point and the year is WY2011. Peaks in the data (upper plot) not captured in the model in February are due to wind/rain events.

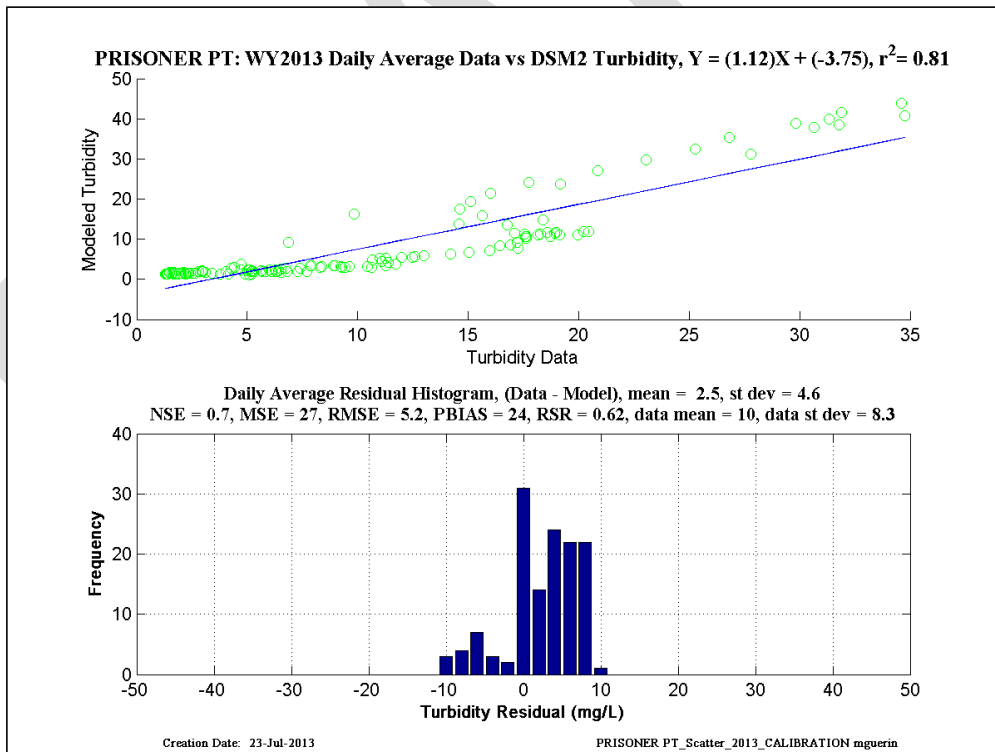
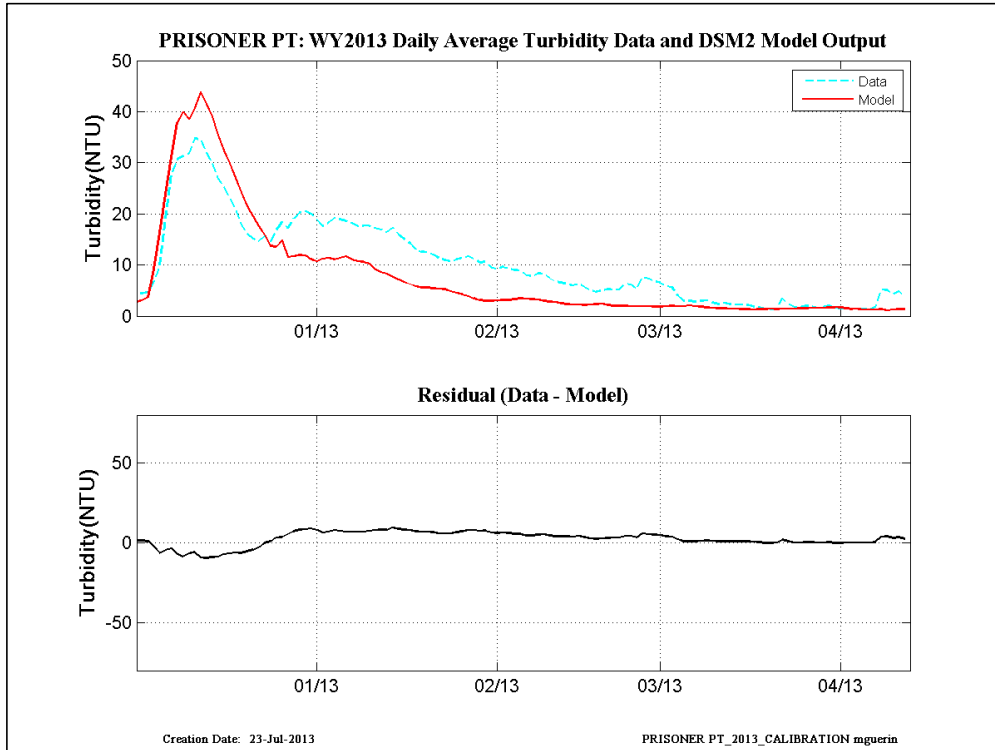


Figure 3-8An illustration of the output prepared for each data location including calibration statistics for each Water Year. This location is the compliance site at Prisoner’s Point and the year is WY2013. The peak in the data (upper plot) not captured in the model in mid-to-late-January is due to resuspension of sediments due to wind.

## 4 Model set-up

### 4.1 High flow period Historical simulations: WY2010, WY2011, WY2013

DSM2 was run with the Mini-calibration set-up and V8.0.6 of HYDRO and QUAL<sup>3</sup>. Gate operations and export flows for HYDRO for the calibration time frames were obtained from the DMS and implemented as received. Boundary conditions were set after a QA/QC step to check, clean, refine and possibly time shift the data. Inflow and stage boundary conditions were set as documented in Table 1. Only winter high flow periods were prepared for use in calibration, January – April for WY2010, December – April for WY2011, and December – April for WY2013<sup>4</sup>. Spin-up periods started in October of each Water Year.

Boundary conditions for turbidity were developed by RMA when data at or near the boundary was available – in WYs 2010 and 2011, downstream data was not available to set turbidity at the Mokelumne and Cosumnes River locations so WARMF model output was used (see: (RMA 2013) for additional information). Details can be found in Table 2 and in the input files for each model run. DICU turbidity return flow concentrations were set at a constant 20 NTU.

For WYs 2010, 2011 and 2013, the turbidity models with newly developed boundary conditions were initially run with the calibration parameters developed in WY2010 (RMA 2013). The results after calibration were then compared with the initial RMA calibration using the residual and regression analyses discussed in Section 3.

Plots illustrating the inflow, export and turbidity boundary conditions for WY2010, WY2011 and WY2013 high flow periods are shown in Figure 4-1 through Figure 4-27.

### 4.2 Long term (1975 – 2011) Historical Simulations

DSM2 was run with the Mini-calibration set-up and V8.0.6 of HYDRO and QUAL. The DMS supplied the historical hydrodynamic model input for the HYDRO runs (gate operations, exports and inflows, and stage at Martinez) for the Water Years 1975 – 2010 and in separate files for the new Historical model through December 2011. The simulations for the Water Years 1975 – 2011 were run in two steps: the “early years” 1975 – 1990, and separately for the “recent years” 1991 – 2011. The “early years” simulations used the DSM2 model set-up supplied with the long-term (1975 – 2010) Historical model (e.g., without Liberty Island), while the “recent years” simulations used a DSM2 Historical model set-up which included Liberty and ran through 2011.

QUAL turbidity model simulation results were prepared using USGS-SSC data at Freeport and Vernalis, and WARMF model calculations to develop boundary conditions at the other inflow boundaries – the Calaveras, Cosumnes, and Mokelumne Rivers and the Yolo Bypass. The Martinez boundary was set at a constant 20 NTU. The nomenclature for this set-up was coined in (RMA 2013) as “Mixed-SSC-WARMF”, and that nomenclature is also used in this document.

---

<sup>3</sup><http://baydeltaoffice.water.ca.gov/modeling/deltamodeling/models/dsm2/dsm2.cfm>

<sup>4</sup> The WY2012 model was developed, but was again found unsuitable. Spin-up periods were not included.

Following the QUAL turbidity calibration discussed in Section 5 below, it was found that setting the Freeport boundary condition by reducing the concentration of SSC data produced slightly better statistical results. No changes were made to the Vernalis turbidity boundary condition. For the Early Years simulation (1975 – 1990), the Freeport boundary condition was set at  $0.85 \times (\text{USGS SSC})$  and for the Later Years simulation (1991 – 2011) it was set at  $0.8 \times (\text{USGS SSC})$ .

Figures documenting the results of the Vernalis and Freeport boundary conditions are illustrated at several locations in model output in comparison with EMP data in Figure 4-28 and Figure 4-29 for the “early” years modeled, and in Figure 4-30 and Figure 4-31 for the “recent years” modeled. To demonstrate the Freeport BC’s the IEP “C3” location at Hood downstream is used, and to demonstrate the Vernalis boundary condition, two locations are used at IEP’s “C7” and “C10” locations at Mossdale and SJR-McCune, respectively.

Two things are notable:

- The Vernalis boundary condition produces reasonable visual matches with the IEP grab-sample data, and the range of IEP data turbidity values is similar to the range of values seen in CDEC 15-minute turbidity data at Vernalis and Mossdale (~50 – 300 NTU, or higher) during periods of high inflow.
- The Freeport boundary condition produces a range of modeled values at Hood that are comparable to the range of values seen in CDEC 15-minute turbidity data at Hood (~50 – 350 NTU, or higher) during periods of high inflow, but the IEP grab-sample data is very low in comparison with the range of CDEC data values.

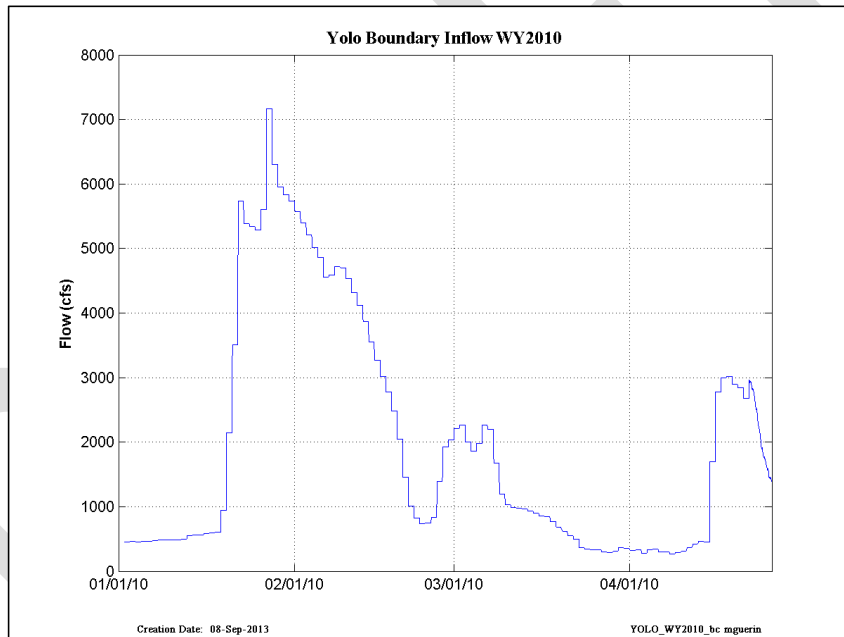
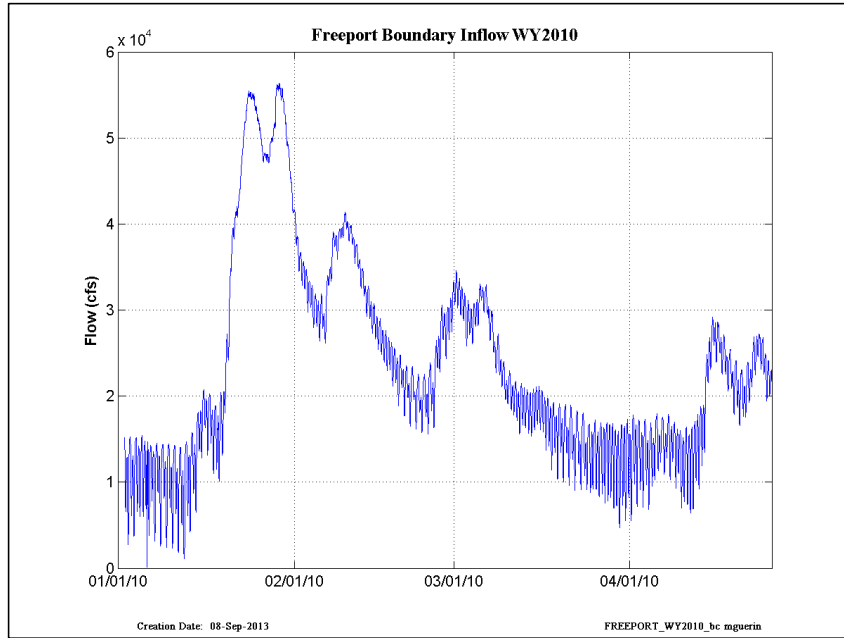
It appears that along the Sacramento River, the IEP data is unreasonable low, possibly indicating that samples were not taken during times when river flows were high, or, perhaps dangerously high for sample acquisition. Thus, although statistical results for the new calibration during these long Historical models will be calculated by comparing model output with IEP data, the magnitude of the IEP data appears suspect, at least in some locations.

**Table 1 Inflow and stage boundary conditions - data sources and shifts in timing.**

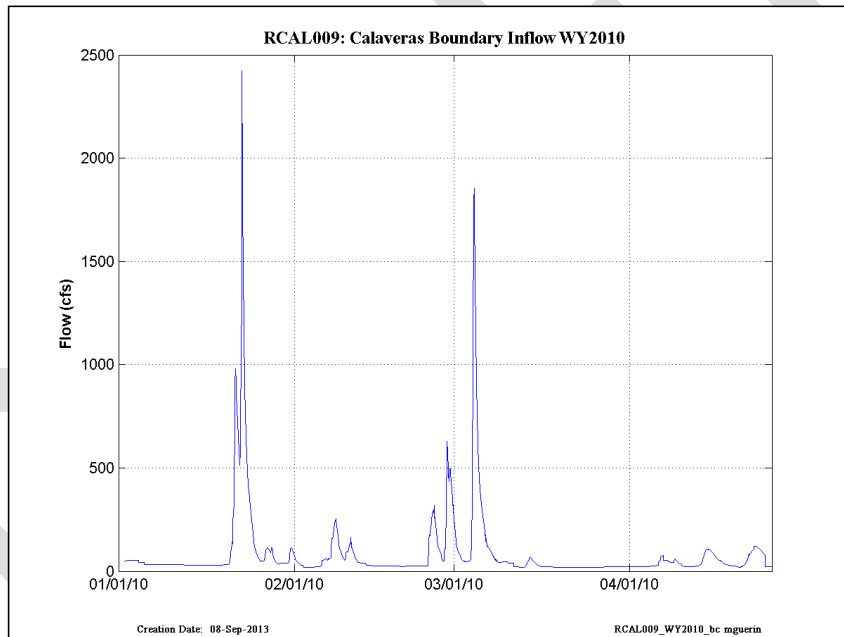
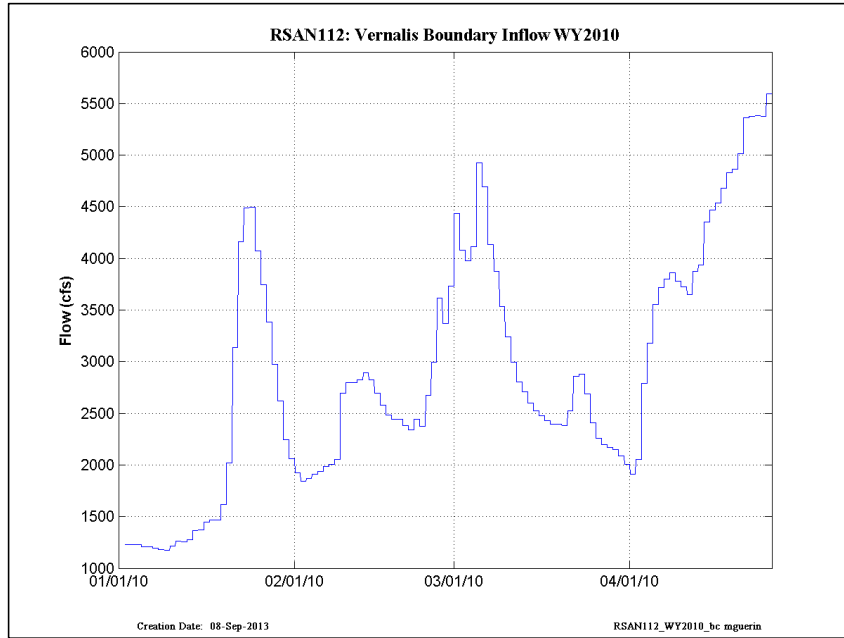
	<b>WY 2010</b>	<b>WY2011</b>	<b>WY2013</b>
<b>Sacramento</b> Source Edit timing	CDEC -	CDEC -	DMS -
<b>Vernalis</b> Source Edit timing	CDEC+DMS -	CDEC+DMS -	DMS -
<b>Yolo</b> Source Edit timing	CDEC+CNRFC+DMS -	CDEC+CNRFC+DMS -	DMS -
<b>Mokelumne</b> Source Edit timing	DMS+O&M Back 1 day	DMS+O&M -	DMS Forward 8 hours
<b>Cosumnes</b> Source Edit timing	DMS+CDEC Back 1 day	DMS+CDEC -	DMS Forward 8 hours
<b>Calaveras</b> Source Edit timing	DMS Forward 1 day	DMS Forward 12 hours	DMS Forward 12 hours
<b>Martinez</b> Source Edit timing	DMS+CDEC Back 30 min.	DMS+CDEC Back 30 min.	DMS+CDEC Back 30 min.

Table 2 Turbidity BC - sources and alterations in timing and magnitude.

	WY 2010	WY2011	WY2013
<b>Sacramento</b> Source Edit timing	CDEC - FPT Back 7 hours	CDEC - FPT Back 7 hours	CDEC - FPT Back 7 hours
<b>Vernalis</b> Source Edit timing	CDEC - SJR -	CDEC - SJR -	CDEC - SJR Back 6 hours
<b>Yolo</b> Source Edit timing	CDEC - RYI -	CDEC - RYI -	CDEC - RYI -
<b>Mokelumne</b> Source Edit timing	WARMF -	WARMF -	CDEC - SMR Back 5 hours
<b>Cosumnes</b> Source Edit timing	WARMF -	WARMF -	CDEC - SMR Back 10 hours
<b>Calaveras</b> Source Edit timing Edit magnitude	CDEC - RRI Forward 12 hours Times 10	CDEC - RRI Forward 12 hours -	CDEC - RRI Forward 12 hours Times 10
<b>Martinez</b> Source Edit timing	CDEC- MRZ -	CDEC- MRZ -	CDEC- MRZ -



**Figure 4-1 WY2010 flow BCs at Freeport and the Yolo Bypass.**



**Figure 4-2 WY2010 flow BCs at Vernalis and on the Calaveras River.**

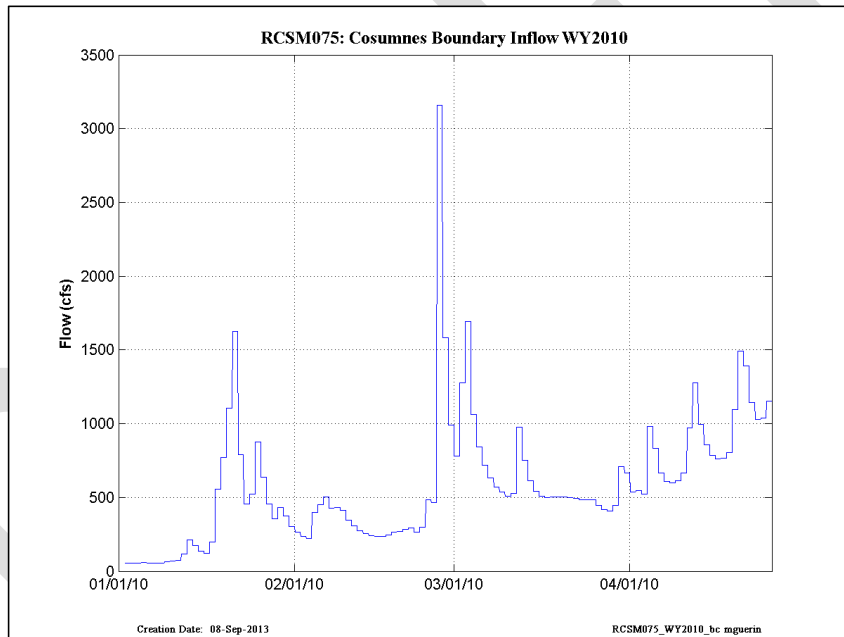
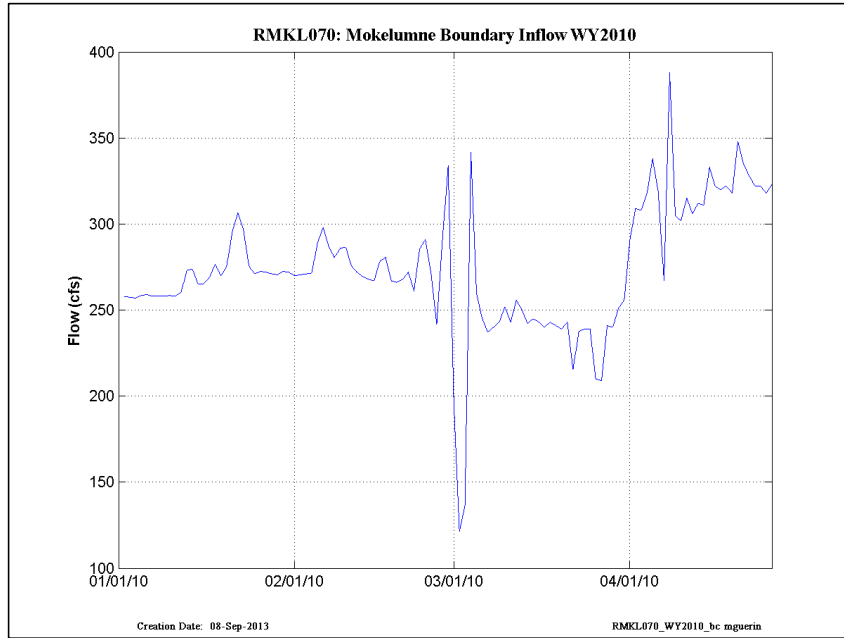


**Figure 4-3 WY2010 flow BCs on the Mokelumne and Cosumnes Rivers.**

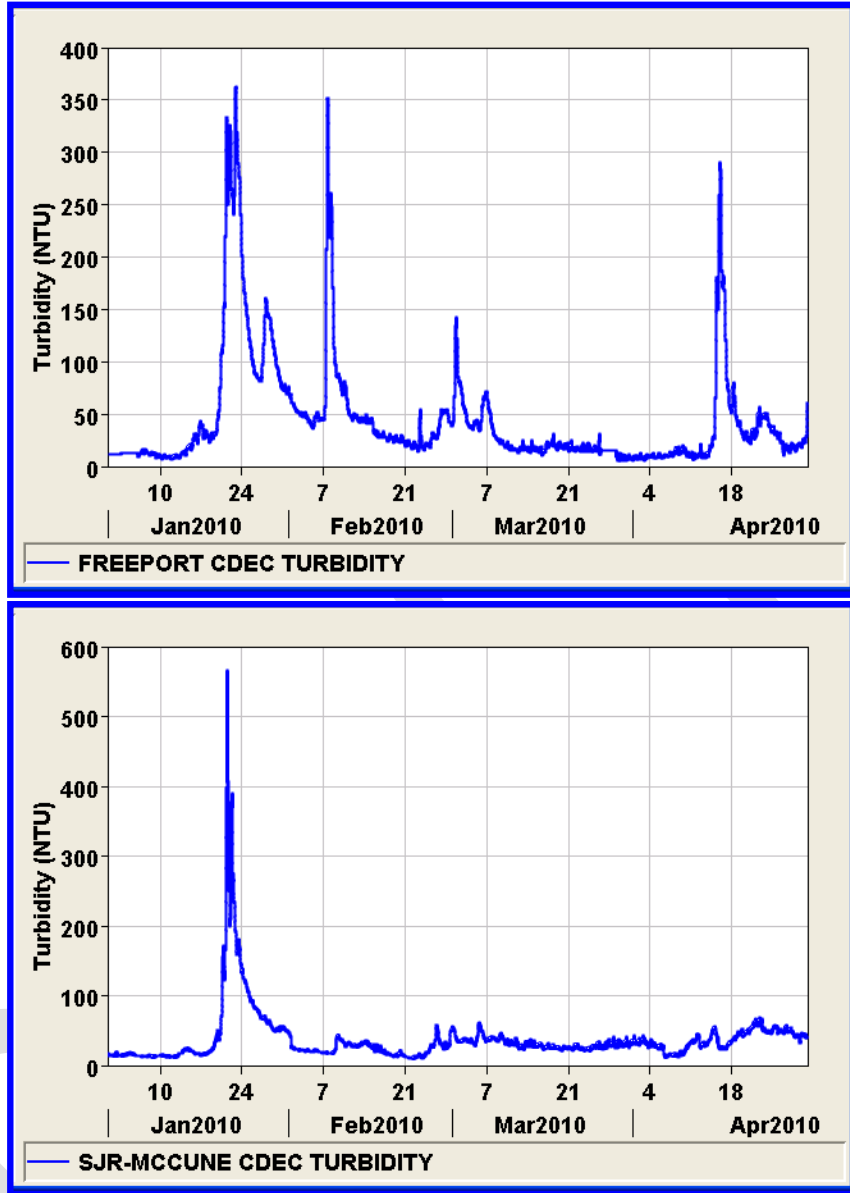


Figure 4-4 WY2010 Turbidity BCs at Freeport and Vernalis.

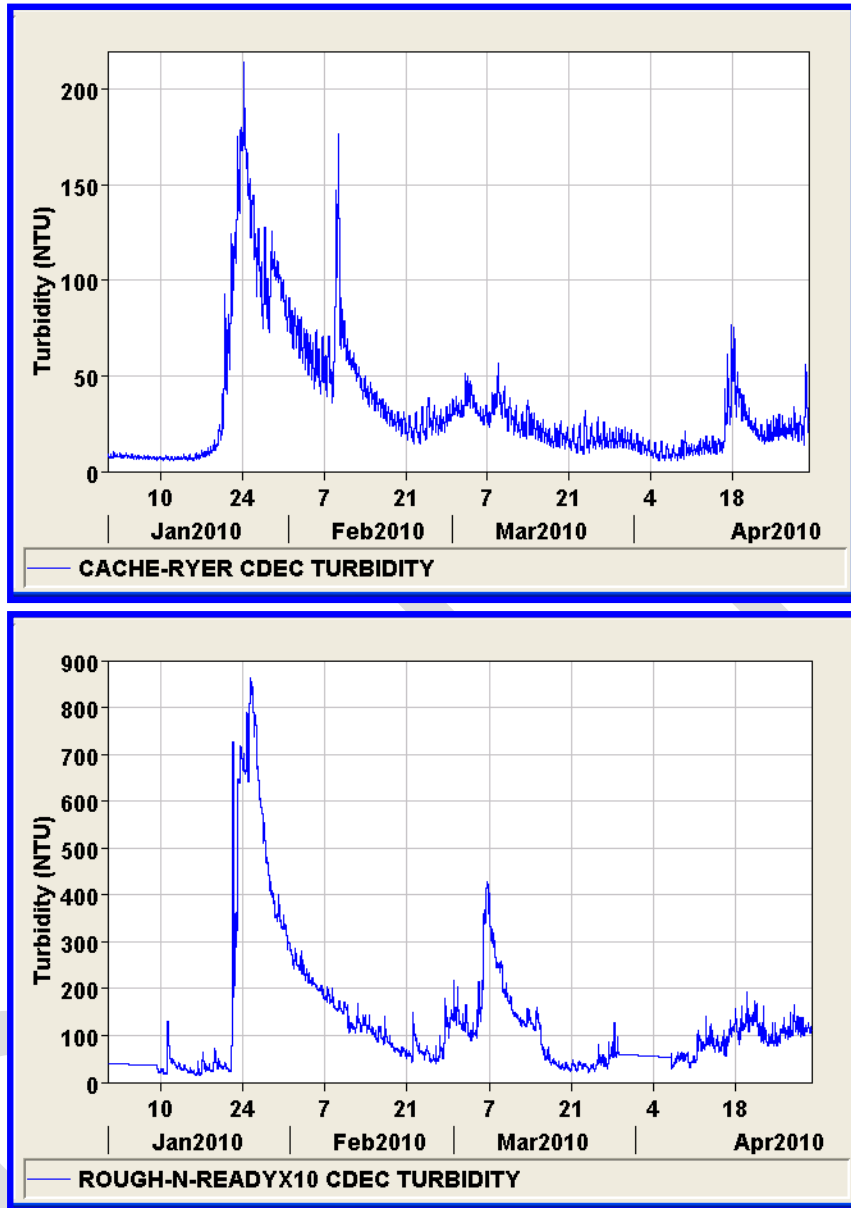


Figure 4-5 WY2010 Turbidity BCs for the Yolo Bypass (upper) and the Calaveras River (lower).

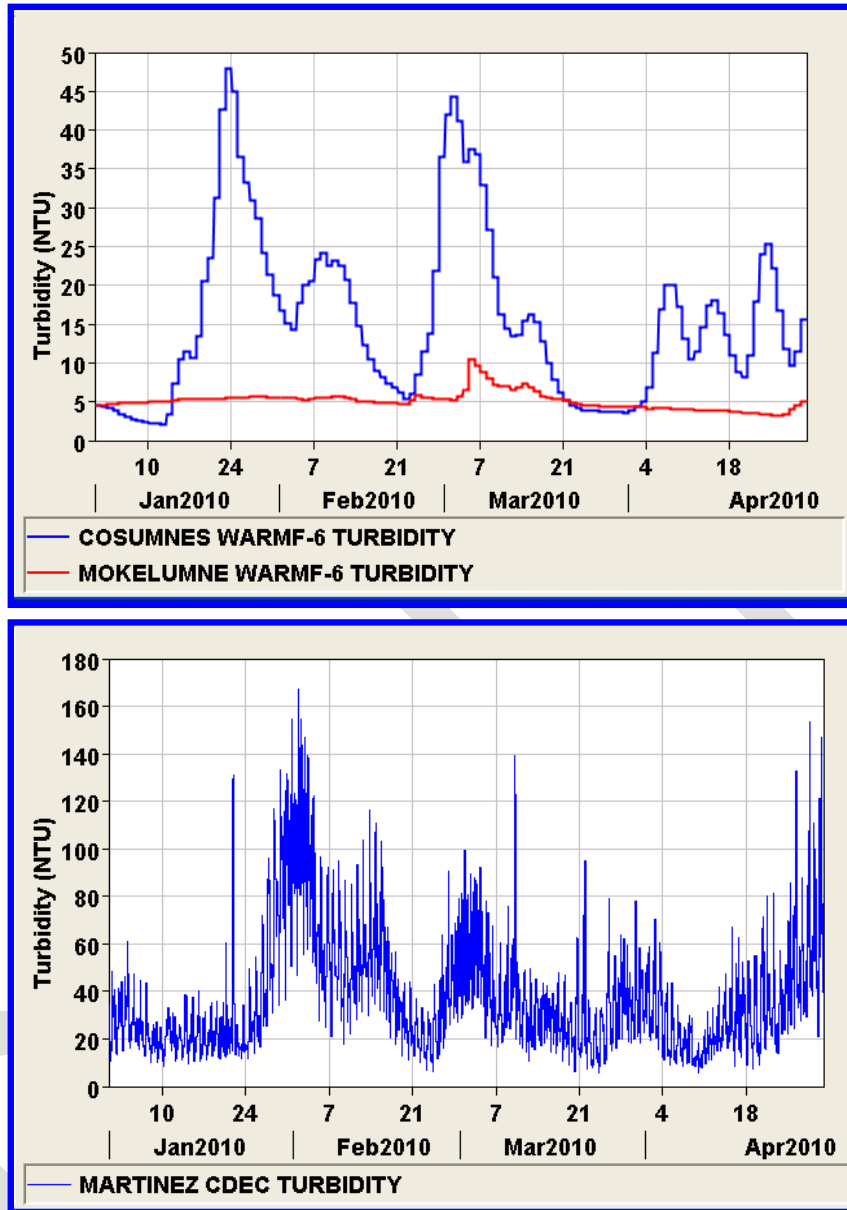


Figure 4-6 WY2010 Turbidity BCs for the Cosumnes and Mokelumne Rivers (upper, sourced from a previous WARMF model) and at Martinez (lower).

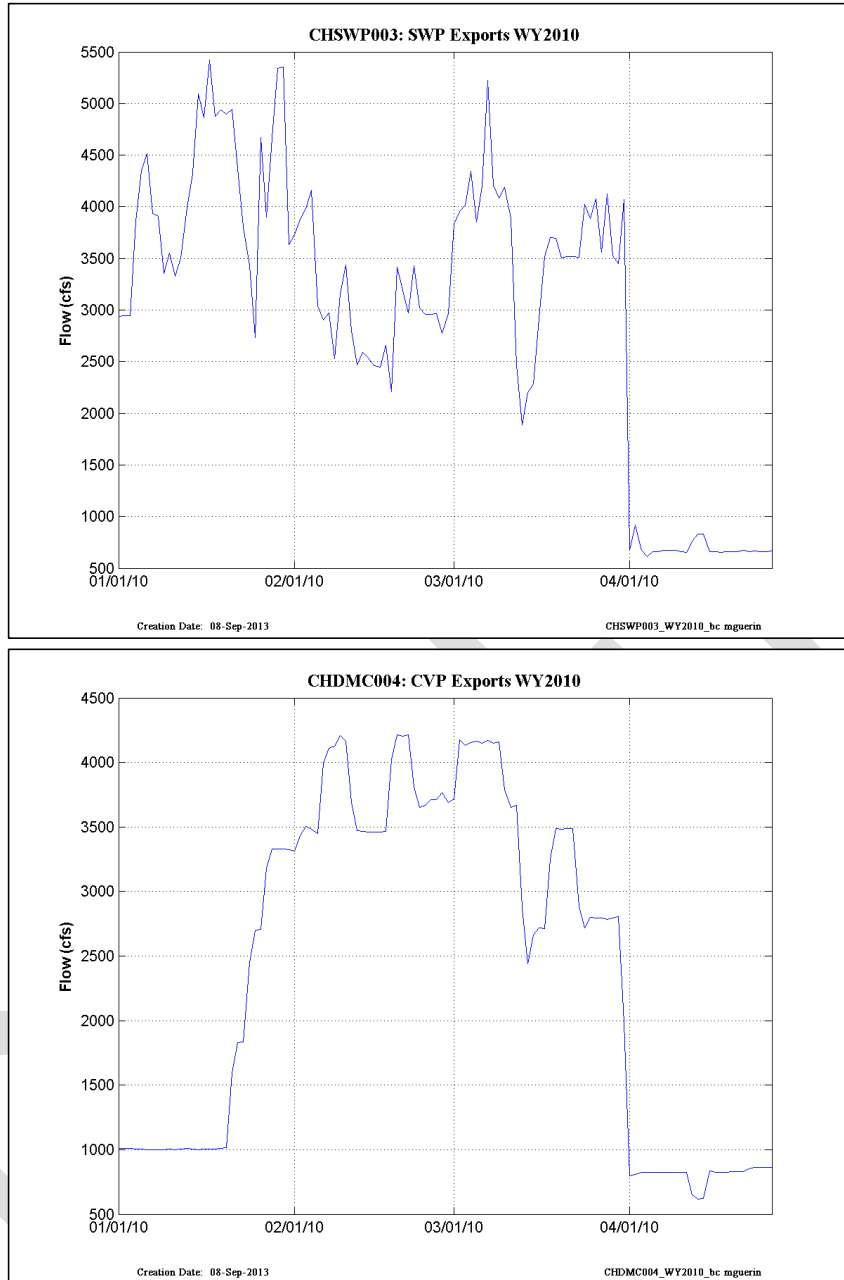
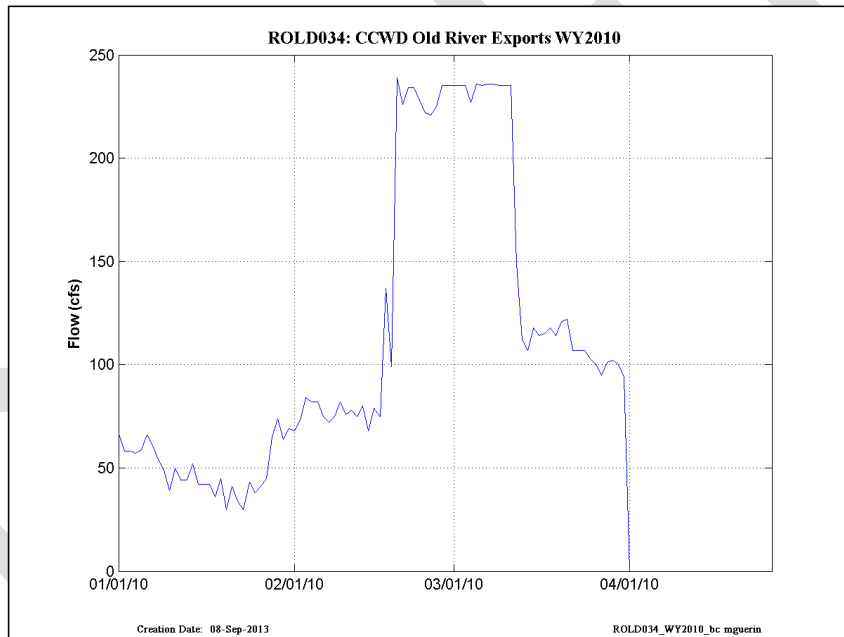
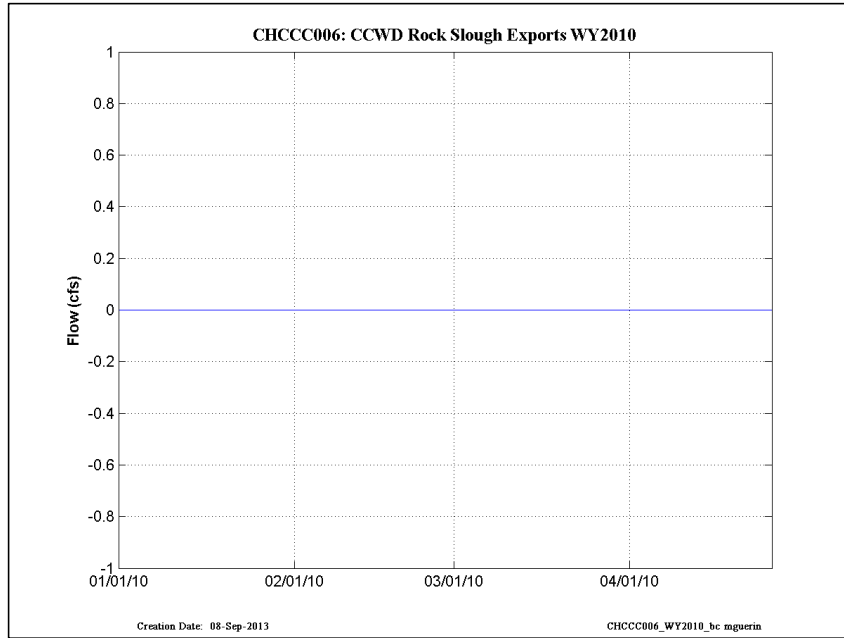
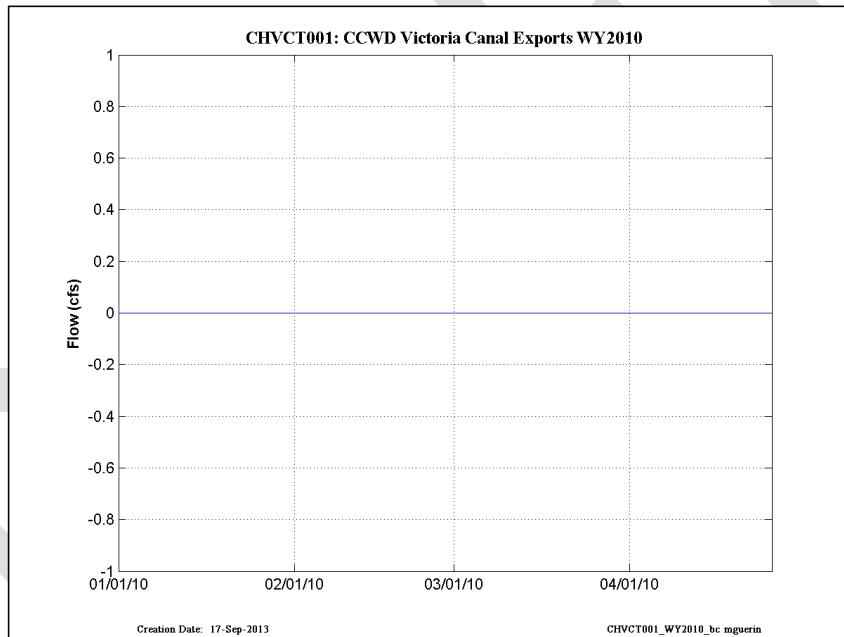
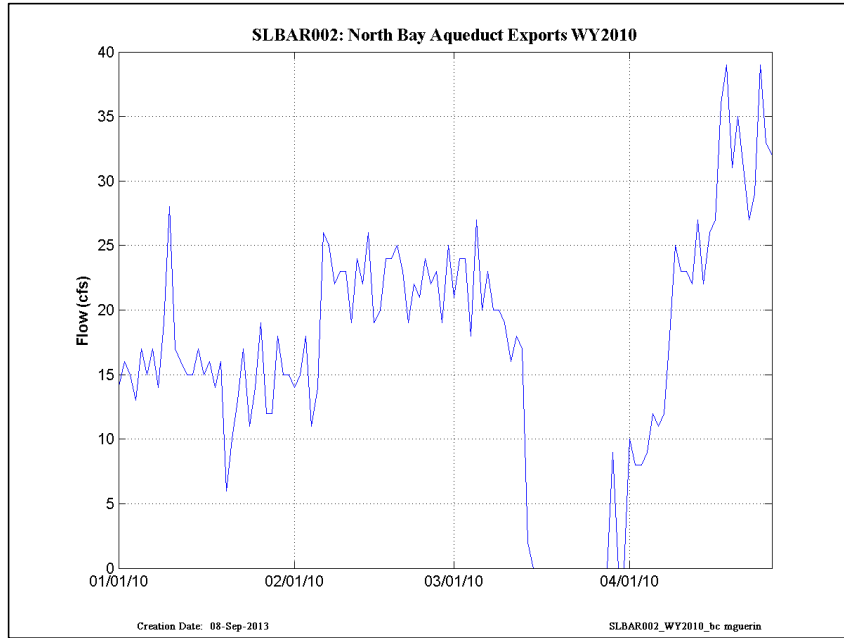


Figure 4-7 WY2010 export BCs at the SWP and CVP locations.



**Figure 4-8 WY2010 export BCs at the CCWD Contra Costa Canal and Old River locations.**



**Figure 4-9 WY2010 export BCs at the North Bay Aqueduct and at the CCWD Victoria Canal location.**

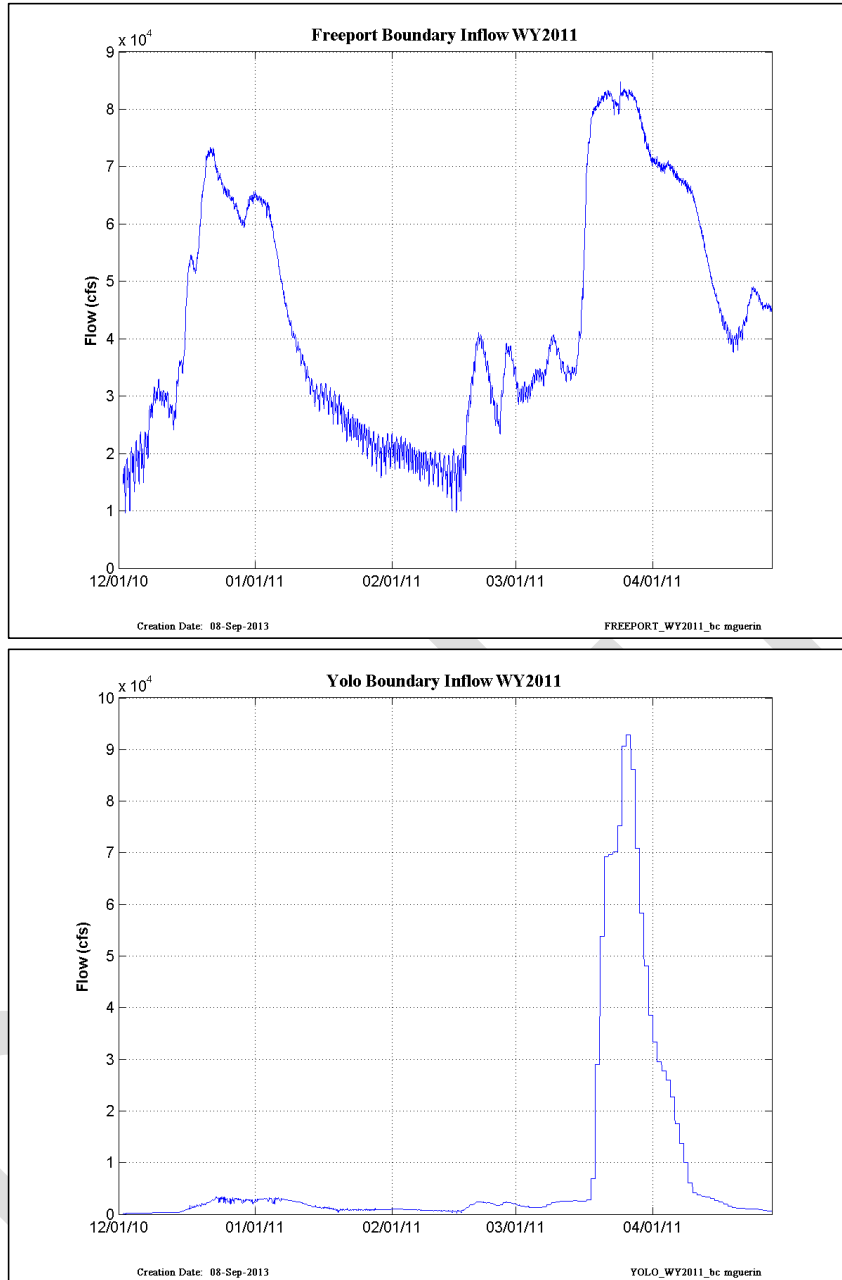


**Figure 4-10 WY2011 flow BCs at the Freeport and Yolo Bypass locations.**

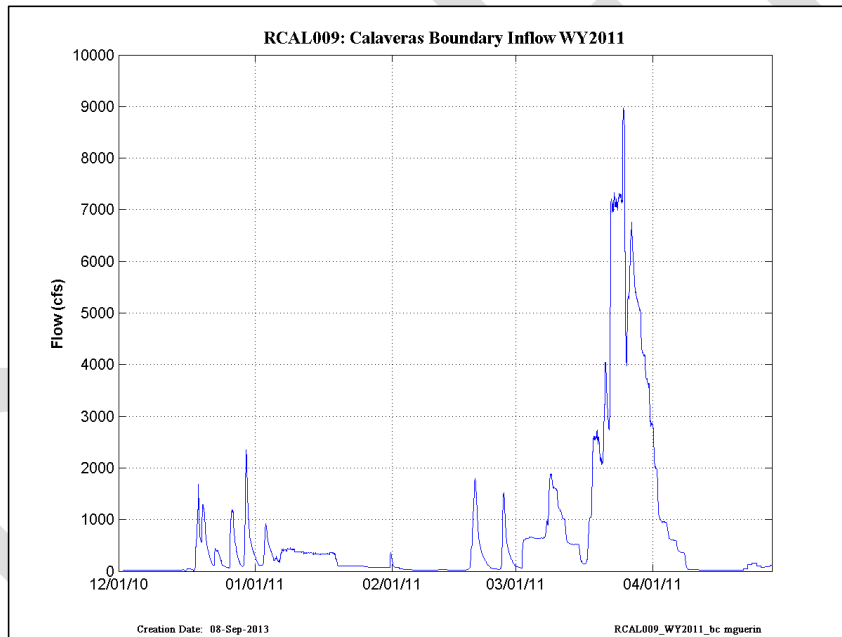
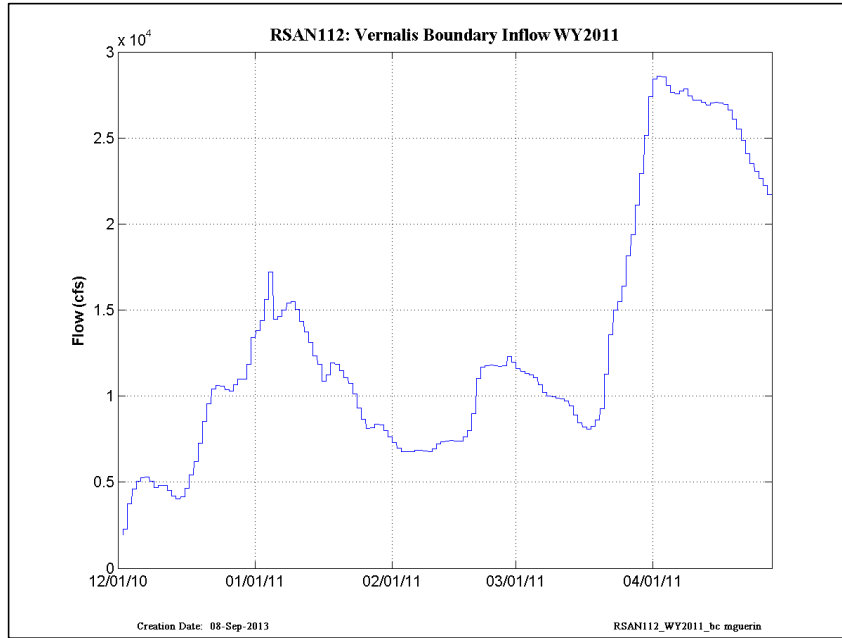


**Figure 4-11 WY2011flow BCs at the Vernalis and Calaveras River locations.**

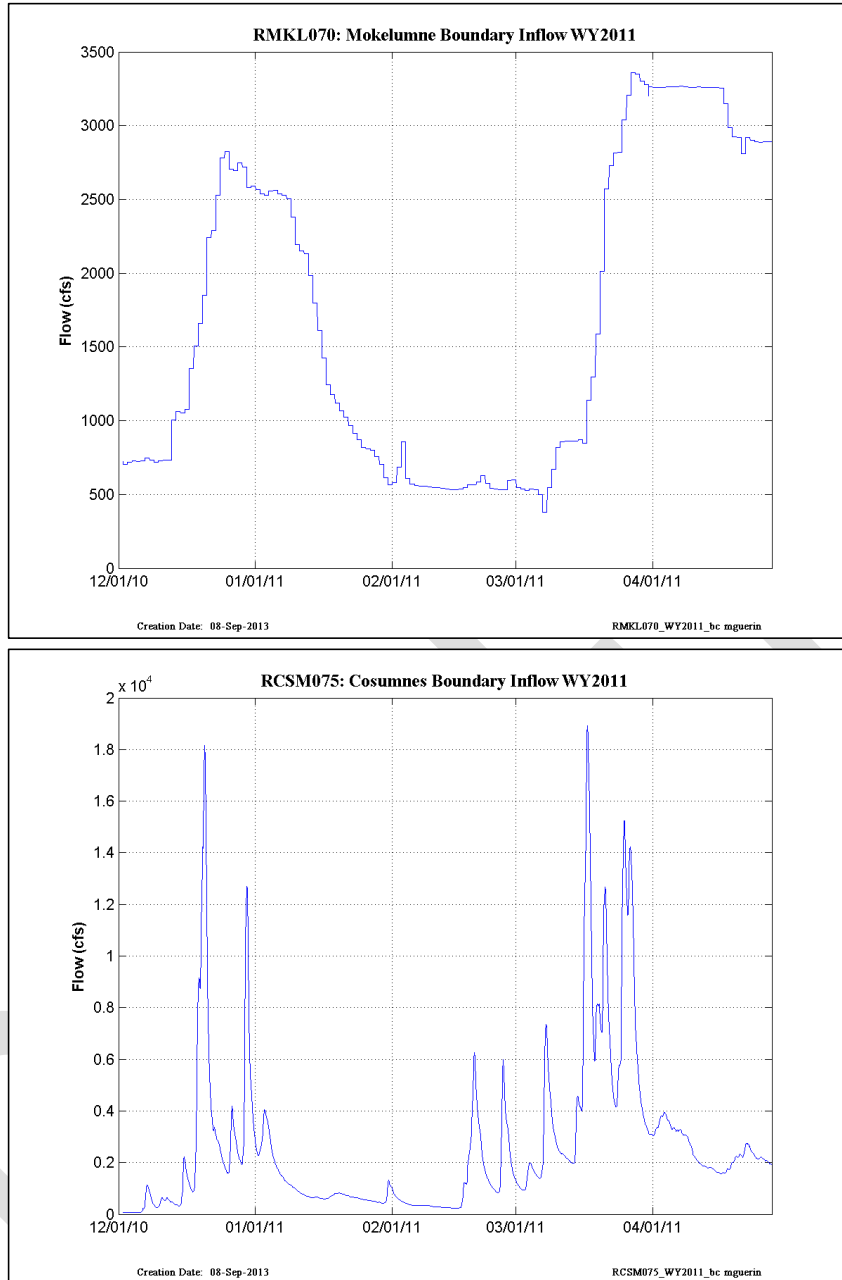


**Figure 4-12 WY2011 flow BCs at the Mokelumne and Cosumnes River locations.**

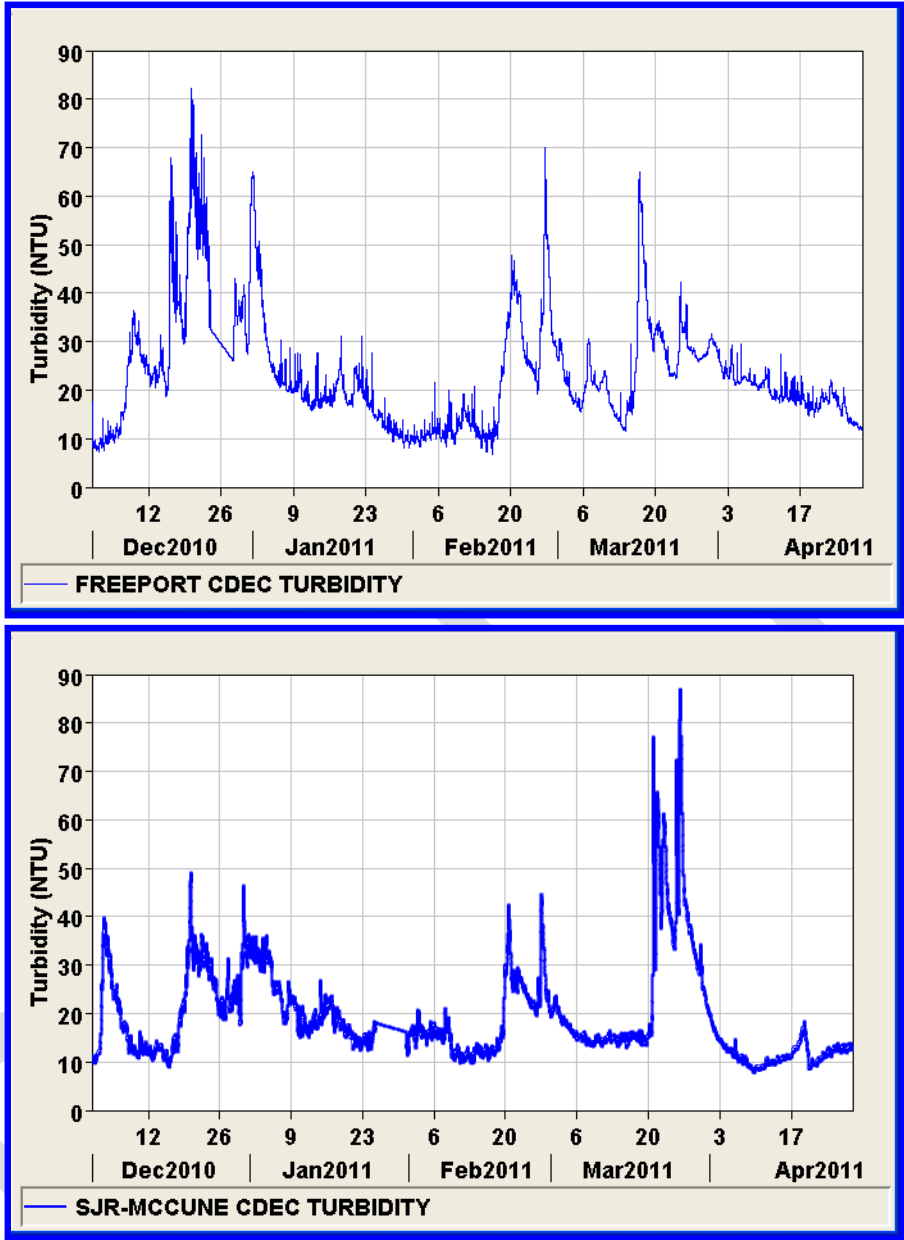


Figure 4-13 WY2011 Turbidity BCs at Freeport and Vernalis.

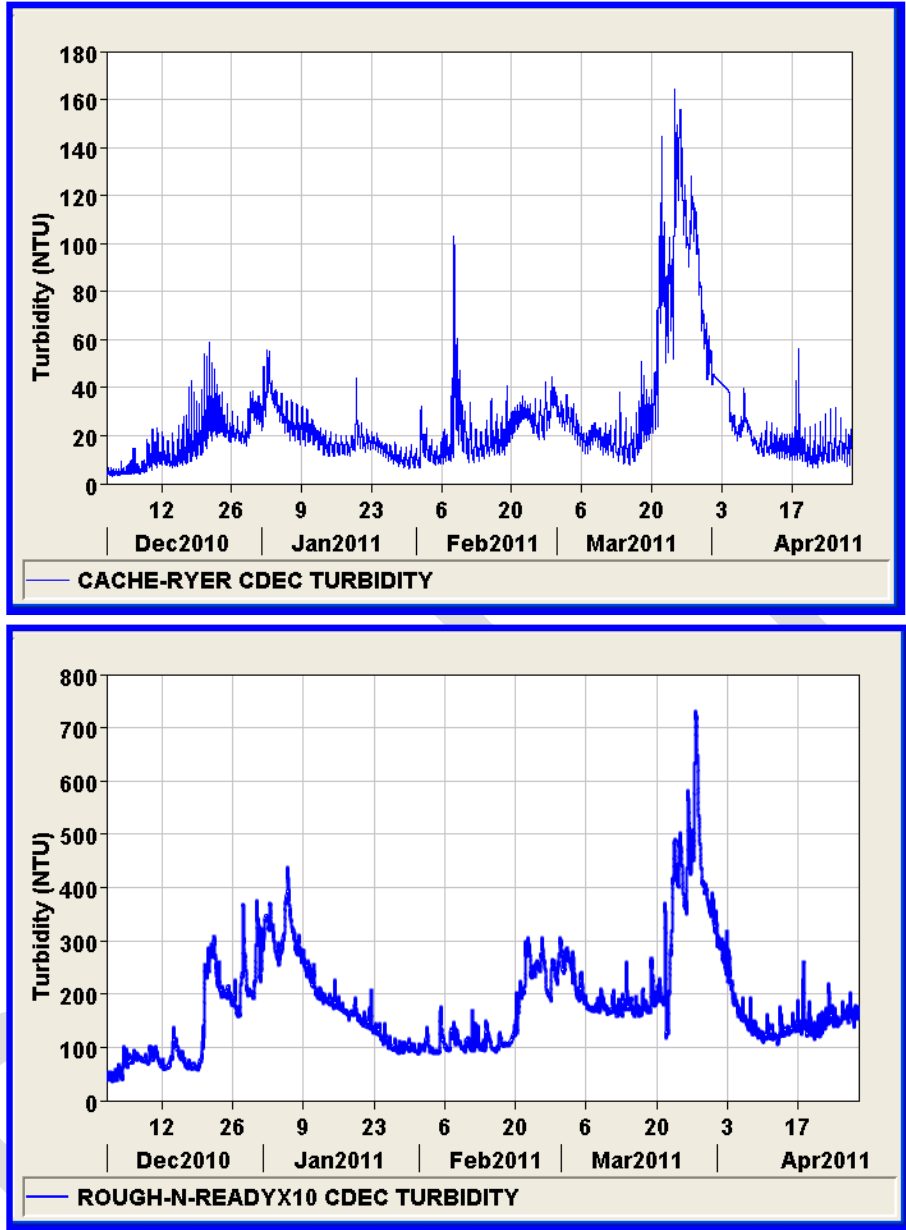


Figure 4-14 WY2011 Turbidity BCs for the Yolo Bypass (upper) and the Calaveras River (lower).

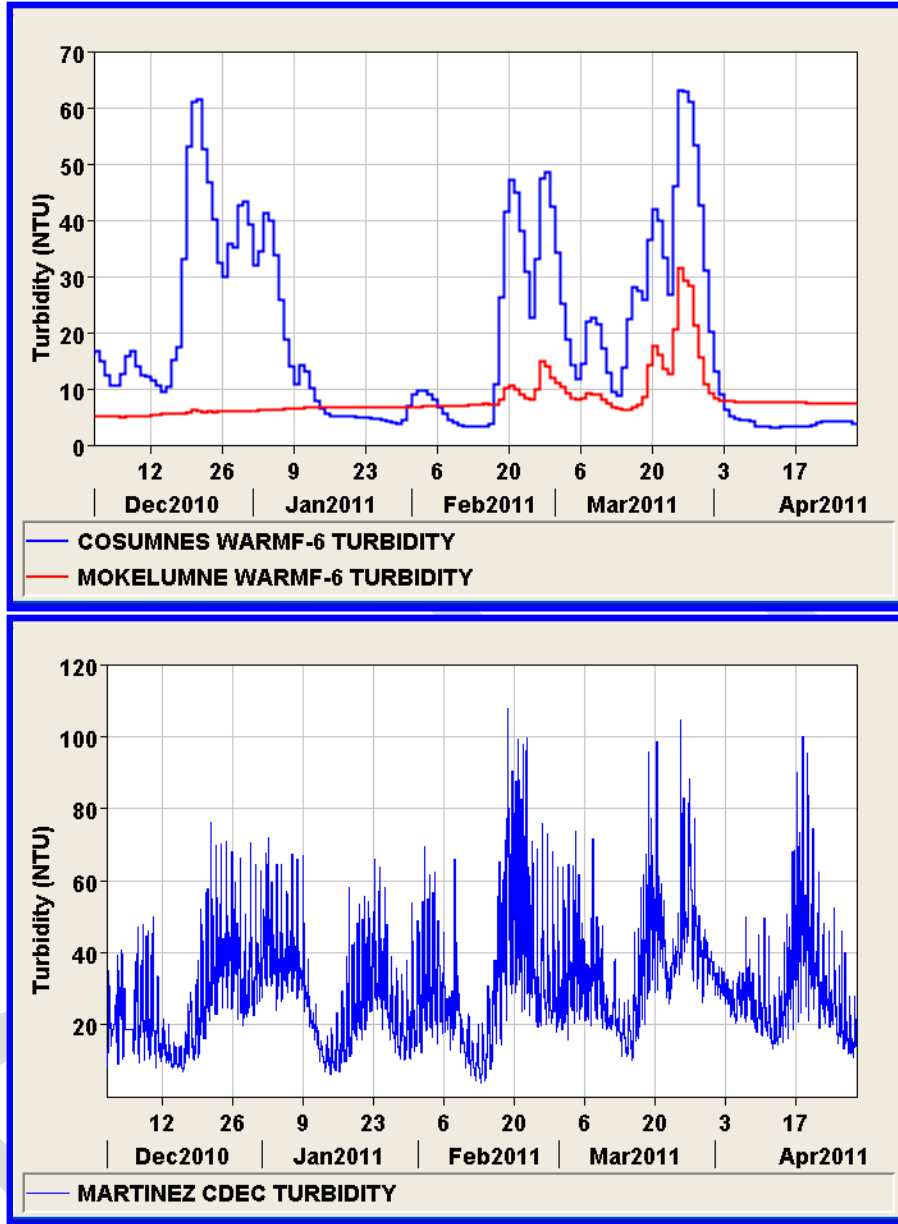
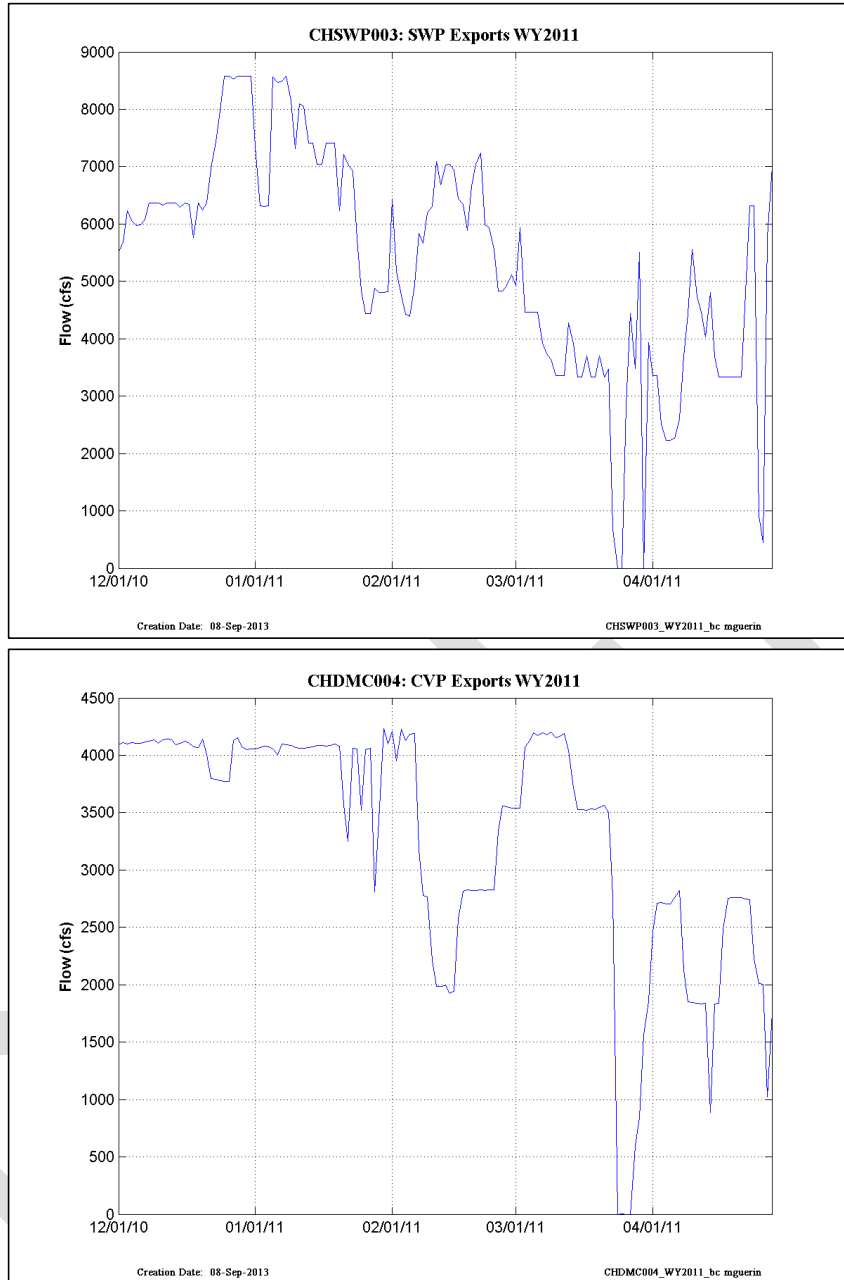
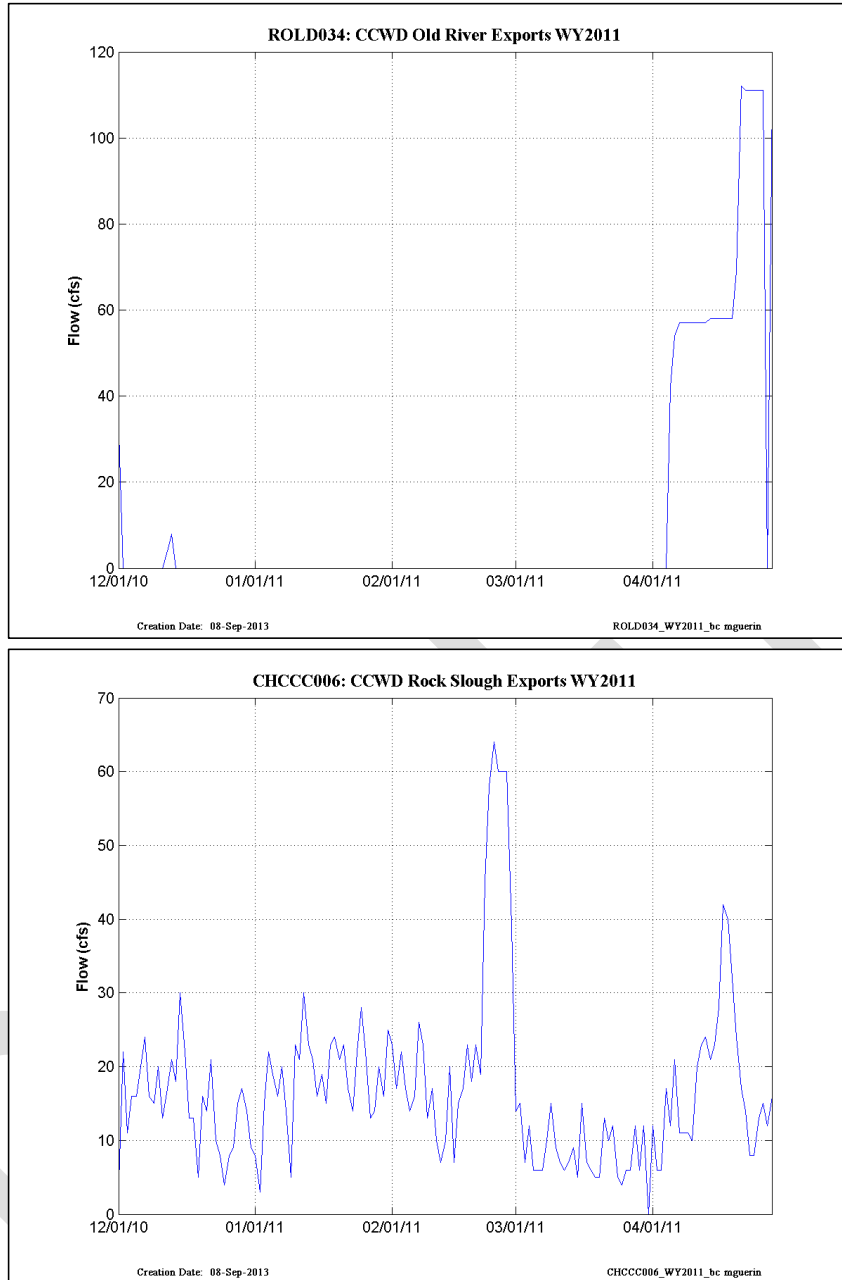


Figure 4-15 WY2011 Turbidity BCs at the Cosumnes and Mokelumne Rivers (upper, sourced from previous WARMF output) and at Martinez (lower).



**Figure 4-16 WY2011 export BCs at the SWP and CVP locations.**



**Figure 4-17 WY2011 export BCs at the CCWD Contra Costa Canal and Old River locations.**

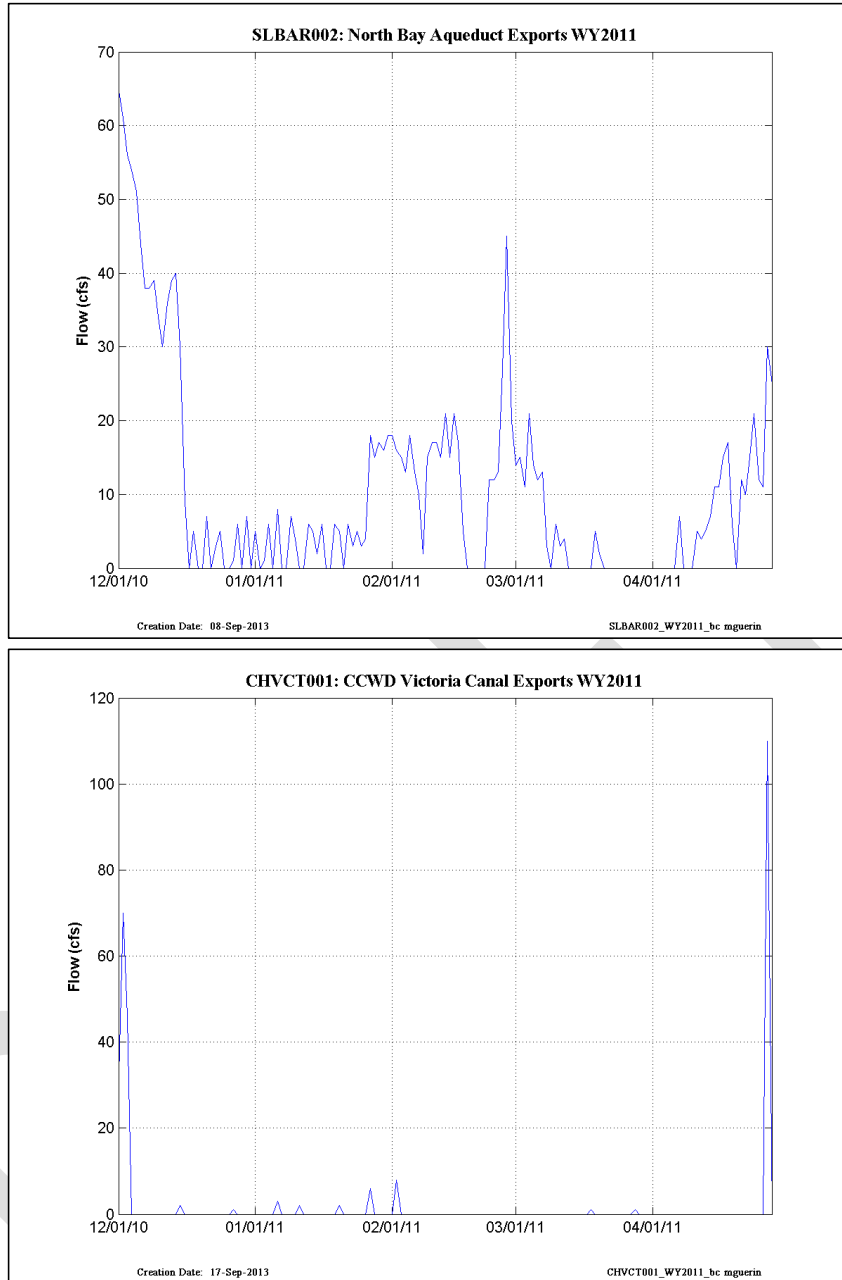


**Figure 4-18 WY2011 export BCs at the North Bay Aqueduct and CCWD Victoria Canal locations.**

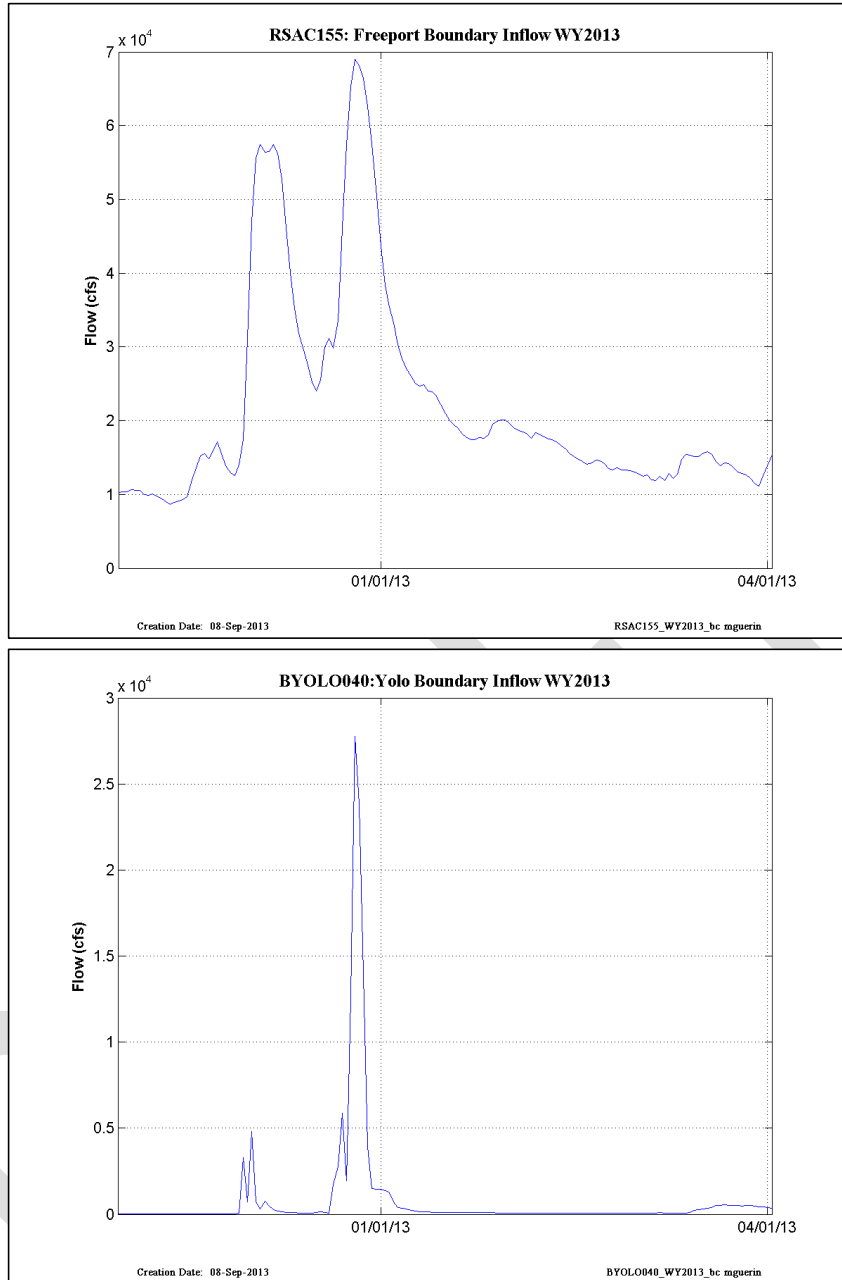
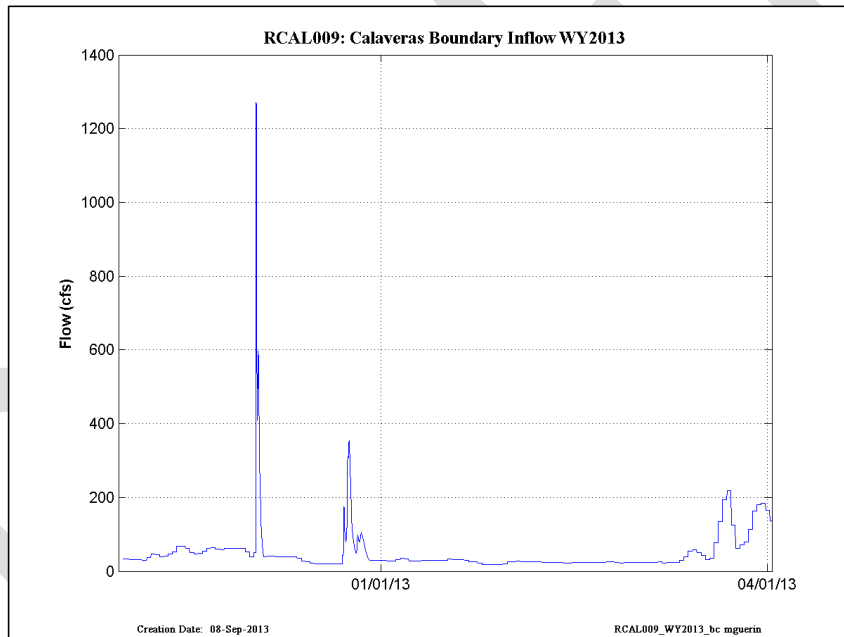
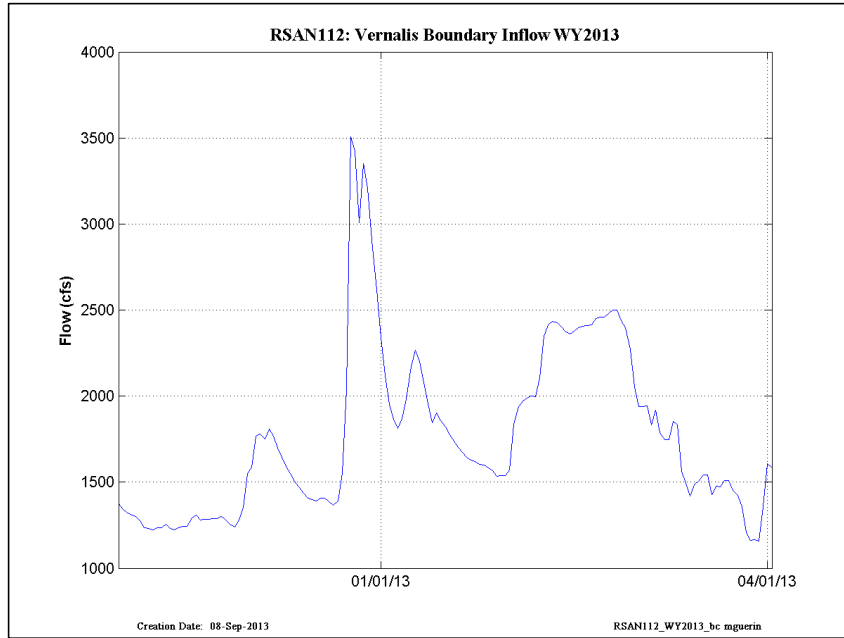
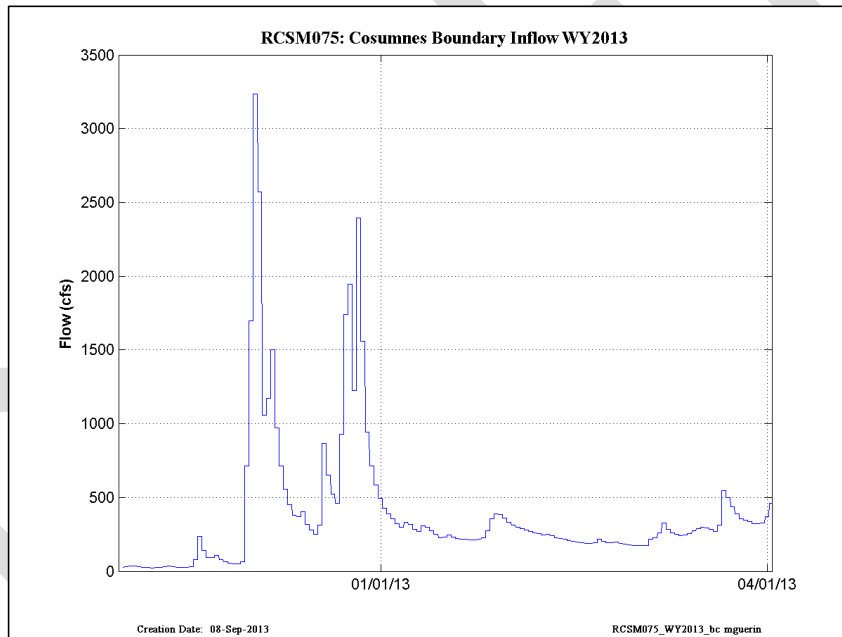
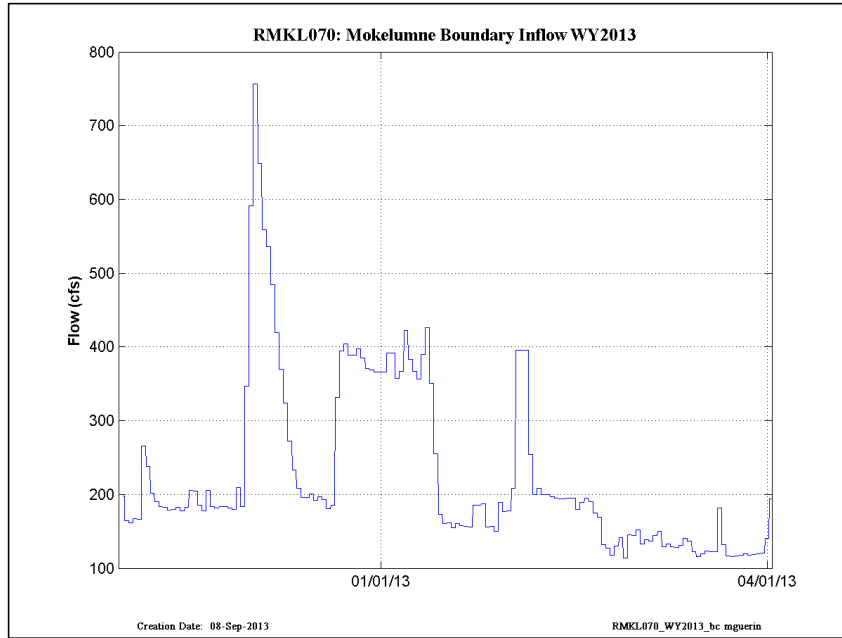


Figure 4-19 WY2013 flow BCs at Freeport and Yolo Bypass locations.



**Figure 4-20 WY2013 flow BCs at the Vernalis and Calaveras River locations.**



**Figure 4-21 WY2013 flow BCs at the Mokelumne and Cosumnes River locations.**

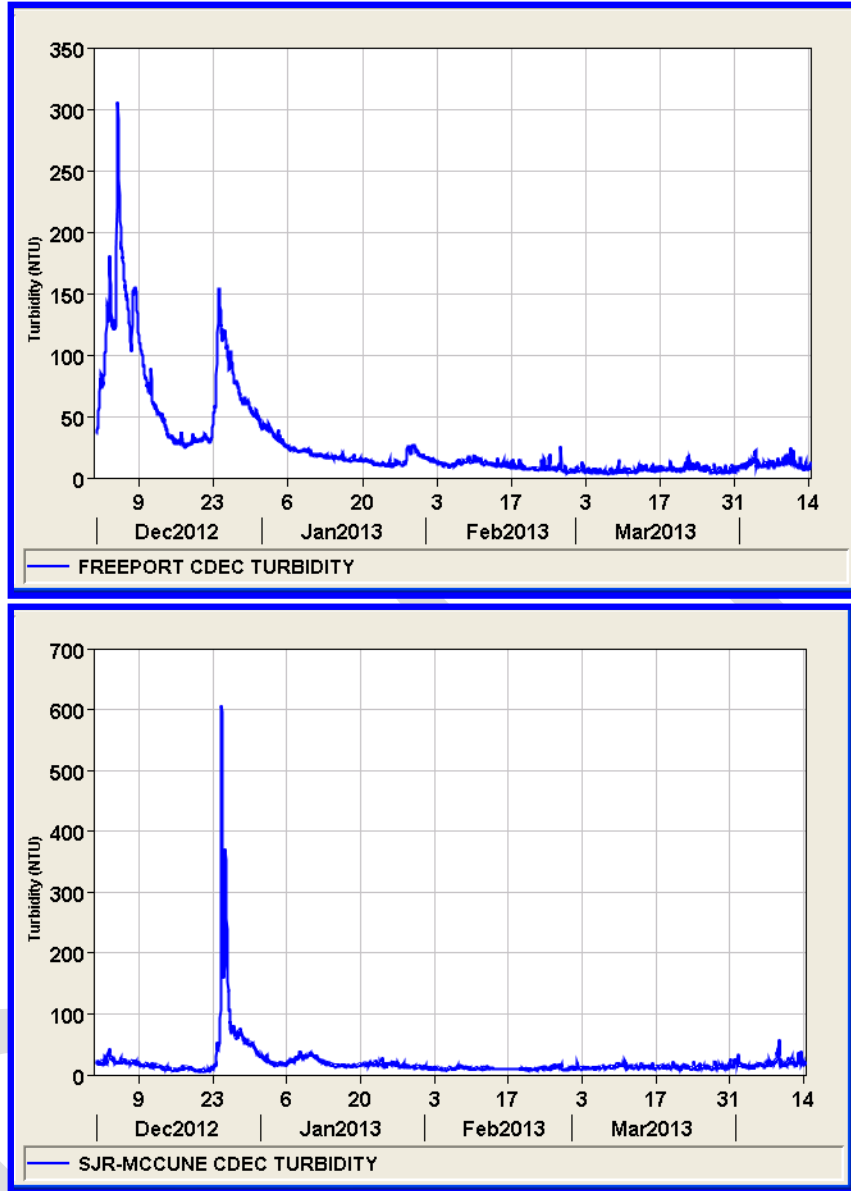


Figure 4-22 WY2013 turbidity BCs at Freeport and Vernalis.

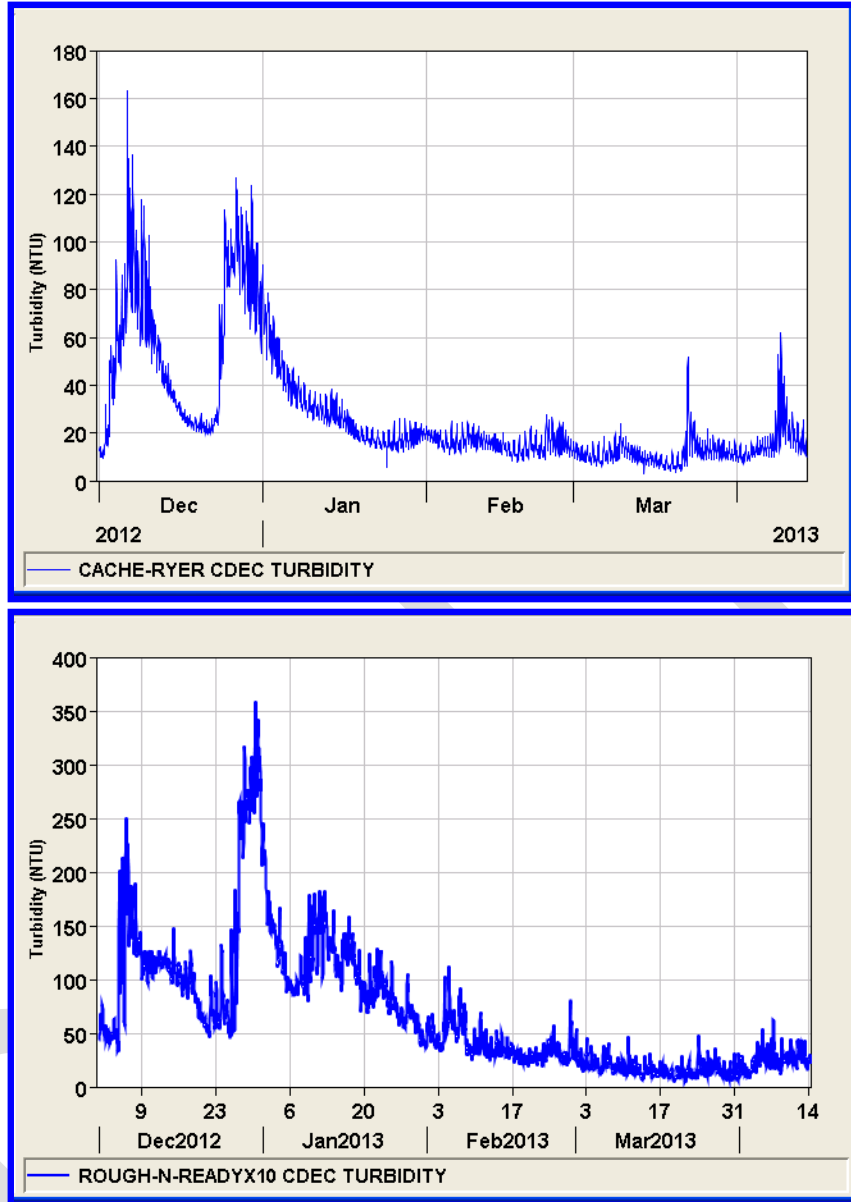


Figure 4-23 Turbidity BCs for the Yolo Bypass (upper) and the Calaveras River (lower).

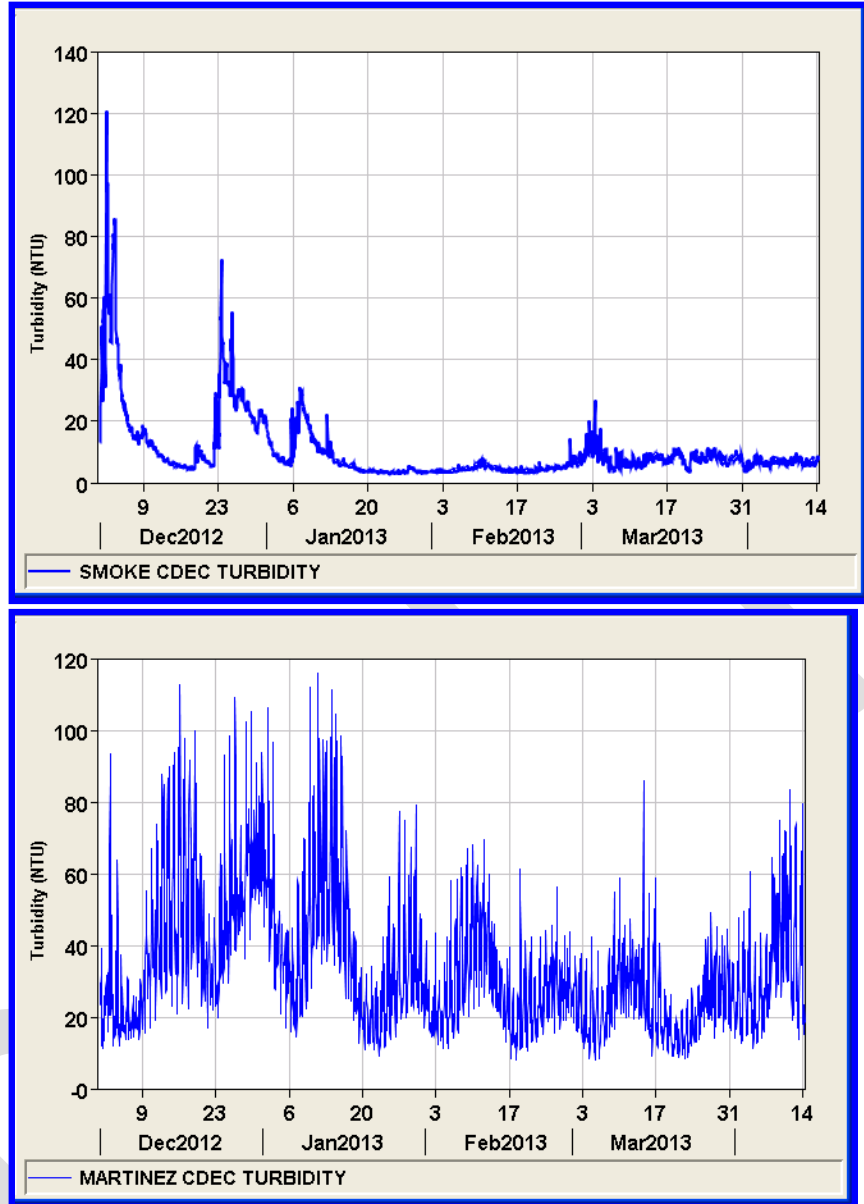


Figure 4-24 WY2013 turbidity BCs for the Mokelumne and Cosumnes Rivers (upper plot) and Martinez (lower plot).

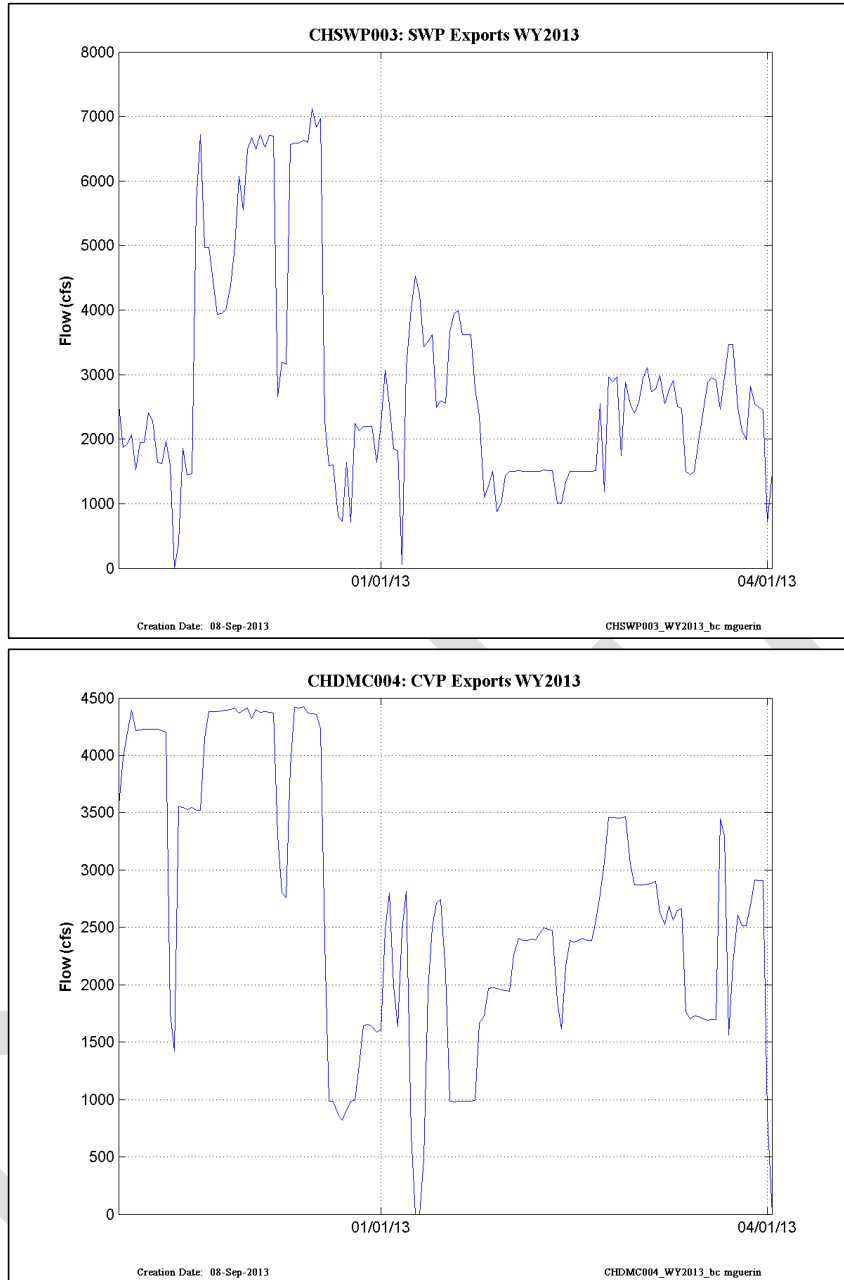


Figure 4-25 WY2013 export BCs at the SWP and CVP locations.

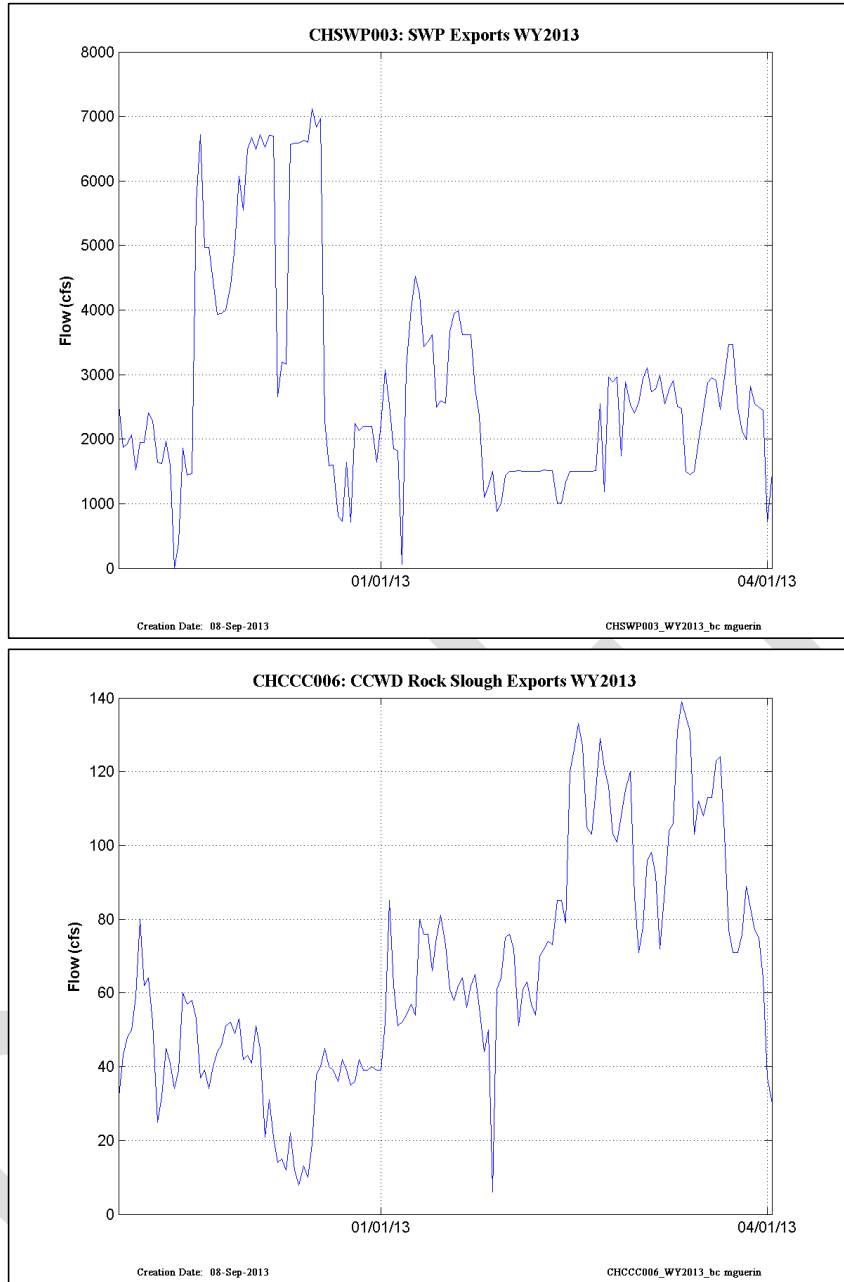
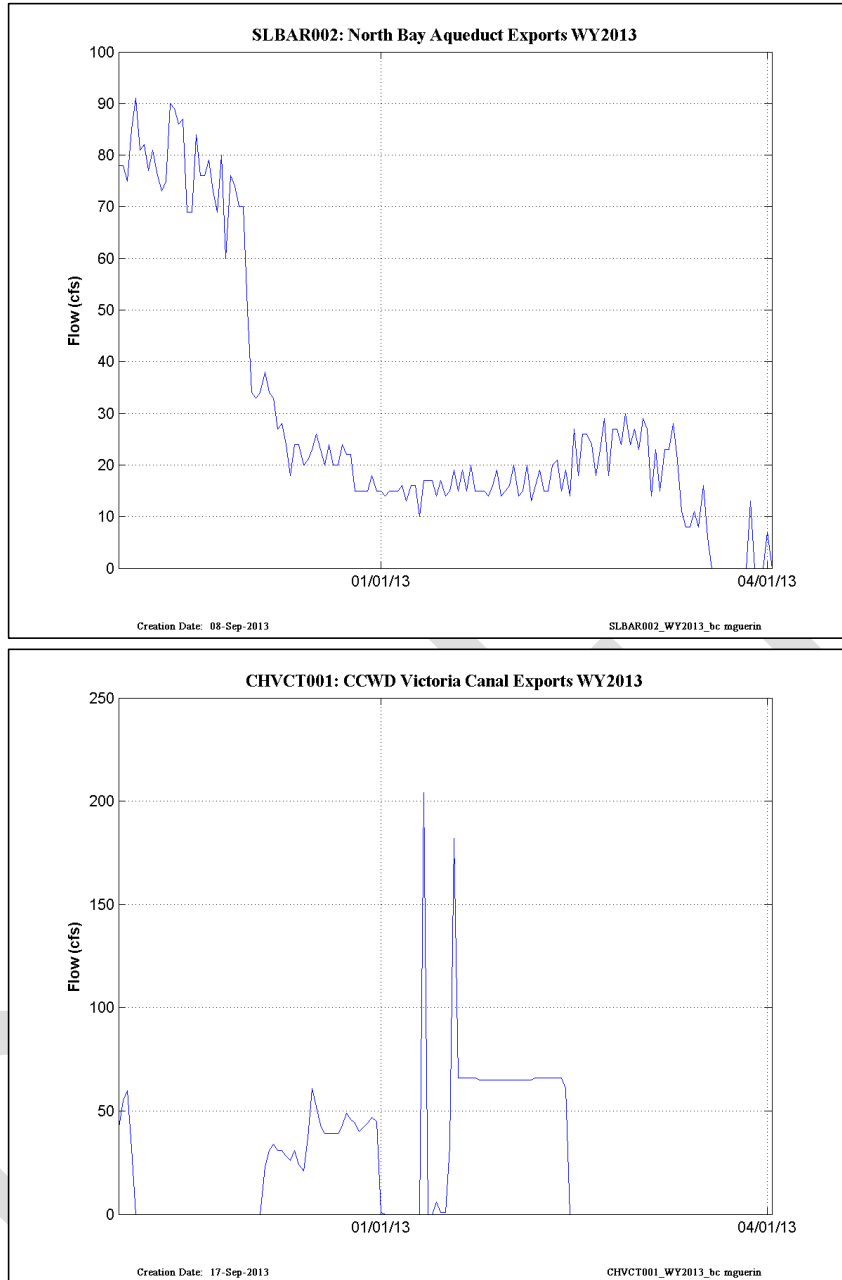


Figure 4-26 WY2013 export BCs at the CCWD Contra Costa Canal and Old River locations.



**Figure 4-27 WY2013 export BCs at the North Bay Aqueduct and CCWD Victoria Canal locations.**

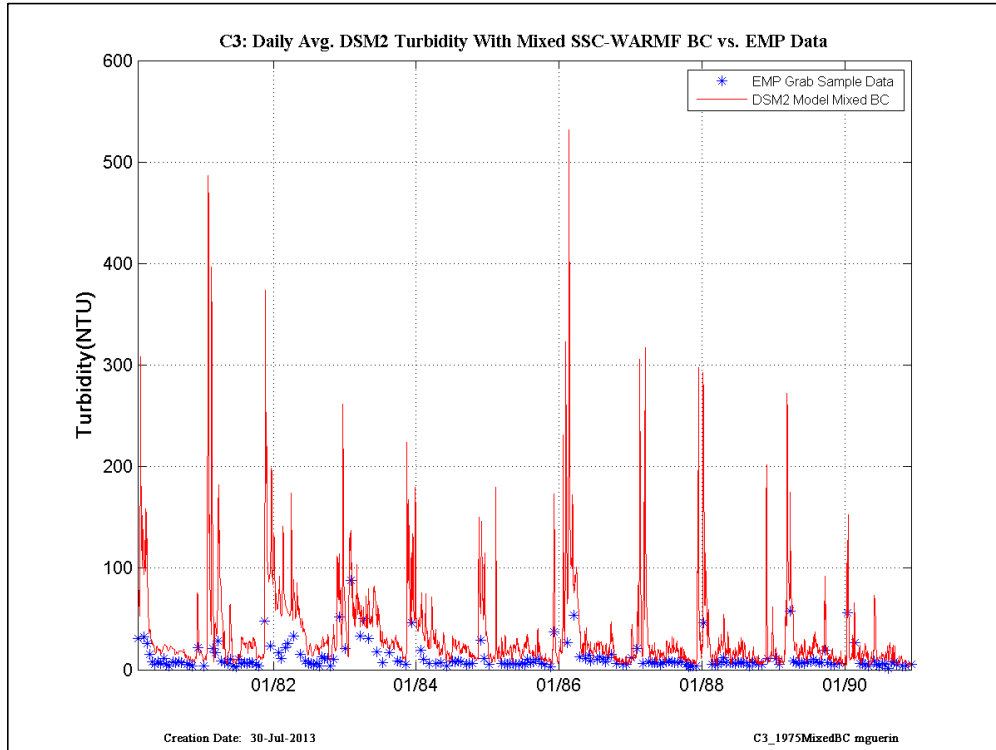


Figure 4-28 Model output and EMP grab-sample data at the IEP “C3” location at Hood for the early period historical model.

DRAFT

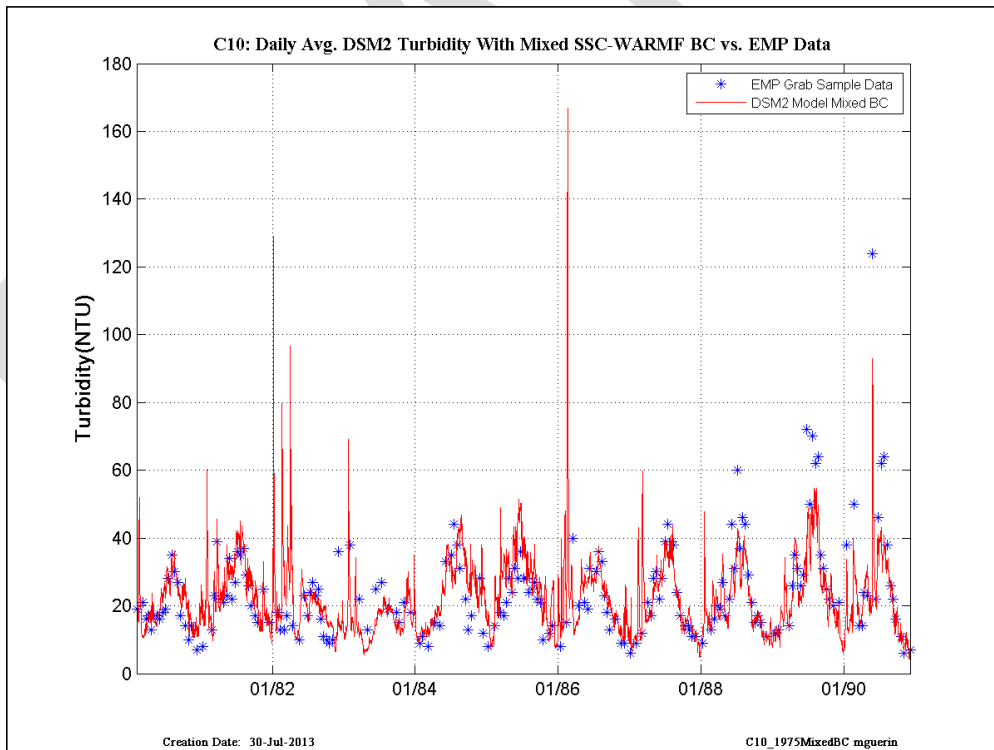
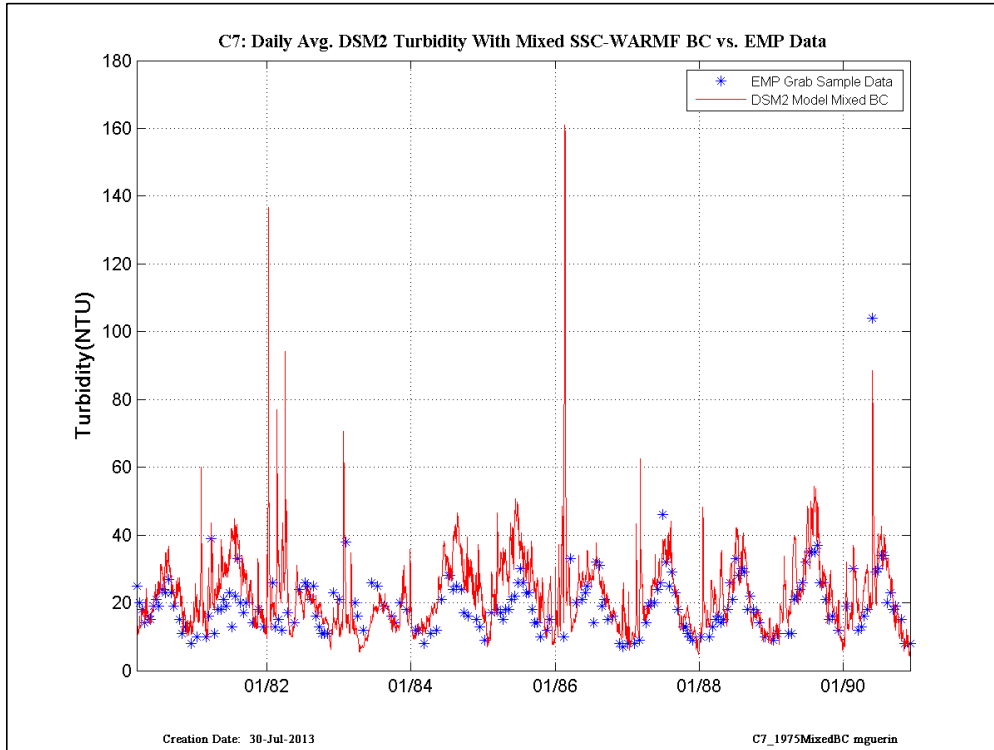


Figure 4-29 Model output and EMP grab-sample data at the IEP “C7” location at Mossdale and the “C10” location at SJR-McCune for the early period historical model.

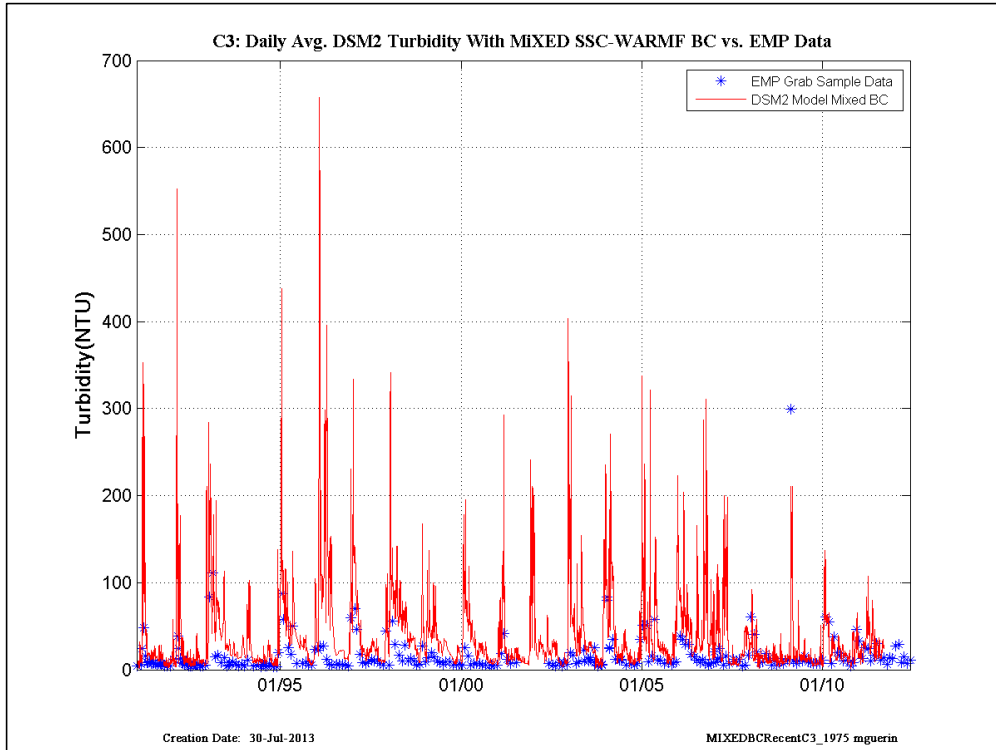


Figure 4-30 Model output and EMP grab-sample data at the IEP “C3” location at Hood for the later period historical model.

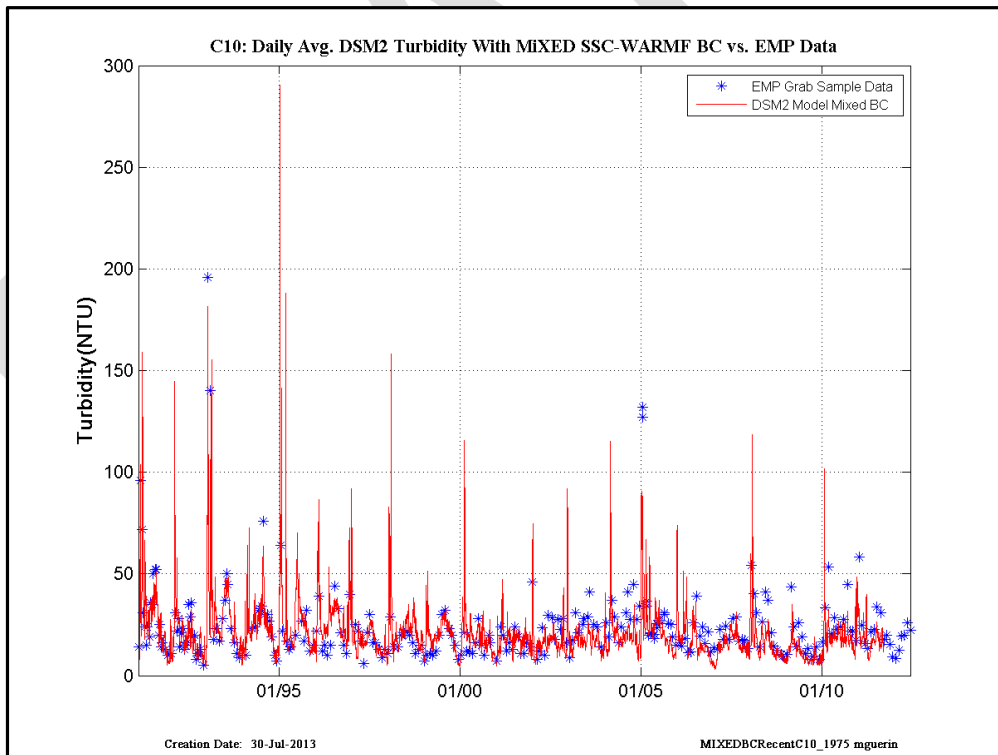
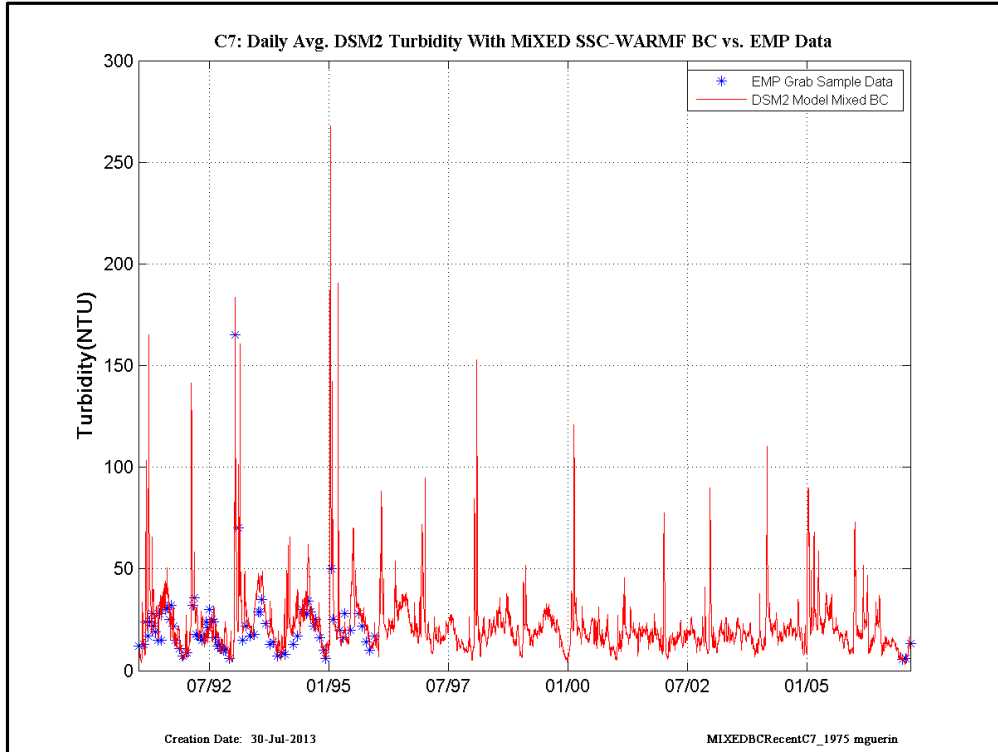


Figure 4-31 Model output and EMP grab-sample data at the IEP “C7” location at Mossdale and the “C10” location at SJR-McCune for the later period historical model.

## 5 Calibration Results

### 5.1 Calibration priorities

There were three major steps in the calibration process. The first step involved iterative calibration for WY2013 alone. Daily-averaged data and model results were used to assess the quality of the calibration statistics in comparison with WY2013 run with the previous RMA calibration. During step two, statistics for WY2010, WY2011 and WY2013 were computed after minor adjustments in the calibration parameters from step one and compared with statistics from the previous RMA model calibration. Step 3 involved comparisons on the setting of the Calaveras inflow turbidity as this time series was varied to obtain a better fit at downstream locations. The final set of settling parameters ( $K_3$ ) used in the calibration can be found in the file “rate\_coefficient\_delta\_ncc\_turbidity\_Run6B2.inp”. A visual representation of these values and their placement in the model grid is seen in Section 3.

During the calibration process, a priority was placed on improving the calibration statistics at the three compliance locations. A particular emphasis was placed on the PBIAS statistic, and considerable effort was undertaken to decrease the absolute value of this statistic without sacrificing the quality of the other statistics at the compliance location, as well as the statistics at other locations used in the calibration process. The reasoning behind this objective was that if forecast modeling of turbidity was used to assist the Delta Smelt Working Group, getting the magnitude of the turbidity as close as possible to reality would best benefit the working group’s ability to influence Delta operations. Additional reasons for minimizing the value of the PBIAS statistic are related to the ability to apply corrections to long-term averaged results – for example, if a given location is generally modeled as higher than data (negative PBIAS), then the interpretation of that model value can be assessed with the additional knowledge given by an average PBIAS value.

### 5.2 Calibration metrics

#### 5.2.1 Model Skill: Two Delta-wide calibration metrics

Background information on the use of “Model Skill” metrics was discussed in previous documentation (RMA 2013). In this section, we supply metrics specific to the current calibration project that quantify model skill as overall, Delta-wide calibration metrics.

Four overall, Delta-wide calibration metrics were calculated for each Water Year:

1. The sum of the absolute value of the PBIAS statistic at the three compliance locations
2. The sum of the absolute value of the PBIAS statistic at all available data locations excluding the compliance locations
3. Sum of the  $r^2$  statistic at the three compliance locations
4. Sum of the  $r^2$  statistic at all available data locations excluding the compliance locations.

Tabular results are presented for WY2010, WY2011 and WY2013 in Section 5.3 for the four Model Skill metrics.

### 5.3 Calibration results for WY2010 and WY2011, comparing revised and original DMS calibration simulations

The following set of four tables – Table 3 through Table 6 – illustrate the calibration comparisons between individual Water Years and the overall (Table 6) calibration metrics and statistics used to assess the revised calibration. The first four tables illustrate the individual statistics used, the PBIAS (percent Bias) and  $r^2$  statistics. The  $r^2$  statistic was chosen as it corresponds with a plotted, visual representation of the model output vs. turbidity data included in Appendices to this report, and is widely used as a measure of calibration success. The color scheme in the Tables is used solely to highlight the difference between the new and revised RMA calibrations and in the overall statistics, *i.e.*, whether a statistic was better (blue) in the comparison between measures of the previous and the current calibration. For WY2010 and WY2011, blue font highlight was only used at the three compliance locations.

The revised calibration made improvements in the overall calibration for WY2011 and WY2013 (Table 4 and Table 5, respectively) and at many individual calibration locations, while in WY2010 (Table 3) the results were mixed with a loss in performance in PBIAS particularly along Old River and at the Holland Cut compliance location. Conversely, results were markedly better along Old River and at the Holland Cut compliance location in WY2011 and WY2013. These particular results clearly indicate the difficulty in this calibration work, as there was a trade-off in performance between these modeled years. In Table 5, the improvement in the calibration is highlighted with blue color font at each location. In the few cases where the original calibration was better, the degradation in the new calibration is minor.

Table 6 documents the overall Model Skill assessment statistics. The statistics clearly indicate that the overall model skill was improved by the recalibration effort in WY2011 and WY2013, with a mix of loss and improvements in WY2010. Note that each of these statistics reflects the subjective decision to bias a specific statistic that was intentionally introduced in the recalibration effort:

1. A bias during the calibration process toward improving the PBIAS statistics over other individual statistics at each location.
2. A bias in the calibration for improving the compliance statistics over the other locations for which statistics were calculated - this is reflected in the “Compliance Only” statistics in Table 6.
3. A bias to the  $r^2$  statistic<sup>5</sup>.

---

<sup>5</sup> This is different than the decision made in the previous RMA calibration (RMA 2013).

Table 3 WY2010 calibration statistics for QUAL turbidity – comparison of New calibration run and Original RMA calibration. Bold font in the name indicates compliance locations; blue font in the statistic denotes a better result at the compliance location.

	<b>PBIAS New RMA</b>	<b>PBIAS Original RMA</b>	<b>R<sup>2</sup> New RMA</b>	<b>R<sup>2</sup> Original RMA</b>
Antioch	-13.6	5.0	0.8	0.8
Cache-Ryer	-11.9	14.6	0.9	0.9
Decker	-0.4	7.3	1.0	1.0
Dutch Slough	20.3	51.4	0.0	0.0
False River	-7.0	21.5	0.7	0.7
Freeport	2.4	2.4	1.0	1.0
Georgiana -Sac	-2.2	-2.1	0.9	0.9
Grant line	0.0	5.4	0.8	0.8
<b>Holland Cut</b>	<b>-64.7</b>	<b>27.6</b>	<b>0.7</b>	<b>0.6</b>
Hood	-8.1	-8.0	1.0	1.0
Little-Potato-SI-Term	14.2	17.6	0.7	0.8
Mallard	6.6	15.9	0.9	0.9
Martinez	-4.1	-3.4	1.0	1.0
Middle-R-Holt	16.4	42.5	0.9	0.9
Middle-at-Middle	-21.3	22.6	0.9	0.7
Miner-SI	-15.1	-14.7	1.0	1.0
Moke-at-SJR	-22.5	-21.5	1.0	1.0
Mosssdale	8.8	8.9	0.8	0.8
Old-R-Bacon	-91.6	27.6	0.7	0.5
Old-R-Hwy4	-46.2	42.8	0.5	0.4
Old-R-Quimbly	-98.4	-17.7	0.6	0.5
<b>Prisoner-Pt</b>	<b>13.3</b>	<b>24.9</b>	<b>0.9</b>	<b>0.9</b>
Rio Vista	-20.2	-4.3	0.9	0.9
Rough-n-Ready	-20.1	-23.6	0.8	0.8
SJR-Garwood	23.0	-2.7	0.6	0.6
SJR-JP	-1.6	22.8	0.8	0.8
SJR-McCune	-4.2	-4.2	1.0	1.0
3Mile-SJR	-7.3	10.0	1.0	1.0
Turner Cut-Holt	-90.5	-70.0	0.9	0.8
<b>Victoria Canal-Byron</b>	<b>-8.9</b>	<b>25.0</b>	<b>0.5</b>	<b>0.4</b>

Table 4 WY2011 calibration statistics for QUAL turbidity – comparison of New calibration run and Original RMA calibration. Bold font in the name indicates compliance locations; blue font in the statistic denotes a better result at the compliance location.

	<b>PBIAS New RMA</b>	<b>PBIAS Original RMA</b>	<b>R<sup>2</sup> New RMA</b>	<b>R<sup>2</sup> Original RMA</b>
Antioch	-1.6	13.8	0.4	0.4
Cache-Ryer	-1.6	16.7	0.9	0.9
Decker	2.4	10.0	0.9	0.8
Dutch Slough	7.2	46.4	0.2	0.2
False River	7.4	26.6	0.3	0.2
Freeport	4.4	4.4	0.9	0.9
Georgiana -Sac	9.2	9.3	1.0	1.0
Grant Line	23.7	23.9	0.8	0.8
<b>Holland Cut</b>	<b>-12.5</b>	<b>38.8</b>	<b>0.0</b>	<b>0.0</b>
Hood	-0.4	-0.3	0.7	0.7
Little-Potato-SI-Term	2.9	7.4	0.8	0.8
Mallard	2.4	11.1	0.5	0.5
Martinez	8.0	8.9	0.9	0.9
Middle-R-Holt	-21.7	3.4	0.7	0.7
Middle-at-Middle	-29.6	-5.0	0.9	0.7
Miner-SI	-15.7	-15.3	0.9	0.9
Moke-at-SJR	-4.3	-3.4	0.9	0.9
Mossdale	15.3	15.4	0.8	0.8
N Mokelumne	3.5	5.9	0.8	0.8
Old-R-Bacon	-23.0	33.8	0.2	0.2
Old-R-Hwy4	14.0	46.4	0.7	0.6
Old-R-Quimbly	-26.4	19.5	0.3	0.3
<b>Prisoner-Pt</b>	<b>13.3</b>	<b>17.7</b>	<b>0.8</b>	<b>0.5</b>
Rio Vista	-2.9	8.2	0.8	0.8
Rough-n-Ready	26.9	24.3	0.8	0.8
SJR-Garwood	36.2	27.9	0.8	0.8
SJR-JP	-0.4	16.6	0.4	0.3
S Mokelumne	0.2	0.9	0.8	0.8
SJR-McCune	0.3	0.3	1.0	1.0
3Mile-SJR	-7.5	3.7	0.9	0.8
Turner Cut-Holt	-15.4	-11.8	0.8	0.6
<b>Victoria Canal-Byron</b>	<b>-8.8</b>	<b>5.5</b>	<b>0.9</b>	<b>0.8</b>

Table 5 WY2013 calibration statistics for QUAL turbidity – comparison of New calibration run and Original RMA calibration. Bold font in the name indicates compliance locations; blue font in the statistic denotes a better result in the calibration comparison.

	PBIAS New RMA	PBIAS Original RMA	R <sup>2</sup> New RMA	R <sup>2</sup> Original RMA
Antioch	4.8	21.1	0.7	0.7
Cache-Ryer	8.2	31.6	0.9	0.9
Decker	10.5	21.0	0.9	0.9
Dutch Slough	29.5	60.6	0.2	0.1
False River	3.1	29.0	0.6	0.5
Freeport	2.0	2.0	1.0	1.0
Georgiana -Sac	2.3	2.4	1.0	1.0
Grant Line	-10.9	-8.6	0.7	0.7
<b>Holland Cut</b>	<b>-16.0</b>	<b>51.9</b>	<b>0.0</b>	<b>0.0</b>
Hood	-8.5	-8.4	1.0	1.0
Little-Potato-SI-Term	23.0	26.6	0.8	0.8
Mallard	10.2	18.4	0.7	0.7
Martinez	-4.9	-4.3	0.9	0.9
Middle-R-Holt	38.2	61.9	0.8	0.8
Middle-at-Middle	25.8	60.7	0.8	0.8
Miner-SI	-13.0	-12.7	1.0	1.0
Moke-at-SJR	-18.2	-16.8	1.0	1.0
Mossdale	-13.2	-12.7	1.0	1.0
N Mokelumne	21.2	27.1	0.2	0.1
Old-R-Bacon	-22.1	56.9	0.6	0.4
Old-R-Hwy4	11.0	72.6	0.6	0.6
Old-R-Quimbly	-25.6	28.8	0.8	0.8
<b>Prisoner-Pt</b>	<b>23.7</b>	<b>33.8</b>	<b>0.9</b>	<b>0.9</b>
Rio Vista	-10.5	5.0	0.5	0.5
Rough-n-Ready	12.8	20.8	0.3	0.3
SJR-Garwood	52.5	25.9	0.6	0.5
SJR-JP	7.2	29.3	1.0	1.0
SJR-McCune	-0.3	-0.3	0.9	0.9
S Mokelumne	10.9	13.9	0.5	0.5
3Mile-SJR	-0.4	16.1	0.9	0.9
Turner Cut-Holt	30.2	46.0	0.5	0.5
<b>Victoria Canal-Byron</b>	<b>39.8</b>	<b>65.9</b>	<b>0.6</b>	<b>0.5</b>

**Table 6 Overall calibration metrics for the New calibration run and the Original RMA calibration run. Blue, bold font indicates a superior calibration result. Black, bold font indicates equivalent results.**

<b>RMA New calibration of QUAL turbidity</b>	<b>WY2010</b>	<b>WY2011</b>	<b>WY2013</b>
Sum Abs(PBIAS) Compliance Only	87.0	<b>34.6</b>	<b>79.5</b>
Sum Abs(PBIAS) w/o compliance	577.4	<b>314.3</b>	<b>430.9</b>
Sum r <sup>2</sup> Compliance Only	<b>2.1</b>	<b>1.7</b>	<b>1.4</b>
Sum r <sup>2</sup> w/o compliance	<b>21.2</b>	<b>20.7</b>	<b>22.0</b>
<b>RMA Original calibration of QUAL turbidity</b>	<b>WY2010</b>	<b>WY2011</b>	<b>WY2013</b>
Sum Abs(PBIAS) Compliance Only	<b>77.4</b>	62.1	151.6
Sum Abs(PBIAS) w/o compliance	<b>483.2</b>	420.6	741.5
Sum r <sup>2</sup> Compliance Only	1.9	1.3	1.3
Sum r <sup>2</sup> w/o compliance	20.6	19.9	21.2

DRAFT

## 6 Evaluation of the Calaveras Boundary Condition and Its Role in Turbidity Bridge Formation

### 6.1 Background

As part of the recalibration process, the set of inflow flow and turbidity boundary conditions was revisited to ensure the best possible model results. As mentioned in Section 3, in addition to checking time shifts needed at the flow boundaries, turbidity boundary conditions were formulated with CDEC turbidity data wherever possible. As a consequence, the Rough-N-Ready data location was used to formulate the Calaveras River turbidity boundary. For WY2013, it was found that increasing the data by a factor of ten (i.e., (CDEC Rough-N-Ready)\*10) produced a reasonable set of turbidity model results in WY2013. In step 2 of the calibration, when WY2010 and WY2011 turbidity models were implemented to refine the recalibration, it was clear that for WY2011 this scale factor was too high, while for WY2010 it appeared reasonable. In the remainder of this section, we illustrate these boundary condition results (Figure 6-1 through Figure 6-18, Table 6-2 and Table 6-3) and then discuss the role of the Calaveras, as well as other boundary conditions, in the creation of a turbidity bridge (Figure 6-19 through Figure 6-24, and Table 6-1).

### 6.2 Calaveras Turbidity Boundary

As documented in Section 3, Table 2, the Calaveras turbidity boundary was set at a multiple of CDEC Rough-N-Ready turbidity – for WY2010 and WY2010, the multiple was a factor of ten, while for WY2011, the multiple was one, i.e., the cleaned turbidity data was applied without scaling. This CDEC location was chosen as it is the closest to the location where the Calaveras joins the San Joaquin, as there is not a measurement of turbidity on the Calaveras itself.

To illustrate the importance of this boundary condition, a series of plots were developed to document the book-end values used in setting the Calaveras turbidity boundary for each Water Year, at the low end of Rough-N-Ready turbidity without scaling and at the upper end scaled up by a factor of ten. In addition, volumetric model output plots are used to identify the potential sources of turbidity, and to investigate the importance of the Calaveras, at seven central and south Delta CDEC station locations used in the model calibration process – Rough-N-Ready, Holland Cut, Prisoner’s Point, Victoria-Canal-Byron, Turner-Cut-Byron, Middle-R-Holt, and Middle-at-Middle.

Figure 6-1 through Figure 6-7 illustrate results for WY2013. In each figure, the upper plot shows the time series for the cleaned-daily-averaged CDEC data (blue dash), the model results using the final settings for the Calaveras River (red line) and the model results for the other book-end Calaveras turbidity boundary condition. The lower plot illustrates volumetric results for the Calaveras (blue line), the sum Mokelumne+Cosumnes (red line), the Sacramento (green line) and the San Joaquin (black line). The volumetric model results begin after the model domain has achieved a good initial condition, i.e., when the sum of all input volumes reaches 100%.

At Rough-N-Ready, Figure 6-1, the output shows that setting the Calaveras boundary at (CDEC Rough-N-Ready)\*10 improves the match between CDEC data and model output at the lower turbidity values,

even though the volume of Calaveras water is low. At Turner-Cut-Holt, Figure 6-5, the Calaveras turbidity has a noticeable effect at the lower turbidity values, with the higher boundary condition improving the fit to data. At each of the other locations- Holland Cut, Prisoner's Point, Victoria-Canal-Byron and the two Middle River locations - the Calaveras boundary has little or no effect on model results.

Figure 6-8 through Figure 6-14 illustrate results for WY2011. As for WY2013, the upper plot illustrates data and model results and the lower plot illustrates volumetric results after the model domain has achieved an acceptable initial condition (the sum of all input volumes reaching 100%). Note that the Calaveras River inflow is quite high during March (Table 6-1). At Rough-N-Ready, Figure 6-8, the output shows that neither setting for the Calaveras boundary has much effect on model results – the water at this location is dominated by San Joaquin water. The result is quite different at each of the other locations, Figure 6-9 through Figure 6-14. Comparing the volumetric plots with the modeled turbidity, it is seen that the volume of Calaveras flow carrying turbidity has a noticeable influence on the modeled turbidity, and that the high Calaveras boundary condition (CDEC Rough-N-Ready)\*10 is much too high, and the lower setting (CDEC Rough-N-Ready)\*1 produces a better match with the CDEC data. For example, at the compliance location Prisoner's Point, (Figure 6-10), the influence of the Calaveras volume reaches about 45% in late March, and the proper setting of this turbidity boundary is crucial to the model result. The effect is similar at the Turner-Cut-Holt location, Figure 6-12.

Figure 6-15 through Figure 6-18 illustrate model results for WY2010. In this year, the volumetric results are not shown as the simulation did not reach 100% anywhere until February. In comparing the model results at the seven locations, the decision on the best Calaveras boundary condition setting is not obvious, as it was in WY2011. In some case the higher results looks more appropriate in others the lower setting does – an example at the two Middle River locations is seen in Figure 6-18. In order to decide on the best setting, calibration statistics were prepared for both settings – the results are documented in Table 6-2 for all of the locations, while the overall metrics are documented in Table 6-3. Examining Table 6-2, it seen that while the number locations with better statistics was found in the lower Calaveras setting, the differences between the two are small in many cases –for example at the three Old River locations. The overall calibration metrics in Table 6-3 document that the higher Calaveras setting has better overall metrics, although the differences are not great.

### **6.3 Turbidity Bridge Formation**

In each of the Water Years investigated, the 12 NTU value at compliance locations, used for potentially changing Delta exports operations, was exceeded during the modeled period, although in some cases very briefly. In this section, we discuss the conditions potentially leading to a turbidity bridge formation which we assume are directly related to these compliance values. Documentation is supplied in Figure 6-19 through Figure 6-24, and in Table 6-1.

Table 6-1 lists the conditions in the month where the compliance values were exceeded. March 2011 stands out in this table as the Calaveras River inflow reached a very high level, and as was seen in Section 6.2, the setting of the Calaveras turbidity boundary condition differed dramatically from the setting in WY2010 and WY2013. In comparing WY2010 and WY2013, we see that the main differences in

the selected months lie in the Sacramento River inflow, low in WY2010, and in the SWP+CVP export levels, high in WY2013.

What can't be seen in these tabular results are the differences in timing of the peaks in flow and turbidity, or the overall distribution of turbidity. However, here the figures give significant intuition on the timing differences. The simplest case, mid-March 2011 is shown as a contour plot in Figure 6-21. Here, although all of the inflows are quite high, the plot shows that in the south Delta, increases in turbidity are due in large part to inflow from the San Joaquin combined with inflow from the Calaveras. This is also seen in the volumetric plots shown in Section 6.2 from the Calaveras River analysis. The high Sacramento River plus Yolo Bypass inflow leads to the increases in turbidity in the central Delta from the north, with the flows shown in Figure 6-22. Influence from the exports decreases and the OMR flow becomes positive as exports are reduced when the compliance locations showed increased levels of turbidity.

In WY2010, Figure 6-19, we see that the northern two compliance locations, Prisoner's Point and Holland Cut are primarily influenced by Sacramento River turbidity despite a low Sacramento inflow, while Victoria-Canal-Byron is primarily influenced by San Joaquin River turbidity. Figure 6-20 shows the Sacramento inflow along with the export levels - the moderate exports are indicated by a nearly constant and moderately negative OMR flow - contribute to the potential for a turbidity bridge.

In WY2013, the information in the contour plot, Figure 6-23, provides a clear picture that the high values at the turbidity compliance locations are from Sacramento turbidity. Here, the timing issue also appears to be important, as the export flow and OMR flow appear (Figure 6-24) to coincide with the potential appearance of a turbidity bridge, as indicated by the turbidity values near the compliance locations.

## 6.4 Summary Discussion

The influence of the Calaveras River on central and south Delta turbidity was illustrated in WY2011 during a period of high Calaveras inflow, in large part due to careful setting of the Calaveras River turbidity boundary condition with data from the CDEC location at Rough-N-Ready. During lower Calaveras inflow years, turbidity boundary conditions on the Calaveras are less crucial as the volume of Calaveras water reaching the central Delta is small. However, the somewhat higher flows in WY2013 showed the need for careful scrutiny of Calaveras turbidity boundary conditions.

The WY2011 results are somewhat problematic, as the CDEC location at Rough-N-Ready showed only a marginal volume of Calaveras water during the time span when this location was used a boundary condition for Calaveras turbidity. This suggests that the source of the sediment that produced this level of turbidity was not necessarily the Calaveras River. However, the turbidity results downstream of this location, for example Figure 6-8 at Prisoner's Point and Figure 6-12 at Turner-Cut-Holt, suggest that the Calaveras water contributes an important component to the turbidity there.

In Section 6, we consider the value of 12 NTU at the three compliance locations to indicate the potential for formation of a turbidity bridge joining the central and south Delta regions. The three Water Years investigated illustrate different modes for turbidity bridge formation. In WY2011, the high flow in March 2011 and (possibly) high turbidity on the Calaveras contributed to the formation of a turbidity bridge,

along with the high flow (and relatively low turbidity) on the San Joaquin. Sacramento and Yolo Bypass turbidity was drawn in to the central Delta, in part due to high export levels early in March, 2011.

In February 2010, the potential formation of a turbidity bridge is influenced by turbidity from the San Joaquin from the south and the Sacramento from the north. Exports appear to play a minor role in this formation, as OMR and exports are relatively constant during this period. In December 2012 (WY2013), the Sacramento River plays the major role in supplying turbidity to the central Delta, and exports appear to play a significant role in drawing the turbidity to the south Delta.

DRAFT

**Table 6-1 Flow and turbidity values for the month in which the three compliance locations exceeded 12 NTU in each Water Year modeled in the recalibration effort.**

	<b>February 2010</b>	<b>March 2011</b>	<b>December 2012</b>
<b>Peak Sac+Yolo Flow (CFS)</b>	~ 40,000	> 91,000	> 96,000
<b>Peak Sac Daily (NTU)</b>	> 220	~ 55	> 220
<b>Peak SJR Flow (CFS)</b>	> 3600	> 20,000	> 3000
<b>Peak SJR Daily (NTU)</b>	~ 43	~ 67	~ 240
<b>Peak Cal Flow (CFS)</b>	~ 50	> 6900	~ 50
<b>Peak Cal Daily (NTU)</b>	N/A	N/A	N/A
<b>Cos+Moke Flow (CFS)</b>	~ 500 to 3500	~ 1400 to 11,000	~ 450 to 4000
<b>Peak S-Moke Daily (NTU)</b>	N/A	74	~ 70 to 120
<b>OMR Daily (CFS)</b>	-5806 to -2343	-2862 to -72	-9880 to 554
<b>SWP+CVP (CFS)</b>	~ 5900 to 7600	0 to ~ 9500	~ 1500 to > 11400

Table 6-2 Comparison of calibration statistics in WY2010 for the lower and higher Calaveras turbidity boundary condition (CDEC Rough-N-Ready)\*10) that was used as the final setting. Bold font indicates a compliance location while blue font indicates a better result in comparison with the other simulation.

	R <sup>2</sup> Low Cal	R <sup>2</sup> High Cal	PBIAS Low Cal	PBIAS High Cal
Antioch	0.83	0.83	-13.6	-13.6
Cache-Ryer	0.95	0.95	-11.9	-11.9
Dutch Slough	0.04	0.04	20.2	20.3
False River	0.74	0.74	-7.0	-7.0
Freeport	1.00	1.00	2.4	2.4
Georgiana -Sac	0.93	0.93	-2.2	-2.2
Grant line	0.83	0.83	0.7	0.0
<b>Holland Cut</b>	<b>0.66</b>	<b>0.66</b>	<b>-64.2</b>	<b>-64.7</b>
Hood	0.97	0.97	-8.1	-8.1
Little-Potato-SI-Term	0.76	0.75	13.8	14.2
Mallard	0.88	0.88	6.6	6.6
Martinez	0.98	0.98	-4.1	-4.1
Middle-R-Holt	0.82	0.92	31.4	16.4
Middle-at-Middle	0.93	0.85	7.0	-21.3
Miner-SI	0.98	0.98	-15.1	-15.1
Moke-at-SJR	0.96	0.96	-22.7	-22.5
Mossdale	0.84	0.84	8.8	8.8
Old-R-Bacon	0.70	0.70	-90.5	-91.6
Old-R-Hwy4	0.52	0.50	-40.0	-46.2
Old-R-Quimbly	0.57	0.58	-98.1	-98.4
<b>Prisoner-Pt</b>	<b>0.92</b>	<b>0.92</b>	<b>14.6</b>	<b>13.3</b>
Rio Vista	0.95	0.95	-20.2	-20.2
Rough-n-Ready	0.65	0.81	2.5	-20.1
SJR-Garwood	0.61	0.61	22.9	23.0
SJR-JP	0.79	0.79	-1.6	-1.6
SJR-McCune	0.99	0.99	-4.2	-4.2
3Mile-SJR	0.95	0.96	-7.3	-7.3
Turner Cut-Holt	0.56	0.87	-5.6	-90.5
<b>Victoria Canal-Byron</b>	<b>0.59</b>	<b>0.54</b>	<b>11.7</b>	<b>-8.9</b>

Table 6-3 Overall calibration metrics for the WY2010 calibration run and with low and high Calaveras turbidity boundary. Blue, bold font indicates a superior calibration result. Black, bold font indicates equivalent results.

RMA New calibration of QUAL turbidity	WY2010 Low Cal BC	WY2010 High Cal BC
Sum Abs(PBIAS) Compliance Only	91	<b>87</b>
Sum Abs(PBIAS) w/o compliance	<b>468</b>	577
Sum r <sup>2</sup> Compliance Only	<b>2.2</b>	2.1
Sum r <sup>2</sup> w/o compliance	20.7	<b>21.2</b>

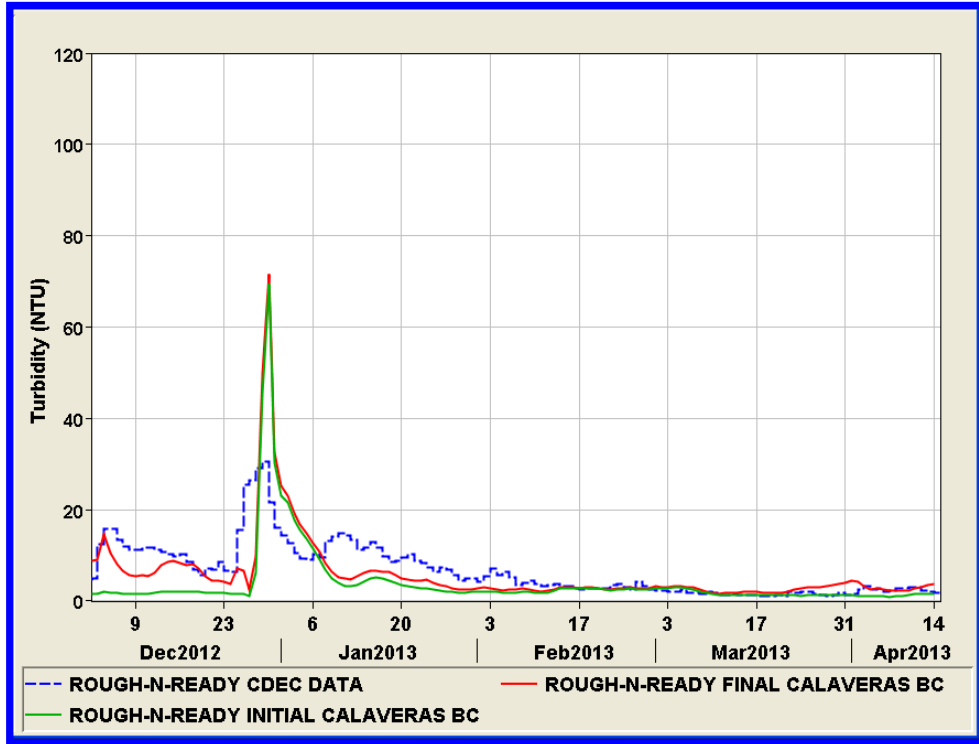


Figure 6-1 WY2013 turbidity data and book-end model output along with volumetric plots at Rough-N-Ready.

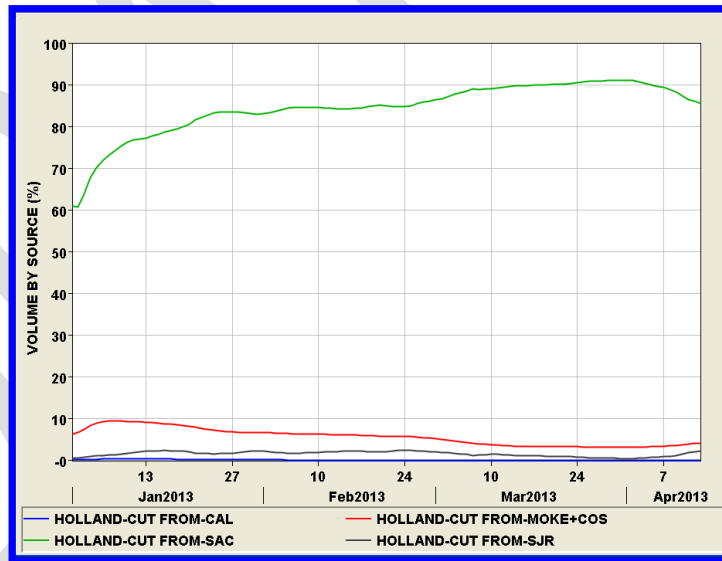
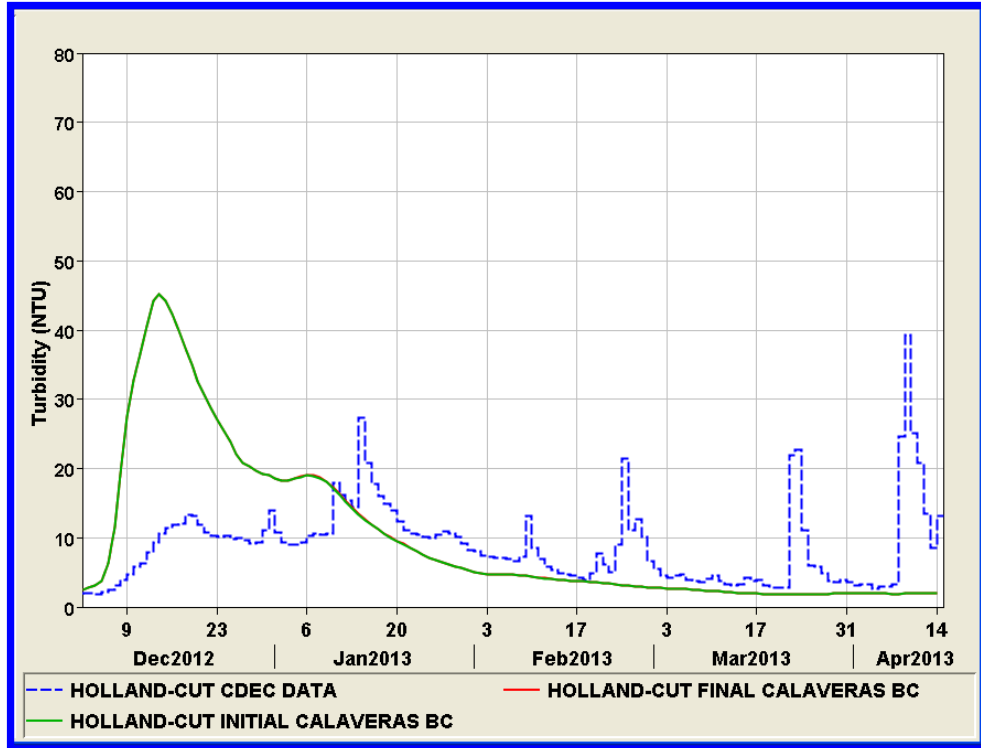


Figure 6-2 WY2013 turbidity data and book-end model output along with volumetric plots at Holland Cut.

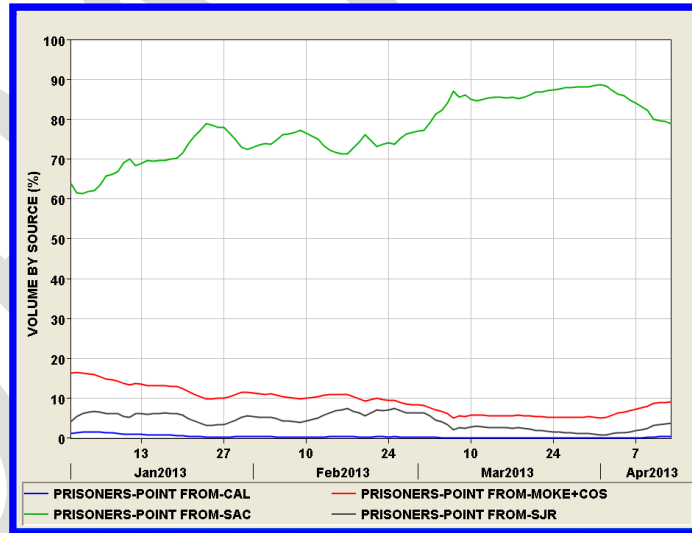
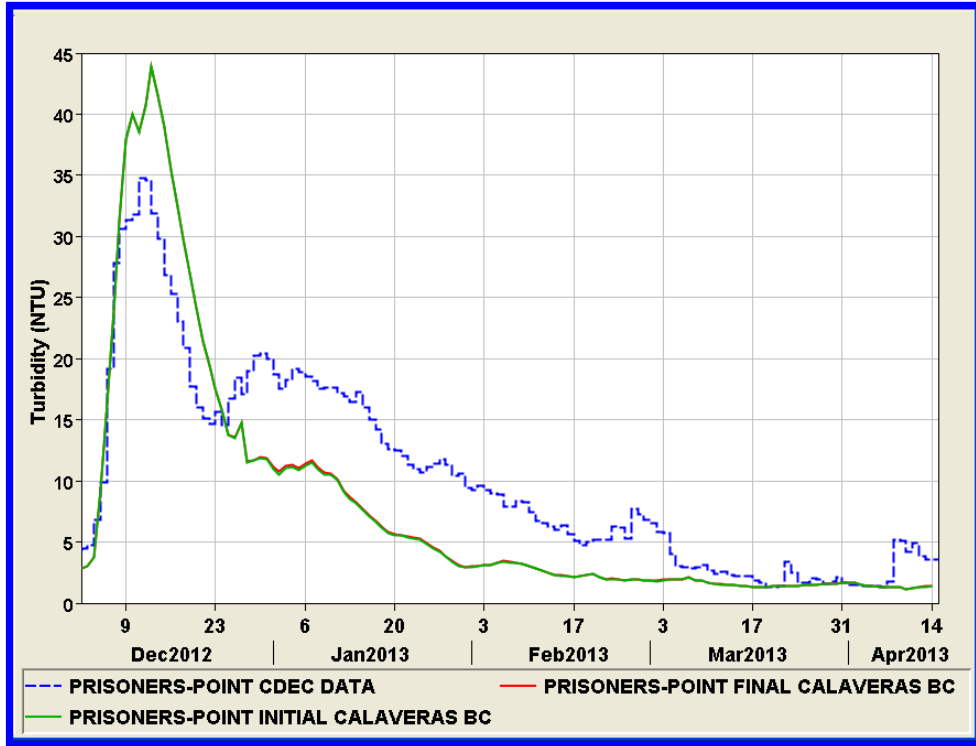


Figure 6-3 WY2013 turbidity data and book-end model output along with volumetric plots at Prisoner's Point.

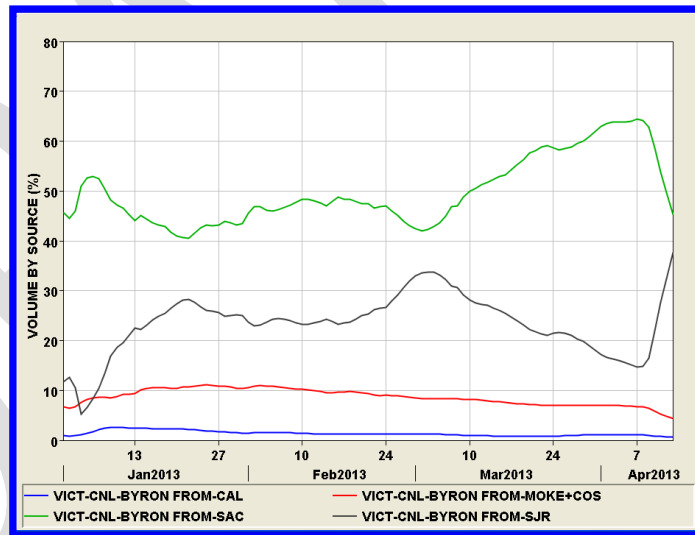


Figure 6-4 WY2013 turbidity data and book-end model output along with volumetric plots at Victoria-Canal-at-Byron.

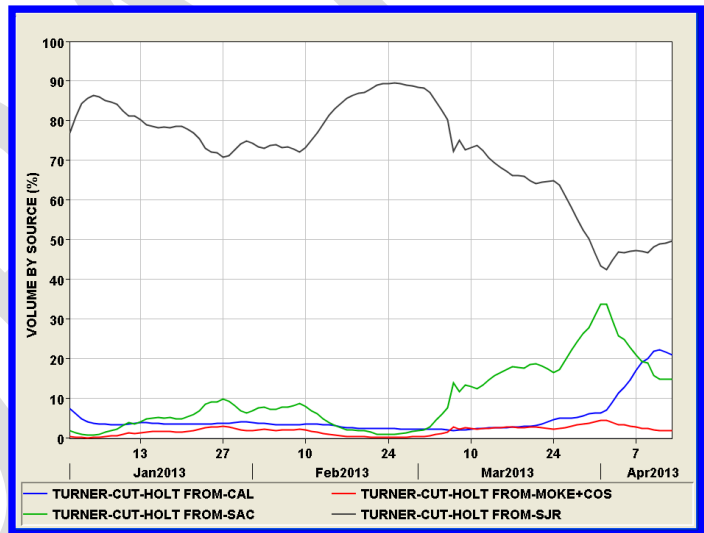
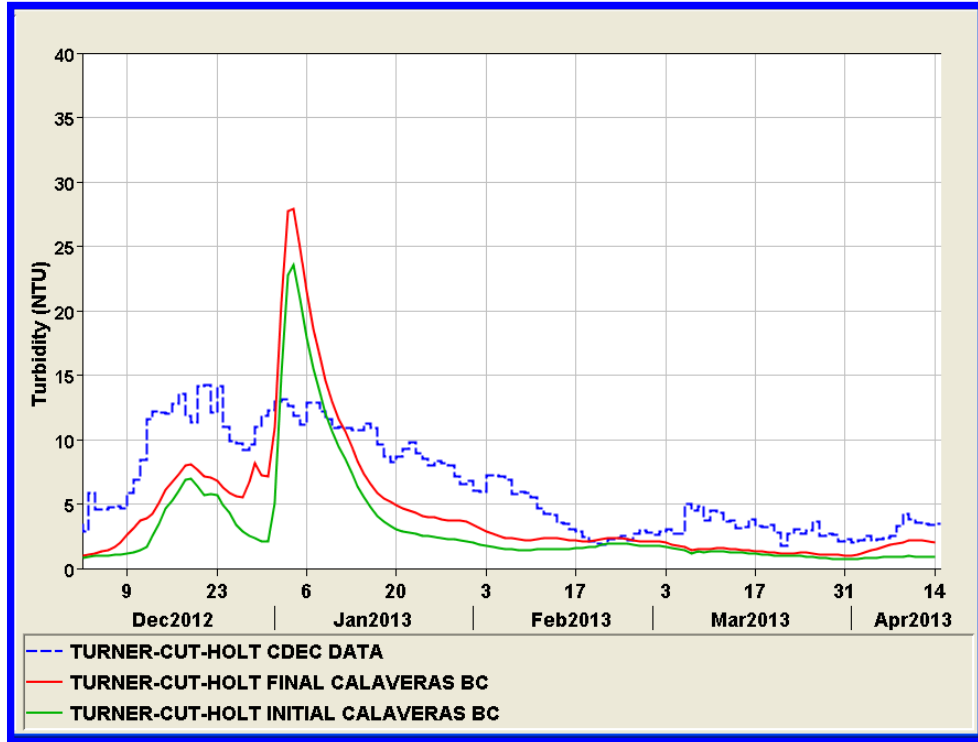


Figure 6-5 WY2013 turbidity data and book-end model output along with volumetric plots at Turner-Cut-Holt.

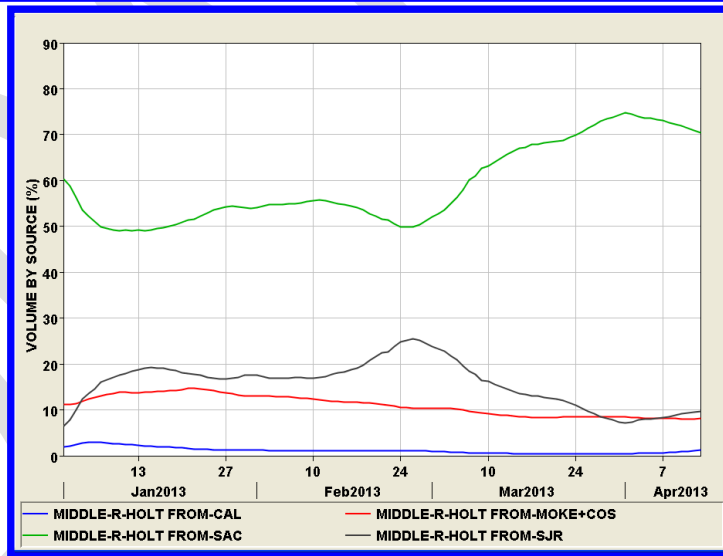
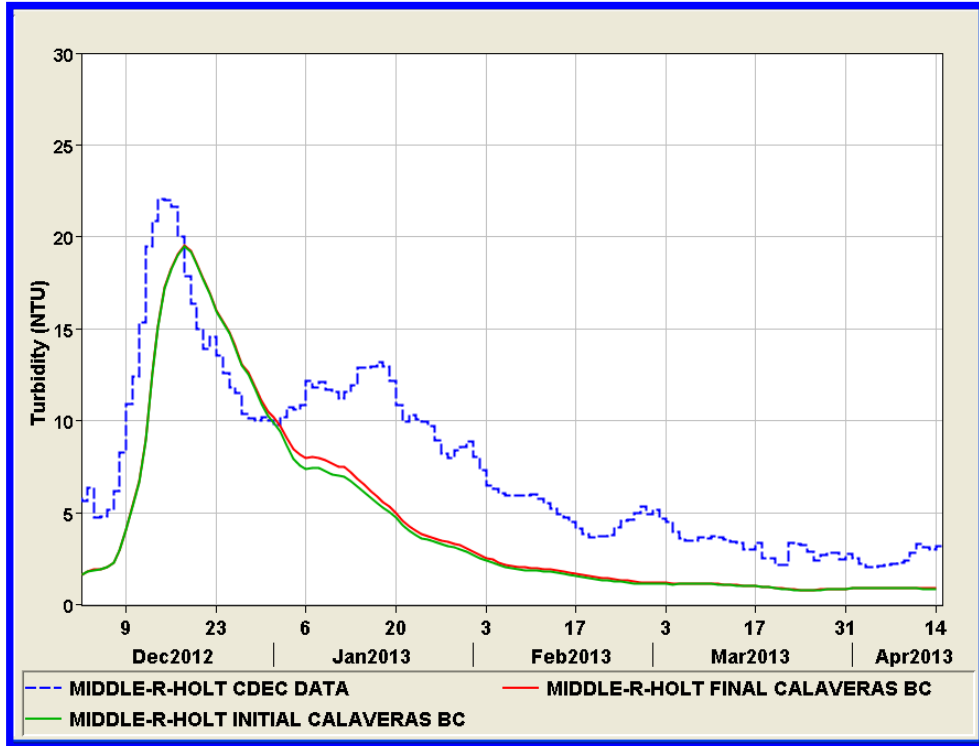


Figure 6-6 WY2013 turbidity data and book-end model output along with volumetric plots at Middle-R-Holt.

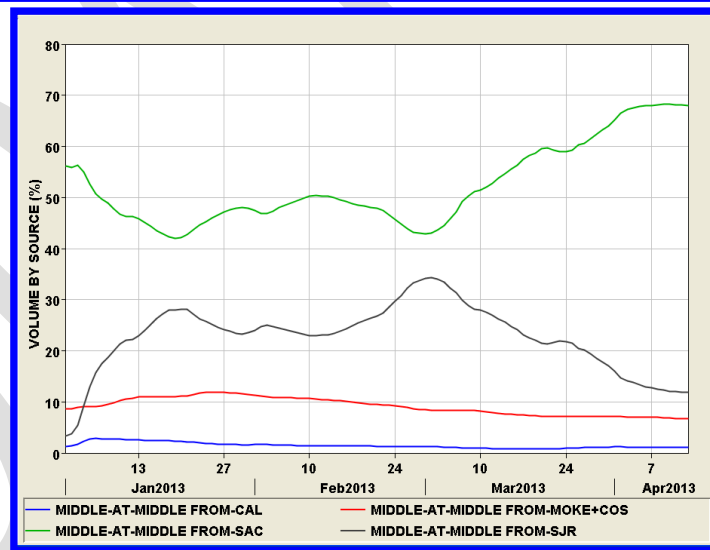
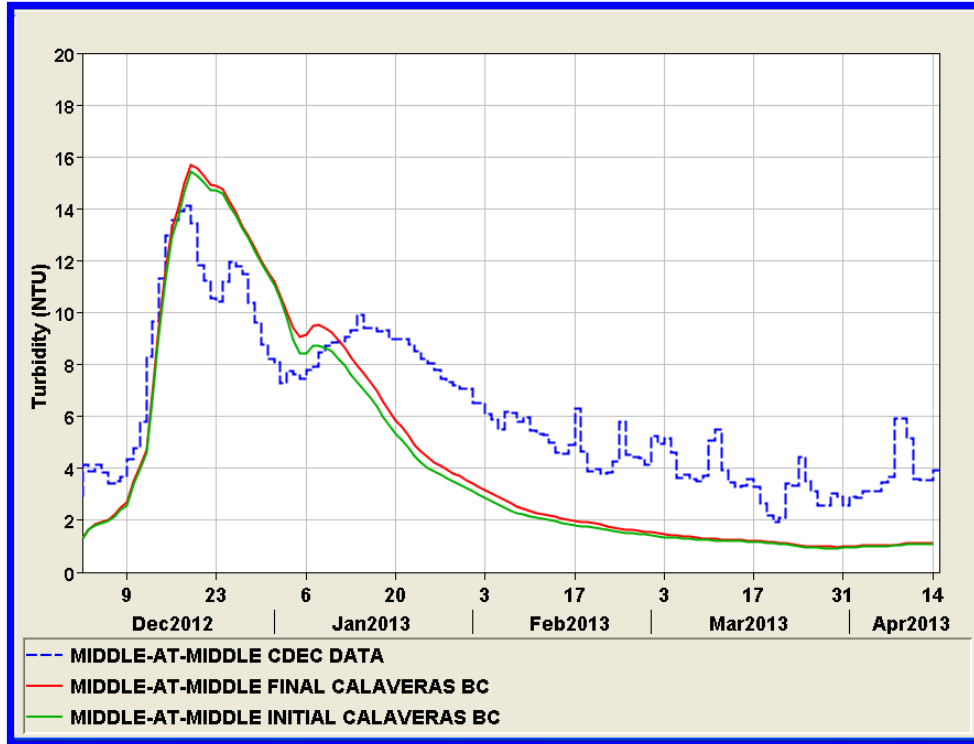


Figure 6-7 WY2013 turbidity data and book-end model output along with volumetric plots at Middle-at-Middle.

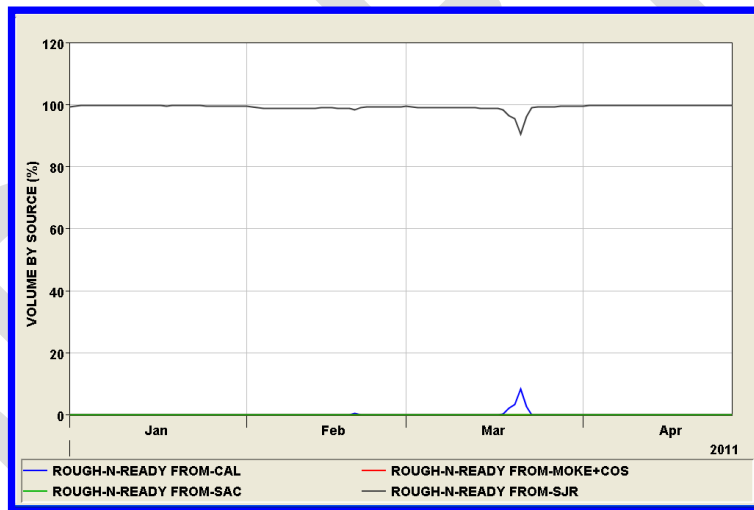


Figure 6-8 WY2011 turbidity data and book-end model output along with volumetric plots at Rough-N-Ready.

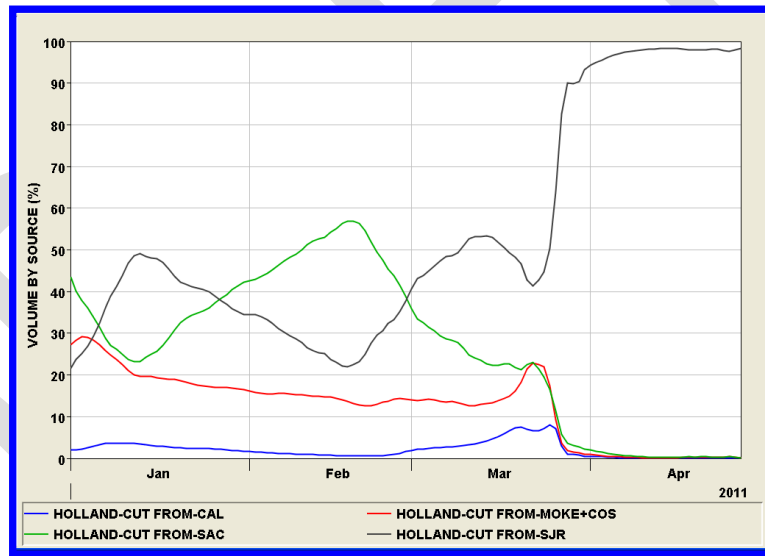
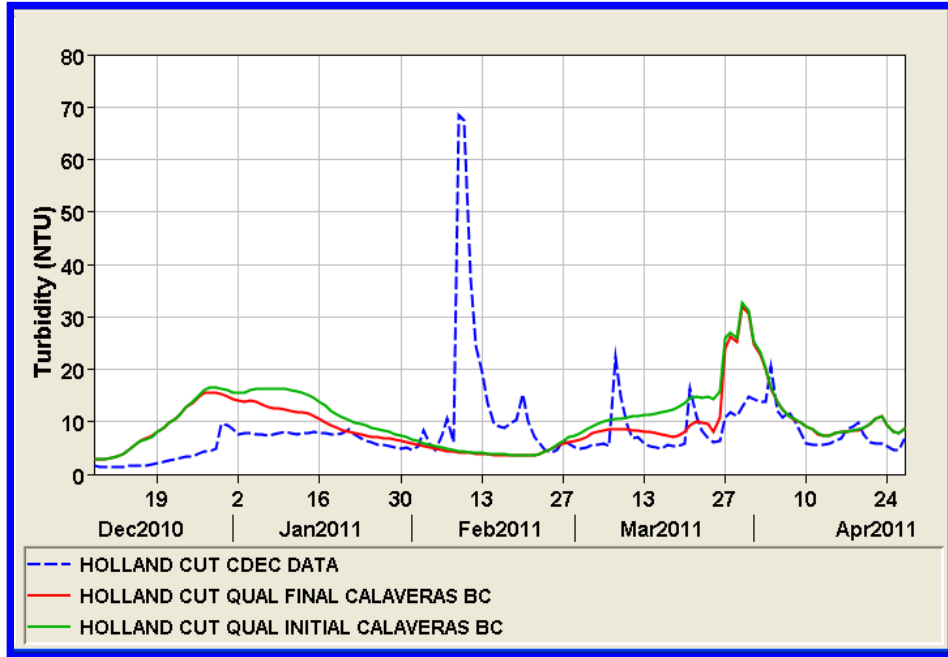


Figure 6-9 WY2011 turbidity data and book-end model output along with volumetric plots at Holland-Cut.

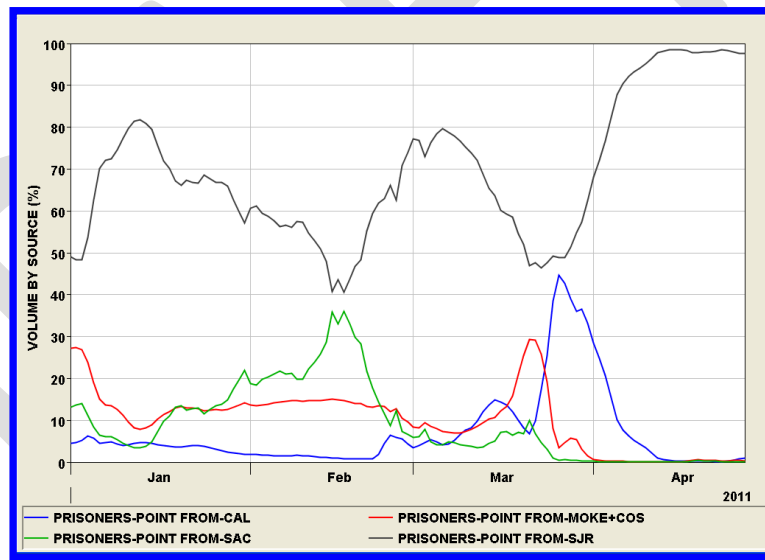
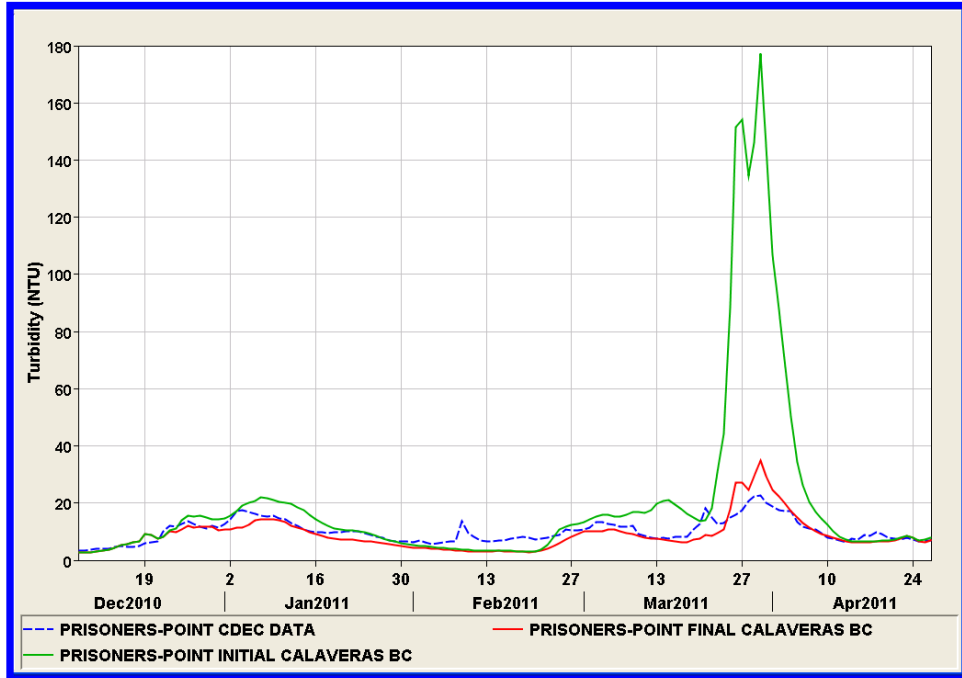


Figure 6-10 WY2011 turbidity data and book-end model output along with volumetric plots at Prisoner's Point.

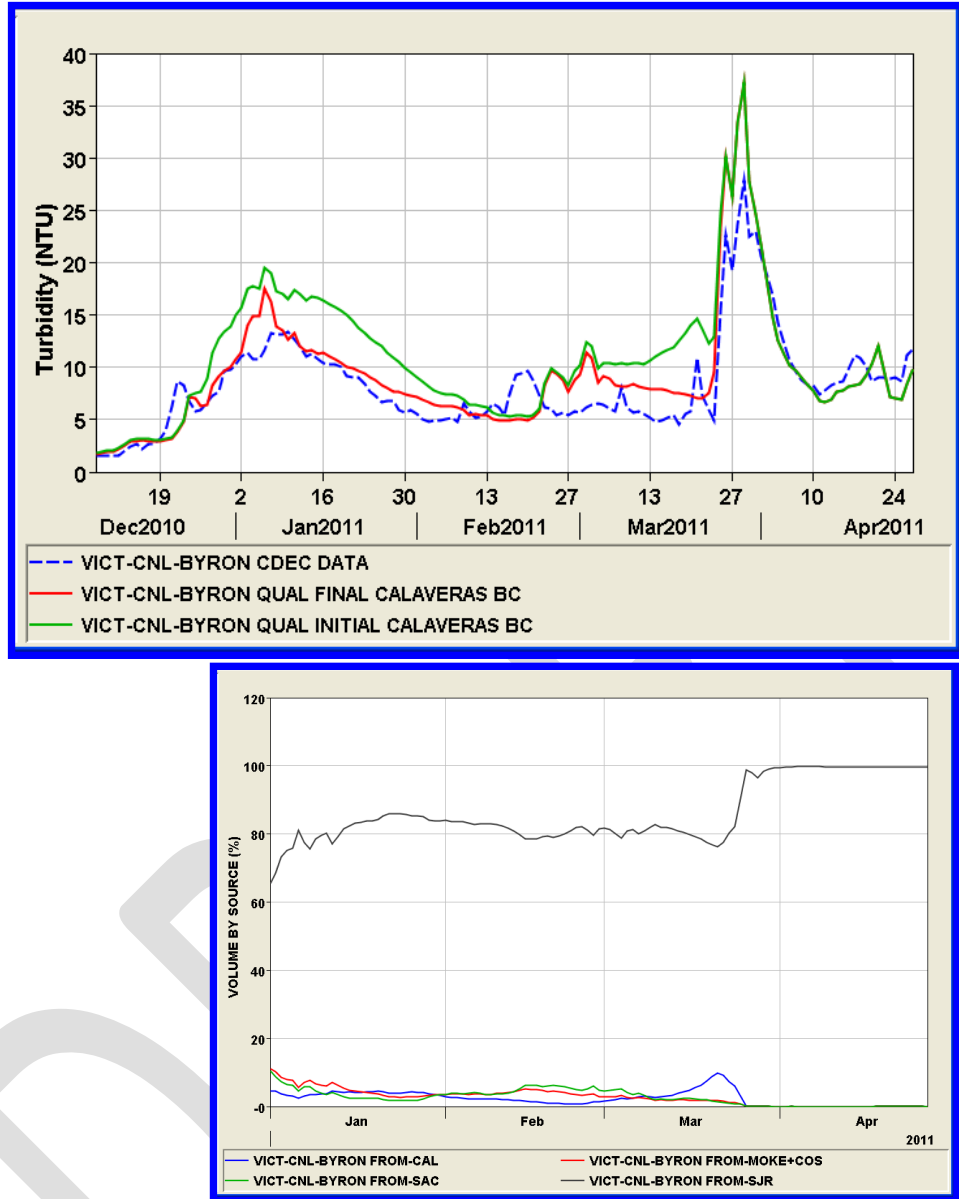


Figure 6-11 WY2011 turbidity data and book-end model output along with volumetric plots at Victoria-Canal-Byron.

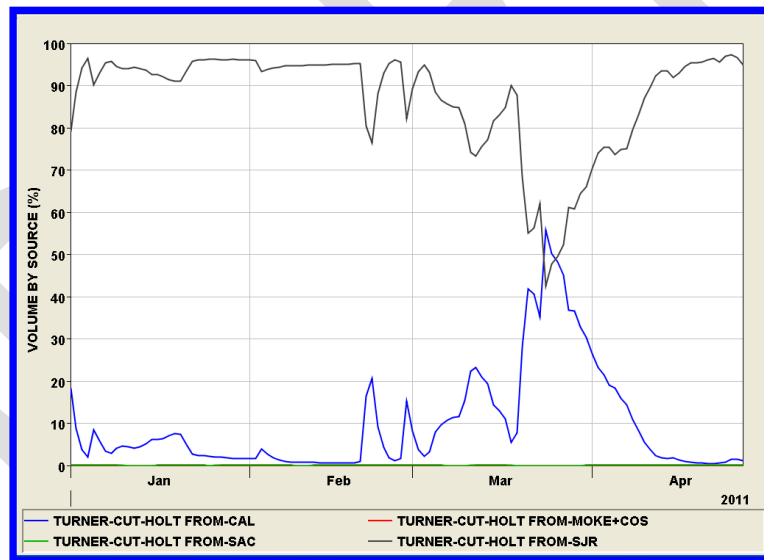
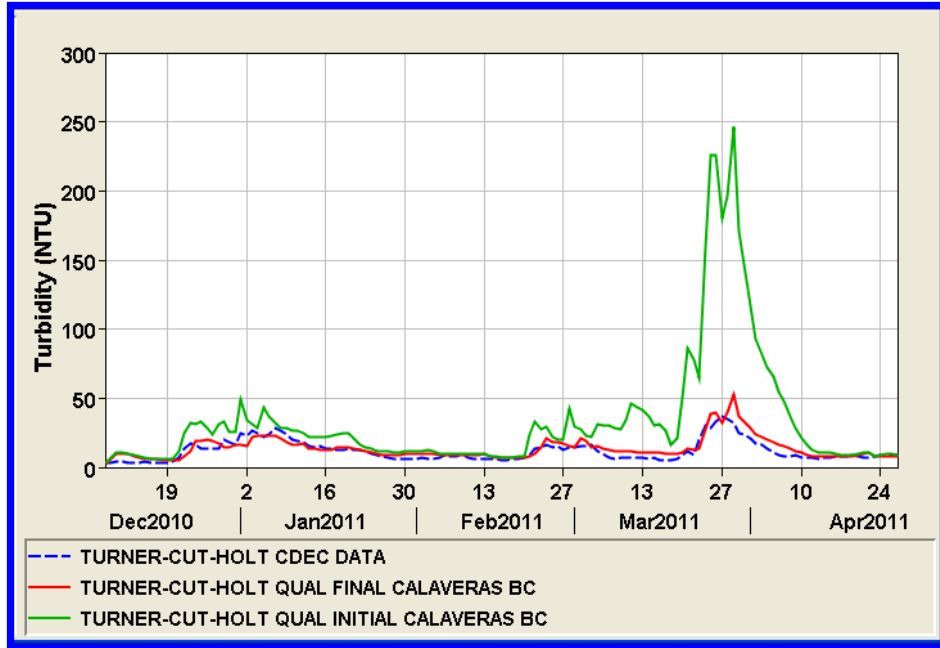


Figure 6-12 WY2011 turbidity data and book-end model output along with volumetric plots at Turner-Cut-Holt.

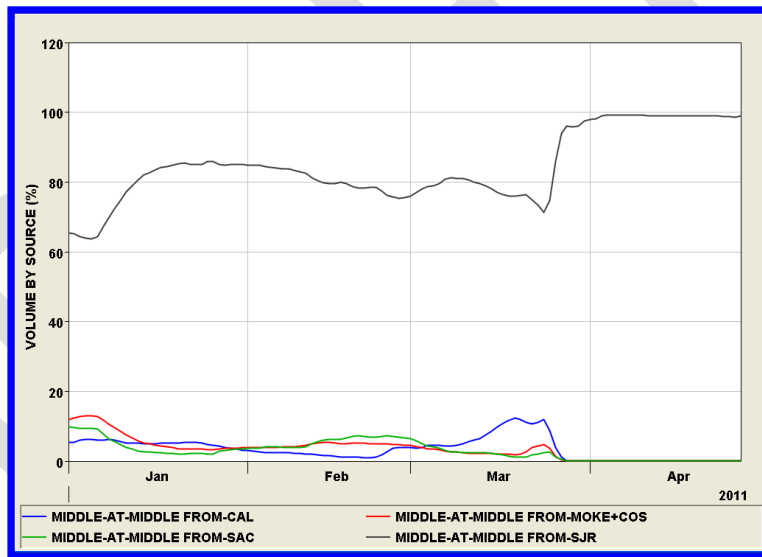
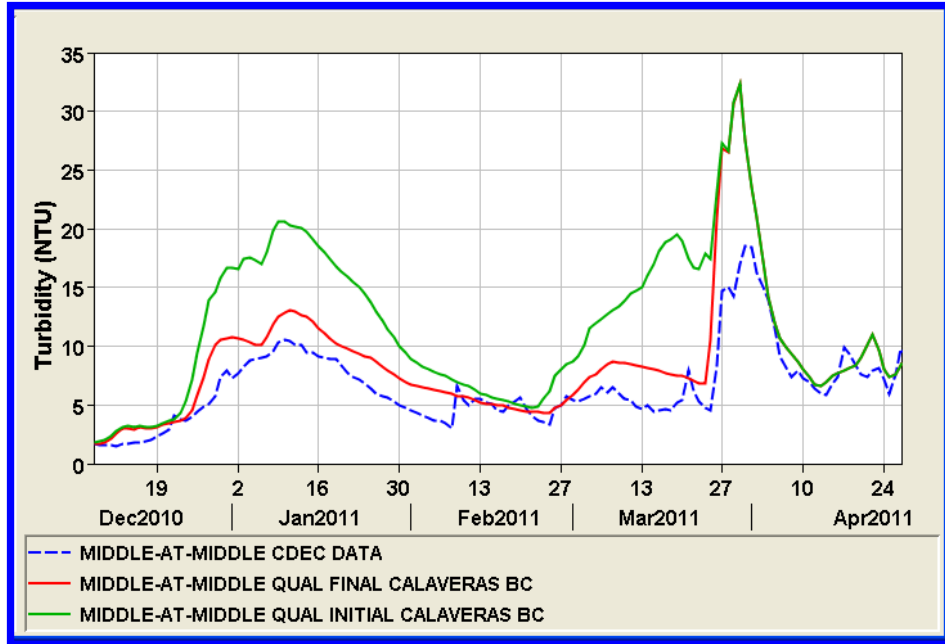


Figure 6-13 WY2011 turbidity data and book-end model output along with volumetric plots at Middle-at-Middle.

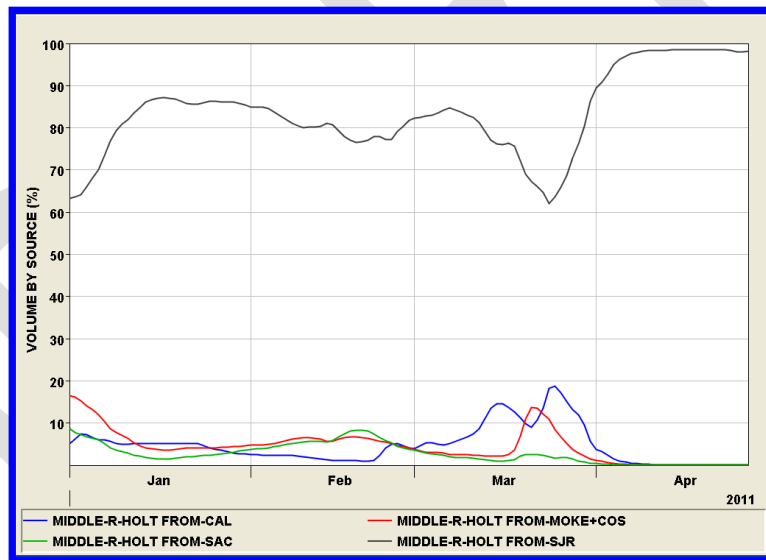


Figure 6-14 WY2011 turbidity data and book-end model output along with volumetric plots at Middle-R-Holt.

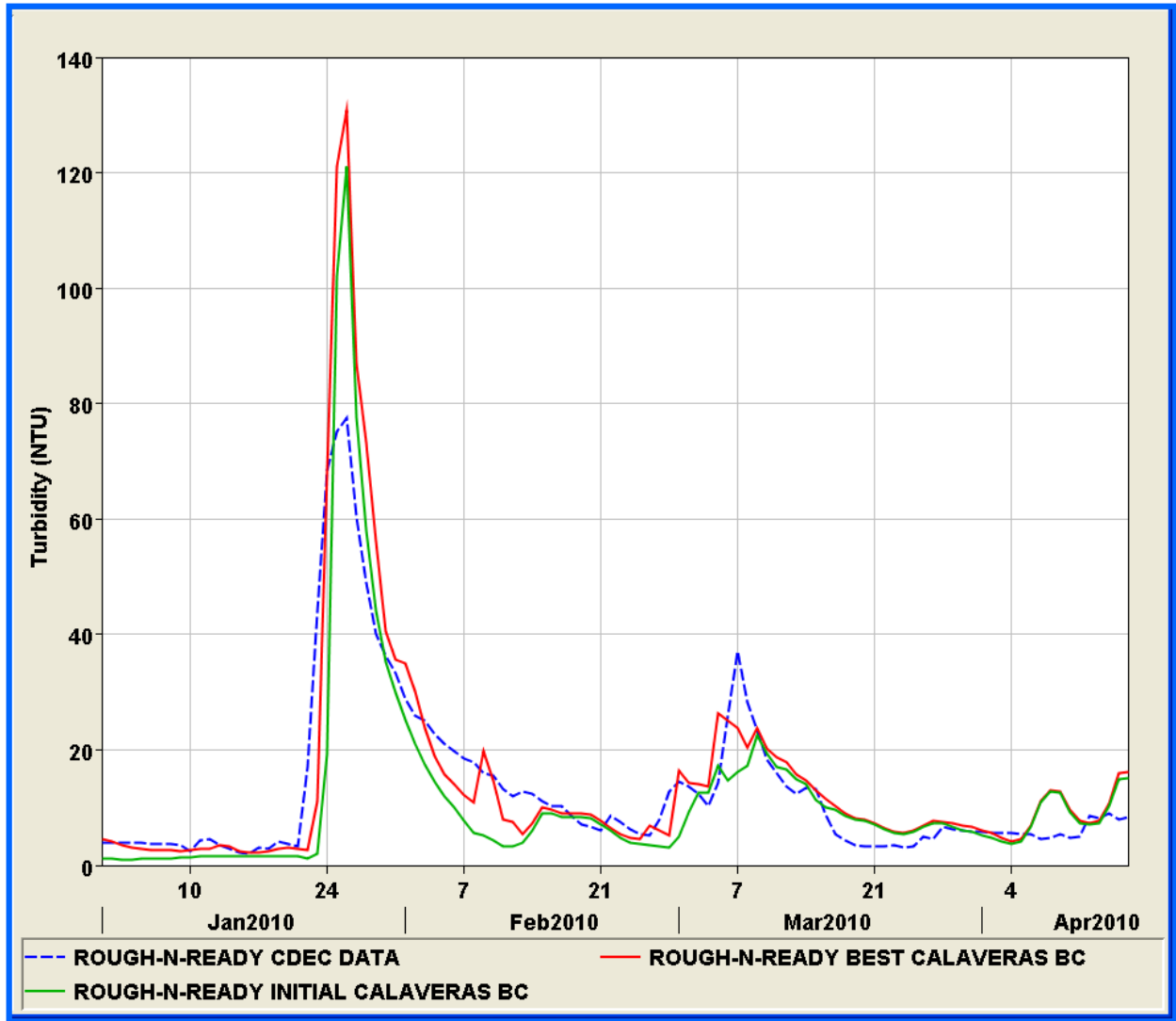


Figure 6-15 WY2010 turbidity data and book-end model output at Rough-N-Ready.

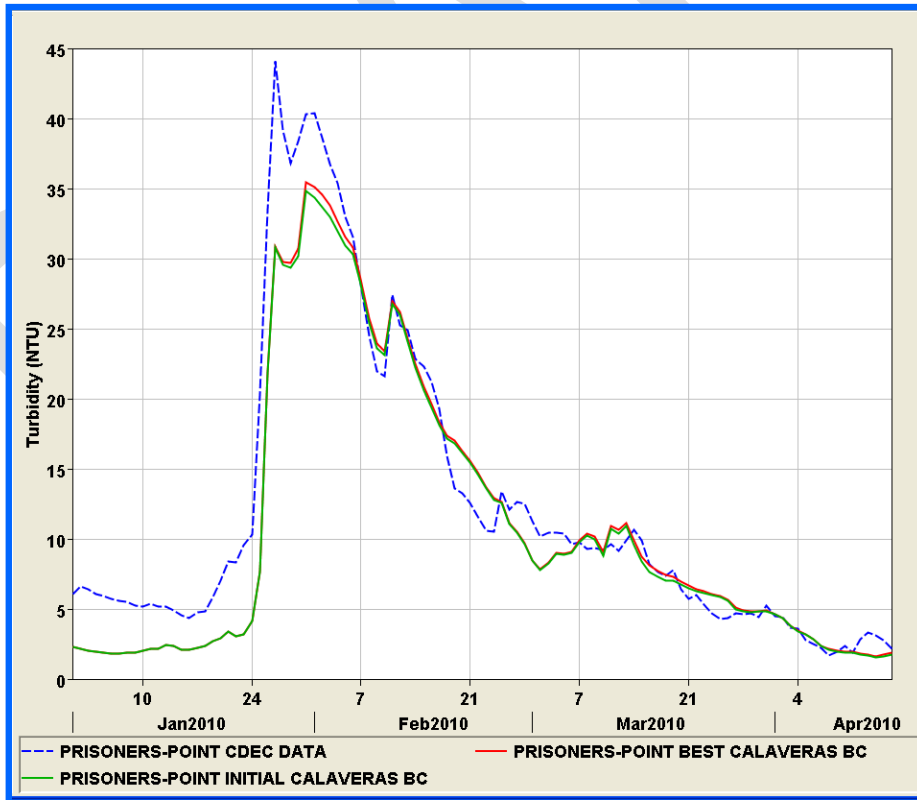
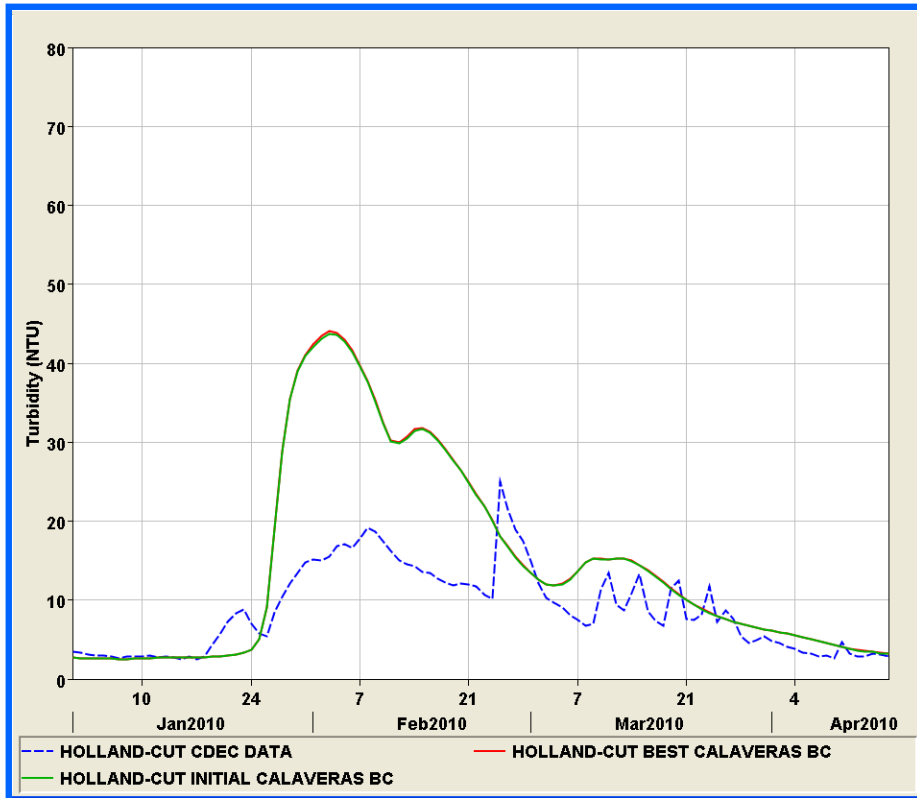


Figure 6-16 WY2010 turbidity data and book-end model output at Holland-Cut (upper) and Prisoner's Point (lower).

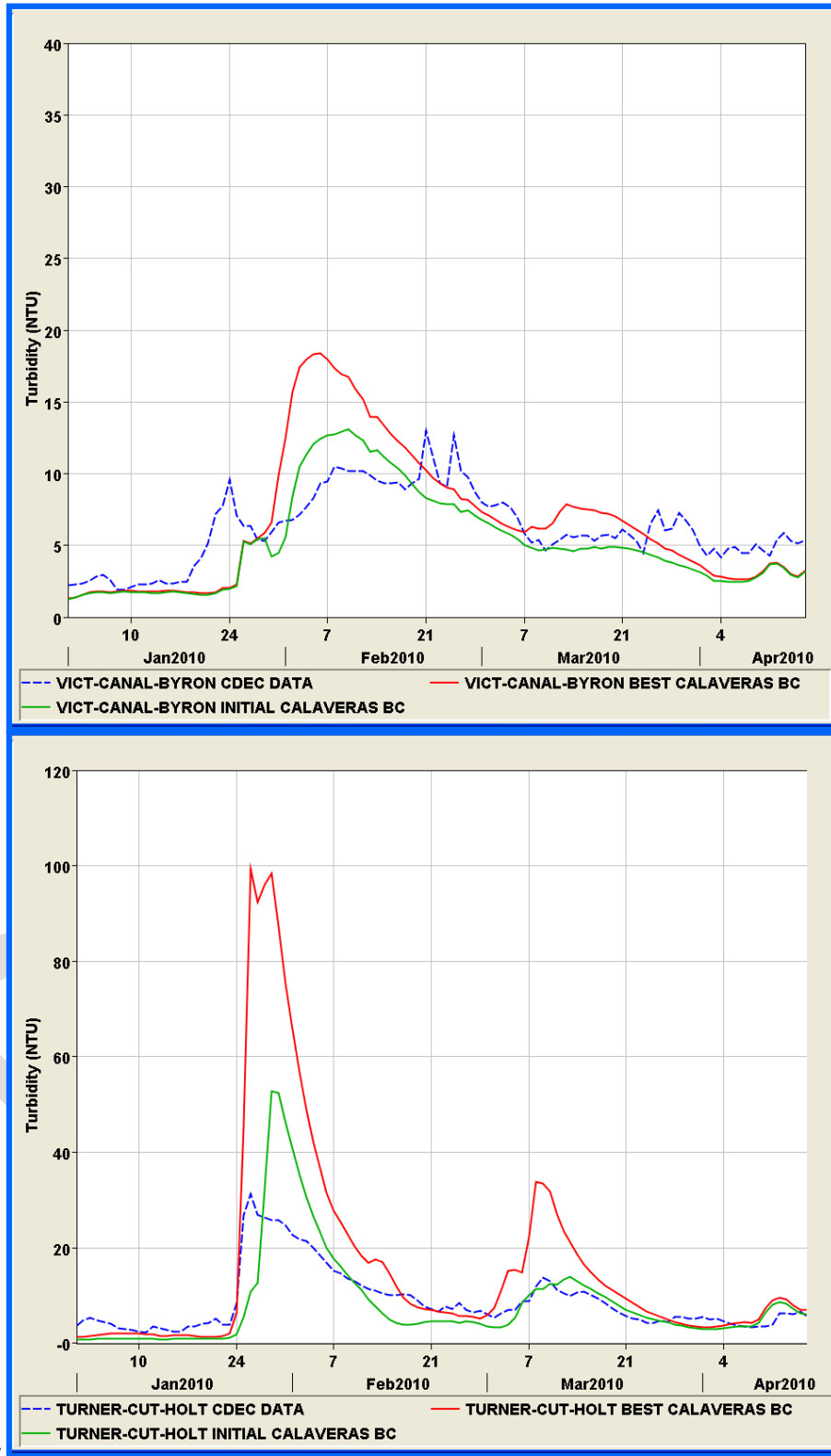


Figure 6-17 WY2010 turbidity data and book-end model output at Victoria-Canal-Byron (upper) and Turner-Cut-Holt (lower).

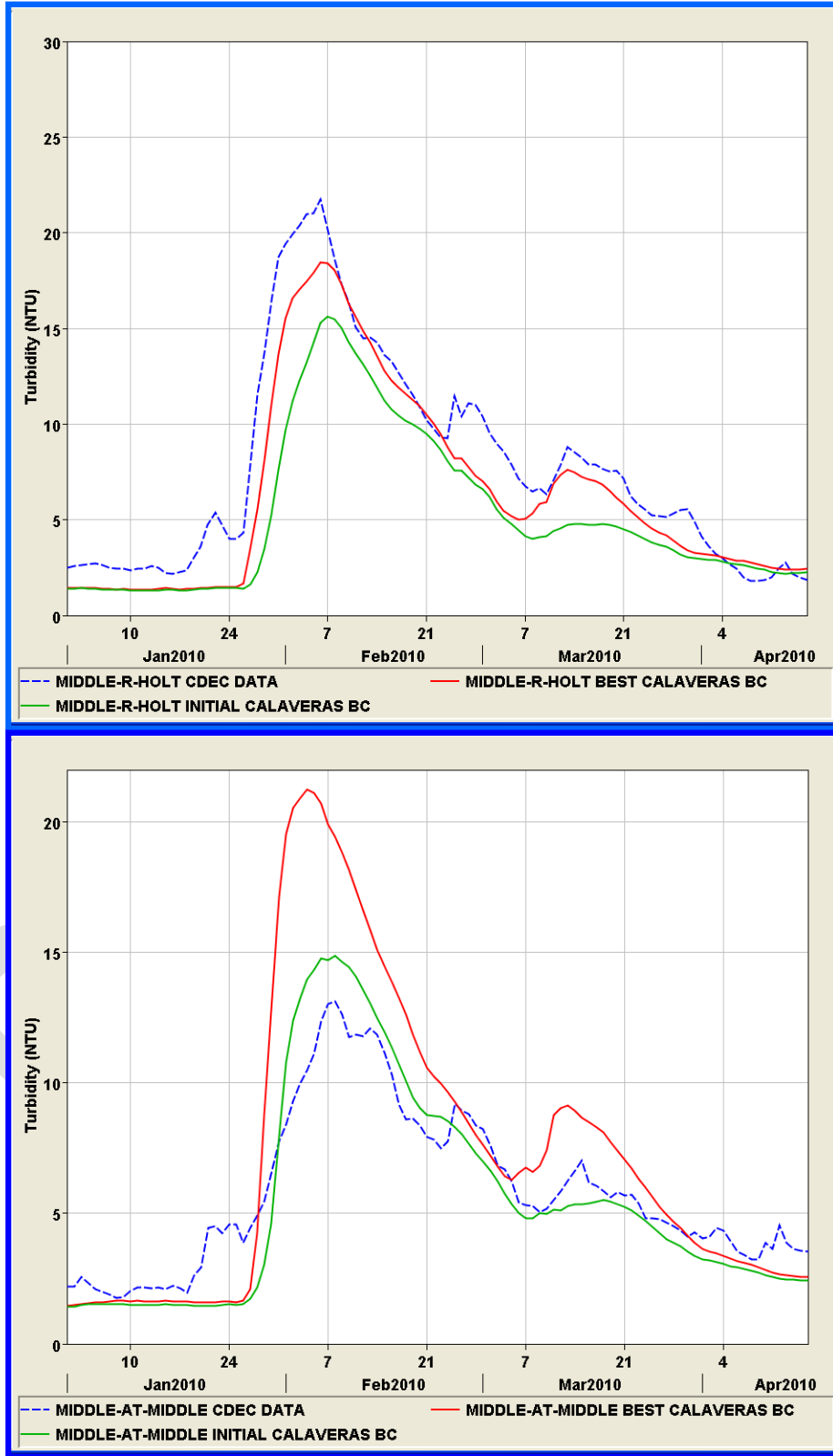


Figure 6-18 WY2010 turbidity data and book-end model output at Middle-R-Holt (upper) and Middle-at-Middle (lower).

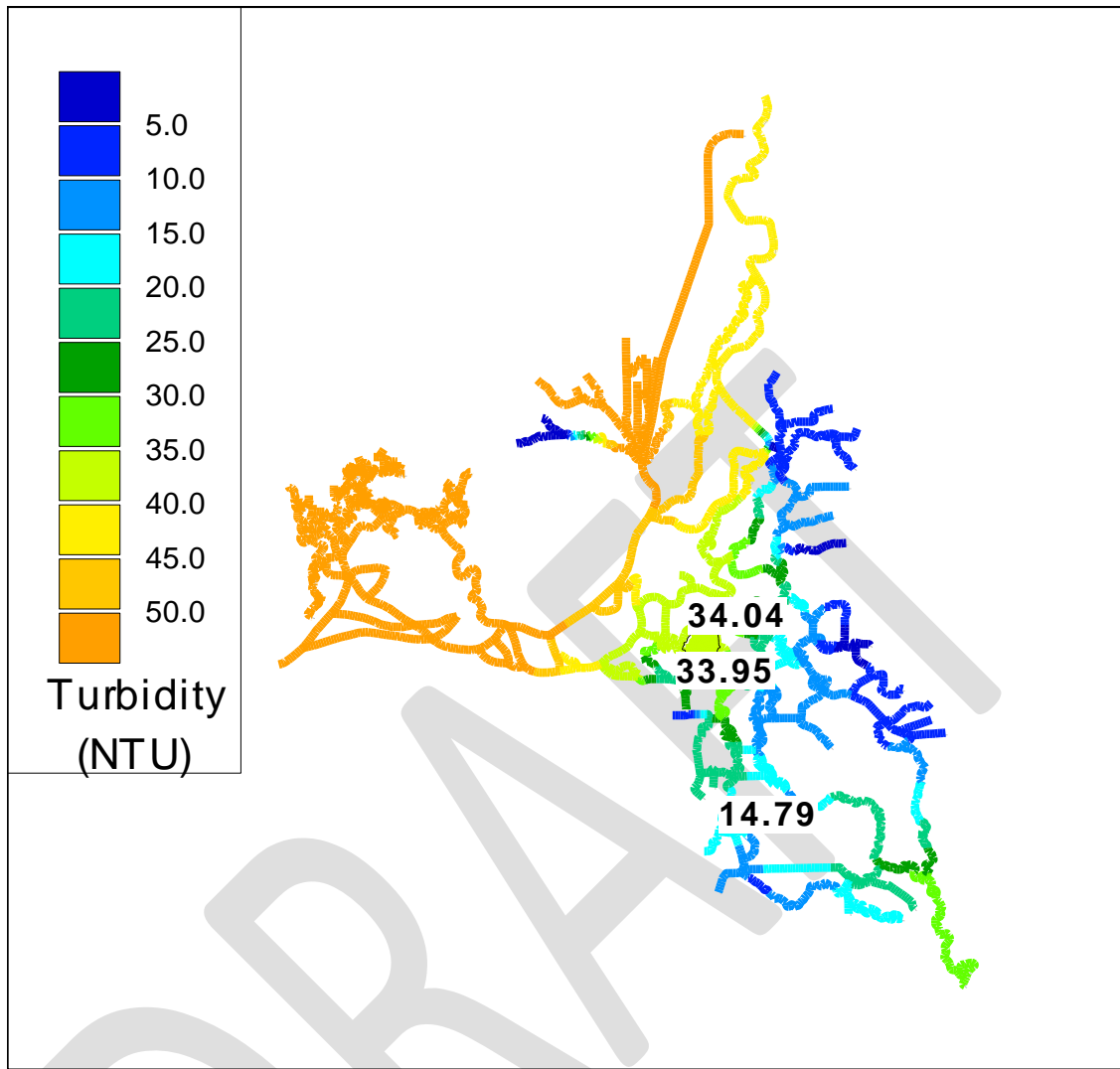


Figure 6-19 WY2010 contour plot showing the modeled distribution of turbidity in February 14, 2010. Values shown are near the compliance locations.

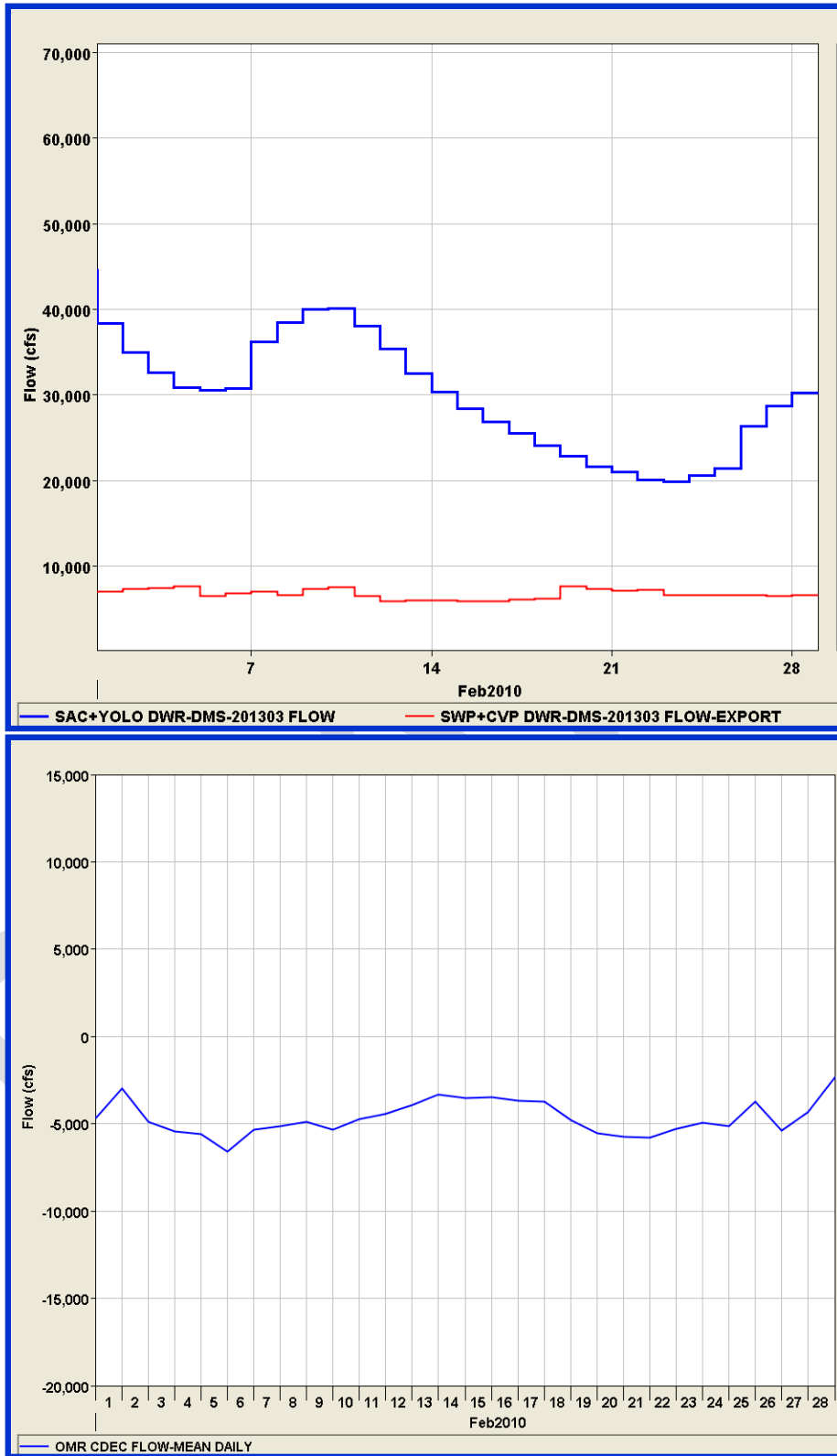


Figure 6-20 Combined flows – inflow from the northern Delta and export flows from the south Delta (upper plot) and OMR flow (lower lot) during February, WY2010.

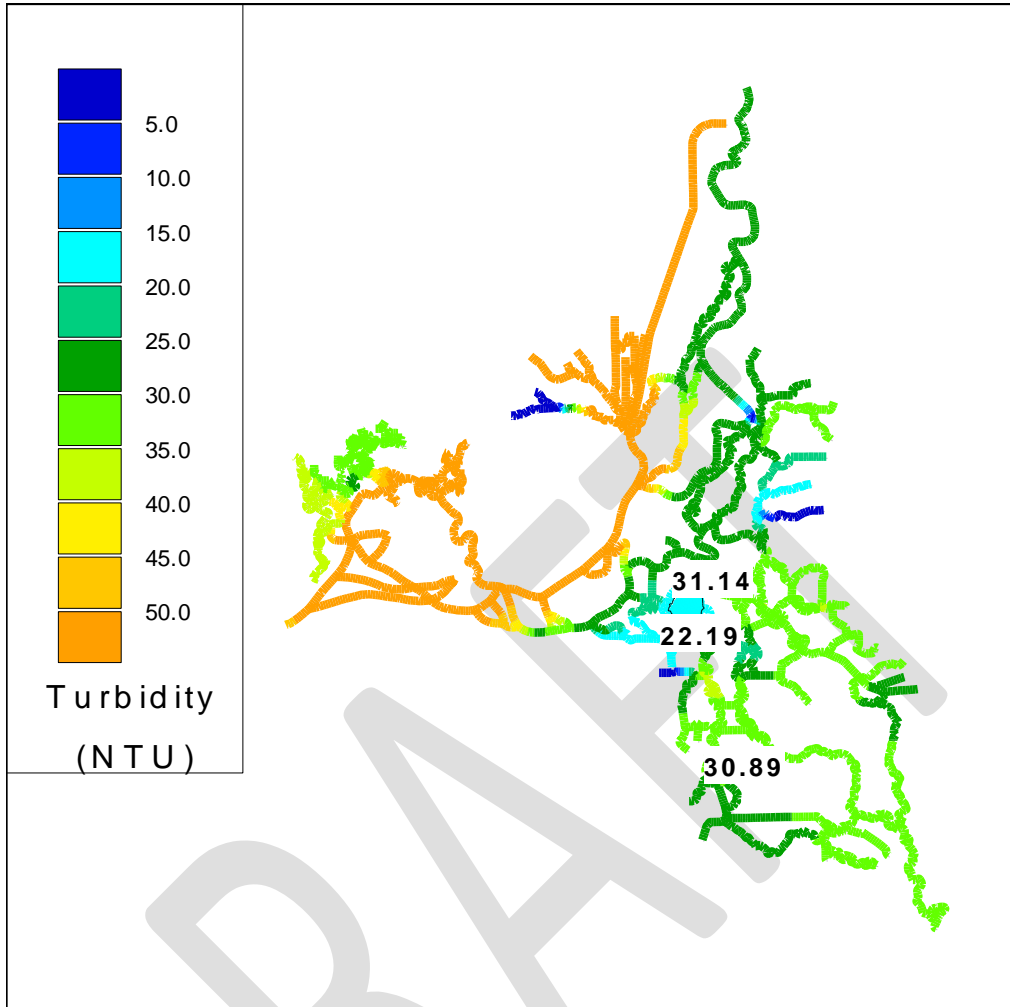


Figure 6-21 WY2011 contour plot showing the modeled distribution of turbidity on March 29, 2011. Values shown are near the compliance locations.

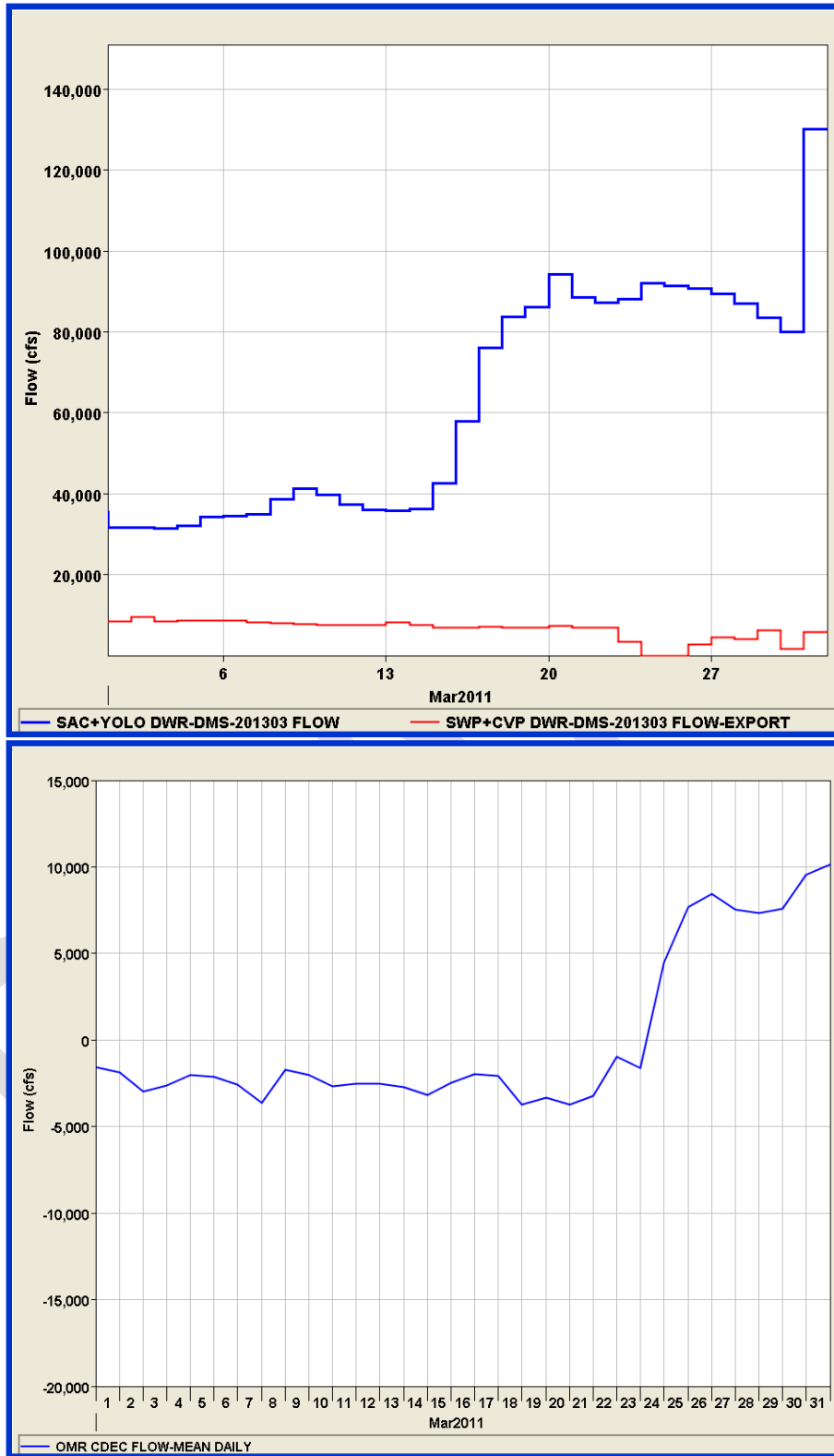


Figure 6-22 Combined flows – inflow from the northern Delta and export flows from the south Delta (upper plot) and OMR flow (lower lot) during March, WY2011.

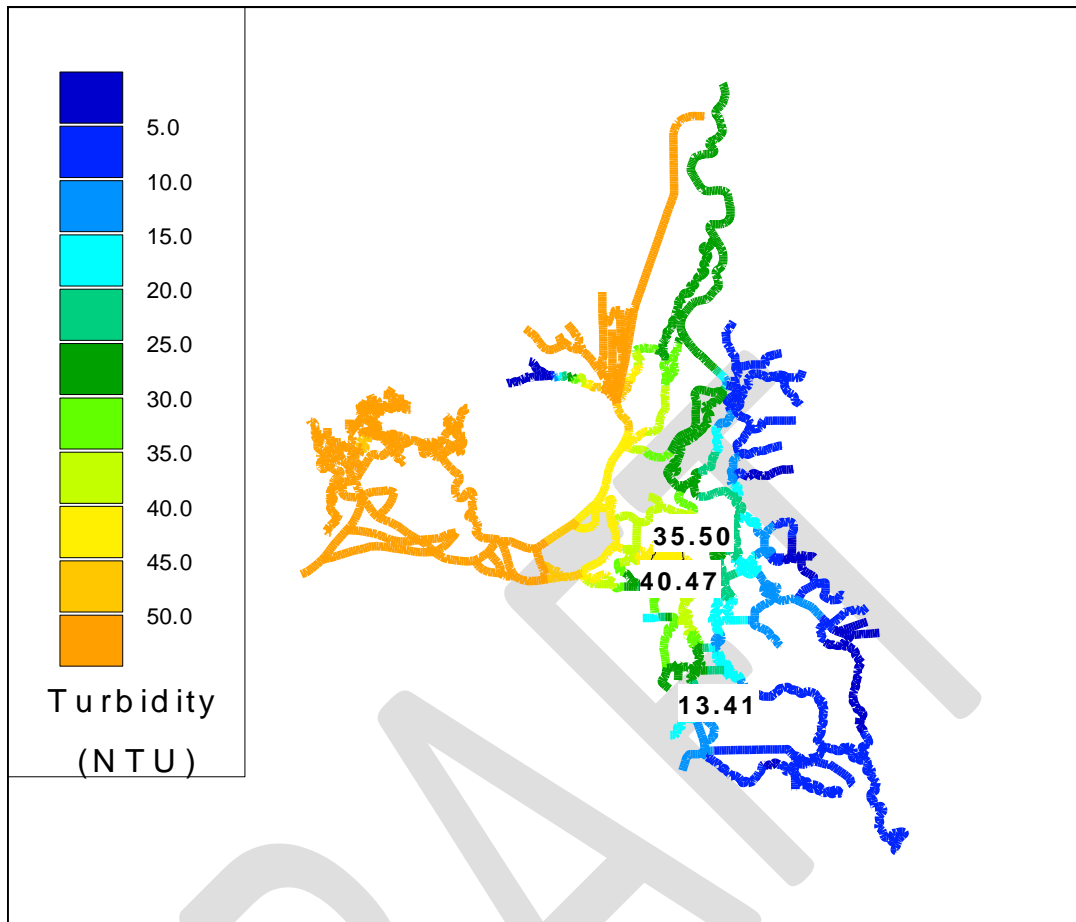


Figure 6-23 WY2013 contour plot showing the modeled distribution of turbidity on Dec. 16, 2012. Values shown are near the compliance locations.

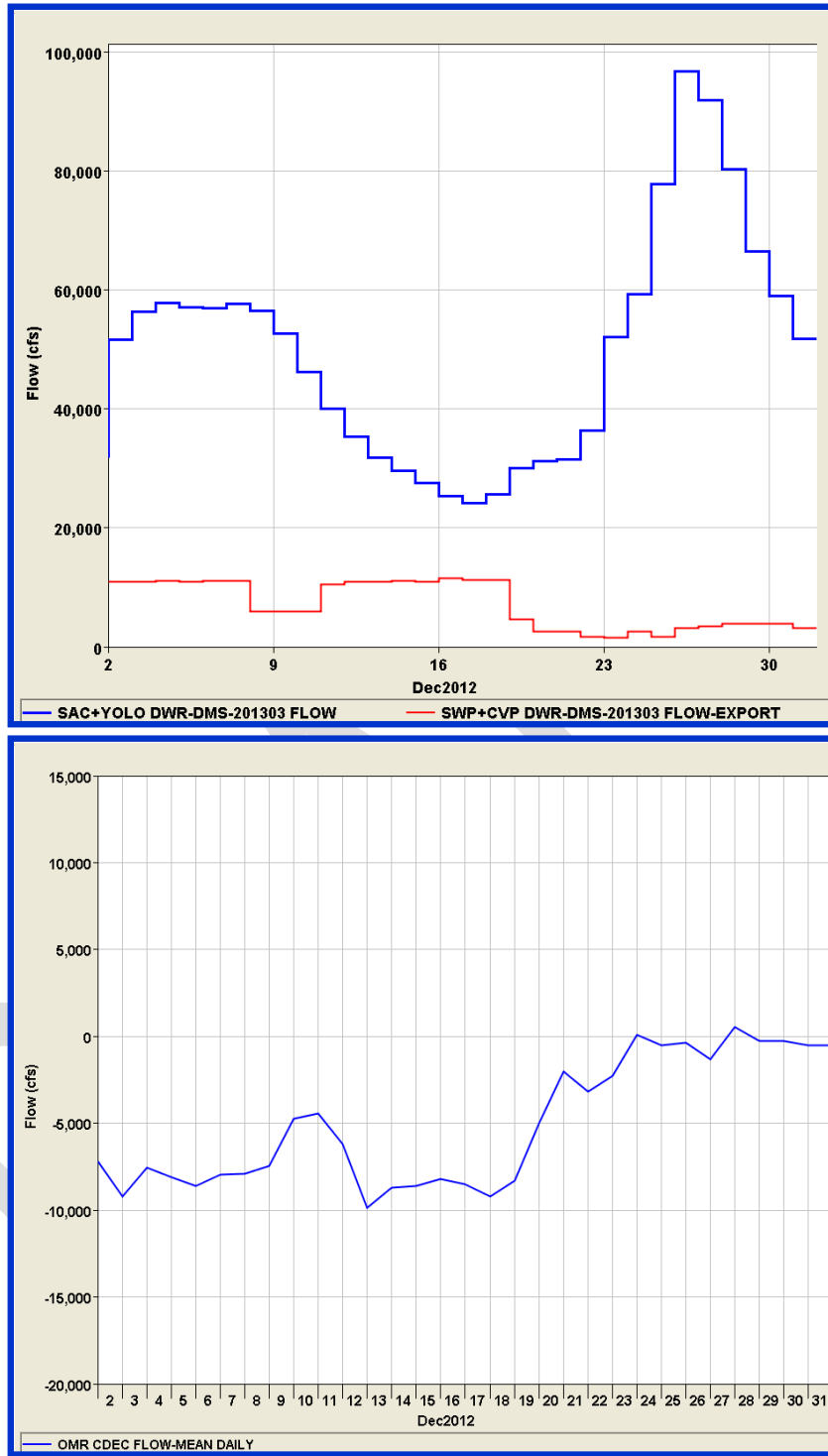


Figure 6-24 Combined flows – inflow from the northern Delta and export flows from the south Delta (upper plot) and OMR flow (lower lot) during December, WY2013.

## 7 Results of the Long Term QUAL Historical Turbidity Simulation – Water Years 1975 - 2011

In the first few subsections of this section, the focus is on satisfying Objective Two of the project - supporting the development of a Turbidity ANN interfacing with the DSM2 QUAL turbidity model output from the recalibrated model. The final section discusses conditions leading to turbidity bridge formation.

The boundary conditions nomenclature for these Historical set-ups was coined in (RMA 2013) as “Mixed-SSC-WARMF”, and that nomenclature is also used in this document. Two simulations were developed, the “early years”, 1975 – 1990, and the “recent years”, 1991 – 2011, model set-ups with the Mixed-SSC-WARMF boundary conditions. Model residual statistics during the high flow periods were calculated using Environmental Monitoring Program (EMP) grab sample data restricted to the period December to March in each Water Year.

The objective of this portion of the work was to further assess the boundary conditions and compute a revised set of statistics. Statistics were computed at each available data location in each time frame (recent years and early years) by comparing EMP with daily averaged model results – note that EMP data did not include the three compliance locations. In these statistics, only the high flow portion of the Water Years from December to March was used.

### 7.1 EMP data

EMP measurements occur approximately monthly at numerous locations in the Delta. The locations for these measurements within the DSM2 model domain have changed over the years, with some locations being phased out and some locations being phased in. Samples are collected from shore-based collection locations and by boat (*i.e.*, from DWR or USBR research vessels). Details on sample collection and field methods are available at the following website:

<http://www.water.ca.gov/bdma/meta/discrete.cfm>

For comparison with EMP data, QUAL long-term turbidity model results were daily averaged. Although the EMP measurements are essentially instantaneous, the collection time was not included in the metadata, only the collection date.

### 7.2 Changes to the Mixed-WARMF-SSC Boundary Conditions

The early and recent versions of the Historical model were rerun with the newly calibrated parameter set and calibration statistics were calculated December to March (each Water Year) using EMP data separately for the early and recent simulation periods. The results along the upper San Joaquin River required no adjustment, so the Vernalis boundary condition was not altered. Along the Sacramento River and locations heavily influenced by Sacramento turbidity, the model results were high so the Freeport boundary condition was adjusted. The process involved increasing and decreasing the scale factor applied to the USGS SSC data for the early years and the recent years separately to improve the statistical results.

As mentioned in Section 7, the IEP grab-sample data is very low in comparison with the range of CDEC 15-minute turbidity data at Hood (~50 – 350 NTU, or higher) so it appears that along the Sacramento River, the IEP data is unreasonable low, possibly indicating that samples were not taken during times when river flows and the associated turbidity were high. Thus, statistical results for the new calibration during these long Historical model periods will be biased to overestimating the IEP data (i.e., negative PBIAS statistic) as the magnitude of the IEP data appears suspect, at least in some locations.

### **7.3 Simulation results – Model residuals and regressions comparing long-term simulations with EMP data**

QUAL model output was specified at all EMP data locations, and the 15-minute model output was daily averaged. The residual (data – model) and regression calculations used the EMP data and daily-averaged model output on the same date, but restricted in each Water Year to the period from December to March. Plots comparing model output and EMP data along with regression plots and residual histograms with detailed statistics were created for each available EMP location. Figure 7-1 and Figure 7-2 illustrate these plots for the EMP location D26, which is also known as SJR at Potato Point, for the Mixed-SSC-WARMF simulation in the recent years and early years time frames, respectively.

Residual statistics, regressions and the associated statistics were calculated using the reduced set of QUAL turbidity output (*i.e.*, only at EMP data dates from December to March). Plots for each EMP location and each time frame are found in Appendix IV Section 13 for each of the simulations.

The statistical results are collated in Table 7-1 and Table 7-2. The final column in each table lists the sign (+ or -) of the PBIAS statistic to allow easy reference as to whether the simulation tends to overestimate the data (negative bias) or underestimate the data (positive bias). Table 7-1 documents the statistical results for the early years (1975 – 1990) simulations and Table 7-2 documents the results for the recent years (1991 – 2011). The final row of each table lists the sum of the statistics in each column – each sum gives an indication of the full-period, Delta-wide skill of the simulation for comparisons. The R<sup>2</sup> statistics is maximized at 1.0, so a higher sum indicates a superior result in the comparison tables. The PBIAS statistic is maximized at zero, so a smaller value indicates a superior result. The absolute value of the PBIAS statistic was summed.

Clearly, both tables show that the model generally overestimates the EMP data. Given the observation that EMP data along the Sacramento seems unreasonably low, this is a reasonable calibration result.

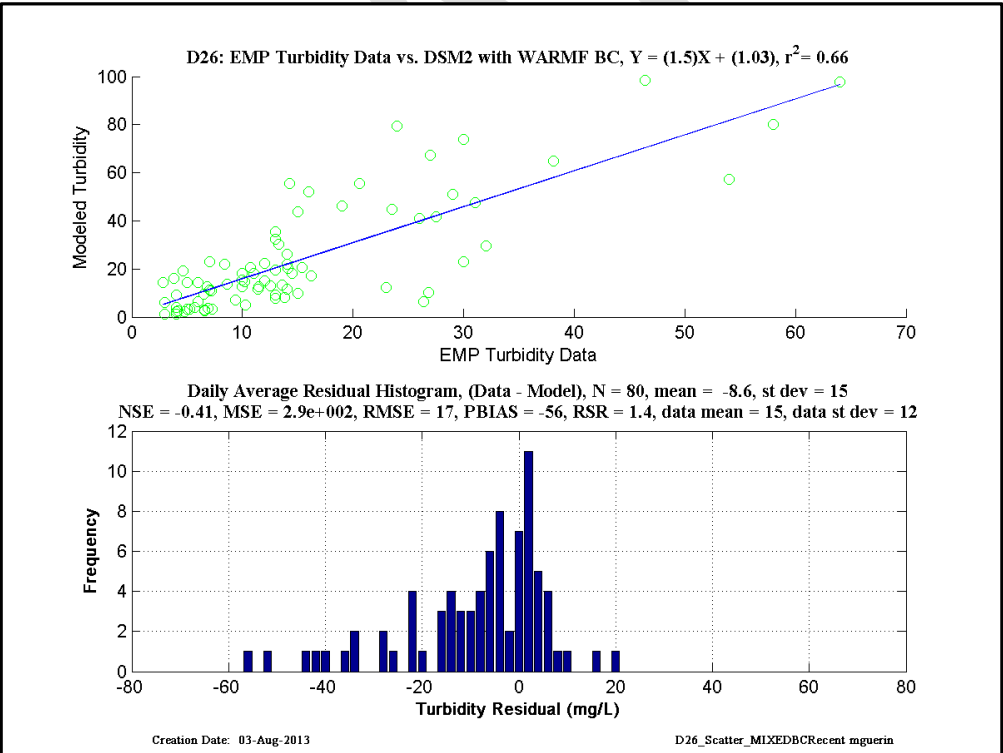
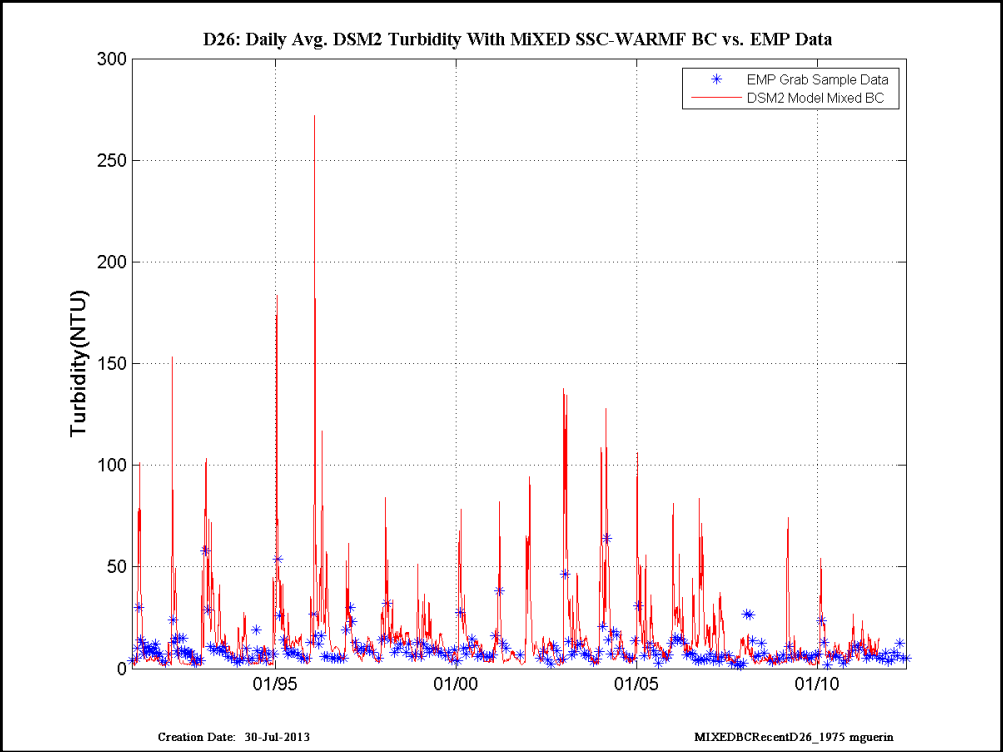


Figure 7-1 Mixed-SSC-WARMF results at D26 in the recent years time frame.

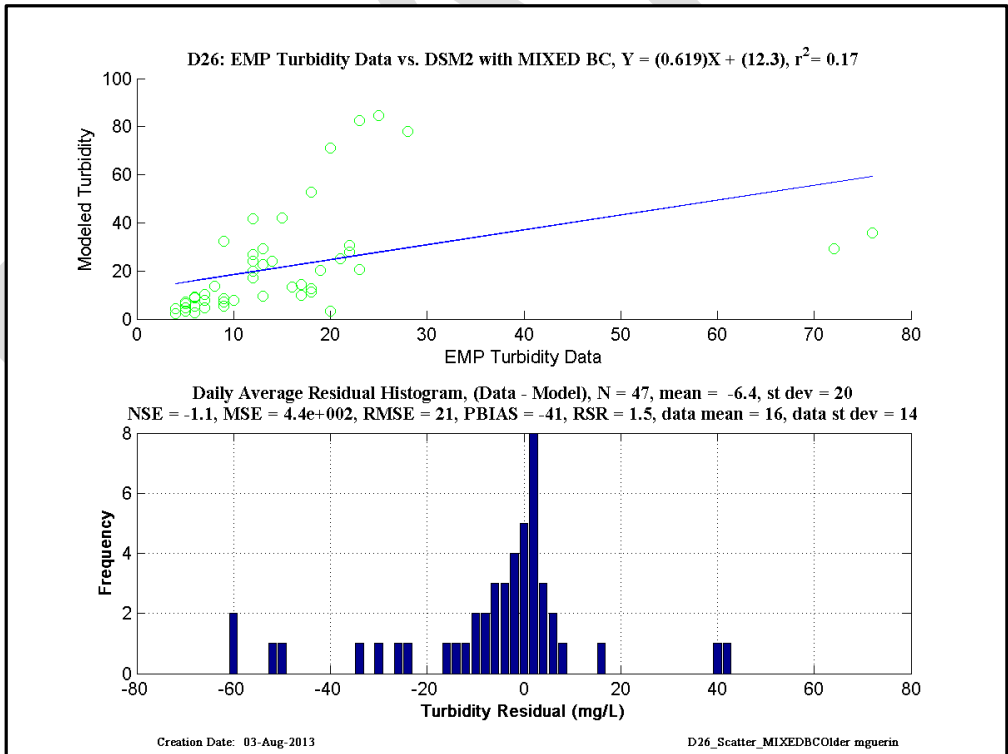
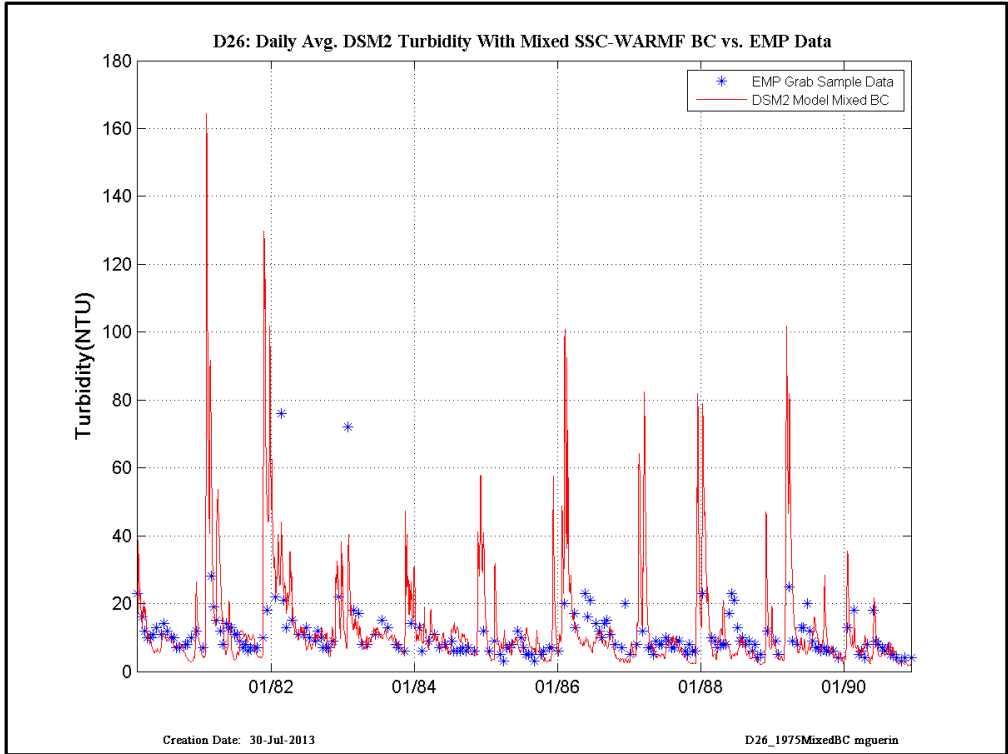


Figure 7-2 Mixed-SSC-WARMF results at D26 in the early years time frame.

Table 7-1 Statistics for the simulation in early years (1975 – 1990) for the Mixed-SSC-WARME simulation.

Common Name Location	EMP Location	R <sup>2</sup>	PBIAS	Sign Bias
GREENES/HOOD	C3	0.61	-185	-
Mossdale	C7	0.33	-17	-
CCFB entrance	C9	0.41	38	+
SJR-McCune	C10	0.35	-9	-
SAC R Above Point SAC	D4	0.22	-79	-
SUISUN BAY NR MTZ	D6	0.47	-60	-
GRIZZLY BAY	D7	0.22	-33	-
SLM001, SUISUN NR NICHOLS	D8	0.25	-74	-
HONKER BAY	D9	0.35	-51	-
Mallard-Sl., RSAC075	D10	0.32	-70	-
SHERMAN ISLAND	D11	0.36	-49	-
RSAN007	D12	0.59	-47	-
BIG BREAK NR OAKLEY	D14A	0.04	-28	-
SJR-JP, RSAN018	D15	0.28	-61	-
RSAN024 TWITCHELL	D16	0.45	-70	-
Franks Tract	D19	0.24	-128	-
Sac at Decker	D22	0.29	-117	-
Rio Vista	D24	0.17	-41	-
SJR AT POTATO PT	D26	0.15	-18	-
OLD-R-BACON, ROLD024	D28A	0.29	-5	-
RSMKLO08,LIT-POT-SL-TERM	MD7A	0.46	74	+
DISAPPOINTMENT SL	MD10	0.43	30	+
SJR BUCKLEY COVE	P8	0.38	37	+
RMID023	P10A	0.23	43	+
ROLD059	P12	0.24	-7	-
SLSUS012, SUSIUN SL S OF VOLANTI	S42	0.61	-185	-
		<b>Sum</b>	<b>Sum(ABS)</b>	
<b>Sum of Statistics</b>		8.1	1370	

Table 7-2 Statistics for the simulation in recent years (1991 – 2011) for the Mixed-SSC-WARMF simulation .

Common Name Location	EMP Location	R <sup>2</sup>	PBIAS	Sign Bias
GREENES/HOOD	C3	0.45	-75	-
Mossdale	C7	0.96	-28	-
CCFB entrance	C9	0.59	26	+
SJR-McCune	C10	0.67	14	+
SAC R Above Point SAC	D4	0.22	-88	-
SUISUN BAY NR MTZ	D6	0.73	-38	-
GRIZZLY BAY	D7	0.46	-21	-
SLM001, SUISUN NR NICHOLS	D8	0.35	-65	-
HONKER BAY	D9	0.54	-18	-
Mallard-SI., RSAC075	D10	0.36	-44	-
SHERMAN ISLAND	D11	0.34	-36	-
RSAN007	D12	0.21	-35	-
BIG BREAK NR OAKLEY	D14A	0.42	-32	-
SJR-JP, RSAN018	D15	0.62	-61	-
RSAN024 TWITCHELL	D16	0.58	-54	-
Sac at Decker	D22	0.52	-92	-
Rio Vista	D24	0.55	-91	-
SJR AT POTATO PT	D26	0.66	-56	-
OLD-R-BACON, ROLD024	D28A	0.22	-76	-
SJR BUCKLEY COVE	P8	0.69	-30	-
RMID023	P10A	0.12	66	+
ROLD059	P12	0.31	25	+
DISAPPOINTMENT SL	MD10	0.61	19	+
RSMKL008,LIT-POT-SL-TERM	MD7A	0.63	38	+
		<b>Sum</b>	<b>Sum(ABS)</b>	
<b>Sum of Statistics</b>		11.8	1129	

## 7.4 Conditions Potentially Leading to “Turbidity Bridges”

In this section, model results from the updated Mixed-SSC-WARMF simulation are used to investigate conditions under which a “turbidity bridge” is formed in the South Delta. Since the condition defining the establishment of a turbidity bridge has not been precisely defined, in this report the compliance value of 12 NTU in daily-averaged model output is used as an indicator of bridge formation at selected south Delta locations (see Figure 7-3). The modeled years 1991 – 2000 are used as a basis to investigate bridge formation conditions, in part because in these years model output generally had decent matches for EMP data, particularly for San Joaquin River turbidity (see Figure 4-29). Although many more years were modeled in these long-term historical simulations, since sediment supply in the Delta has been decreasing since 1957, as documented by Wright and Schoellhamer (2004), these modeled years were selected as representing a broad variation in inflow boundary conditions that are more likely representative of current conditions than earlier years. Note that with the new calibration and boundary conditions, the simulation tends to overestimate turbidity, so although we are using a 12 NTU metric, there are cases where “professional judgment” was used to decide whether or not a turbidity bridge actually formed

### 7.4.1 Analysis methodology

Modeled boundary conditions for inflows, exports, and turbidity concentration along with modeled OMR (Old+Middle River) flow were surveyed to establish general trends relating modeled turbidity values in the central and south Delta with the boundary conditions in Water Years 1991 – 2000. Only the high flow/high turbidity periods during the months December to March were included for analysis, although some years had multiple high flow events. The analysis only considered modeled conditions, not the relationship between turbidity and delta smelt.

A turbidity animation (see (RMA 2013) for details) using daily-averaged model output was developed for the analysis period and used to identify the establishment of a 12 NTU bridge between the central and south Delta in contour plots. Six locations were chosen to monitor during this period, both in contour plots and as daily-averaged time series – the locations are identified in Figure 7-3 and are shown as numerical turbidity concentrations (NTU) in each of the contour plots and in time series graphs of modeled turbidity. For the purposes of this report, a turbidity bridge was deemed to have formed when a 12 NTU route was established either through Middle River or through Old River linking the turbidity output locations in the central and south Delta. During the high flow/high turbidity period, approximate values or a ranges of values were documented in a table for the most important parameters used in the analysis.

### 7.4.2 Results

Table 7-3 through Table 7-5 and Figure 7-3 through Figure 7-28 summarize the results of the analysis. Figure 7-4 through Figure 7-6 illustrate the modeled value at the three compliance locations in each Water Year. A turbidity bridge formed in each Water Year except 1994 and 1999 – these years are highlighted in grey in the tables. The tables also indicate the primary route and driver(s) for turbidity bridge formation (second to last line in each table), and whether or not the three compliance locations exceeded 12 NTU in the simulation (final line). In WY1995 and WY1999 there were multiple high

flow/turbidity events. Note that in the years when either the Cosumnes or Mokelumne had a high flow event (e.g., 1995, 1997 and 1998), the Sacramento River and Yolo Bypass also had high flows so the contribution of these rivers to increased central Delta turbidity was masked. The Calaveras River did not have a high flow event during this period.

Note that the results with the new calibration are somewhat different from the previous RMA calibration (RMA 2013), although the main features are similar. There are several modes for turbidity bridge formation, which are discussed in the subsequent paragraph:

- Predominantly from the North into the central Delta with high north Delta inflow.
- Predominantly from the south when San Joaquin flow is high, initially favoring increased turbidity along Middle River.
- When export flows are high – this occurred mainly during the very high Sacramento+Yolo inflow periods but also occurred during a couple of moderate to high San Joaquin inflow periods.

During several of the years, high turbidity originating on the Sacramento side first intruded down Old River. As the simulation progressed, the turbidity moved into Middle River, with a partial bridge first forming along Old River and eventually along on Middle River (e.g., WYs 1993 and 1995). When San Joaquin River inflow and turbidity was dominant source for forming the bridge (e.g., 1995, 1998, and 2000), turbidity tended to travel into the central Delta through Middle River to form a bridge along that route, with the full bridge eventually forming along Old River.

In WYs 1994 and 1999 when turbidity bridges did NOT form, San Joaquin inflow and turbidity were low, and exports and negative OMR flow were low at least periodically during the highest flow and turbidity periods investigated. Sacramento+Yolo inflow was also low during at least part of those periods.

### 7.4.3 Summary of Analysis

It should be noted that this analysis is based on a turbidity model developed with synthetic (*i.e.*, scaled USGS-SSC data) or externally calculated (*i.e.*, from WARMF results) boundary conditions, so some skepticism is warranted when interpreting results. In general, the analysis shows that there are several modes under which a turbidity bridge is likely to form, which depend on the relative magnitudes of the Sacramento and San Joaquin River inflows and on the magnitude of the exports, or, equivalently, the sign and magnitude of the OMR flow.

Table 7-3 Turbidity bridge decision variables, 1991 – 1994. Bold font indicates primary driver(s) for turbidity, shaded column indicates no bridge formed.

	March 1991	Feb. 1992	January 1993	January 1994
Peak Sac/Yolo Flow (CFS)	~ <b>47,000/</b> ~ <b>3100</b>	> 47,000 / > 2600	~ <b>80,000/</b> > <b>46,000</b>	~ 30,000 / >1500
Peak Sac/Yolo NTU	< 370 / < 320	> 570/ > 950	~ 311 / ~ 545	~ 100/ < 50
Peak SJR Flow (CFS)	~ 3900	> <b>5100</b>	> 9500	> 2700
Peak SJR NTU	> 90	> 140	> 200	~ 80
Peak Cal Flow (CFS)	~ 60	~ 40	< 50	~ 90
Peak Cal NTU	~ 11	~ 12	< 10	< 40
Peak Cos+Moke Flow (CFS)	> 3500	> 3200	~ 7300	~ 400
Peak Cos/Moke NTU	~ 72	~100	< 10	< 10
OMR (CFS)	< -8000	~ -6000	~ -6000 to -8000	~ -3000 to -6000
SWP+CVP (CFS)	> <b>10,000</b>	> <b>10,000</b>	<b>8000 to &gt; 14000</b>	3400 to 10,000
Primary route	<b>Old - N</b>	Old - S, Mid - S	<b>Old - N, Mid - S</b>	N/A
Three Compliance > 12 NTU	Yes	Yes	Yes	No

Table 7-4 Turbidity bridge decision variables, 1995 – 1997. Bold font indicates primary driver(s) for turbidity.

	January 1995	March 1995	January 1996	Dec./Jan. 1997
Peak Sac/Yolo Flow (CFS)	< <b>96,000 /</b> ~ <b>143,000</b>	~ 100,000 / > 266,000	~ 88,000 / > 52,000	> 113,200 / > 401,000
Peak Sac/Yolo NTU	~ 450/ ~ 360	> 100 / > 200	> 640 / > 400	> 320 / ~ 115
Peak SJR Flow (CFS)	> 11,000	< <b>26,000</b>	~ 2300 to <b>16,000</b>	> 53,000
Peak SJR NTU	> 300	> 210	> 80	> 100
Peak Cal Flow (CFS)	~ 70	> 2100	~ 3000	~ 6900
Peak Cal NTU	~ 50	< 60	> 50	< 100
Peak Cos+Moke Flow (CFS)	> 12,000	> 20,000	~ 9000	> 50,000
Peak Cos/Moke NTU	~ 210	> 100	< 150	> 100
OMR (CFS)	~ -7000	~ 4500 to 9000	~ -7800 to 3400	~ 20,000
SWP+CVP (CFS)	<b>10000 to 12000</b>	0 to 5000	~ <b>4700 to 11,000</b>	~ 3700 to 10,400
Primary route	<b>Old - N, Mid - S</b>	<b>Old S, Mid S</b>	Old/Middle - N and S	Old - S, Mid S
Three Compliance > 12 NTU	Yes	Yes	Yes	Yes

Table 7-5 Turbidity bridge decision variables, 1998 – 2000. Bold font indicates primary driver(s) for turbidity, shaded columns indicate no bridge formed.

	Jan./Feb. 1998	Dec./Jan. 1999	Feb 1999	Jan./Feb.2000
<b>Peak Sac/Yolo Flow (CFS)</b>	~ 94,000 / > 187,000	~ 67,000 / 0	> 86,000 / ~ 56,000	~ 88,000 / > 85,000
<b>Peak Sac/Yolo NTU</b>	~ 350 / ~ 340	< 160 / < 150	~ 130 / < 70	~ 200 / ~ 100
<b>Peak SJR Flow (CFS)</b>	> <b>35,000</b>	~ 7700	~ 15,500	> <b>14,000</b>
<b>Peak SJR NTU</b>	> 160	< 50	> 50	> 130
<b>Peak Cal Flow (CFS)</b>	~ 7900	< 3000	~ 3900	~ 5000
<b>Peak Cal NTU</b>	> 50	> 50	< 50	< 25
<b>Peak Cos+Moke Flow (CFS)</b>	~ 20,000	< 5000	~ 14,500	> 10,000
<b>Peak Cos/Moke NTU</b>	< 150	< 50	< 60	~ 120
<b>OMR (CFS)</b>	0 to 13,000	~ -4000 to 0	~ -2800 to 1800	< -8500
<b>SWP+CVP (CFS)</b>	800 to 4000	2000 to 7100	4300 to 8200	<b>7000 to 13,000</b>
<b>Primary route</b>	<b>Old - S, Mid S</b>	N/A	?	Old N/ Mid S
<b>Three Compliance &gt; 12 NTU</b>	Yes	Barely	Barely	Yes

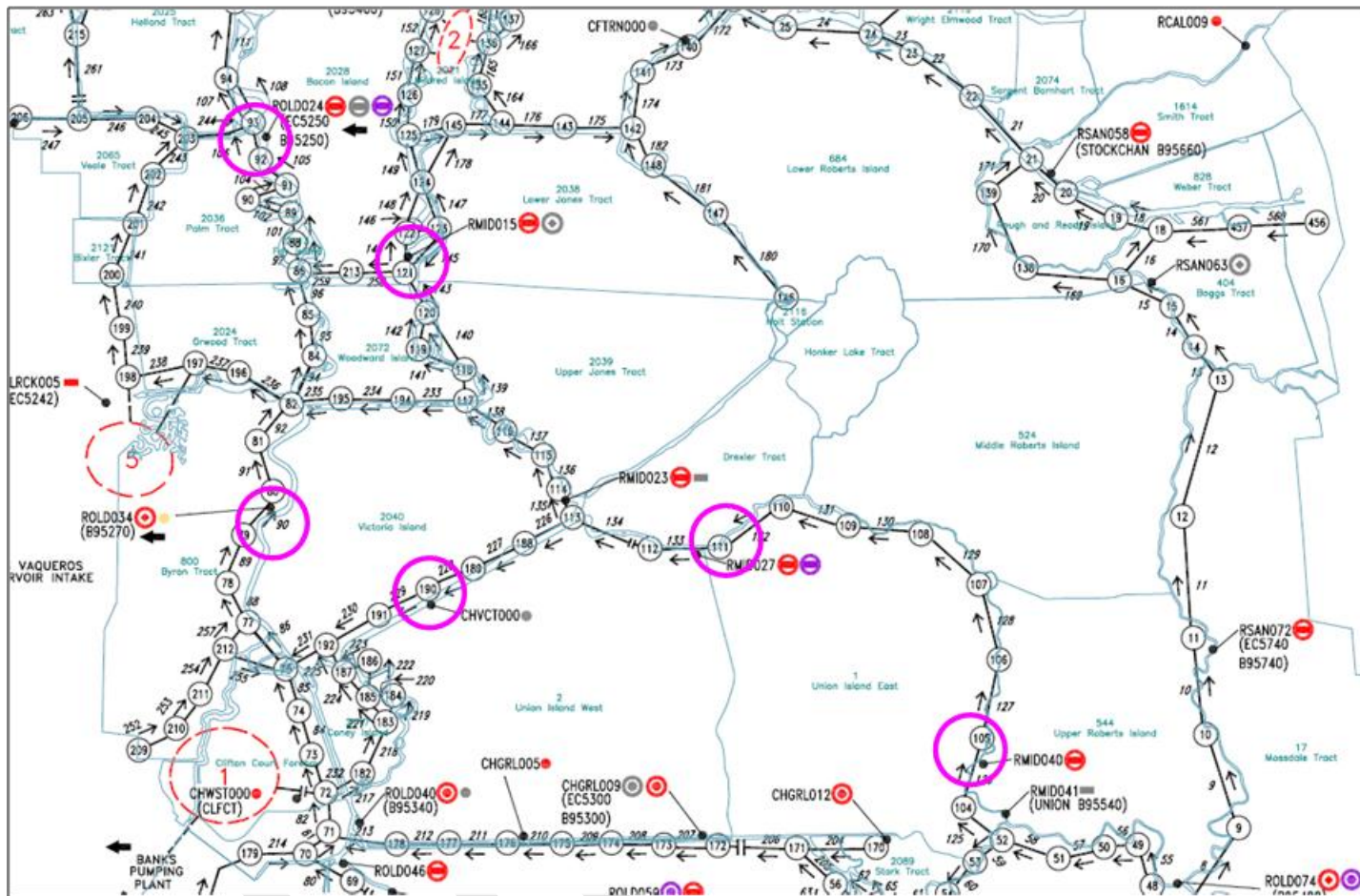


Figure 7-3 Locations used to investigate the formation of a turbidity bridge in the south Delta illustrated in the DSM2 grid.

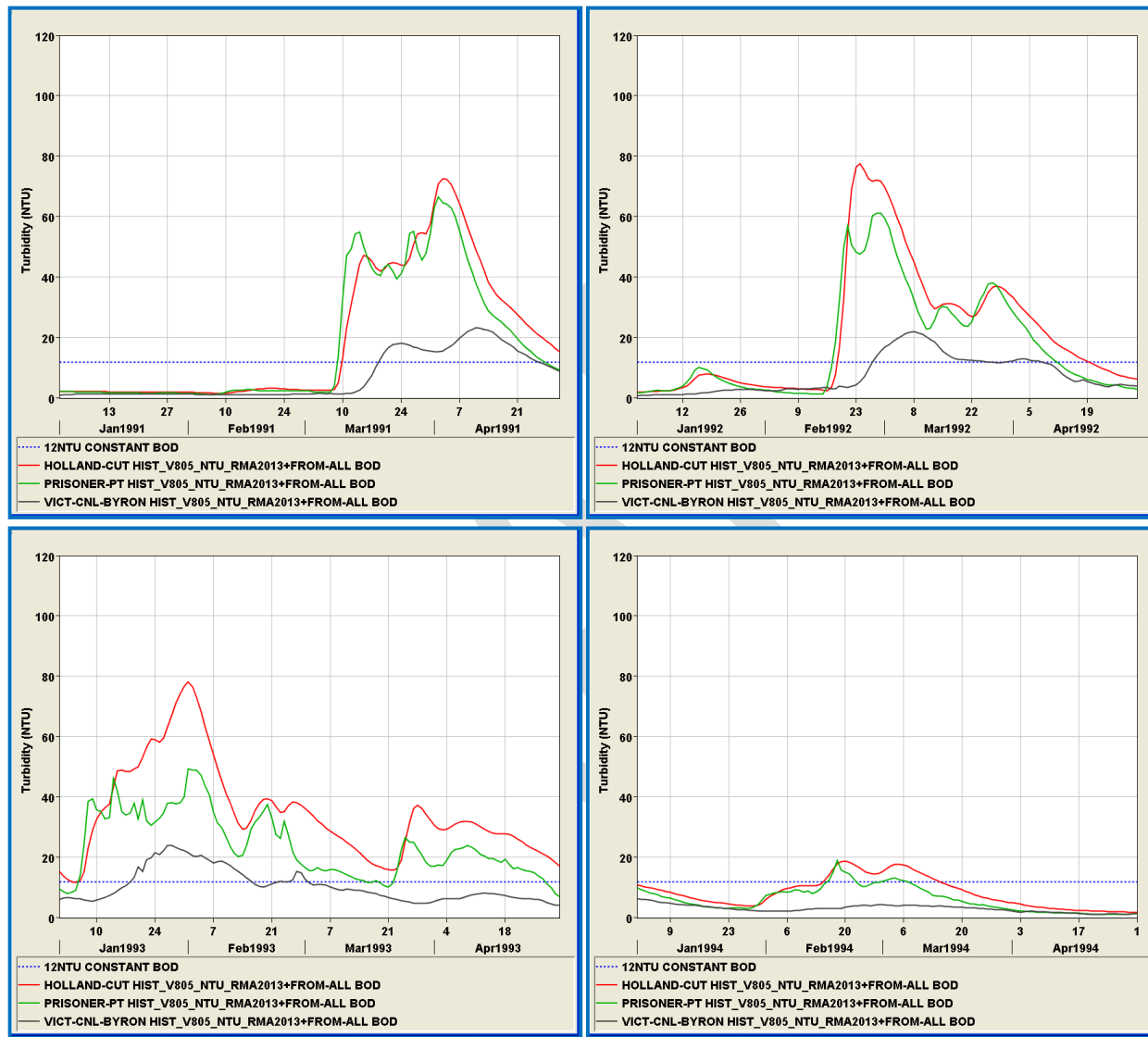


Figure 7-4 Plots show the modeled turbidity output at the three compliance locations along with the 12 NTU compliance value for WYs 1991 – 1994.

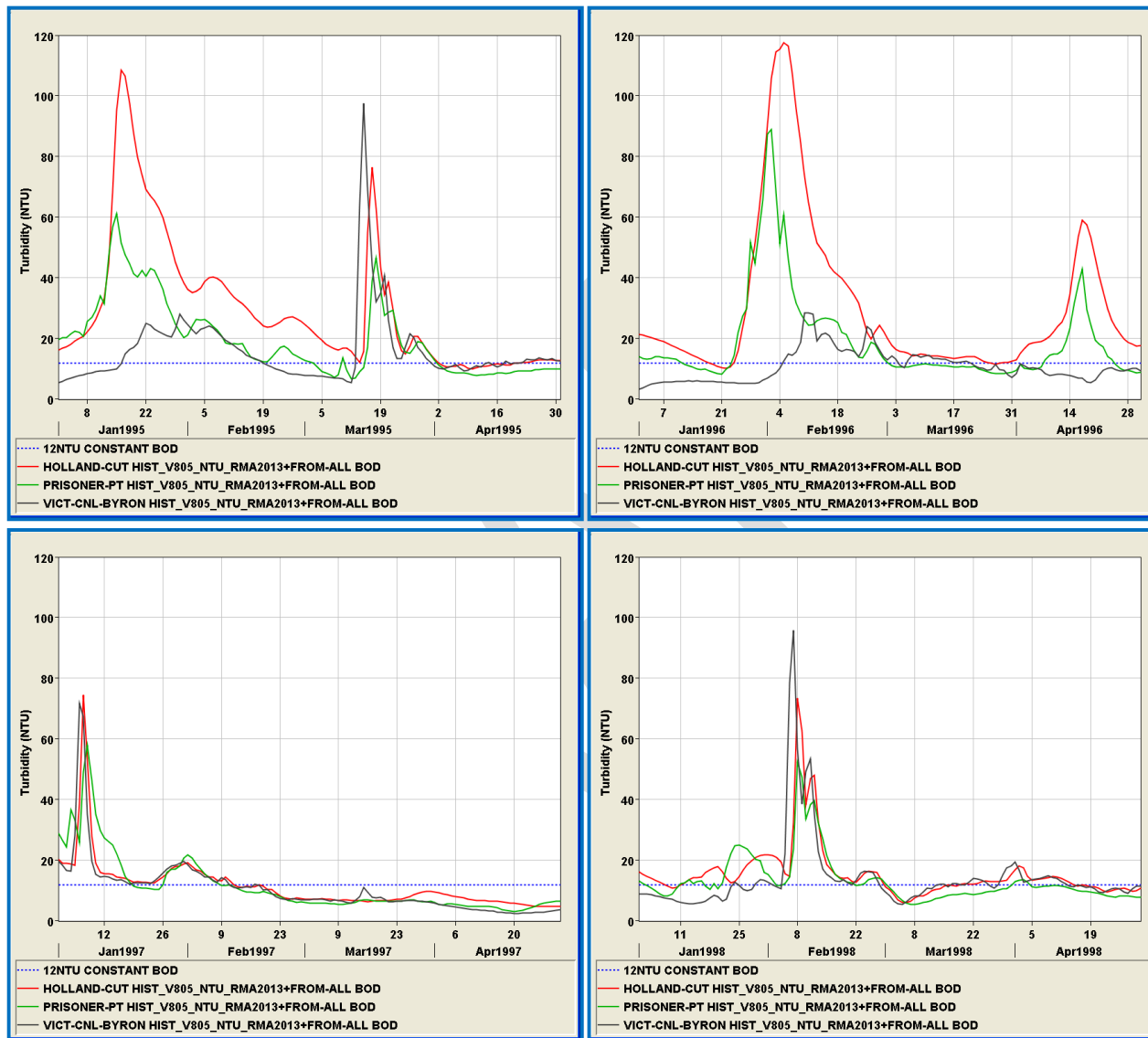


Figure 7-5 Plots show the modeled turbidity output at the three compliance locations along with the 12 NTU compliance value for WYs 1995 – 1998.

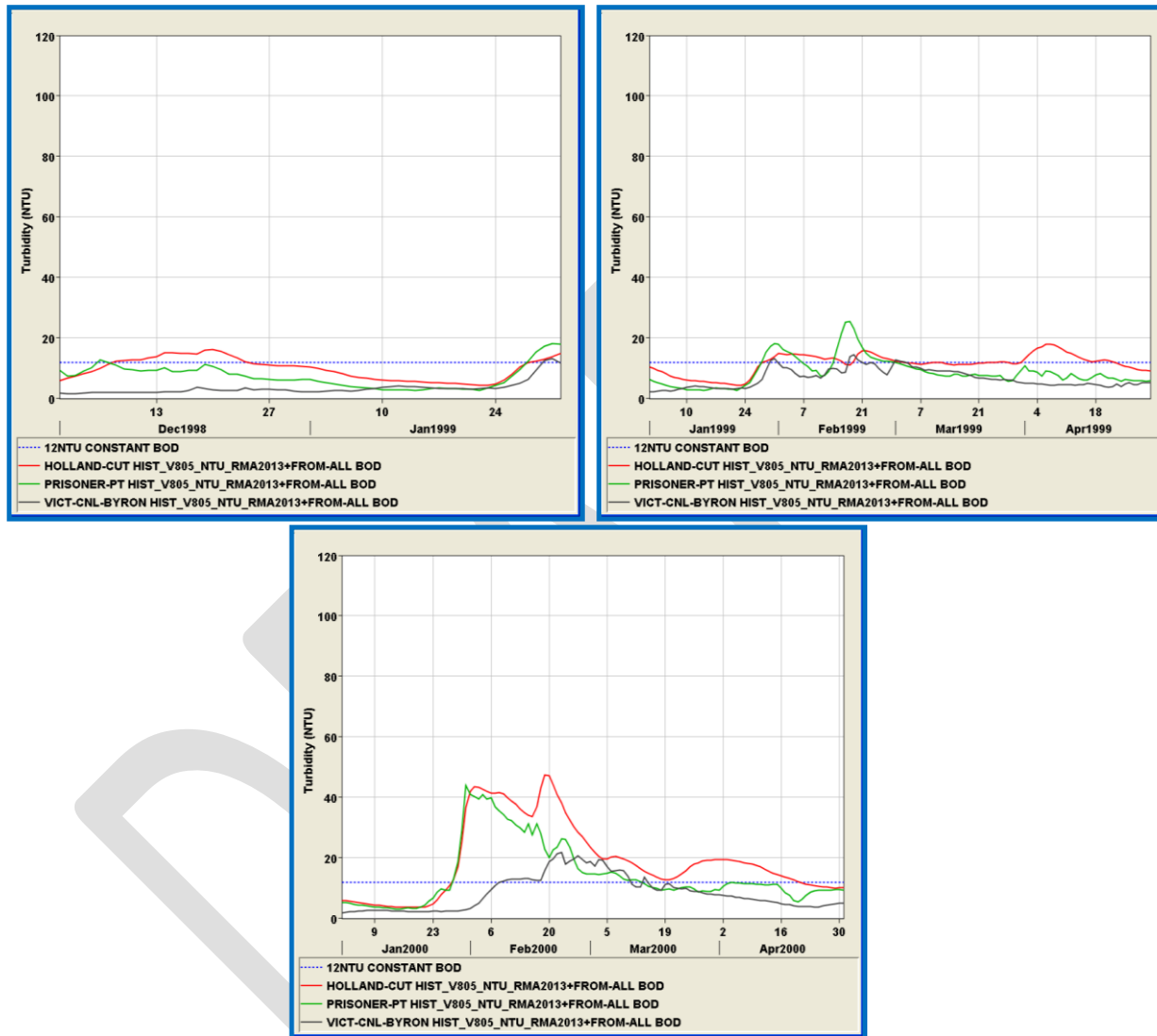


Figure 7-6 Plots show the modeled turbidity output at the three compliance locations along with the 12 NTU compliance value for WYs 1999 – 2000.

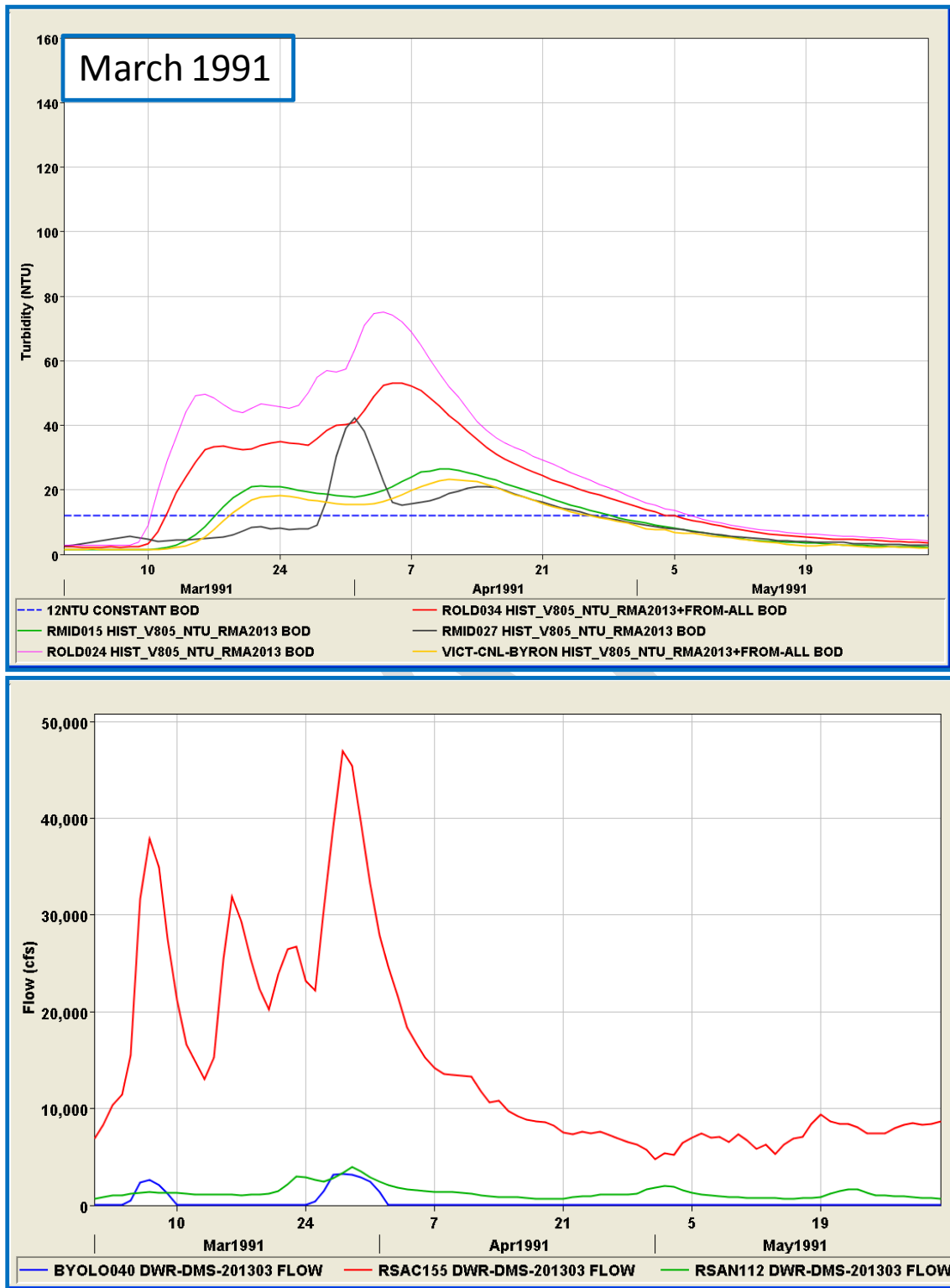


Figure 7-7 Turbidity time series at six key “bridge” locations (upper), and Sacramento, Yolo Bypass and San Joaquin inflow (lower) in WY 1991.

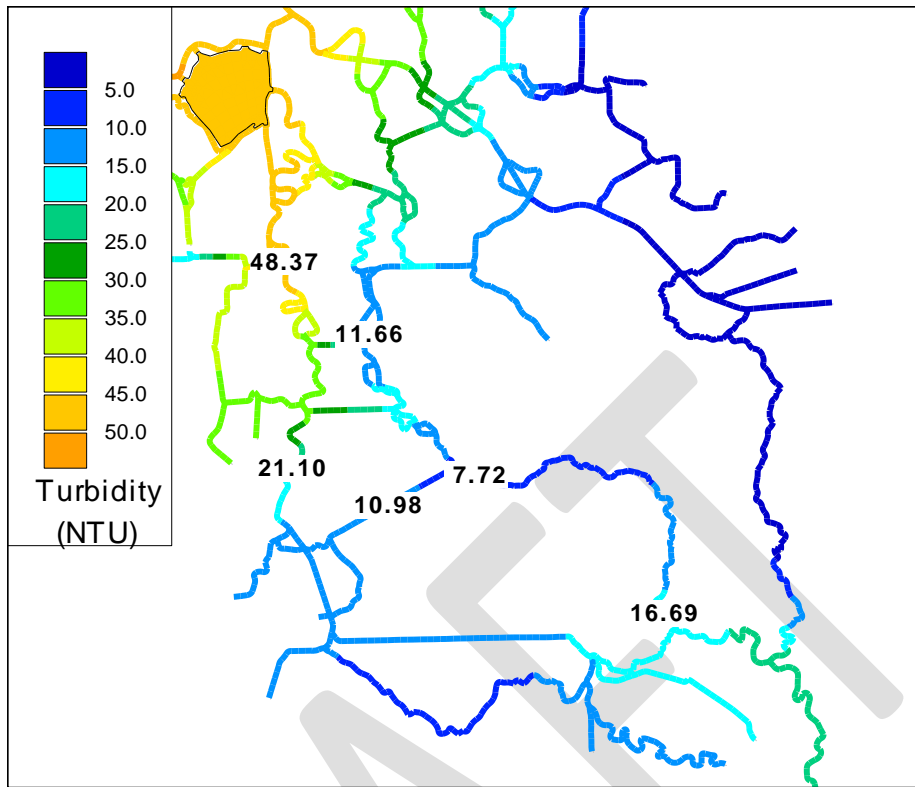


Figure 7-8 March 16, 1991 contour plot showing values at the six key locations. Turbidity is travelling south down Old River, and then east into Middle River.

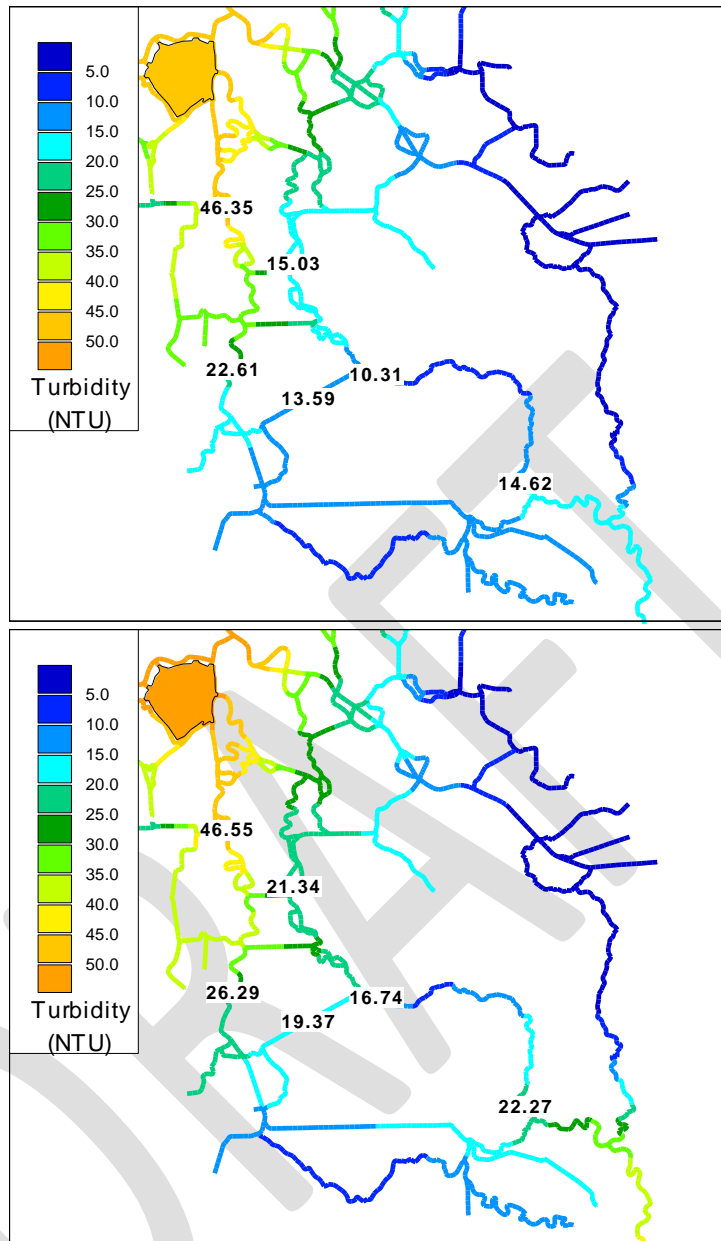


Figure 7-9 March 17 (upper) and 21 (lower) 1991 contour plots showing values at the six key locations and the predominant progression of the turbidity pulse southwards down Old River into Middle River, and also intruding into the south Delta and northwards from San Joaquin flow.

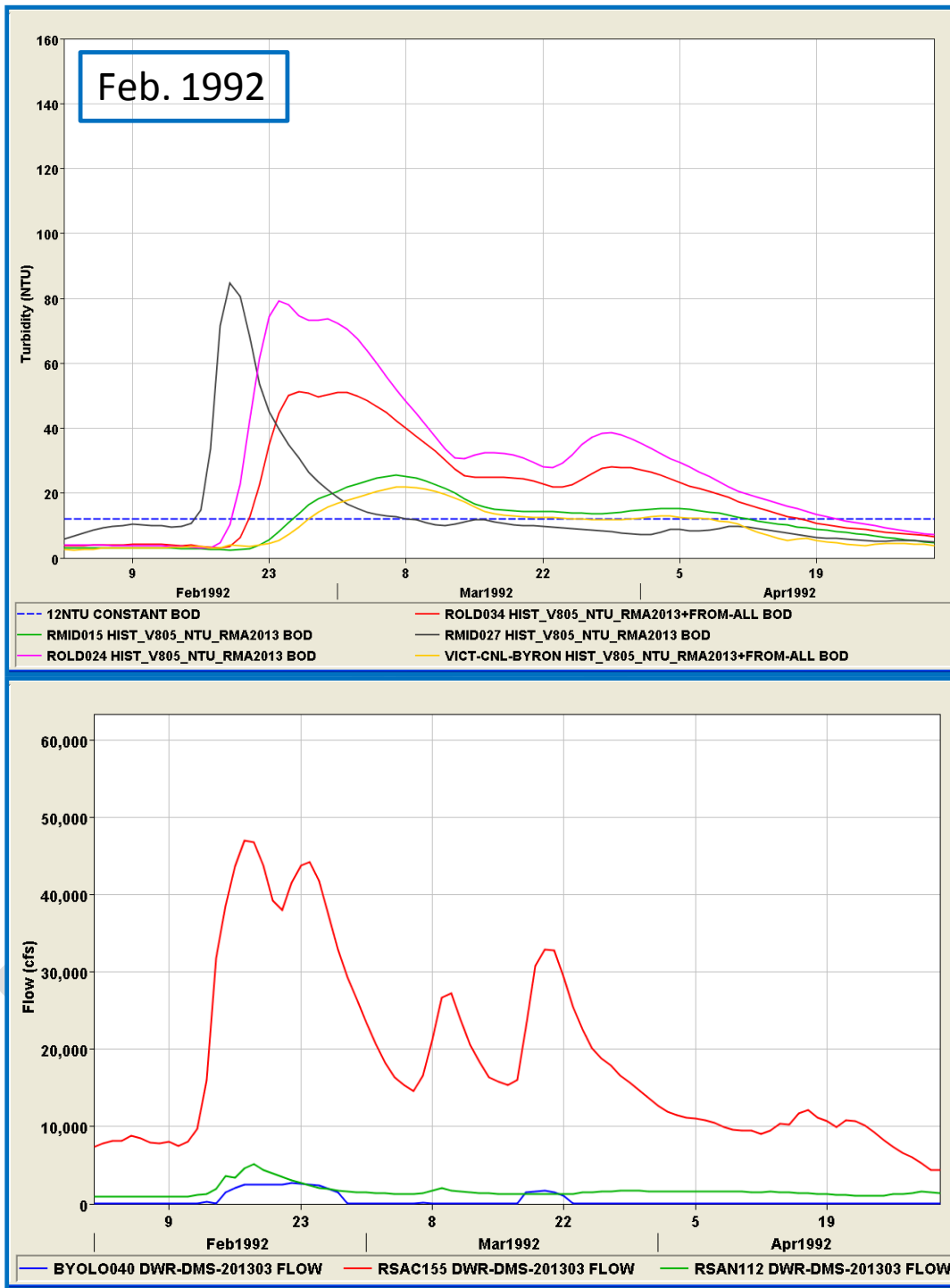


Figure 7-10 Turbidity time series at six key “bridge” locations (upper), and Sacramento, Yolo Bypass and San Joaquin inflow (lower) in WY 1992.

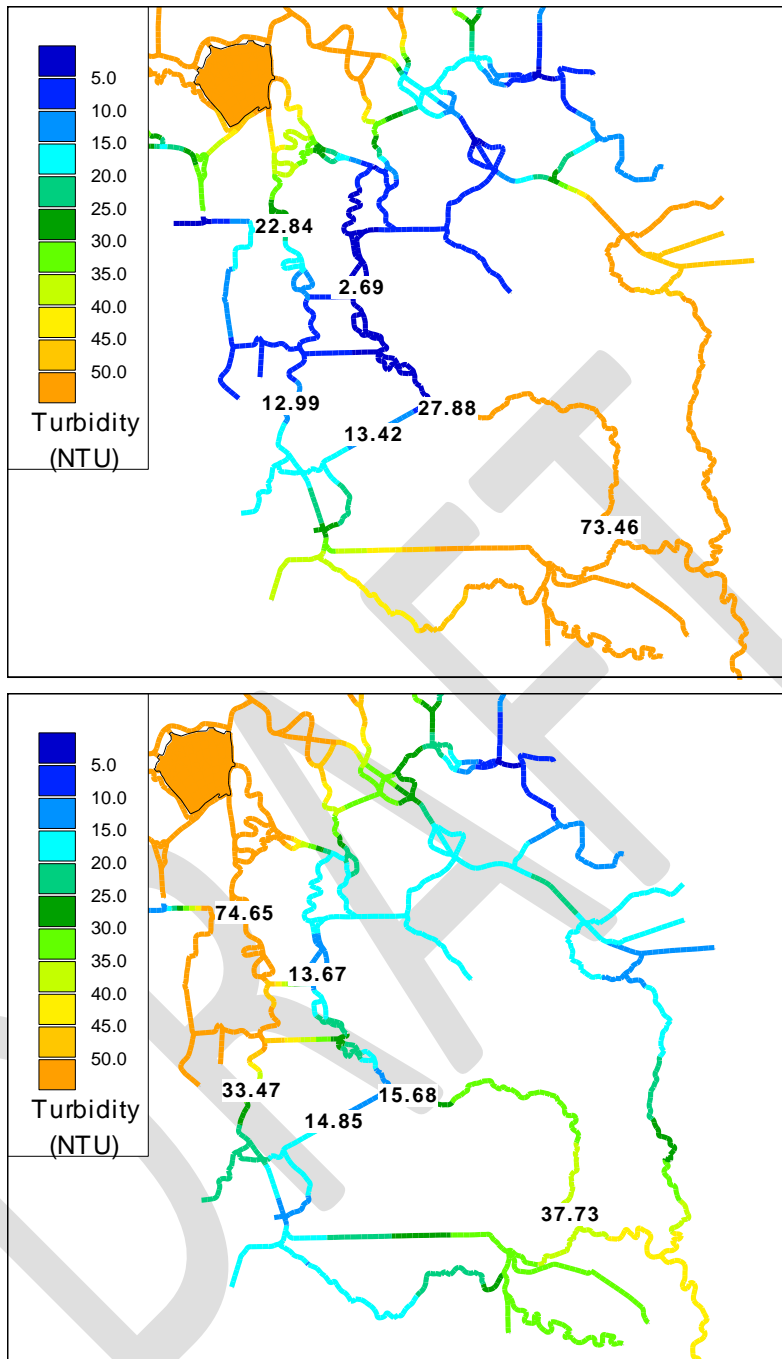


Figure 7-11 February (upper) and 25 (lower) 1992 contour plots showing values at the six key locations and the progression of the predominant turbidity pulse along Old and Middle Rivers from the south (upper), and then is joined in the central Delta by turbidity traveling south from both San Joaquin sources from the East and Sacramento sources from the north.

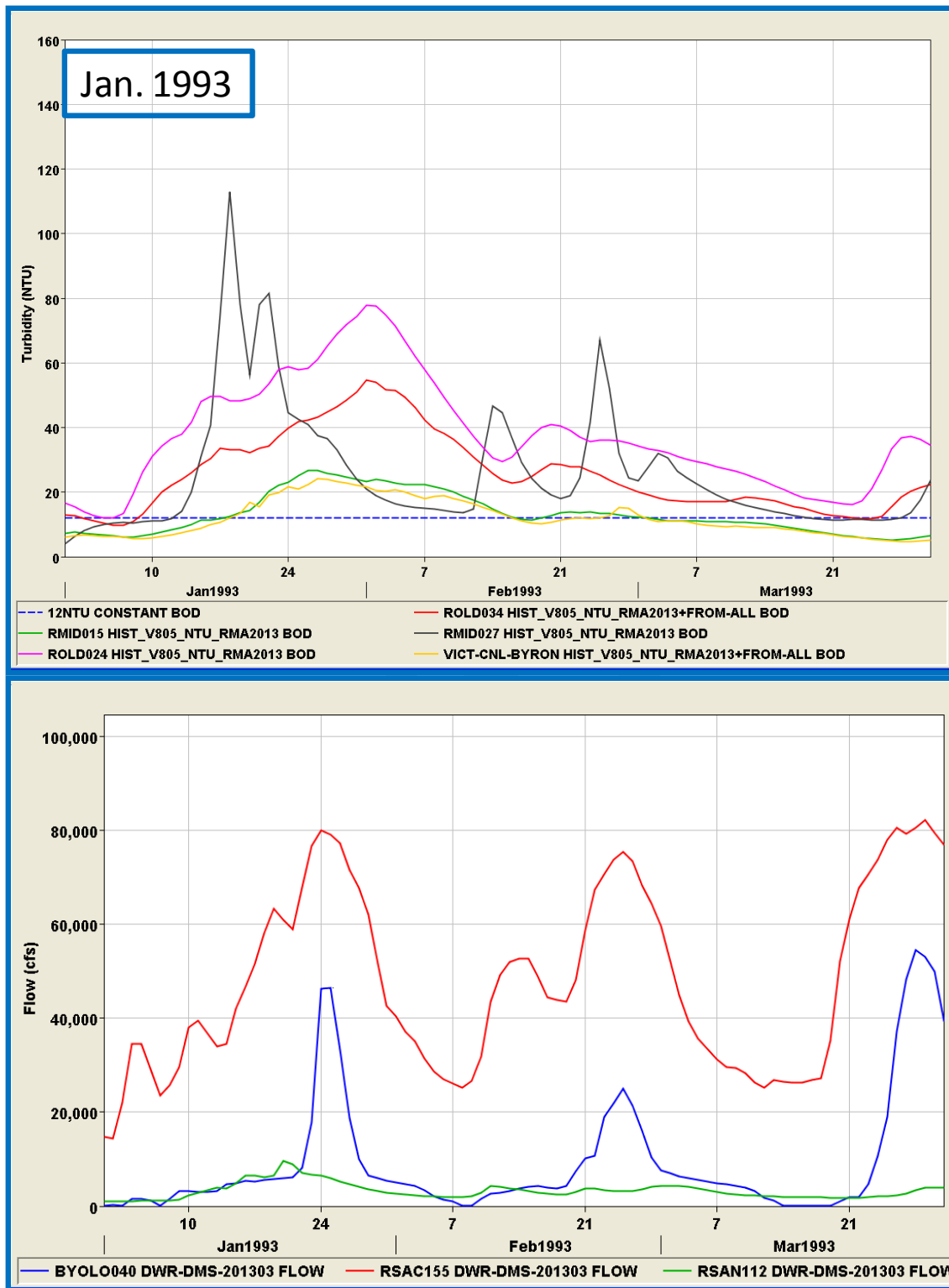


Figure 7-12 Turbidity time series at six key “bridge” locations (upper), and Sacramento, Yolo Bypass and San Joaquin inflow (lower) in WY 1993.

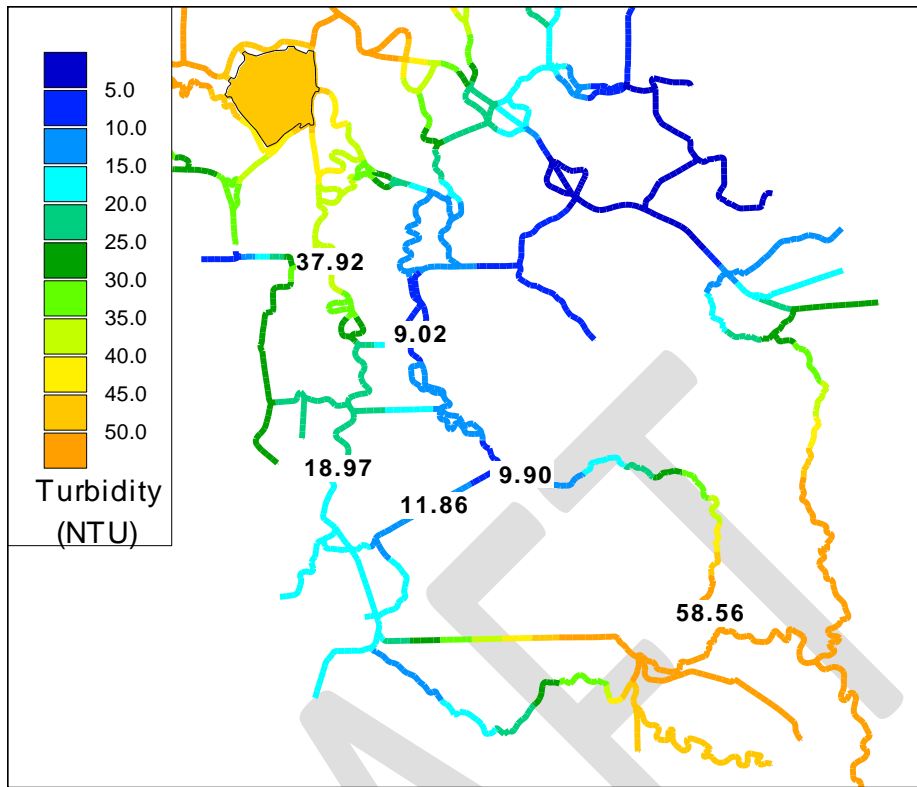


Figure 7-13 January 12, 1993 contour plot showing values at the six key locations. Turbidity is predominantly travelling south down Old River, and additionally traveling northwards from the south into Old and Middle Rivers.

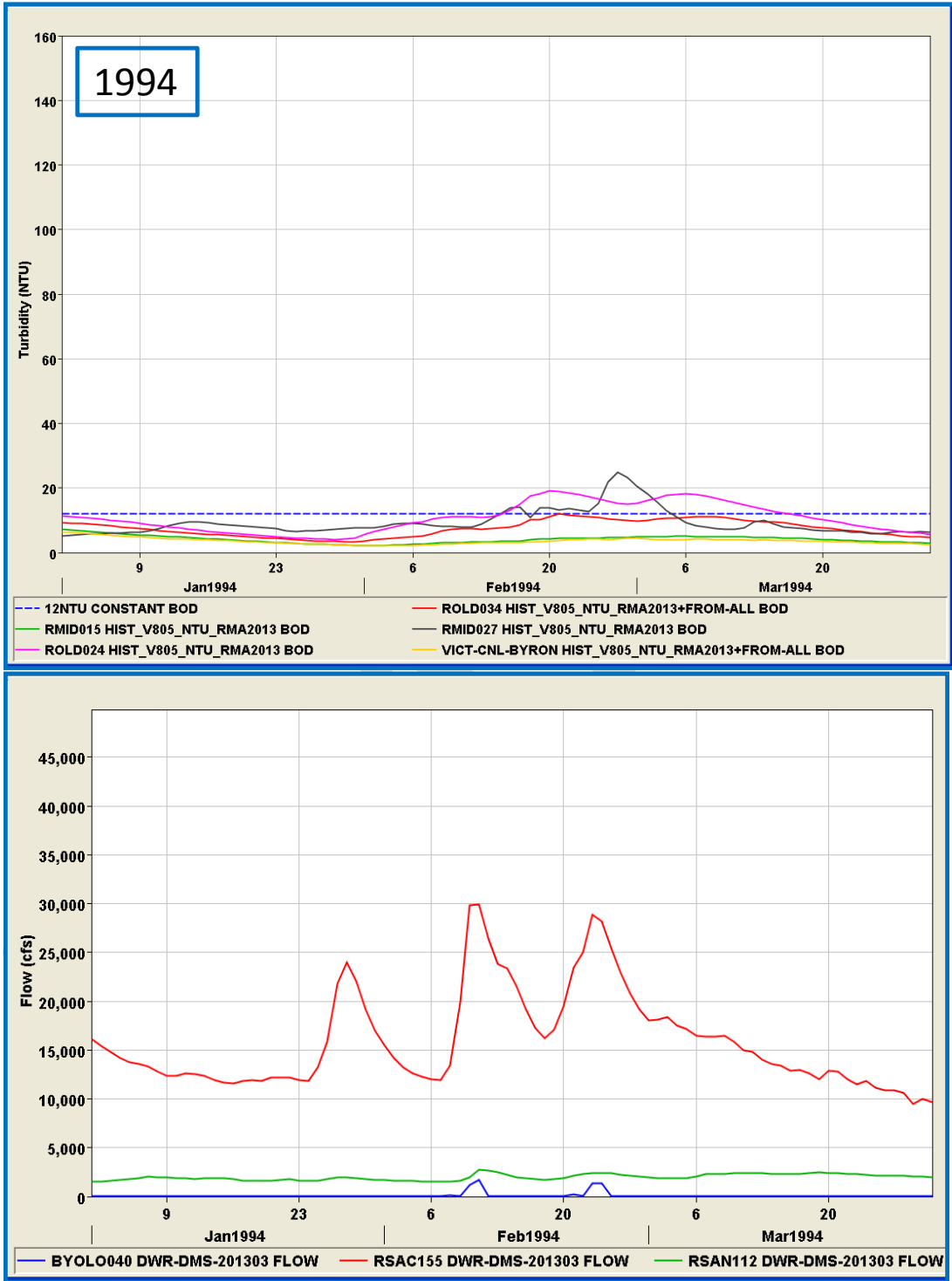


Figure 7-14 Turbidity time series at six key “bridge” locations (upper), and Sacramento, Yolo Bypass and San Joaquin inflow (lower) in WY 1994.

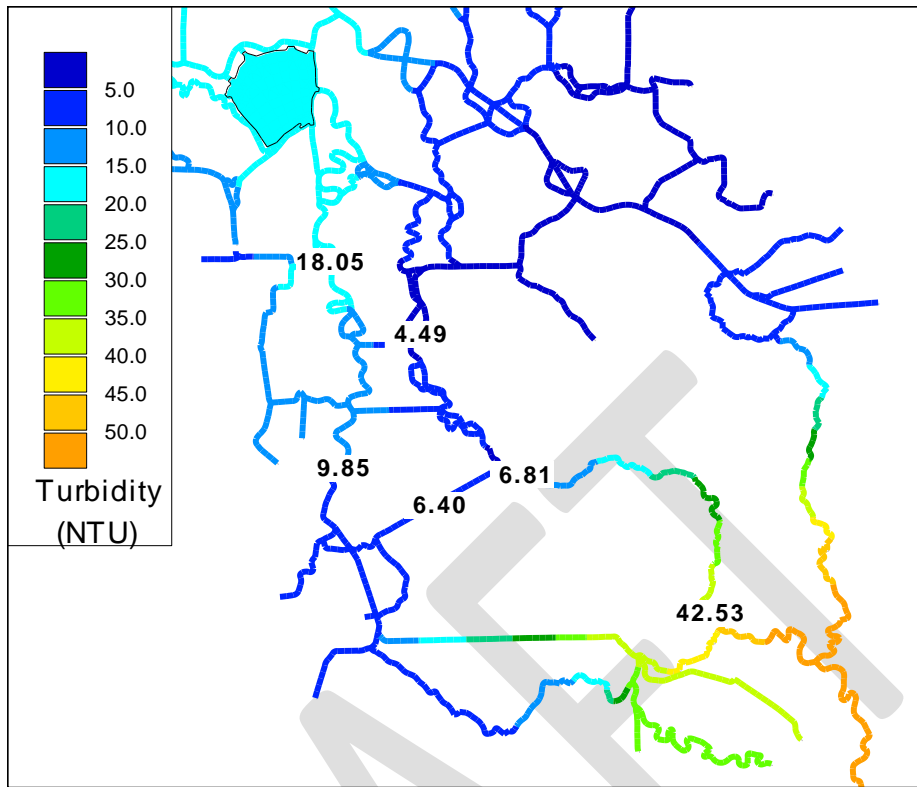


Figure 7-15 February 22, 1994 contour plot showing values at the six key locations. A turbidity bridge did not form.

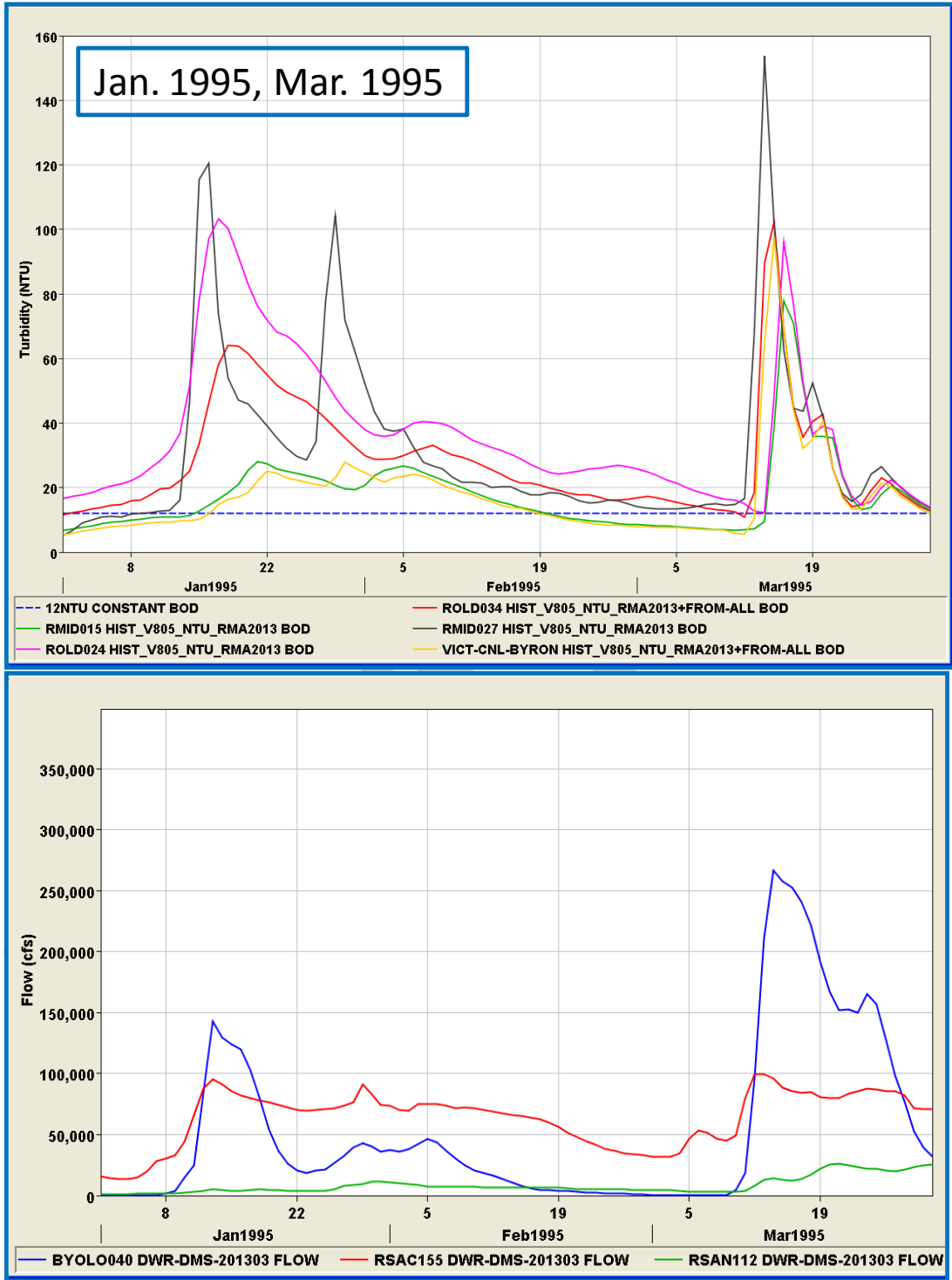


Figure 7-16 Turbidity time series at six key “bridge” locations (upper), and Sacramento, Yolo Bypass and San Joaquin inflow (lower) in WY 1995.

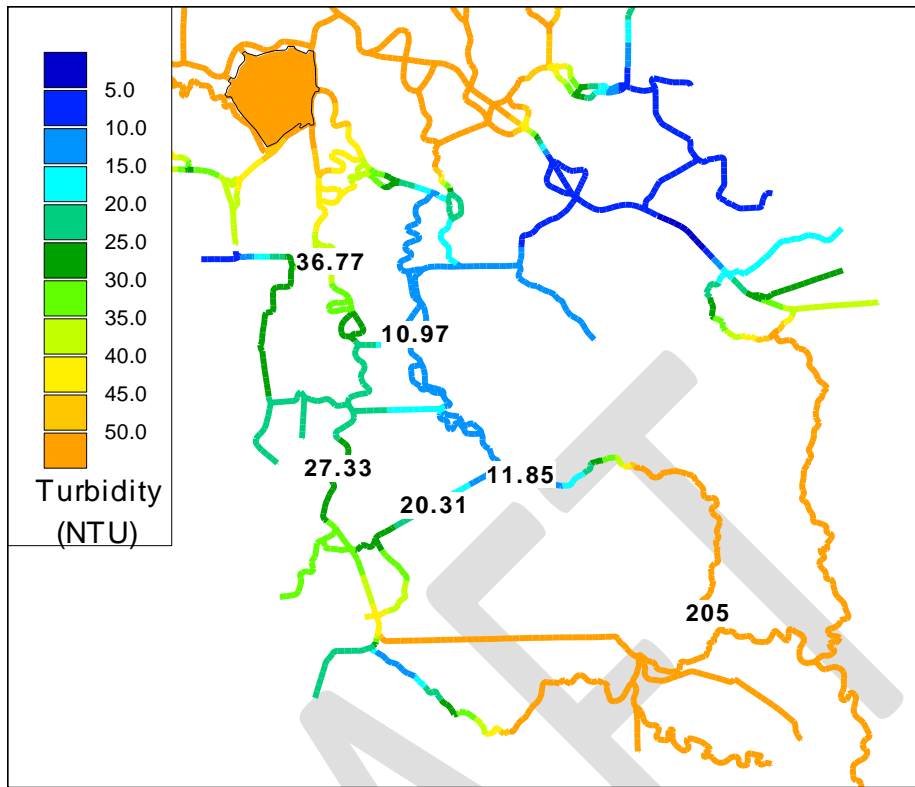


Figure 7-17 January 12, 1995 contour plot showing values at the six key locations. This is the progression predominantly from the north down Old River for the first turbidity pulse this wet season. The San Joaquin pulse also contributes to the bridge from the south.

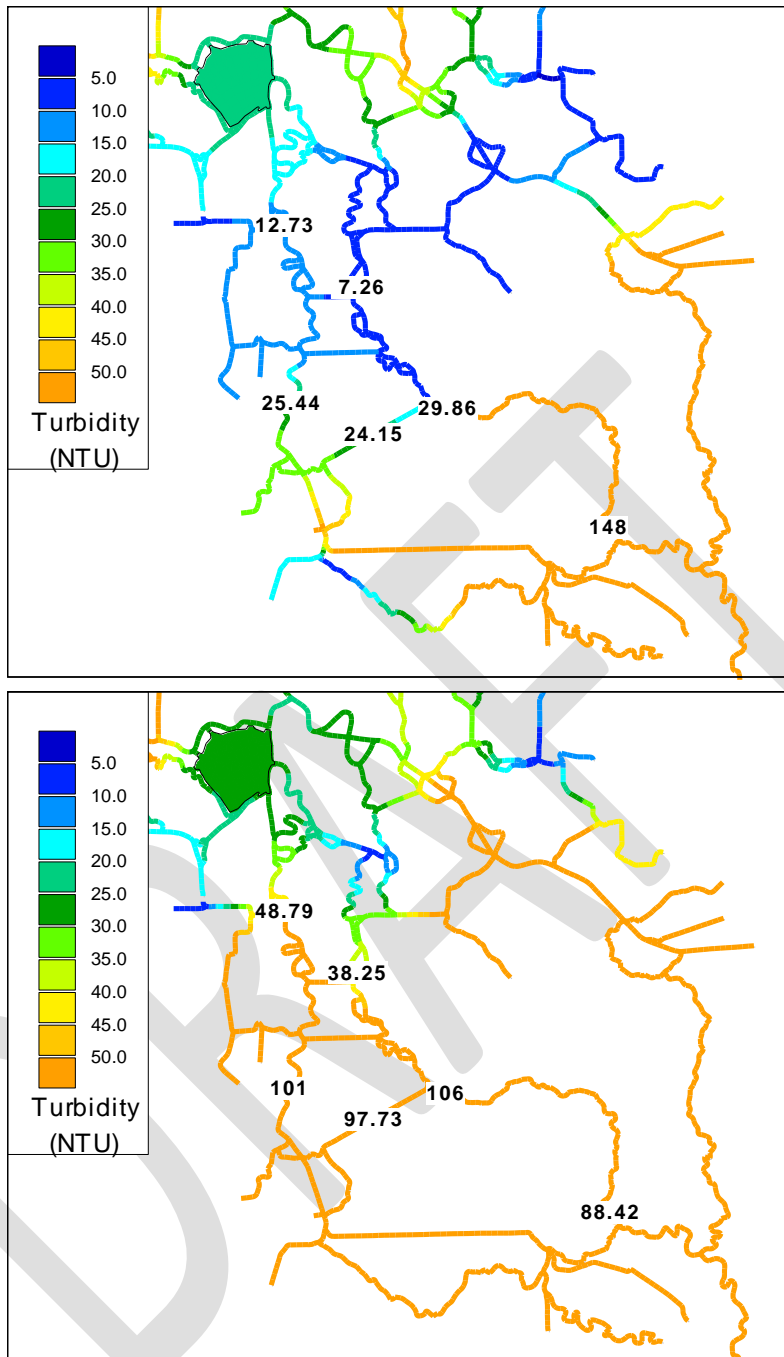


Figure 7-18 March 12 (upper) and 14 (lower) contour plots showing values at the six key locations for the second turbidity pulse of this season - the progression of the predominant turbidity pulse is northward along Old and Middle Rivers from the south (upper).

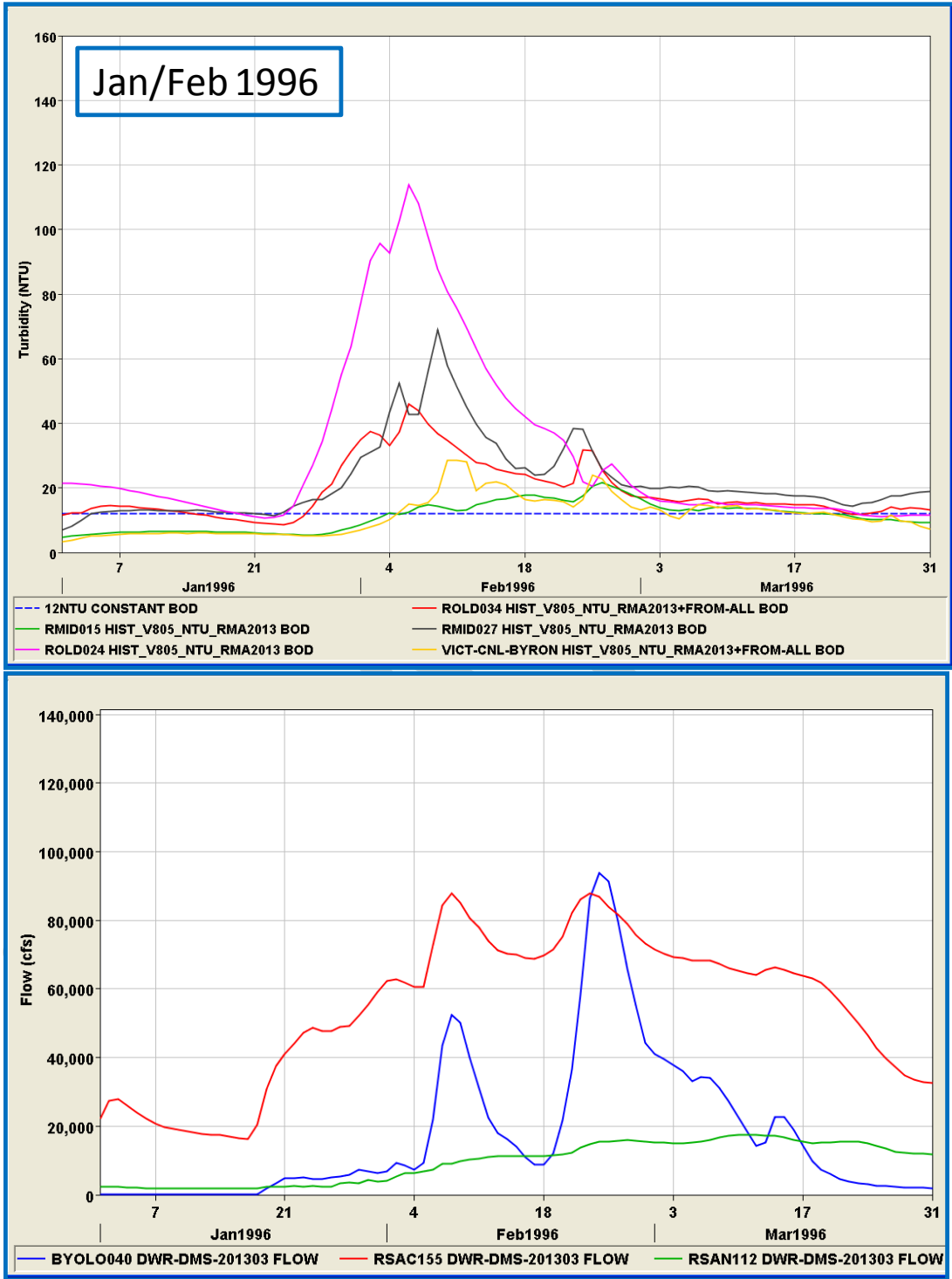


Figure 7-19 Turbidity time series at six key “bridge” locations (upper), and Sacramento, Yolo Bypass and San Joaquin inflow (lower) in WY 1996.

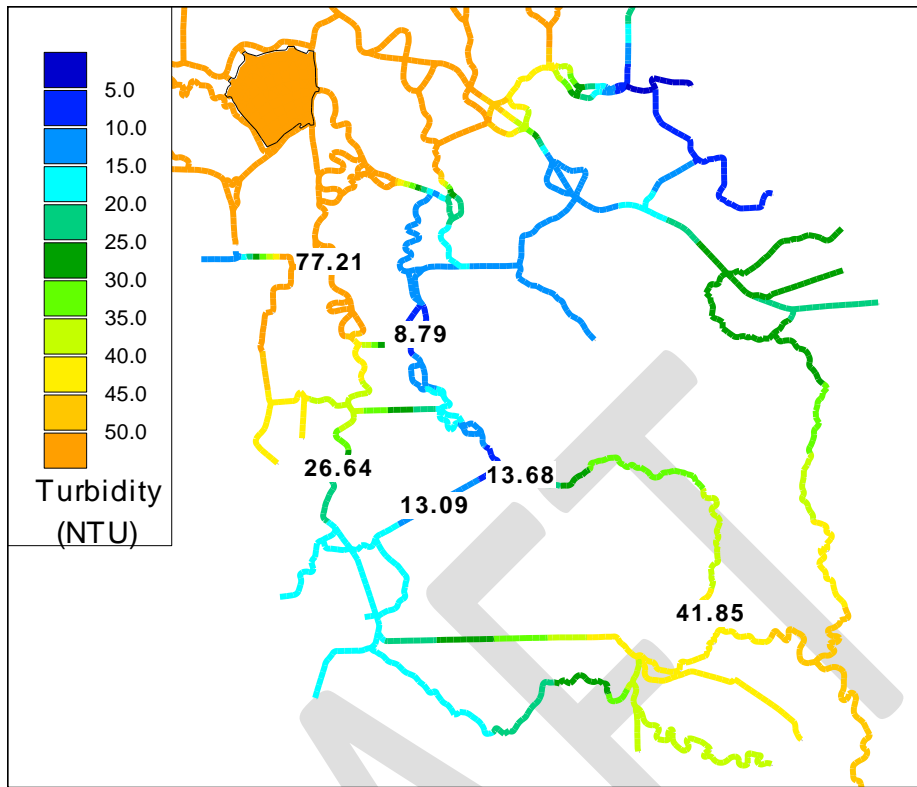


Figure 7-20 January 13, 1996 contour plot showing values at the six key locations. This is the progression equally from the north and south along Old and Middle Rivers.

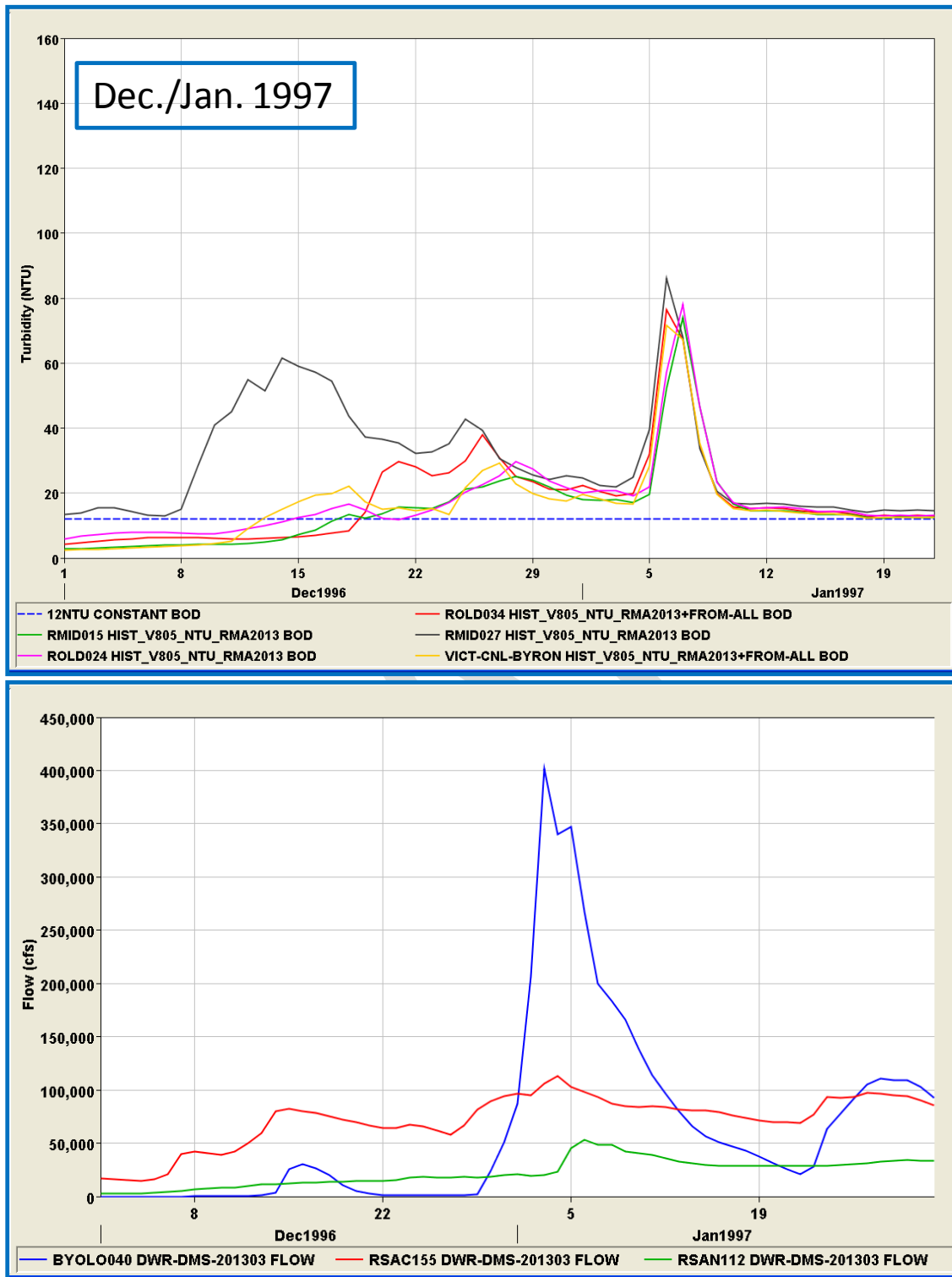


Figure 7-21 Turbidity time series at six key “bridge” locations (upper), and Sacramento, Yolo Bypass and San Joaquin inflow (lower) in WY 1997.

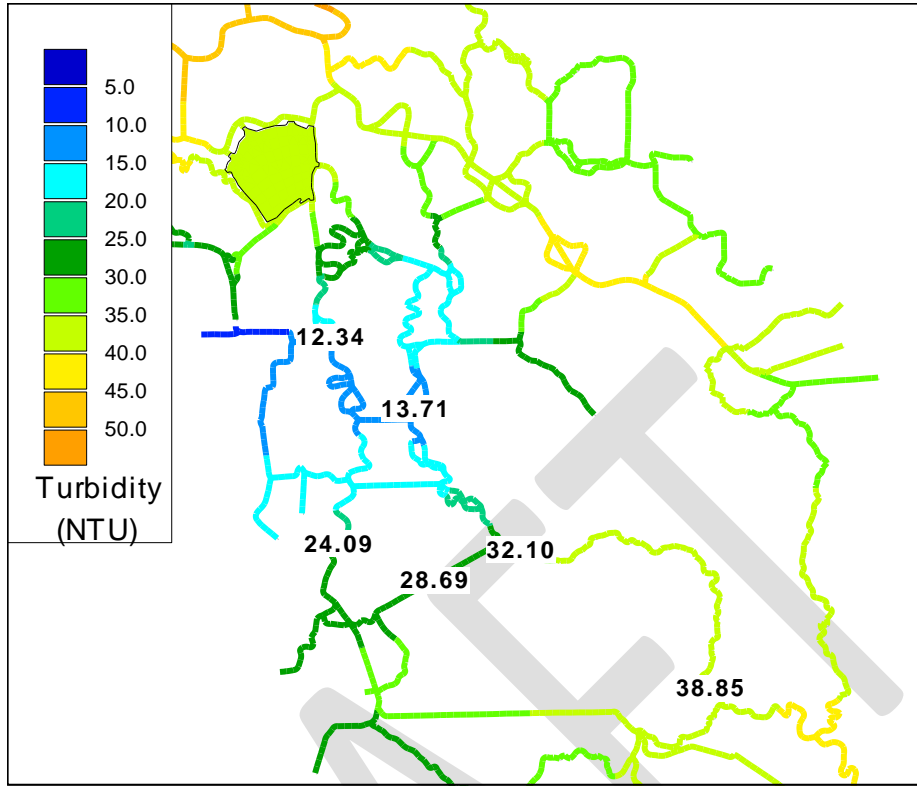


Figure 7-22 December 19, 1996 contour plot showing values at the six key locations. This is the progression primarily from the south and east from the high San Joaquin River inflow.

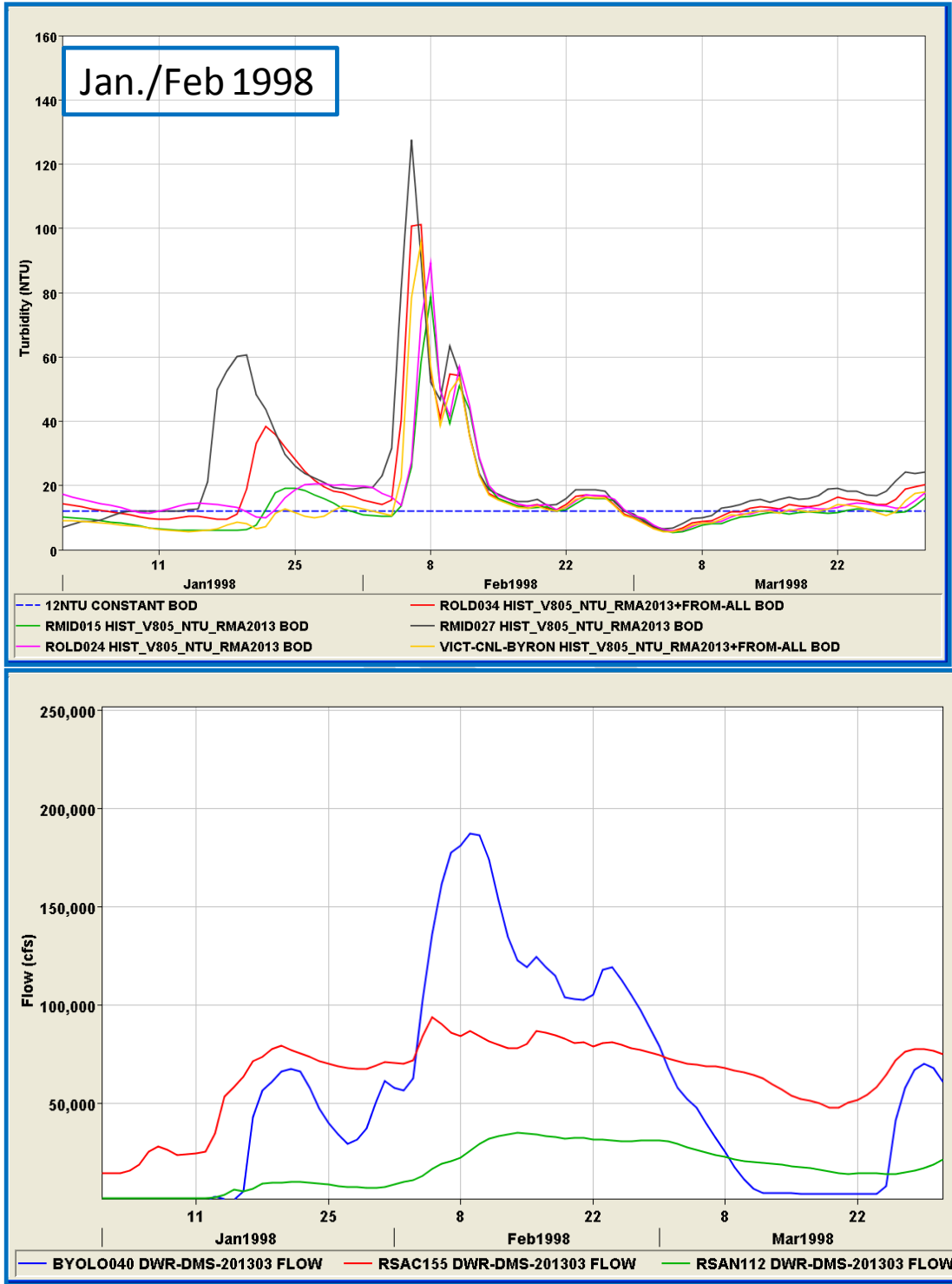


Figure 7-23 Turbidity time series at six key “bridge” locations (upper), and Sacramento, Yolo Bypass and San Joaquin inflow (lower) in WY 1998.

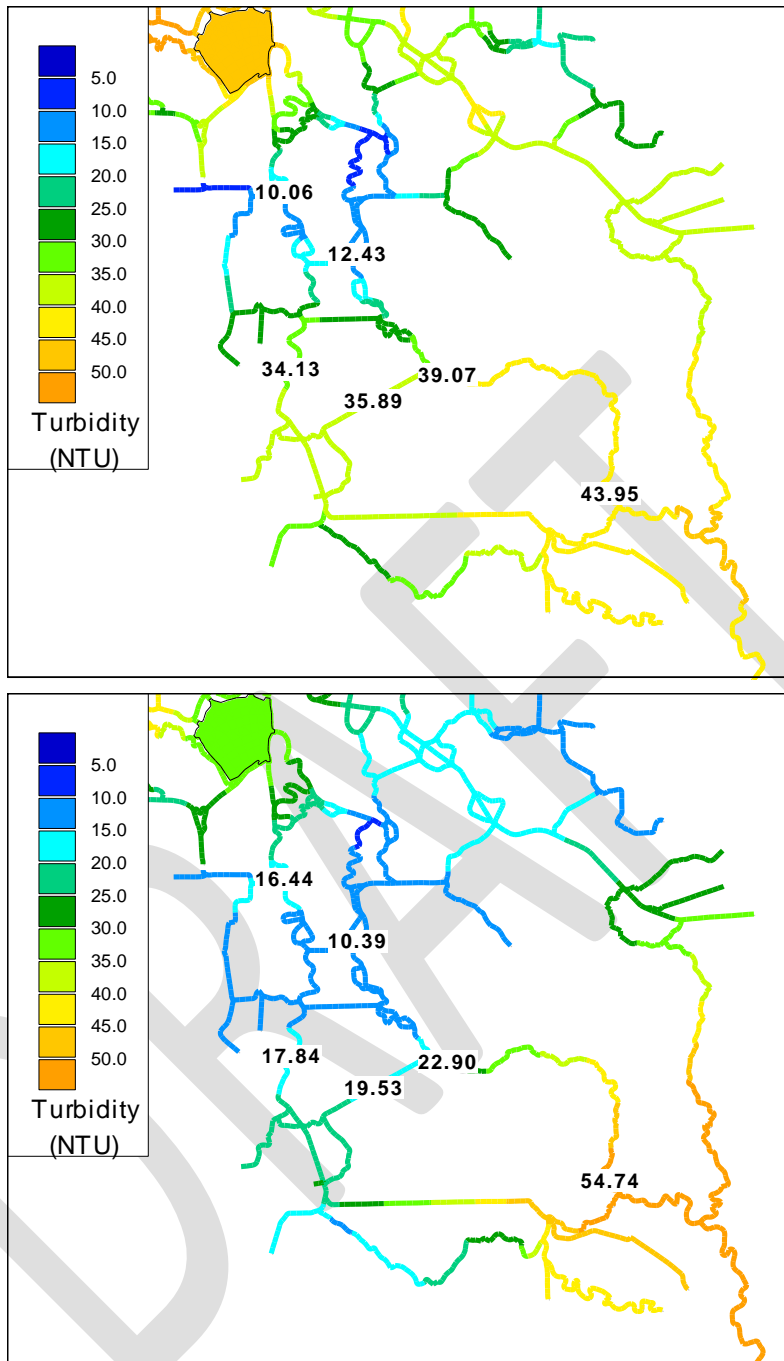


Figure 7-24 January 21 (upper) and February 3 (lower) 1998 contour plots showing values at the six key locations for the two turbidity pulses of this season - the progression of the predominant turbidity pulse is northward along Old and Middle Rivers from the south due to the high San Joaquin River inflow.

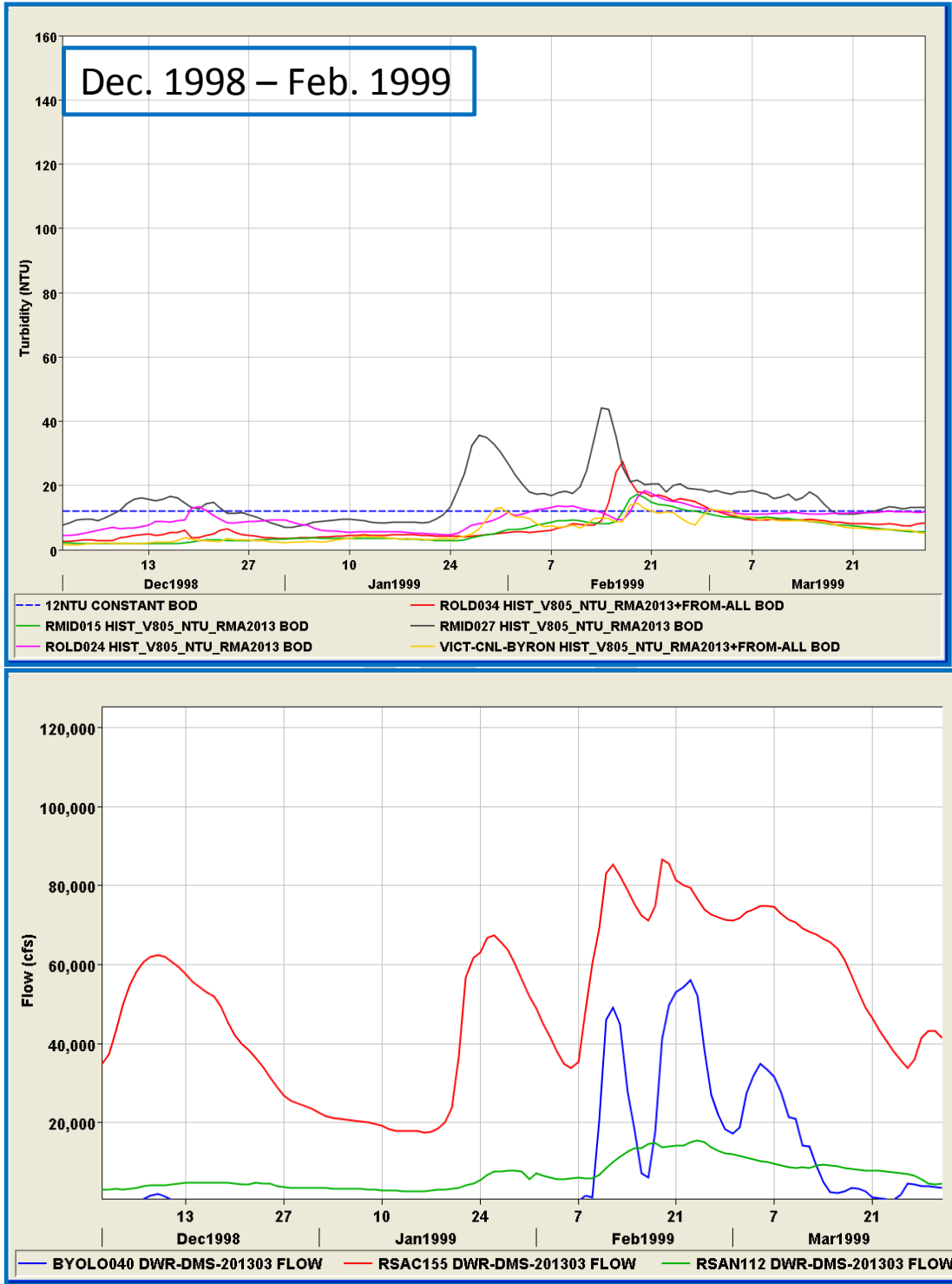


Figure 7-25 Turbidity time series at six key “bridge” locations (upper), and Sacramento, Yolo Bypass and San Joaquin inflow (lower) in WY 1999.

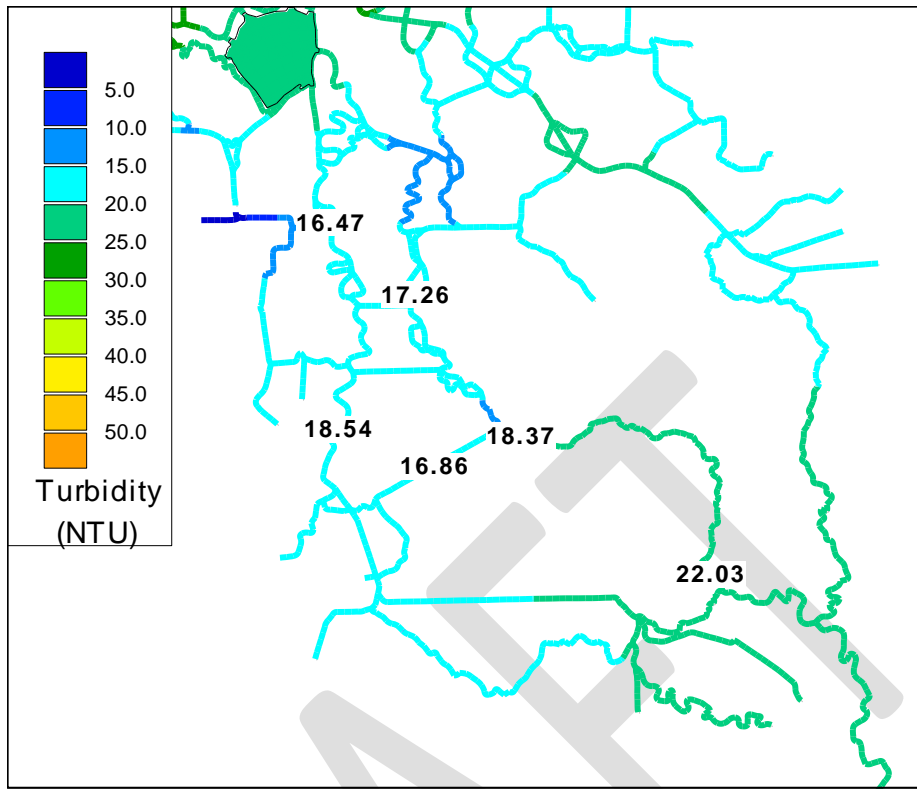


Figure 7-26 February 18, 1999 contour plot showing values at the six key locations. A turbidity bridge just barely formed this year, and this may simply be considered an artifact of the bias toward high turbidity values.

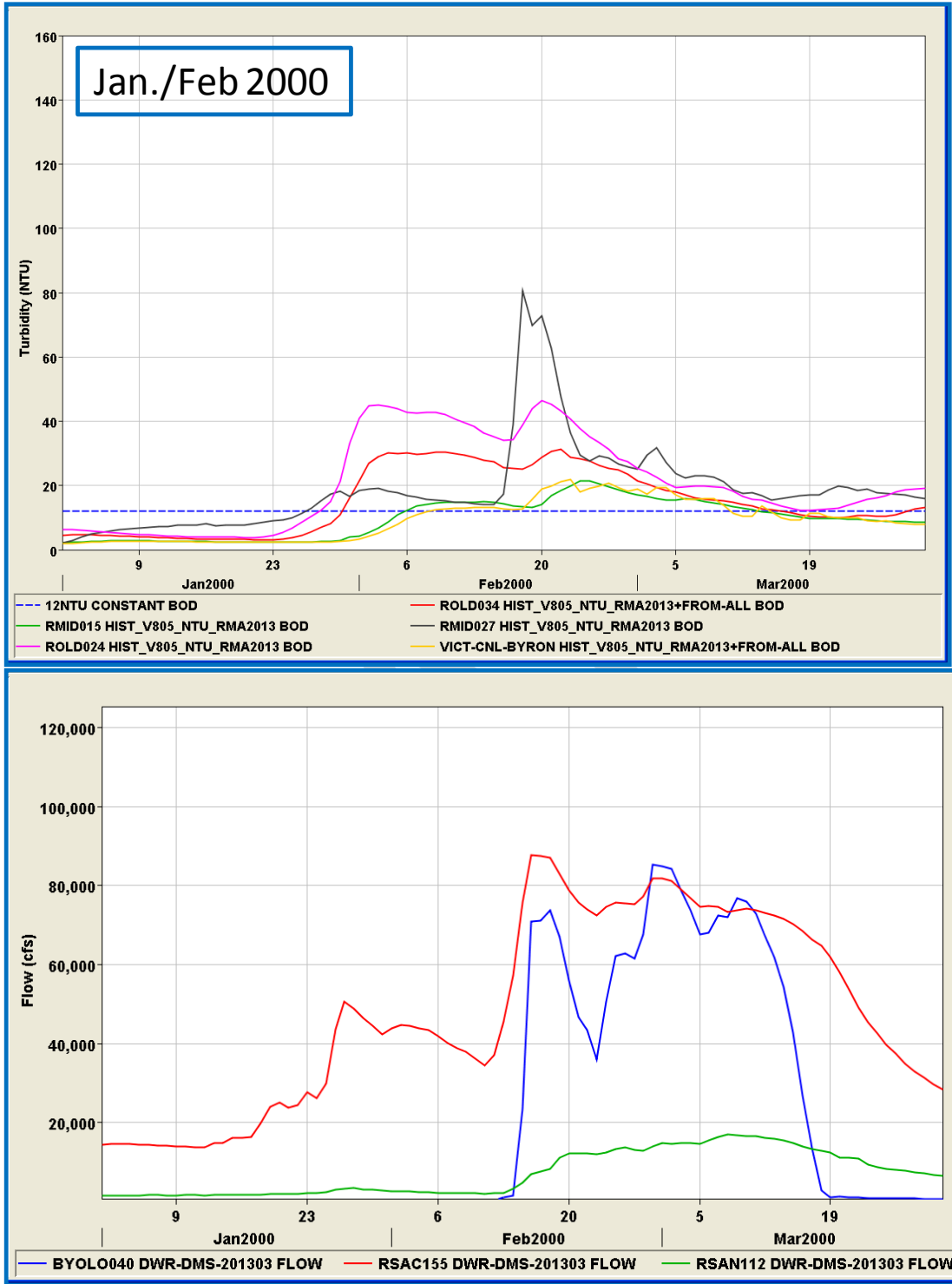


Figure 7-27 Turbidity time series at six key “bridge” locations (upper), and Sacramento, Yolo Bypass and San Joaquin inflow (lower) in WY 2000.

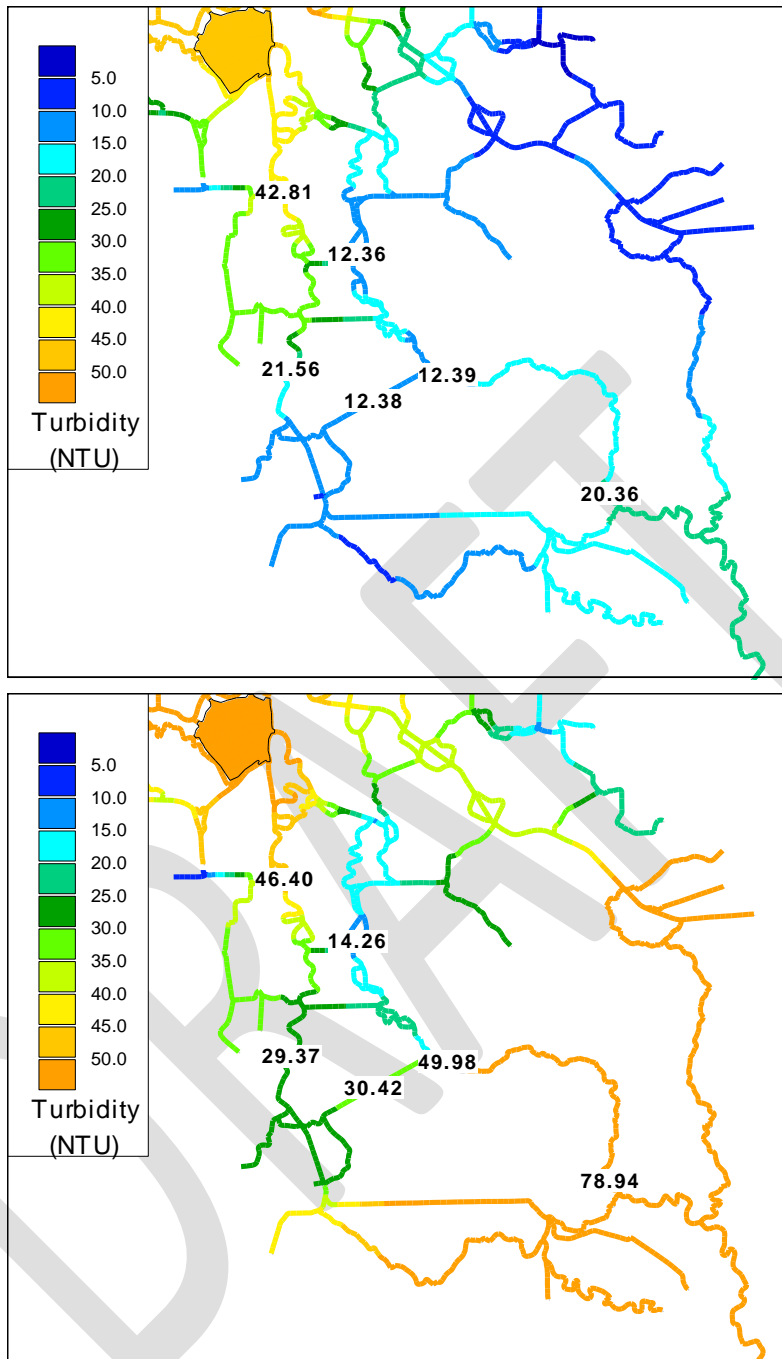


Figure 7-28 February 5 (upper) and 19 (lower) 200 contour plots showing values at the six key locations for the two turbidity pulses of this season - the progression of the predominant turbidity pulse is initially southward along Old and Middle Rivers, and later from the south due to the increased San Joaquin River inflow.

## 8 Summary and Conclusions

As described in previous sections of this report, the model results described herein support three main objectives: updating and refining the previous QUAL turbidity transport model calibration (RMA 2013); refining the long-term (1975 – 2011) turbidity simulation to support training of a Turbidity ANN and calculating wet-season statistics in comparison with EMP grab-sample turbidity data; and, investigating conditions leading to the creation of a “turbidity bridge” joining the central and south Delta with turbidity values of 12 NTU or greater. To document the accomplishment of the first two objectives, statistical measures were employed to quantify the success of the modeling efforts. Metrics to quantify “model skill” were defined for the results of the first objective as an aid in appropriate model application with a focus on decision support. In this application, the decision support objective was realized with a focus on maximizing model skill (*i.e.*, minimizing model error) at the three in-Delta turbidity compliance locations - at Holland Cut, Prisoner Point and Victoria Canal at Byron – as turbidity levels at these locations have the potential to influence decisions changing Delta operations.

The QUAL turbidity model calibration was refined using data available during the wet seasons of WY2010, WY2011 and WY2013. The simulation process started with the development of flow, stage and turbidity BCs that were carefully QA'd, and subject to time shifts or corrections to best match CDEC flow, stage and turbidity data. The calibration process started with WY2013, as the Historical results in that time span were poor using the parameter set from (RMA 2013). After iterative calibration simulation tests failed to produce better statistics in WY2013, calibration in WY2010 and WY2011 was revisited along with the setting of the Calaveras boundary turbidity.

Minimizing the magnitude of the model bias, whether positive or negative, was given a priority over improving other statistics, as mentioned in Section 5, and in addition minimizing the degradation of the other statistics where possible. Particular attention was paid to the three compliance locations and the model bias at these locations due to their important role influencing Delta operations. Reducing model bias has the general effect of minimizing the magnitude of the difference between the model and reality (*i.e.*, the measured turbidity). An additional reason for minimizing the value of the PBIAS statistics is related to the ability to apply corrections to long-term averaged results – for example, if a given location is generally modeled as higher than data (negative PBIAS), then the interpretation of that model value can be assessed with the additional knowledge .

The calibration statistics document that the recalibration substantially improved the representation of Delta turbidity in WY2013 and WY2011 and mixed results in WY2010 at the three turbidity measurement compliance locations in the central and south Delta – Holland Cut, Prisoner Point and Victoria Canal at Byron. In WY2010 there was a loss in the results for the PBIAS statistic particularly along Old River and at the Holland Cut compliance location. Conversely, results were markedly better along Old River and at the Holland Cut compliance location in WY2011 and WY2013. These particular results clearly indicate the difficulty in this calibration work, as there was a clear trade-off in performance between these modeled years. The Model Skill assessment indicates that the overall model skill was improved by the recalibration effort in WY2011 and WY2013, with a mix of loss and improvements in WY2010.

The new set of calibration parameters was then applied to both the “early” and “recent” simulations in the long-term Historical model used in training the Turbidity ANN. The Mixed-SSC-WARMF set of turbidity boundary condition for the San Joaquin and Sacramento Rivers were reviewed, and although the San Joaquin boundary was found to retain a good match, the Sacramento boundary conditions was revised. The revised Freeport boundary condition produces a range of modeled values at Hood that are comparable to the range of values seen in CDEC 15-minute turbidity data at Hood (~50 – 350 NTU, or higher) during periods of high inflow, but the IEP grab-sample data is very low in comparison with the range of CDEC data values. Thus, although statistical results for the new calibration during these long Historical models were be calculated by comparing model output with IEP data, the magnitude of the IEP data appears suspect, at least in some locations. The calibration results indicate that, in comparison with EMP data, the long Historical model overestimates the data (the PBIAS is generally negative) – however, given the questions surrounding the EMP turbidity data, this is considered an acceptable result.

The newly calibrated model in the wet seasons of WY2010, WY2011 and WY2013 and the Mixed-SSC-WARMF simulation in the wet seasons of WYs 1991 - 2000 were used for the third objective to analyze the modeled conditions under which a turbidity bridge linking the central and south Delta was likely to form. The high flow/high turbidity periods of Water Years 1991 – 2000 were selected, as they were in (RMA 2013), as they represent a wide range of conditions in the Mixed-SSC-WARMF simulation.

The conditions under which a turbidity bridge might form were slightly different for the two cases – for WYs 2010, 2011 and 2013 where CDEC data was available as a test, a turbidity bridge was deemed to have formed when the 12 NTU value was exceeded in the daily-averaged data (even for a single day) at the compliance locations. For the Mixed-SSC-WARMF simulation the conditions were more stringent as the results are less reliable, since the boundary conditions were either obtained from WARMF model output or synthesized from USGS-SSC data and the EMP data available for calibration was clearly low in many Delta locations.

In general the analysis shows that there is more than one mode under which a turbidity bridge is likely to form which depend on the magnitude of the primary drivers (Sacramento or San Joaquin River inflow, export flows) and their timing. It should be noted that this analysis is based on a turbidity model developed with synthetic or externally calculated (i.e., from WARMF results or SSC) boundary conditions, so results should be interpreted with caution. The results from the WY2010, 2011 and 2013 simulations are therefore are better indicator of the conditions under which a turbidity bridge may form, although limited in scope. In addition, in these recent wet season simulations it was seen that high Calaveras River flows can be important driver in establishing a turbidity bridge. For the longer term simulation, it was found that the change in the calibration parameters changed the results somewhat from the previous turbidity bridge analysis in (RMA 2013), but the general trends were similar.

Finally, as suggested in previous RMA documentation (RMA 2010b, 2011, 2012b) and in Section 2.3 development of a true suspended sediment model should be considered. The capability of a suspended sediment model to include wind-driven re-suspension of sediments, tidally-influenced suspension of sediments, variations in the character of suspended sediment composition at model boundaries, and

other factors that are not considered in these turbidity model calculations, has the potential to improve the quality of model results. In addition, as the Calaveras River can have an important influence on central and south Delta turbidity, as seen in WY2011, it would be helpful to have an additional CDEC turbidity monitoring station along the Calaveras River.

DRAFT

## 9 References

- Department of Water Resources (DWR), 2011. Internal DMS Memorandum: Turbidity Modeling with DSM2 Version 8.
- Fitzpatrick, J.J. Assessing skill of eutrophication models for water quality managers. Water Environment Federation, 2009.
- Hetland, R.D. Event-driven model skill assessment. *Ocean Modelling*. 11(2006): 214-223.
- King, I.P., 1995. RMA11 – A two-dimensional finite element quality model, Resource Management Associates.
- Joliff, J.K., J.C. Kindle, I. Shulman, B. Penta, M. A.M. Fredrichs, R. Helber, R.A. Arnone. Summary diagrams for coupled hydrodynamic-ecosystem skill assessment. *J of Marine Systems*. 76(2009): 64-82.
- Keenlyside, N.S., M. Latif, J. Jung, Claus, L. Kornlueh, E. Roeckner. Advancing decadal-scale climate prediction in the North-Atlantic sector. *Nature*, Vol. 453, May 2008. 84-88.
- Moriasi, D.N., J.G. Arnold, M.W. Van Liew, R.L. Bingner, R.D. Harmel, and T.L. Vieth. 2007. Model evaluation guidelines for systematic quantification of accuracy in watershed simulations. *Transactions of the ASABE*. Vol. 50(3).
- Resource Management Associates, Inc. (RMA), 2008. "San Francisco Bay-Delta Turbidity Modeling", prepared for Metropolitan Water District of Southern California.
- Resource Management Associates, Inc. (RMA), 2009a "Particle Tracking and Analysis of Adult and Larval/Juvenile Delta Smelt for 2-Gates Demonstration Project", prepared for Metropolitan Water District of Southern California.
- Resource Management Associates, Inc. (RMA), 2009b. "Numerical Modeling in Support of Suisun Marsh PEIR/EIS: Technical Appendix", prepared for Jones and Stokes Associates.
- Resource Management Associates, Inc. (RMA), 2010a. Spatial Animation of Observed Turbidity Time Series for the Sacramento-San Joaquin Delta.
- Resource Management Associates, Inc. (RMA), 2010b. Turbidity and Adult Delta Smelt Forecasting with RMA 2-D Models: December 2009 – May 2010.
- Resource Management Associates, Inc. (RMA), 2011. Turbidity and Adult Delta Smelt Forecasting with RMA 2-D Models: December 2010 – February 2011.
- Resource Management Associates, Inc. (RMA), 2012a. RMA/Systech Collaboration to Improve WARMF Model Turbidity Estimates.
- Resource Management Associates, Inc. (RMA), 2012b. Turbidity and Adult Delta Smelt Modeling with RMA 2-D Models: December 2011 – February 2012.

Stow, C.A., J. Joliff, D.J. McGillicuddy Jr, S.C. Doney, J.I. Allen, M. A.M. Friedrichs, K.A. Rose, P. Wallhead. Skill assessment for coupled biological/physical models of marine systems. *J of Marine Systems*. 76(2009): 4-15.

Taylor, K.E. Summarizing multiple aspects of model performance in a single diagram. PCMDI Report No 55 (Revised), Sept. 2000.

Trucano, T.G., L.P. Swiler, T. Igusa, W.L. Oberkampf, M. Pilch. 2006. Calibration, validation, and sensitivity analysis: What's what. *Reliability Engr. & System Safety*. Vol. 91: 10-11. pp 1331 – 1357.

DRAFT

## 10 Appendix I

### 10.1 Model Skill

#### 10.1.1 Background

In this section, information is presented on model skill. A number of publically-available articles were identified as pertinent background information for the project. This information constitutes a brief overview of the topic of model skill, and is not considered or intended to be comprehensive. Instead, this assessment is intended to supply some basic definitions and to note recent applications of model skill metrics, with a focus on water quality applications

Given the nature of the turbidity model as a proxy for suspended sediment transport, a model calibration step might improve the quality of the calibration in some locations in one year, but deteriorate the quality in those locations in a different year. Thus, it was necessary to define at least one metric for the model domain that could be used to quantify calibration progress and to determine a criterion for model selection.

The motivation behind the investigation of current practice in model skill assessment is the potential that the DSM2 turbidity model output might be used to as a tool to support decisions on Delta operations, potentially in forecasting situations. In general, in those cases where model output may be used in decision support, an assessment of model accuracy is important as decision-makers must weigh the importance they attach to forecasting results and the possible outcome of alternative actions (Stow *et al.* 2009, Fitzpatrick 2009).

The definition of model skill was not universal in the articles reviewed, but in this document we adopt the definition that “model skill” is a measure of the accuracy of a model (Stow *et al.* 2009) – other authors have similarly defined model skill as “fidelity to the truth” (Joliffet *al.* 2009). Since the observations used to assess model skill are imperfect, essentially the “Truth” cannot be known (Joliff *et al.* 2009) so quantification or assessment of observational error is an important component in the overall assessment of model skill. It was noted (as of 2009) that the routine application of rigorous model skill assessment was not broadly reflected in the refereed literature, and that the “community standard” of model-to-data comparisons was the basic visual time series comparison plot (Stow *et al.* 2009).

All authors proposed the use of some sort of model skill metric, either using known statistical measures or in some cases novel assessment metrics (Taylor 2000, Joliffet *al.* 2009, Hetland2006, Fitzpatrick 2009). Model skill was used both to provide information for model selection and implementation (Stow *et al.* 2009). Given the diversity of application and selection of model metrics, it was apparent that the choice of metrics applied and level of skill necessary for a given application were dependent on the context, goals and the spatial and temporal scales of importance (Stow *et al.* 2009, Fitzpatrick 2009).

It was apparent in the articles reviewed that some measure of subjectivity in the metrics chosen for model skill assessment was inevitable. For example, although a model should be able to simulate both

the amplitude and the pattern of variability, the decision of which of these factors is more important is dependent on the application (Taylor 2000).

For univariate comparisons of model output and observations, both graphical techniques (*e.g.*, time series plots) and quantitative metrics were recommended, frequently using residuals and the associated statistics as well as direct comparisons (*e.g.*, correlation coefficient). An interesting graphical technique was developed for multivariate comparisons (Taylor 2000) that was used to monitor overall model performance as a model evolved and in assessing the merits of competing models. Some authors used somewhat more advanced statistical techniques (Hetland 2006, Keenlyside *et al.* 2008)

### **10.1.2 Decisions on model skill assessment for this report**

Two statistics were chosen as basic to calibration accuracy at the locations where CDEC data was available - Percent Bias (PBIAS) calculated using model residuals and the  $R^2$  goodness of fit statistic calculated from the regression equation between model output and data. The utility of all of the residual statistics is presented in (Moriasi *et al.*, 2007). Note that these statistics are among the selection of quantitative metrics noted as useful in the assessment of model skill (Stow *et al.* 2009). Other statistics were calculated, and visual representations of the data-model fit and of the histogram of residuals were presented along with additional residual statistics and the data-model regression plot.

At the outset of the current calibration effort, a decision was made as a model skill criterion to optimize the accuracy of the model at the three Delta turbidity compliance locations – at Holland Cut, Prisoner Point and Victoria Canal at Byron – and to minimize the magnitude of the model bias without sacrificing the desired values of the other residual statistics if possible. Additional detail on the model skill assessment metrics chosen for this project is presented in Section 5.2.1. It is noted that the quantification of observational error (of the turbidity measurements) was not considered, nor were the statistical characteristics of the data specifically considered at measurement locations. In future applications, it would be valuable to specifically consider the statistical characteristics of the observations independent of the residual calculations at the outset of the model skill evaluation process as the “true” state of the modeled system, although unknown, can be assumed to lie within the bounds of observational uncertainty (Stow *et al.* 2009).

## **11 Appendix II – Updated QUAL Turbidity calibration statistics**

### **11.1 Daily-averaged CDEC data and model output – WY2013**

DRAFT

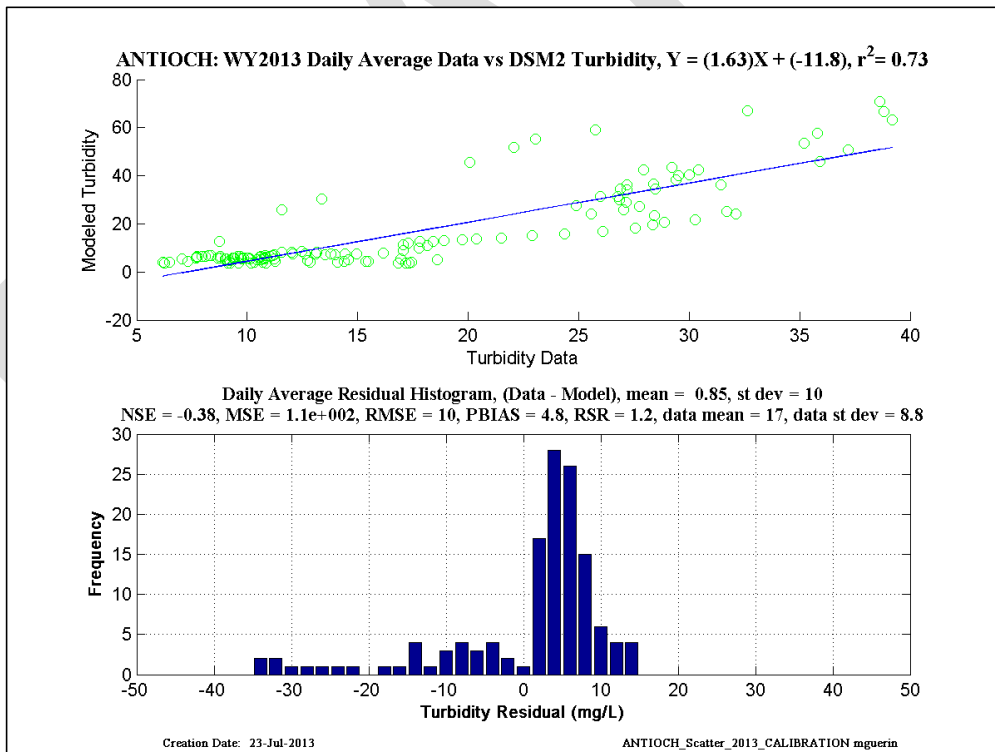
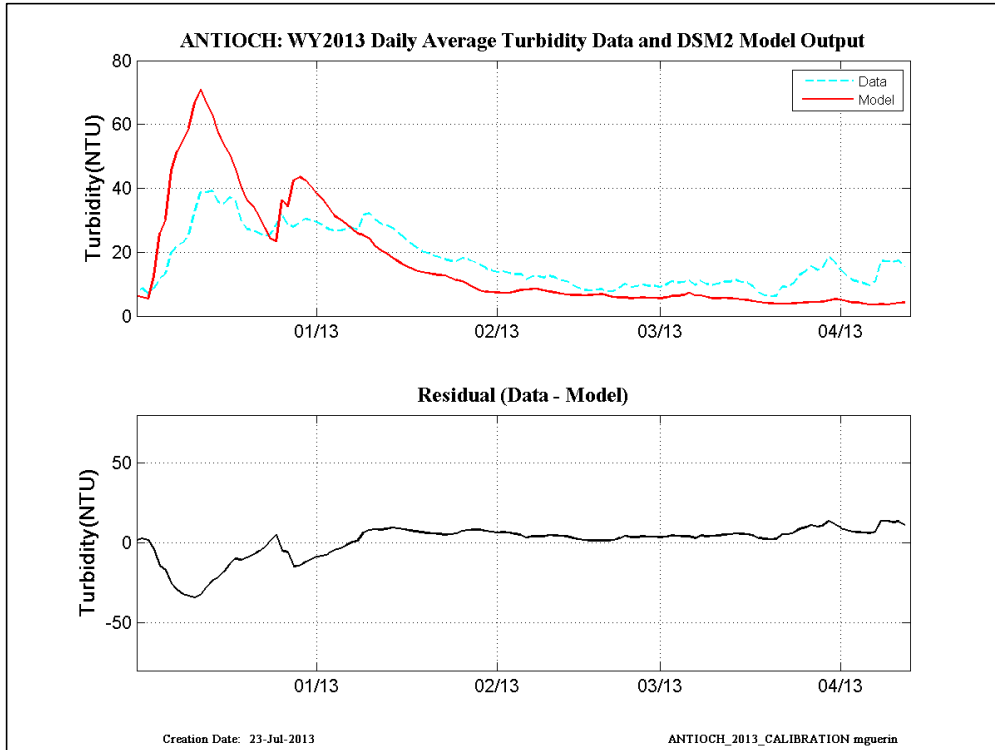


Figure 11-1 WY2013 new RMA calibration results at Antioch.

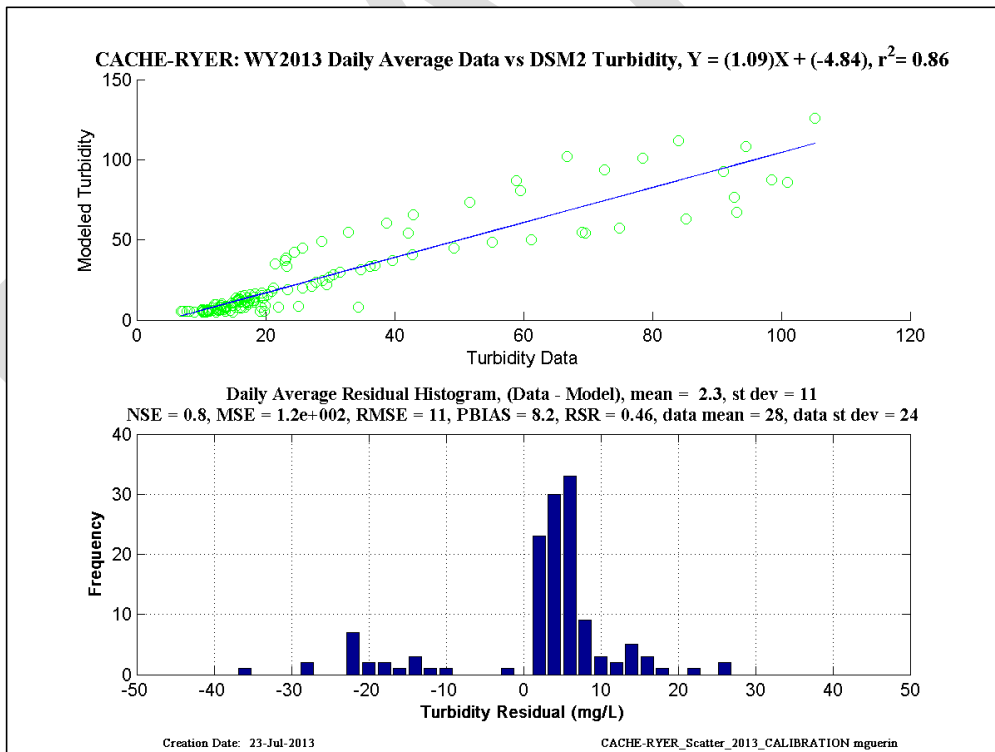
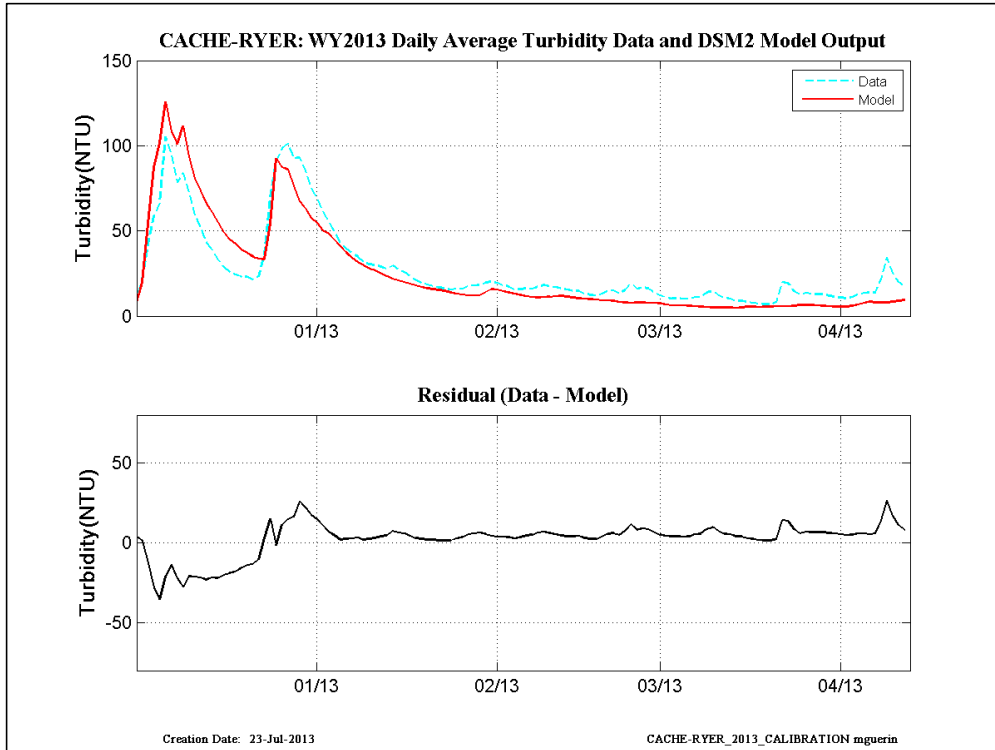


Figure 11-2 WY2013 new RMA calibration results at Cache-Ryer.

## 11.2 Daily-averaged CDEC data and model output - WY2011

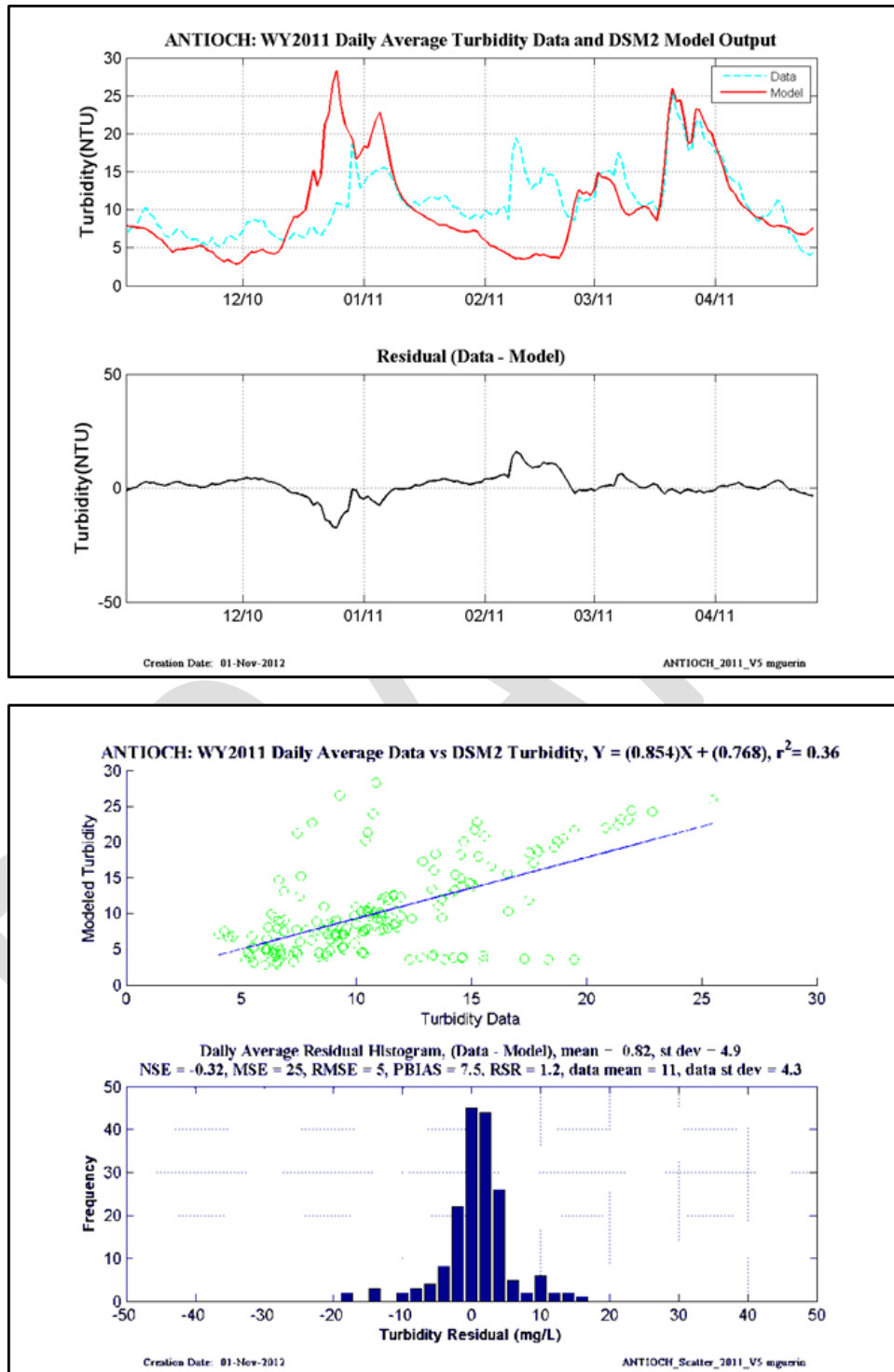


Figure 11-3 WY2011 revised calibration results at Antioch.

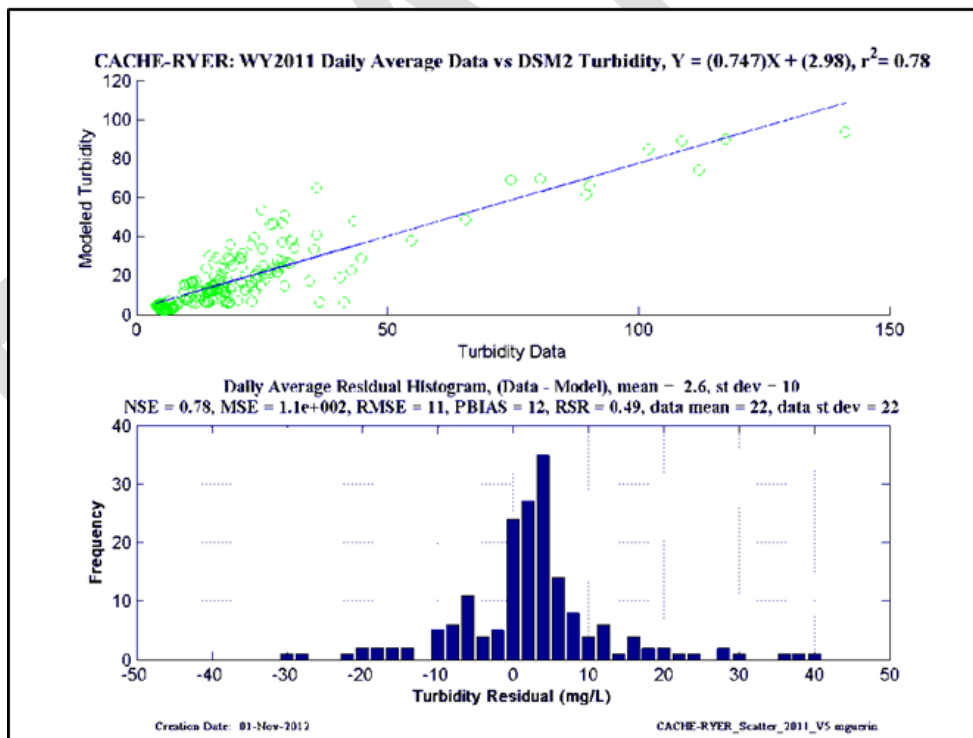
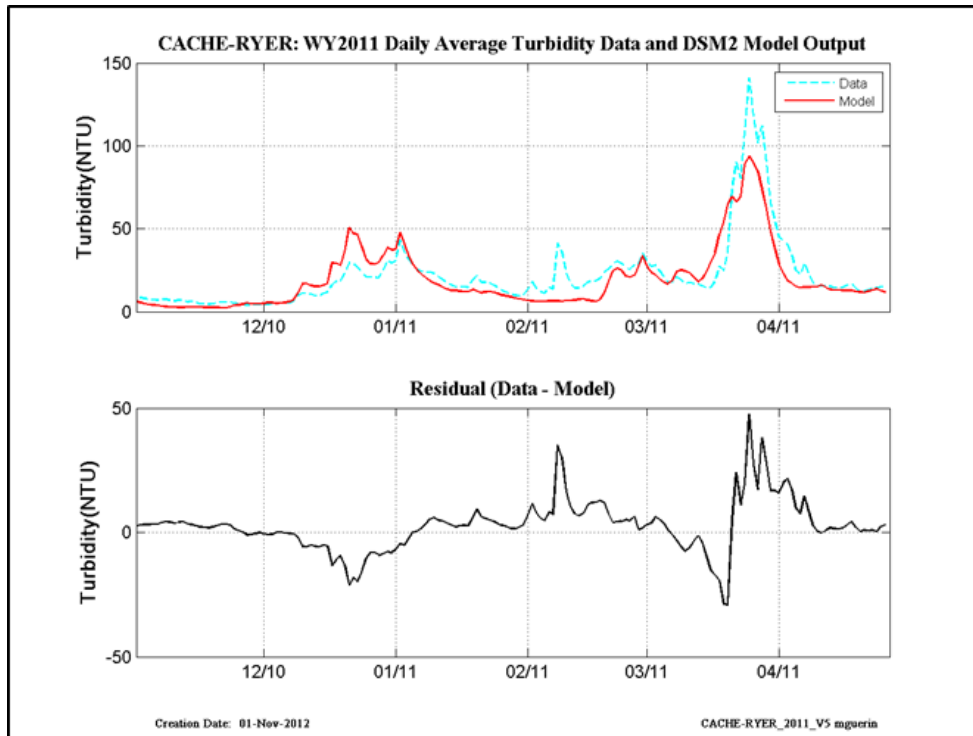


Figure 11-4 WY2011 revised calibration results at Cache-Ryer.

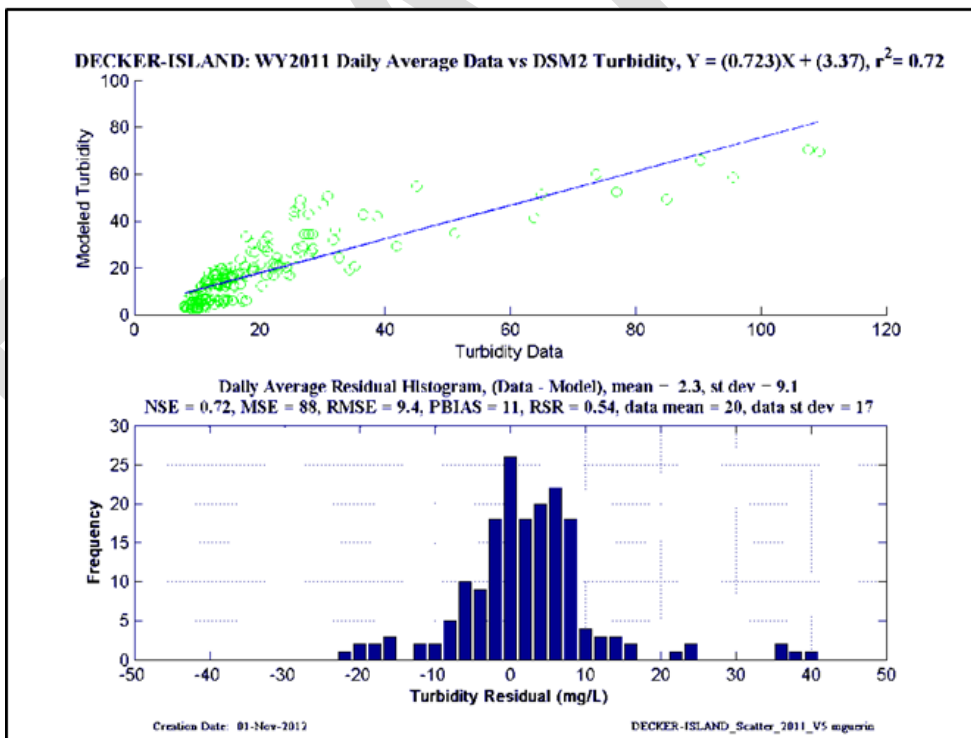
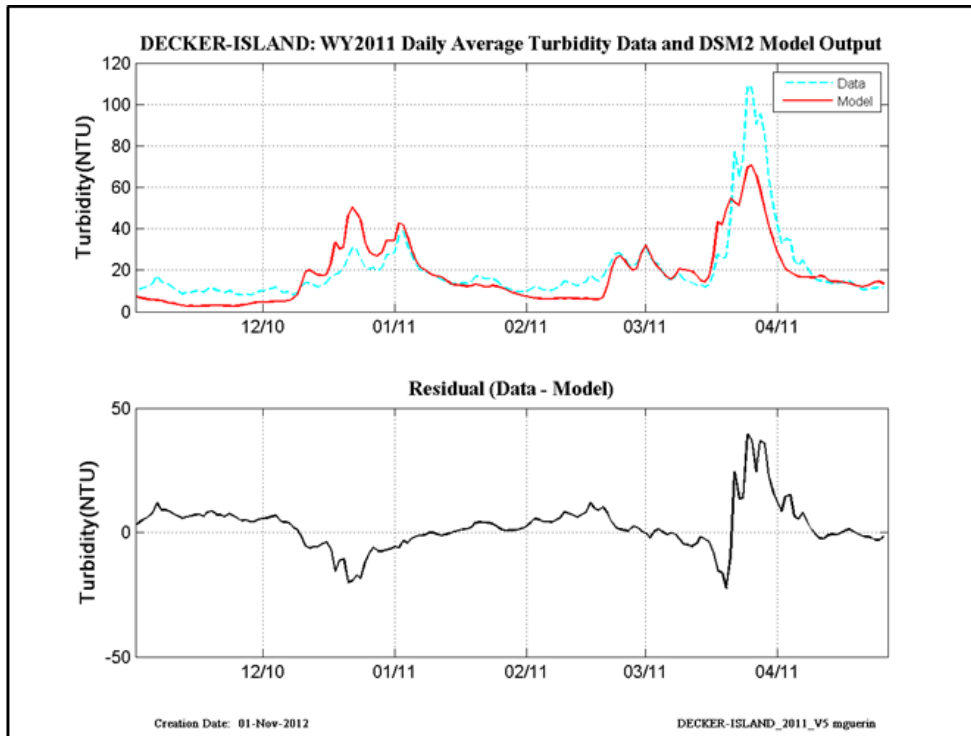


Figure 11-5 WY2011 revised calibration results at Decker Island.

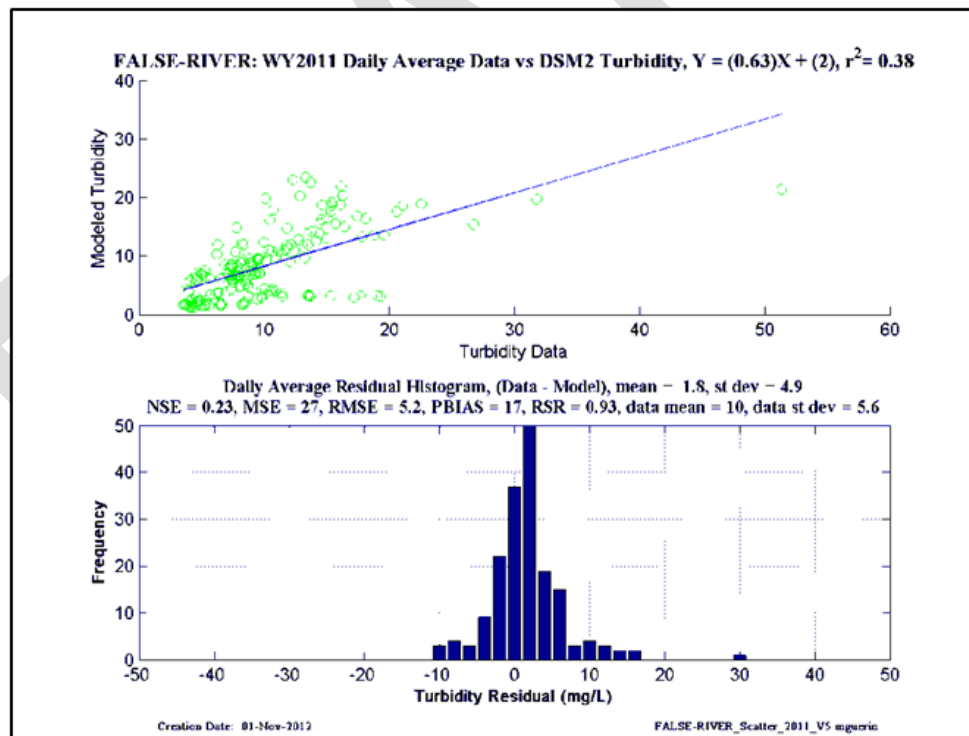
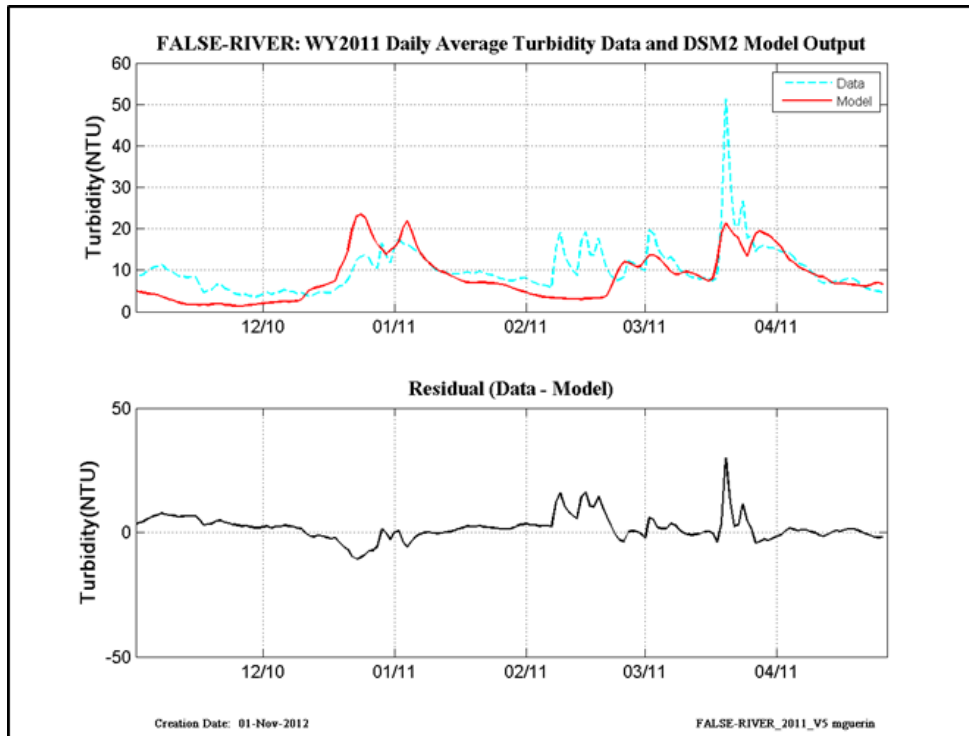


Figure 11-6 WY2011 revised calibration results at False River.

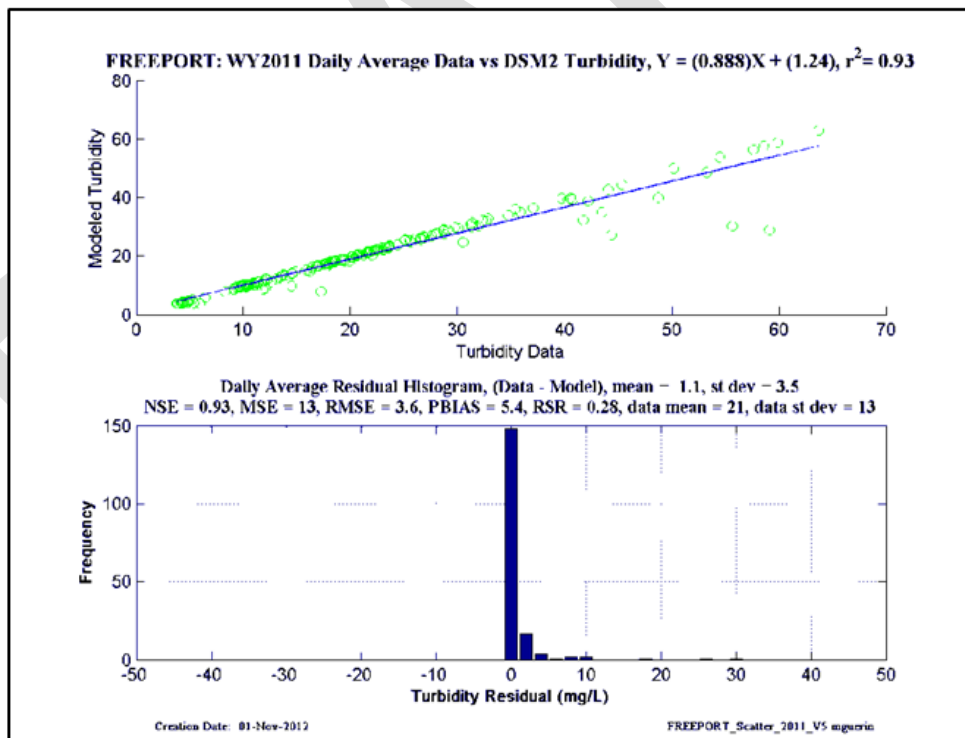
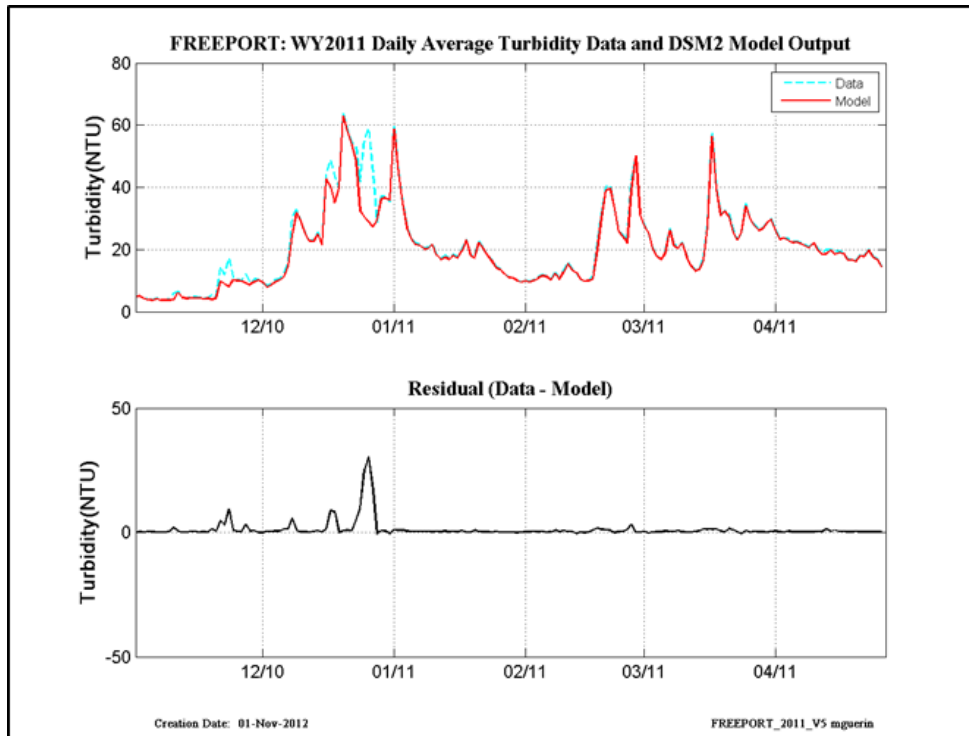


Figure 11-7 WY2011 revised calibration results at Freeport.

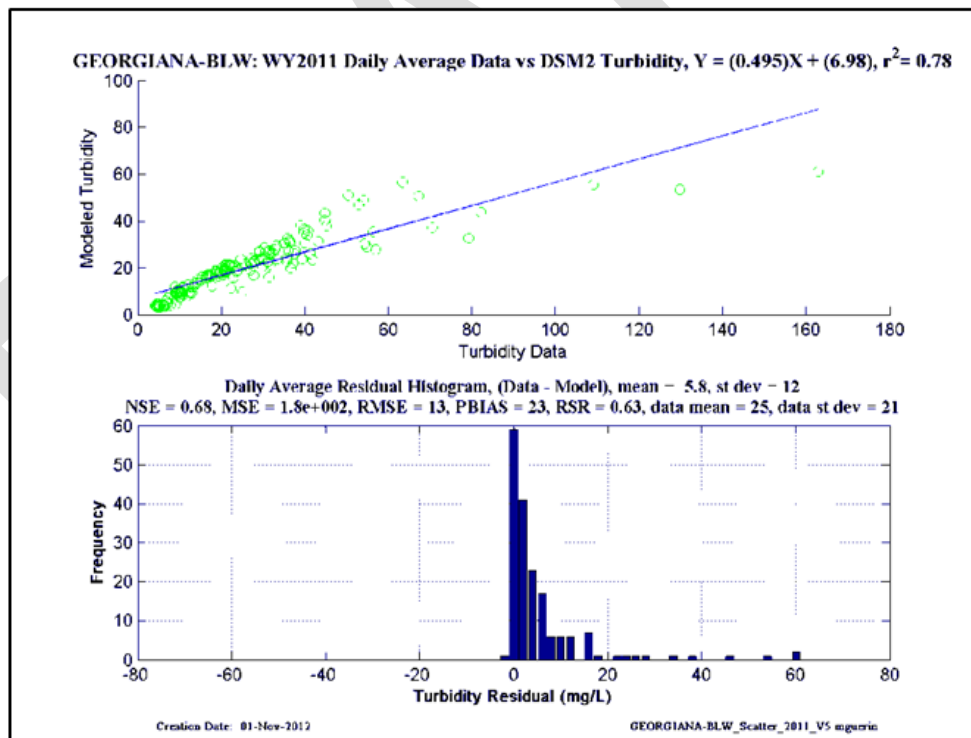
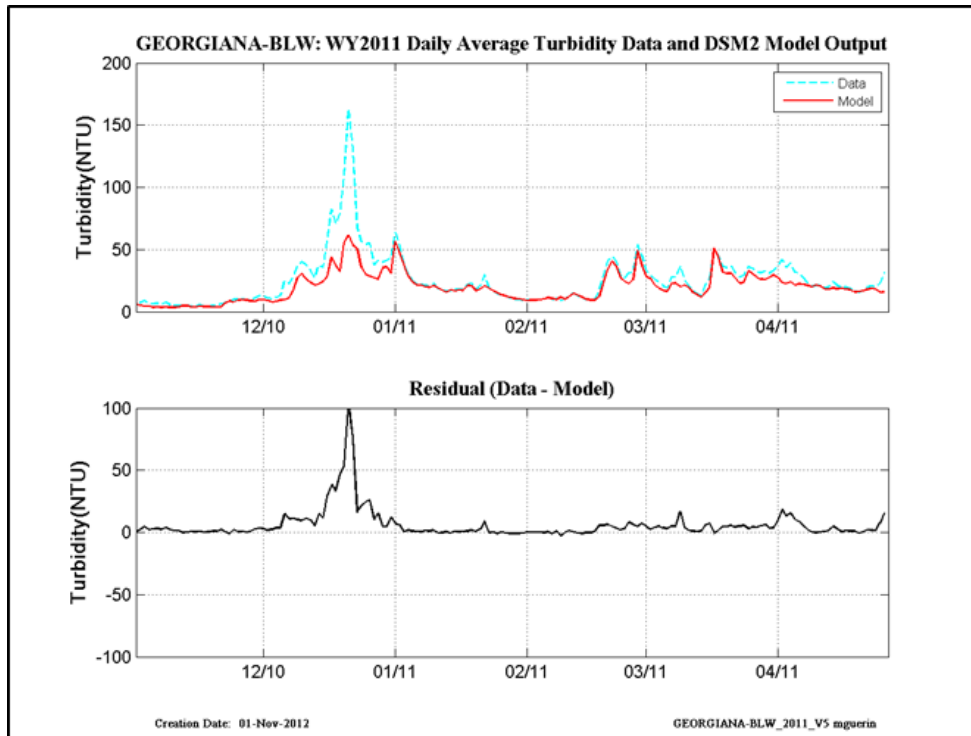


Figure 11-8 WY2011 revised calibration results at Georgiana-Below-Sac.

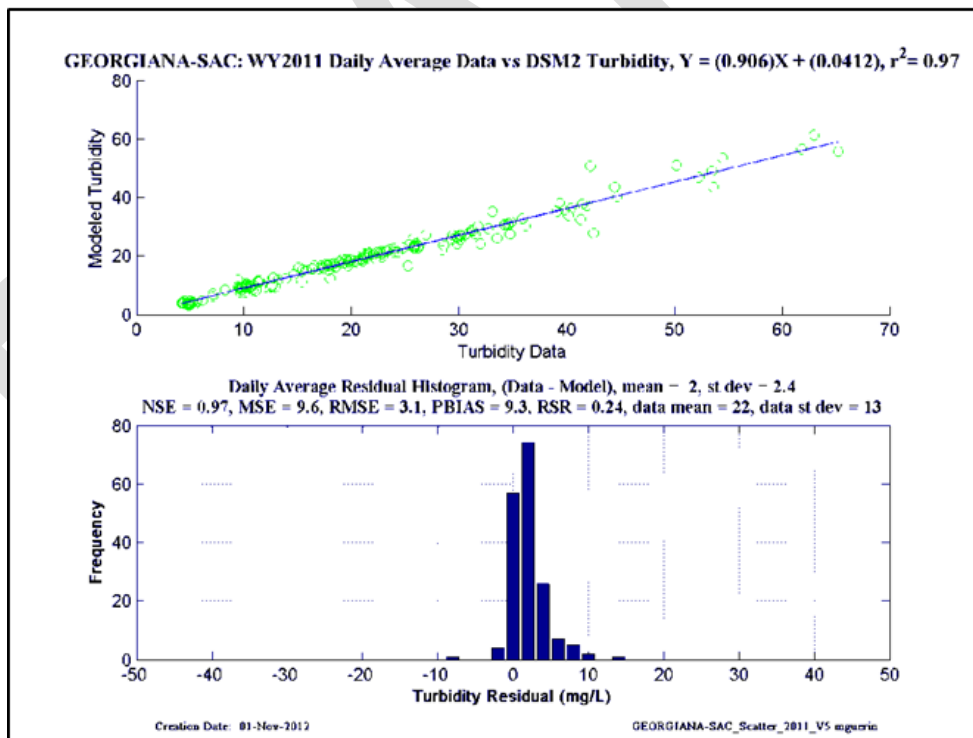
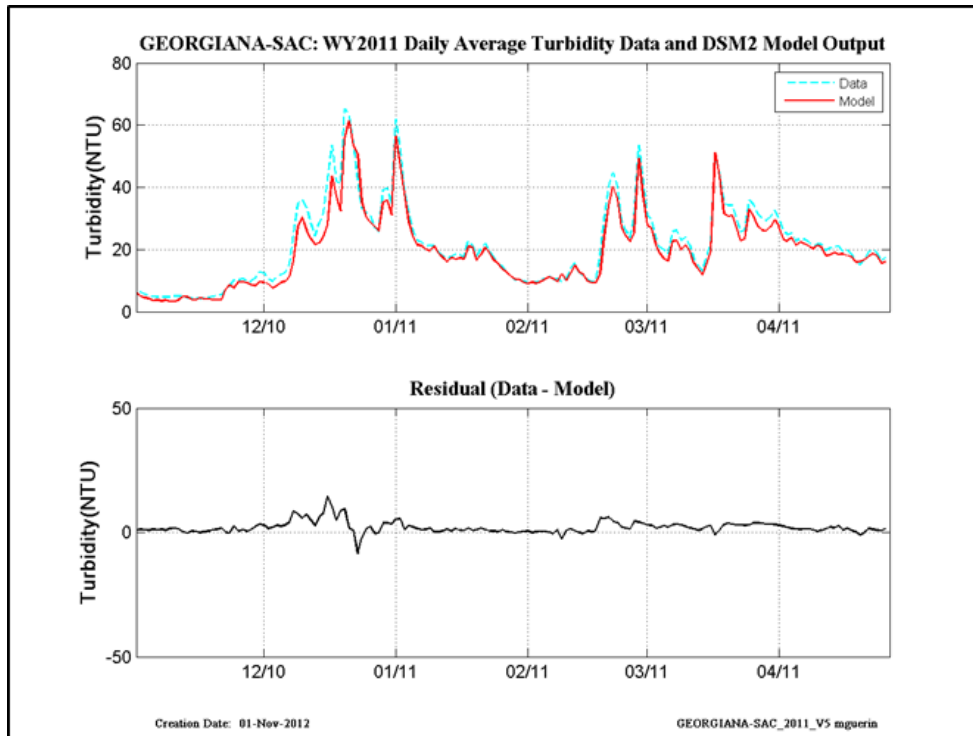


Figure 11-9 WY2011 revised calibration results at Georgiana-at-Sac.

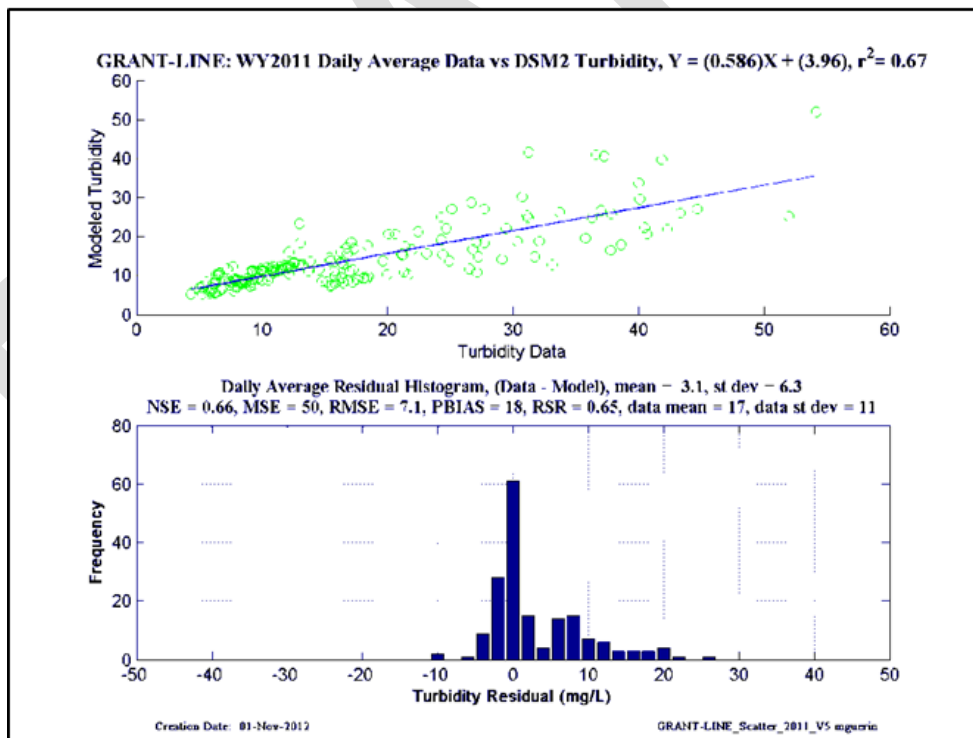
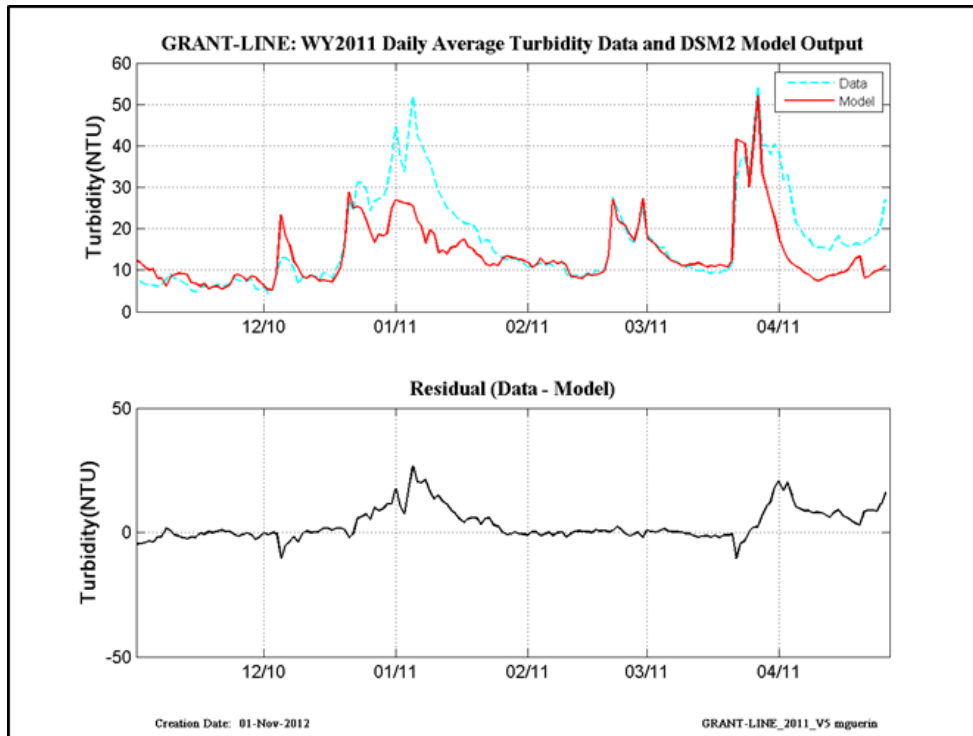


Figure 11-10 WY2011 revised calibration results at Grant Line.

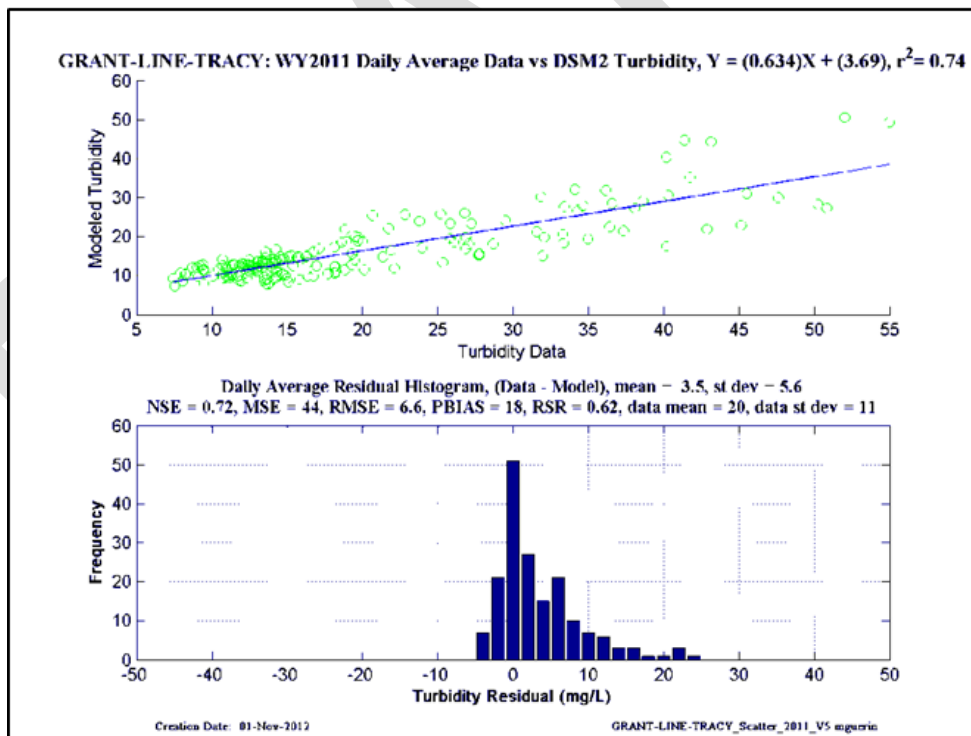
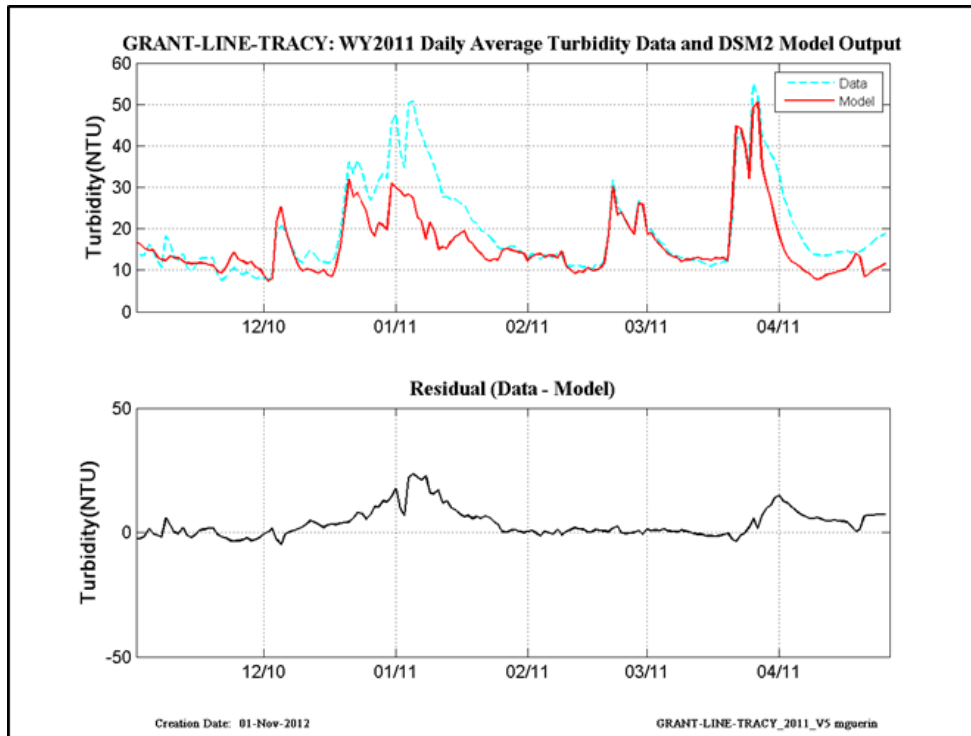


Figure 11-11 WY2011 revised calibration results at Grant-Line Tracy.

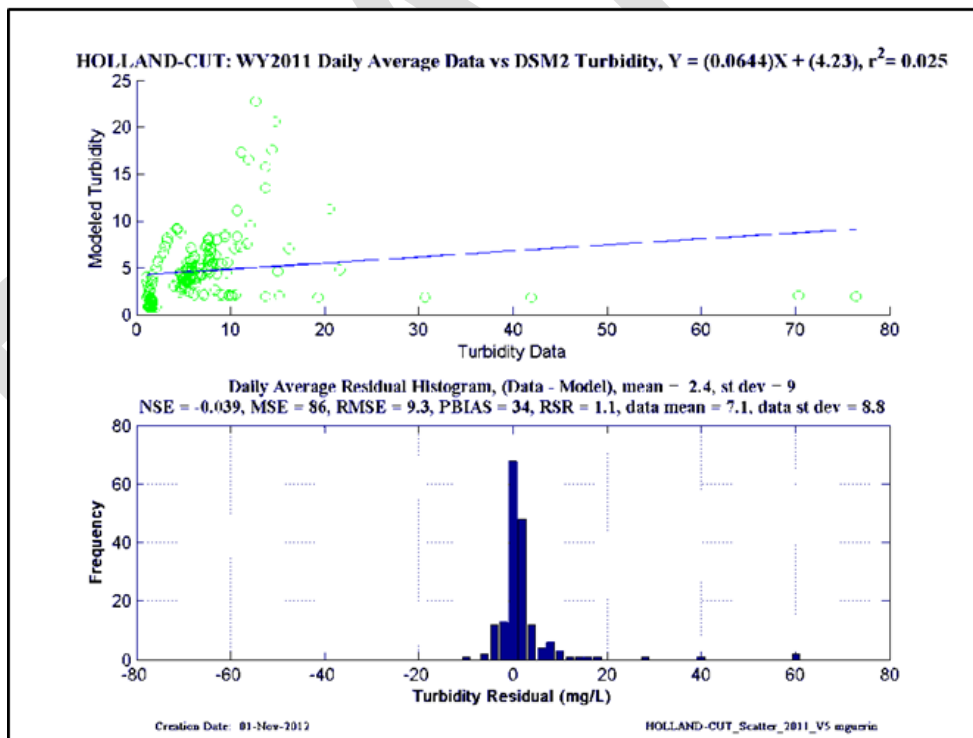
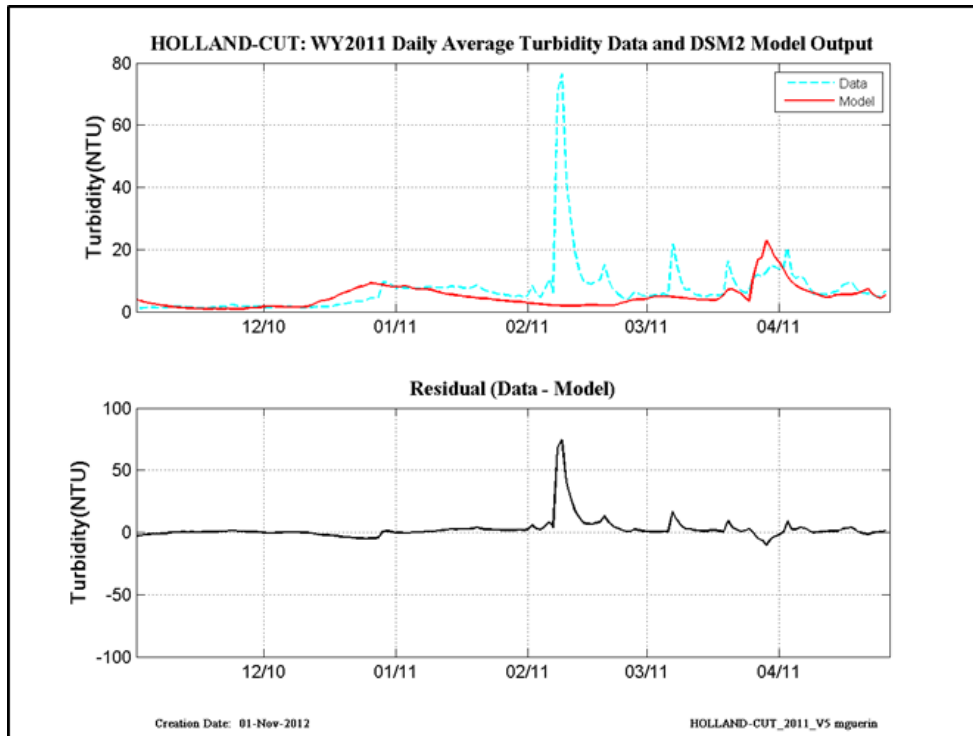


Figure 11-12 WY2011 revised calibration results at Holland Cut.

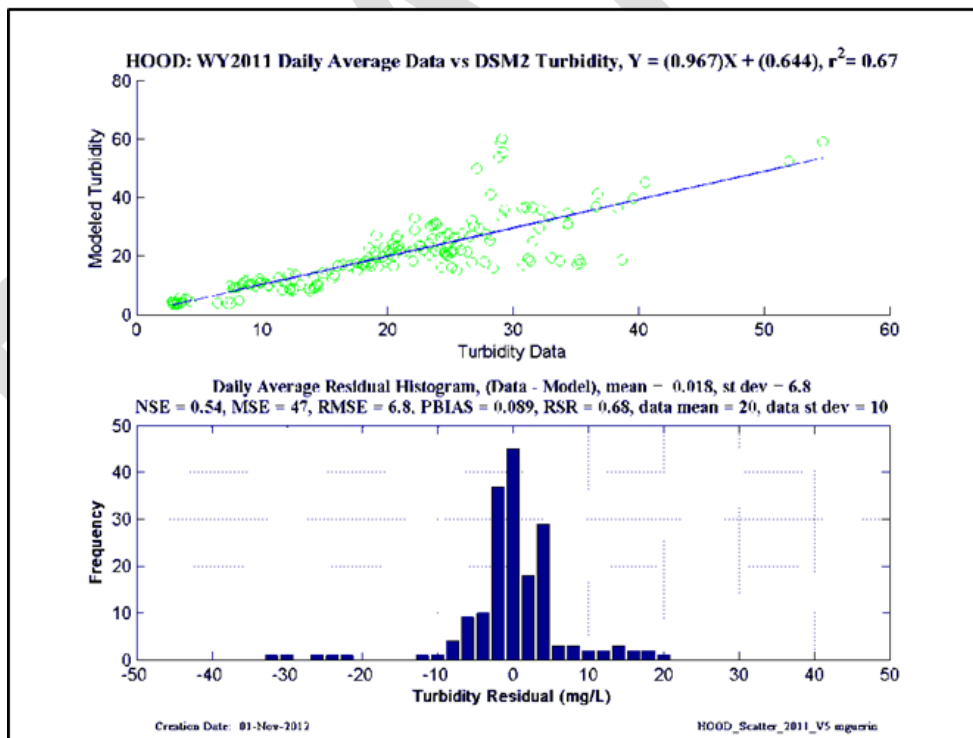
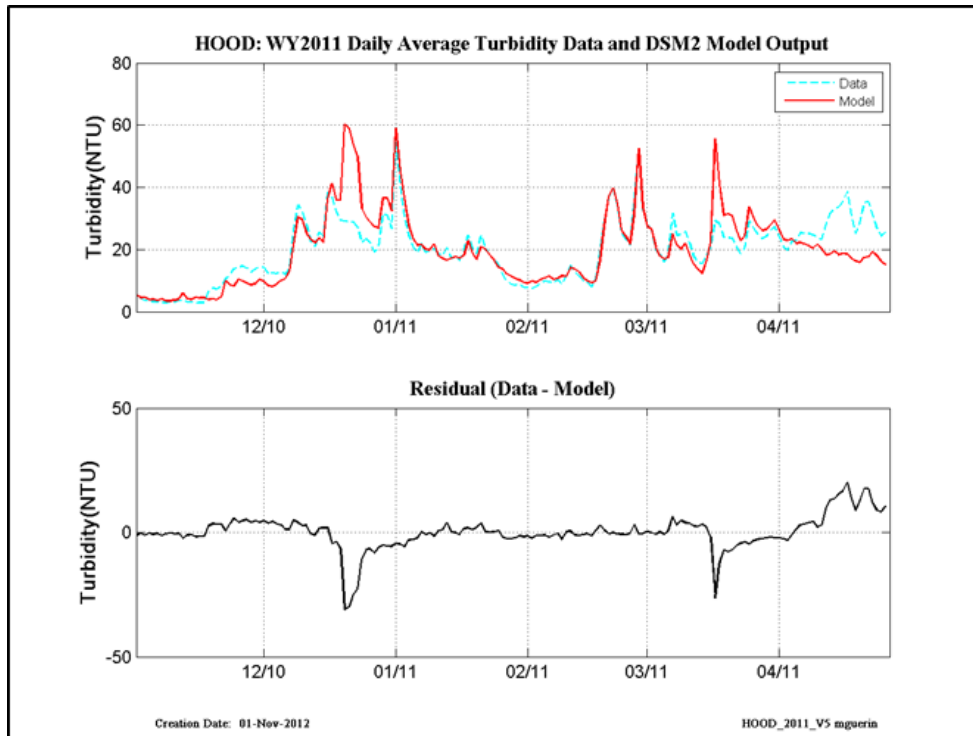


Figure 11-13 WY2011 revised calibration results at Hood.

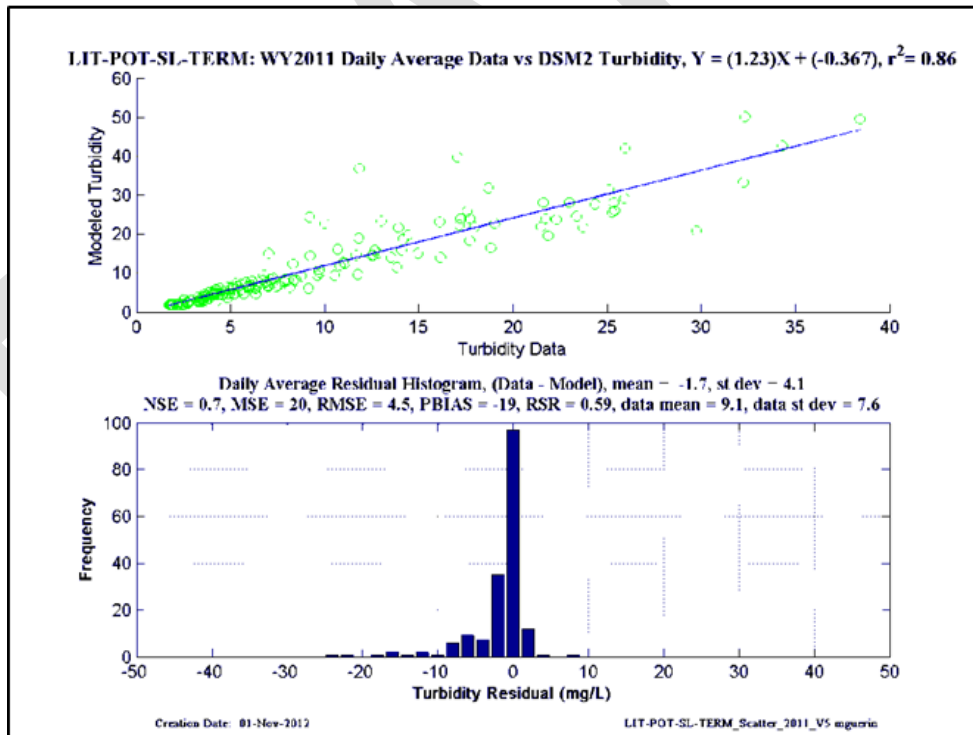
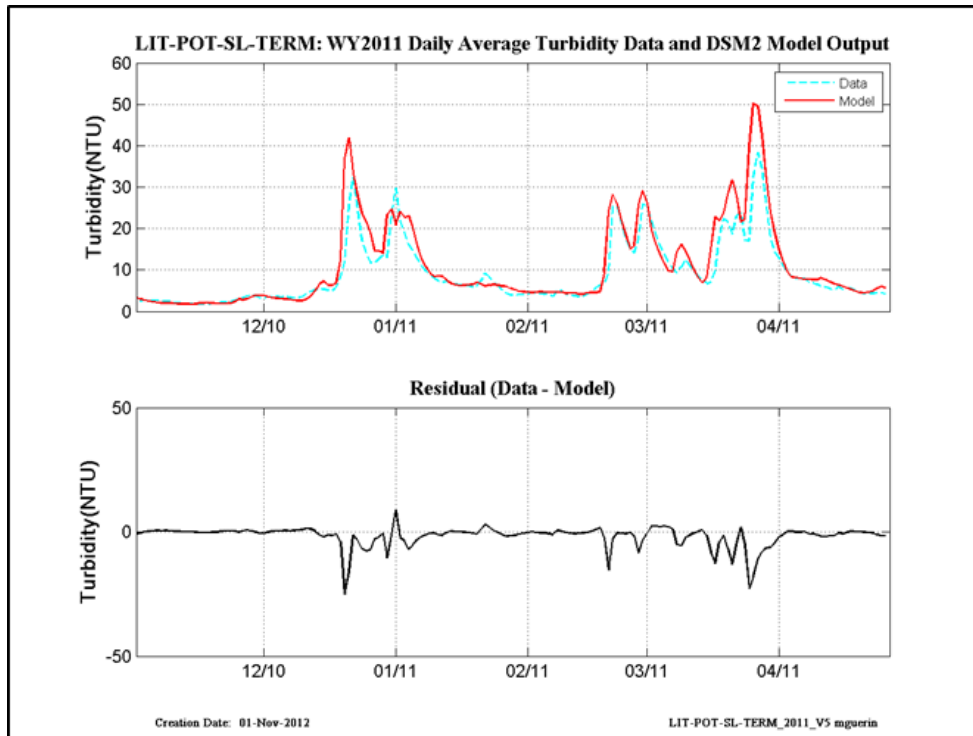


Figure 11-14 WY2011 revised calibration results at Little Potato Slough-at-Terminus.

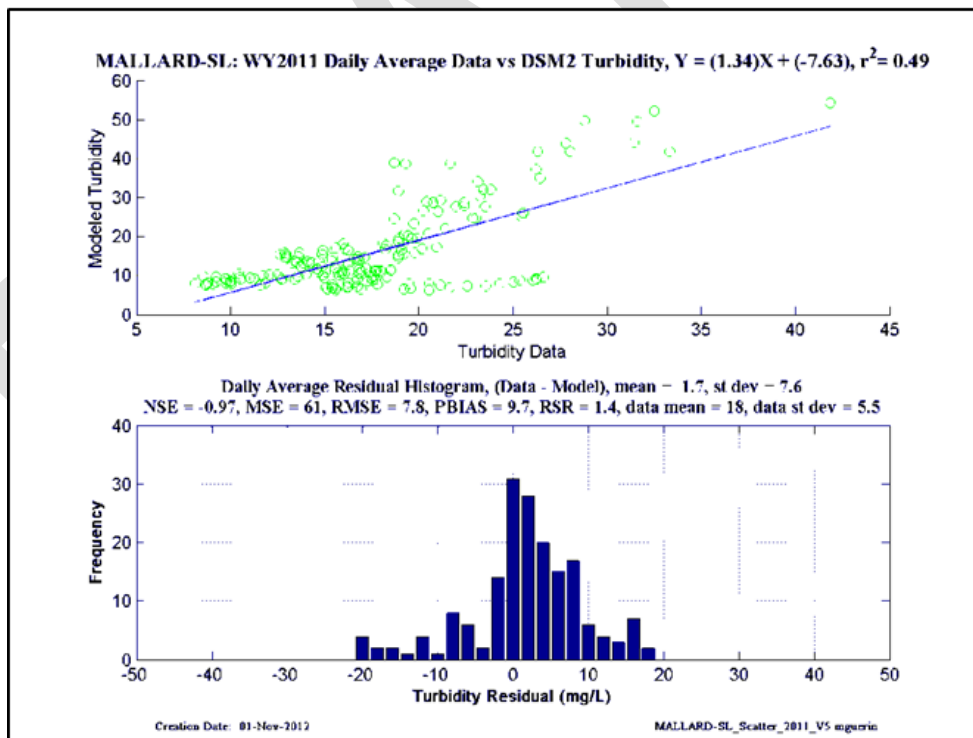
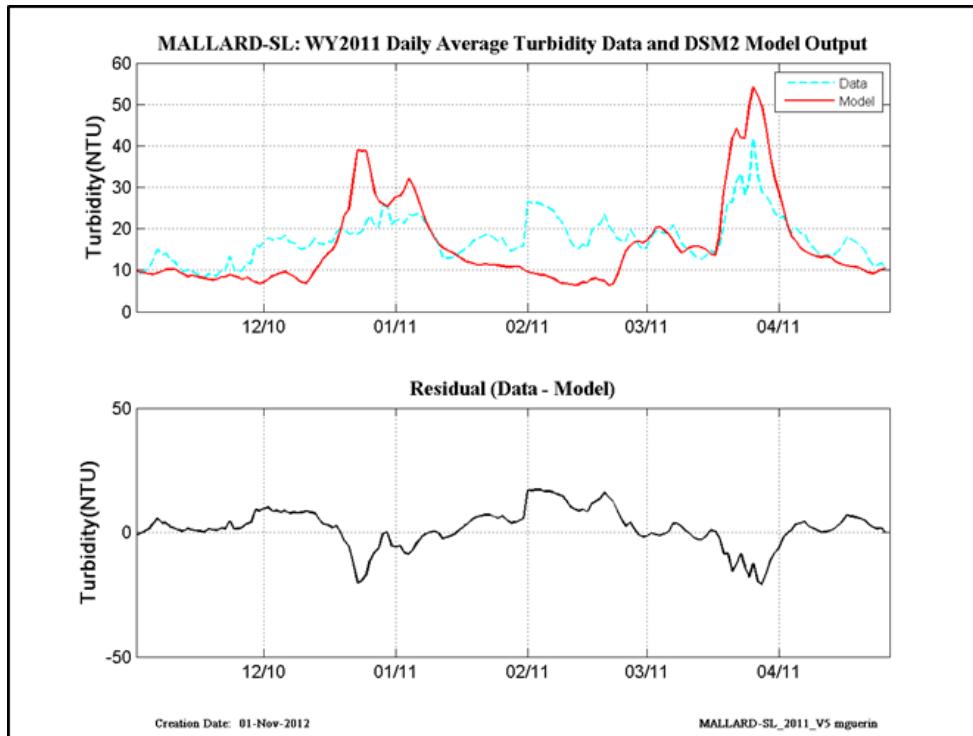


Figure 11-15 WY2011 revised calibration results at Mallard Slough.

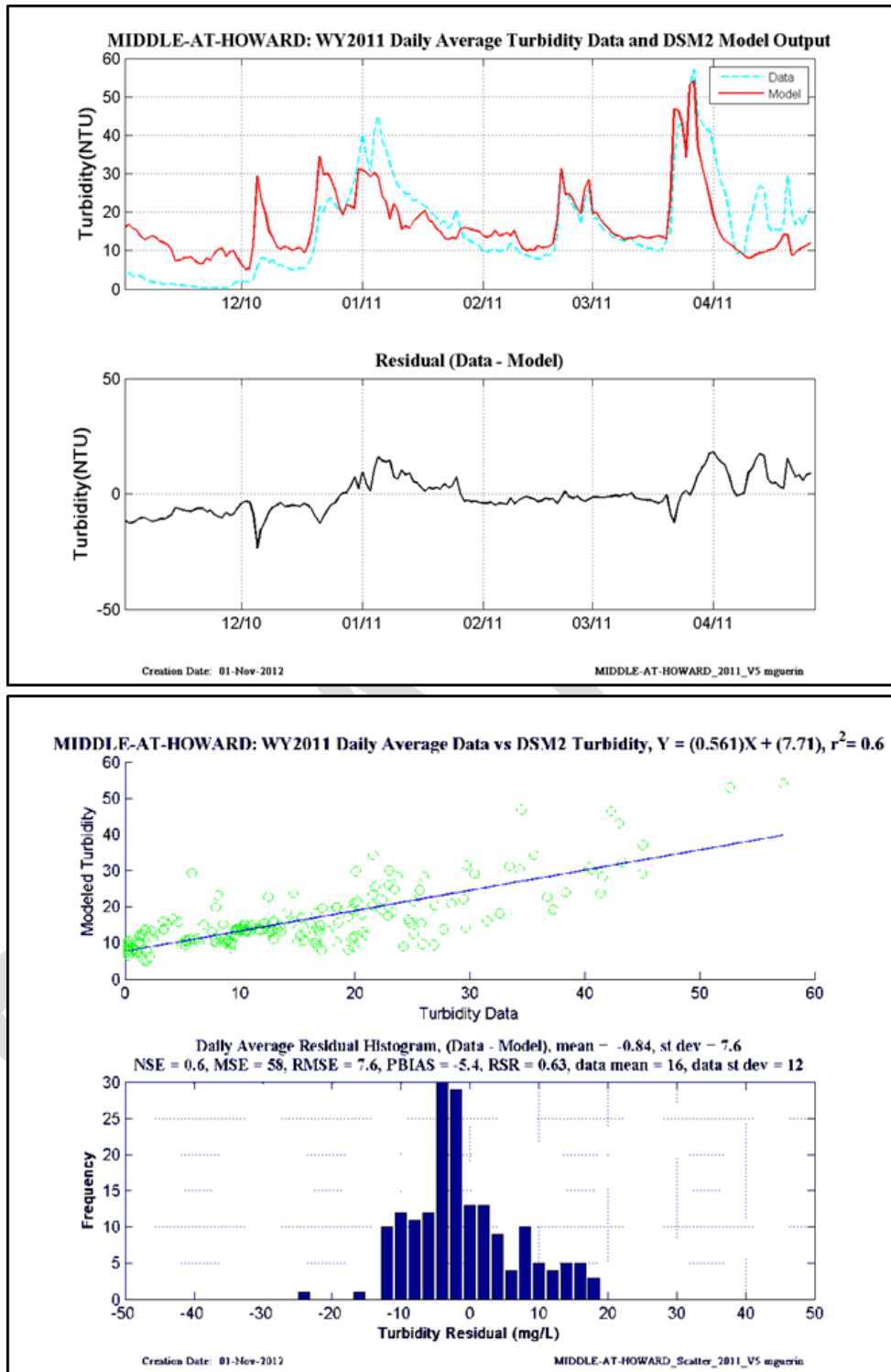


Figure 11-16 WY2011 revised calibration results at Middle River-at-Howard Rd.

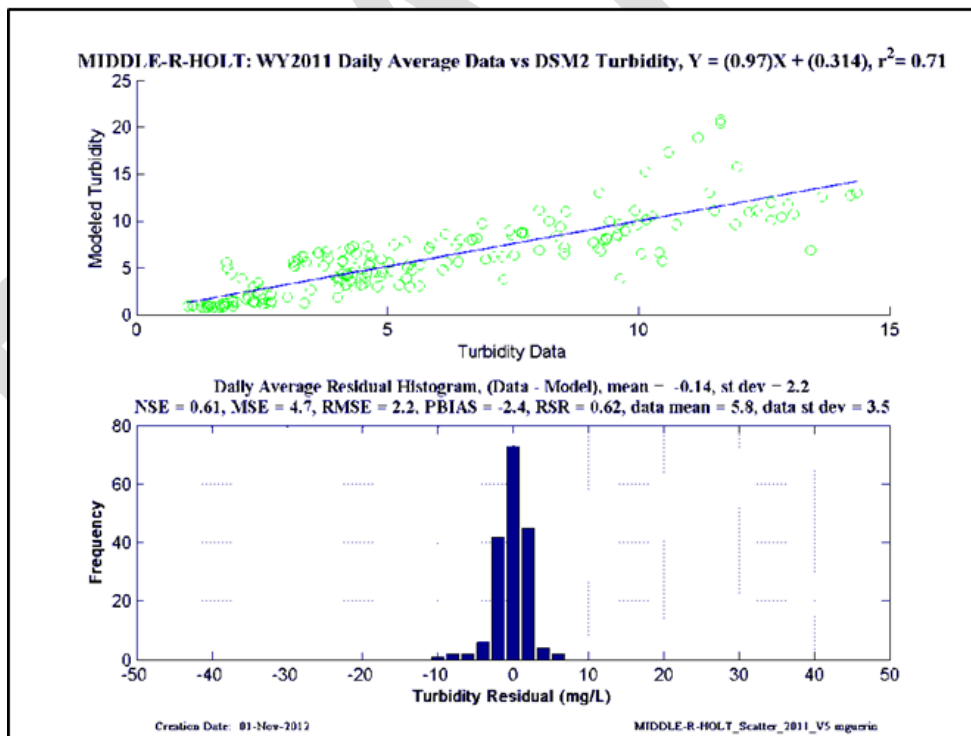
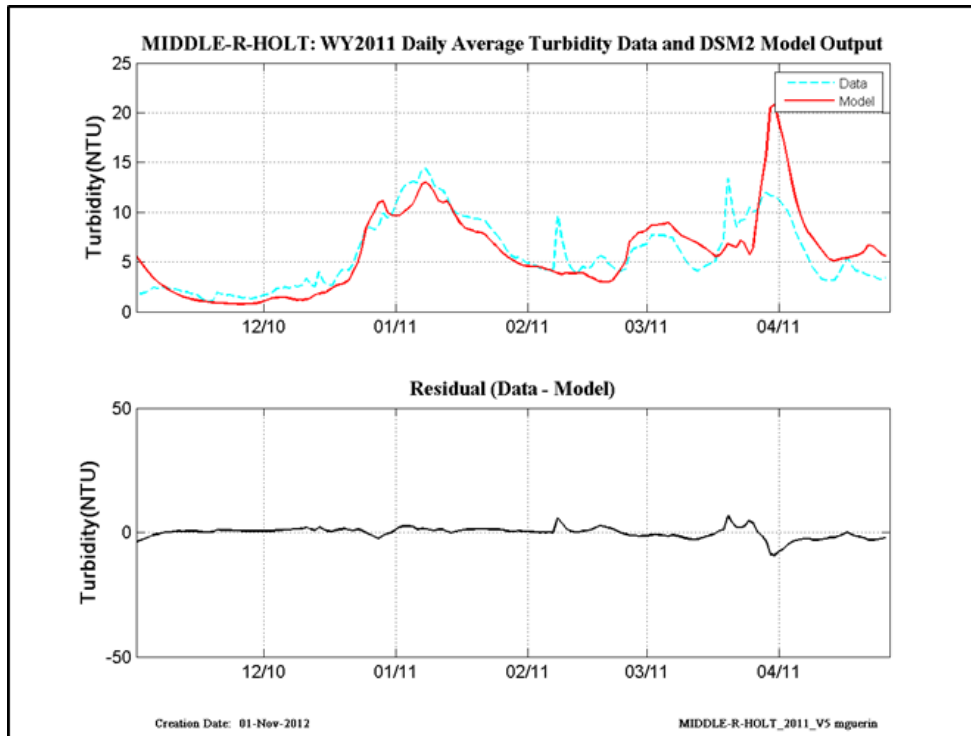


Figure 11-17 WY2011 revised calibration results at Middle River-at-Holt.

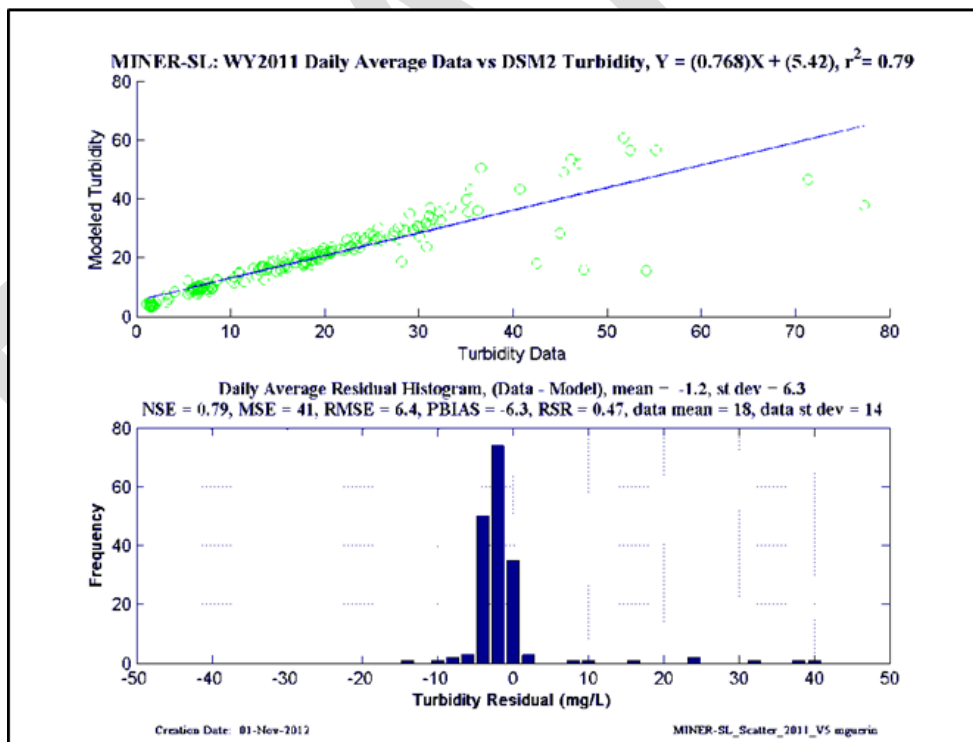
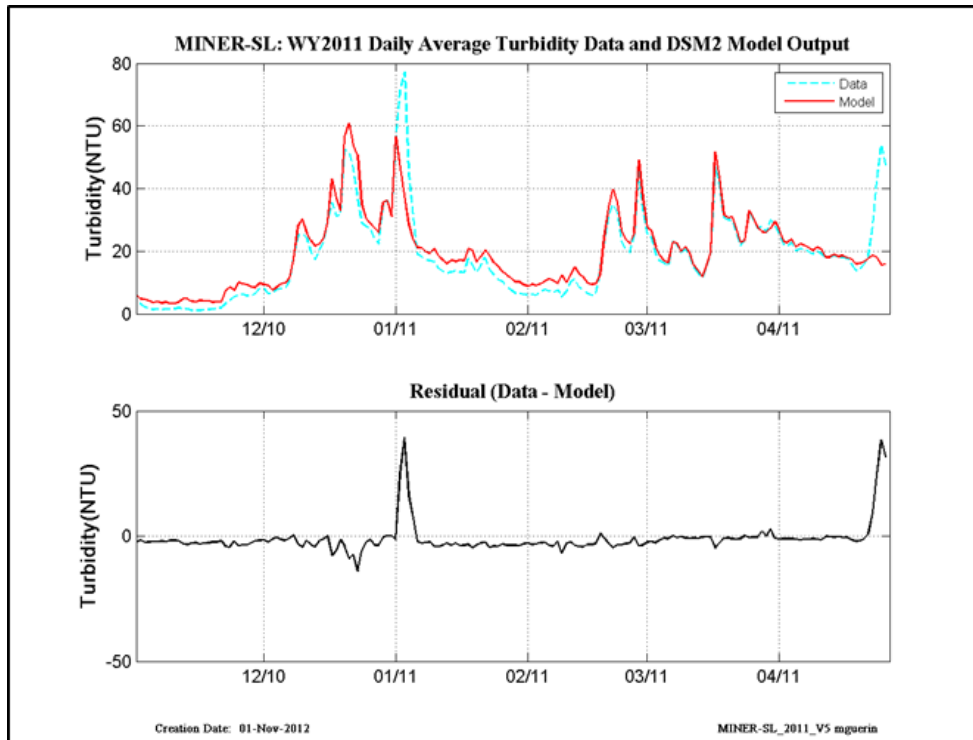


Figure 11-18 WY2011 revised calibration results at Miner Slough.

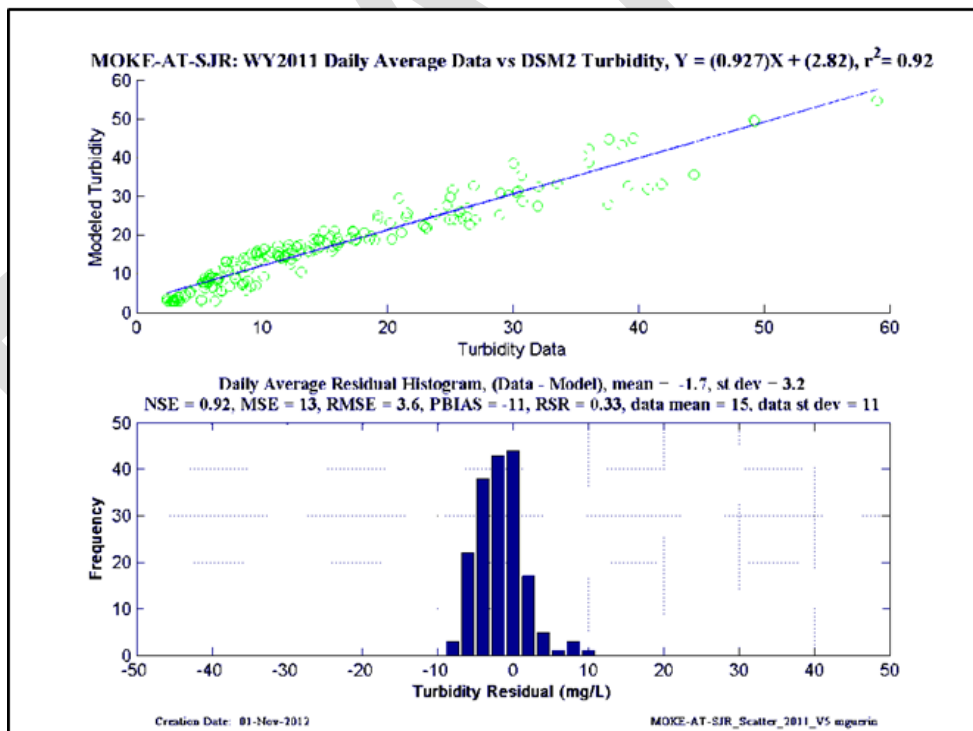
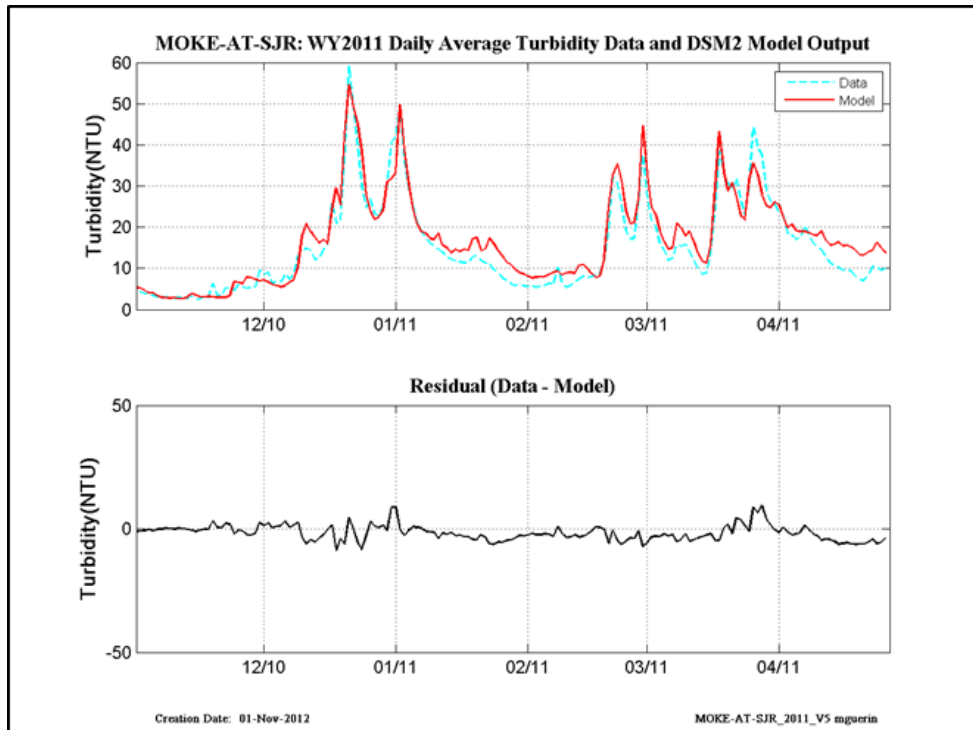


Figure 11-19 WY2011 revised calibration results at Mokelumne-at-San Joaquin.

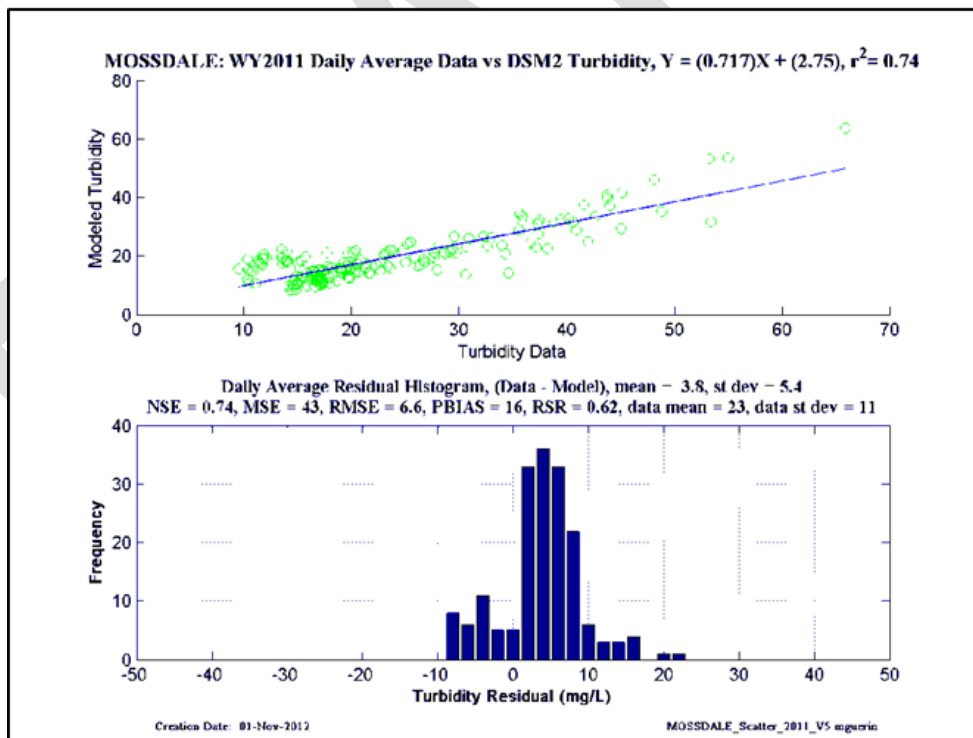
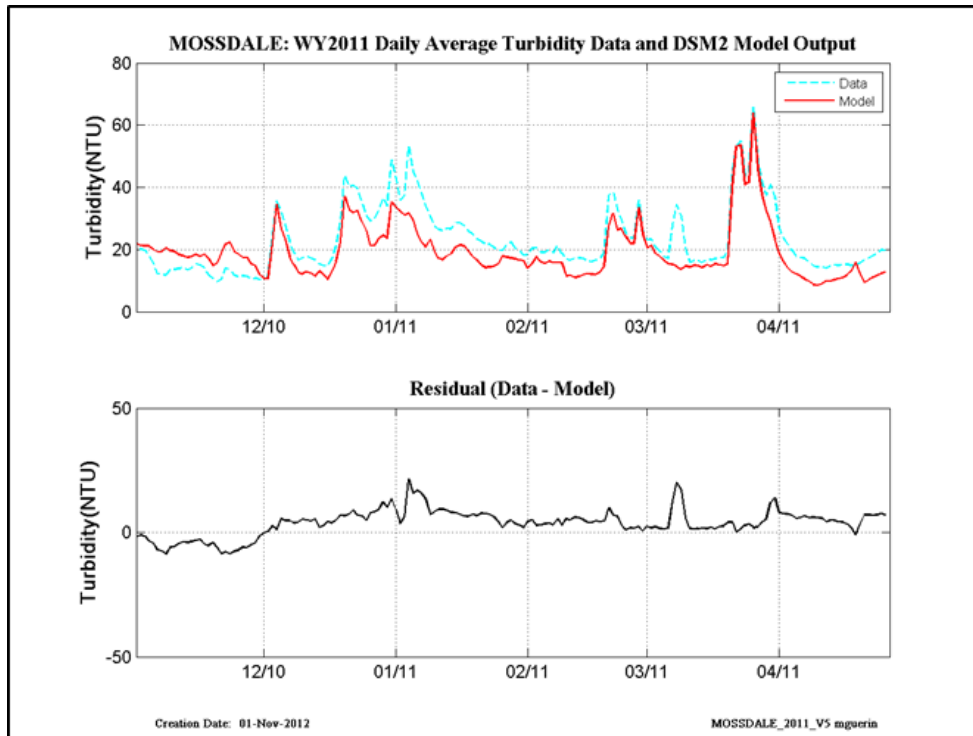


Figure 11-20 WY2011 revised calibration results at Mossdale.

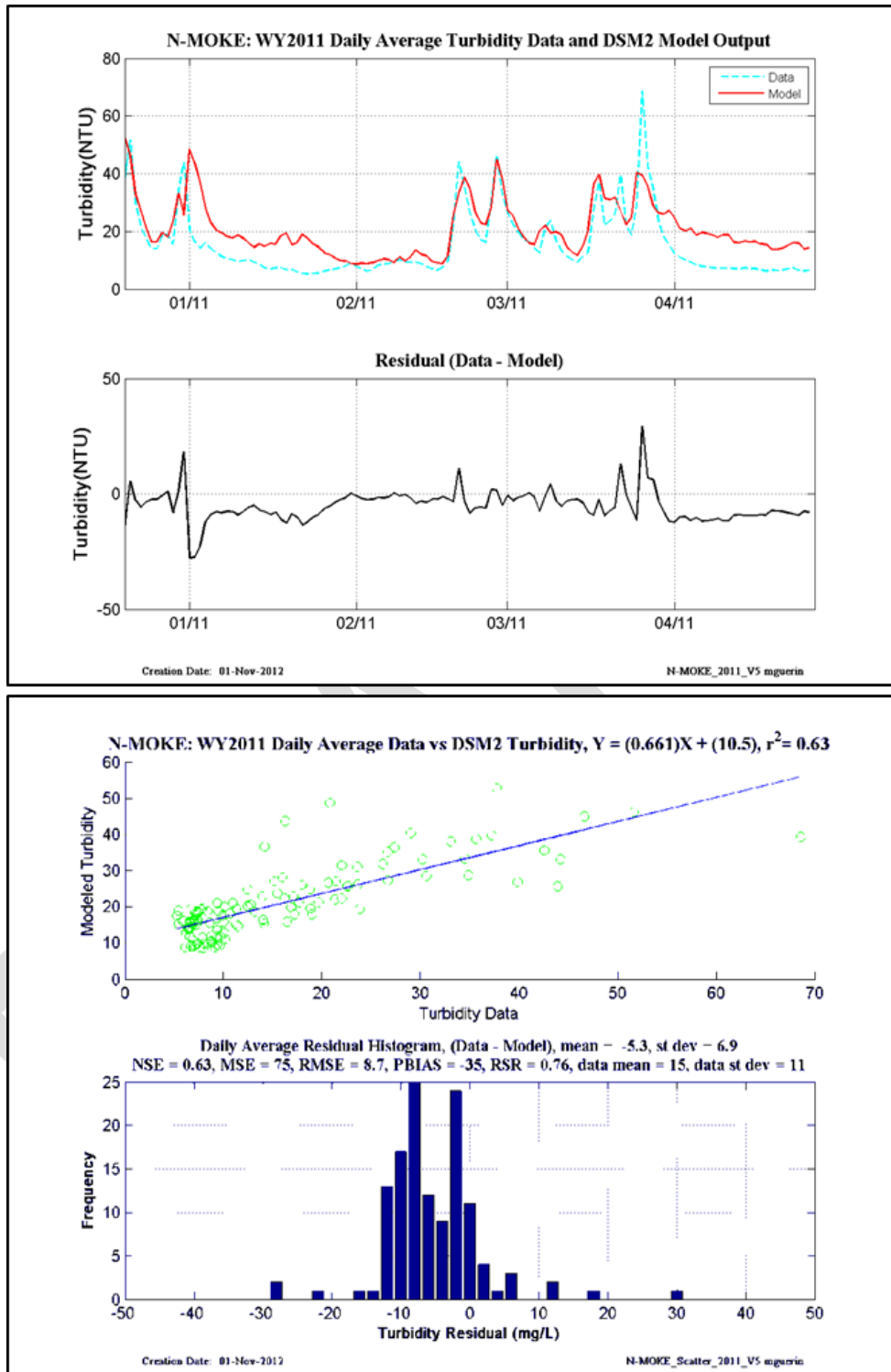


Figure 11-21 WY2011 revised calibration results at North Mokelumne.

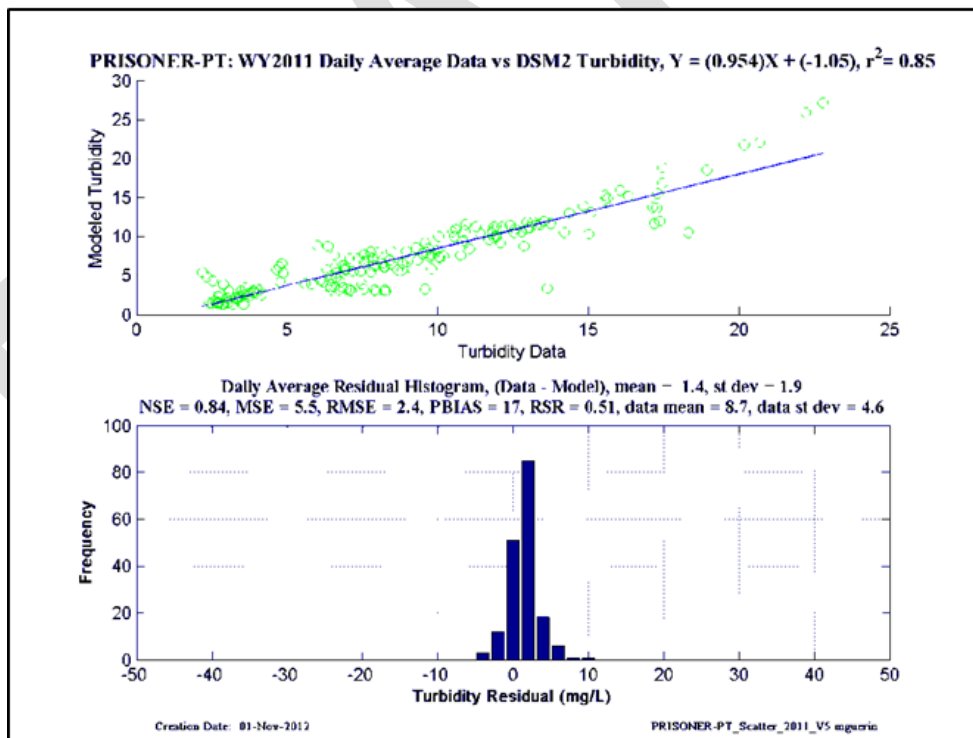
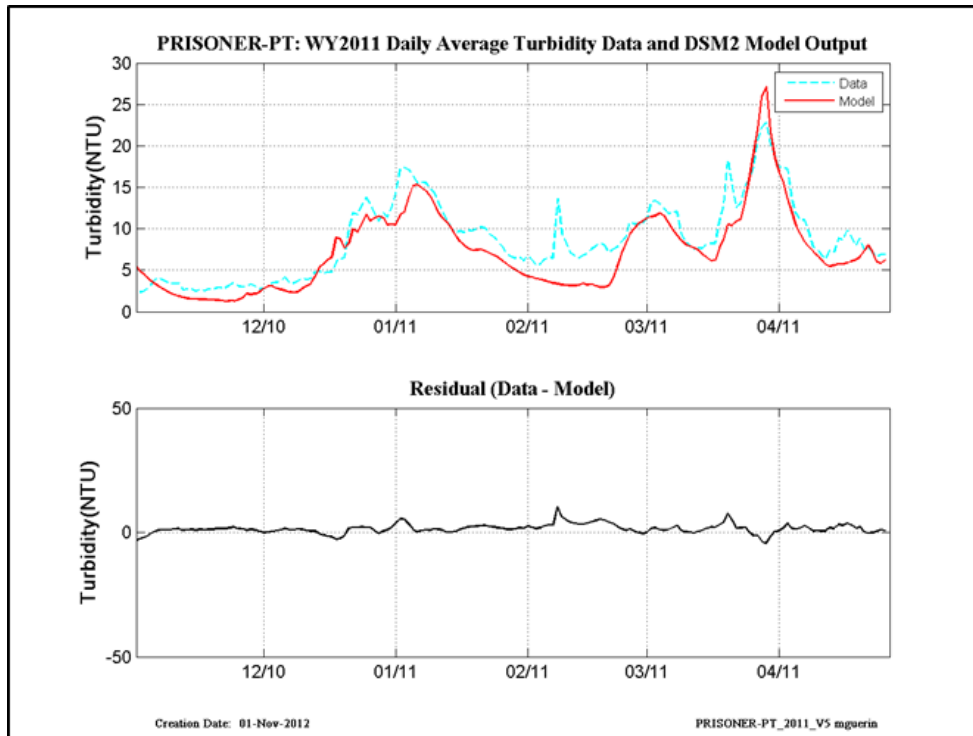


Figure 11-22 WY2011 revised calibration results at Prisoner Point.

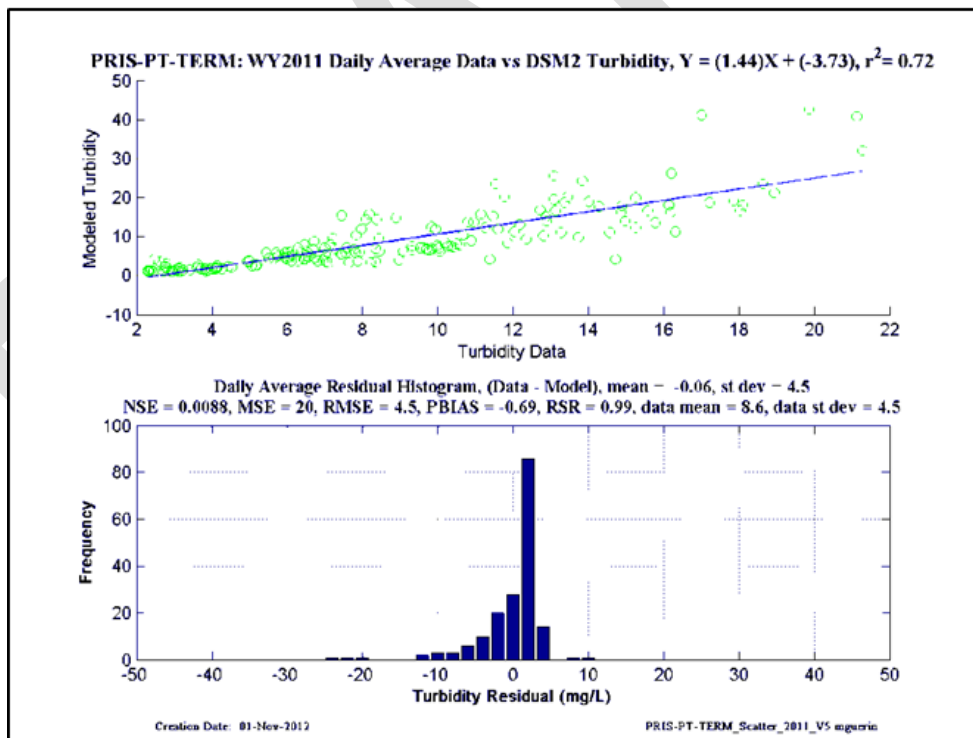
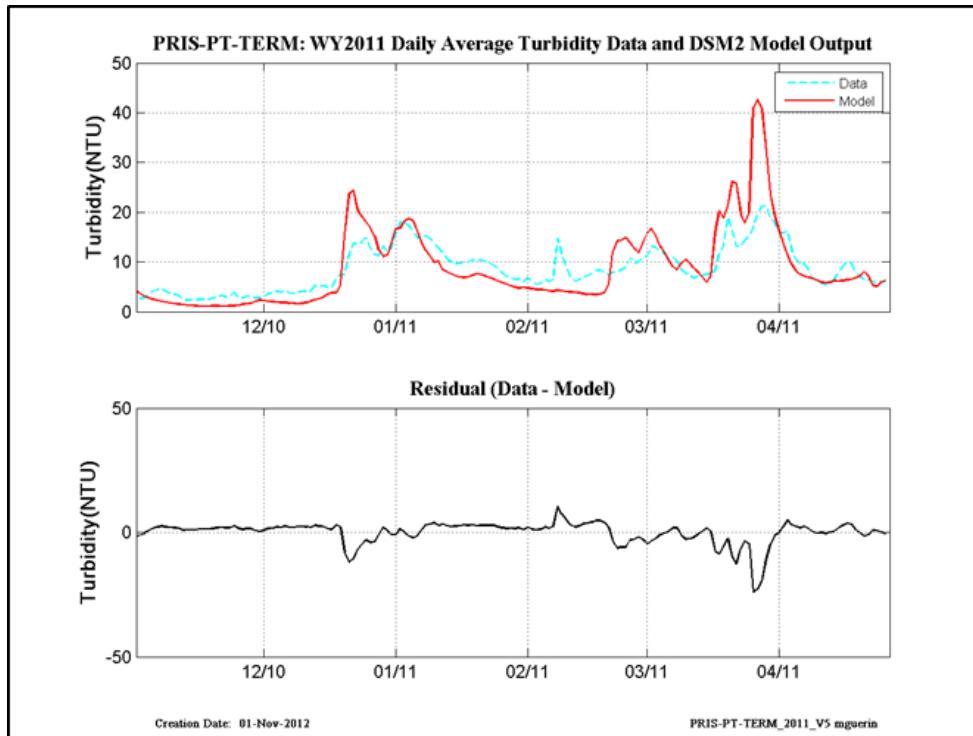


Figure 11-23 WY2011 revised calibration results at Prisoner Point-at-Terminus.

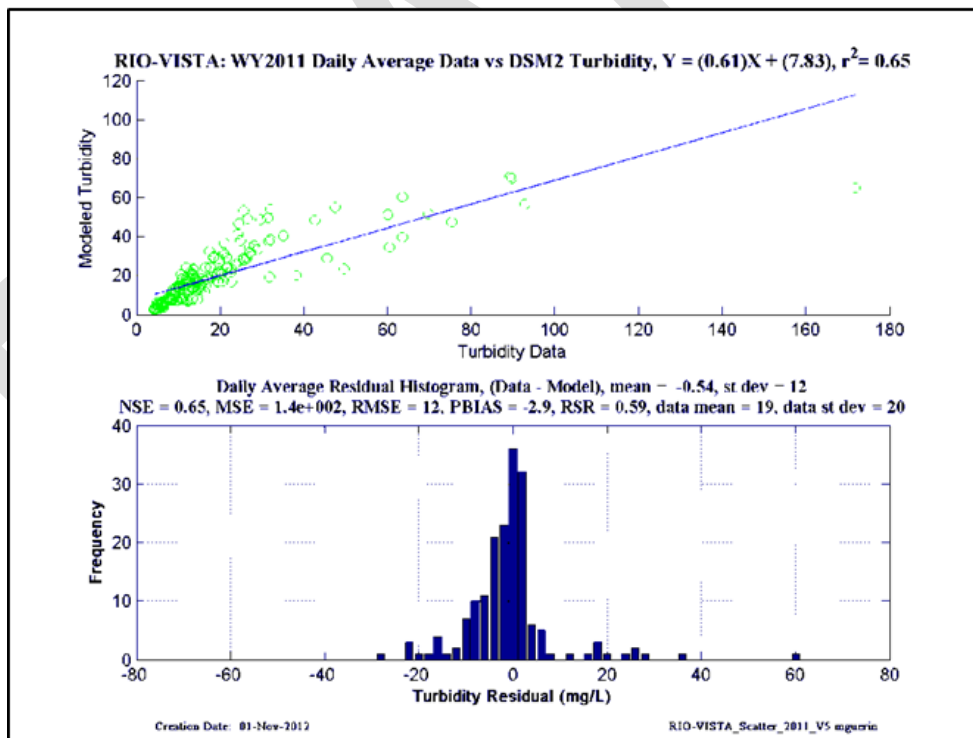
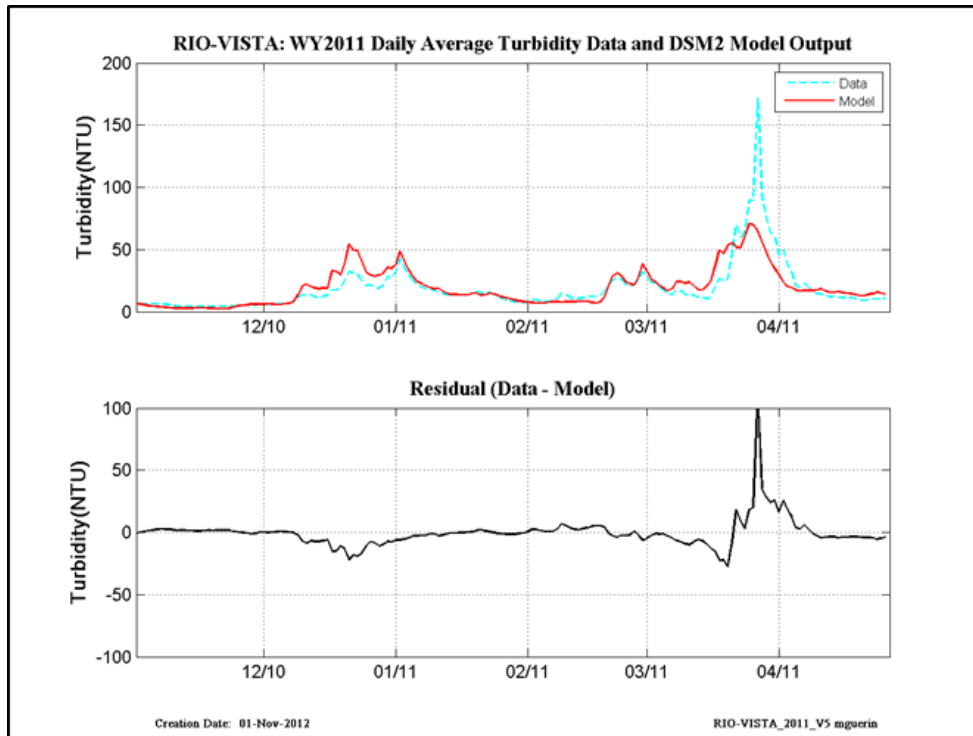


Figure 11-24 WY2011 revised calibration results at Rio Vista.

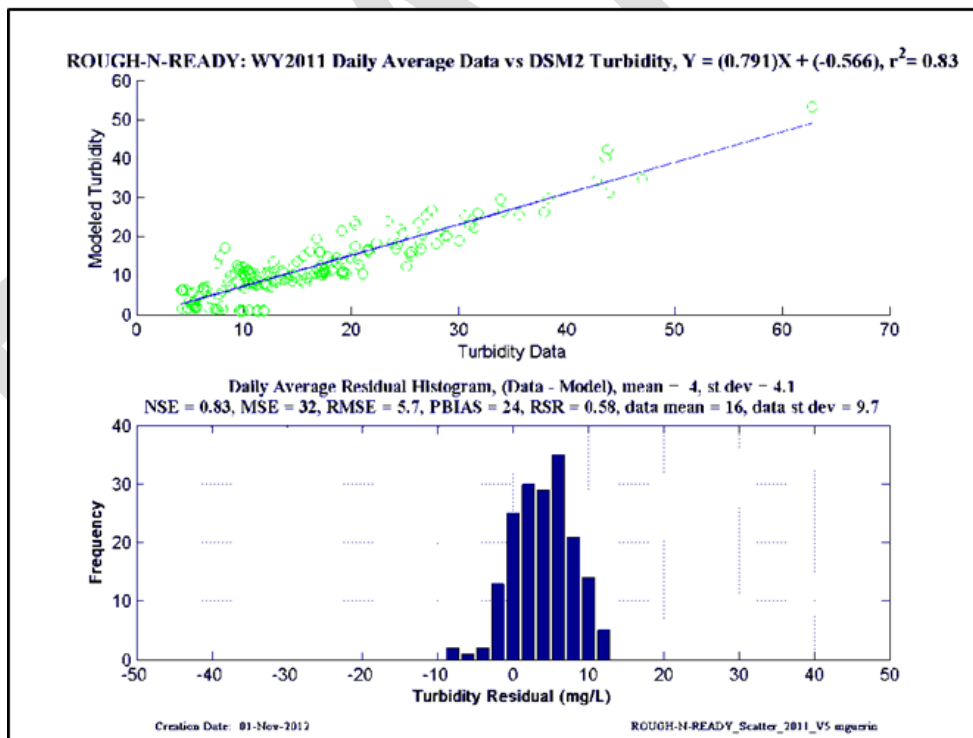
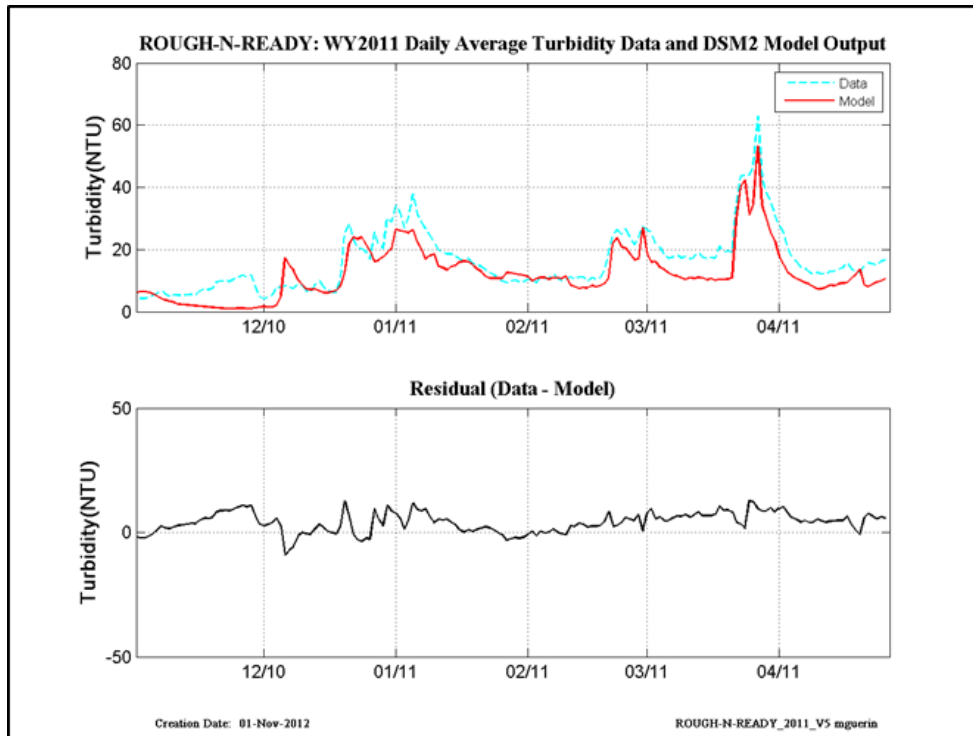


Figure 11-25 WY2011 revised calibration results at Rough-N-Ready Island.

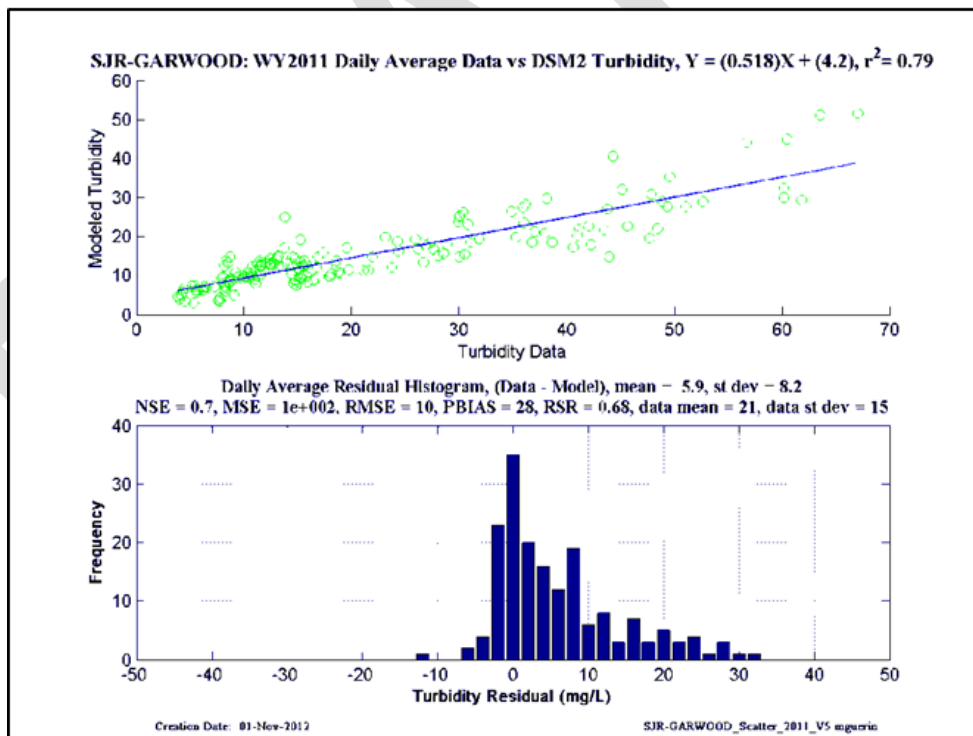
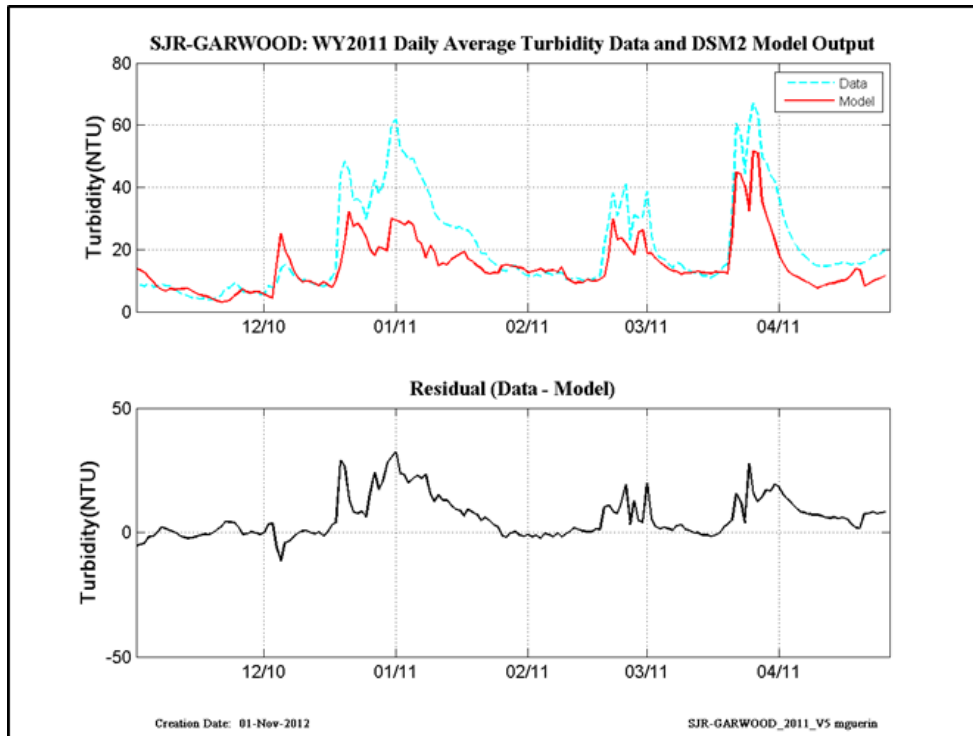


Figure 11-26 WY2011 revised calibration results at San Joaquin-at-Garwood.

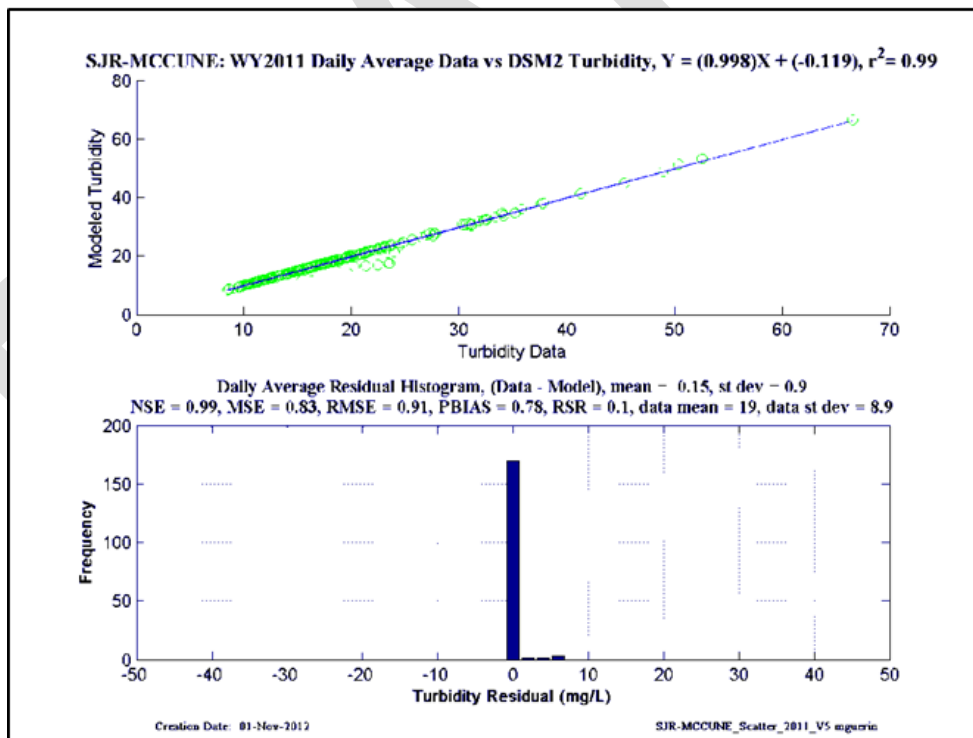
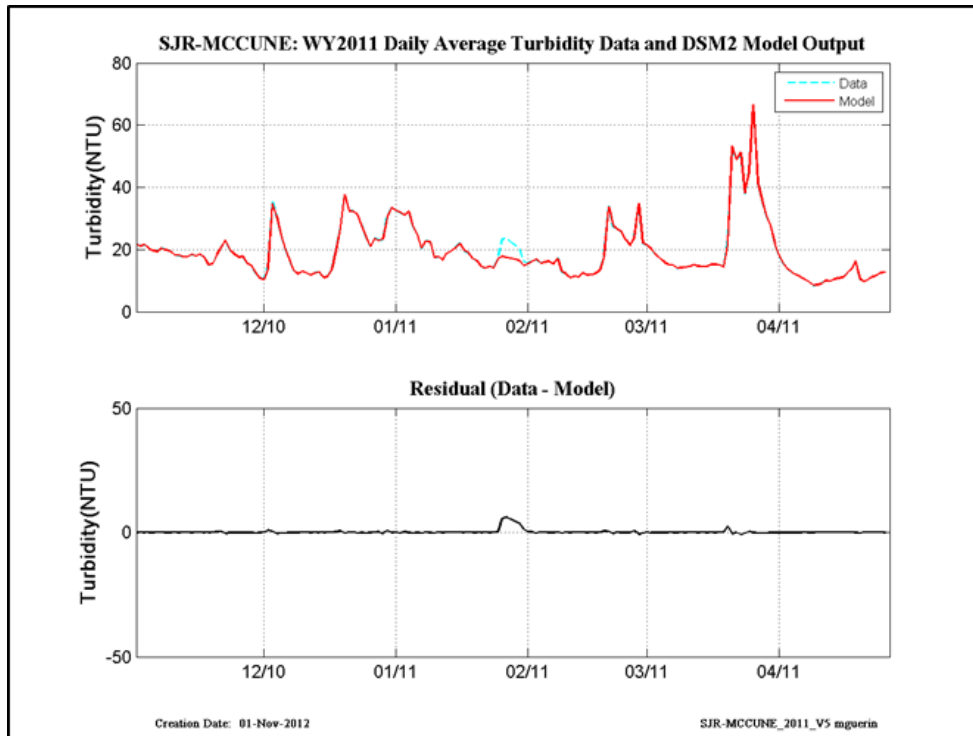


Figure 11-27 WY2011 revised calibration results at San Joaquin-at-McCune (Vernalis).

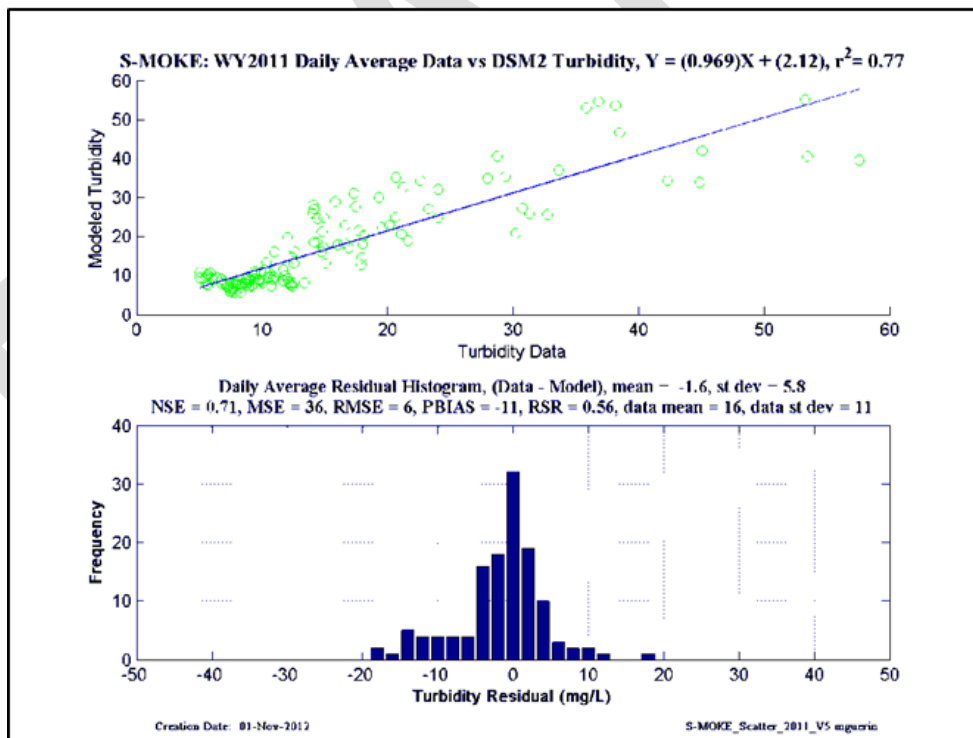
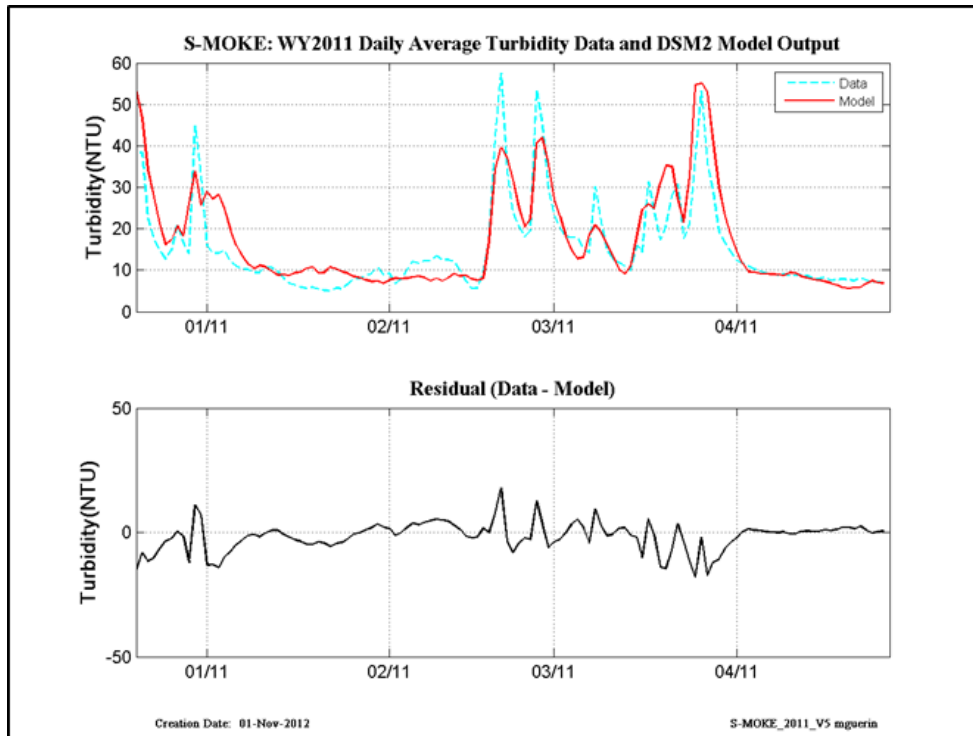


Figure 11-28 WY2011 revised calibration results at South Mokelumne.

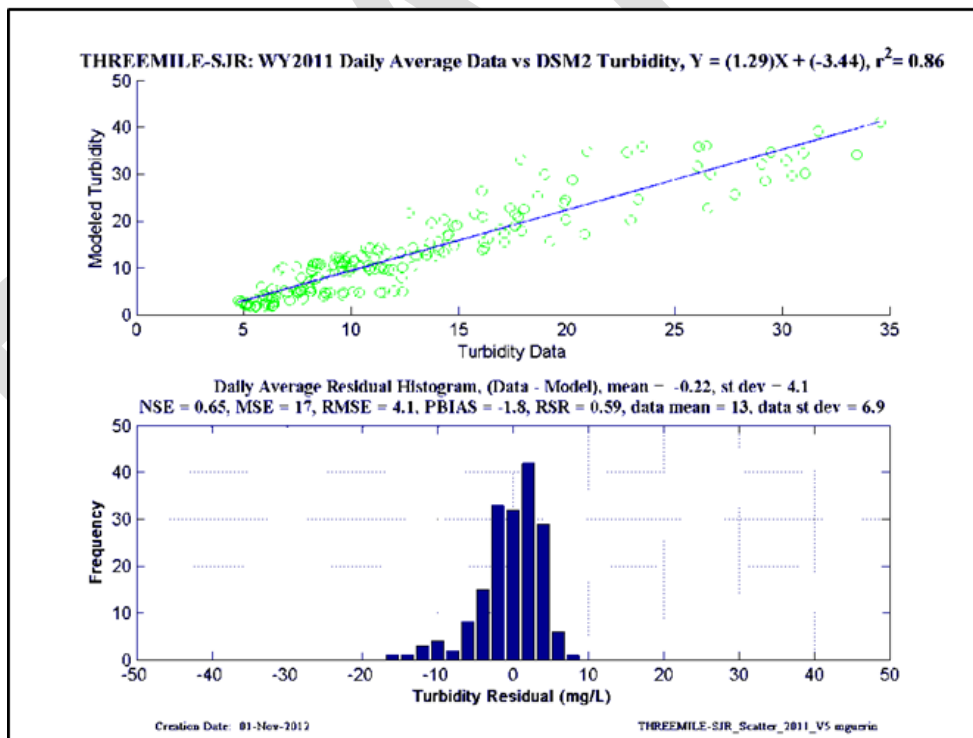
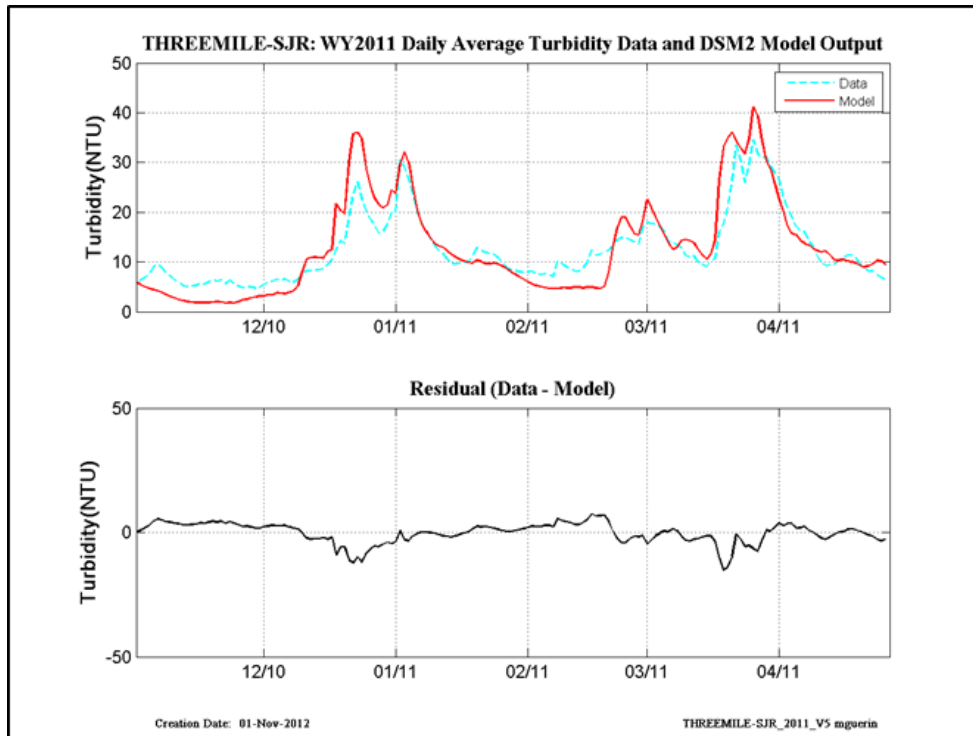


Figure 11-29 WY2011 revised calibration results at Threemile-Slough-at-San Joaquin.

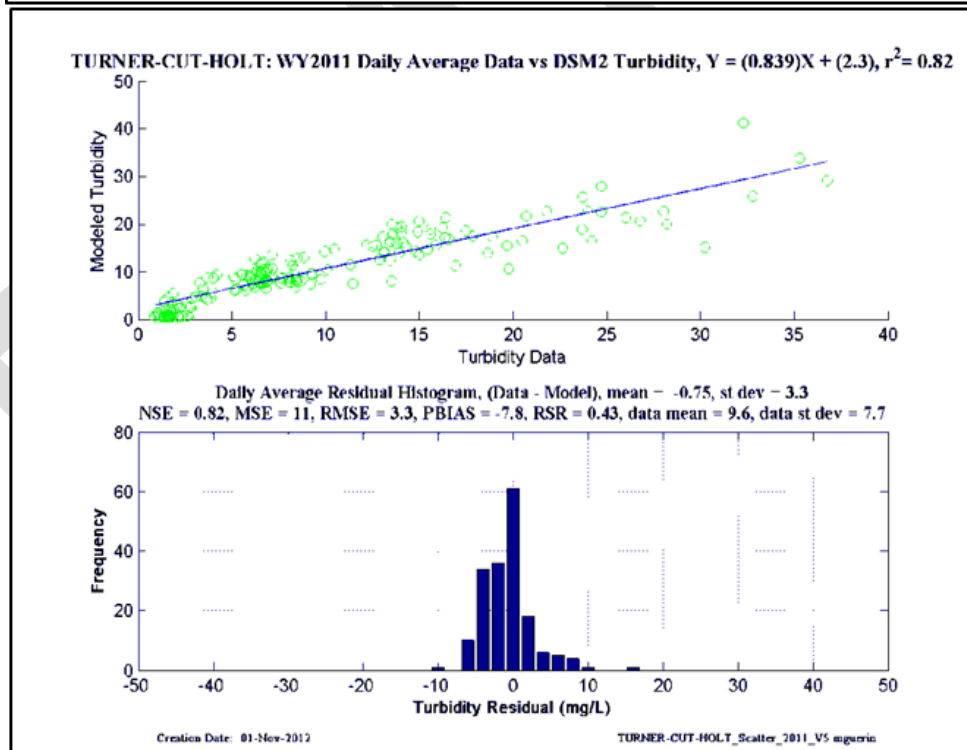
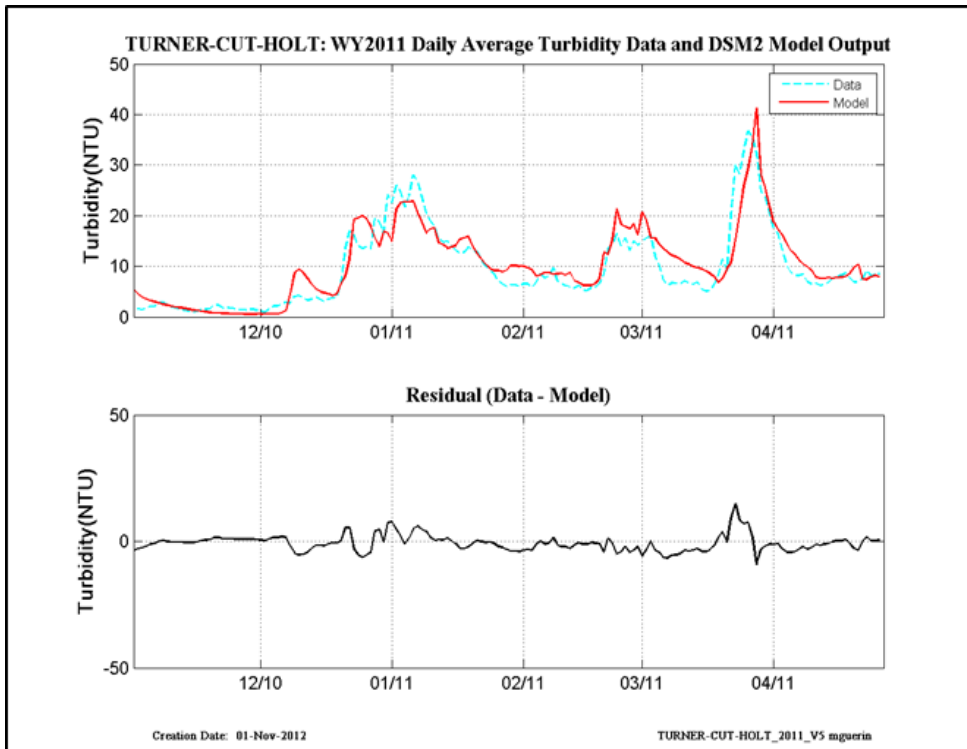


Figure 11-30 WY2011 revised calibration results at Turner Cut-at-Holt.

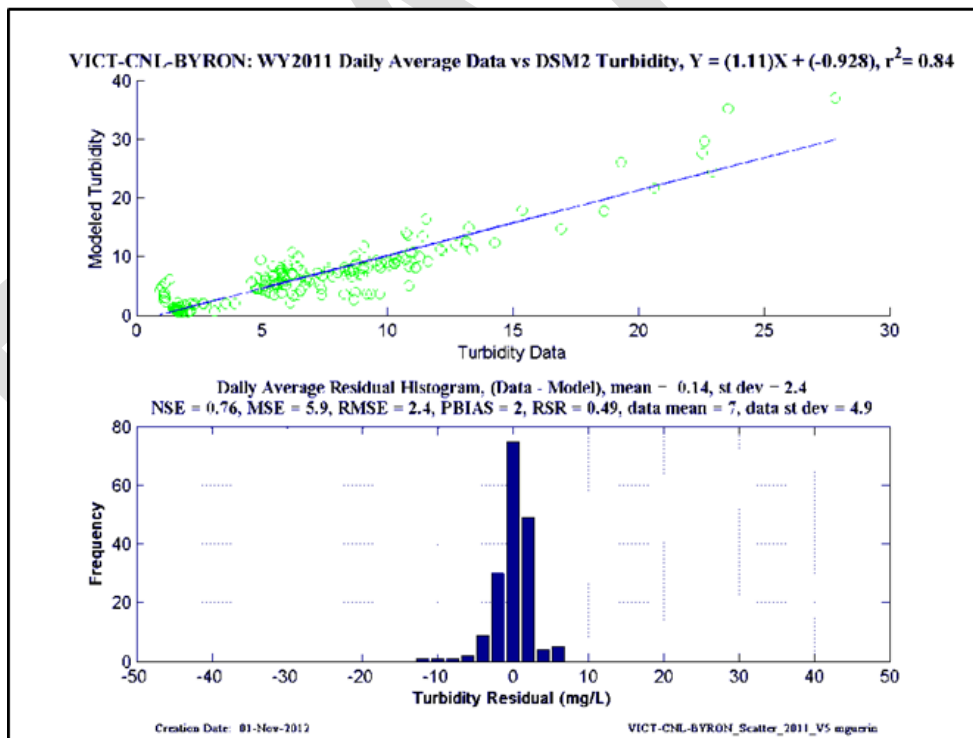
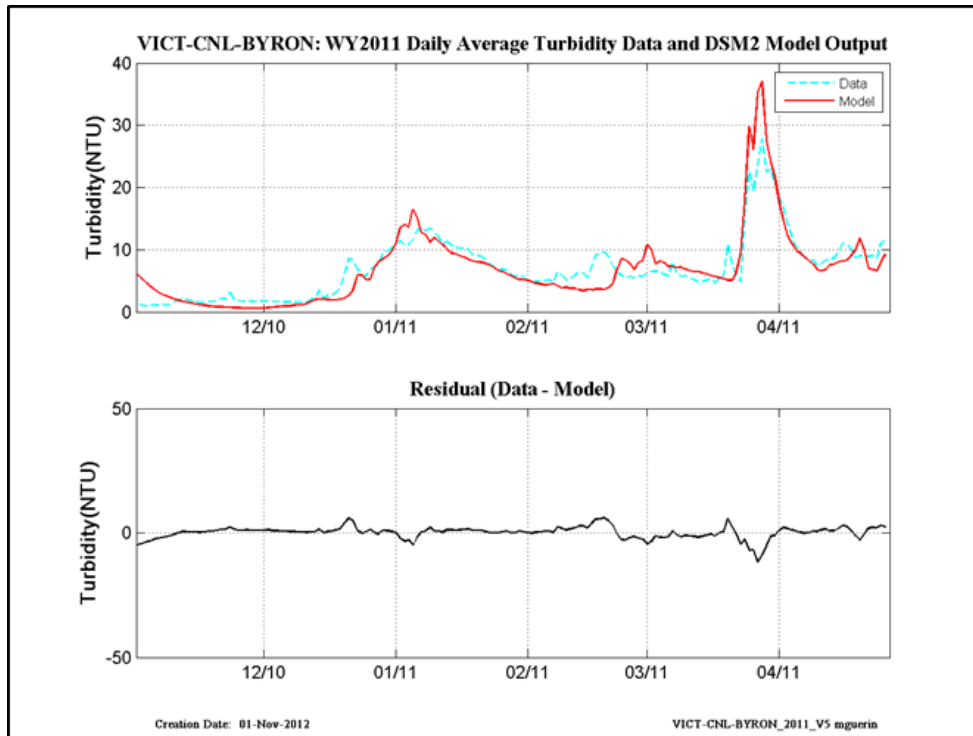


Figure 11-31 WY2011 revised calibration results at Victoria Canal-at-Byron.

### 11.3 Daily-averaged CDEC data and model output - WY2010

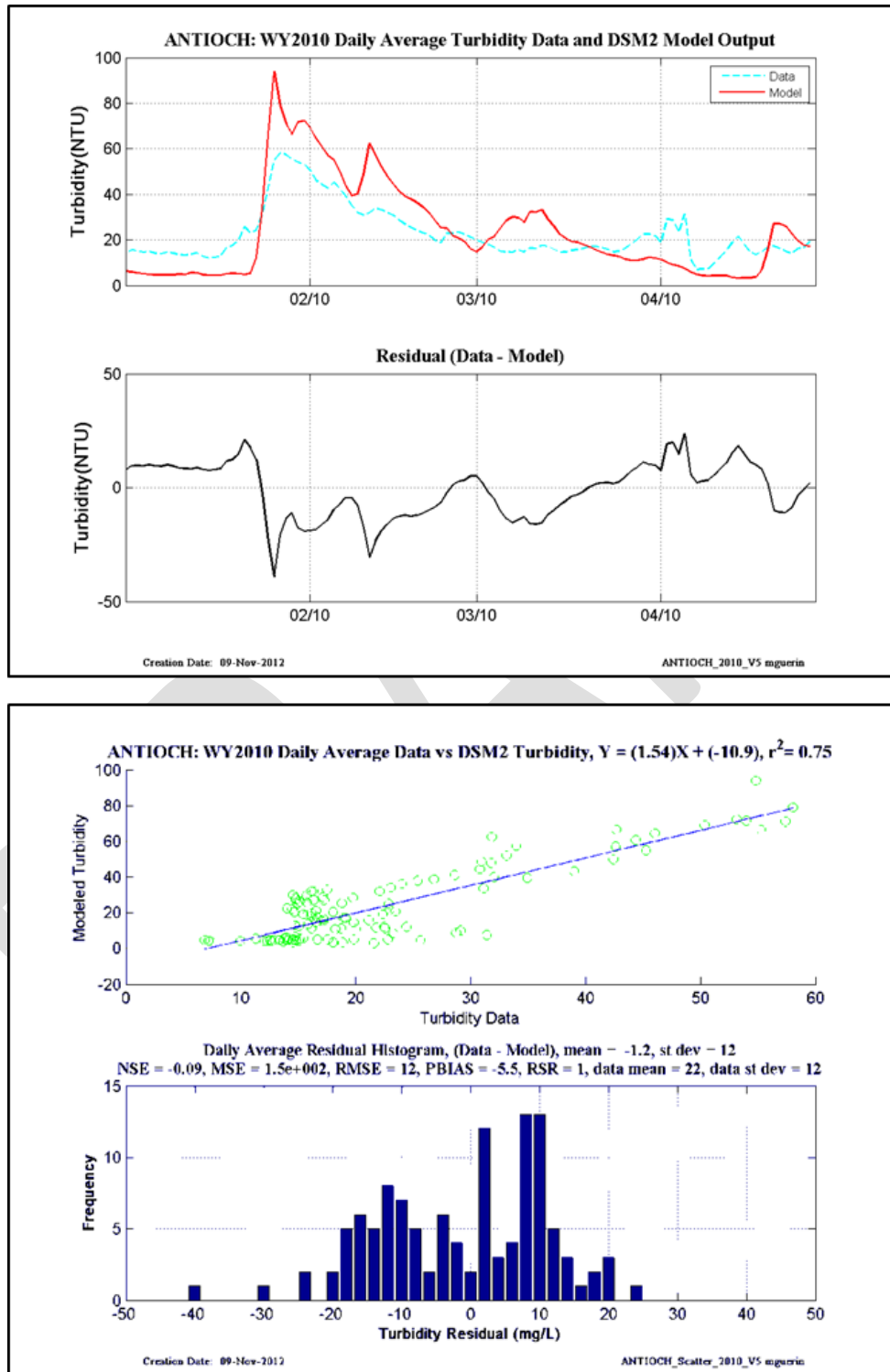


Figure 11-32 WY2010 revised calibration results at Antioch.

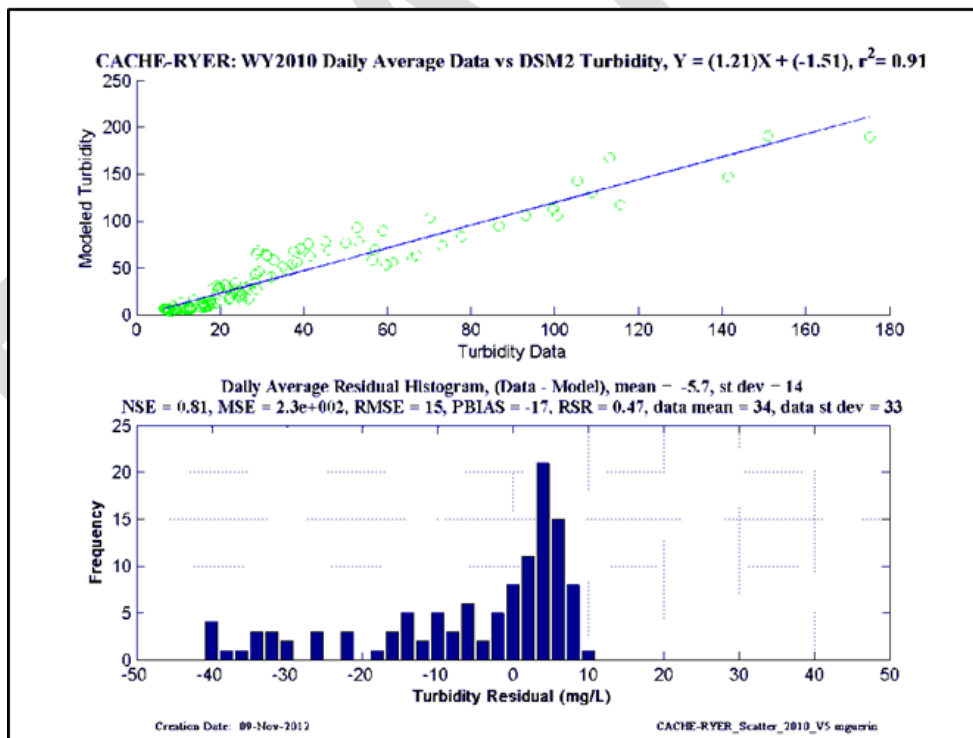
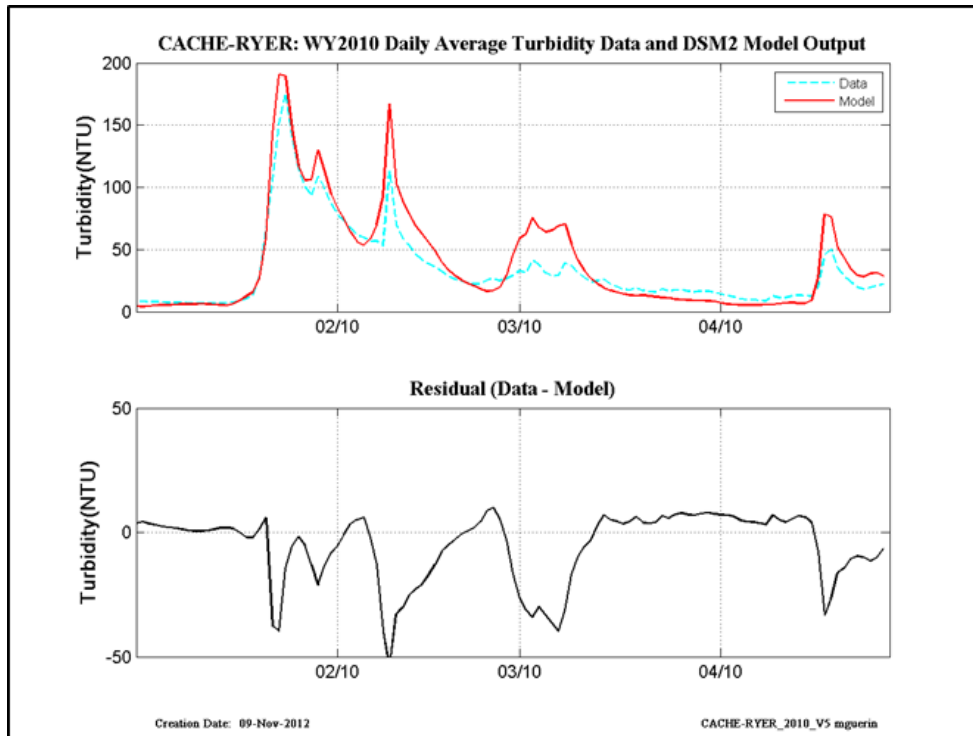


Figure 11-33 WY2010 revised calibration results at Cache-at-Ryer Island.

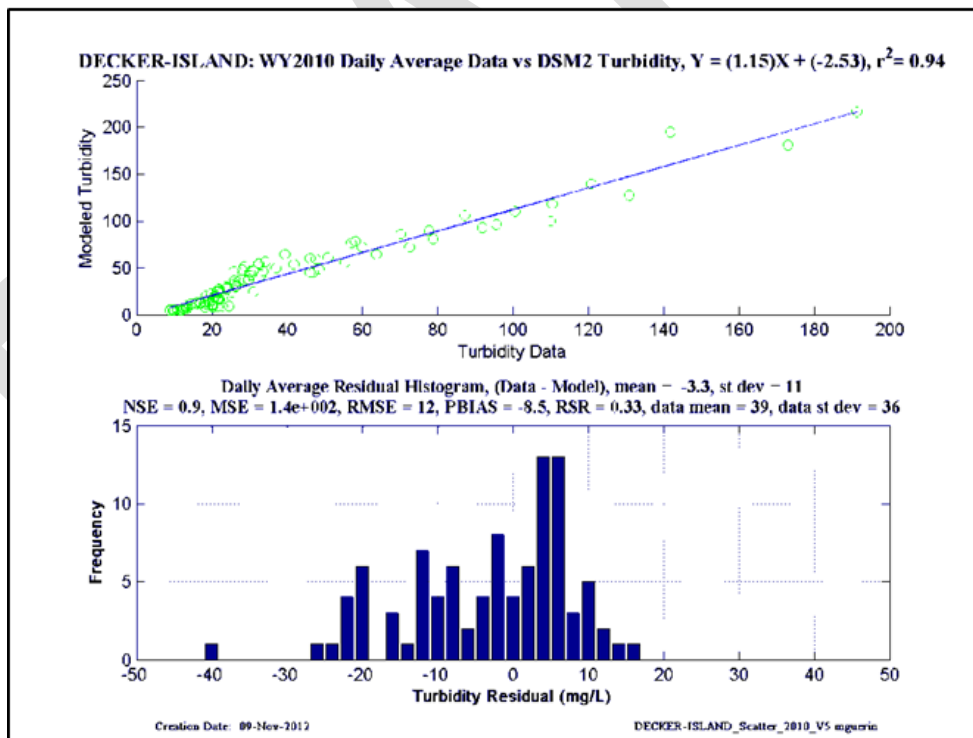
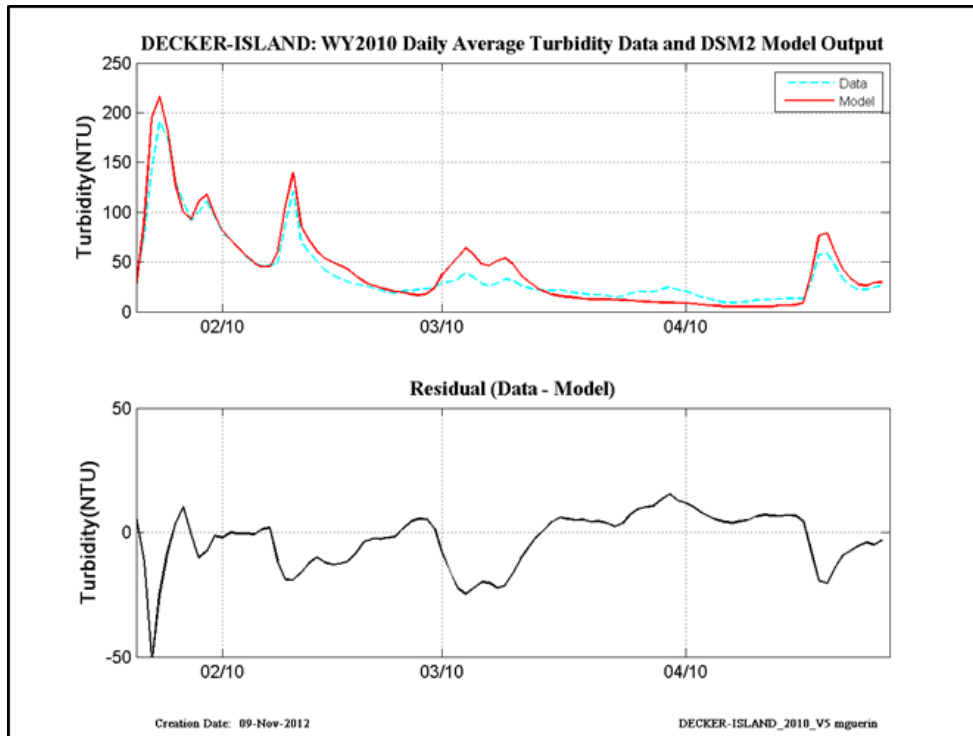


Figure 11-34 WY2010 revised calibration results at Decker Island.

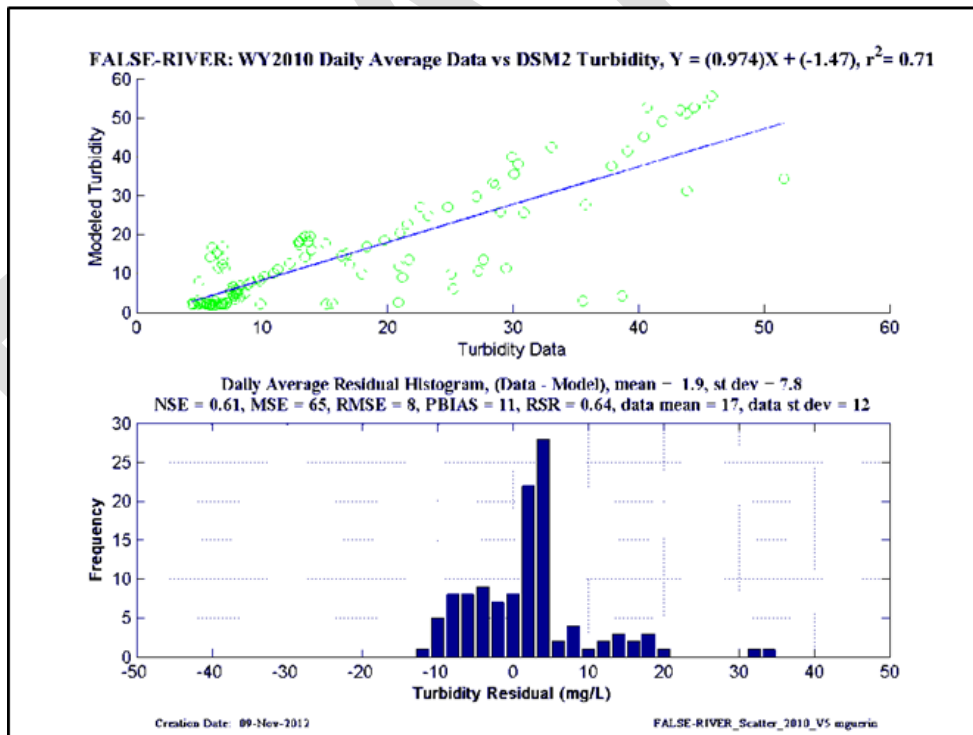
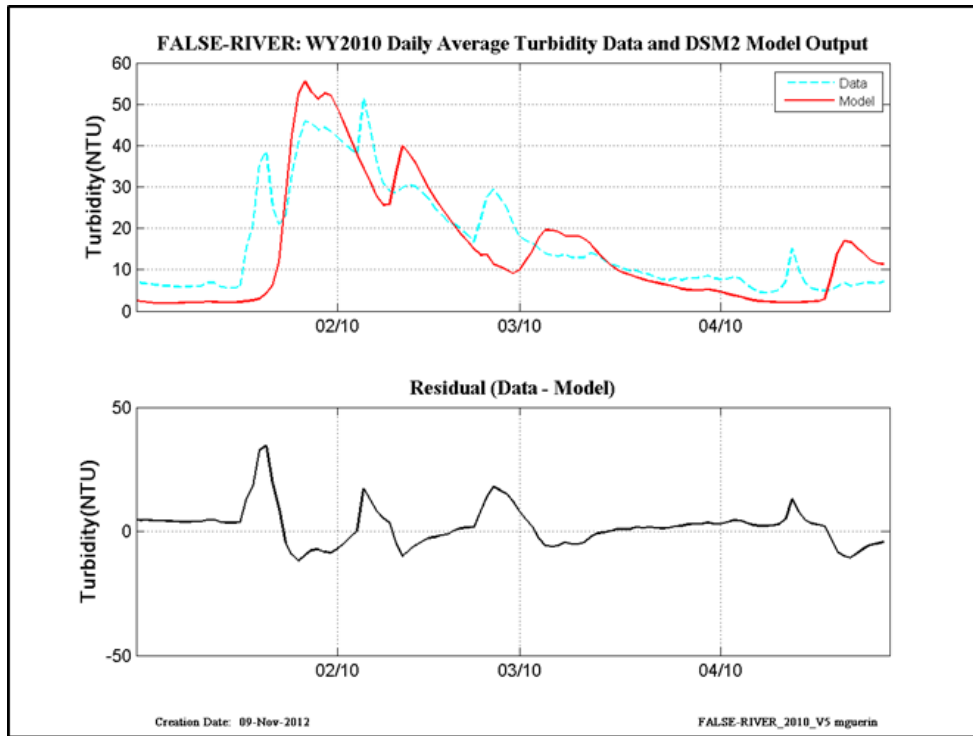


Figure 11-35 WY2010 revised calibration results at False River.

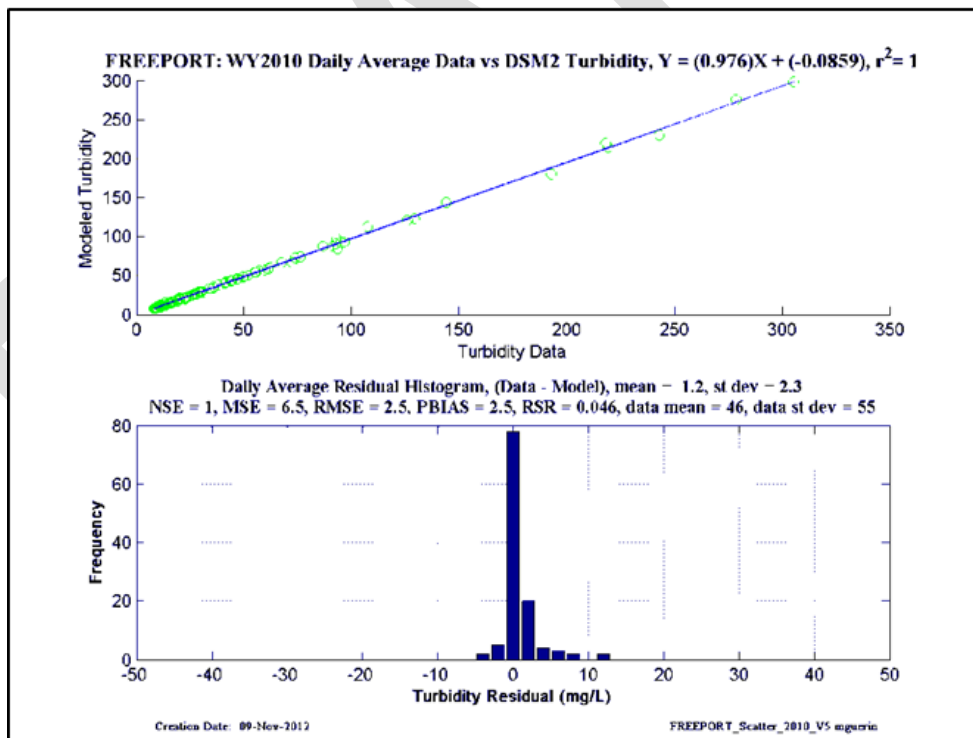
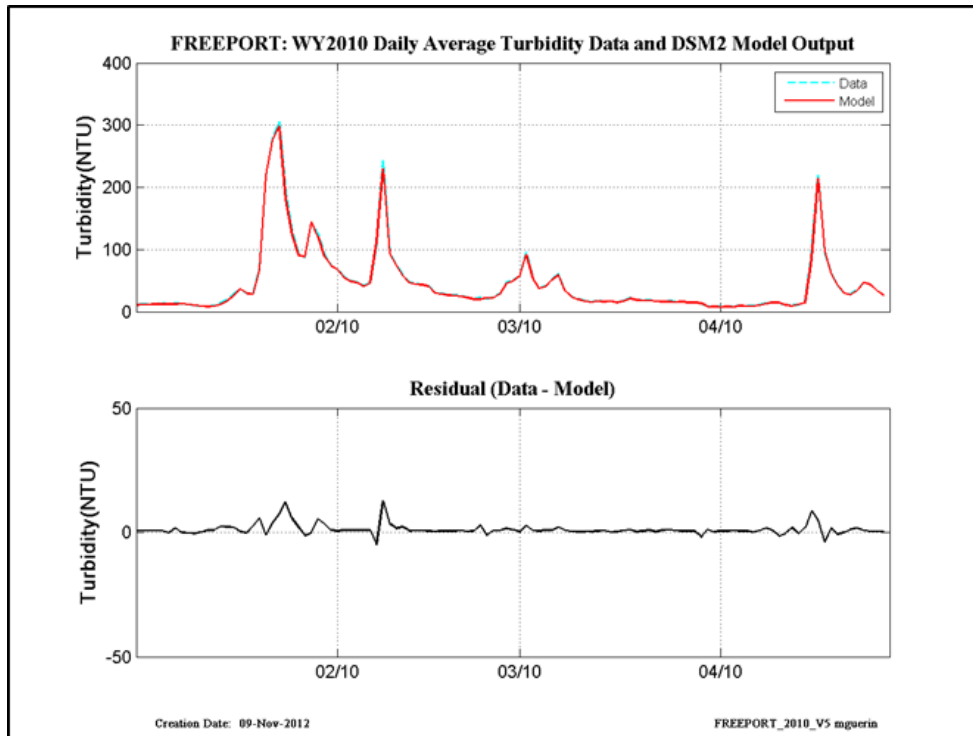


Figure 11-36 WY2010 revised calibration results at Freeport.

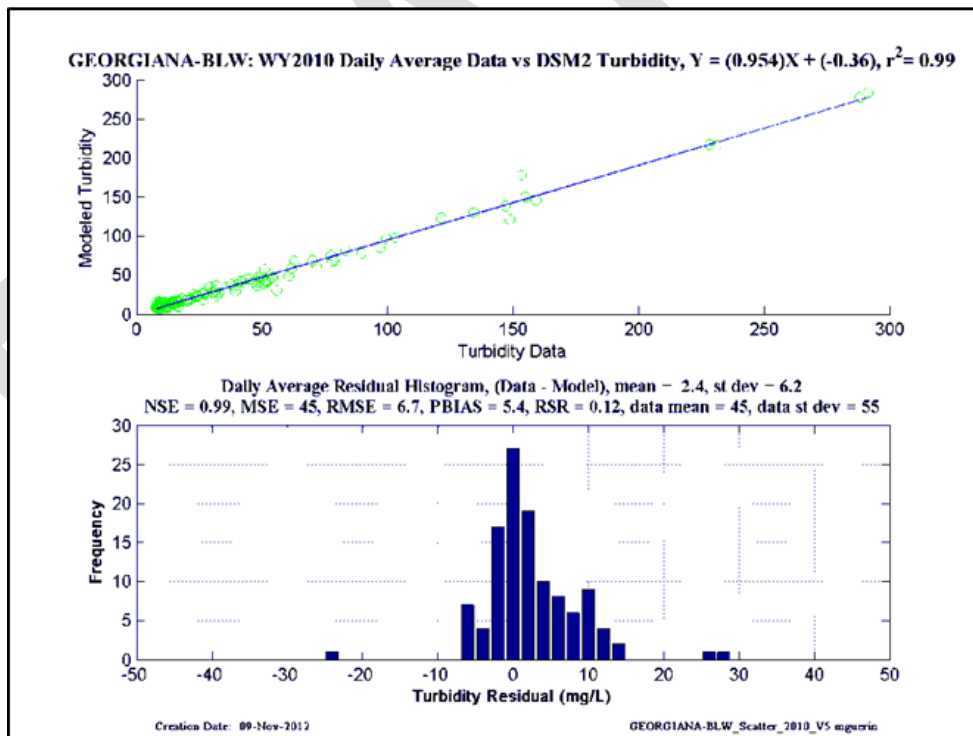
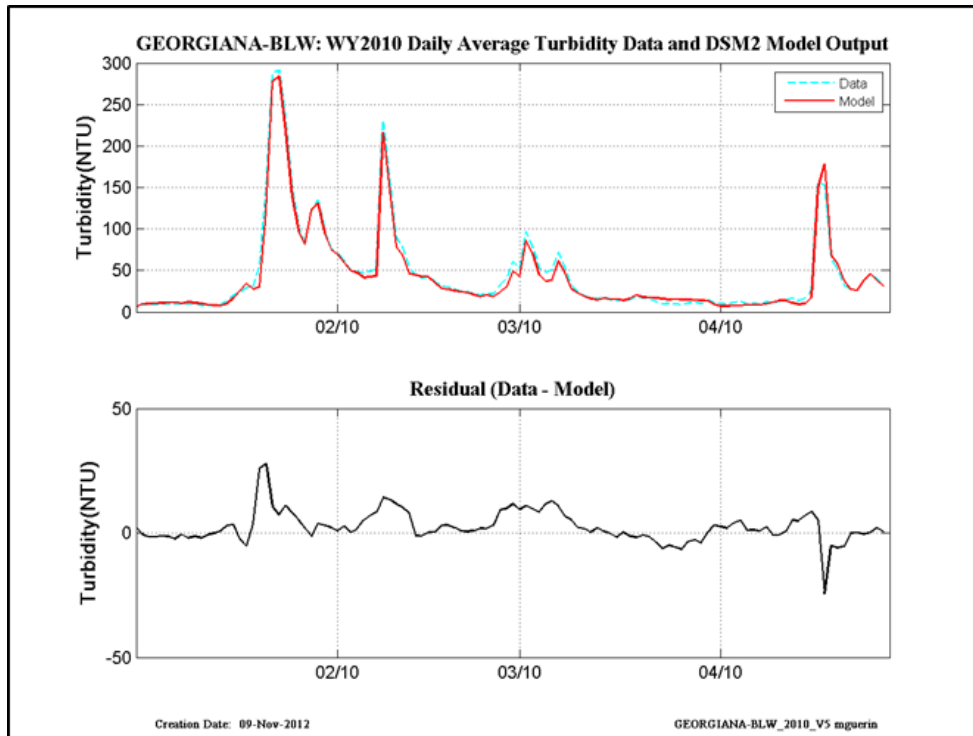


Figure 11-37 WY2010 revised calibration results at Georgiana-Below-Sac.

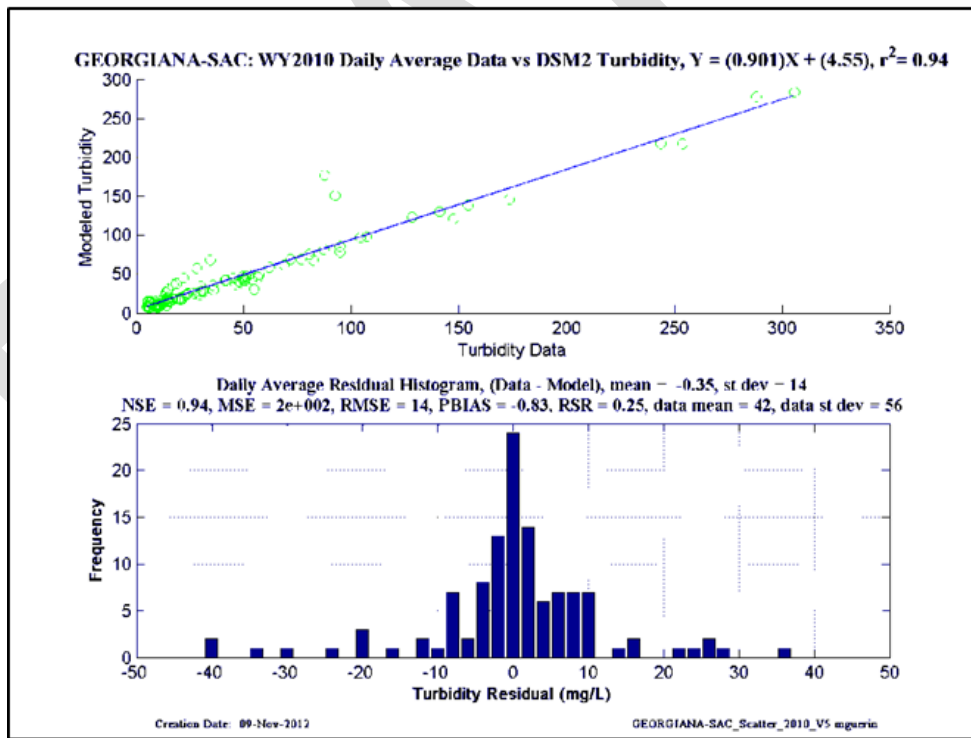
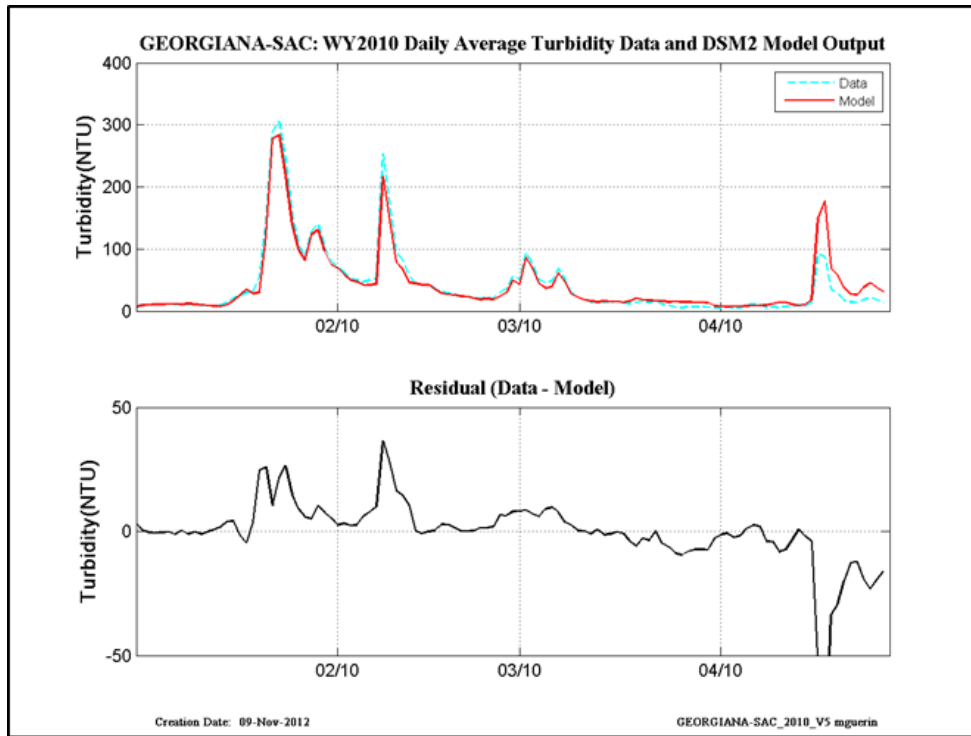


Figure 11-38 WY2010 revised calibration results at Georgiana-Sac.

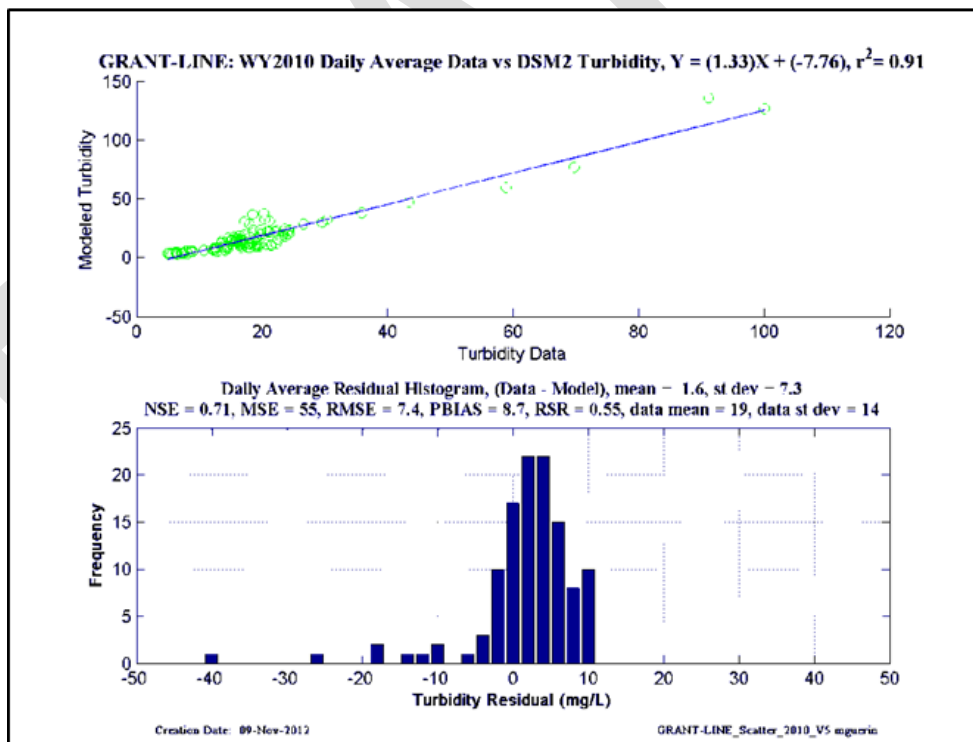
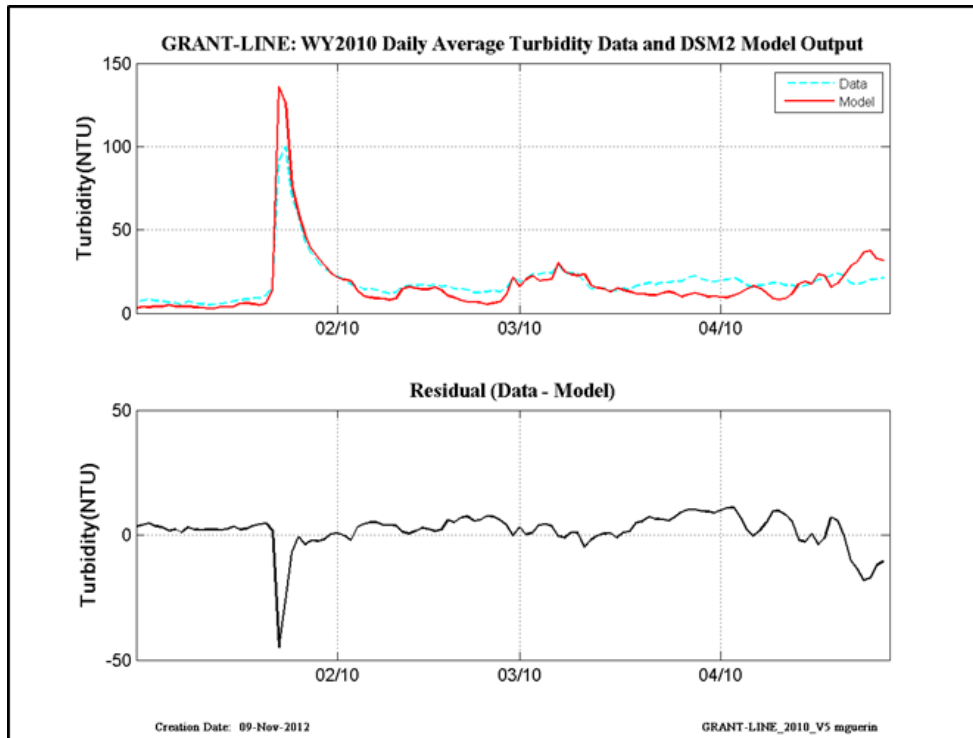


Figure 11-39 WY2010 revised calibration results at Grant Line.

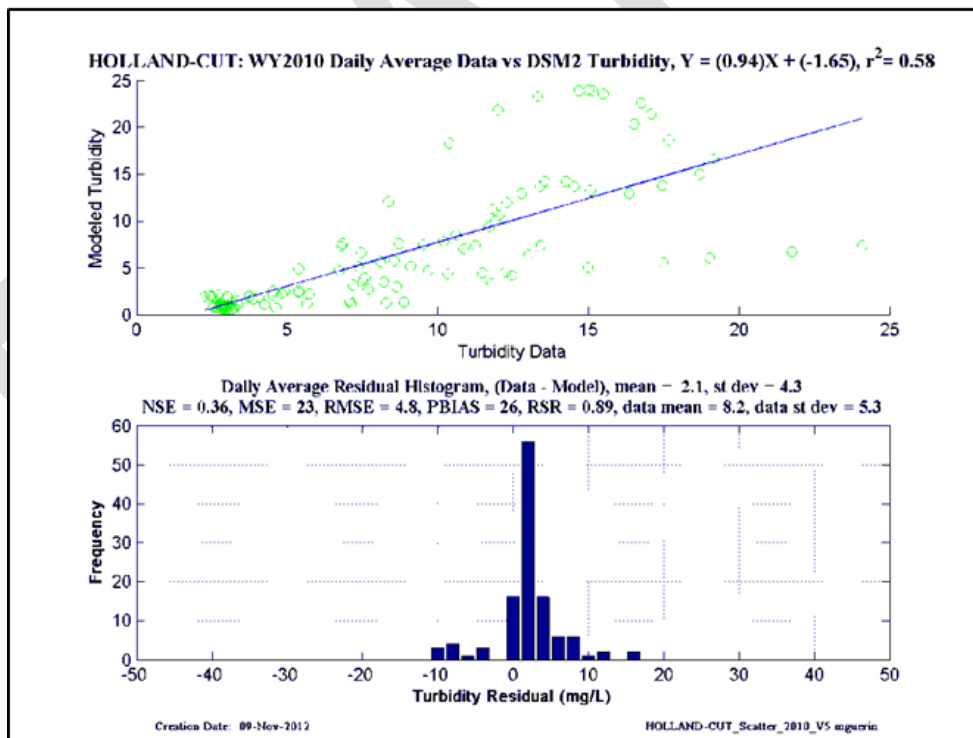
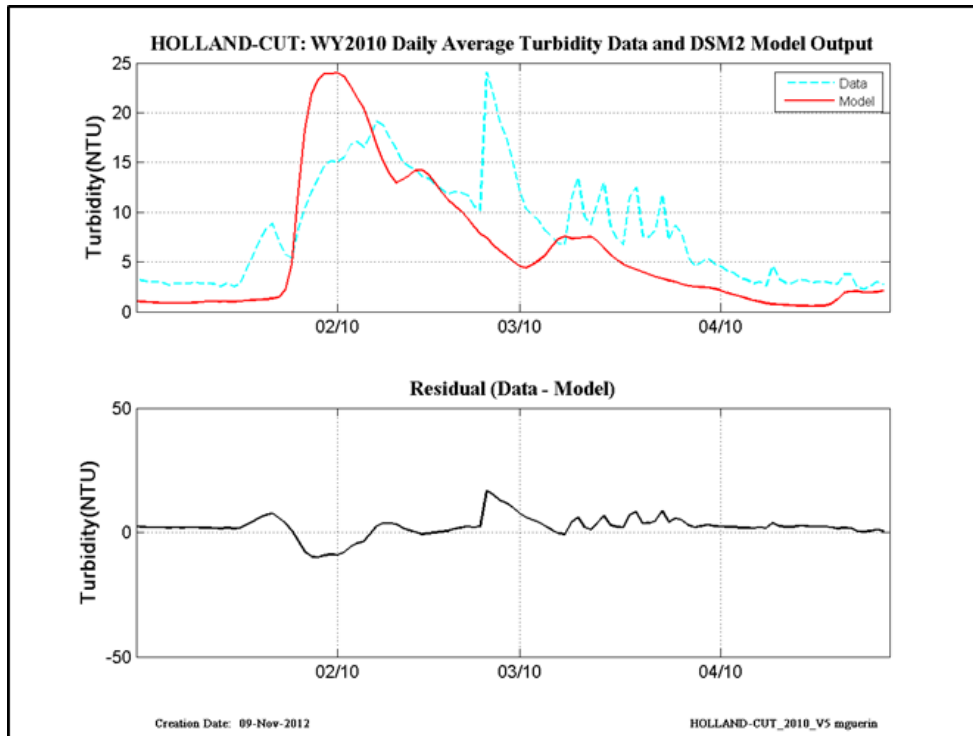


Figure 11-40 WY2010 revised calibration results at Holland Cut.

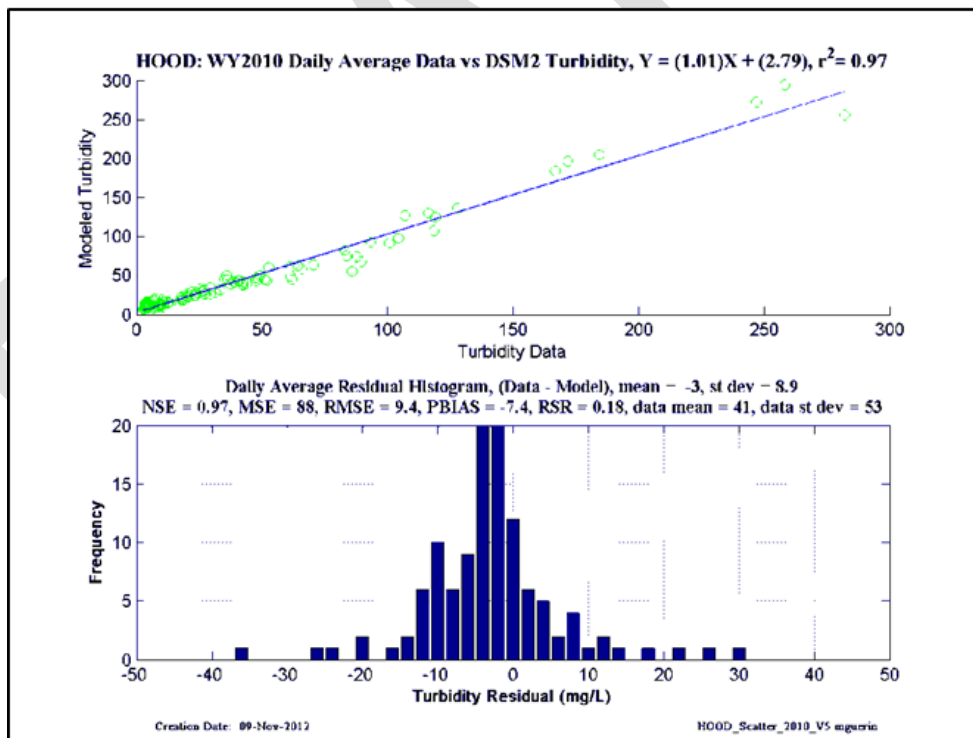
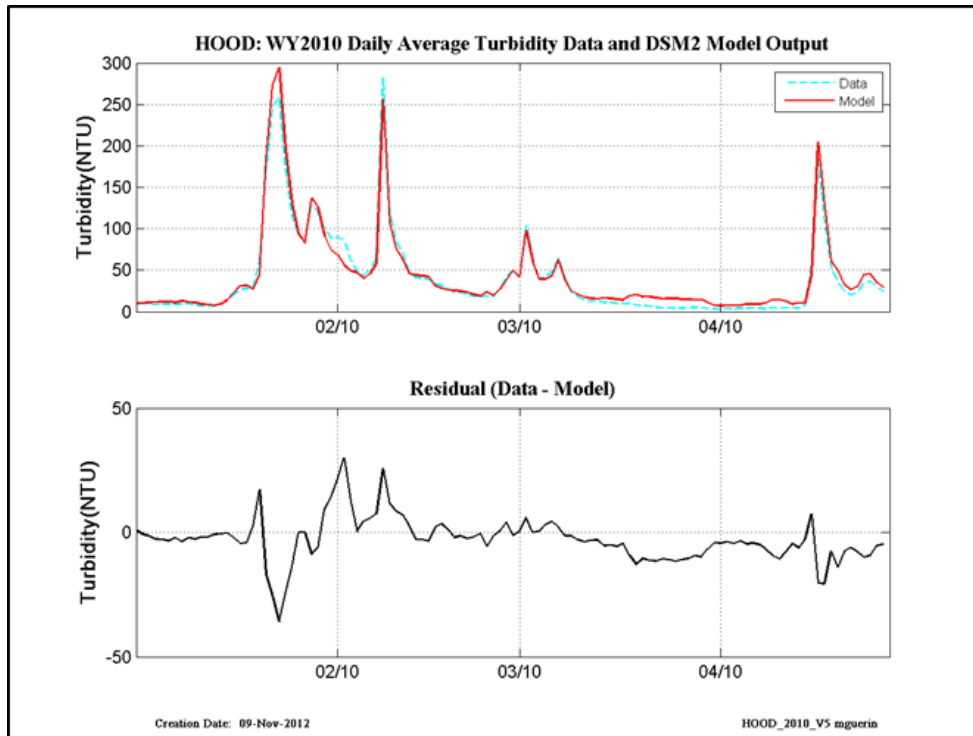


Figure 11-41 WY2010 revised calibration results at Hood.

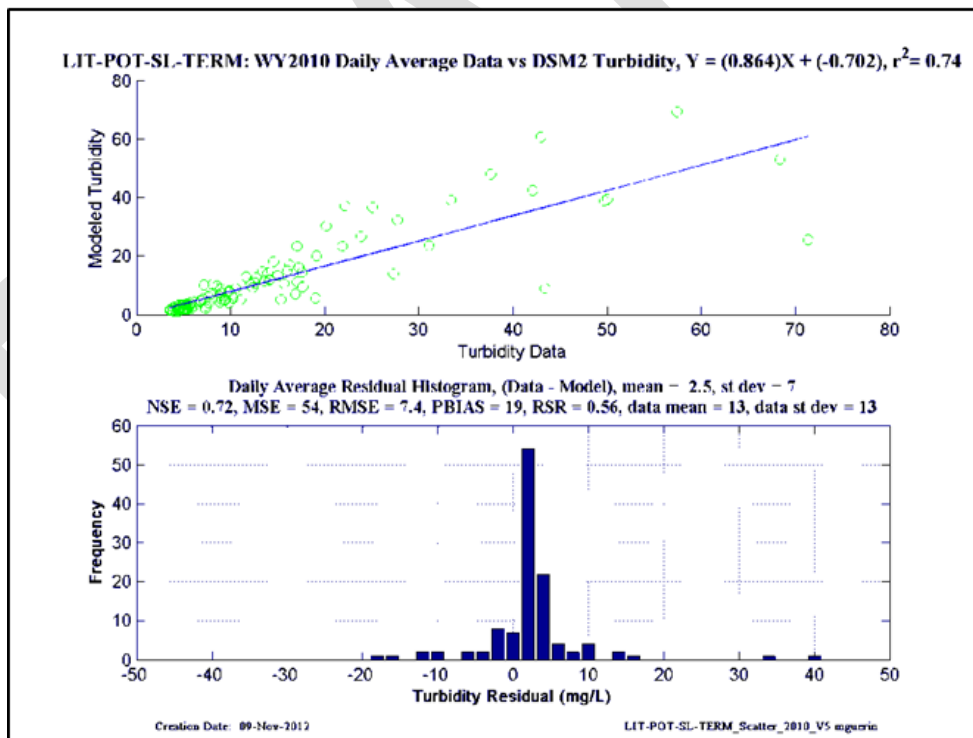
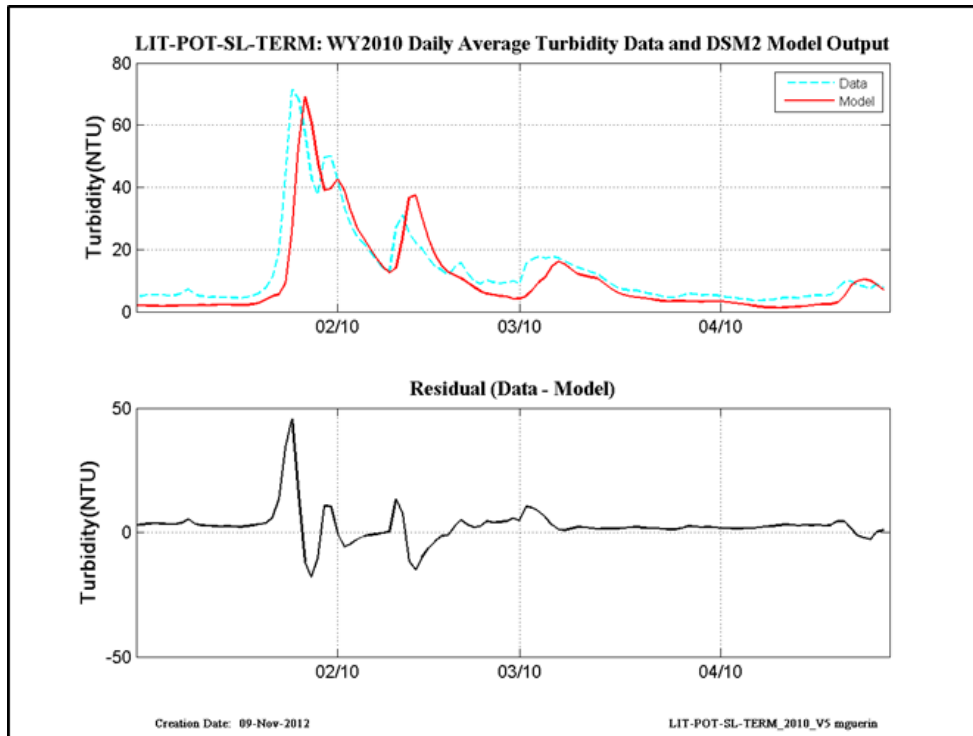


Figure 11-42 WY2010 revised calibration results at Little Potato Slough-at-Terminus.

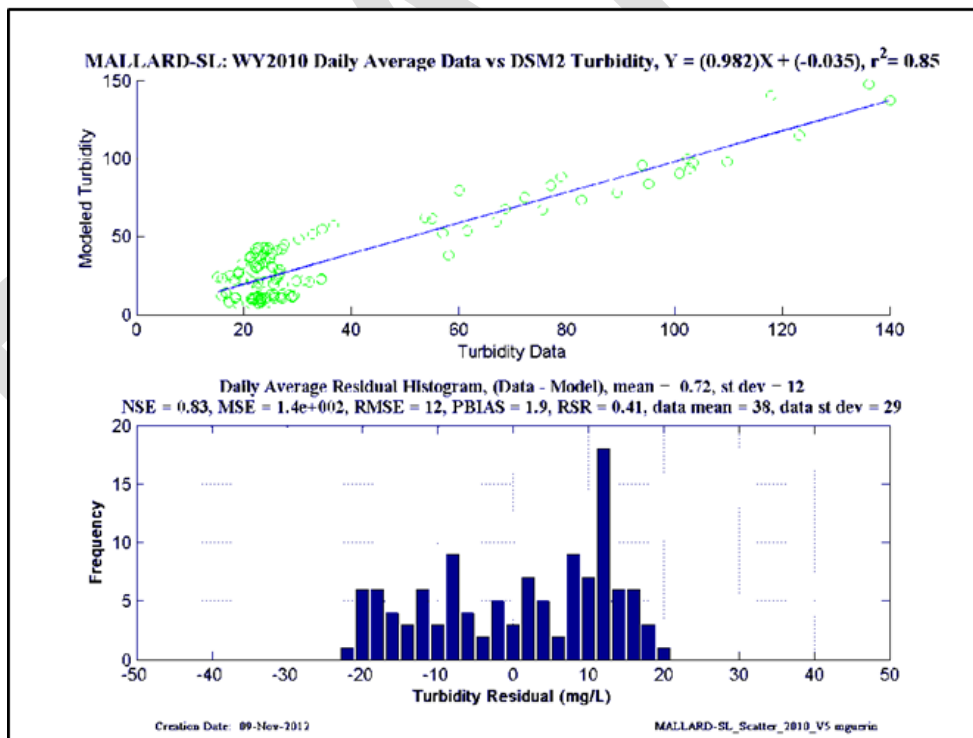
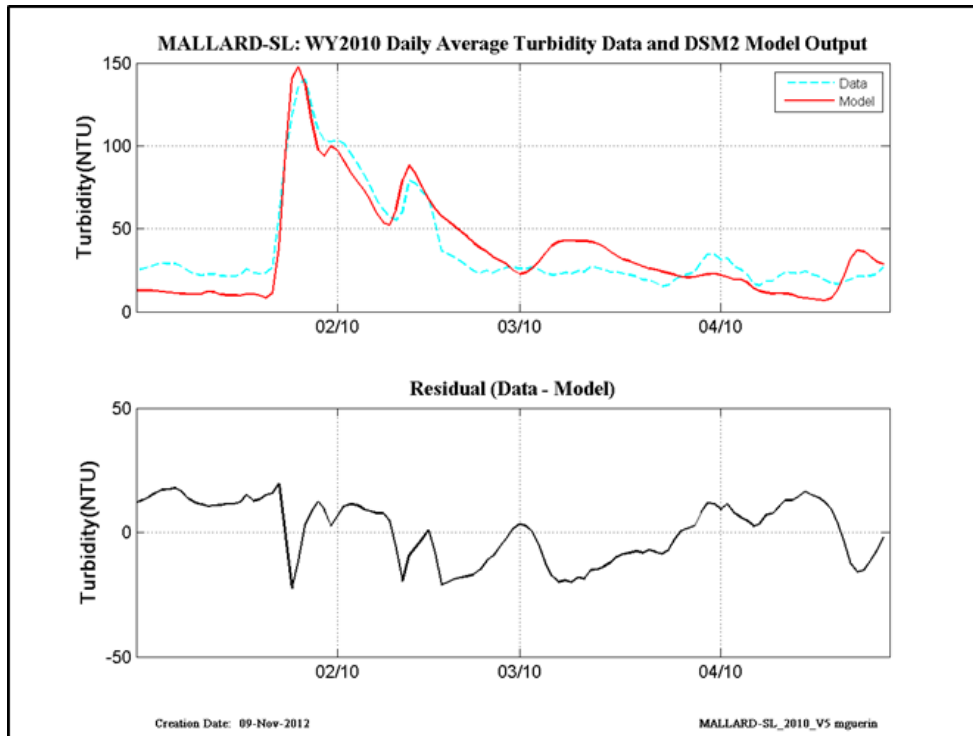


Figure 11-43 WY2010 revised calibration results at Mallard Slough.

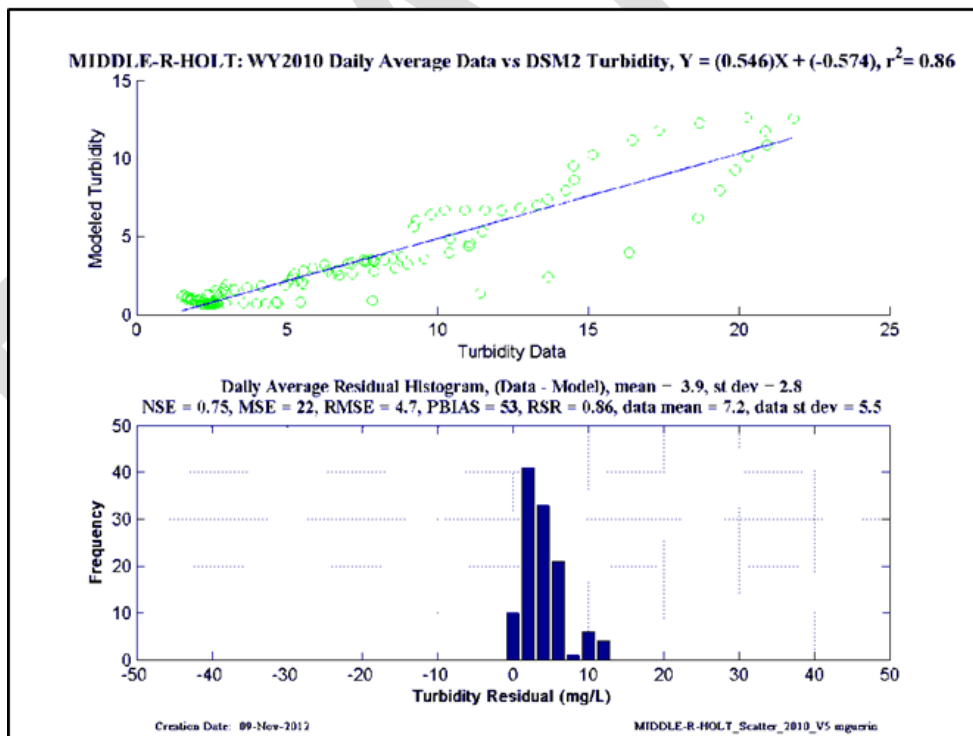
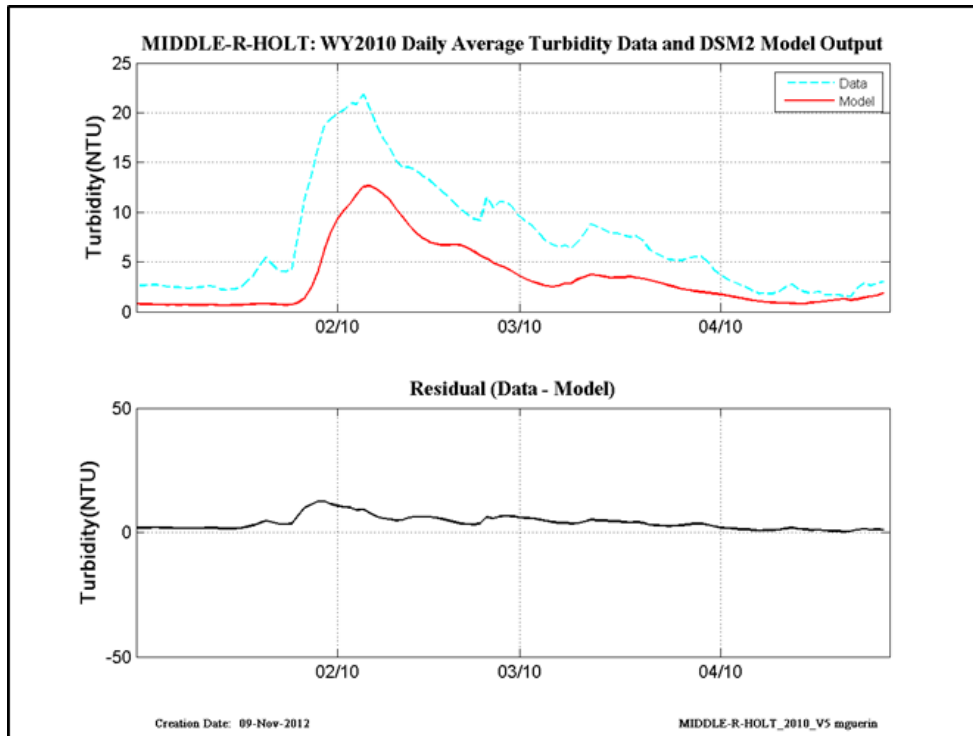


Figure 11-44 WY2010 revised calibration results at Middle River-at-Holt.

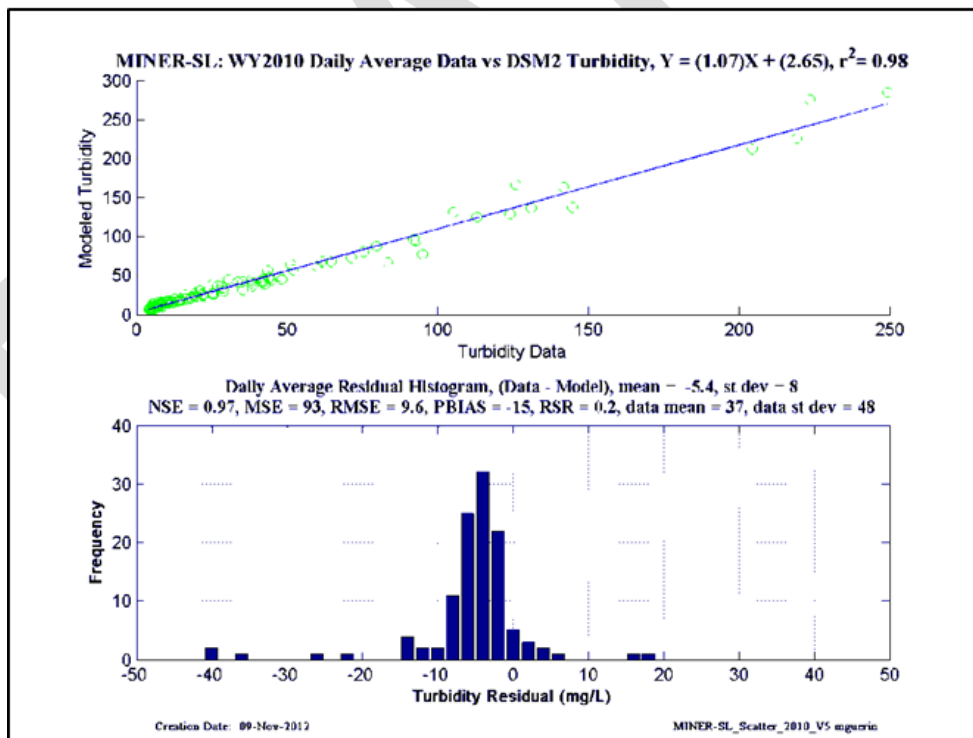
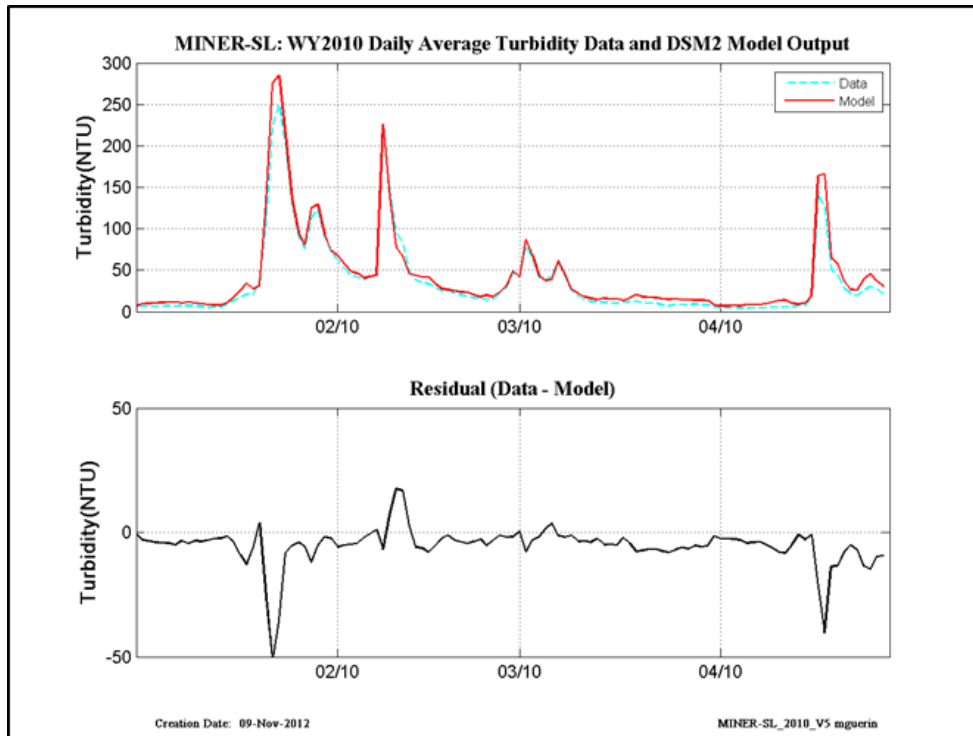


Figure 11-45 WY2010 revised calibration results at Miner Slough.

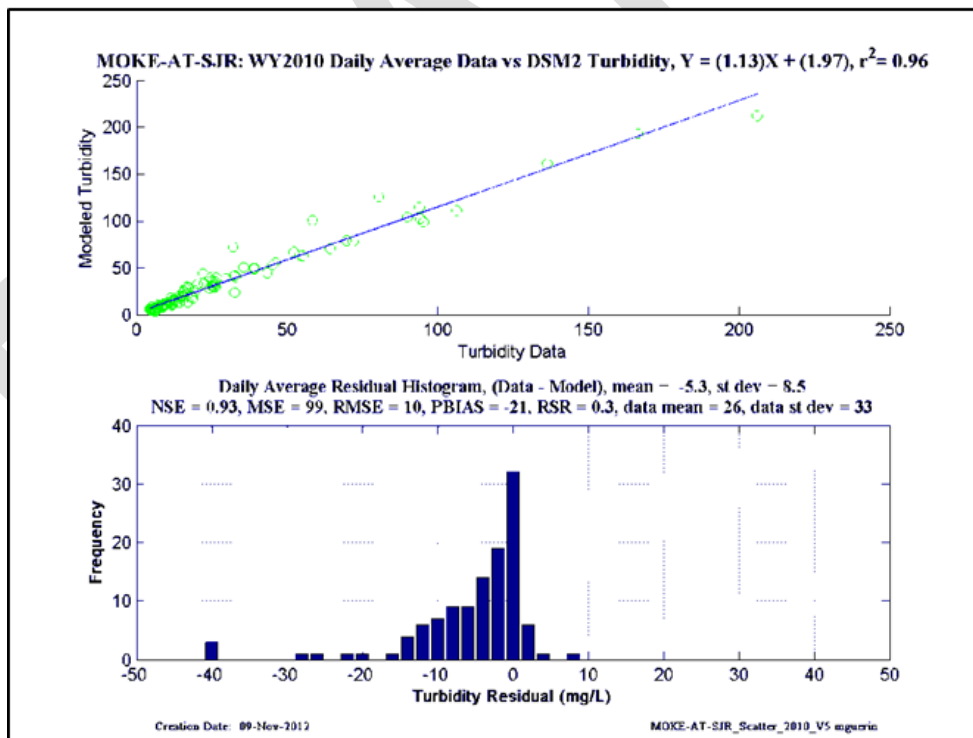
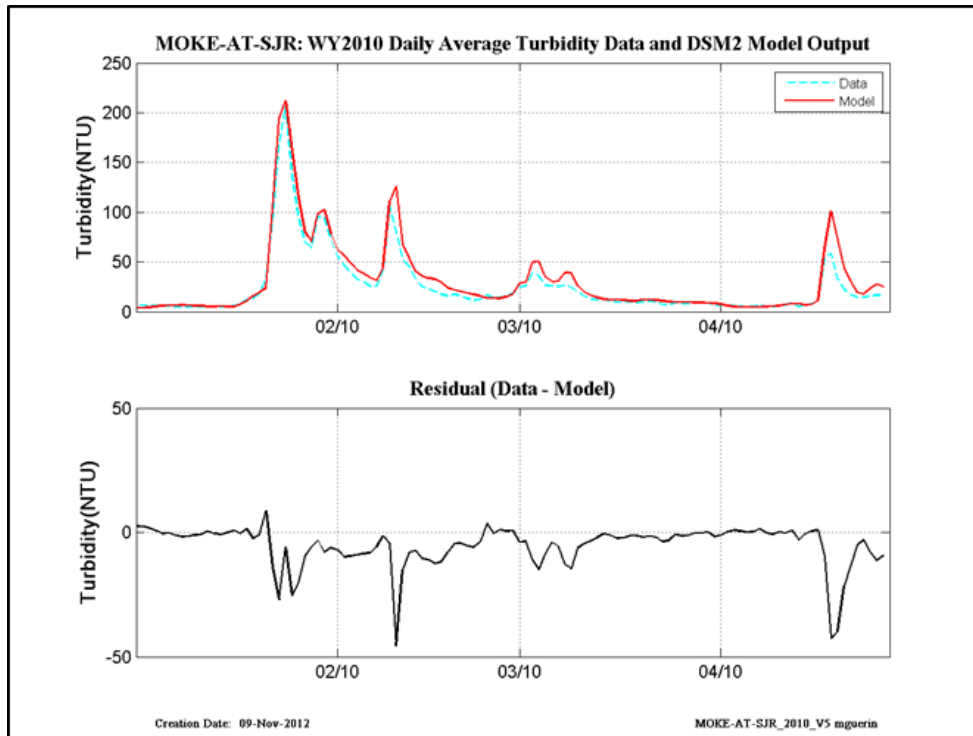


Figure 11-46 WY2010 revised calibration results at Mokelumne-at-San Joaquin.

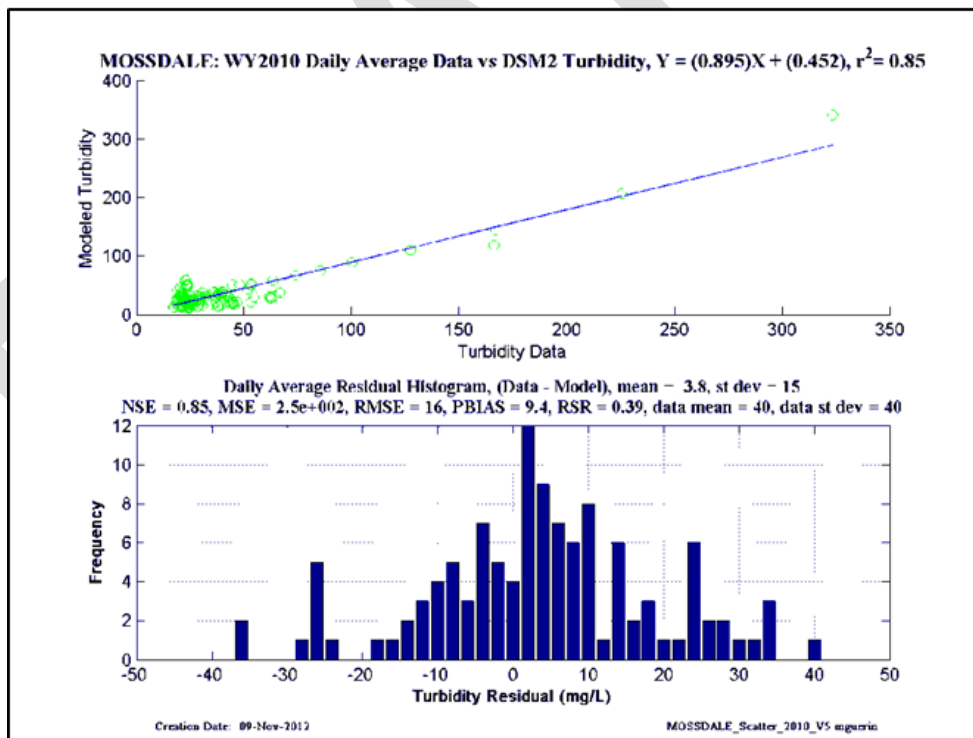
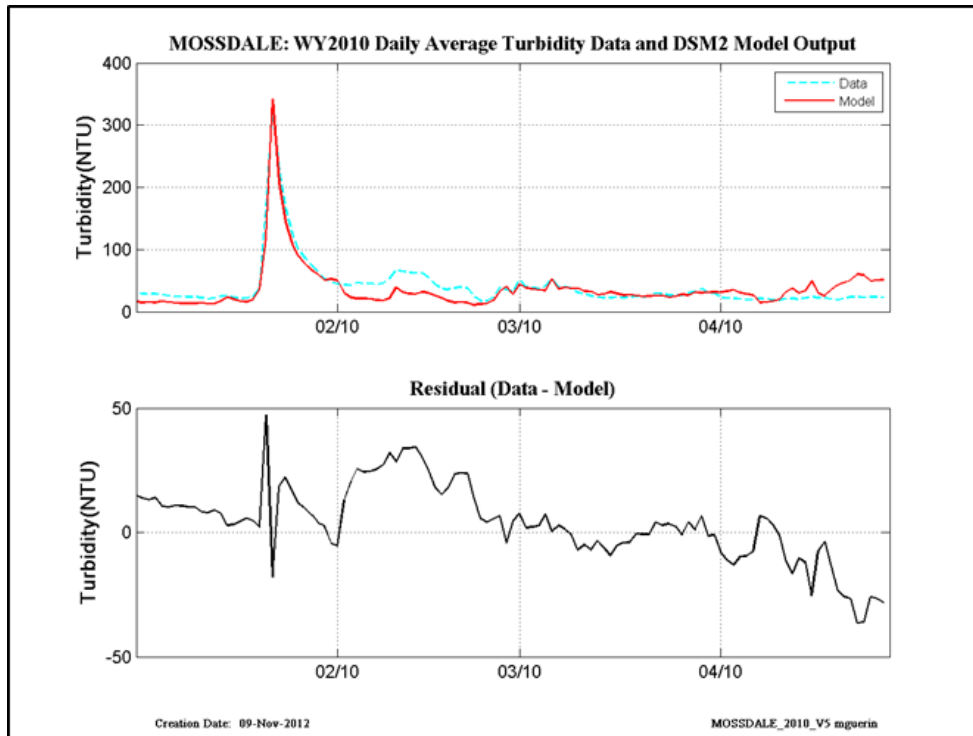


Figure 11-47 WY2010 revised calibration results at Mossdale.

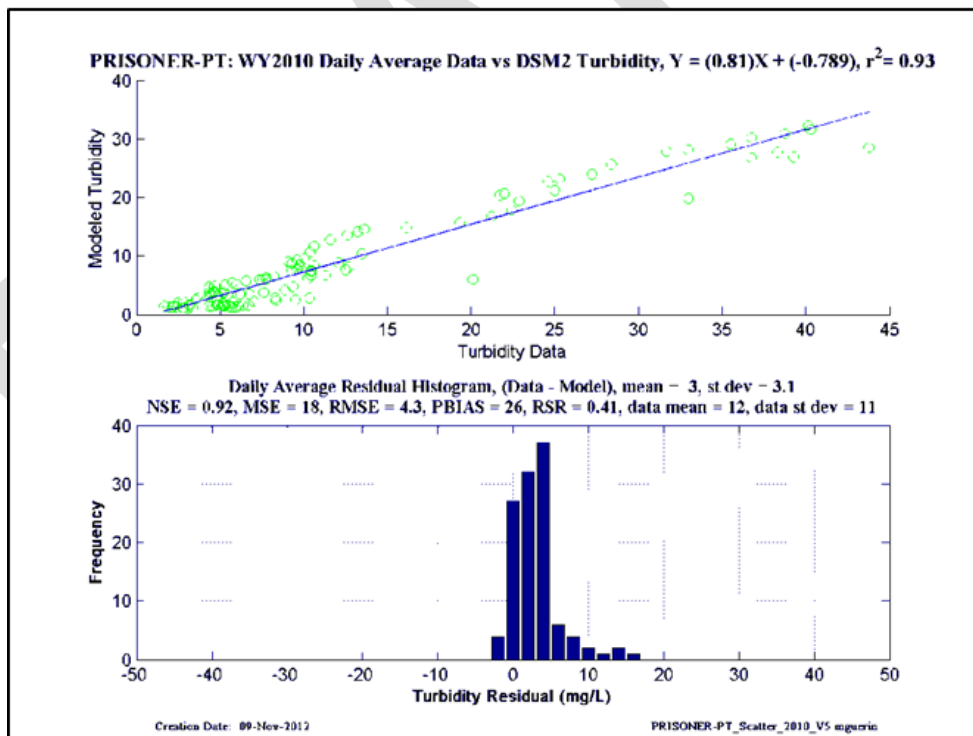
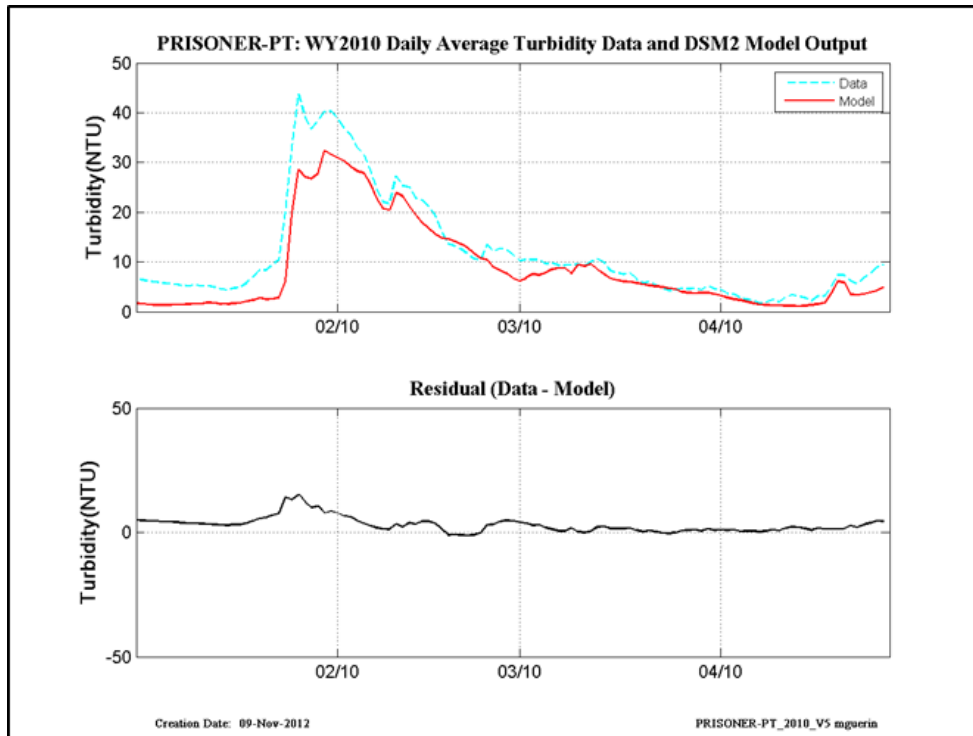


Figure 11-48 WY2010 revised calibration results at Prisoner Point.

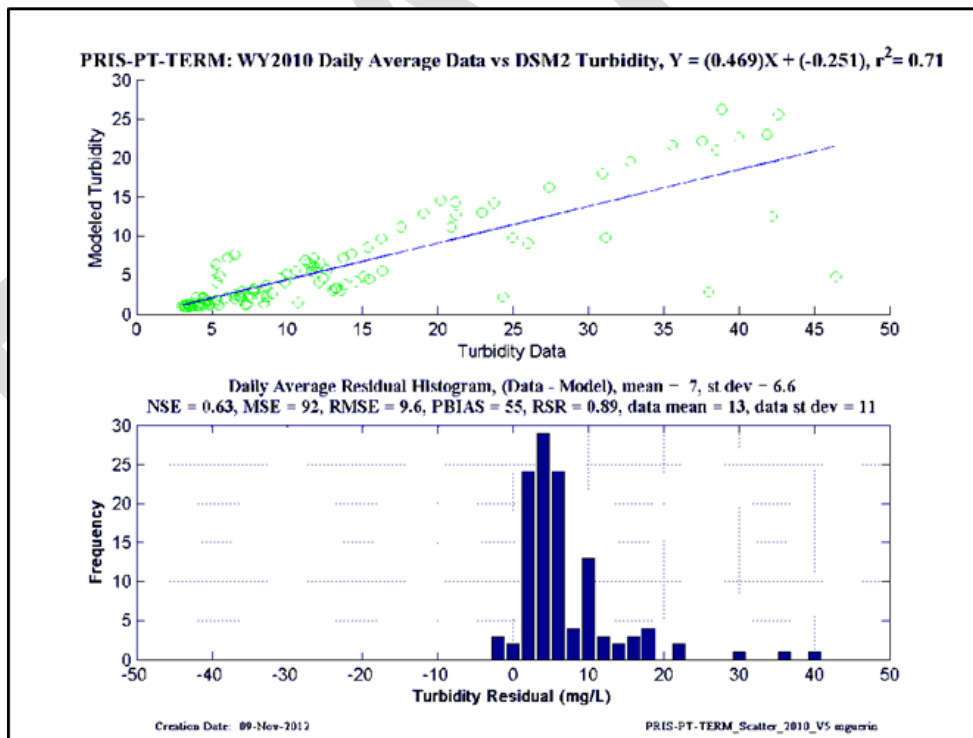
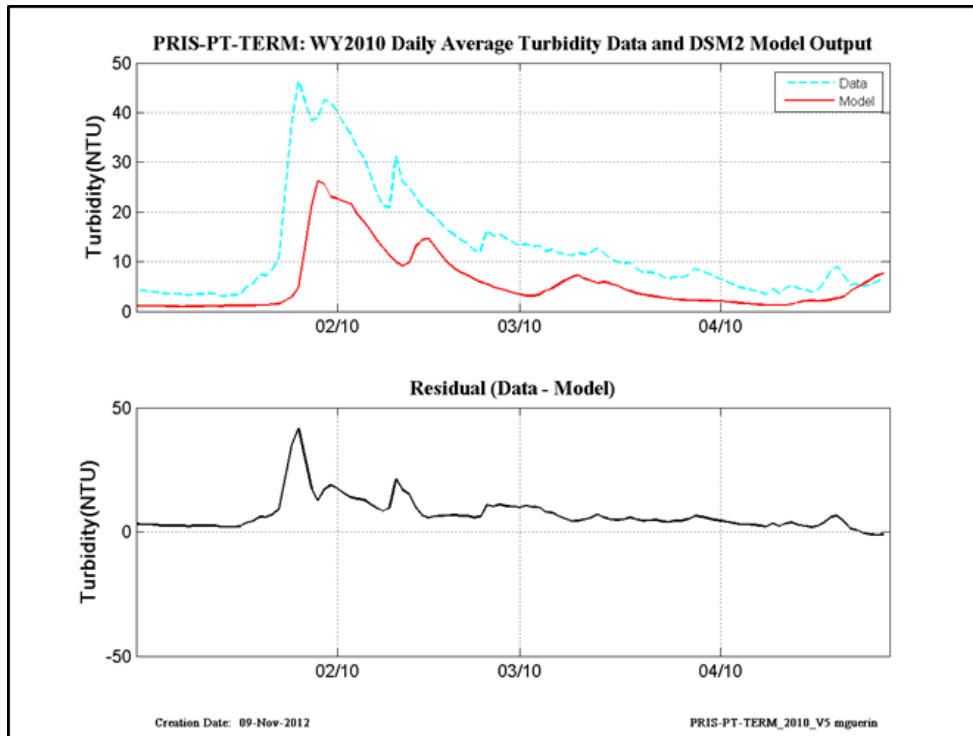


Figure 11-49 WY2010 revised calibration results at Prisoner Point-at-Terminus.

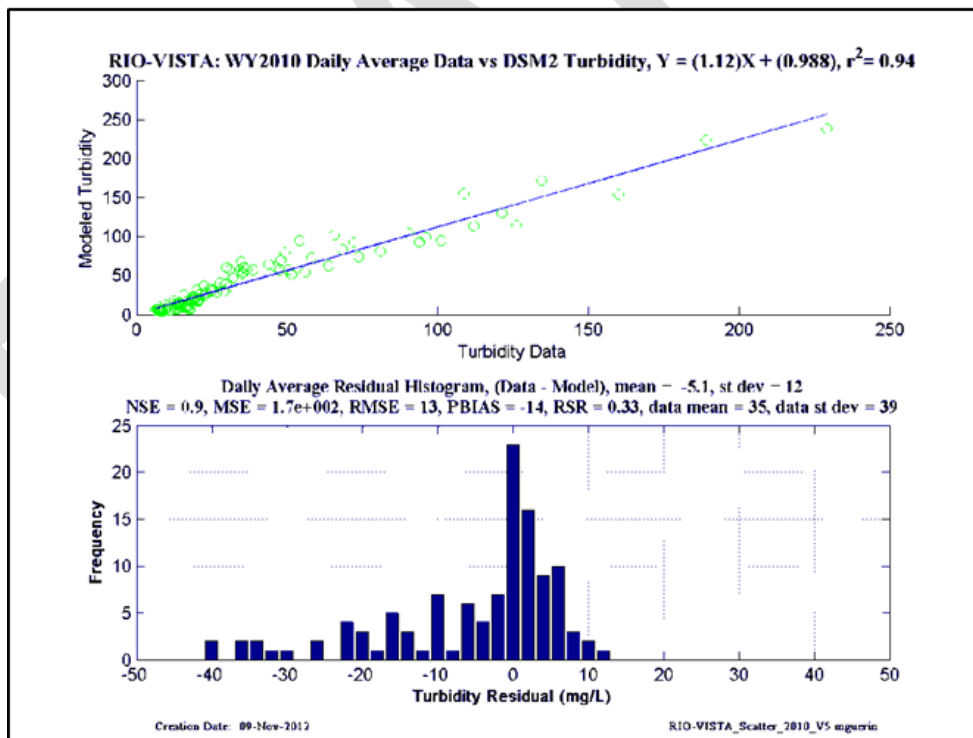
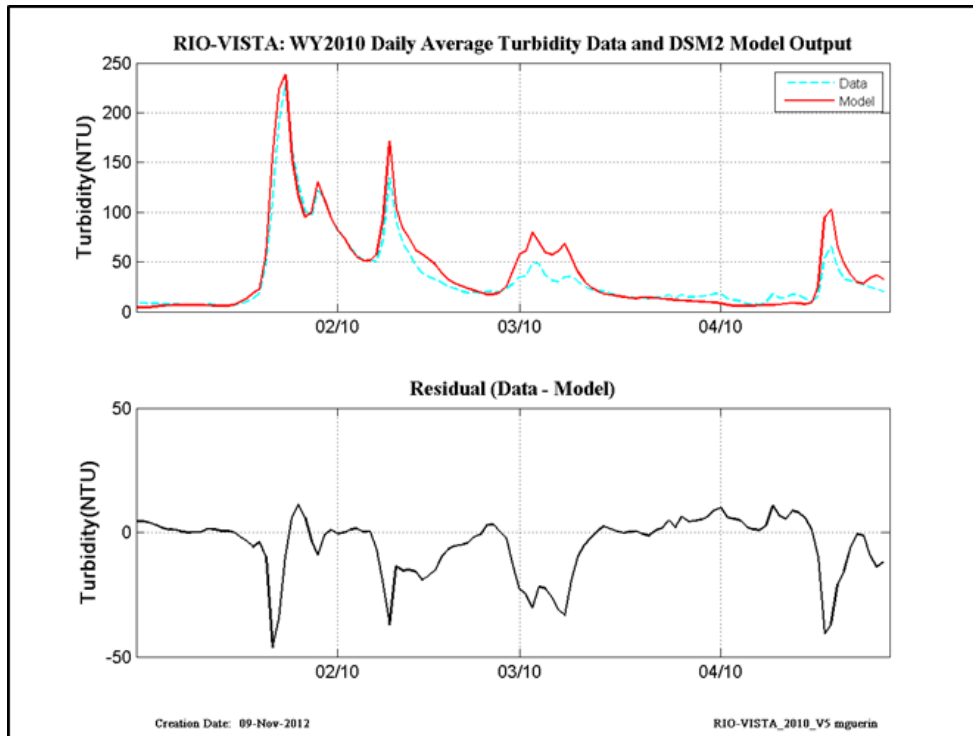


Figure 11-50 WY2010 revised calibration results at Rio Vista.

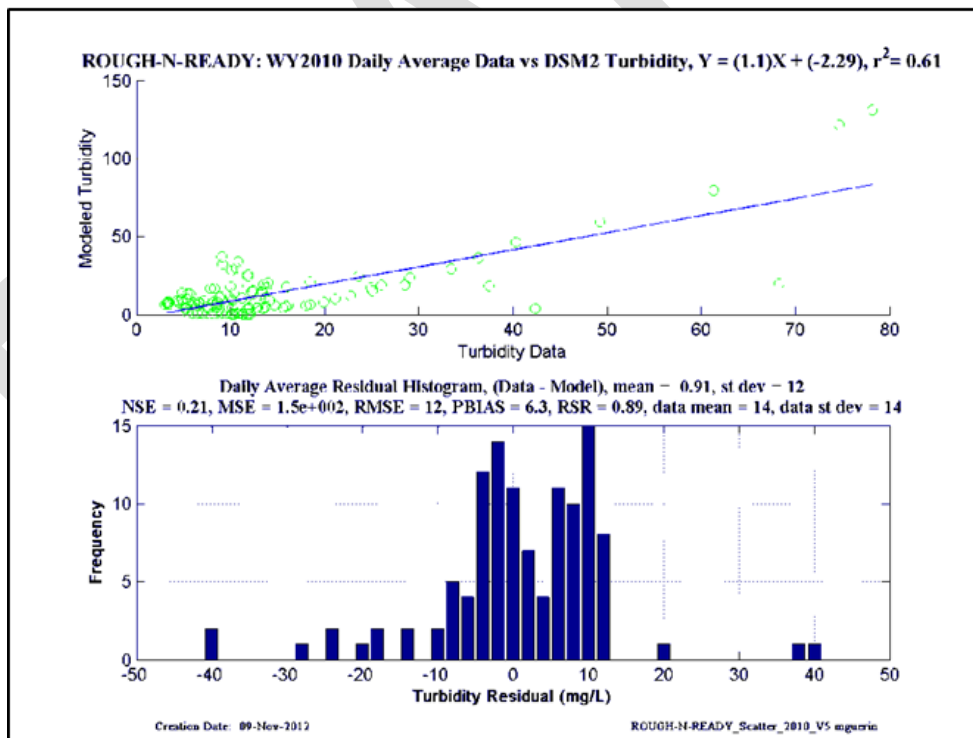
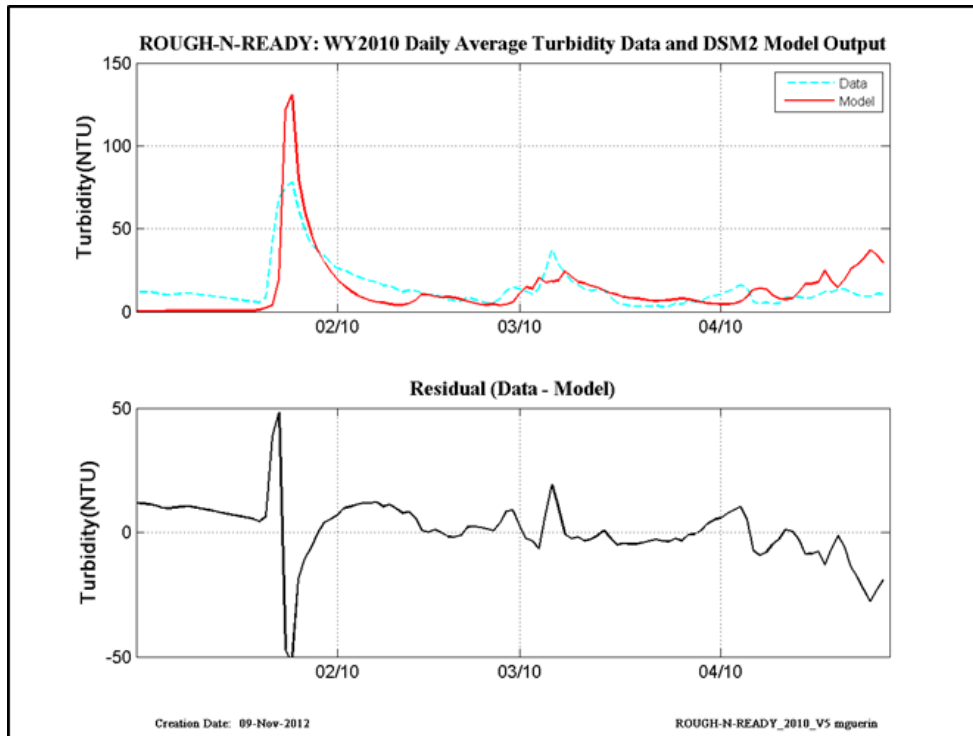


Figure 11-51 WY2010 revised calibration results at Rough-N-Ready Island.

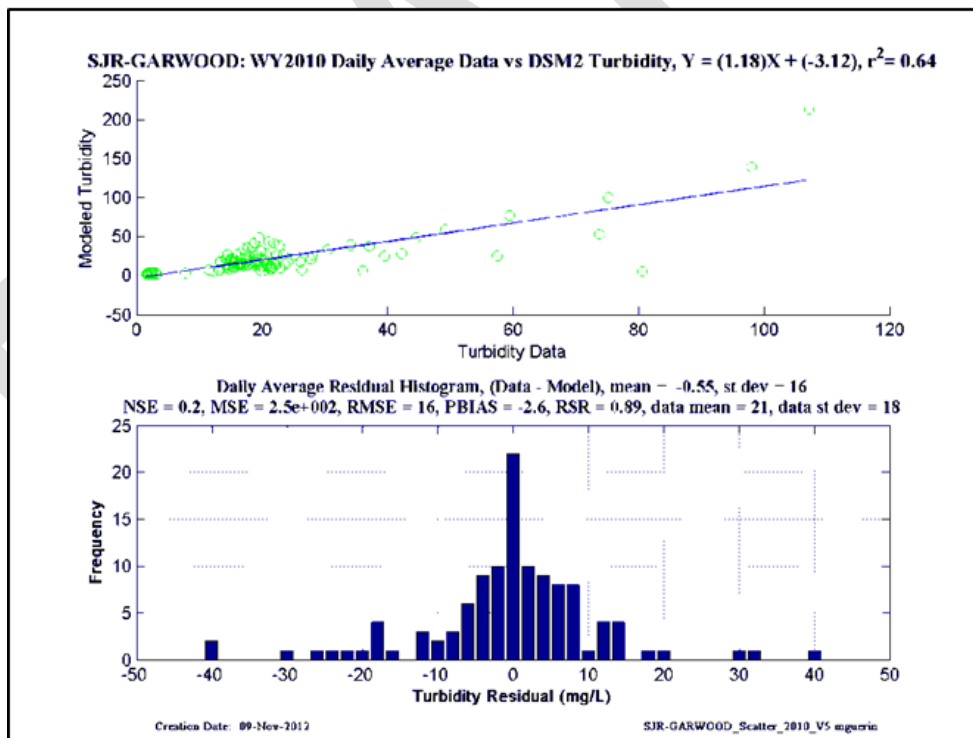
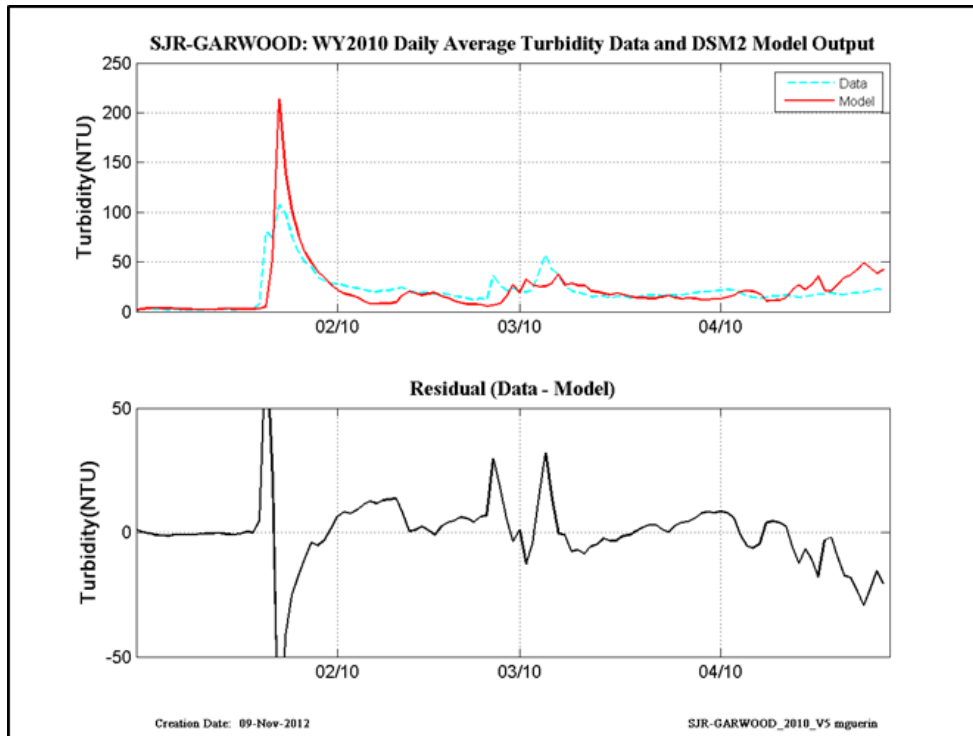


Figure 11-52 WY2010 revised calibration results at San Joaquin-at-Garwood.

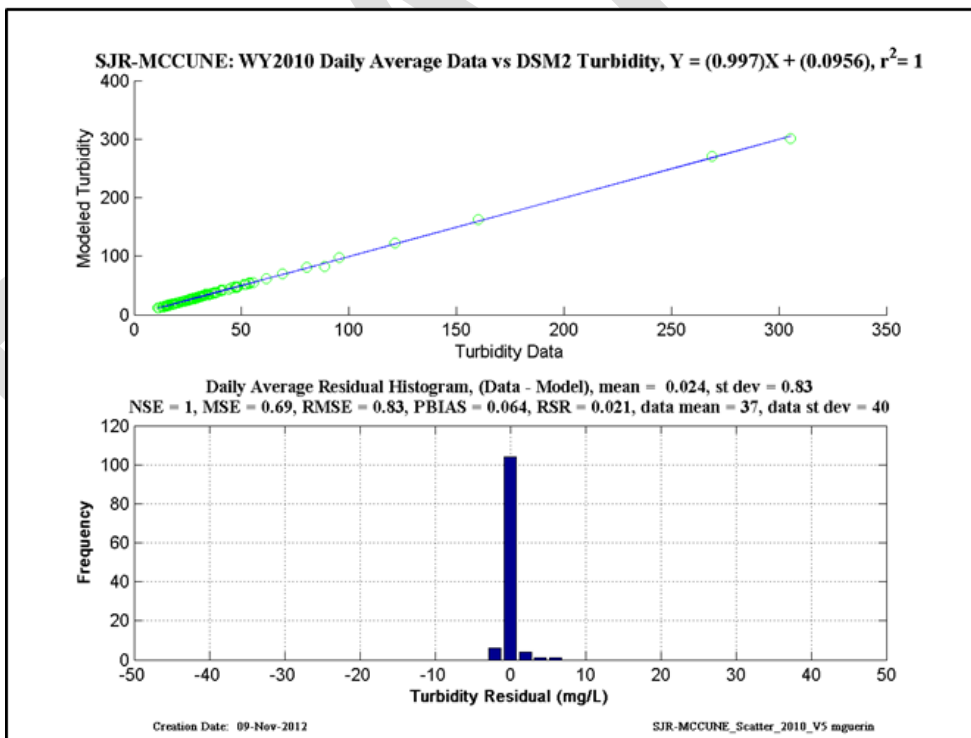
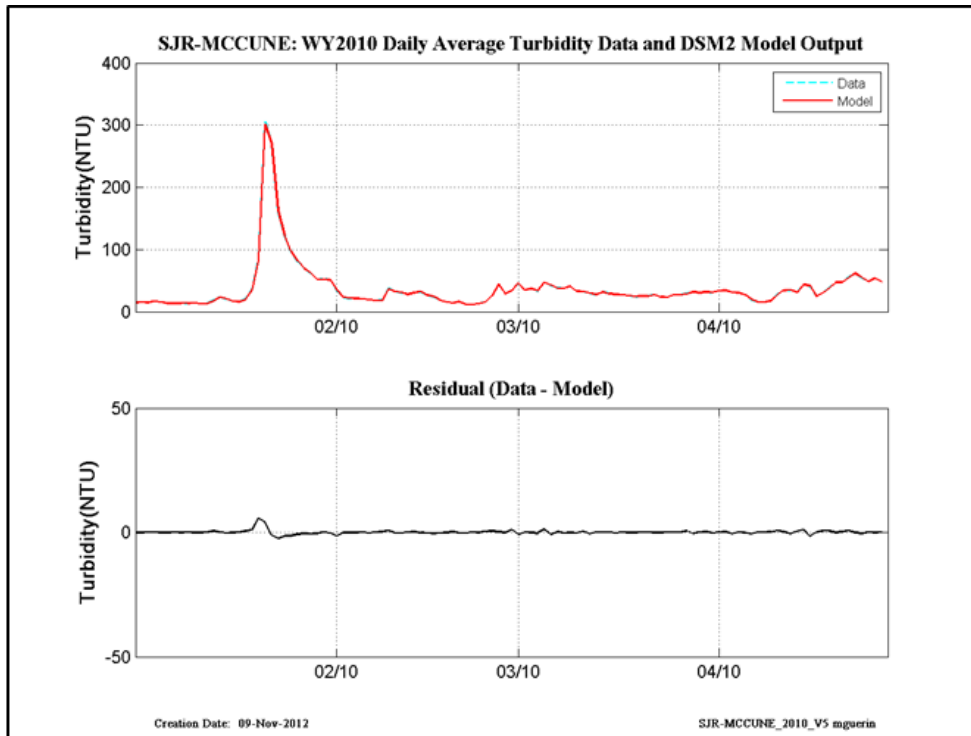


Figure 11-53 WY2010 revised calibration results at San Joaquin-at-McCune (Vernalis).

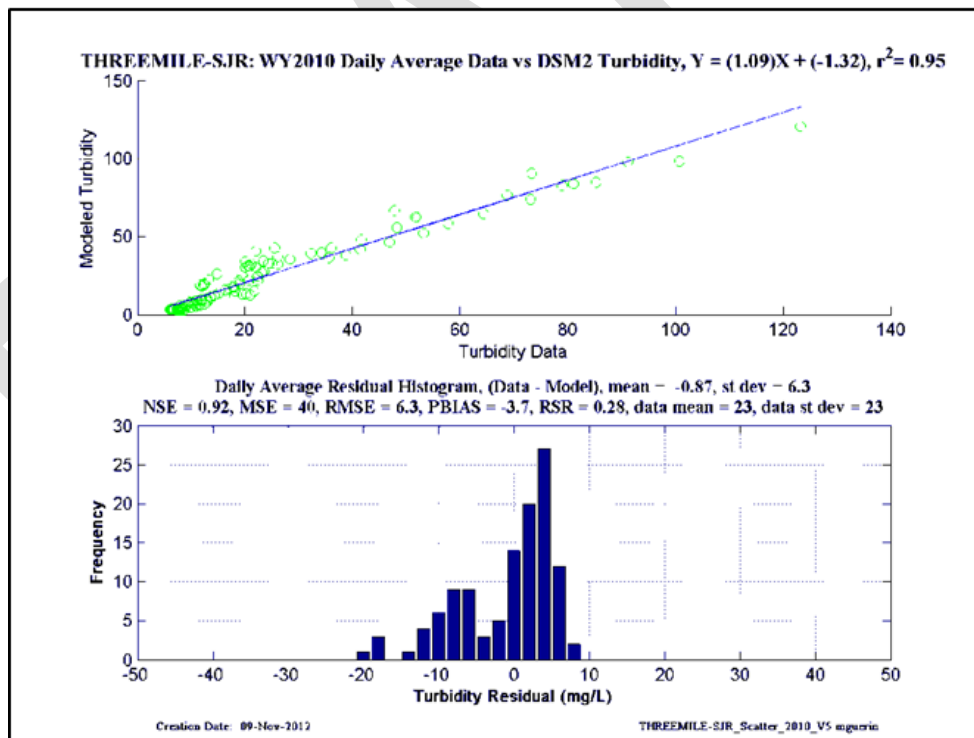
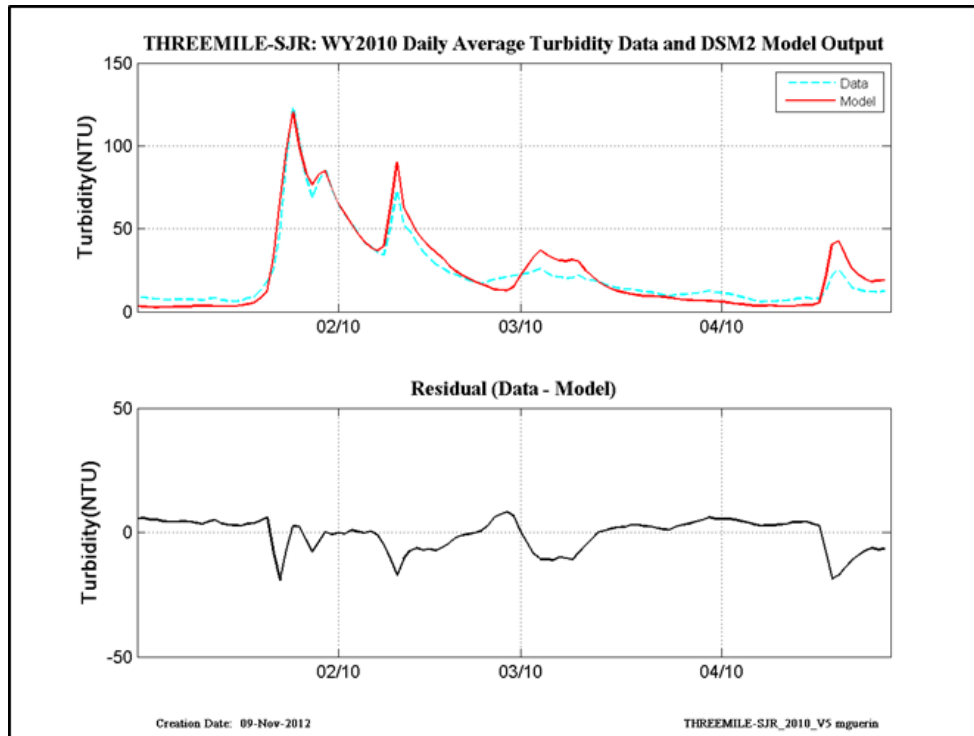


Figure 11-54 WY2010 revised calibration results at Threemile-Slough-at-San Joaquin.

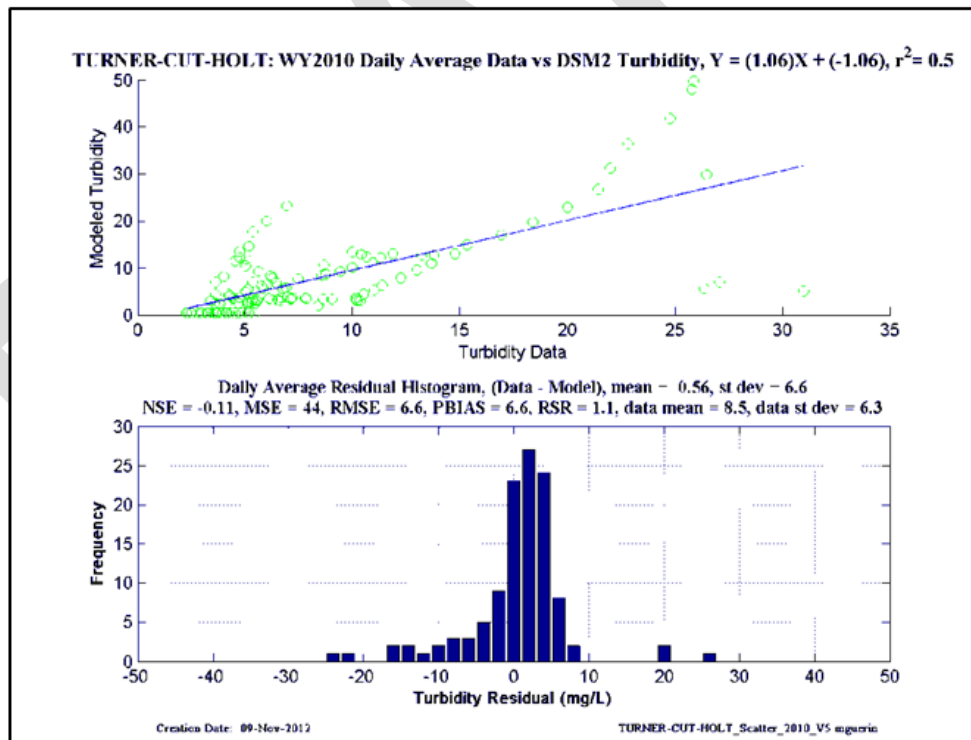
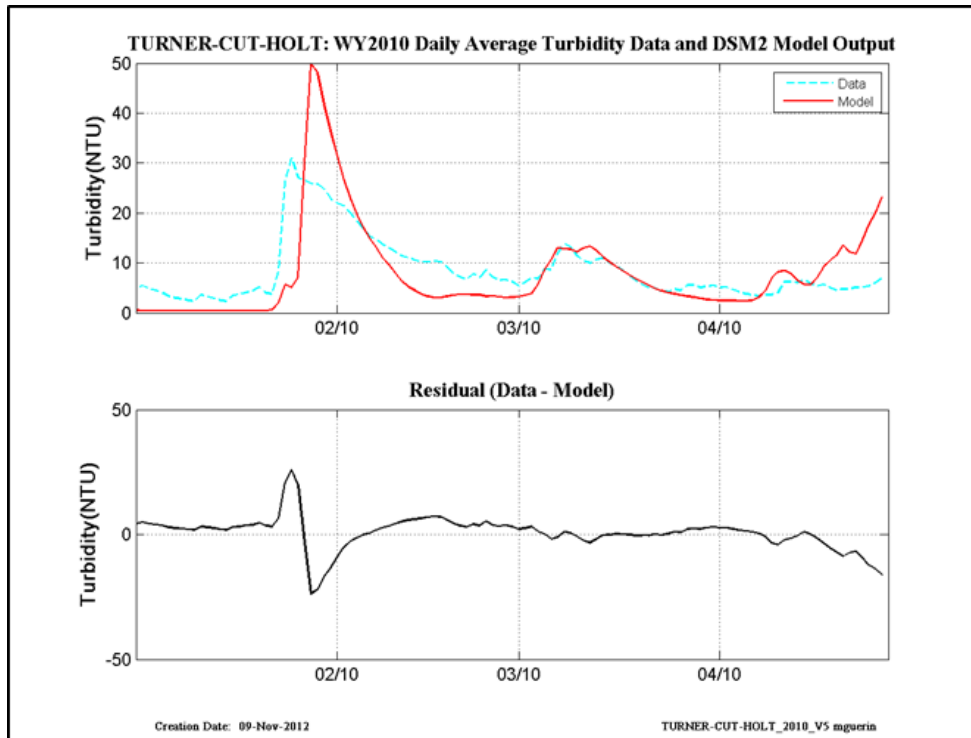


Figure 11-55 WY2010 revised calibration results at Turner Cut-at-Holt.

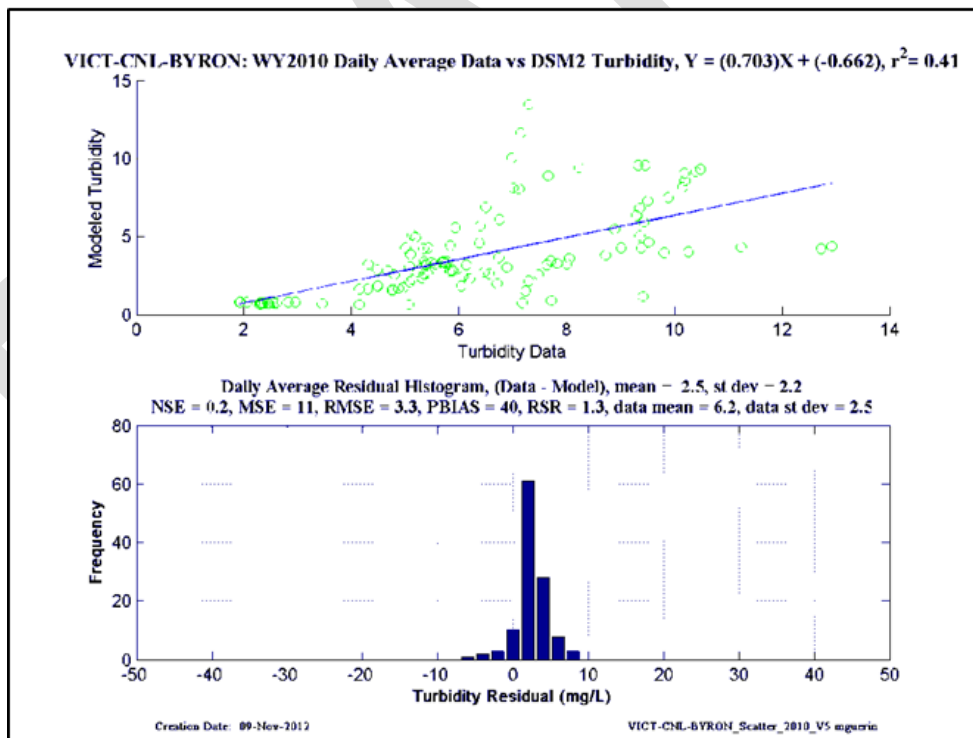
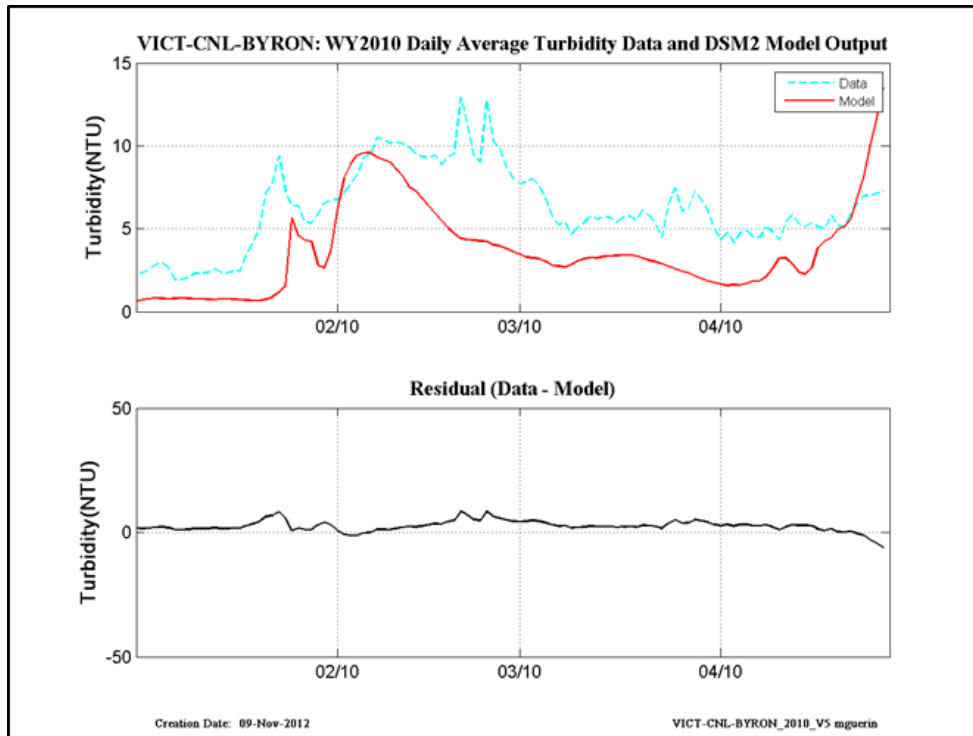


Figure 11-56 WY2010 revised calibration results at Victoria Canal-at-Byron.

## **12 Appendix III - Updated QUAL Turbidity calibration statistics, 15-min**

### **12.1 Fifteen Minute CDEC data and model output - WY2013**

DRAFT

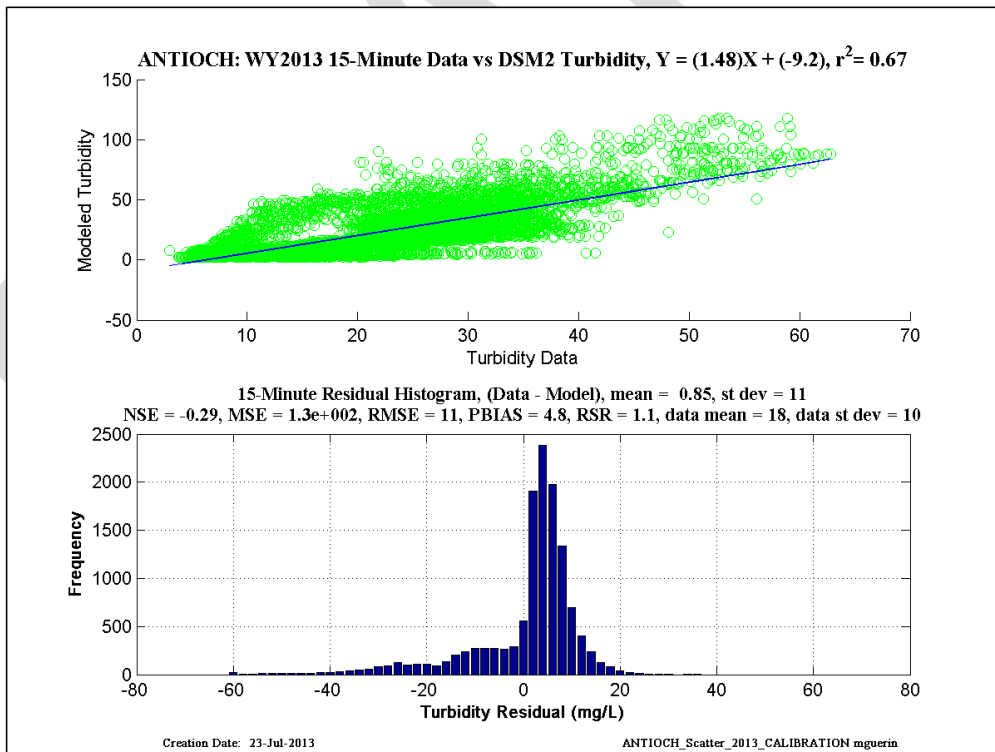
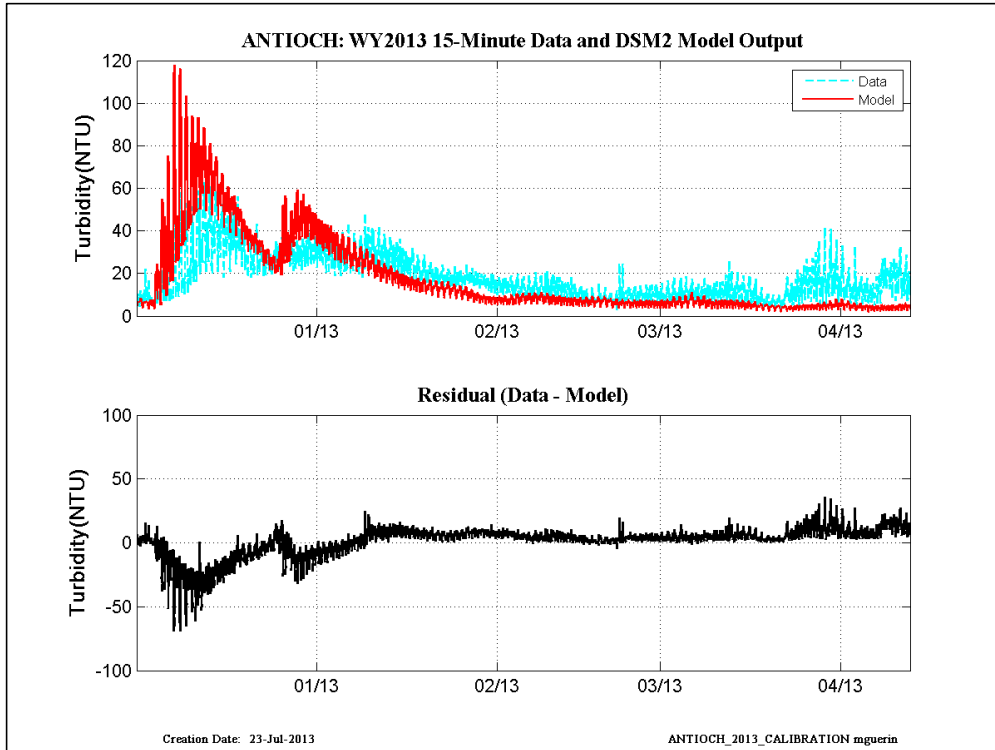


Figure 12-1 WY2013 15-min RMA new calibration results at Antioch.

**12.2 Fifteen Minute CDEC data and model output - WY2011**

DRAFT

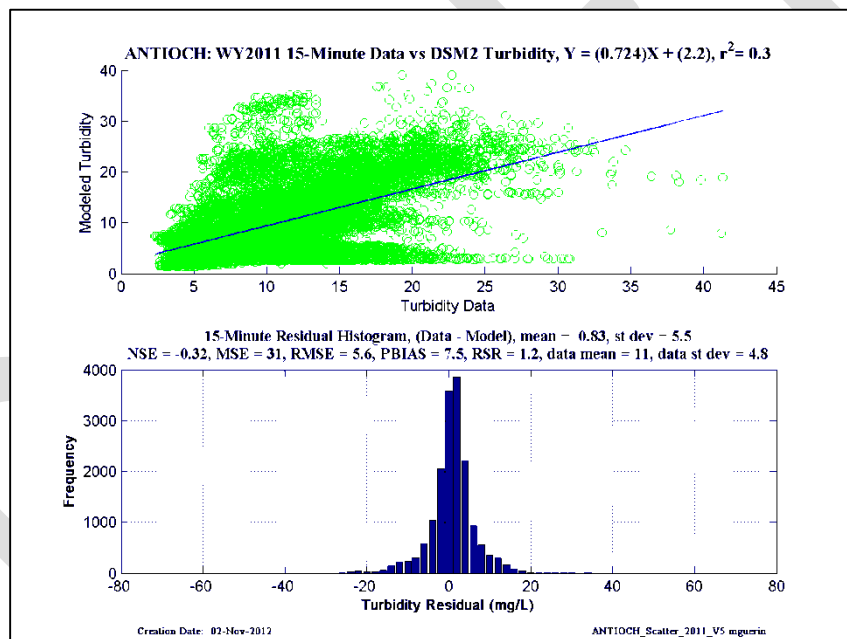
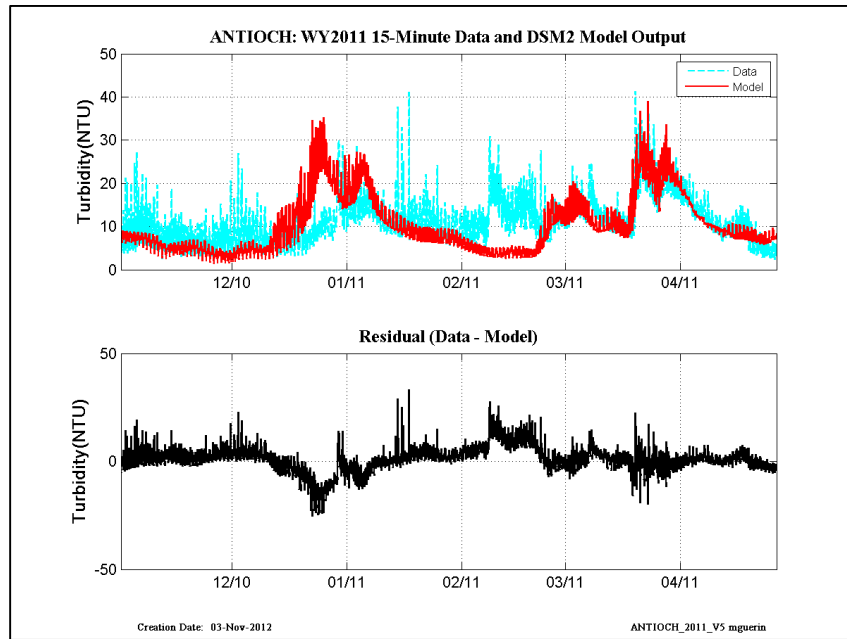


Figure 12-2 WY2011 15-min revised calibration results at Antioch.

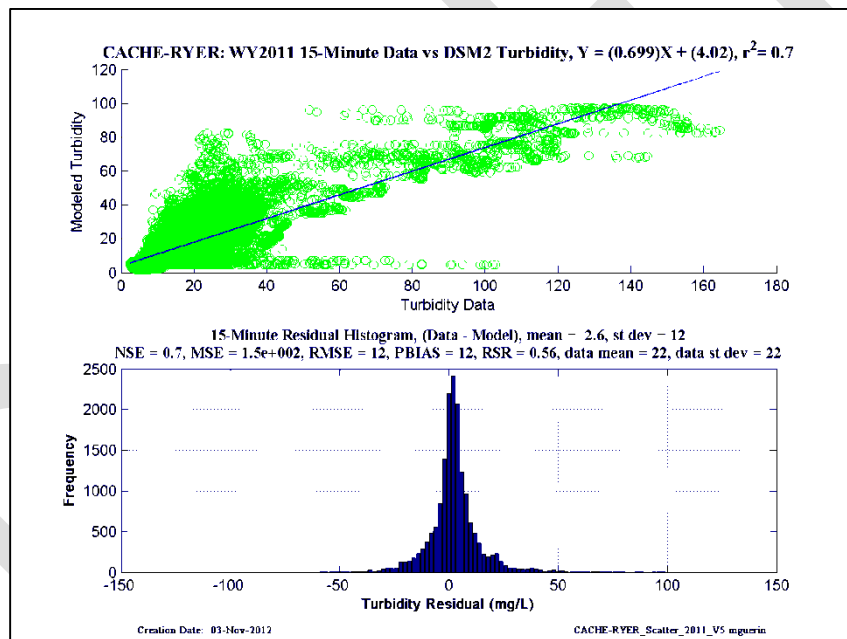
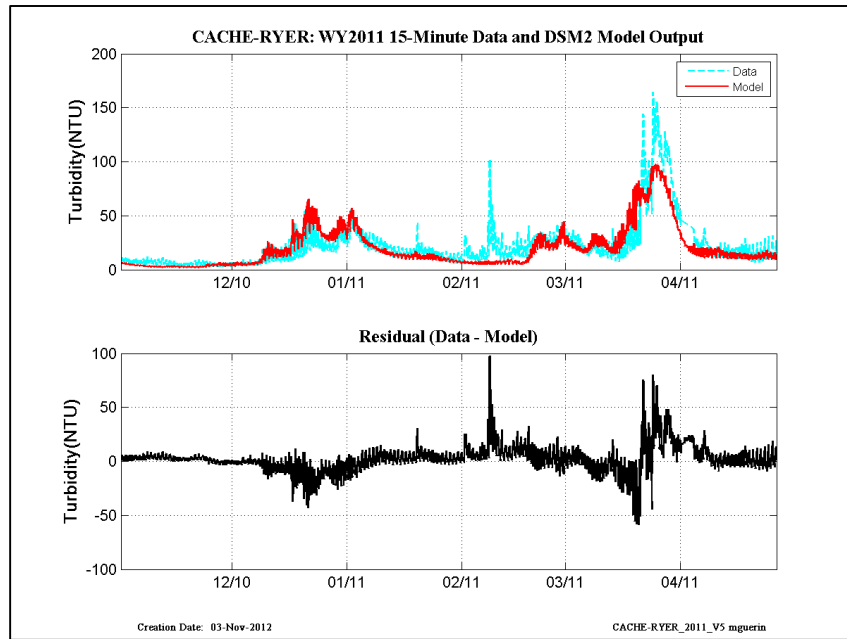


Figure 12-3 WY2011 15-min revised calibration results at Cache-Ryer.

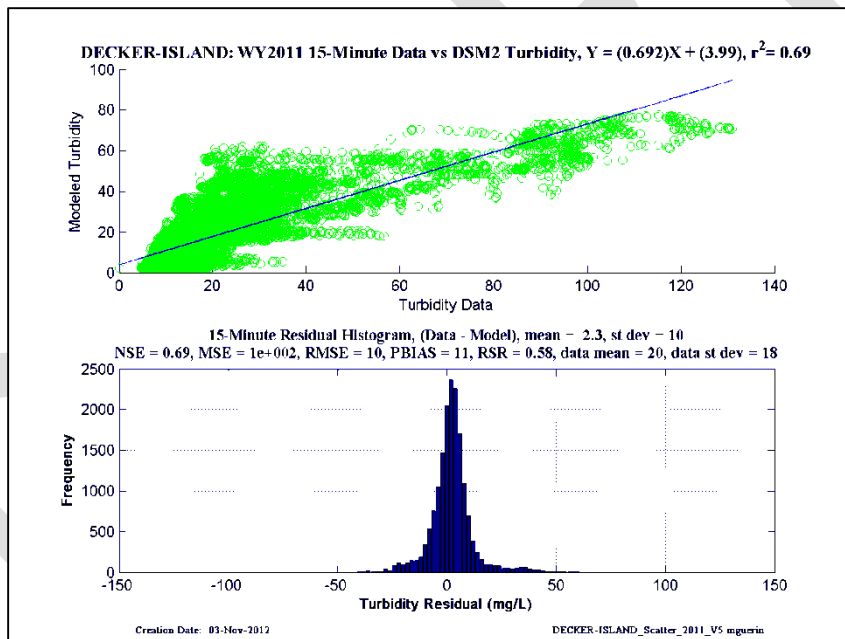
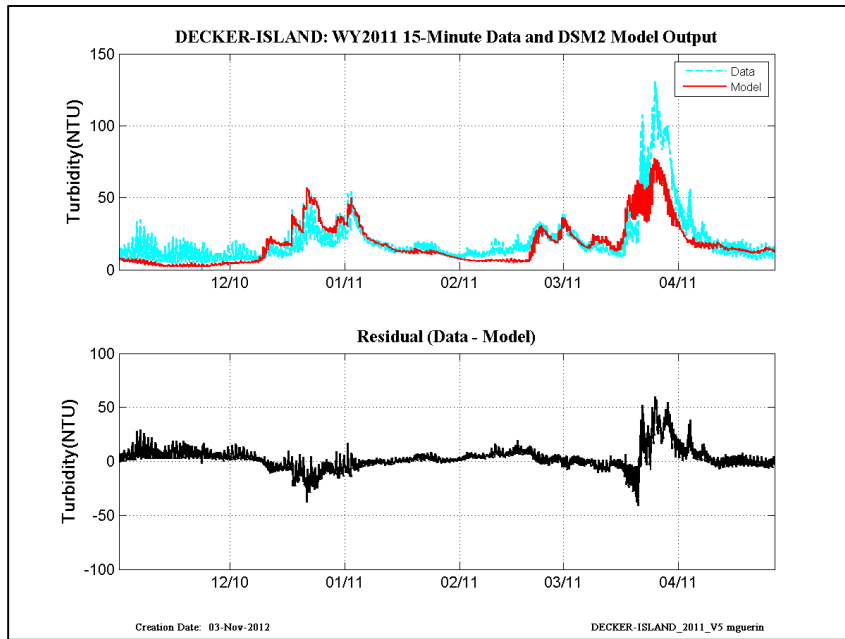


Figure 12-4 WY2011 15-min revised calibration results at Decker Island.

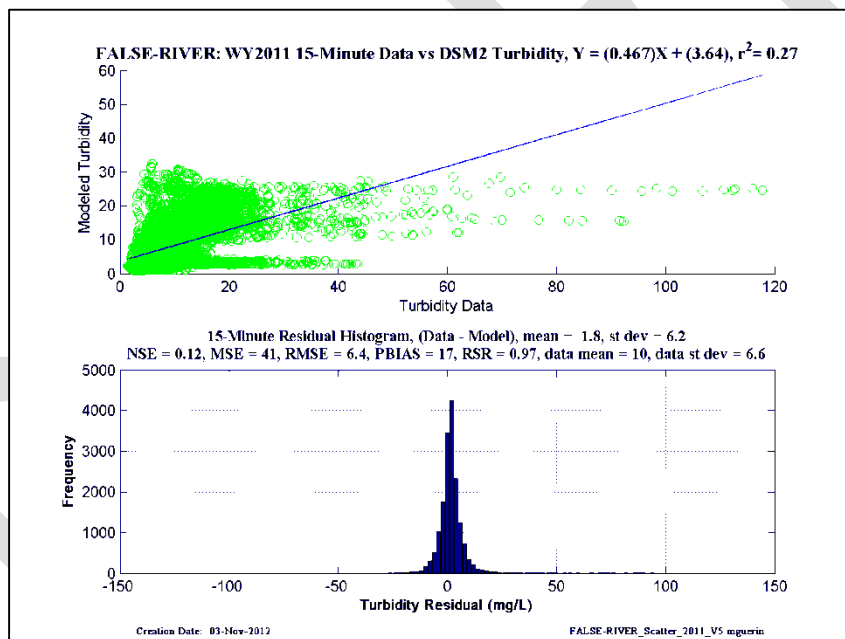
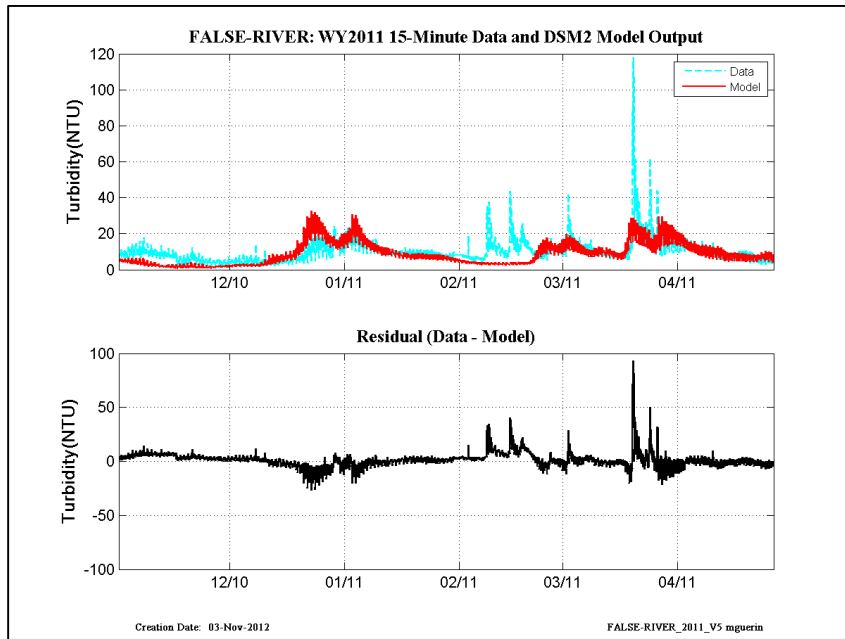


Figure 12-5 WY2011 15-min revised calibration results at False River.

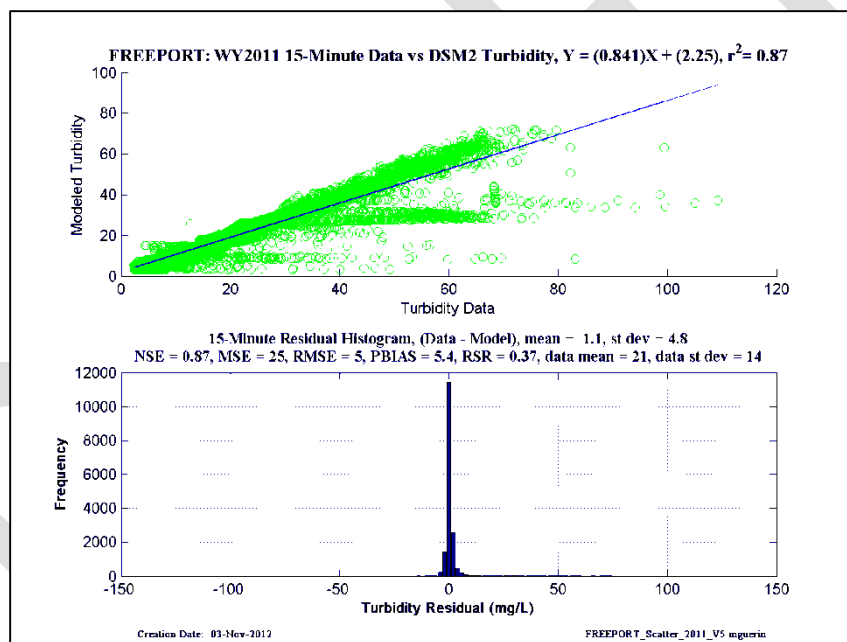
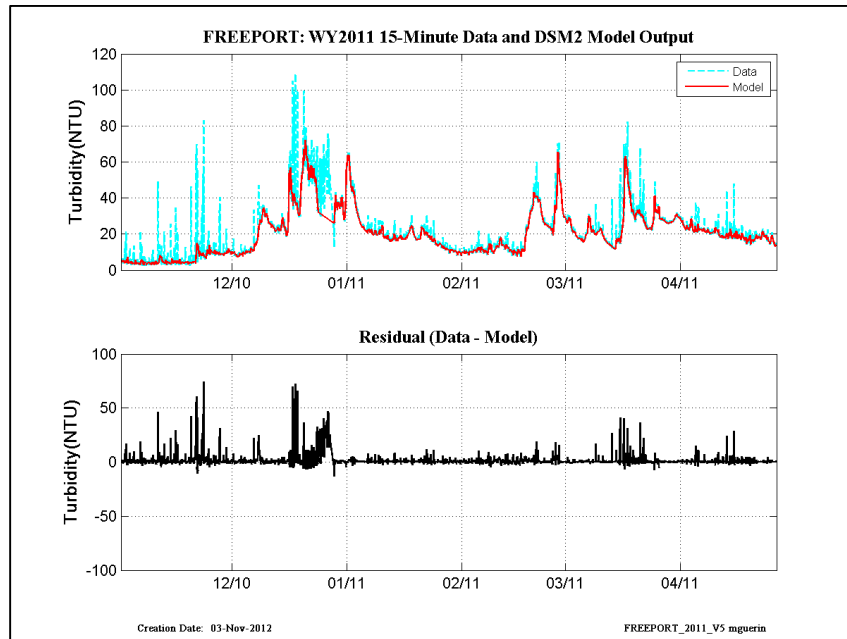


Figure 12-6 WY2011 15-min revised calibration results at Freeport.

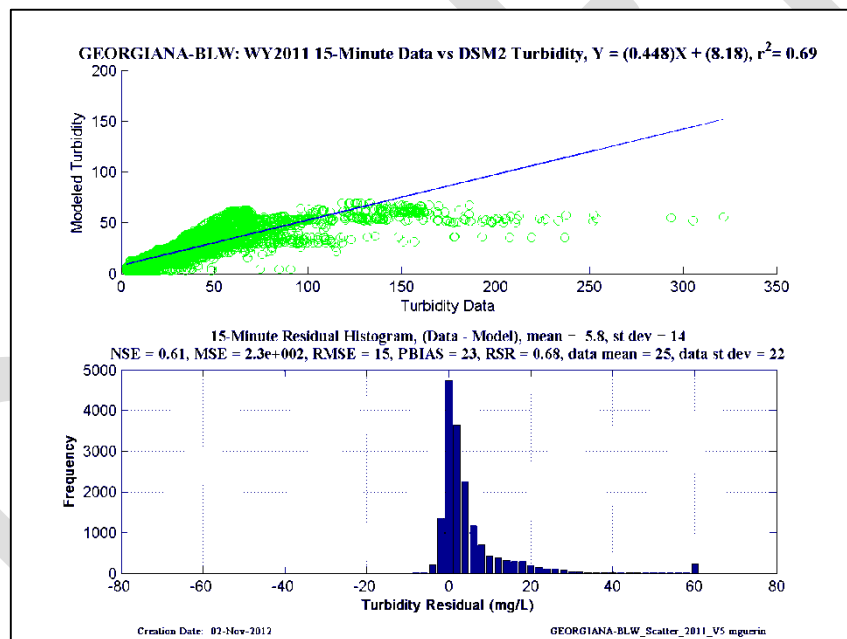
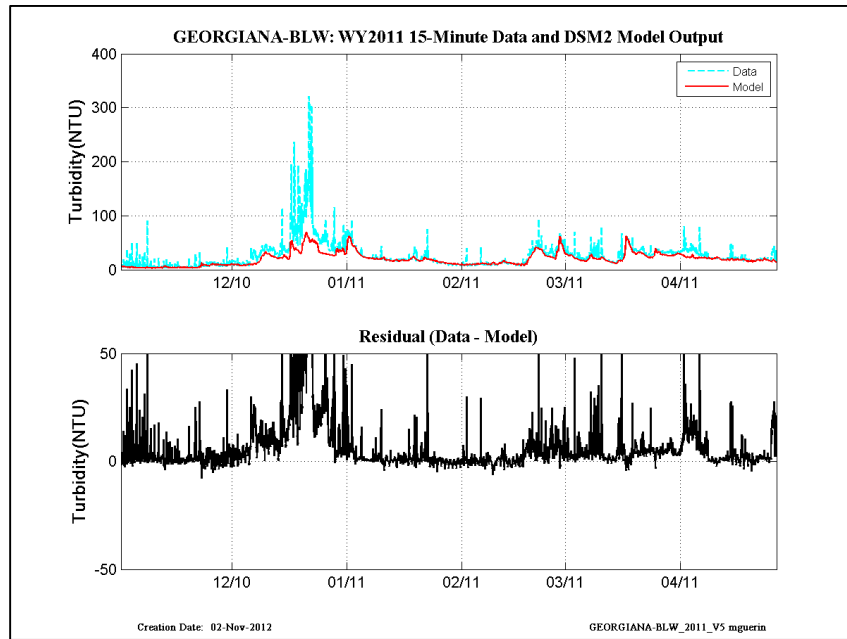


Figure 12-7 WY2011 15-min revised calibration results at Georgiana-Below-Sac.

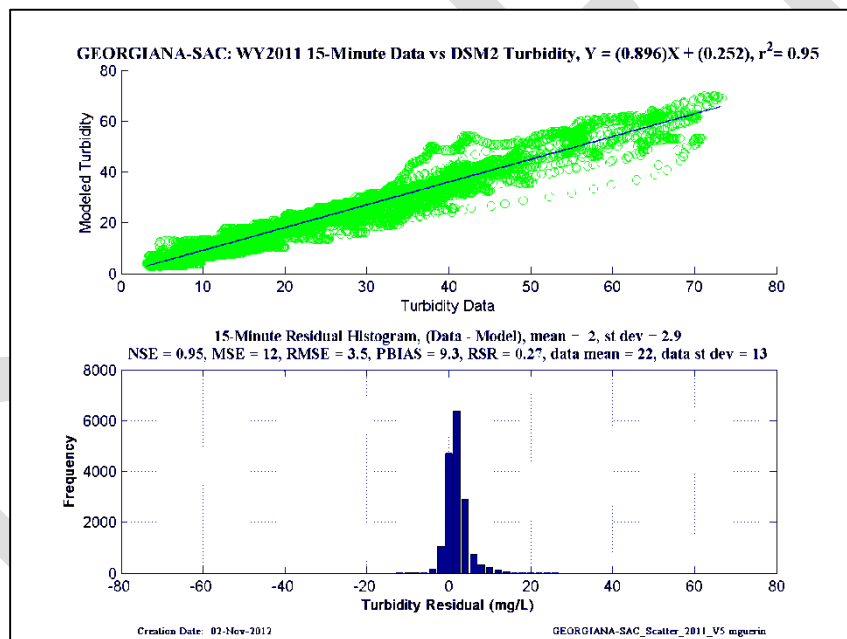
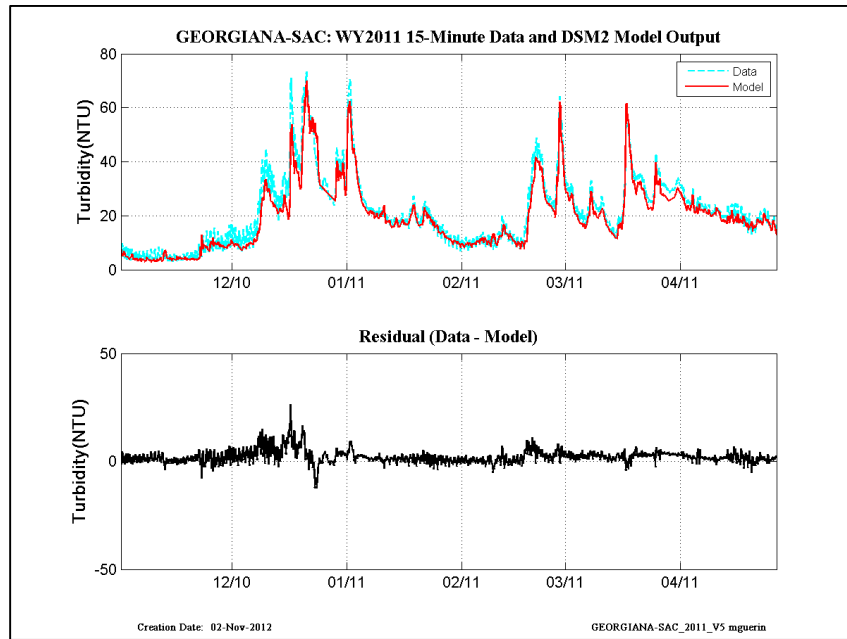


Figure 12-8 WY2011 15-min revised calibration results at Georgiana-at-Sac.

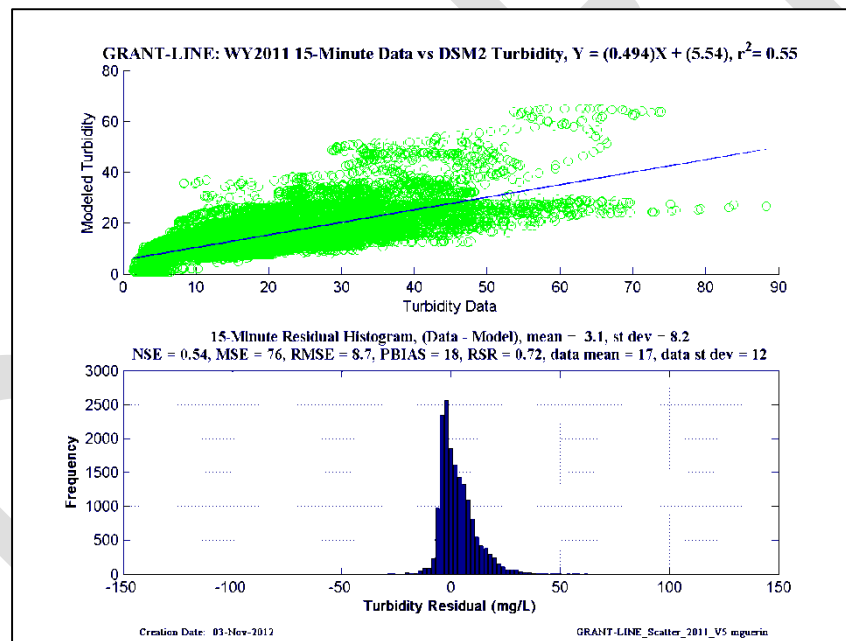
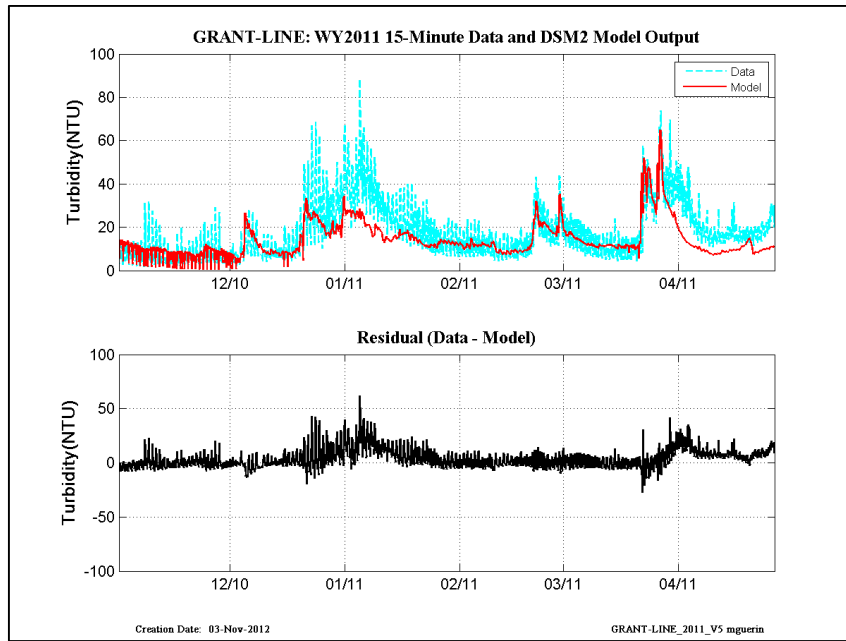


Figure 12-9 WY2011 15-min revised calibration results at Grant Line.

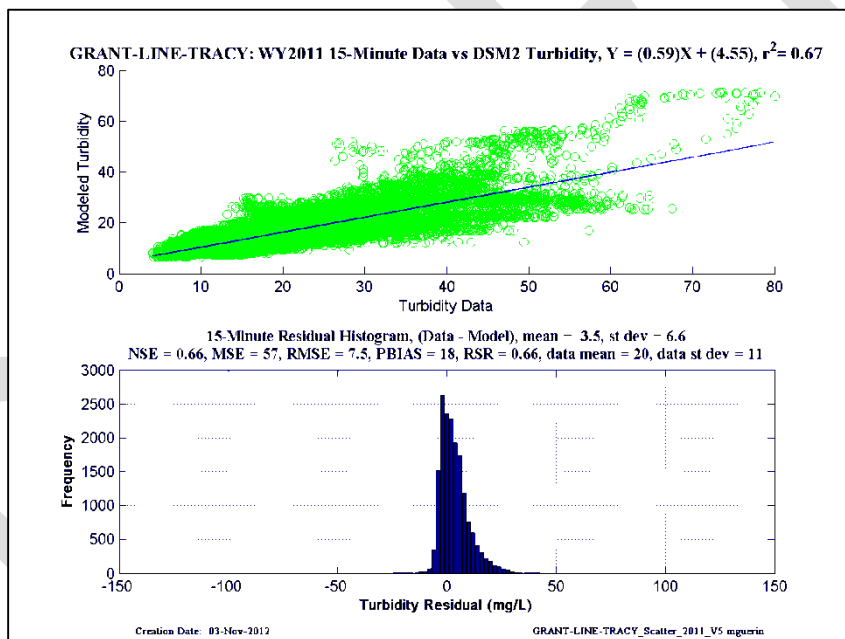
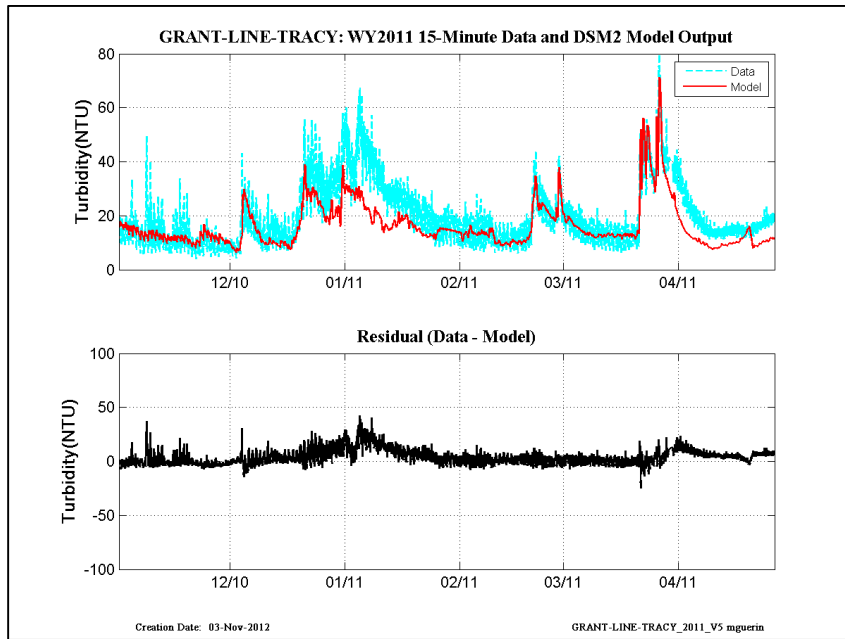


Figure 12-10 WY2011 15-min revised calibration results at Grant-Line Tracy.

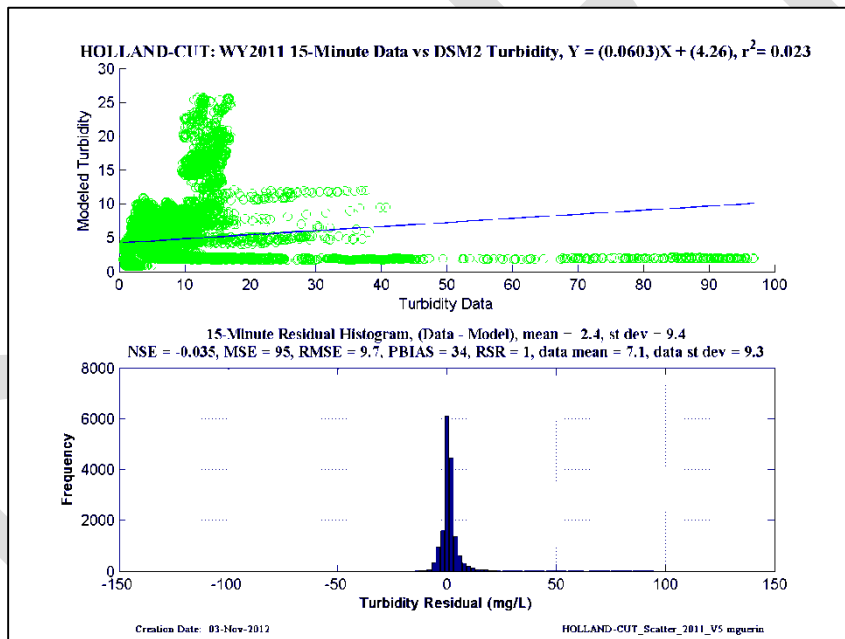
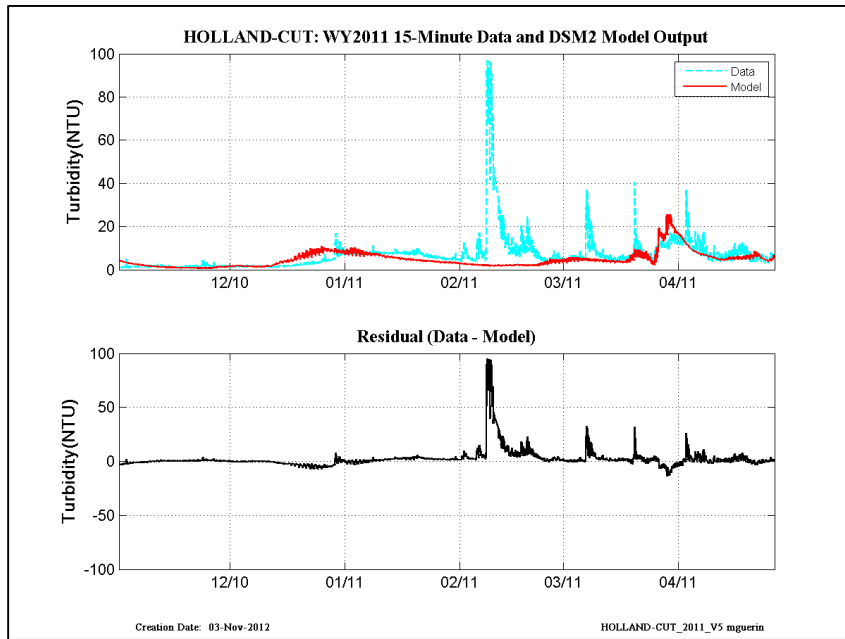


Figure 12-11 WY2011 15-min revised calibration results at Holland Cut.

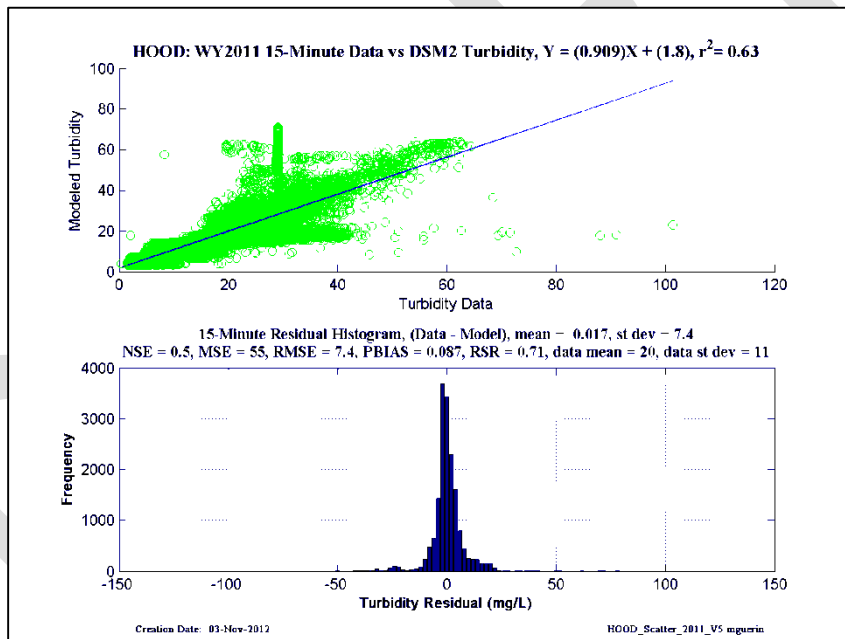
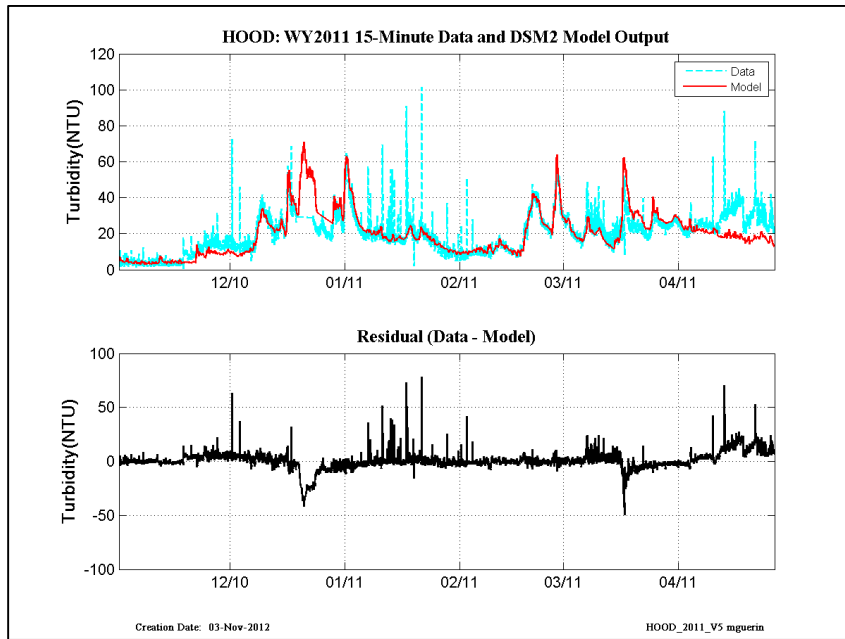


Figure 12-12 WY2011 15-min revised calibration results at Hood.

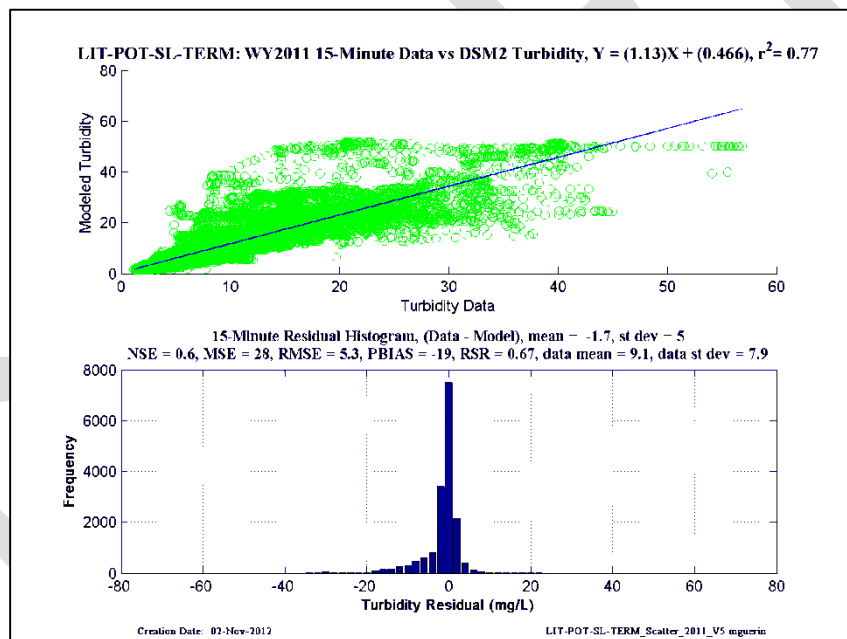
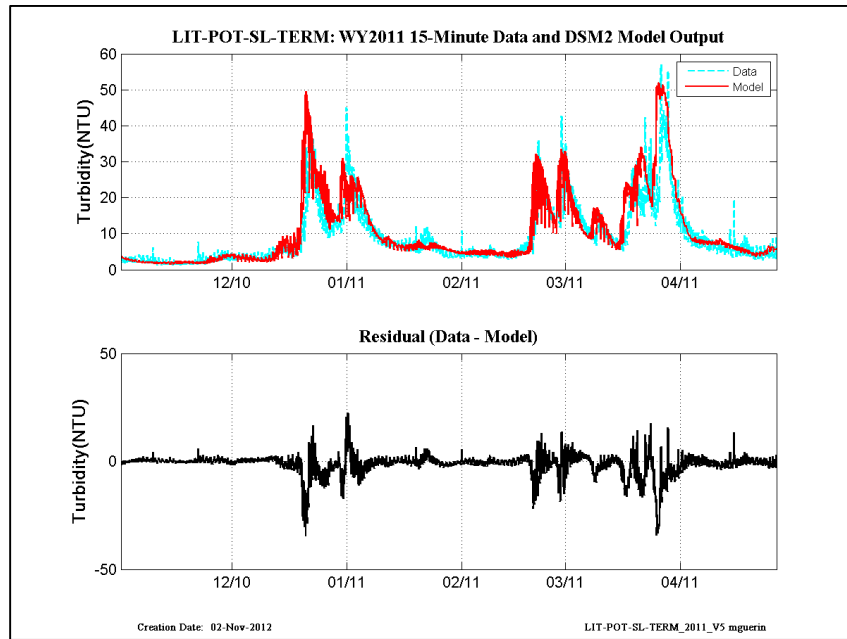


Figure 12-13 WY2011 15-min revised calibration results at Little Potato Slough-at-Terminus.

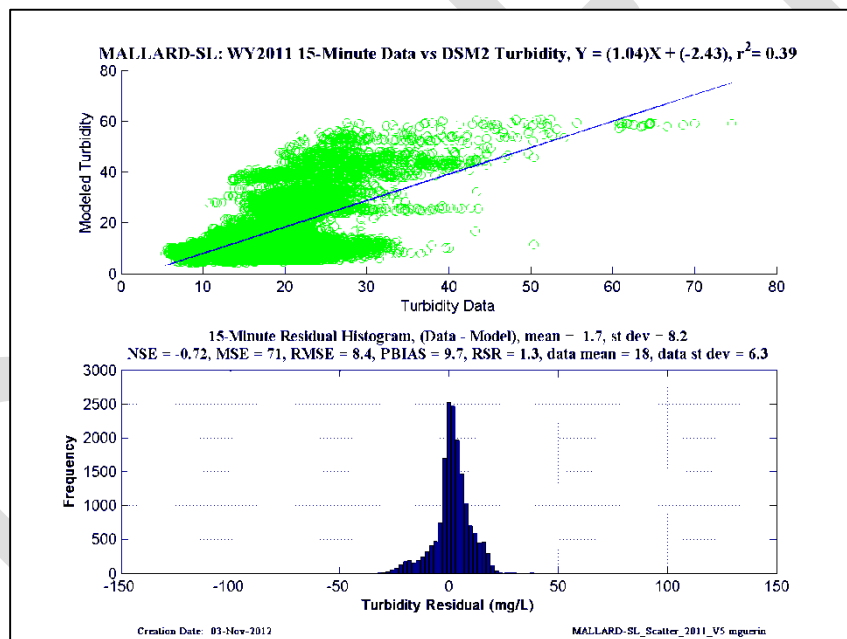
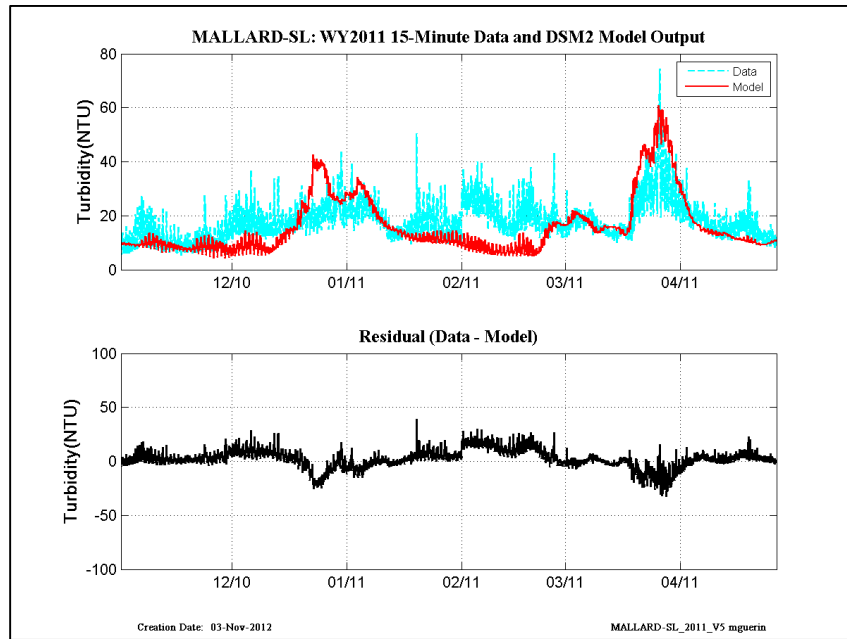


Figure 12-14 WY2011 15-min revised calibration results at Mallard Slough.

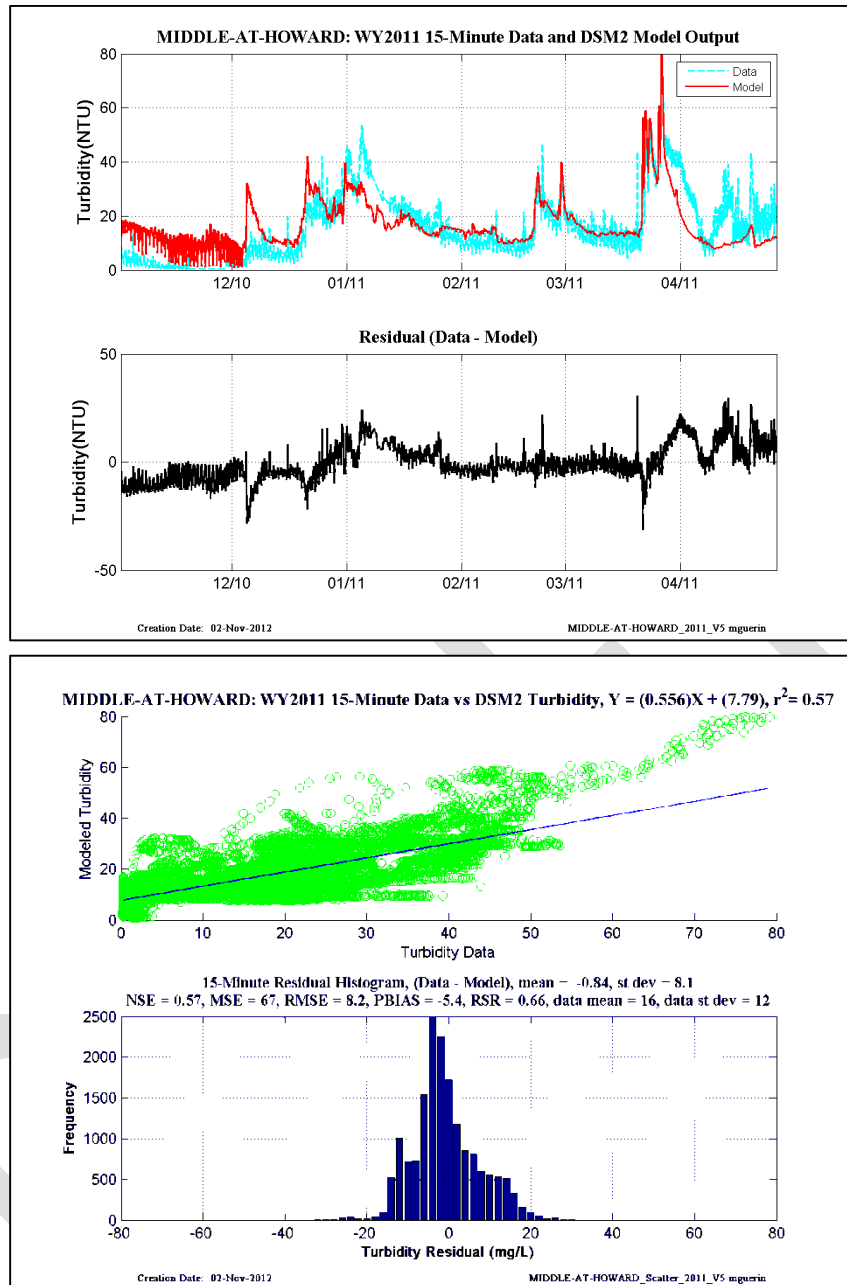


Figure 12-15 WY2011 15-min revised calibration results at Middle River-at-Howard Rd.

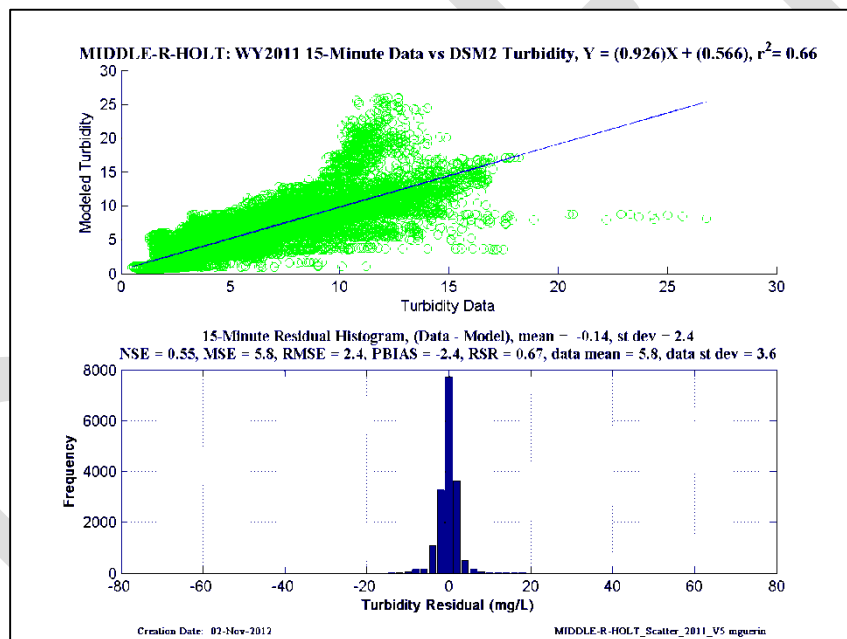
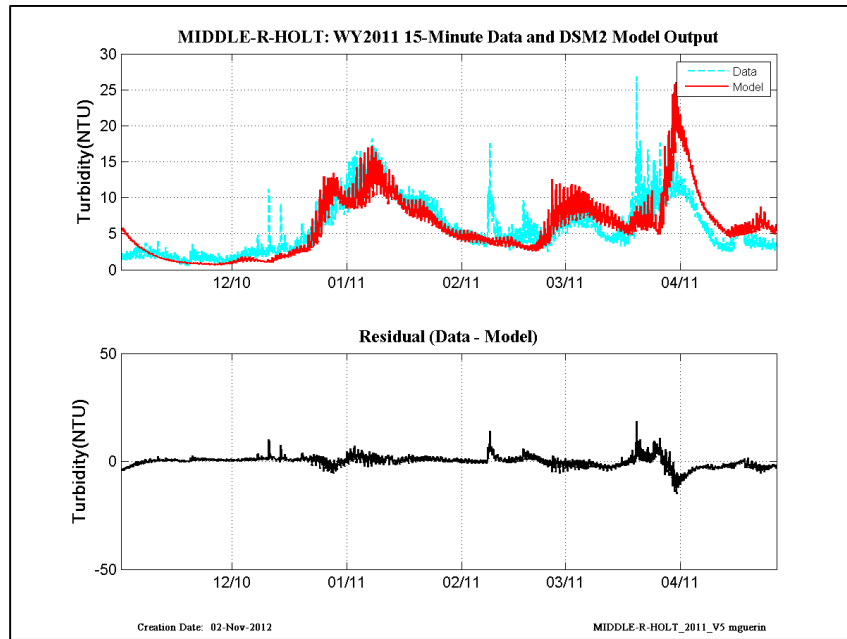


Figure 12-16 WY2011 15-min revised calibration results at Middle River-at-Holt.

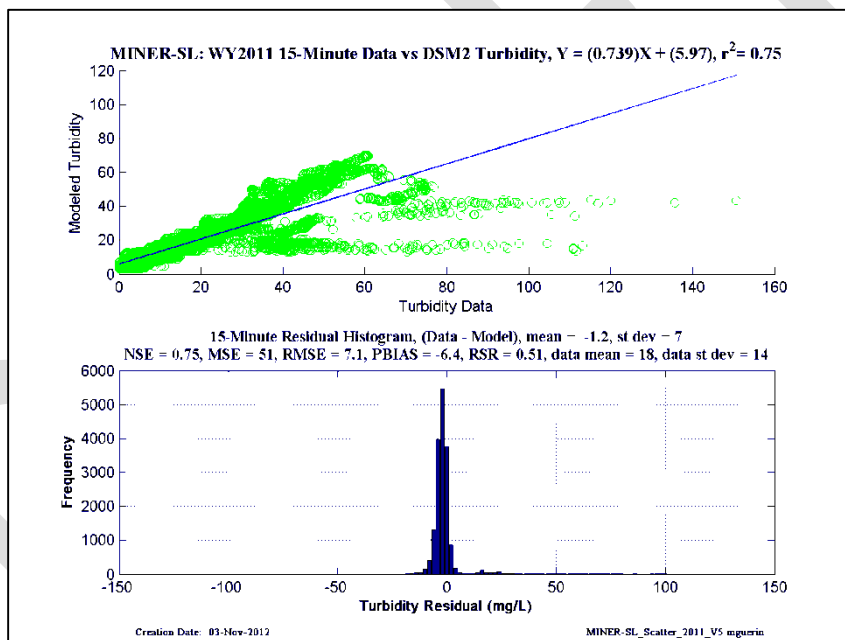
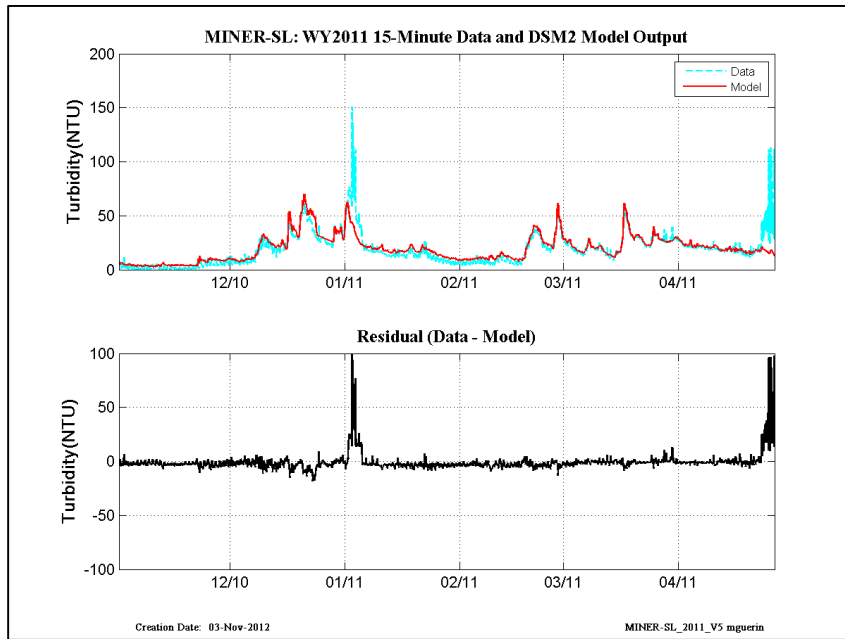


Figure 12-17 WY2011 15-min revised calibration results at Miner Slough.

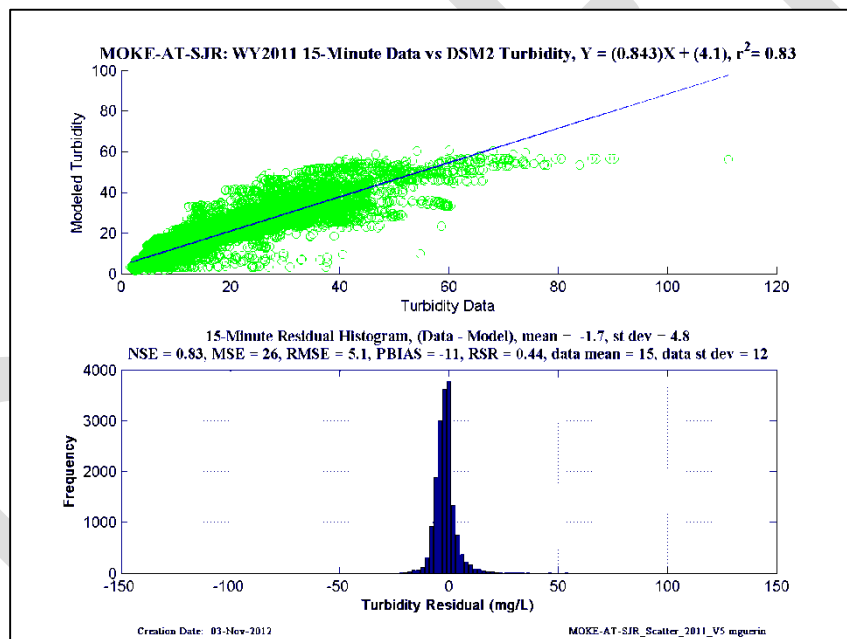
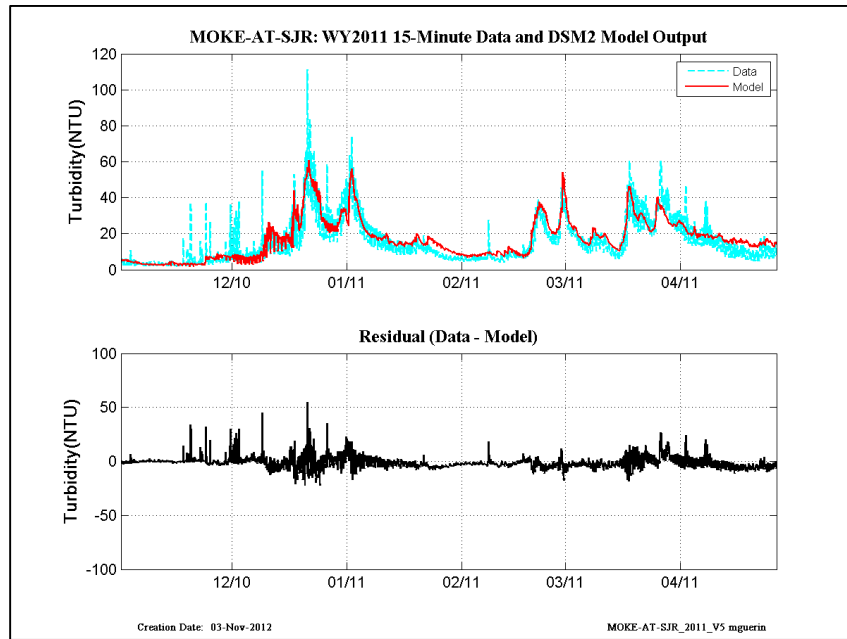


Figure 12-18 WY2011 15-min revised calibration results at Mokelumne-at-San Joaquin.

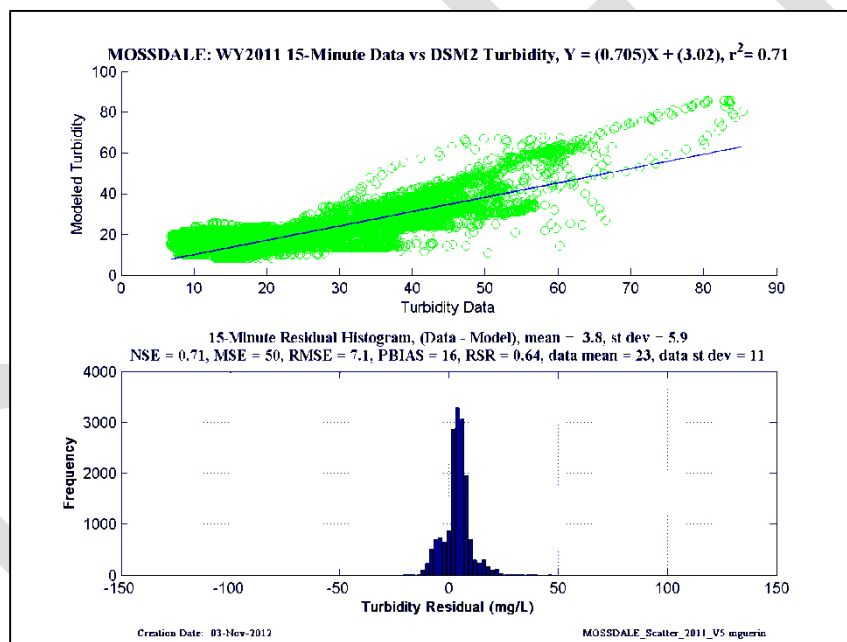
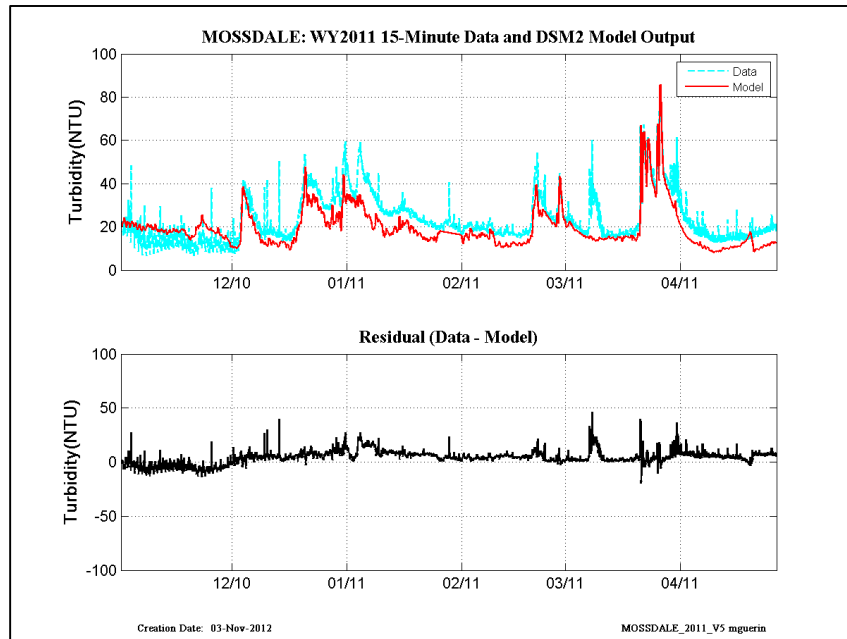


Figure 12-19 WY2011 15-min revised calibration results at Mossdale.

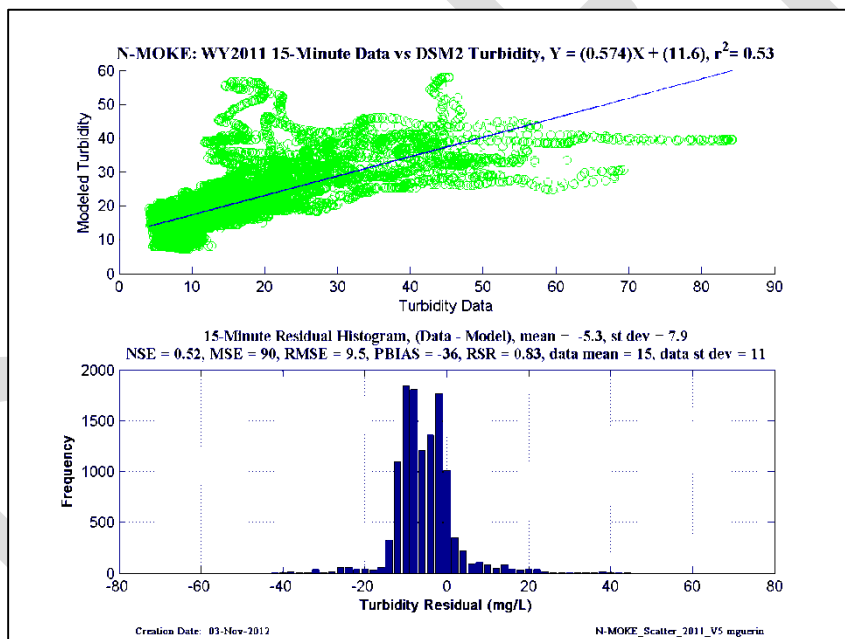
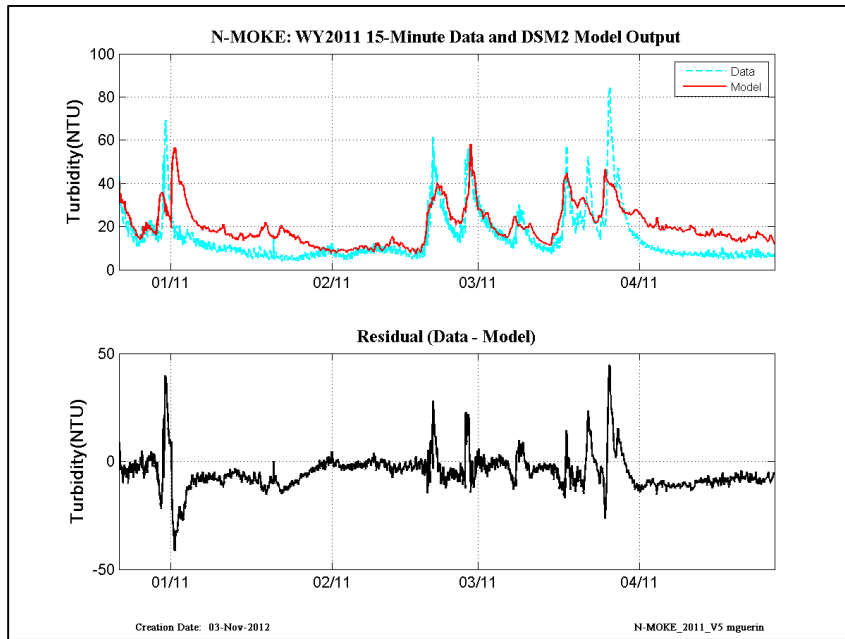


Figure 12-20 WY2011 15-min revised calibration results at North Mokelumne.

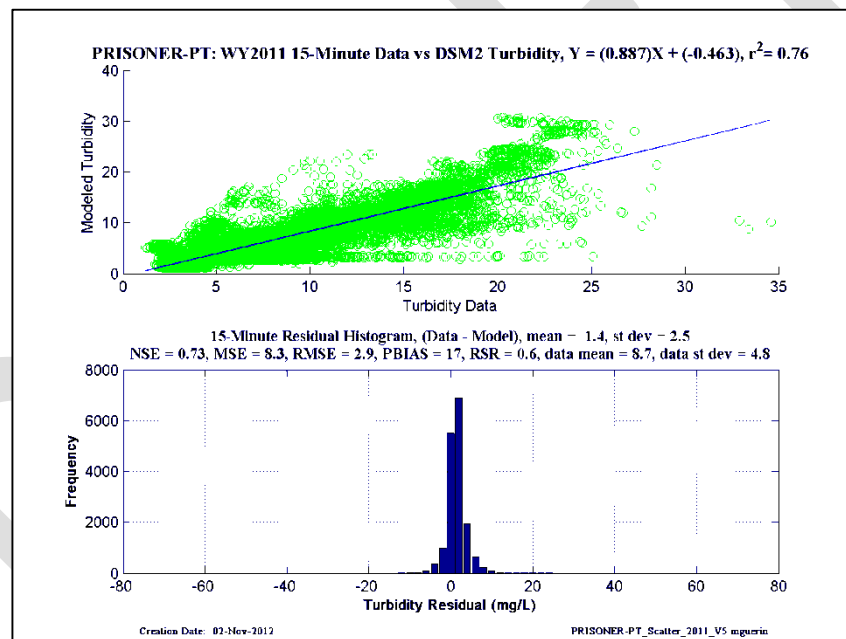
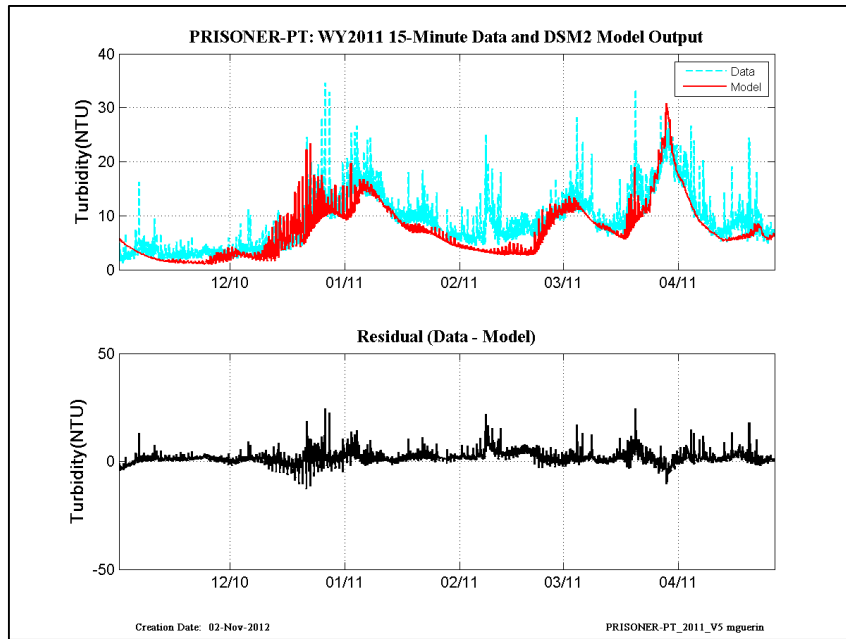


Figure 12-21 WY2011 15-min revised calibration results at Prisoner Point.

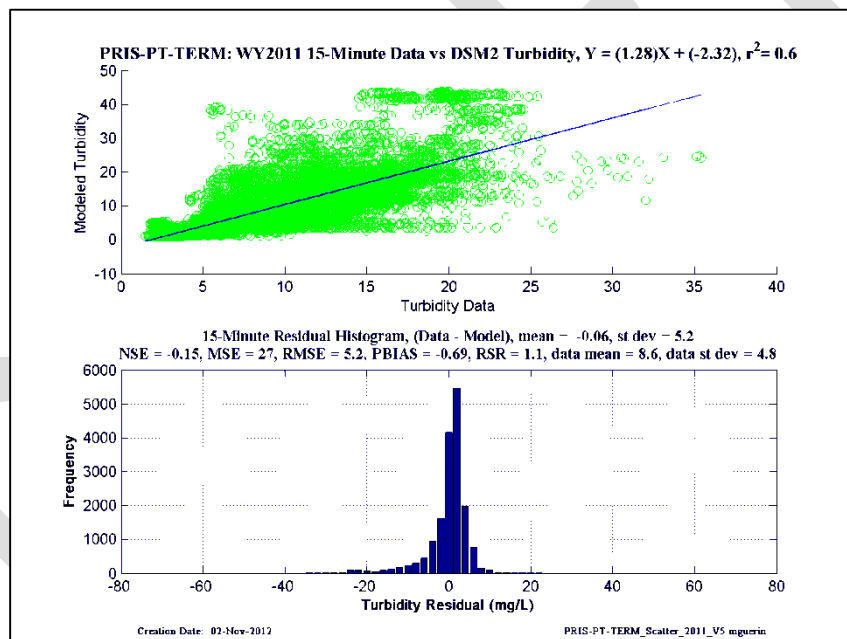
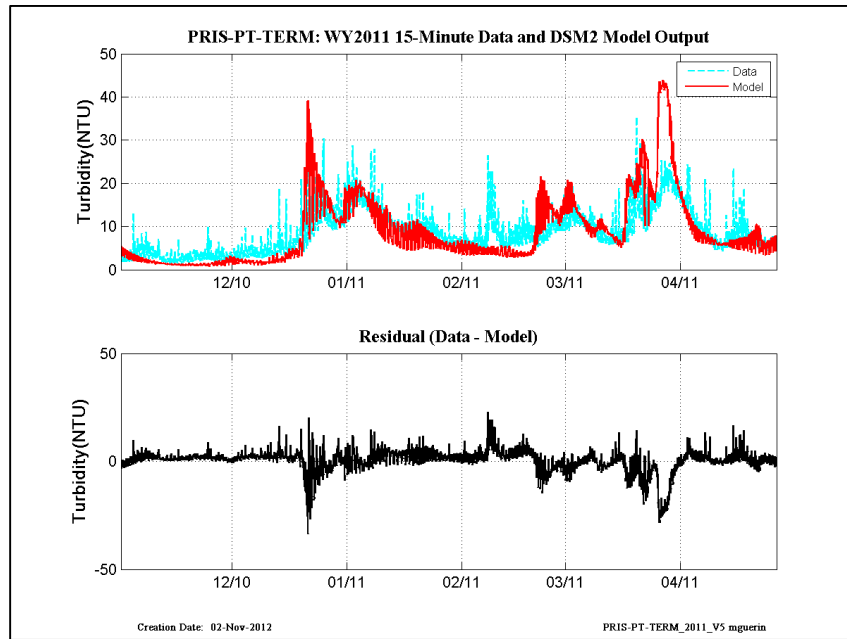


Figure 12-22 WY2011 15-min revised calibration results at Prisoner Point-at-Terminus.

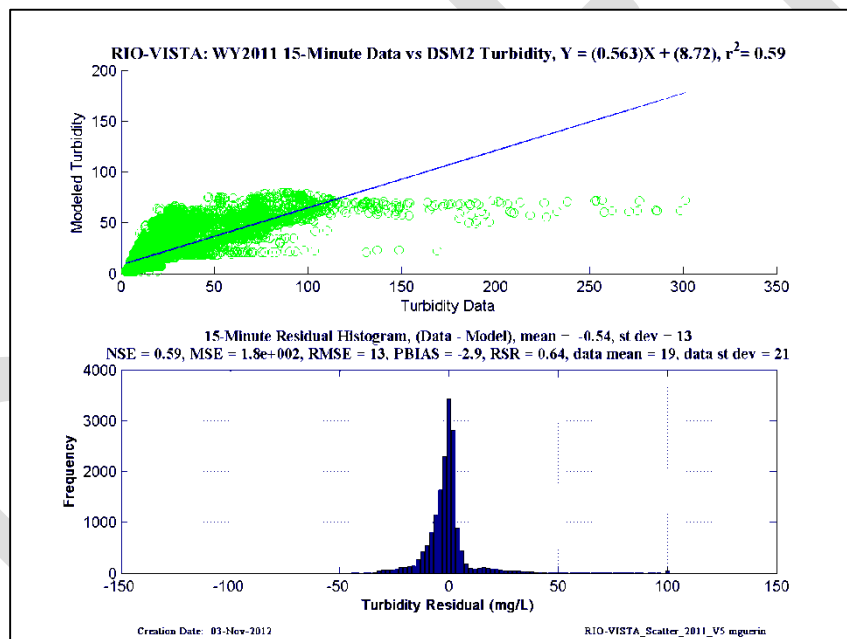
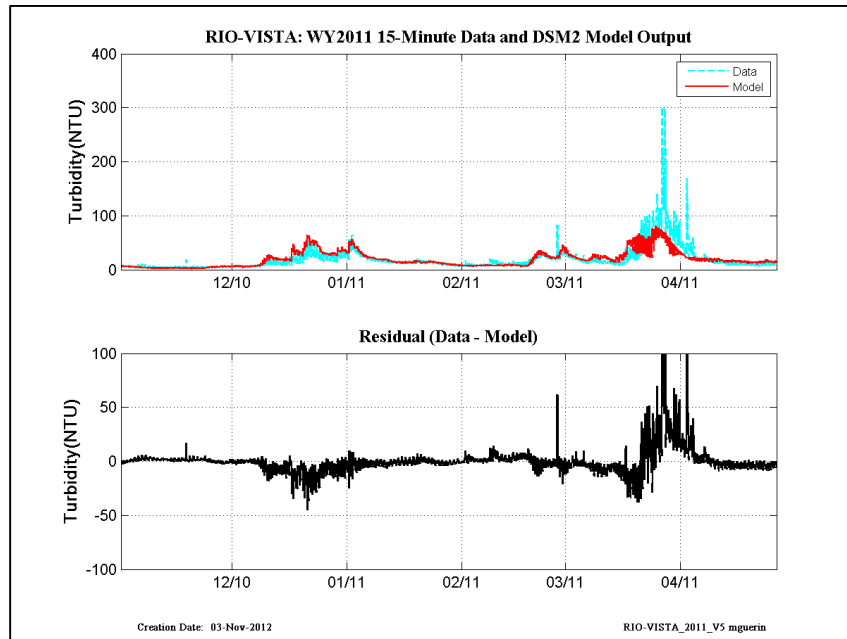


Figure 12-23 WY2011 15-min revised calibration results at Rio Vista.

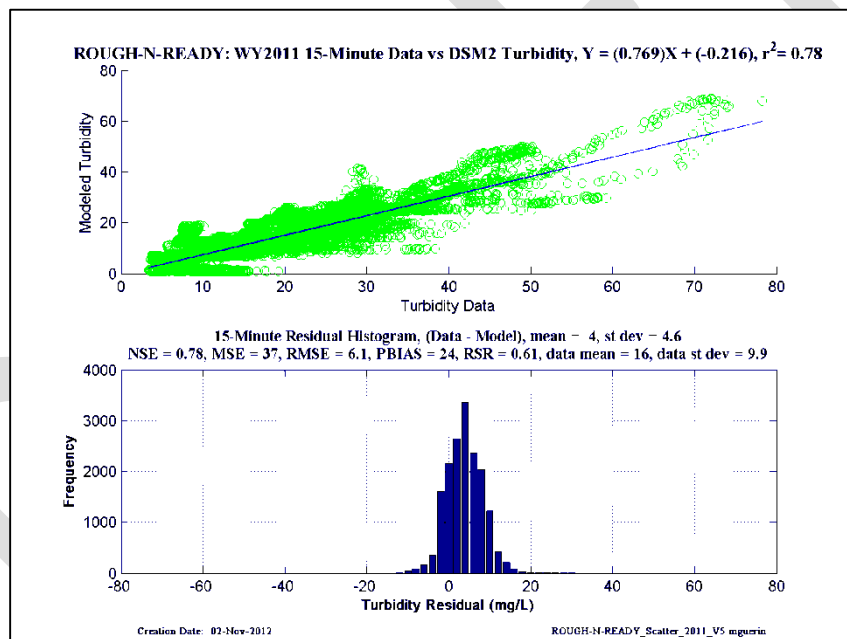
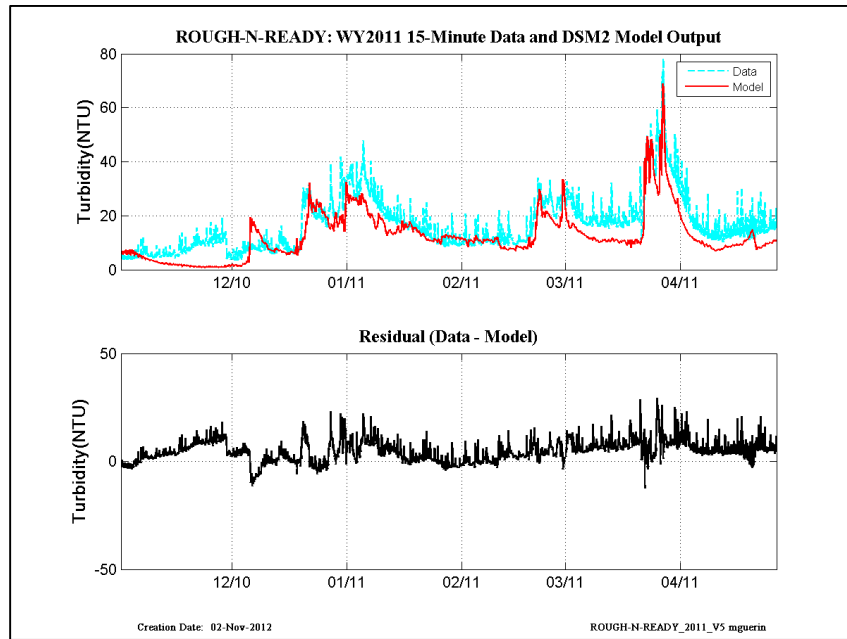


Figure 12-24 WY2011 15-min revised calibration results at Rough-N-Ready Island.

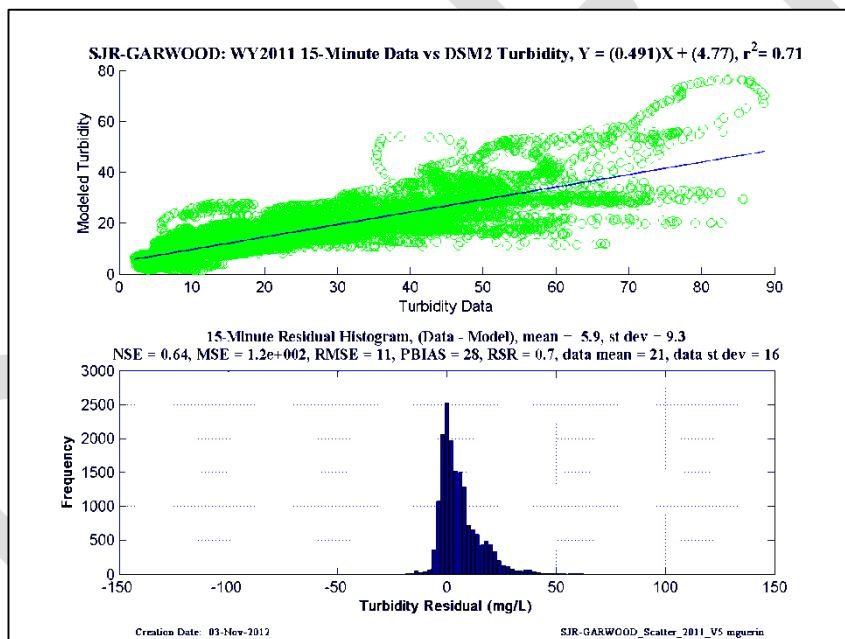
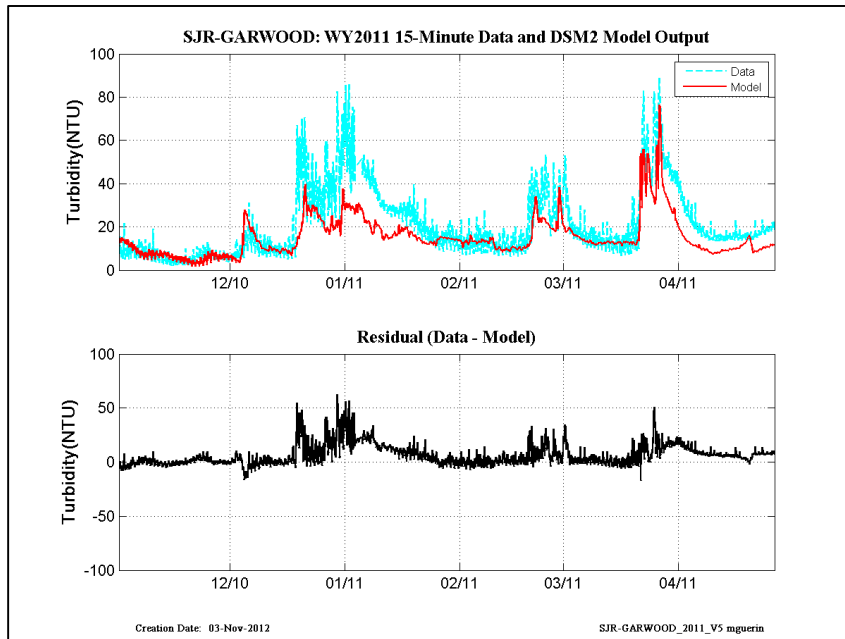


Figure 12-25 WY2011 15-min revised calibration results at San Joaquin-at-Garwood.

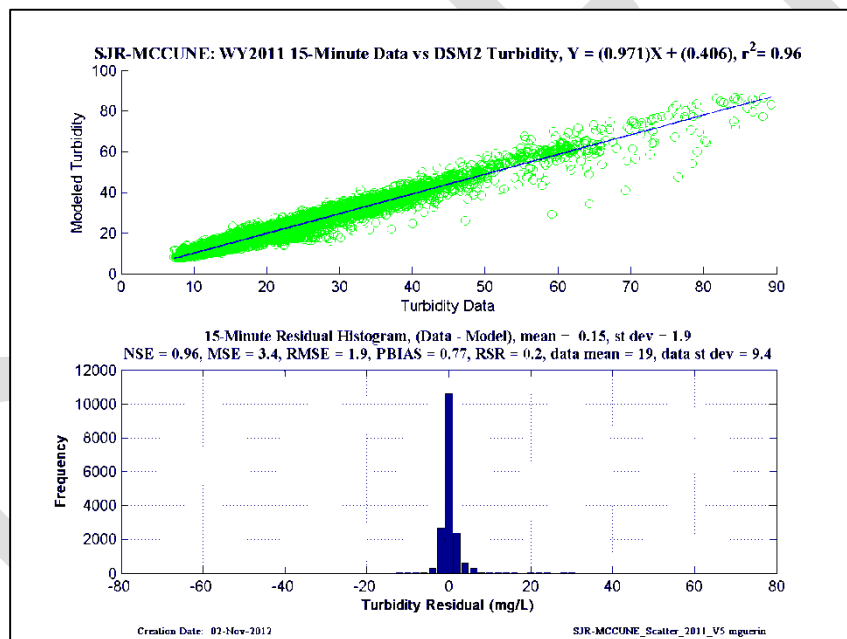
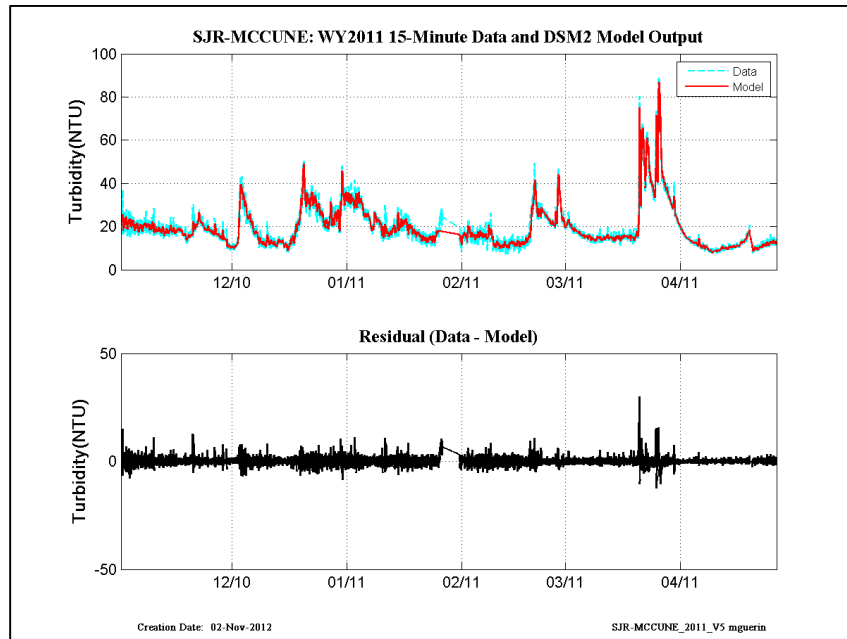


Figure 12-26 WY2011 15-min revised calibration results at San Joaquin-at-McCune (Vernalis).

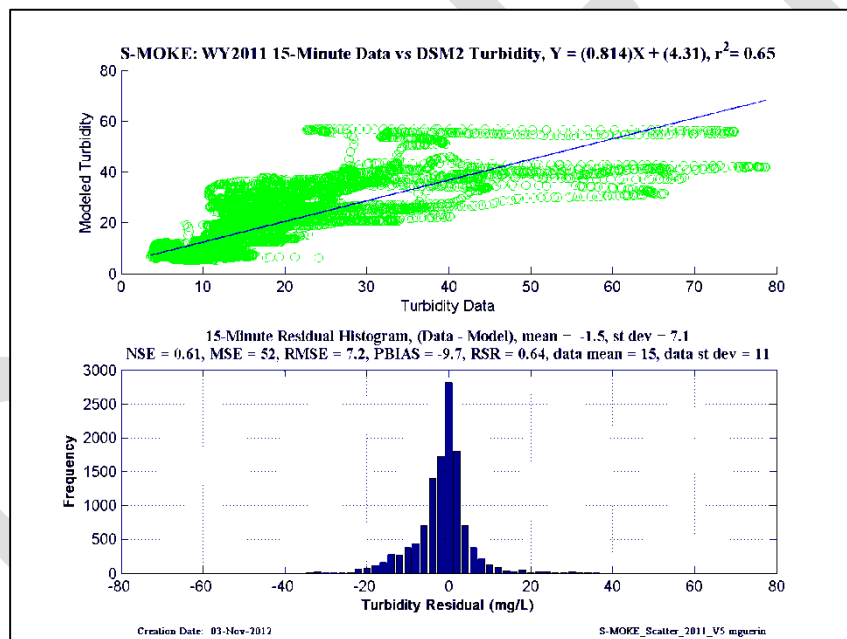
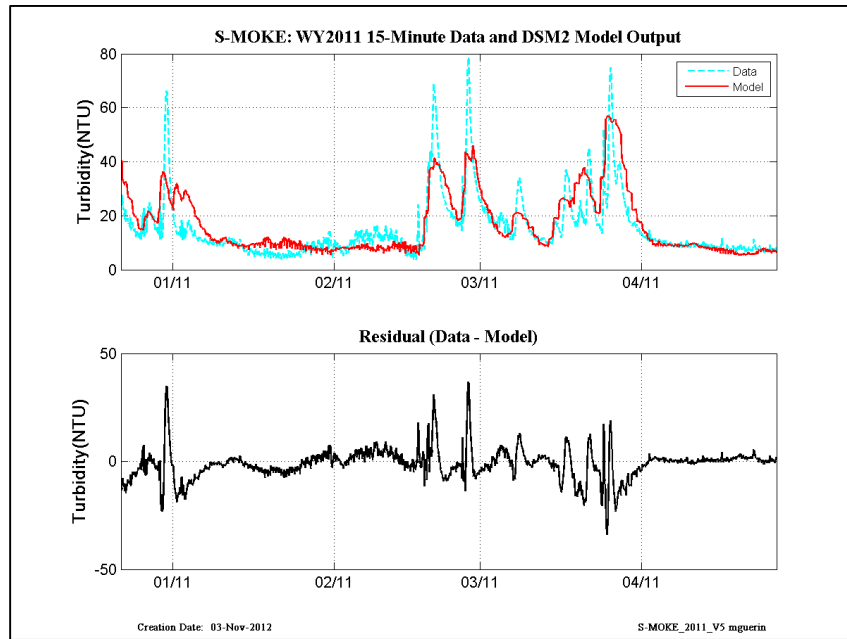


Figure 12-27 WY2011 15-min revised calibration results at South Mokelumne.

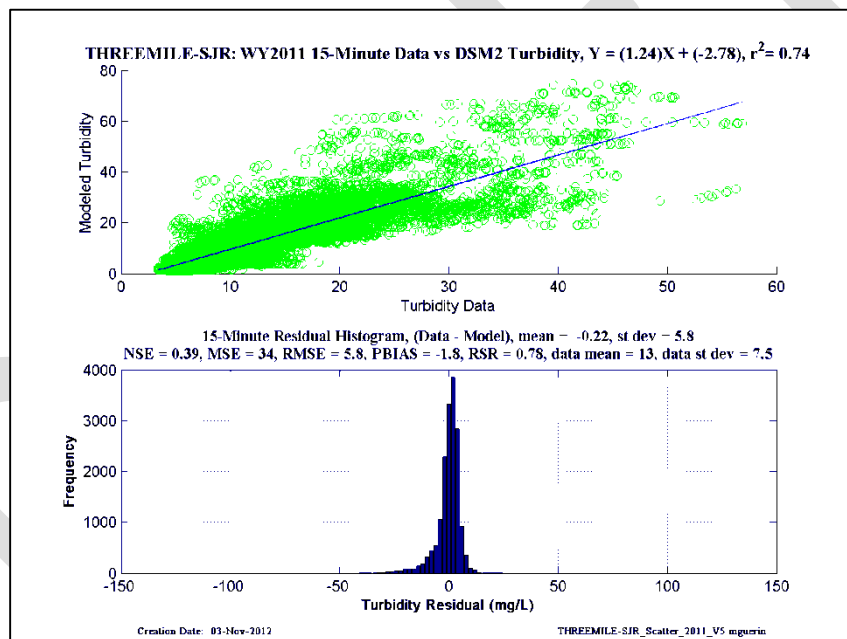
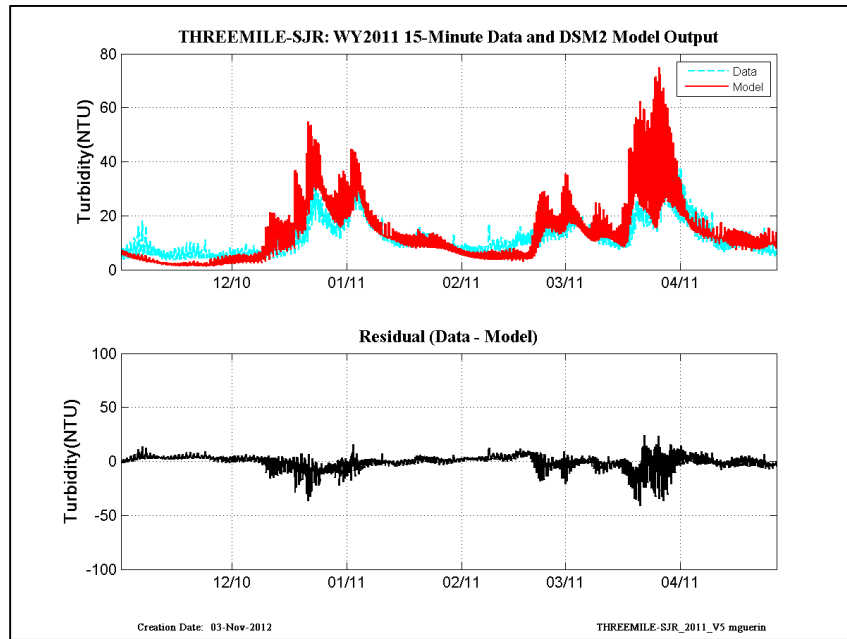


Figure 12-28 WY2011 15-min revised calibration results at Threemile-Slough-at-San Joaquin.

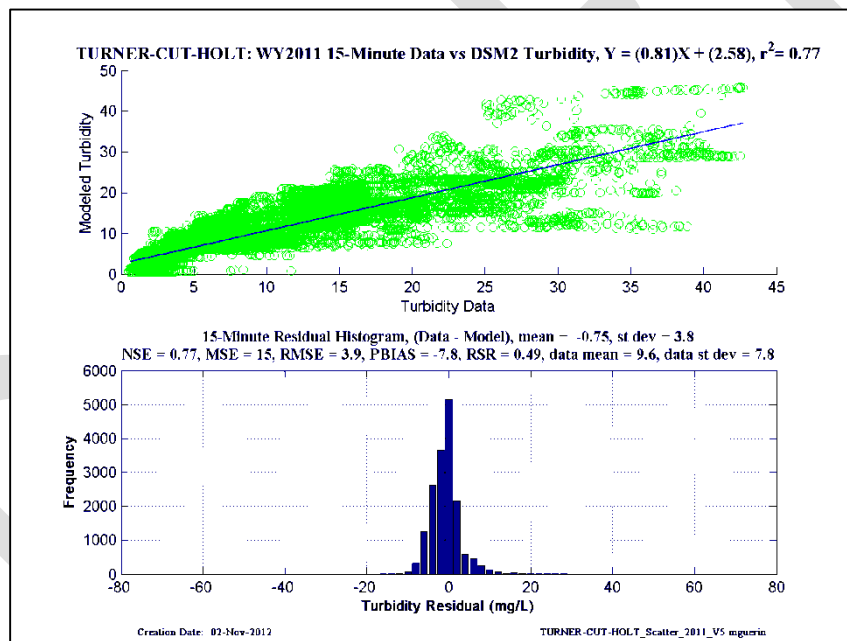
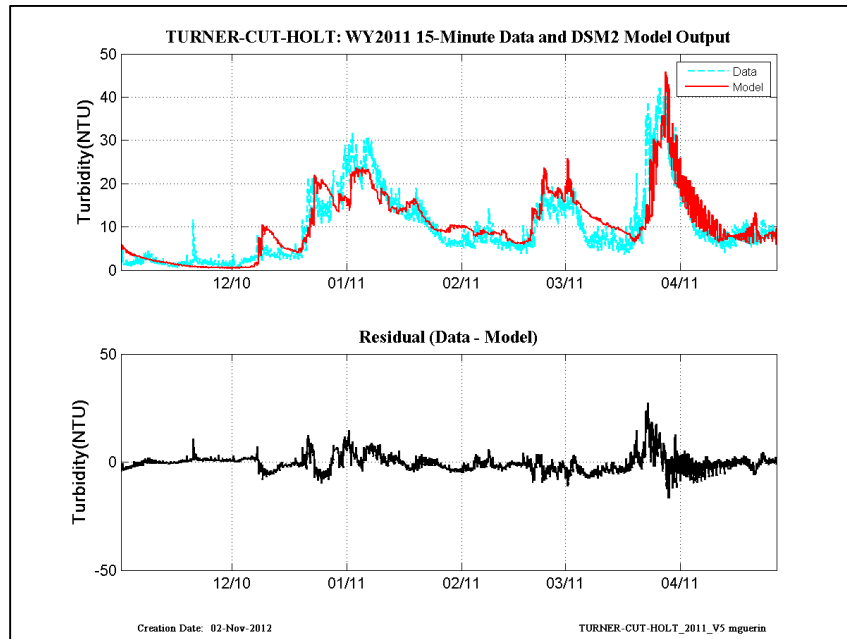


Figure 12-29 WY2011 15-min revised calibration results at Turner Cut-at-Holt.

yy

Figure 12-30 WY2011 15-min revised calibration results at Victoria Canal-at-Byron.

### 12.3 Fifteen minute CDEC data and model output – WY2010

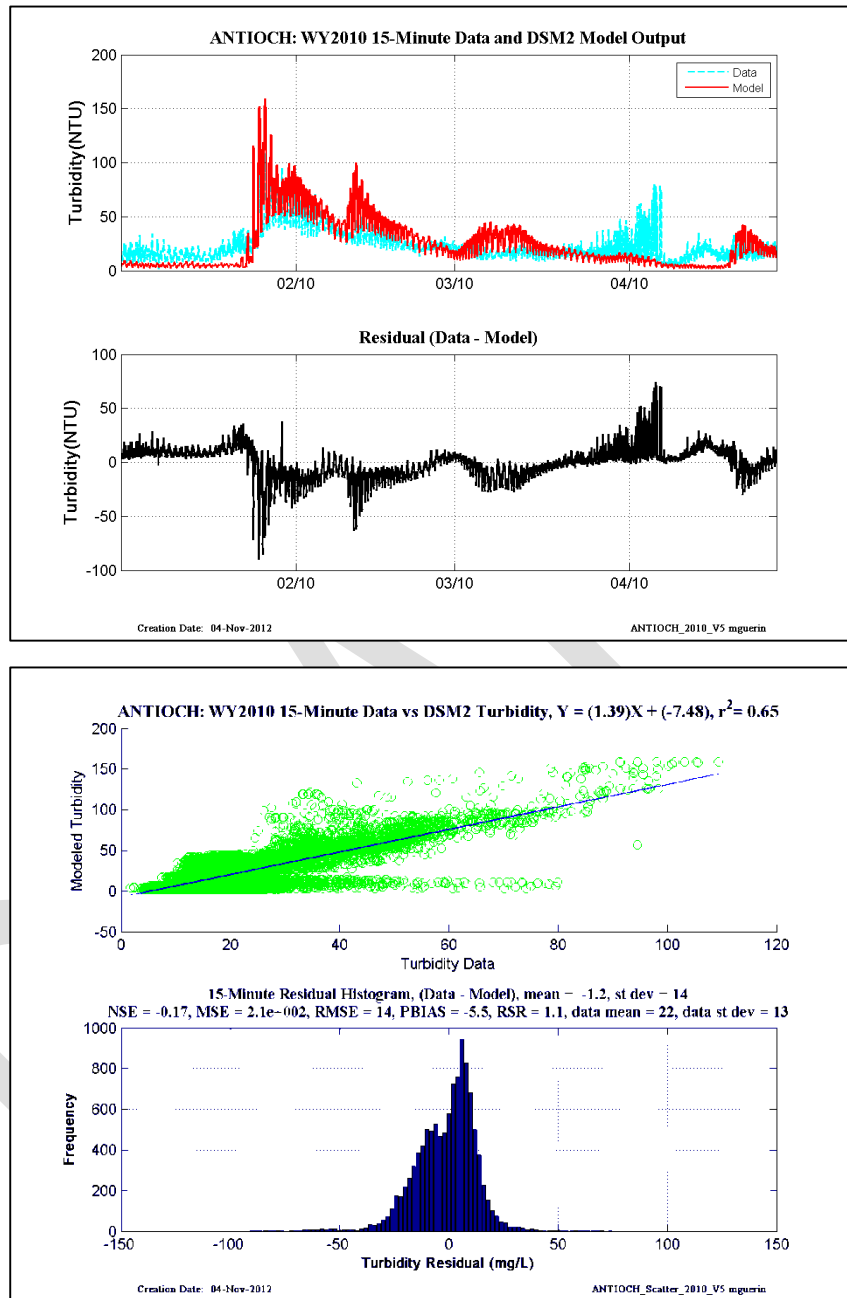


Figure 12-31 WY2010 15-min revised calibration results at Antioch.

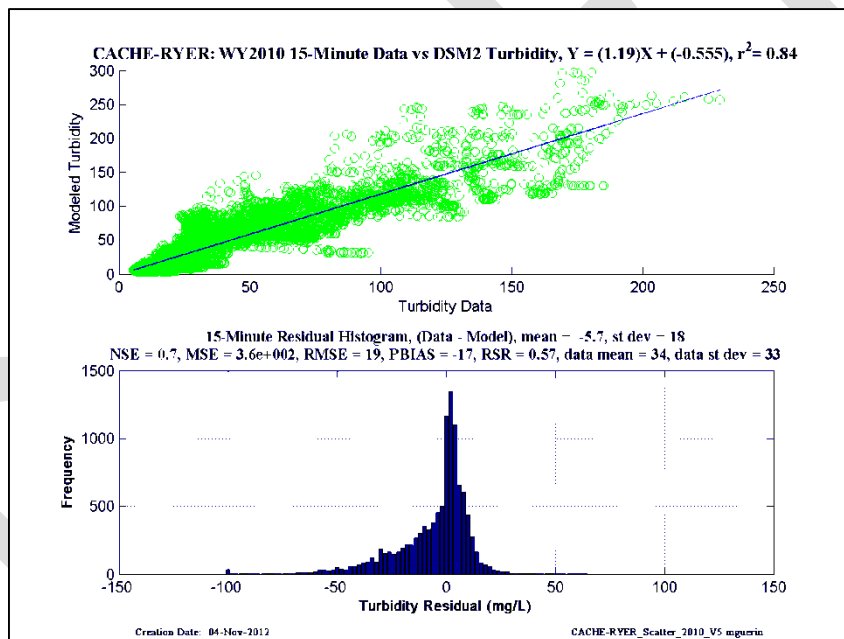
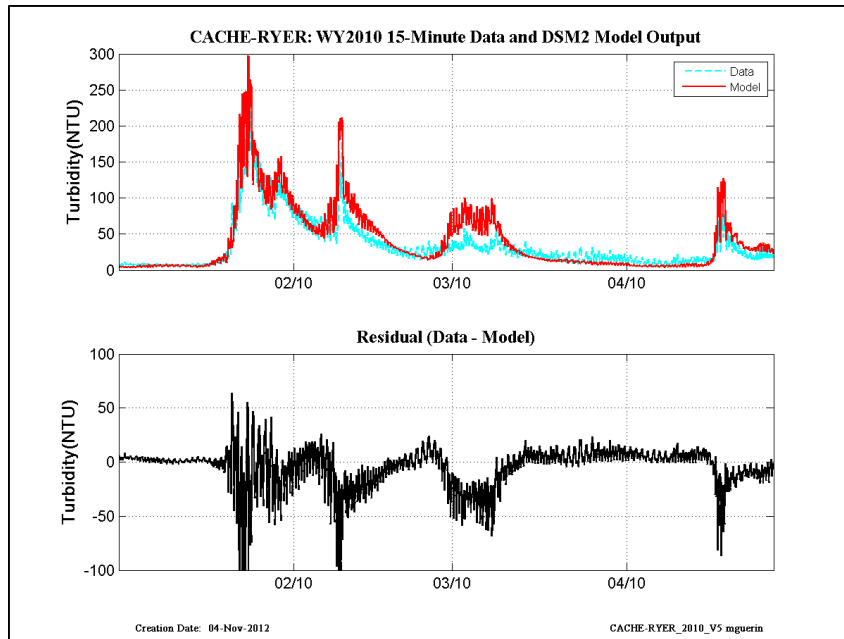


Figure 12-32 WY2010 15-min revised calibration results at Cache-at-Ryer Island.

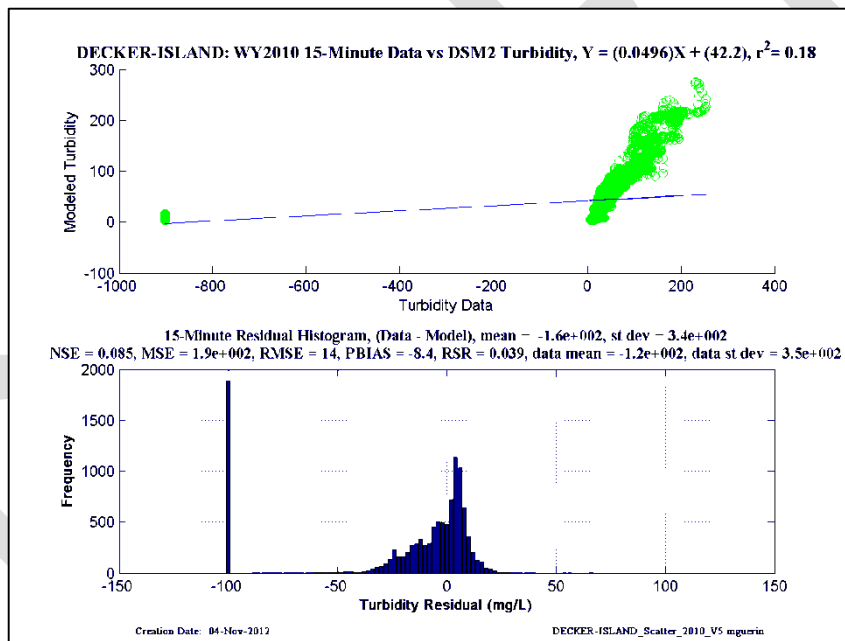
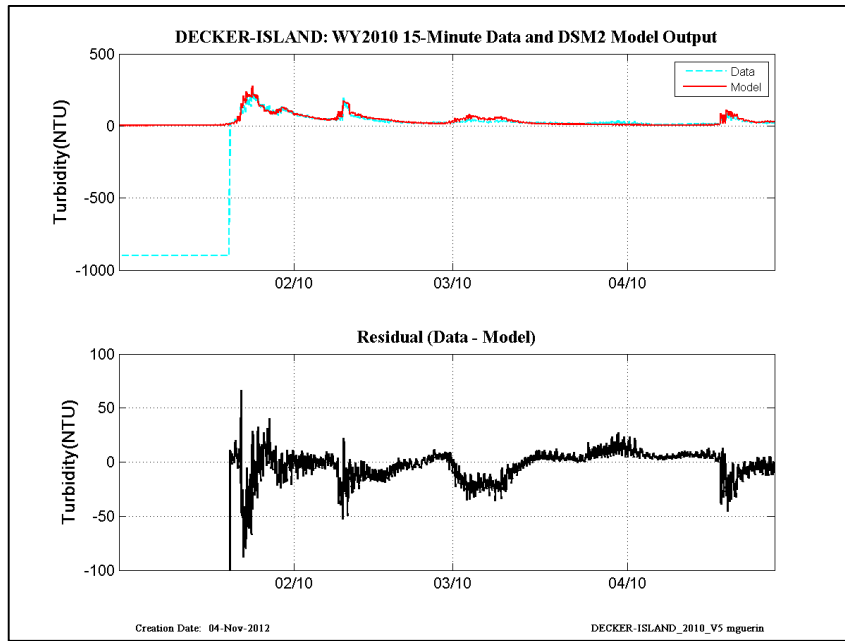


Figure 12-33 WY2010 15-min revised calibration results at Decker Island.

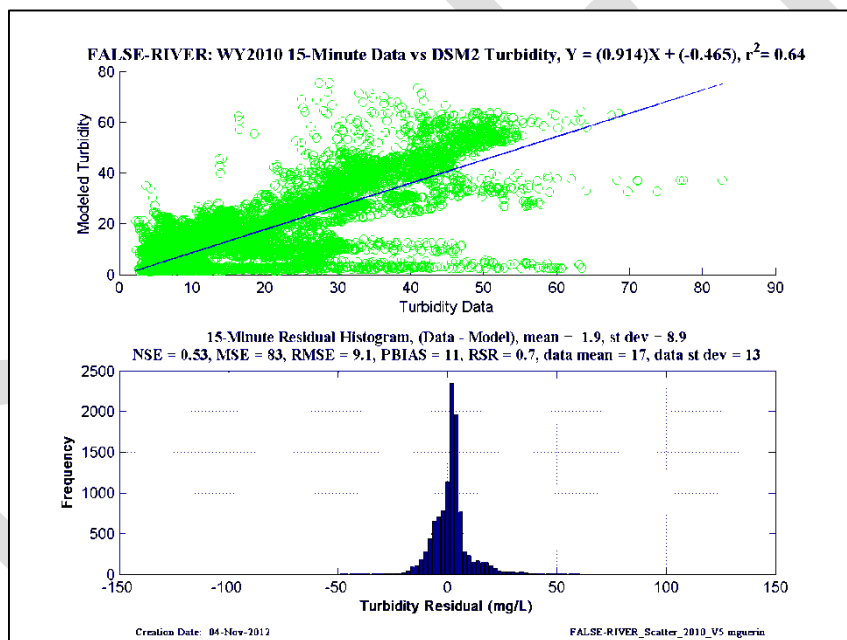
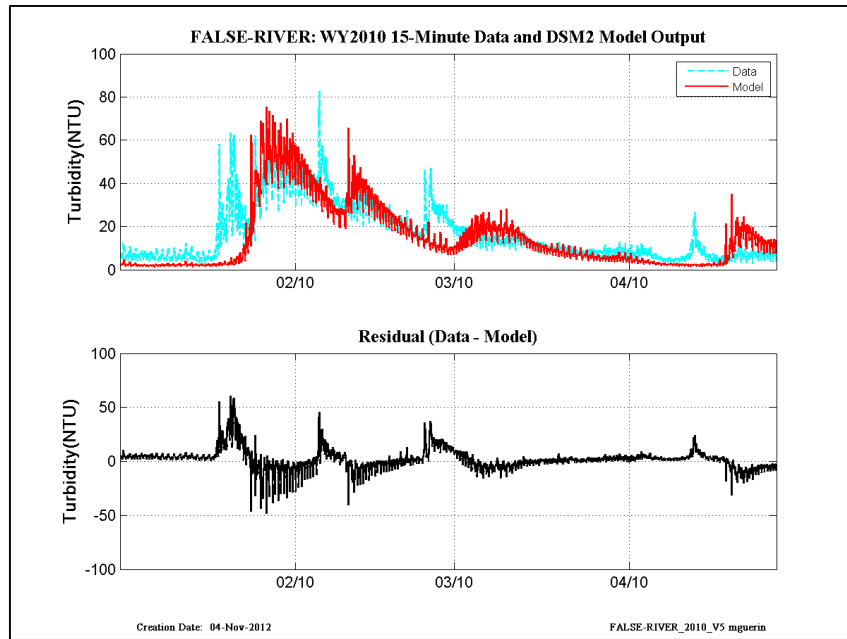


Figure 12-34 WY2010 15-min revised calibration results at False River.

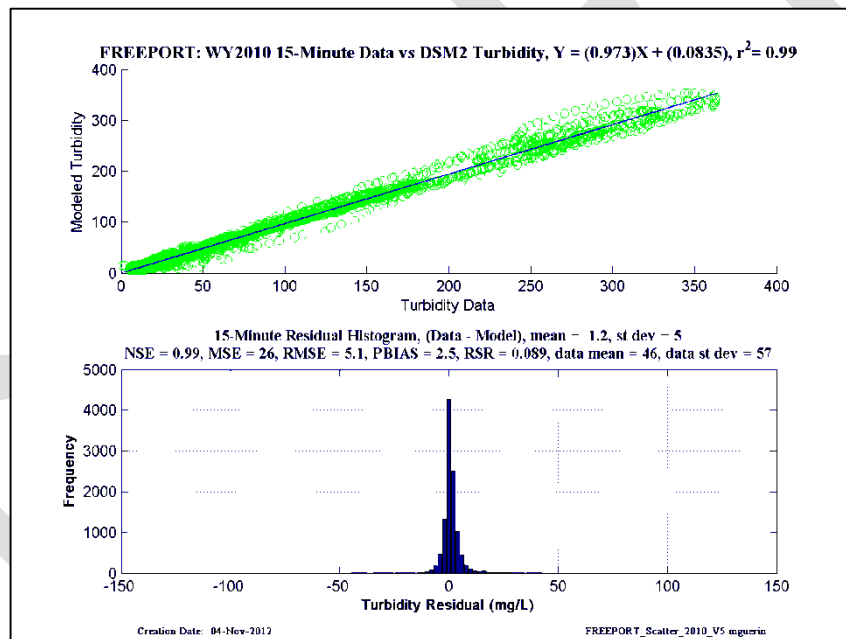
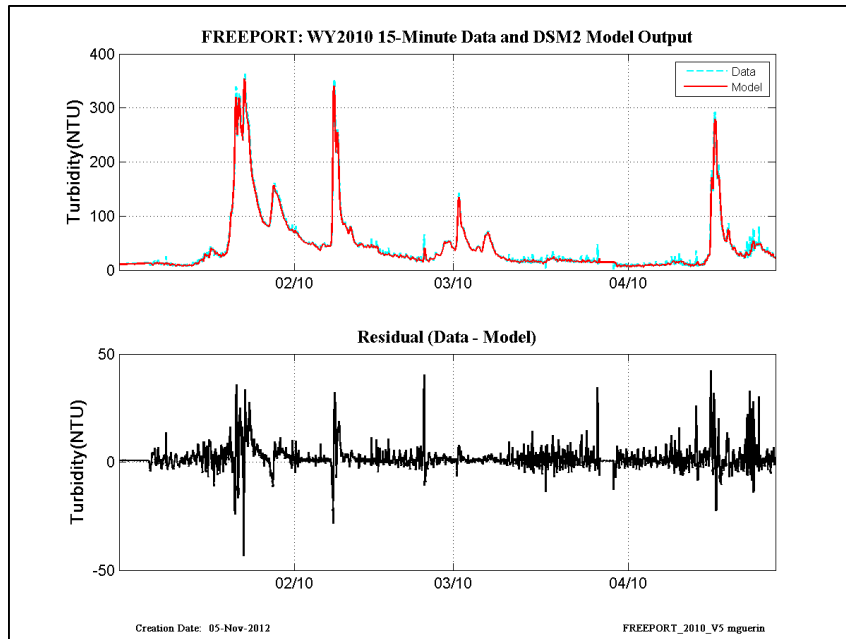


Figure 12-35 WY2010 15-min revised calibration results at Freeport.

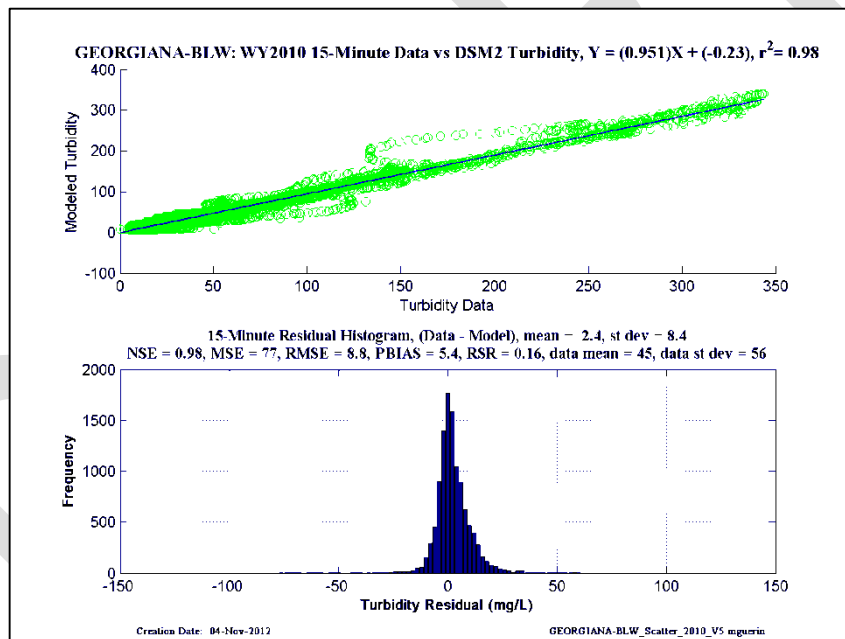
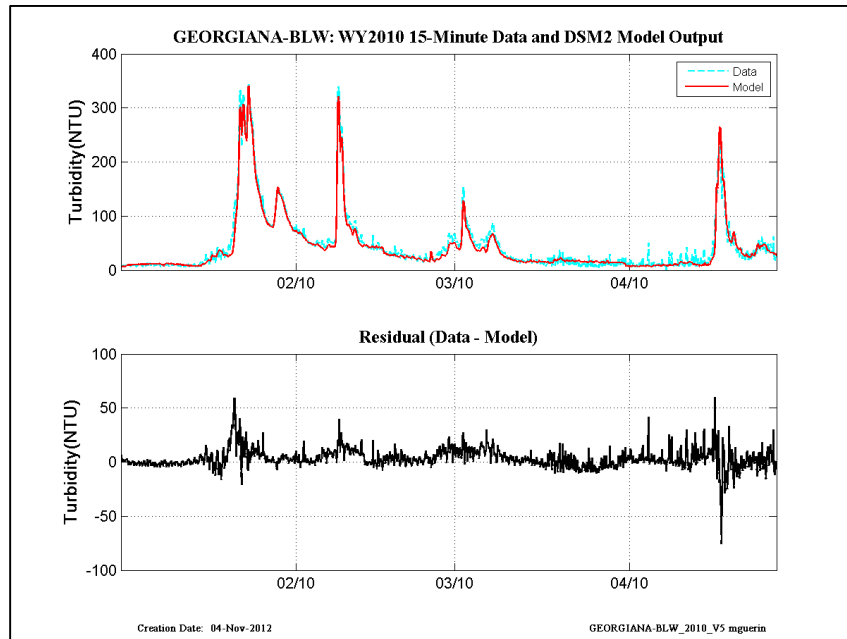


Figure 12-36 WY2010 15-min revised calibration results at Georgiana-Below-Sac.

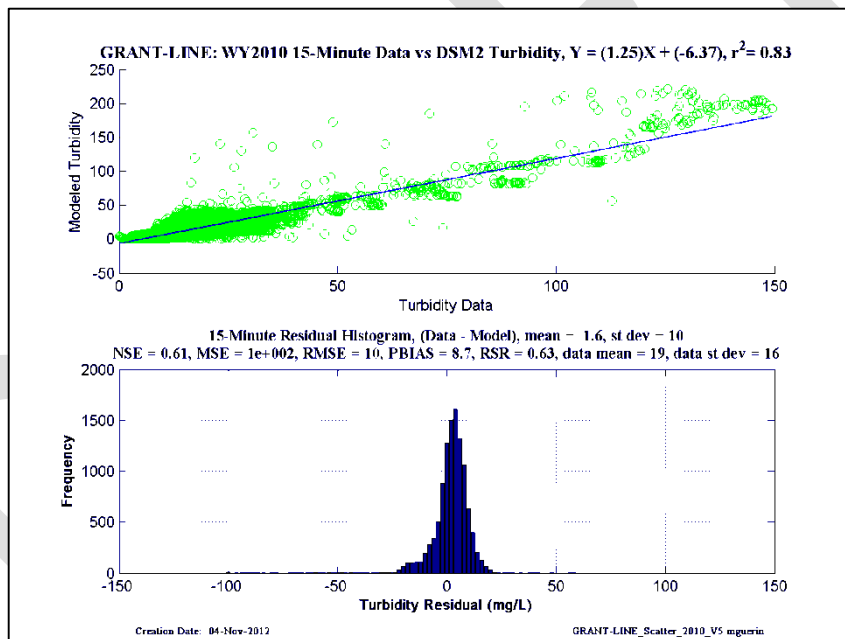
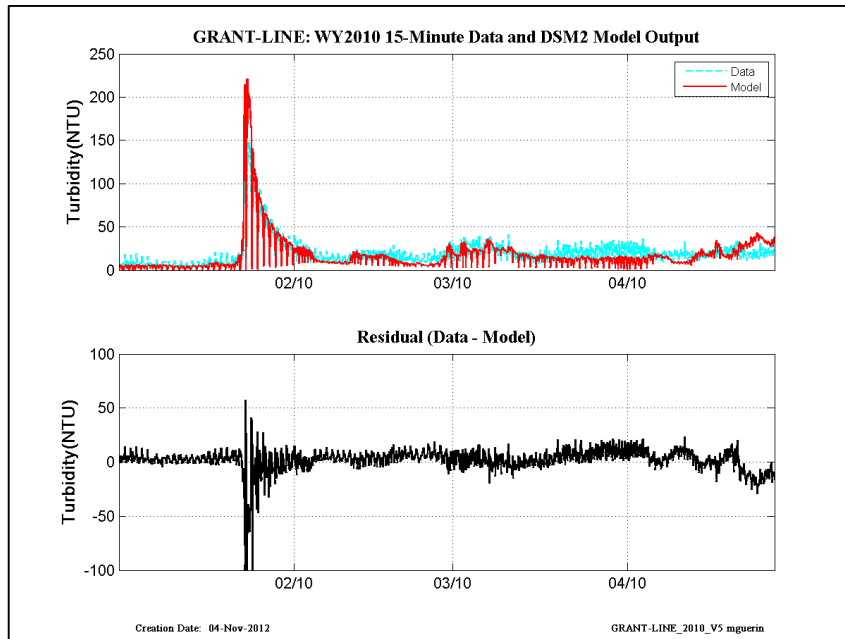


Figure 12-37 WY2010 15-min revised calibration results at Grant Line.

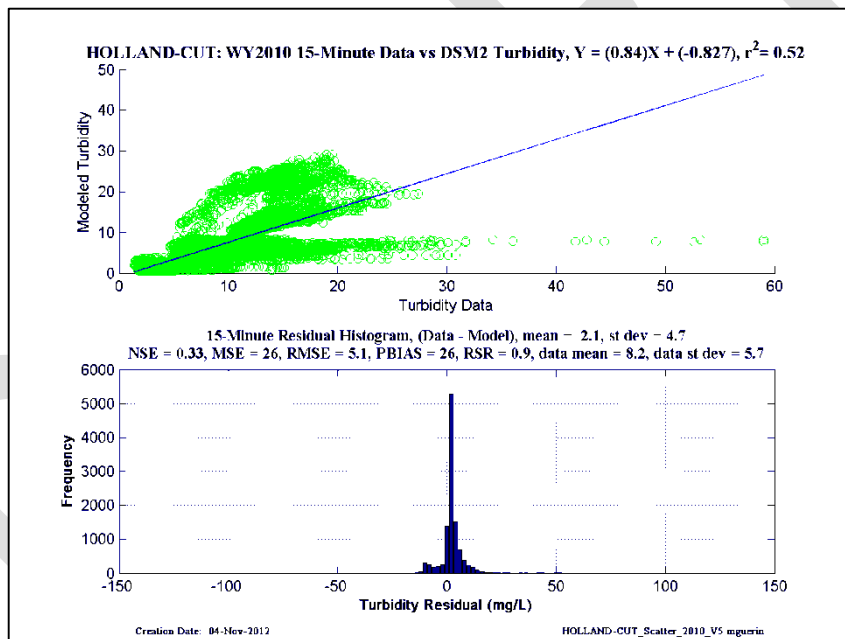
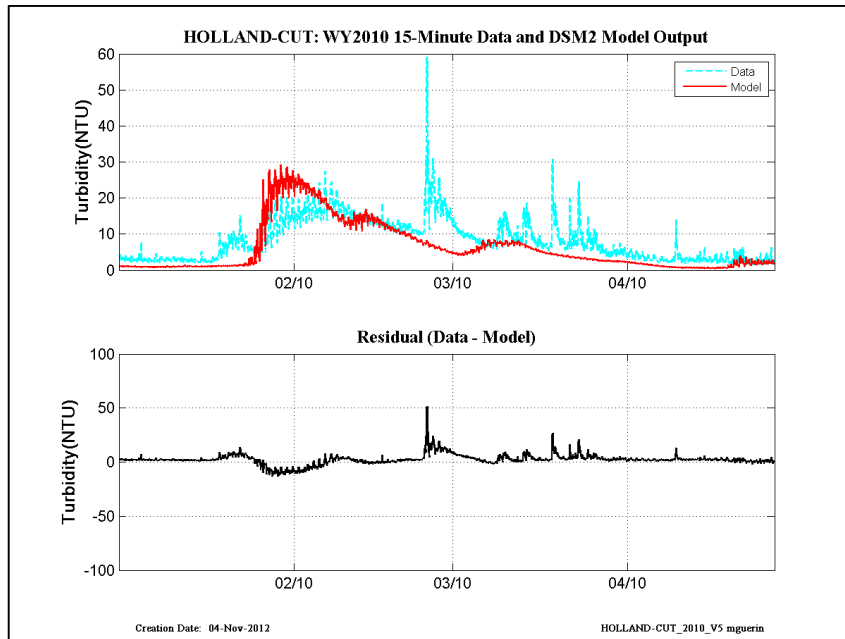


Figure 12-38 WY2010 15-min revised calibration results at Holland Cut.

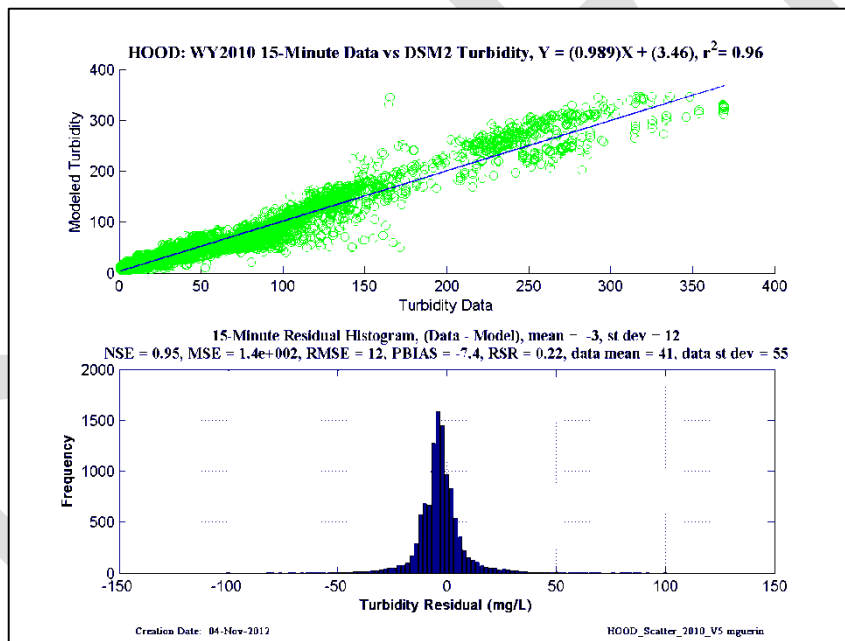
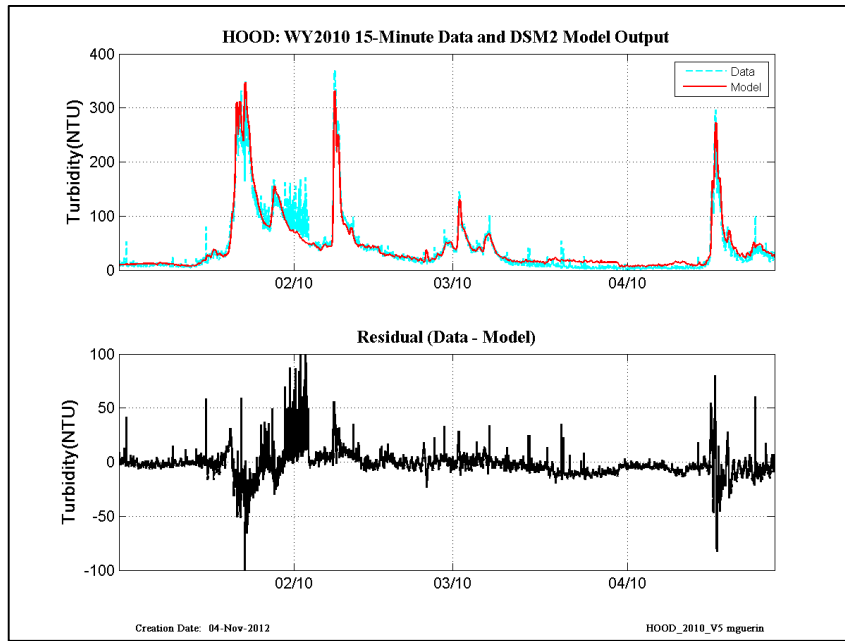


Figure 12-39 WY2010 15-min revised calibration results at Hood.

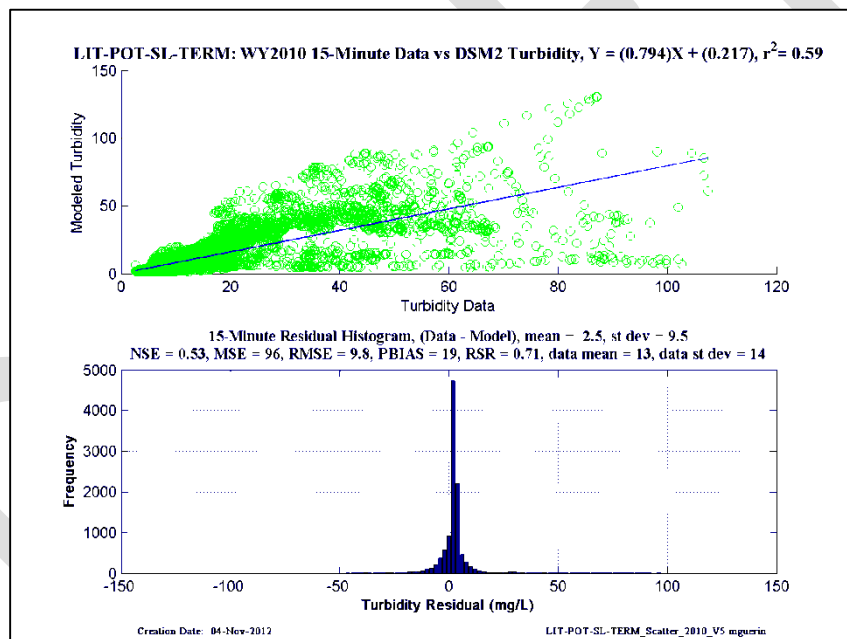
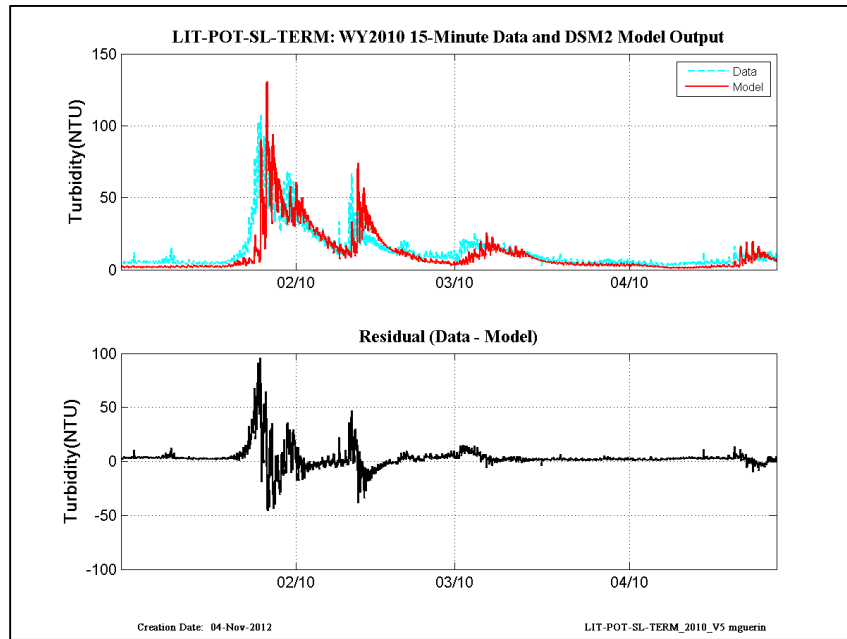


Figure 12-40 WY2010 15-min revised calibration results at Little Potato Slough-at-Terminus.

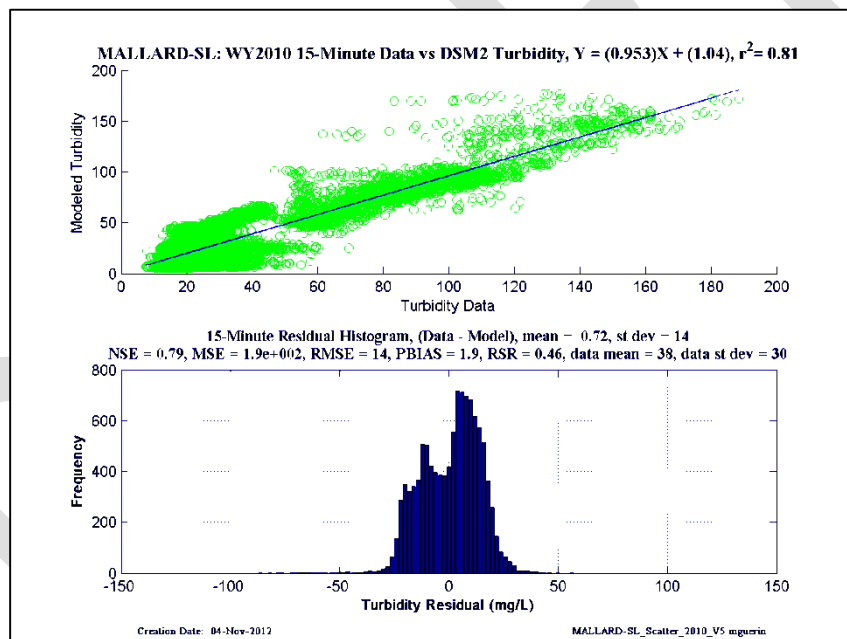
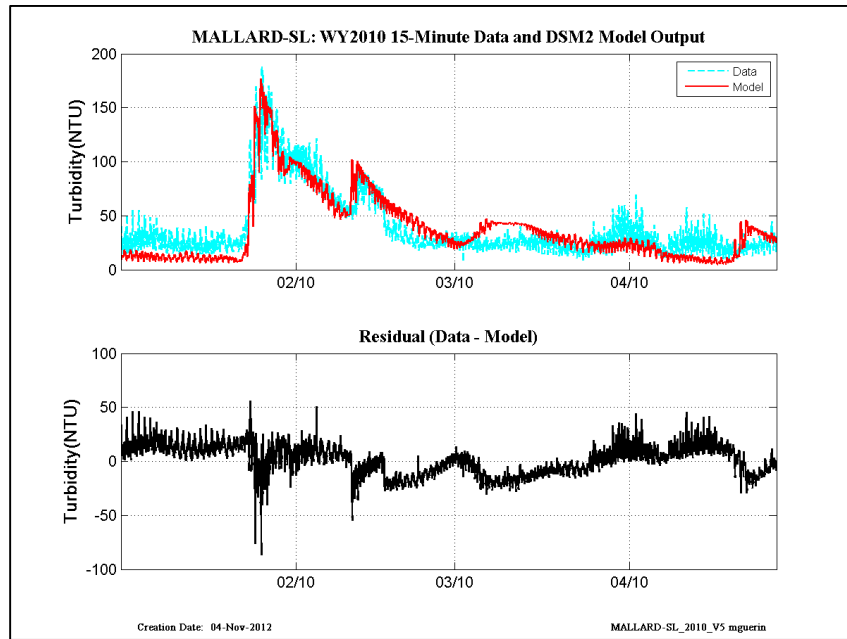


Figure 12-41 WY2010 15-min revised calibration results at Mallard Slough.

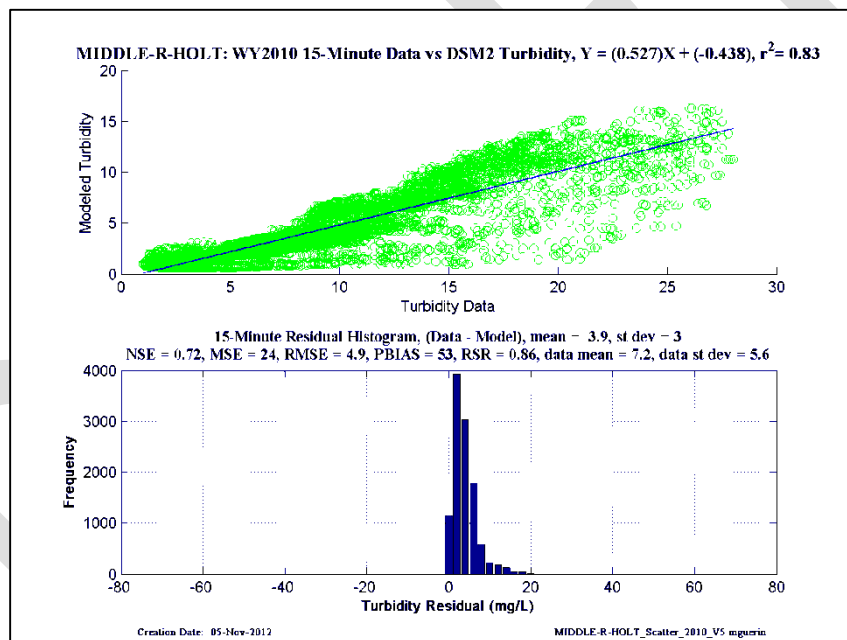
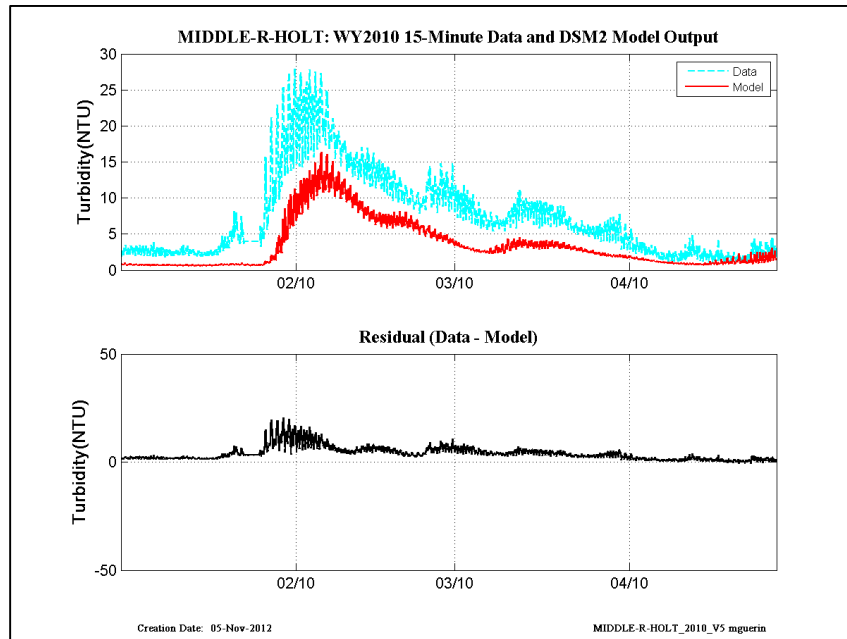


Figure 12-42 WY2010 15-min revised calibration results at Middle River-at-Holt.

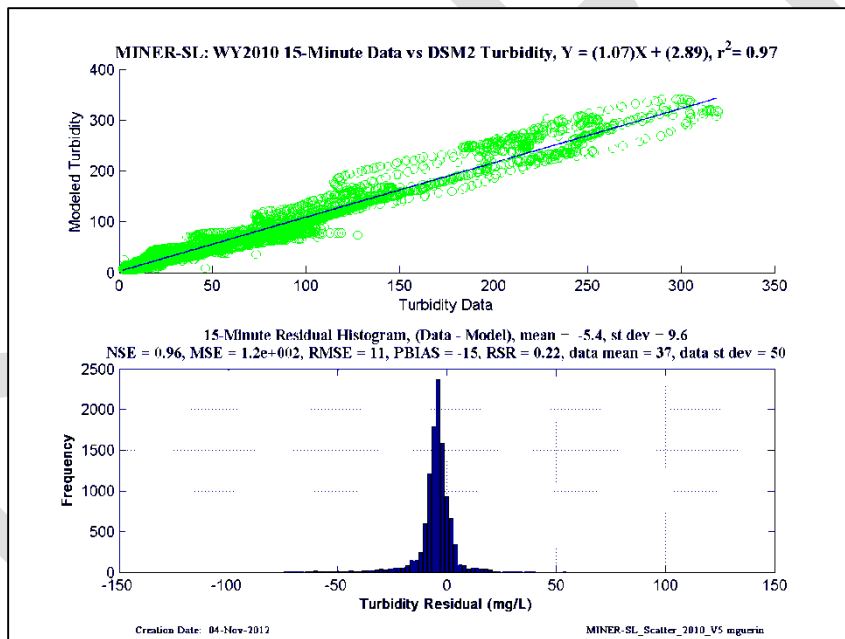
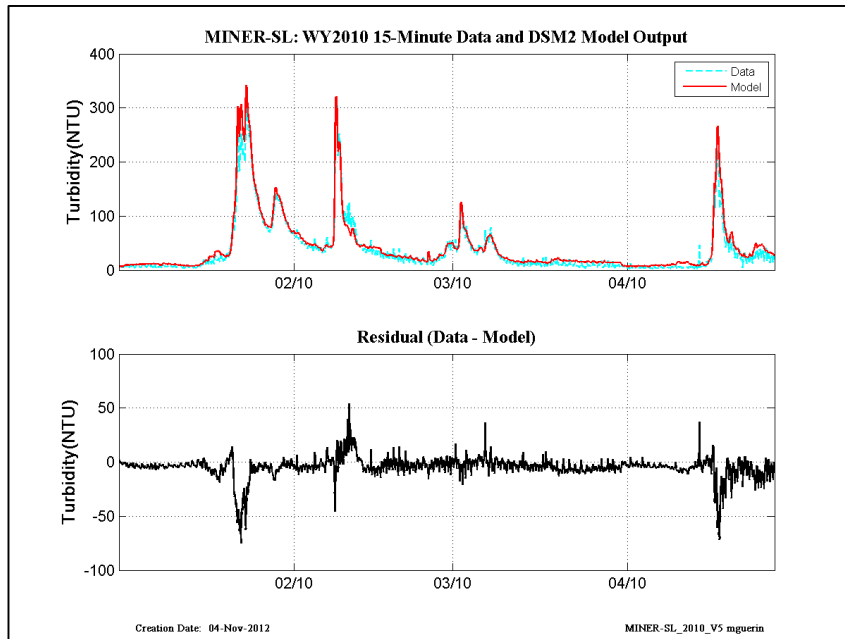


Figure 12-43 WY2010 15-min revised calibration results at Miner Slough.

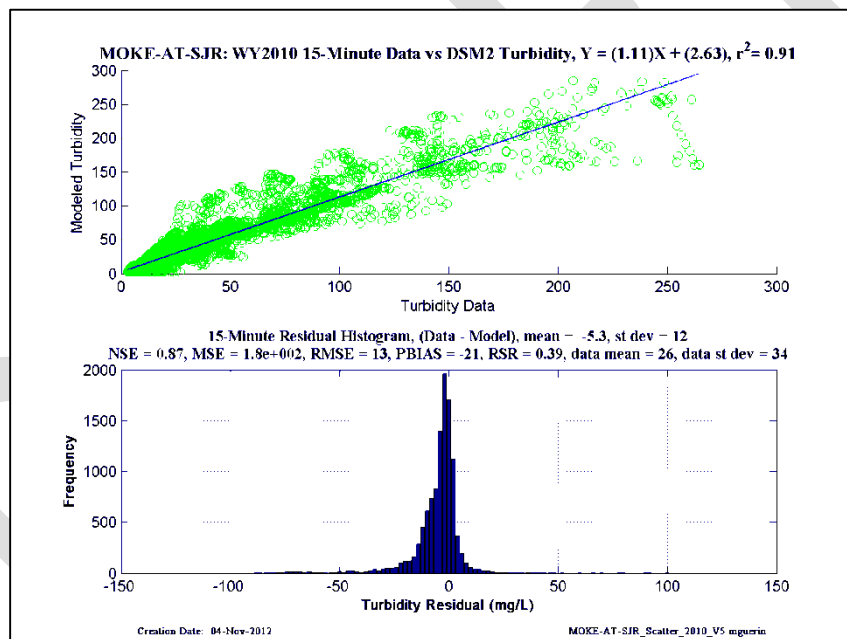
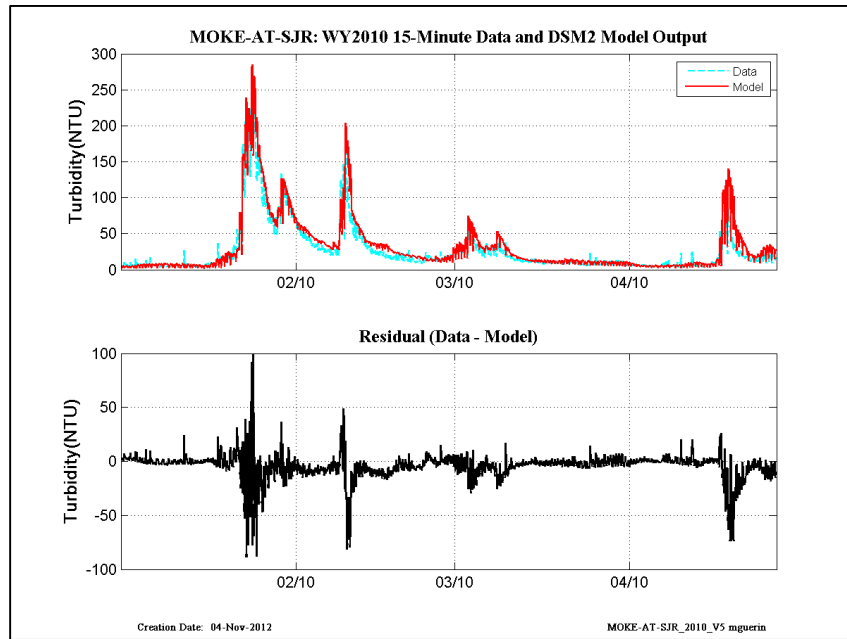


Figure 12-44 WY2010 15-min revised calibration results at Mokelumne-at-San Joaquin.

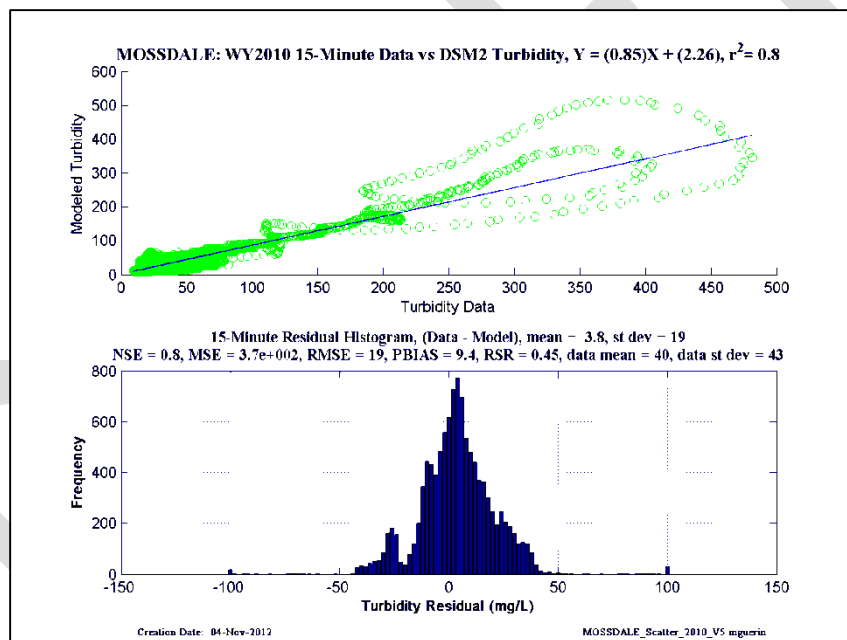
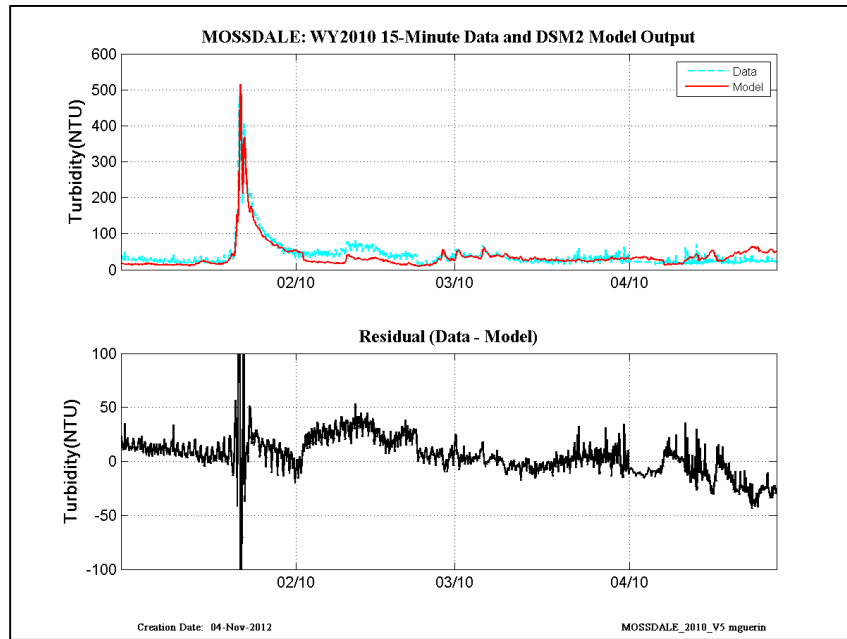


Figure 12-45 WY2010 15-min revised calibration results at Mossdale.

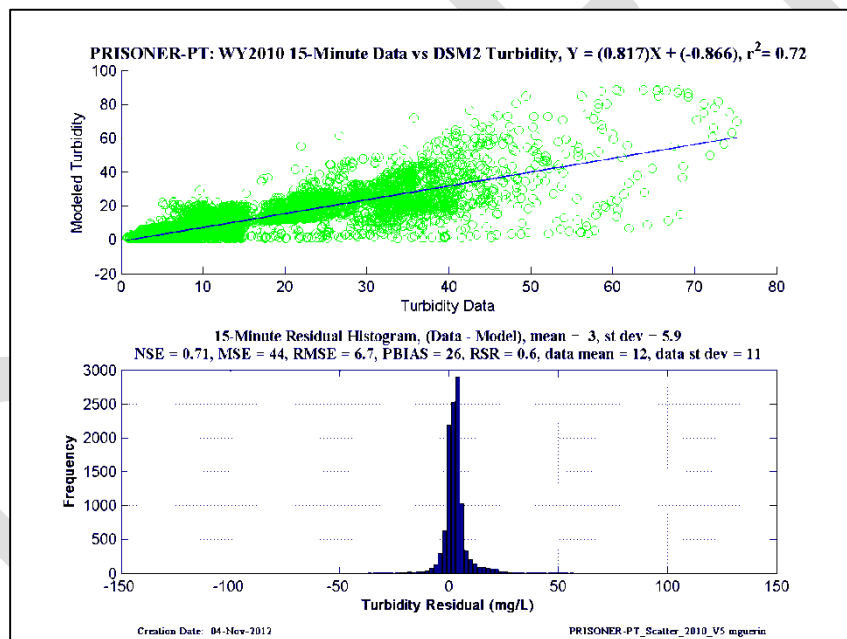
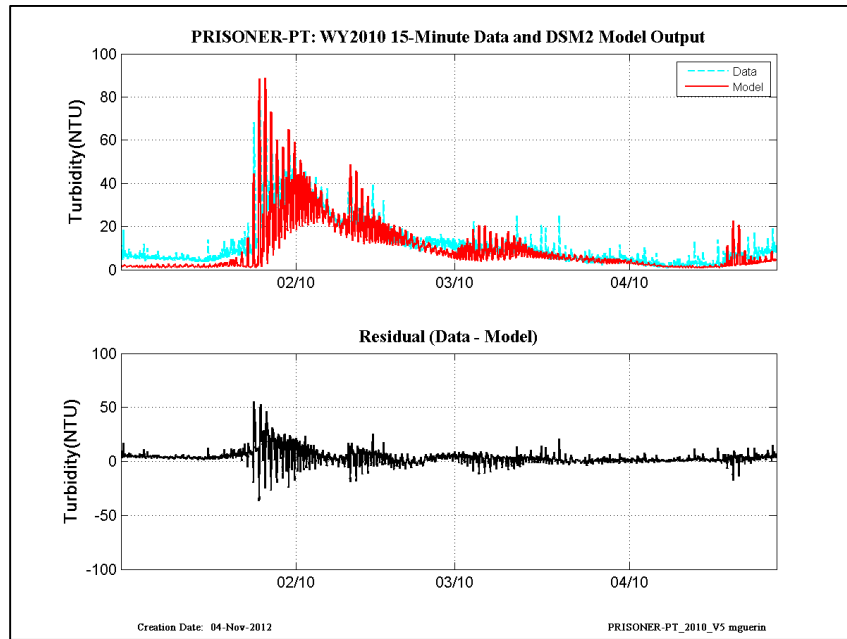


Figure 12-46 WY2010 15-min revised calibration results at Prisoner Point.

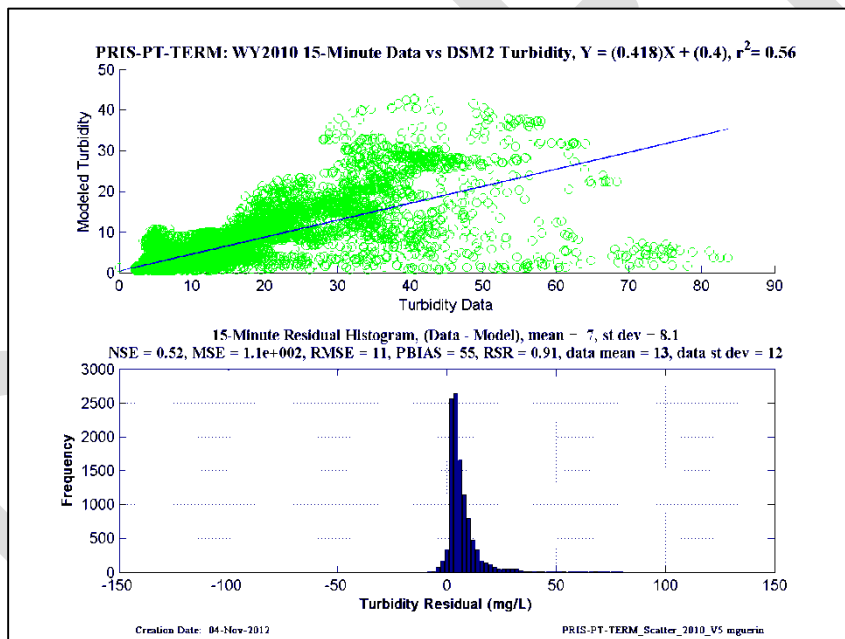
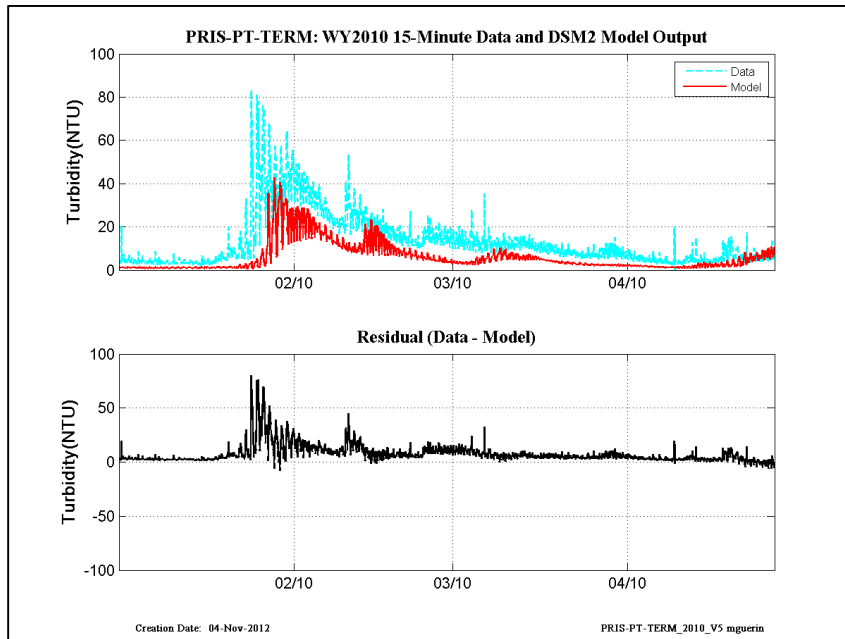


Figure 12-47 WY2010 15-min revised calibration results at Prisoner Point-at-Terminus.

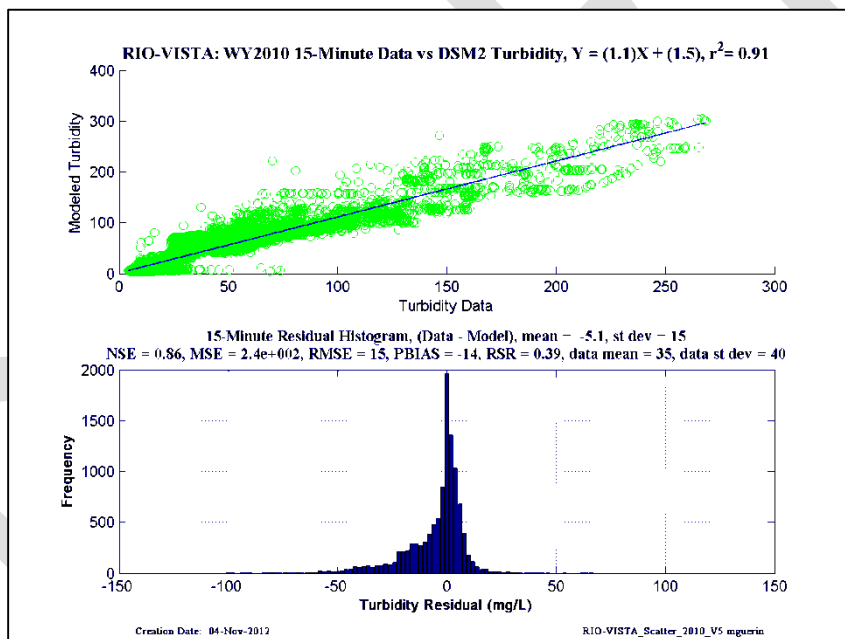
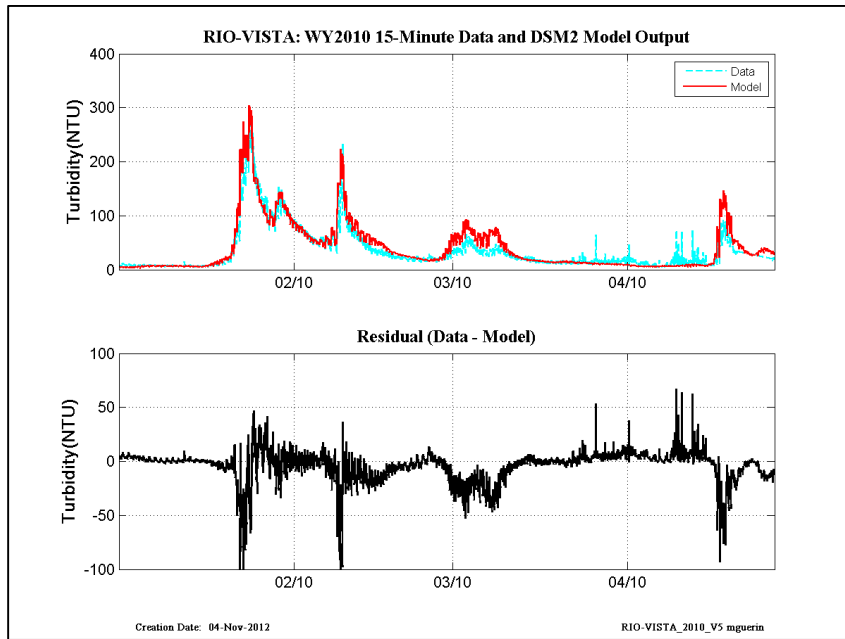


Figure 12-48 WY2010 15-min revised calibration results at Rio Vista.

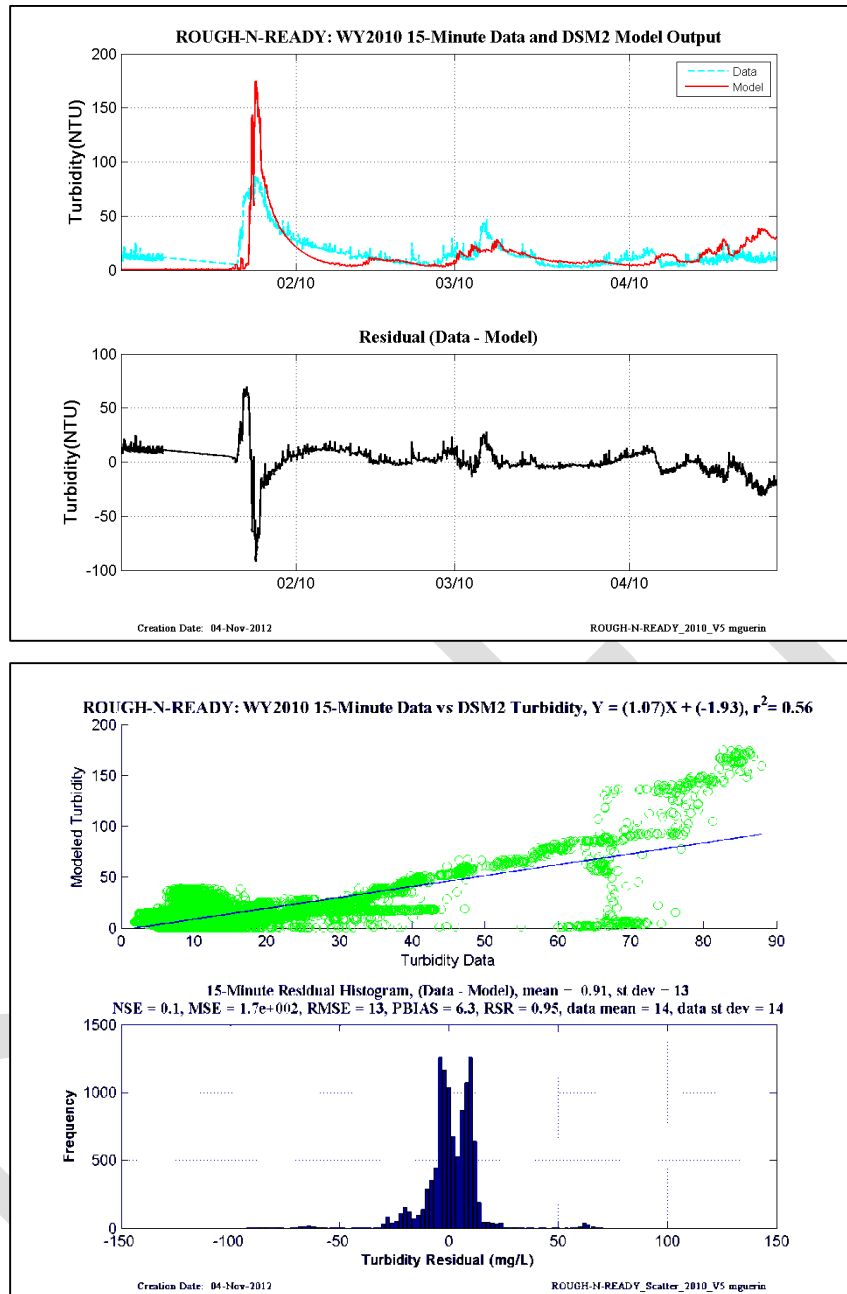


Figure 12-49 WY2010 15-min revised calibration results at Rough-N-Ready Island.

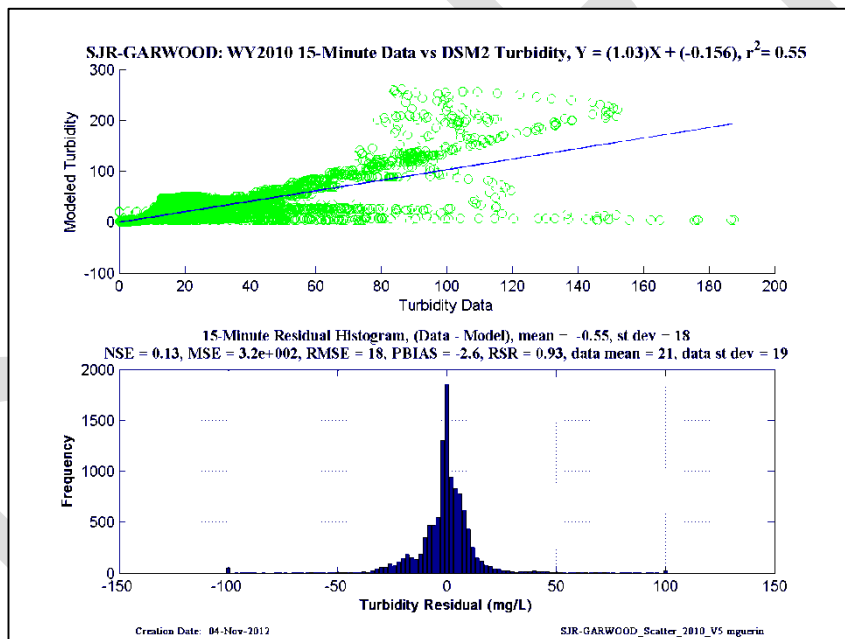
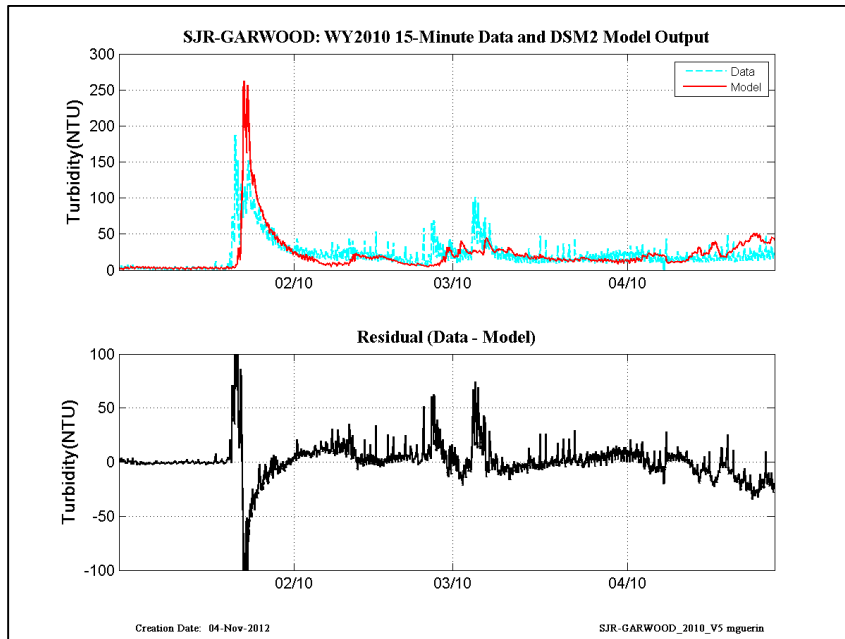


Figure 12-50 WY2010 15-min revised calibration results at San Joaquin-at-Garwood.

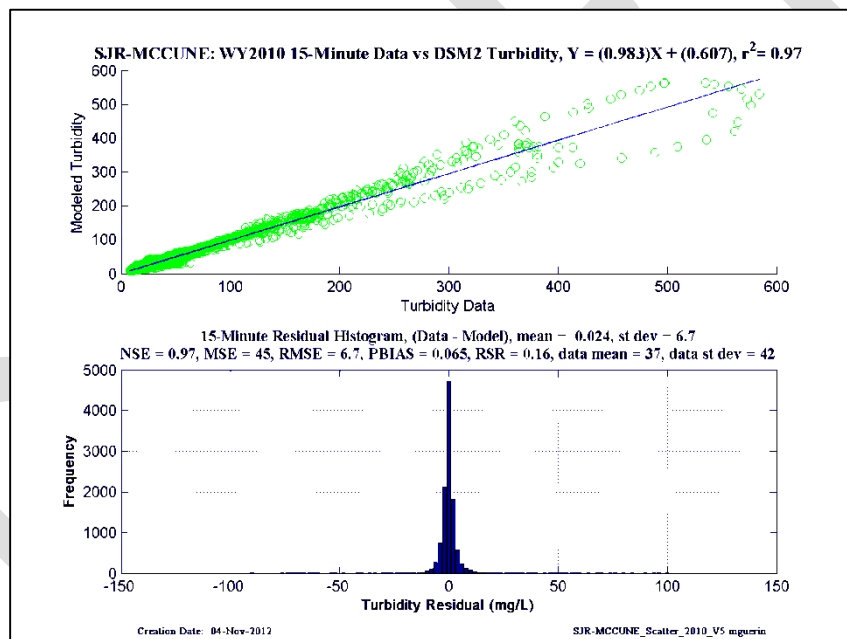
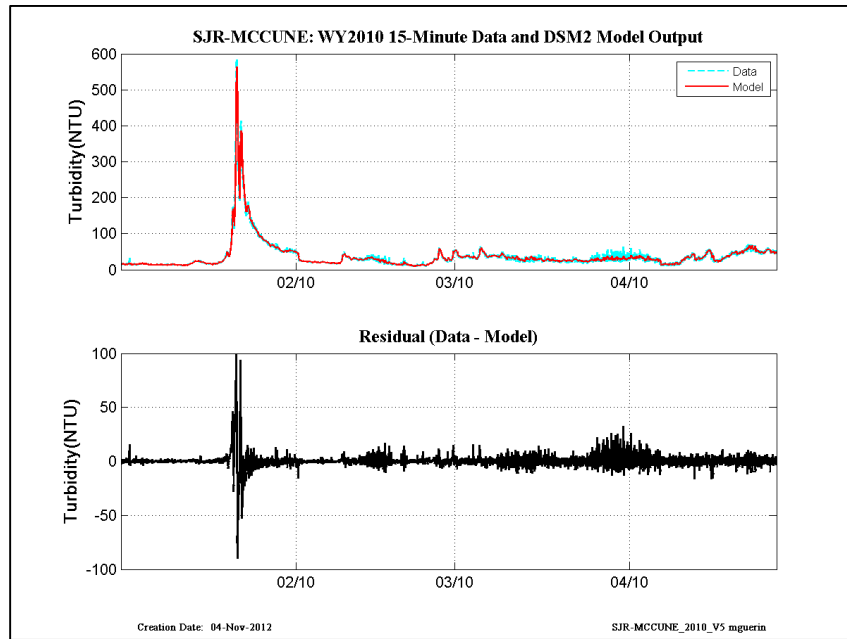


Figure 12-51 WY2010 15-min revised calibration results at San Joaquin-at-McCune (Vernalis).

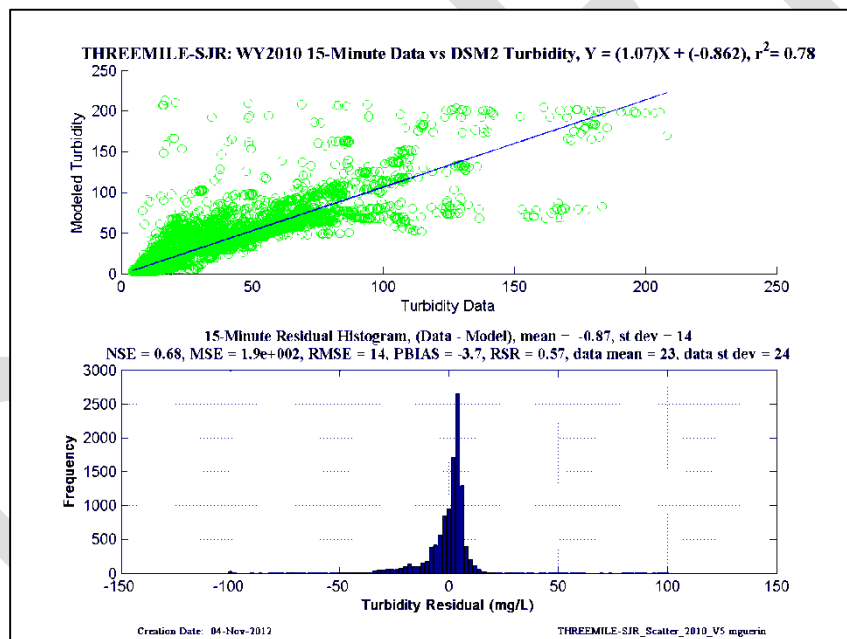
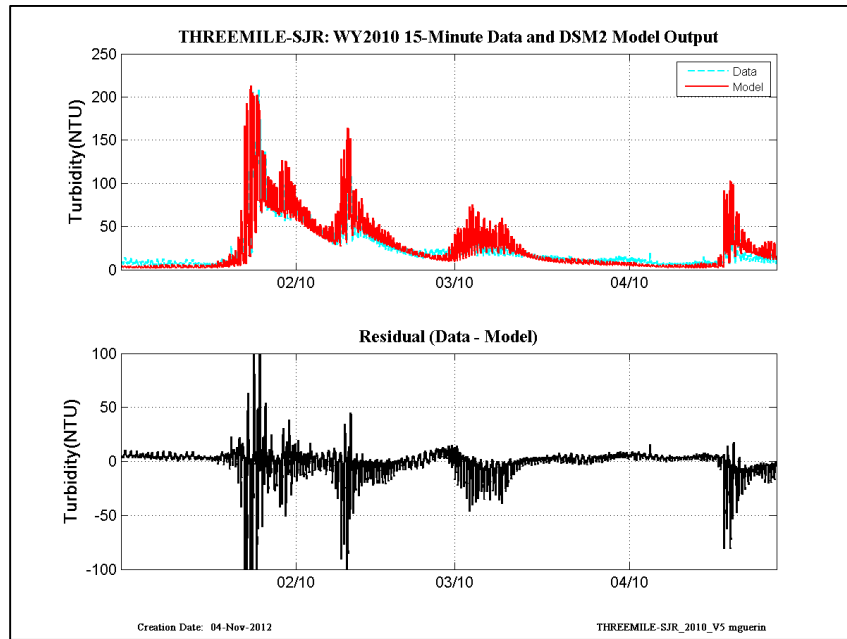


Figure 12-52 WY2010 15-min revised calibration results at Threemile-Slough-at-San Joaquin.

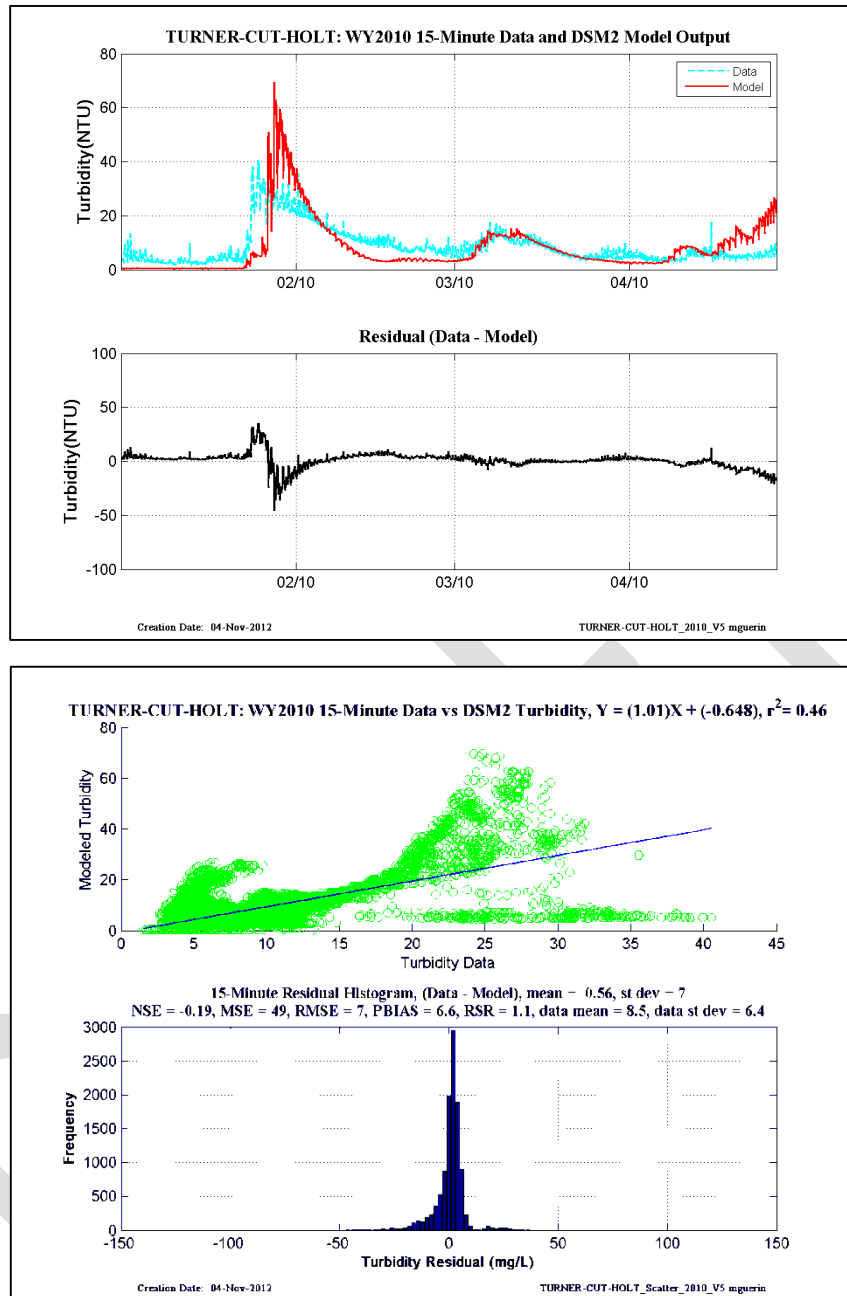


Figure 12-53 WY2010 15-min revised calibration results at Turner Cut-at-Holt.

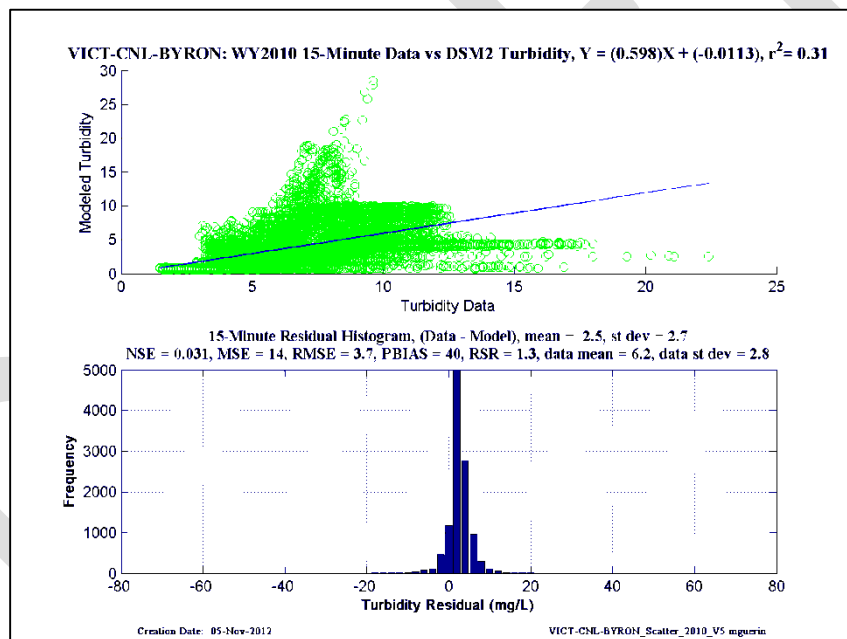
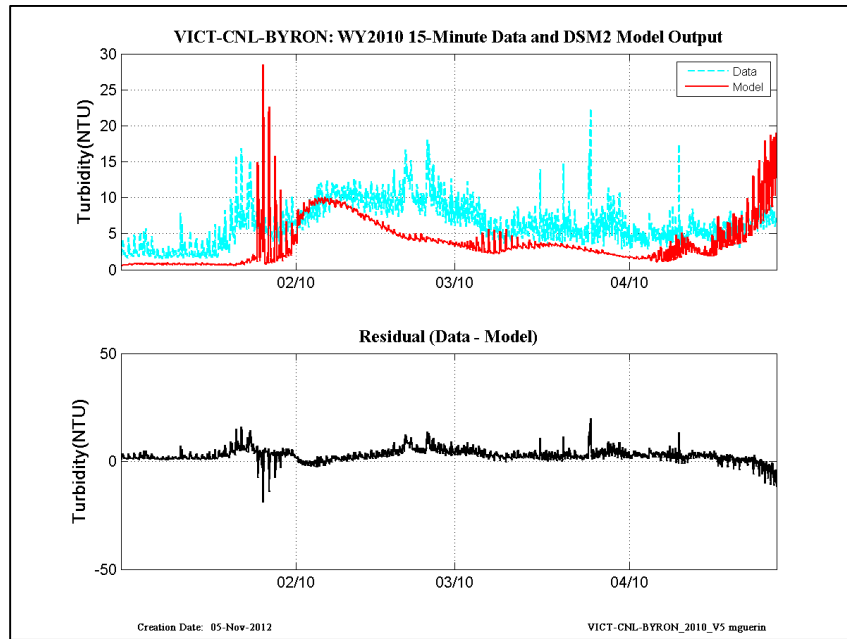


Figure 12-54 WY2010 15-min revised calibration results at Victoria Canal-at-Byron.

## **13 Appendix IV– Figures and Statistics Documenting DSM2 QUAL Historical 1975 – 2011 Turbidity Model Application with Mixed SSC-WARMF Boundary Conditions**

### **13.1 Early years: 1975 -1990**

DRAFT

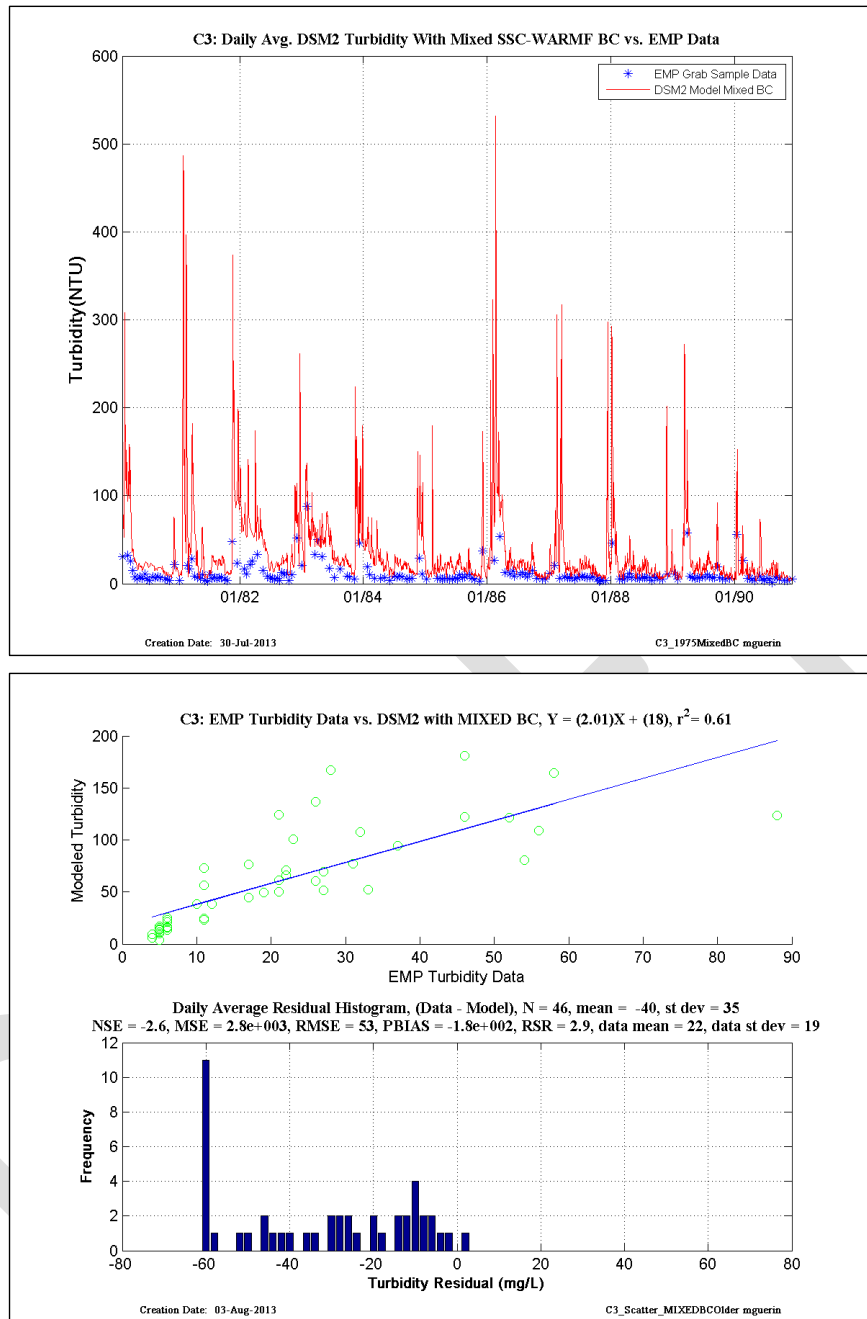


Figure 13-1 DSM2 daily-averaged turbidity model results using USGS-SSC at Freeport and Vernalis, and WARMF turbidity at other inflow boundaries compared to EMP grab-sample data, early years— location is EMP C3.

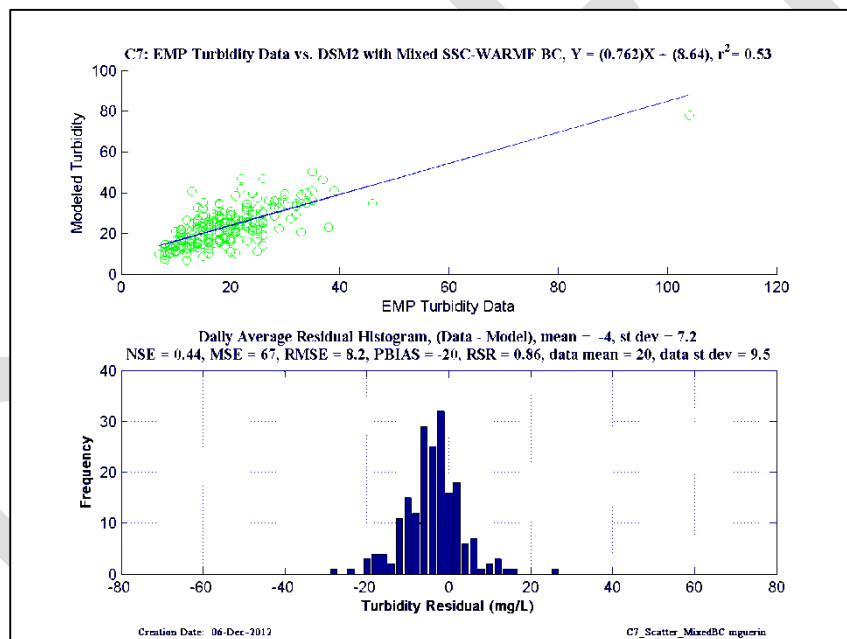
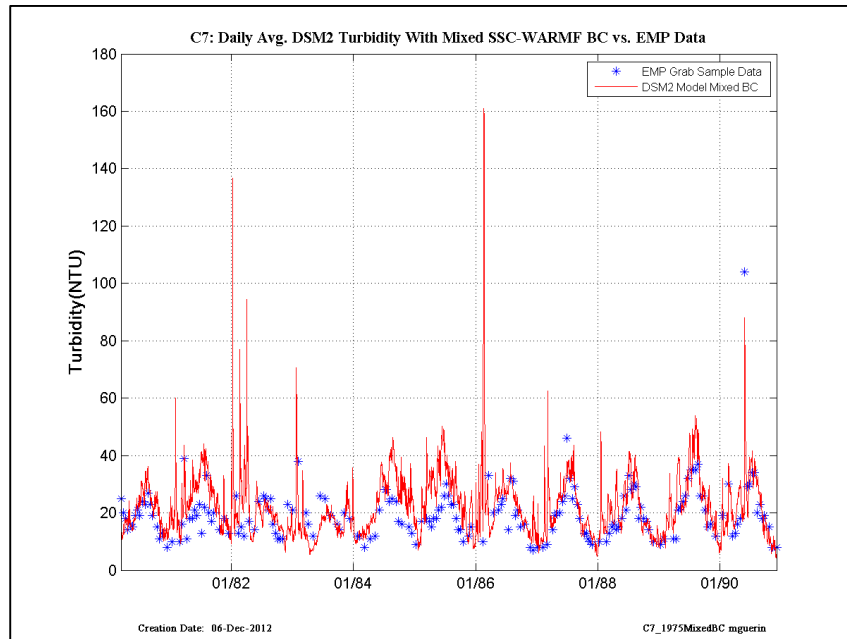


Figure 13-2 DSM2 daily-averaged turbidity model results using USGS-SSC at Freeport and Vernalis, and WARMF turbidity at other inflow boundaries compared to EMP grab-sample data, early years– location is EMP C7.

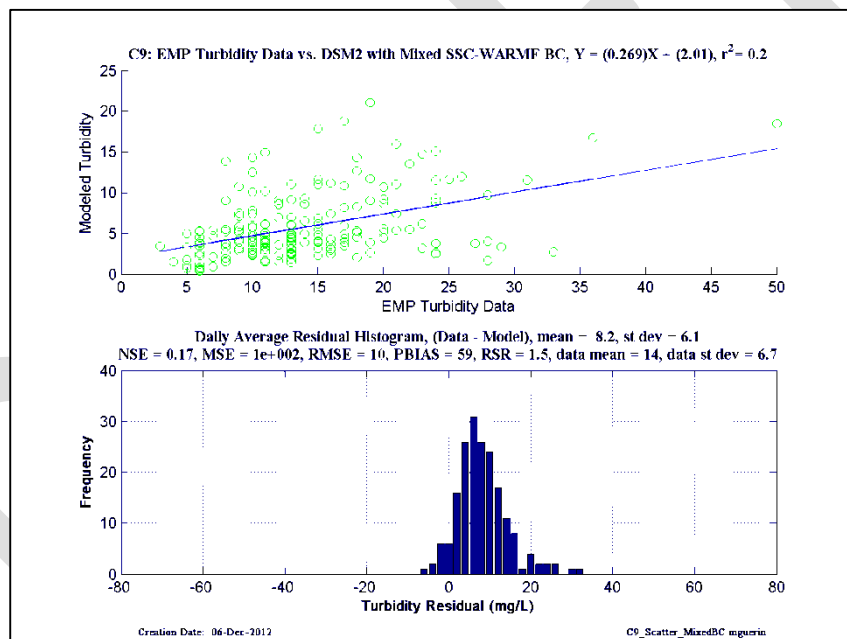
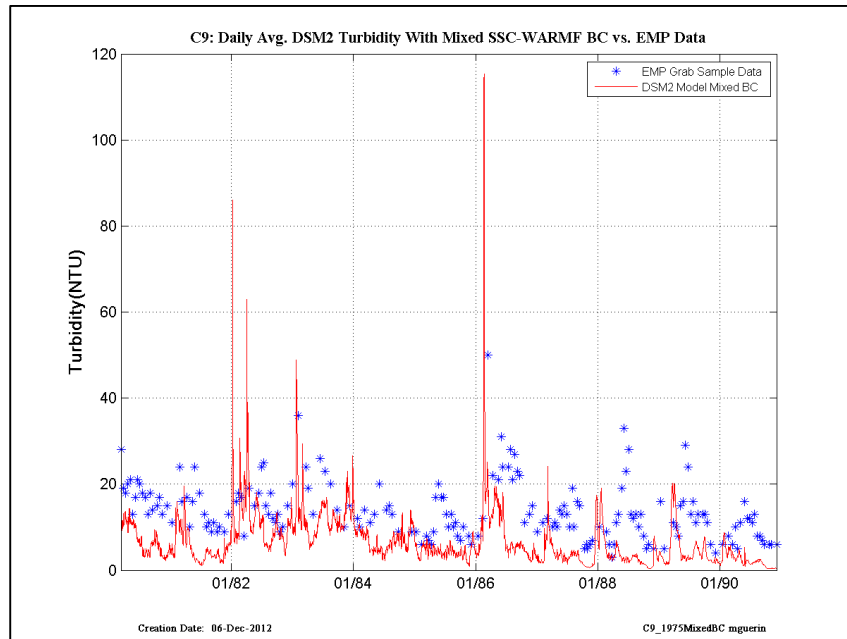


Figure 13-3 DSM2 daily-averaged turbidity model results using USGS-SSC at Freeport and Vernalis, and WARMF turbidity at other inflow boundaries compared to EMP grab-sample data, early years– location is EMP C9.

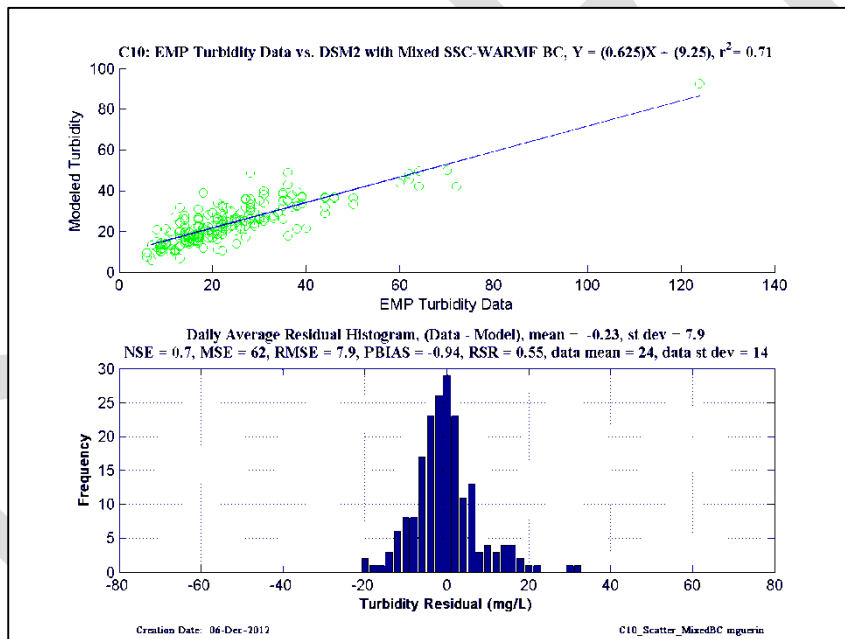
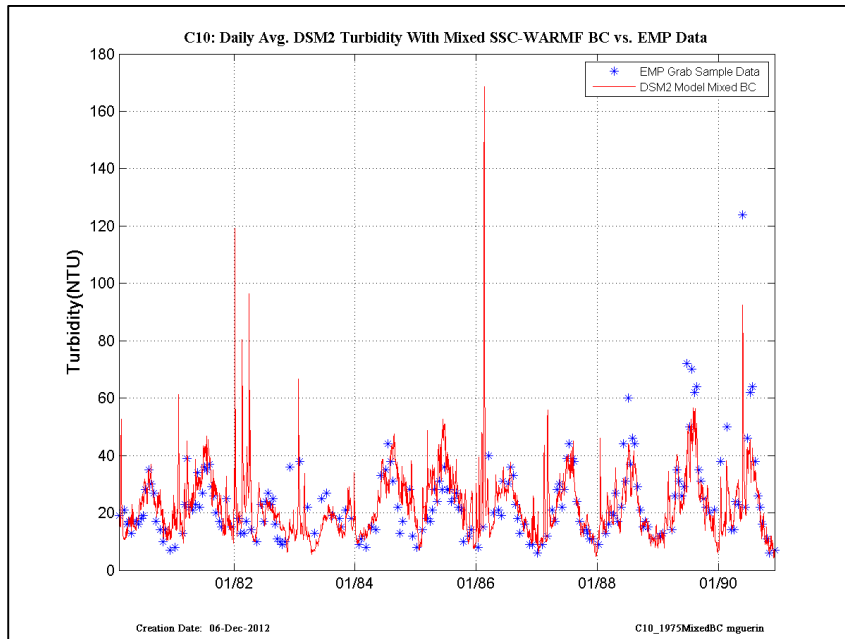


Figure 13-4 DSM2 daily-averaged turbidity model results using USGS-SSC at Freeport and Vernalis, and WARMF turbidity at other inflow boundaries compared to EMP grab-sample data, early years– location is EMP C10.

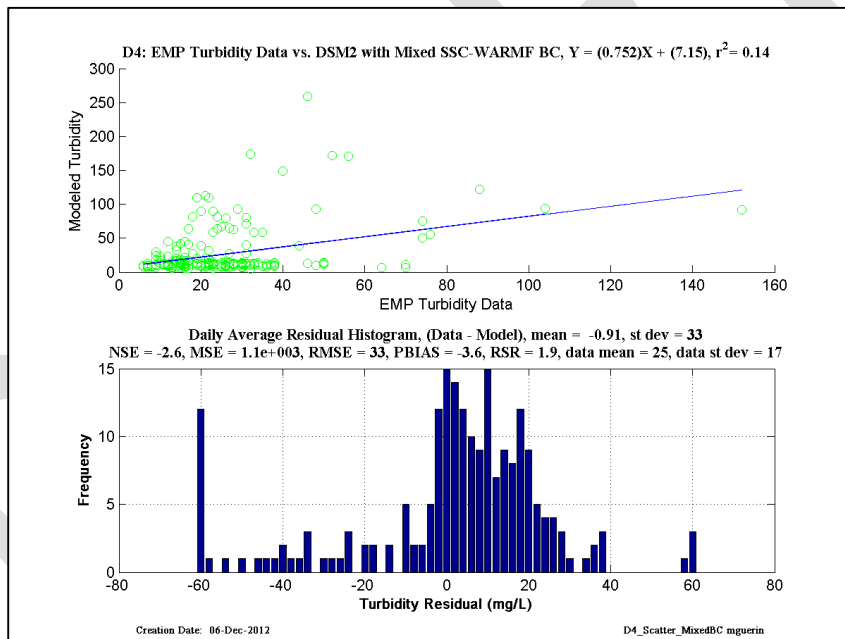
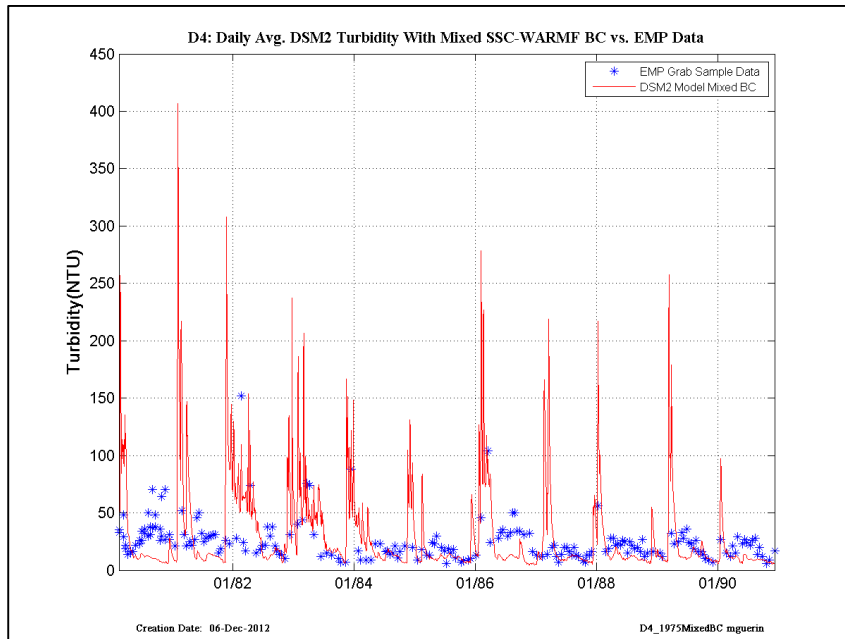


Figure 13-5 DSM2 daily-averaged turbidity model results using USGS-SSC at Freeport and Vernalis, and WARMF turbidity at other inflow boundaries compared to EMP grab-sample data, early years— location is EMP D4.

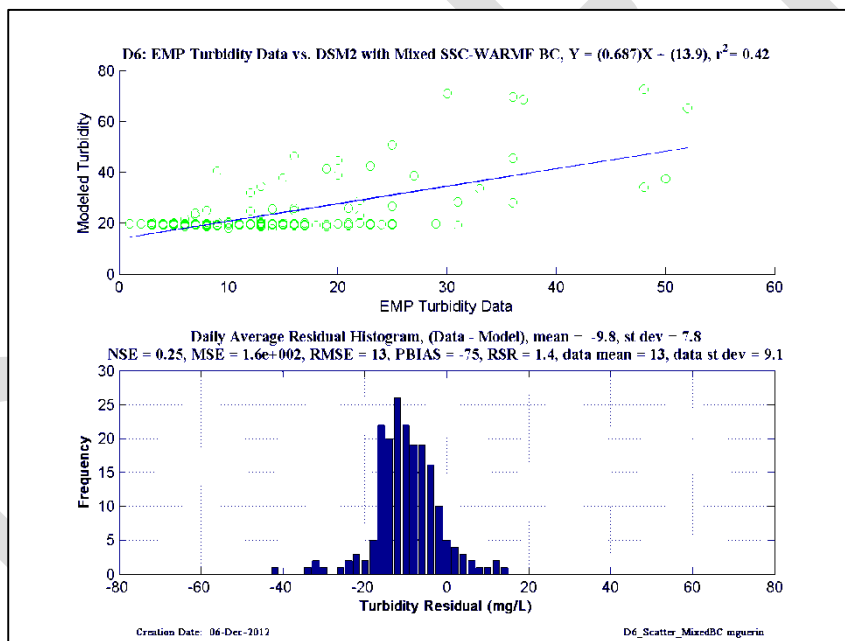
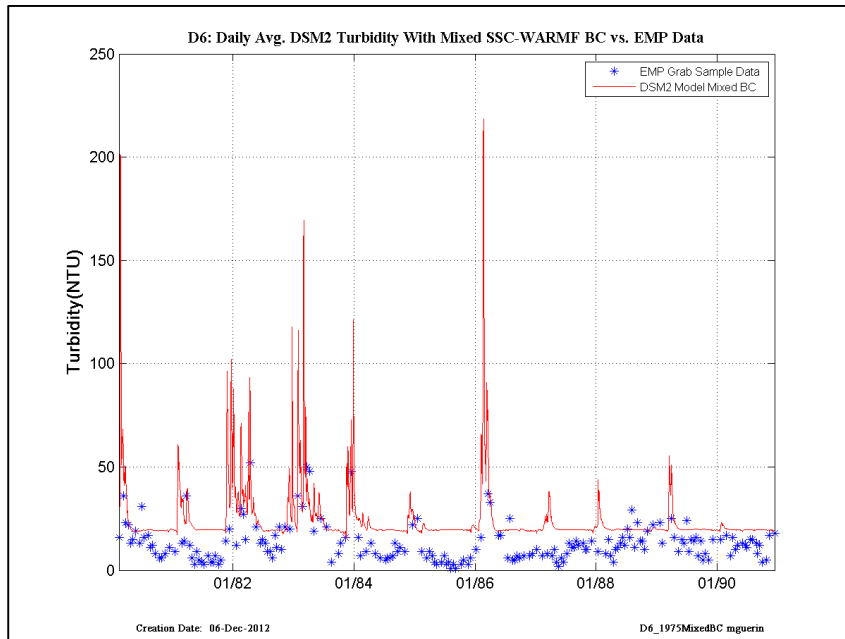


Figure 13-6 DSM2 daily-averaged turbidity model results using USGS-SSC at Freeport and Vernalis, and WARMF turbidity at other inflow boundaries compared to EMP grab-sample data, early years– location is EMP D6.

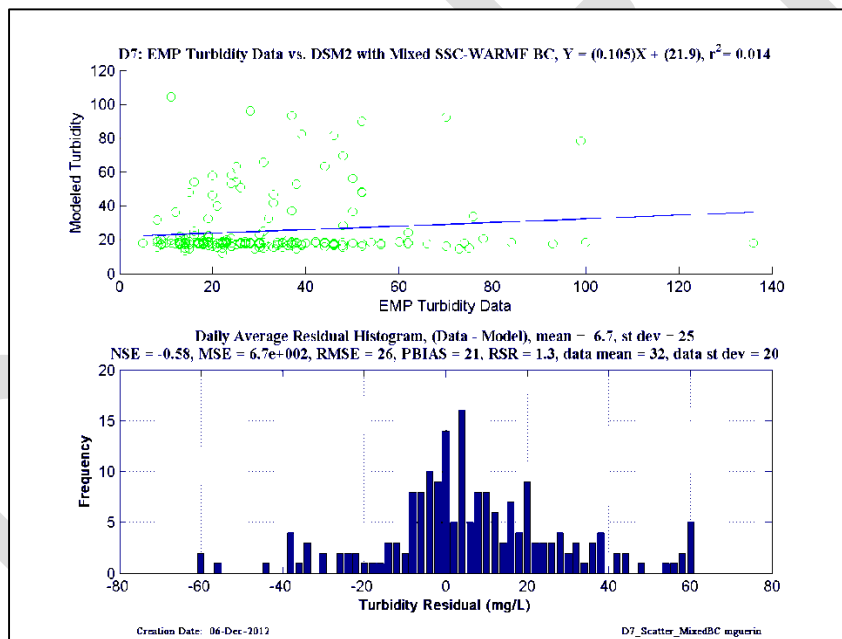
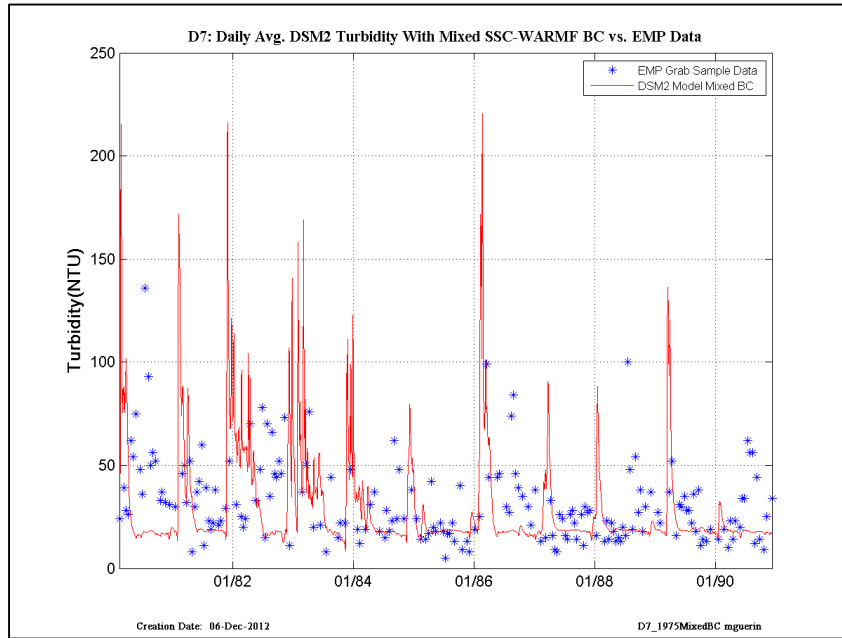


Figure 13-7 DSM2 daily-averaged turbidity model results using USGS-SSC at Freeport and Vernalis, and WARMF turbidity at other inflow boundaries compared to EMP grab-sample data, early years– location is EMP D7.

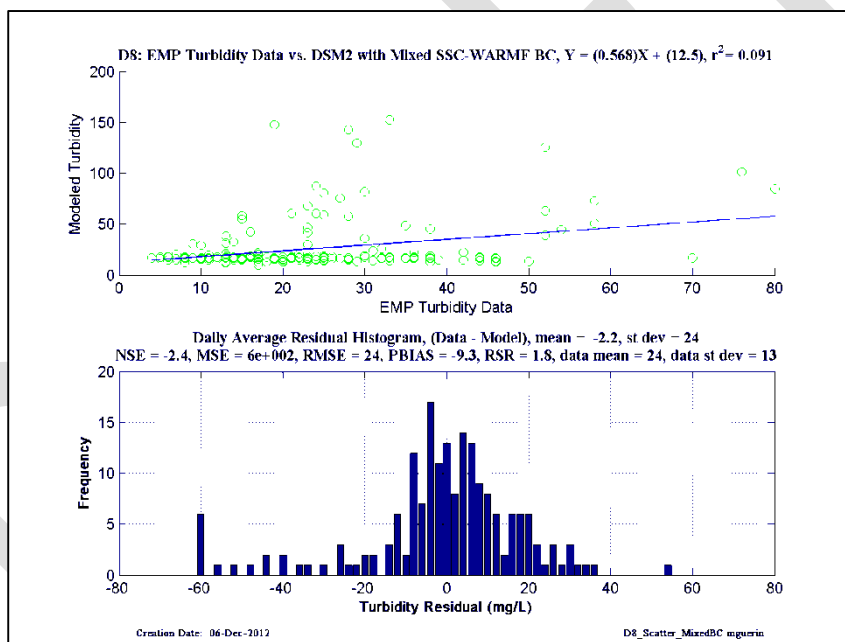
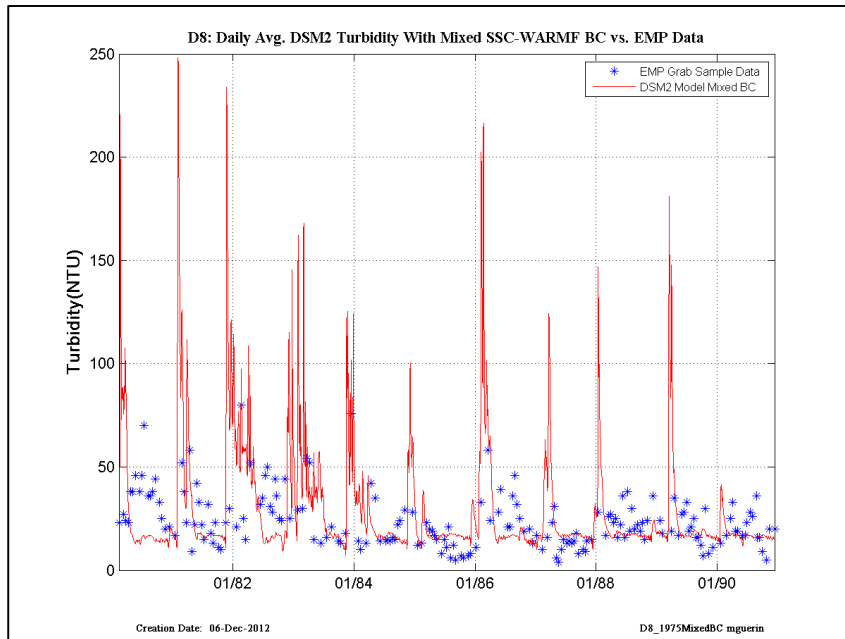


Figure 13-8 DSM2 daily-averaged turbidity model results using USGS-SSC at Freeport and Vernalis, and WARMF turbidity at other inflow boundaries compared to EMP grab-sample data, early years—location is EMP D8.

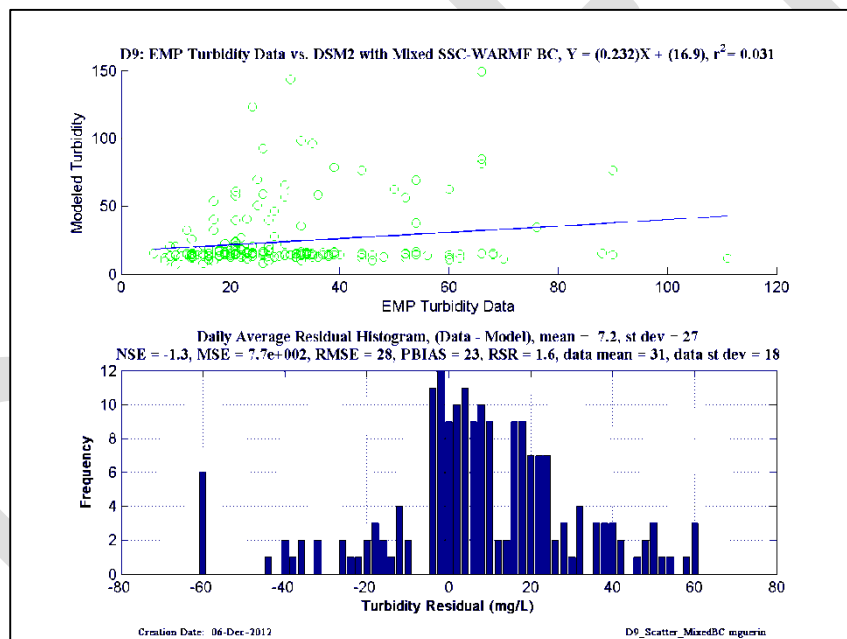
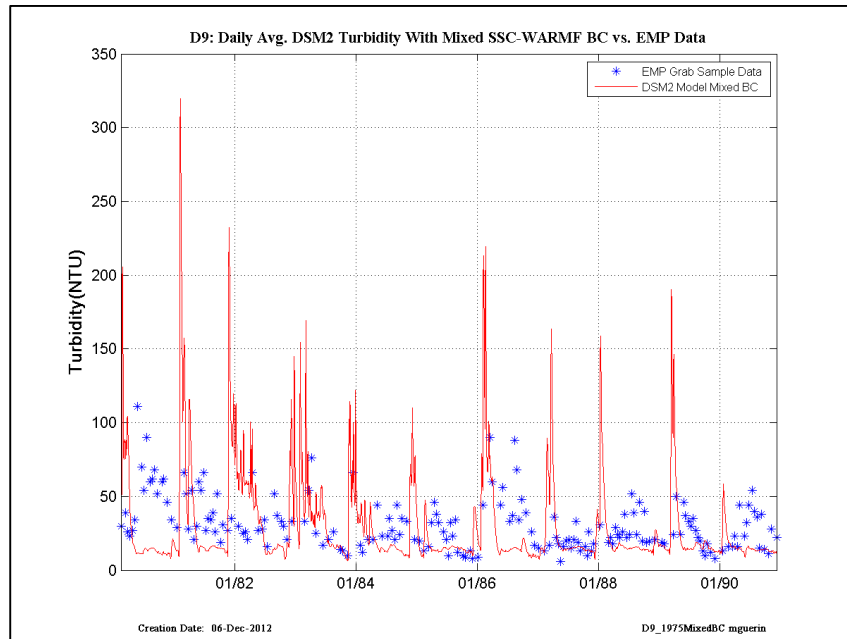


Figure 13-9 DSM2 daily-averaged turbidity model results using USGS-SSC at Freeport and Vernalis, and WARMF turbidity at other inflow boundaries compared to EMP grab-sample data, early years— location is EMP D9.

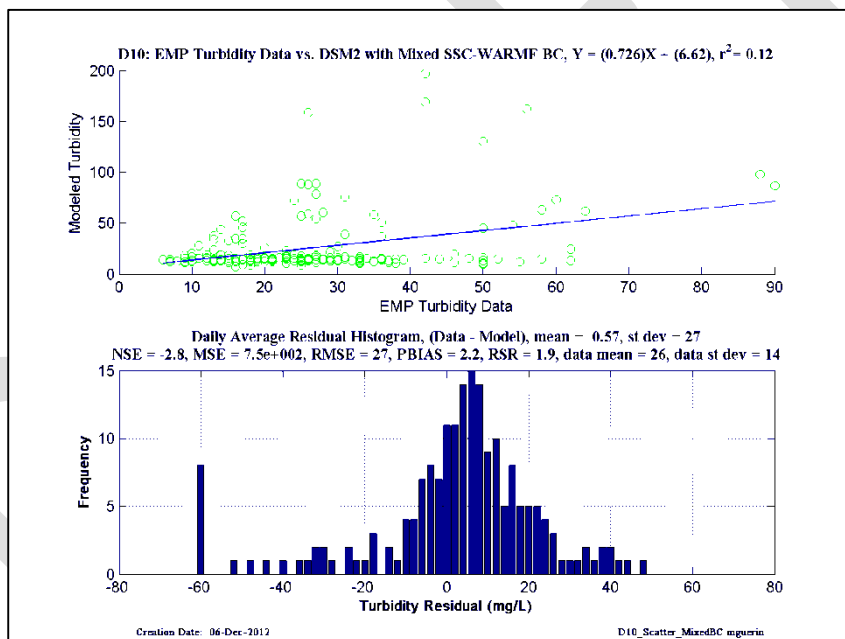
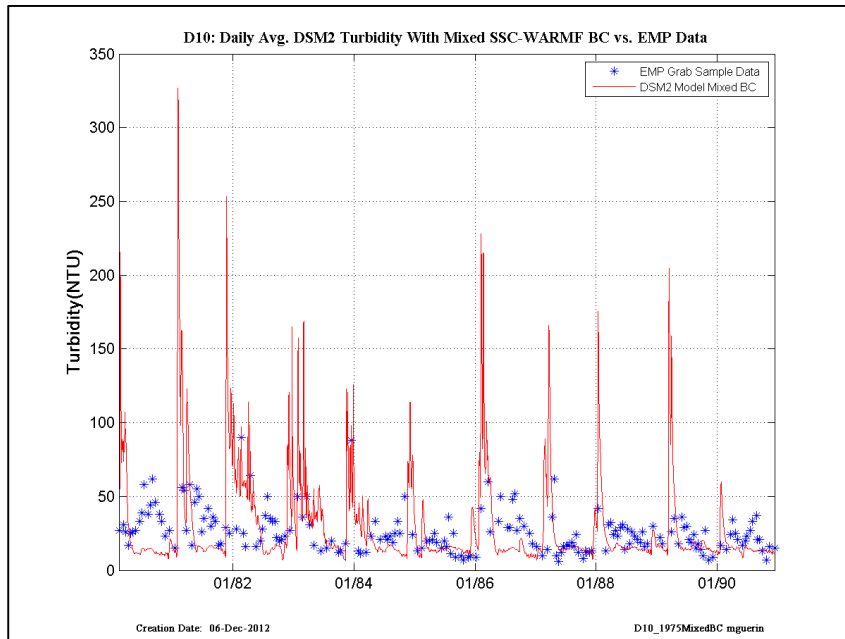


Figure 13-10 DSM2 daily-averaged turbidity model results using USGS-SSC at Freeport and Vernalis, and WARMF turbidity at other inflow boundaries compared to EMP grab-sample data, early years— location is EMP D10.

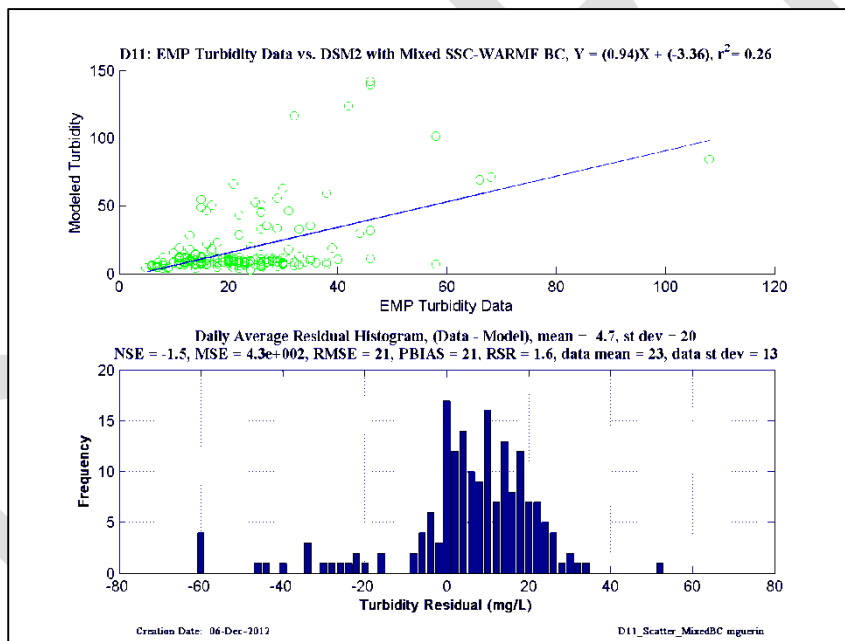
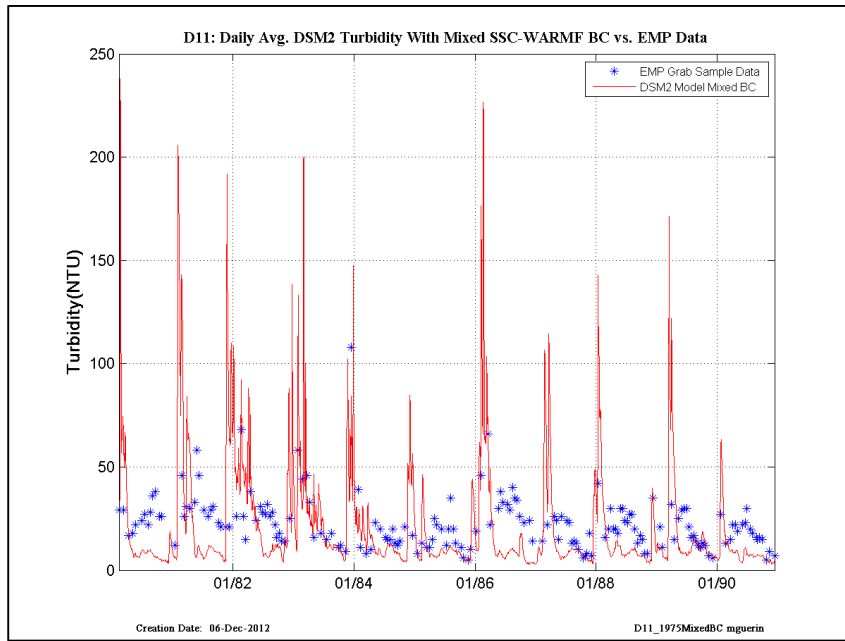


Figure 13-11 DSM2 daily-averaged turbidity model results using USGS-SSC at Freeport and Vernalis, and WARMF turbidity at other inflow boundaries compared to EMP grab-sample data, early years– location is EMP D11.

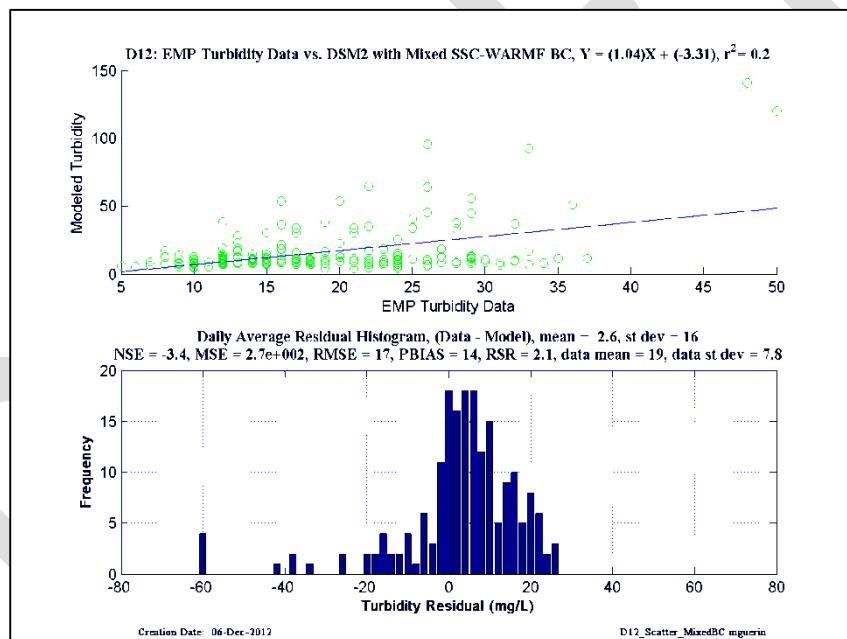
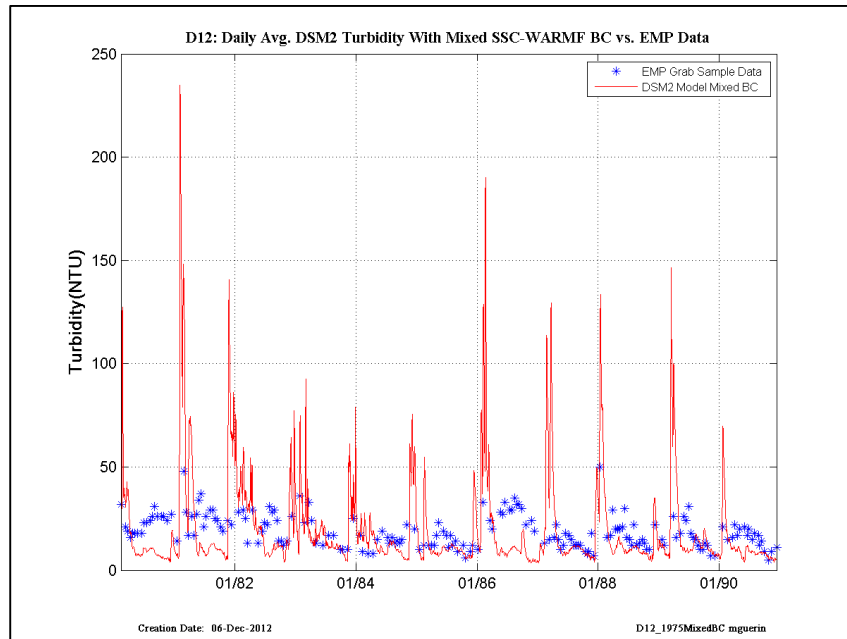


Figure 13-12 DSM2 daily-averaged turbidity model results using USGS-SSC at Freeport and Vernalis, and WARMF turbidity at other inflow boundaries compared to EMP grab-sample data, early years– location is EMP D12.

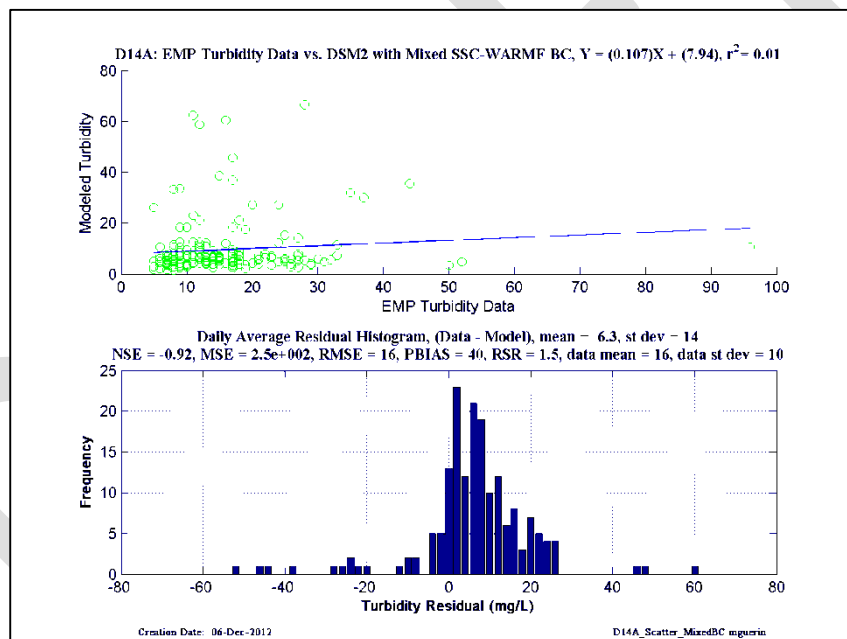
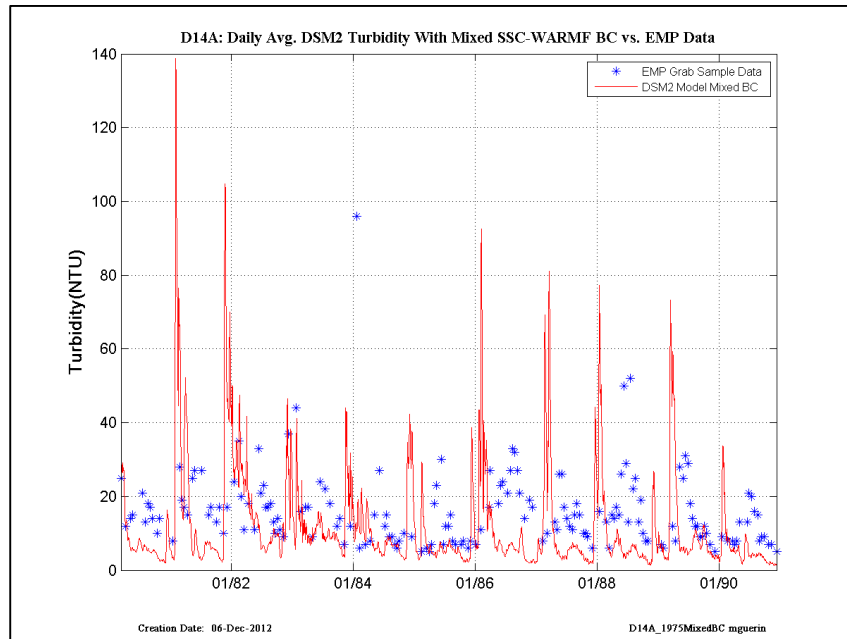


Figure 13-13 DSM2 daily-averaged turbidity model results using USGS-SSC at Freeport and Vernalis, and WARMF turbidity at other inflow boundaries compared to EMP grab-sample data, early years– location is EMP D14A.

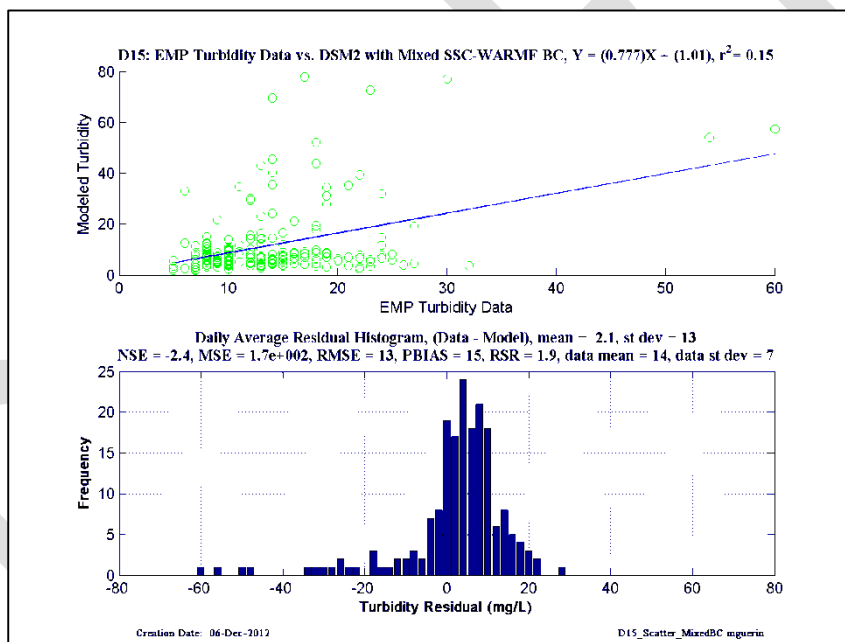
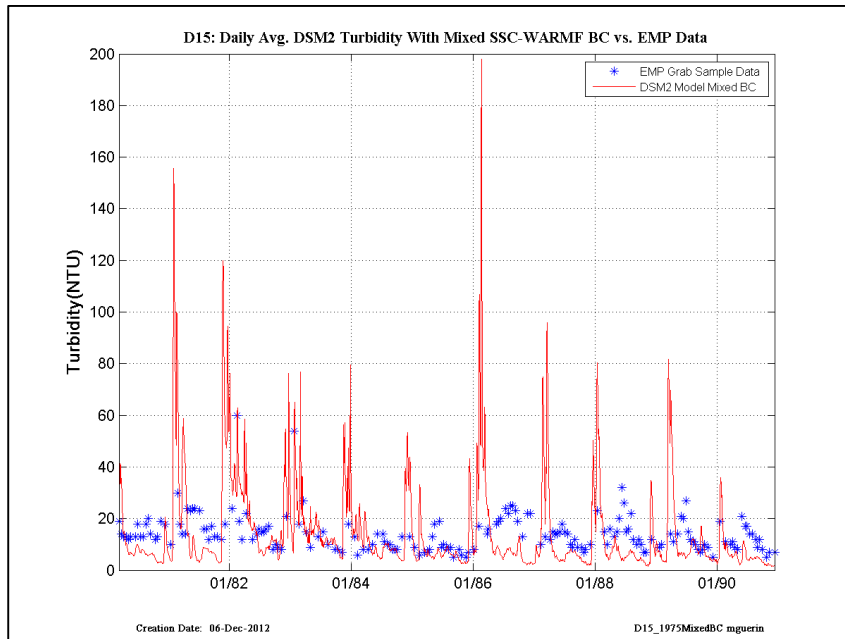


Figure 13-14 DSM2 daily-averaged turbidity model results using USGS-SSC at Freeport and Vernalis, and WARMF turbidity at other inflow boundaries compared to EMP grab-sample data, early years– location is EMP D15.

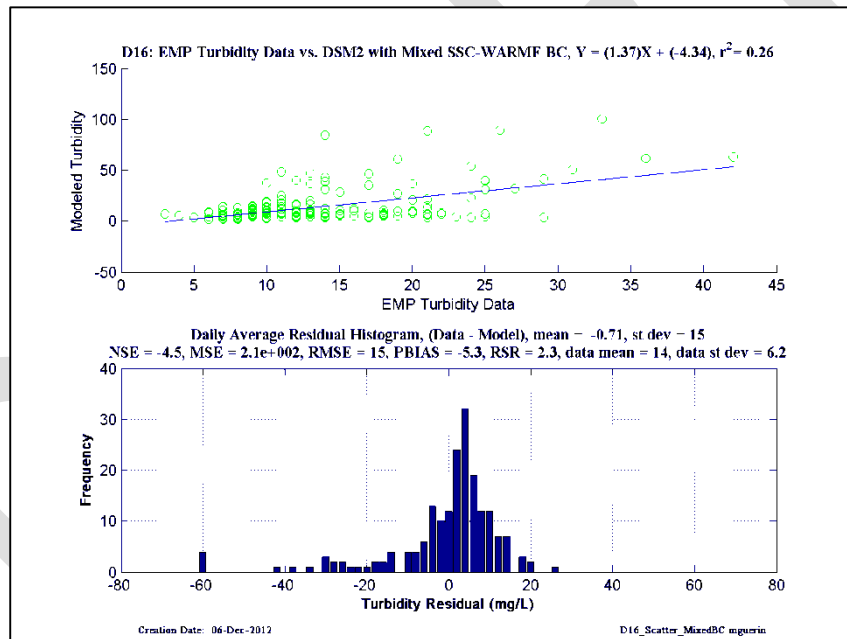
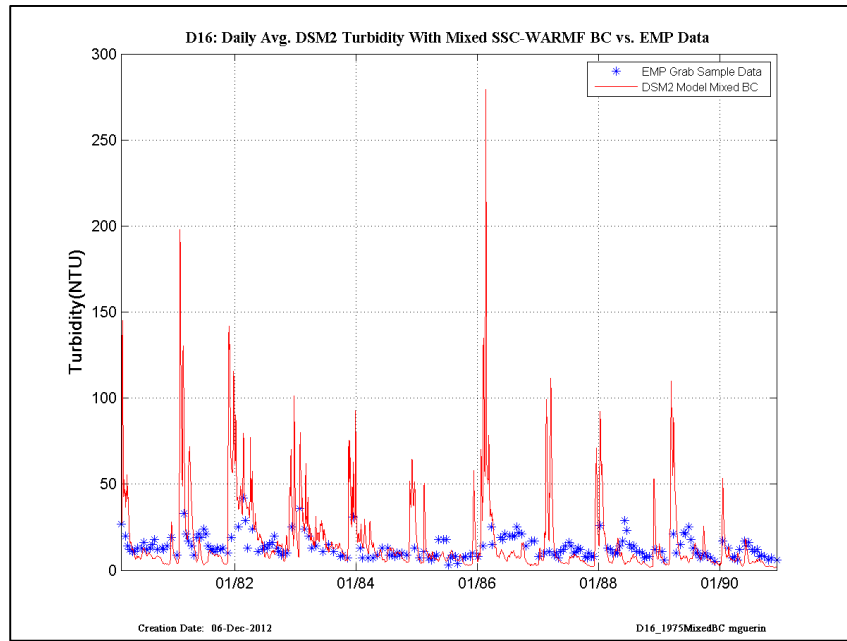


Figure 13-15 DSM2 daily-averaged turbidity model results using USGS-SSC at Freeport and Vernalis, and WARMF turbidity at other inflow boundaries compared to EMP grab-sample data, early years– location is EMP D16.

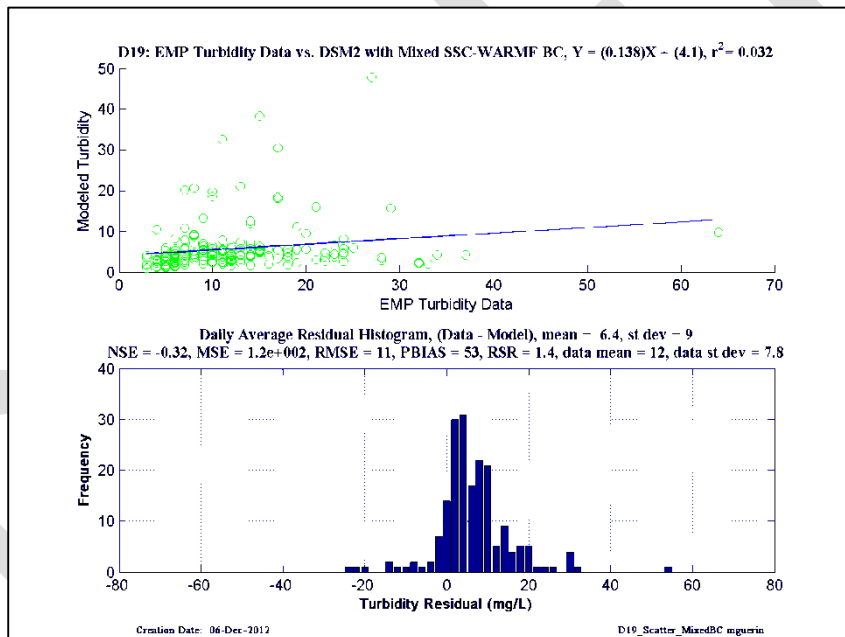
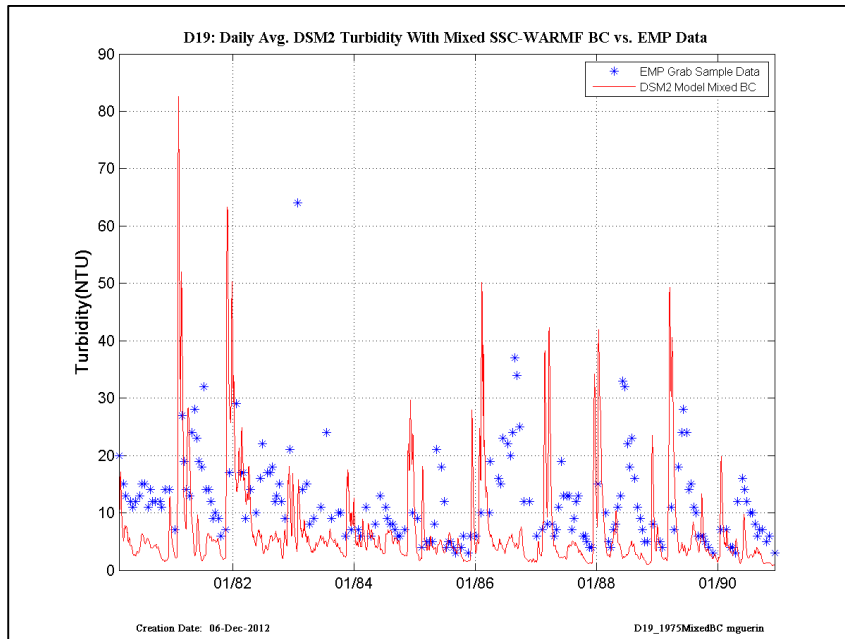


Figure 13-16 DSM2 daily-averaged turbidity model results using USGS-SSC at Freeport and Vernalis, and WARMF turbidity at other inflow boundaries compared to EMP grab-sample data, early years– location is EMP D19.

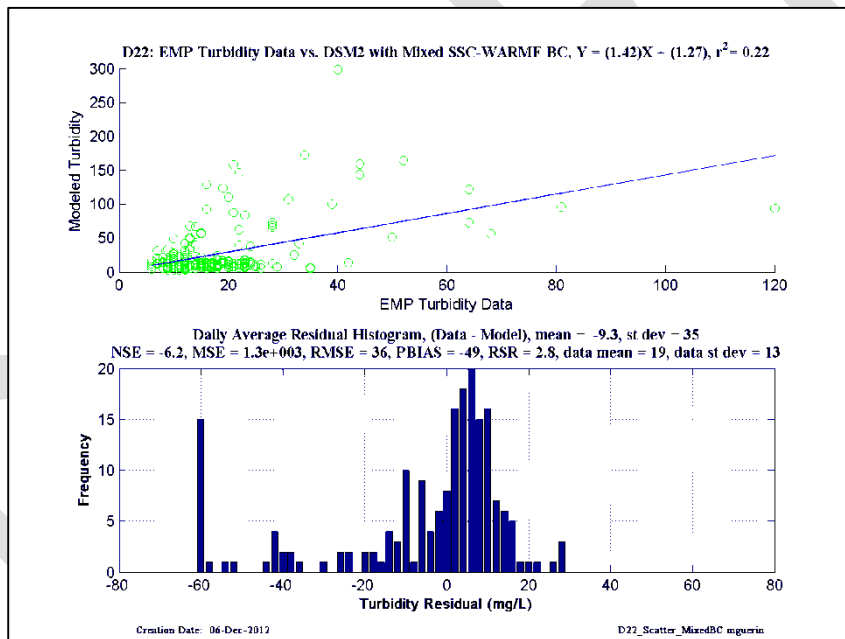
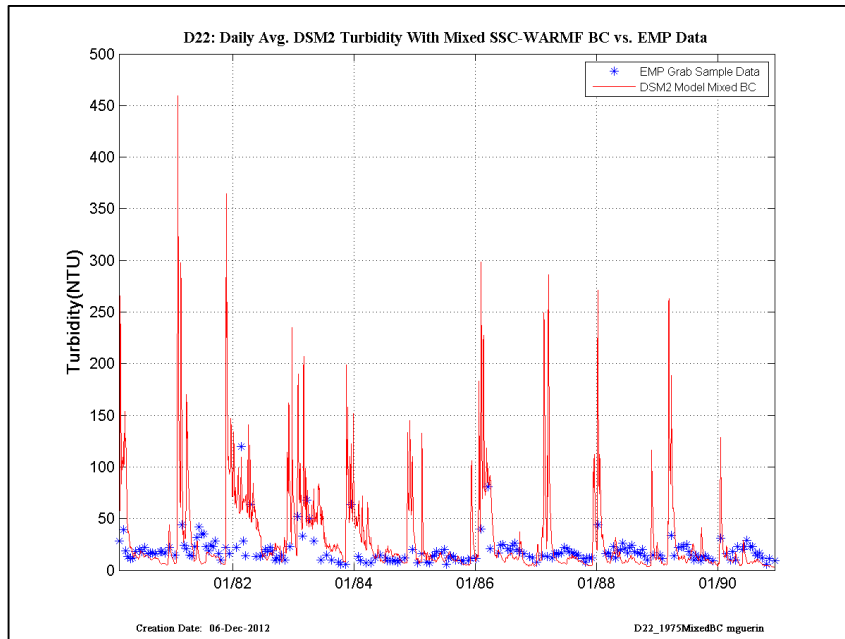


Figure 13-17 DSM2 daily-averaged turbidity model results using USGS-SSC at Freeport and Vernalis, and WARMF turbidity at other inflow boundaries compared to EMP grab-sample data, early years– location is EMP D22.

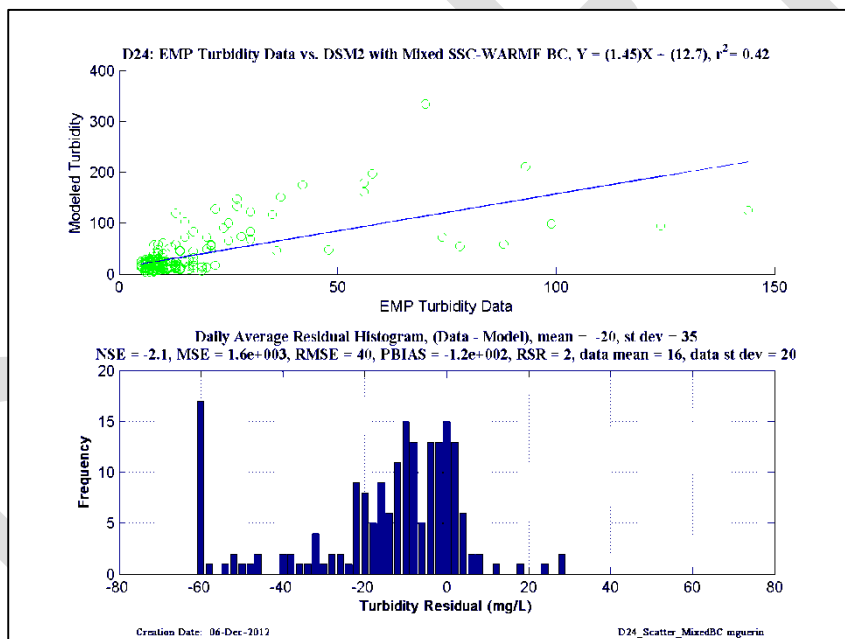
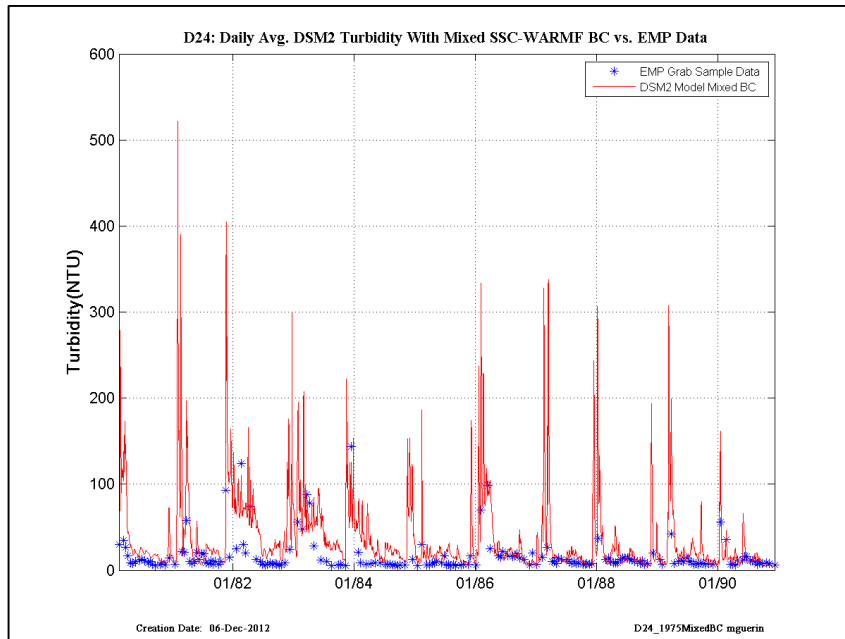


Figure 13-18 DSM2 daily-averaged turbidity model results using USGS-SSC at Freeport and Vernalis, and WARMF turbidity at other inflow boundaries compared to EMP grab-sample data, early years— location is EMP D24.

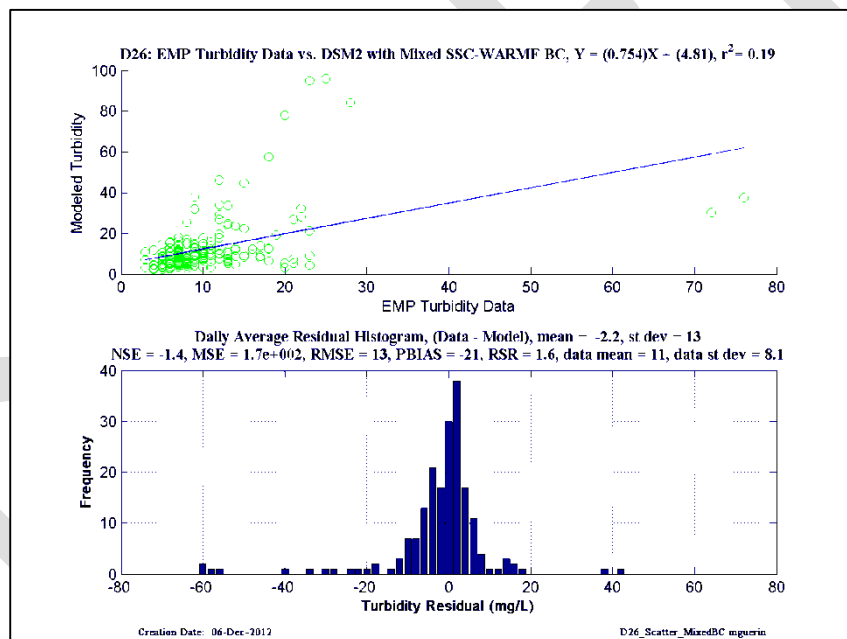
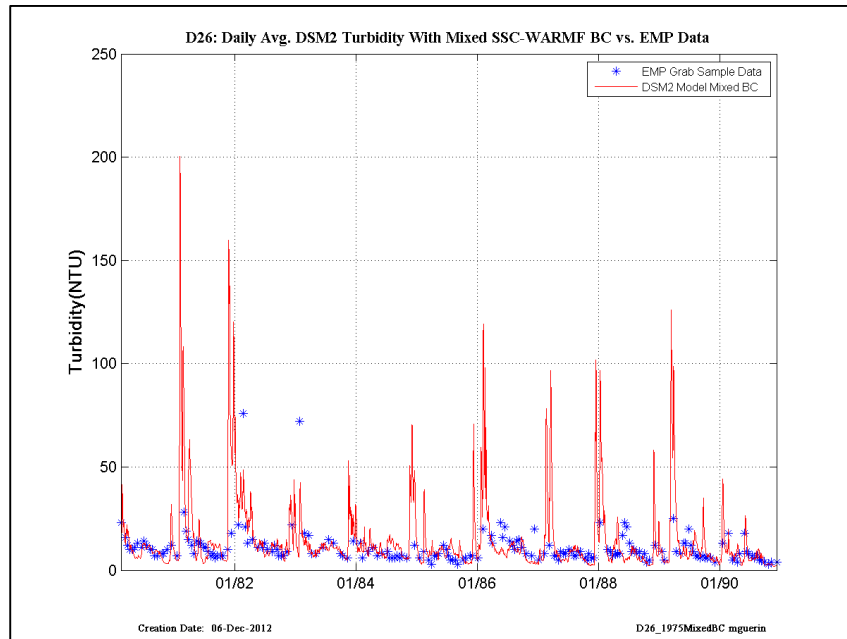


Figure 13-19 DSM2 daily-averaged turbidity model results using USGS-SSC at Freeport and Vernalis, and WARMF turbidity at other inflow boundaries compared to EMP grab-sample data, early years— location is EMP D26.

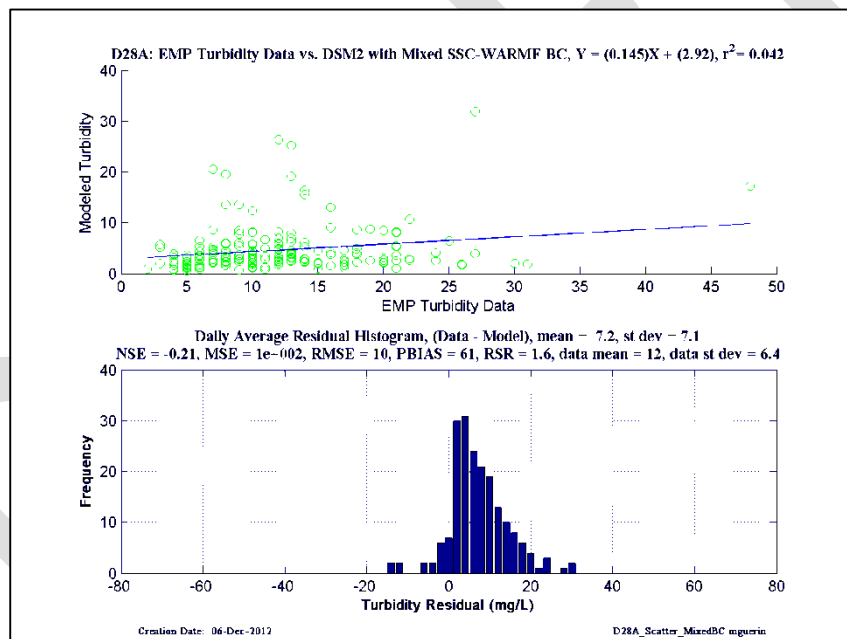
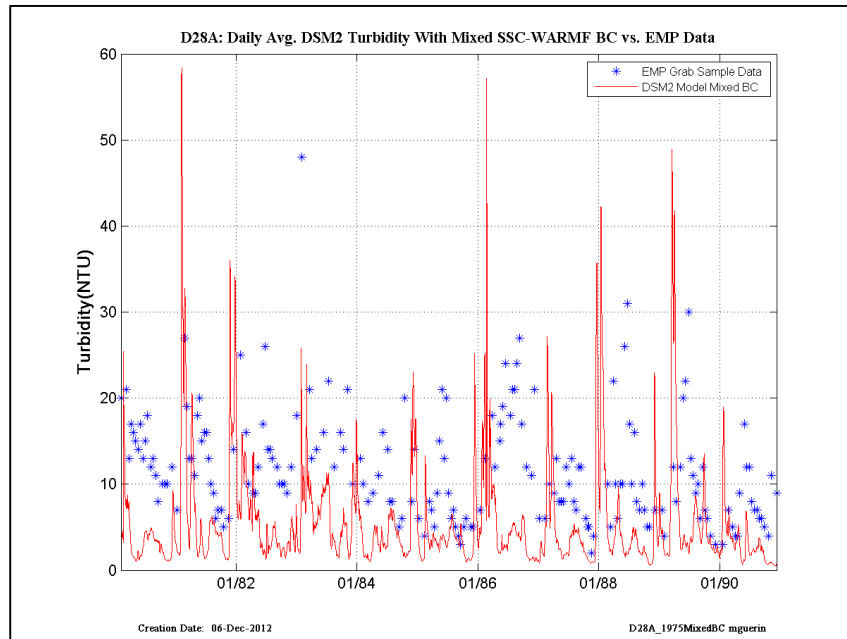


Figure 13-20 DSM2 daily-averaged turbidity model results using USGS-SSC at Freeport and Vernalis, and WARMF turbidity at other inflow boundaries compared to EMP grab-sample data, early years— location is EMP D28A.

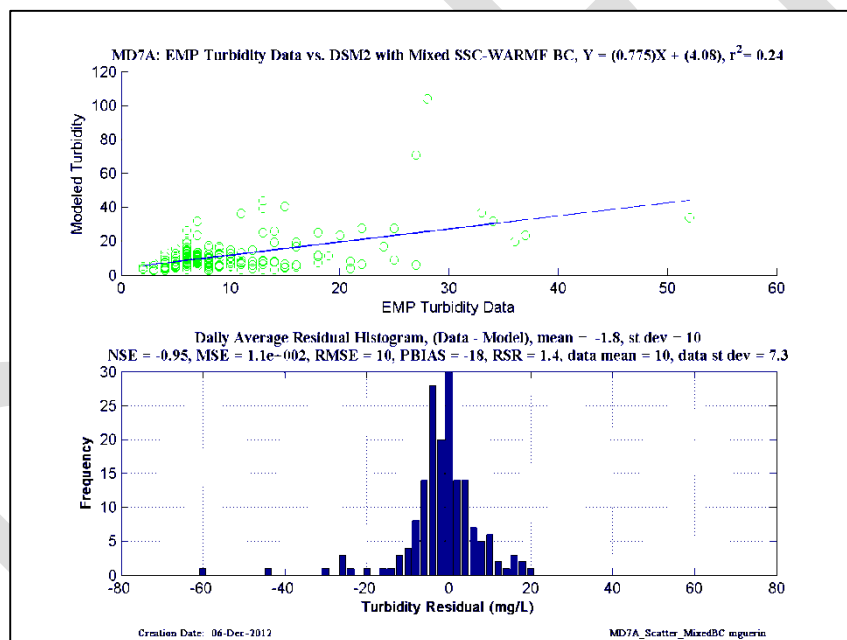
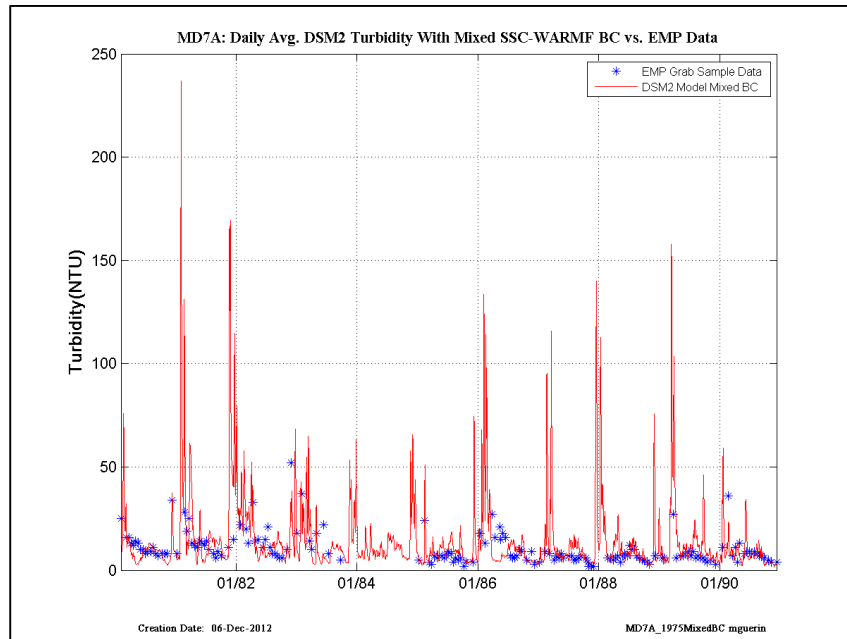


Figure 13-21 DSM2 daily-averaged turbidity model results using USGS-SSC at Freeport and Vernalis, and WARMF turbidity at other inflow boundaries compared to EMP grab-sample data, early years—location is EMP MD7A.

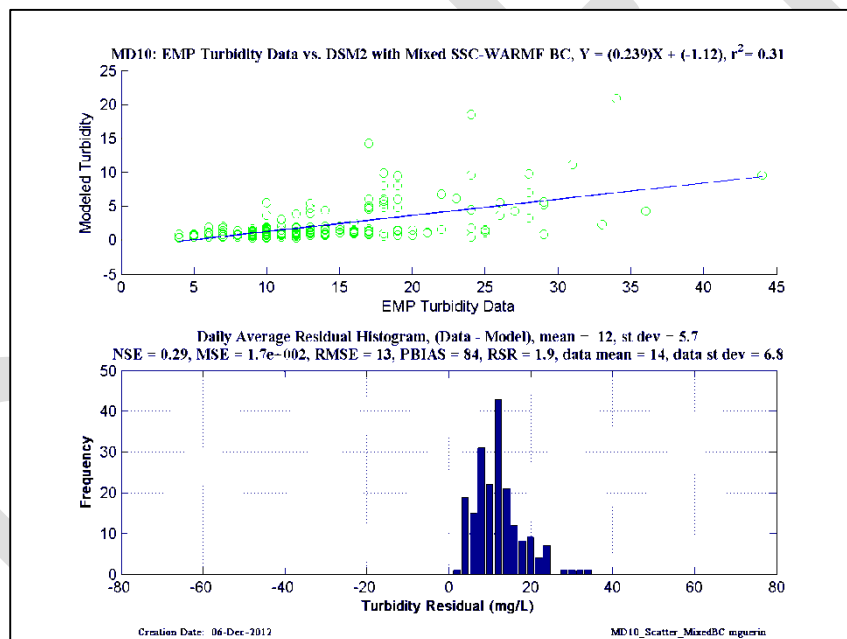
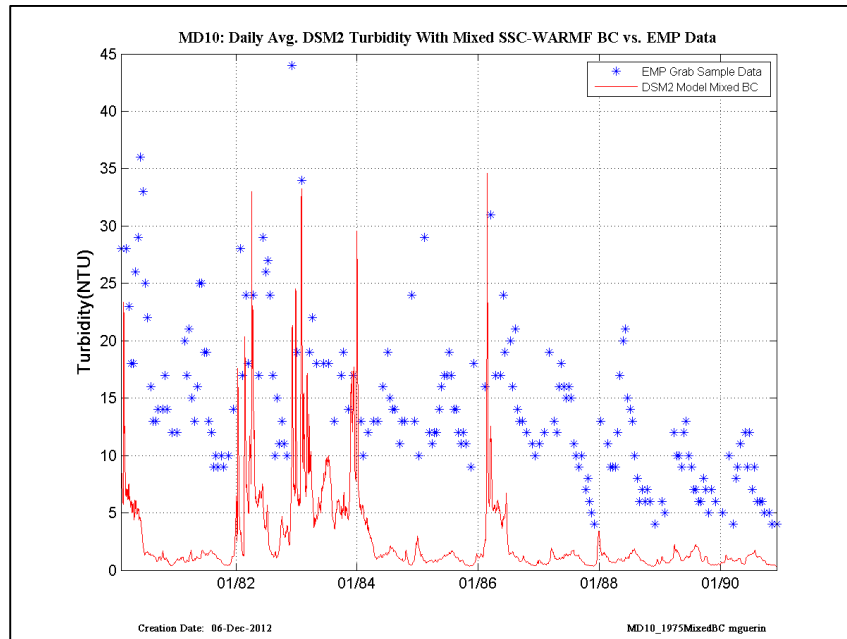


Figure 13-22 DSM2 daily-averaged turbidity model results using USGS-SSC at Freeport and Vernalis, and WARMF turbidity at other inflow boundaries compared to EMP grab-sample data, early years—location is EMP MD10.

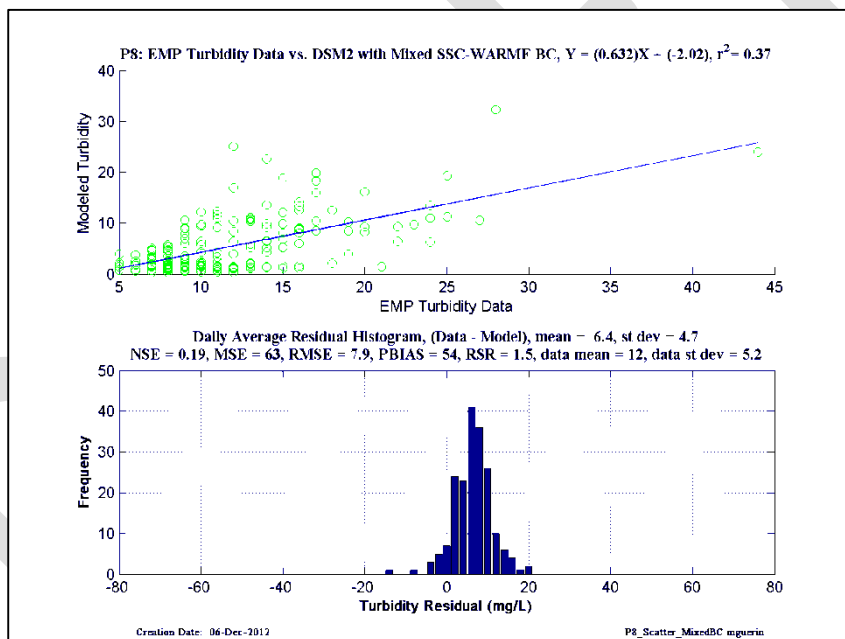
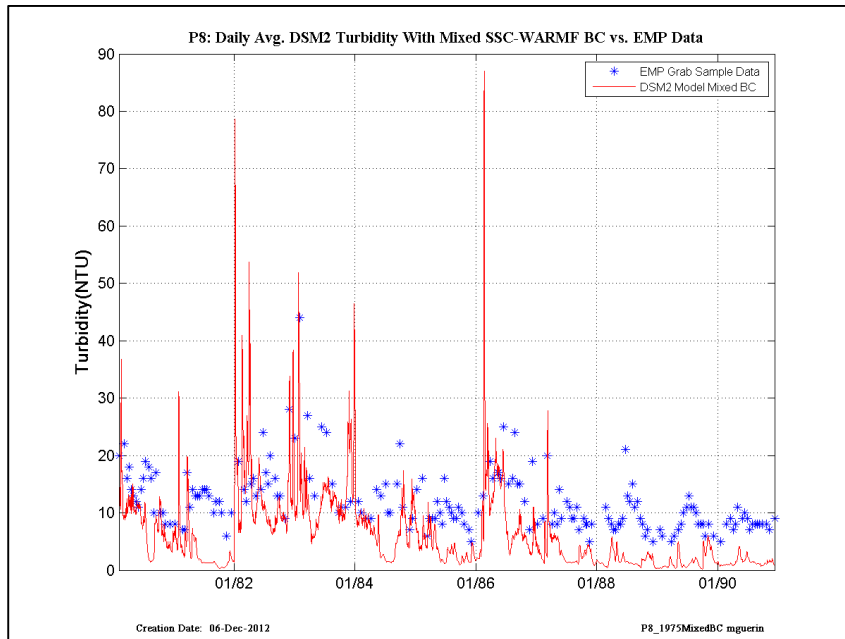


Figure 13-23 DSM2 daily-averaged turbidity model results using USGS-SSC at Freeport and Vernalis, and WARMF turbidity at other inflow boundaries compared to EMP grab-sample data, early years– location is EMP P8.

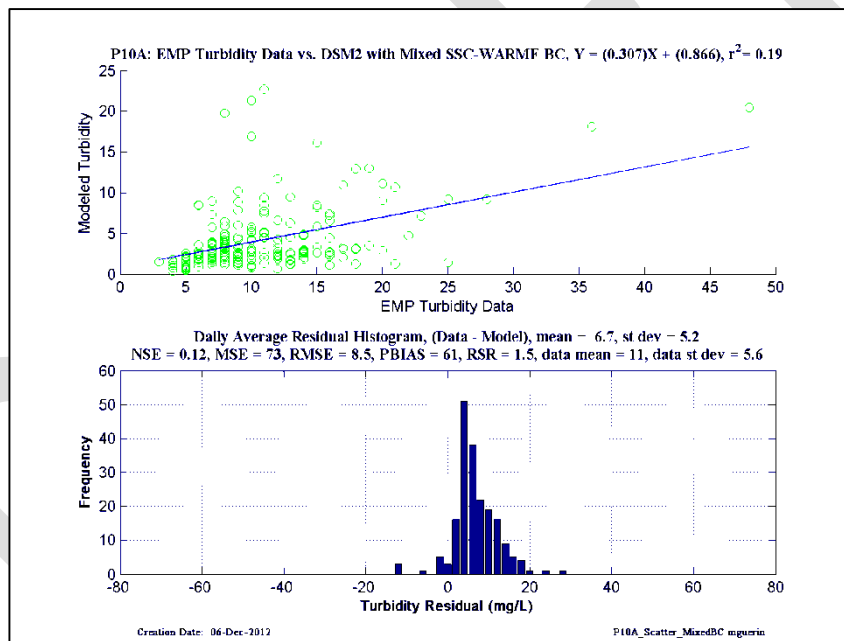
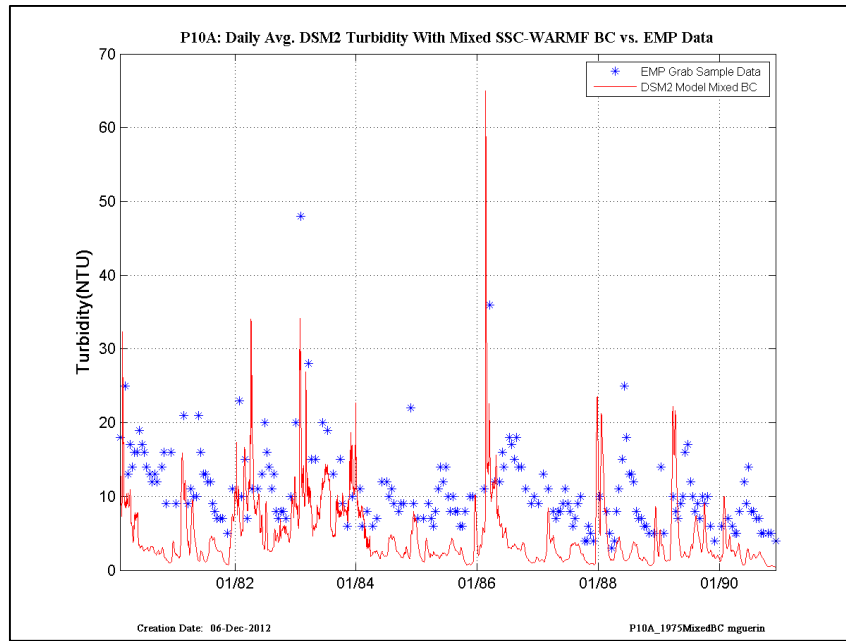


Figure 13-24 DSM2 daily-averaged turbidity model results using USGS-SSC at Freeport and Vernalis, and WARMF turbidity at other inflow boundaries compared to EMP grab-sample data, early years— location is EMP P10A.

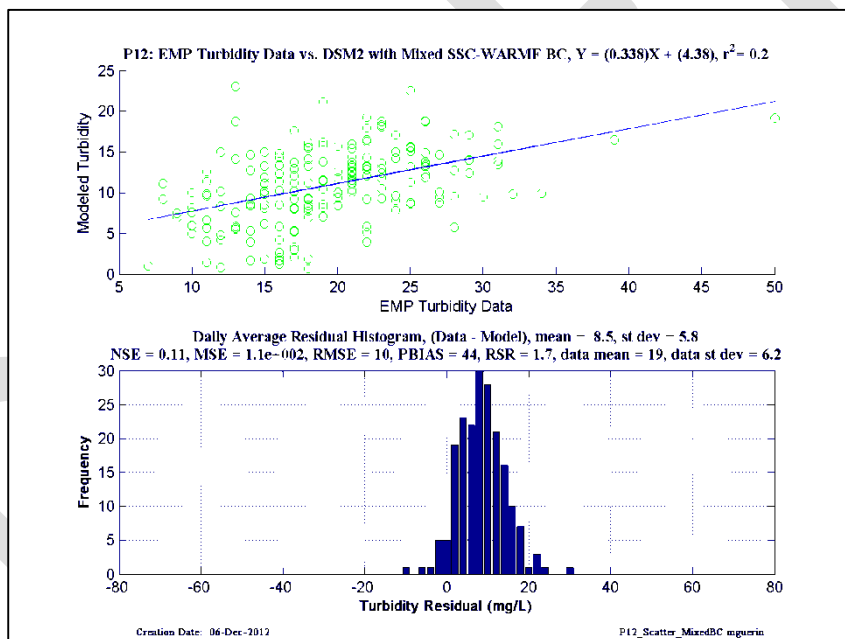
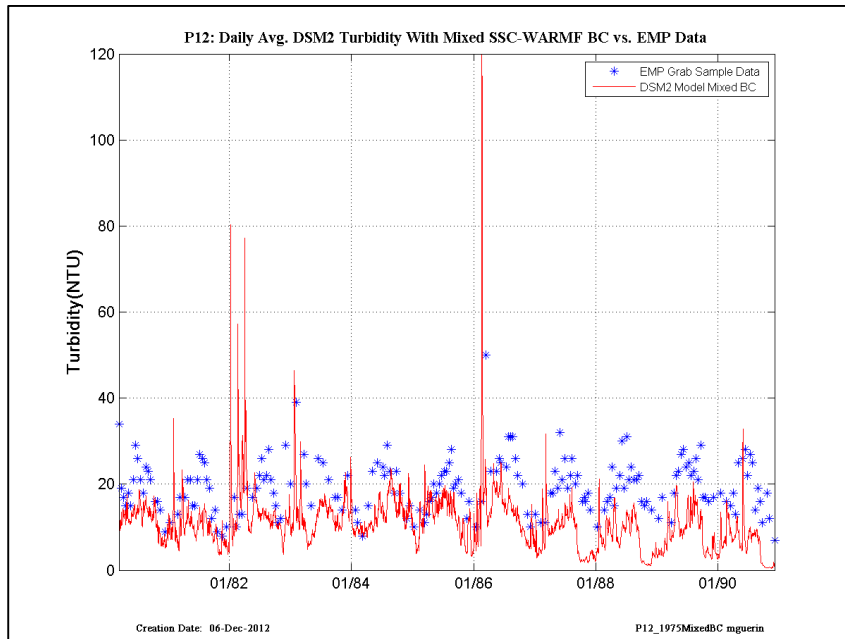


Figure 13-25 DSM2 daily-averaged turbidity model results using USGS-SSC at Freeport and Vernalis, and WARMF turbidity at other inflow boundaries compared to EMP grab-sample data, early years– location is EMP P12.

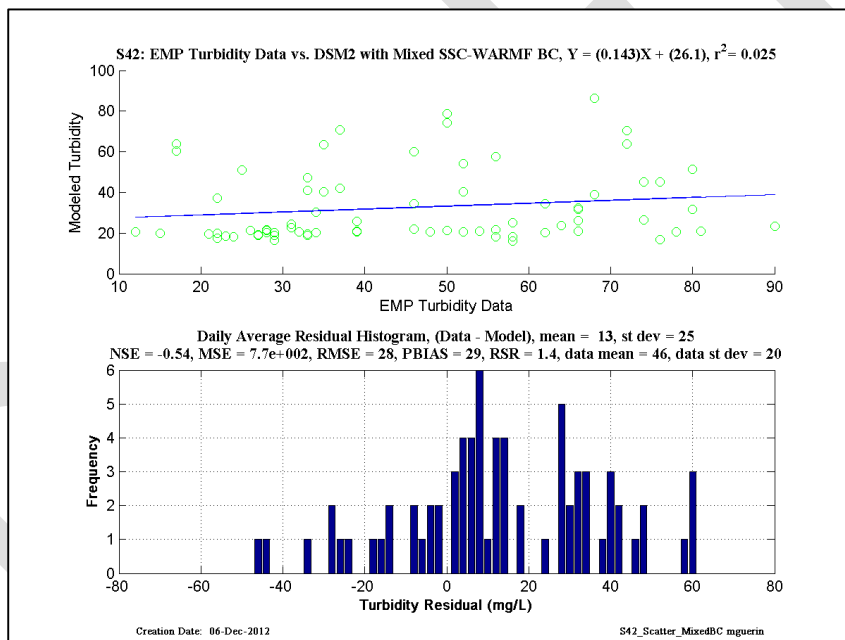
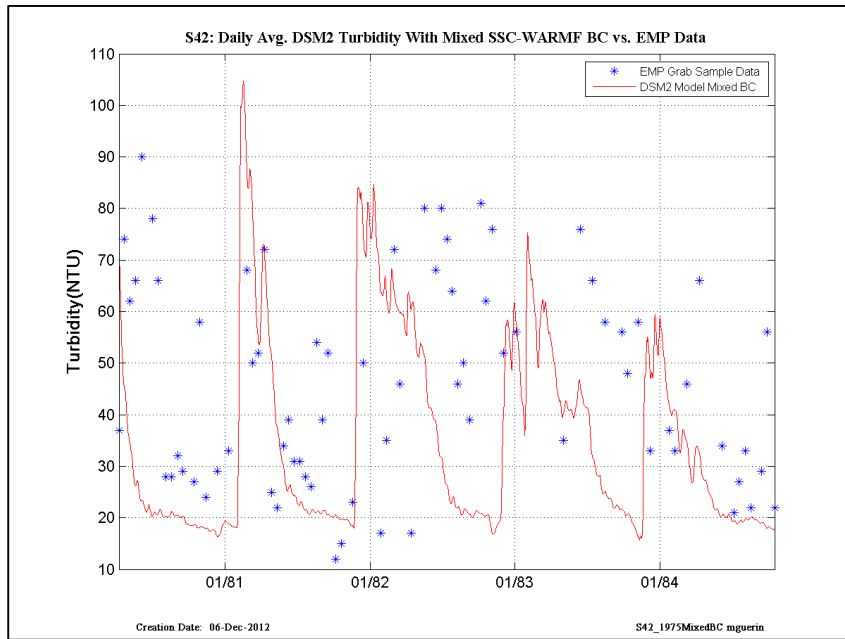


Figure 13-26 DSM2 daily-averaged turbidity model results using USGS-SSC at Freeport and Vernalis, and WARMF turbidity at other inflow boundaries compared to EMP grab-sample data, early years—location is EMP S42.

**12.4 Recent years: 1991 - 2011**

DRAFT

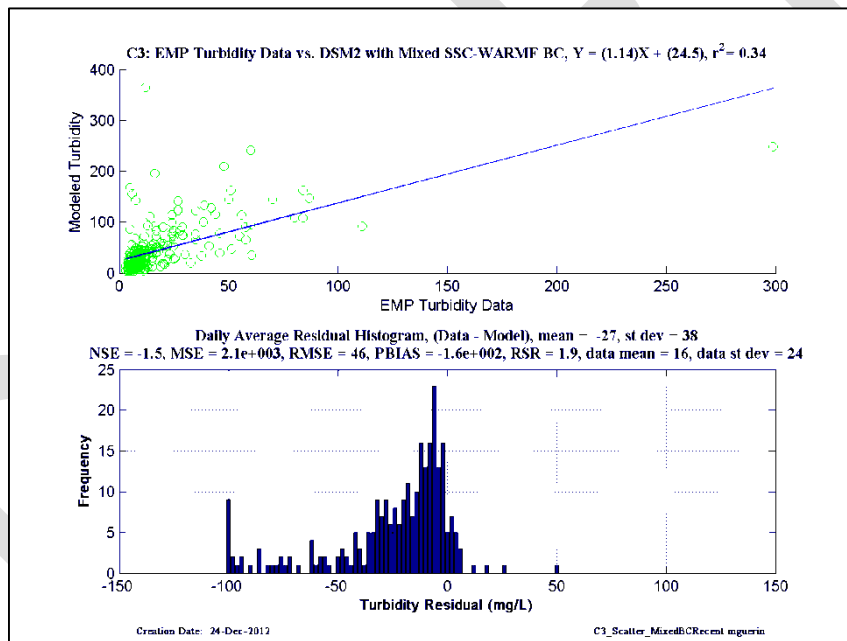
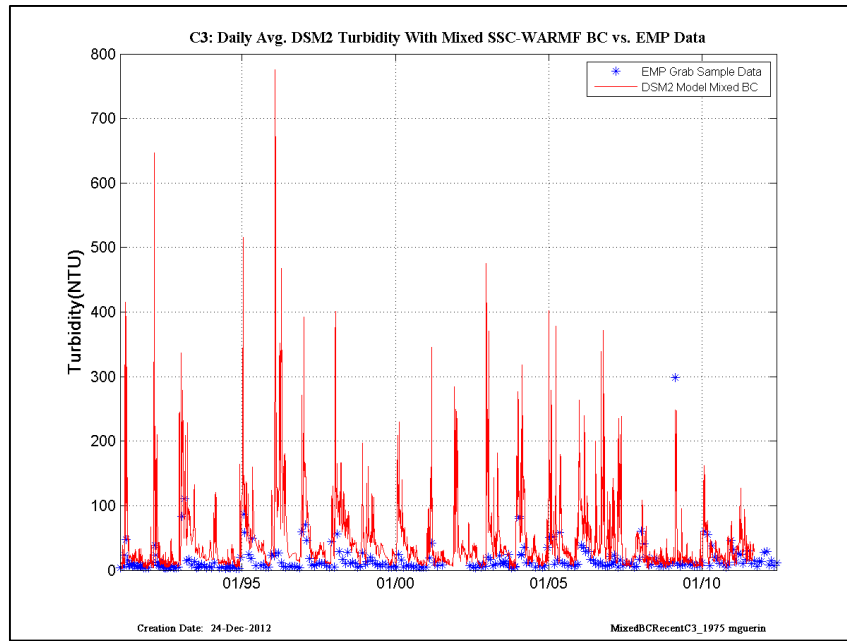


Figure 13-27 DSM2 daily-averaged turbidity model results using USGS-SSC at Freeport and Vernalis, and WARMF turbidity at other inflow boundaries compared to EMP grab-sample data, recent years— location is EMP C3.

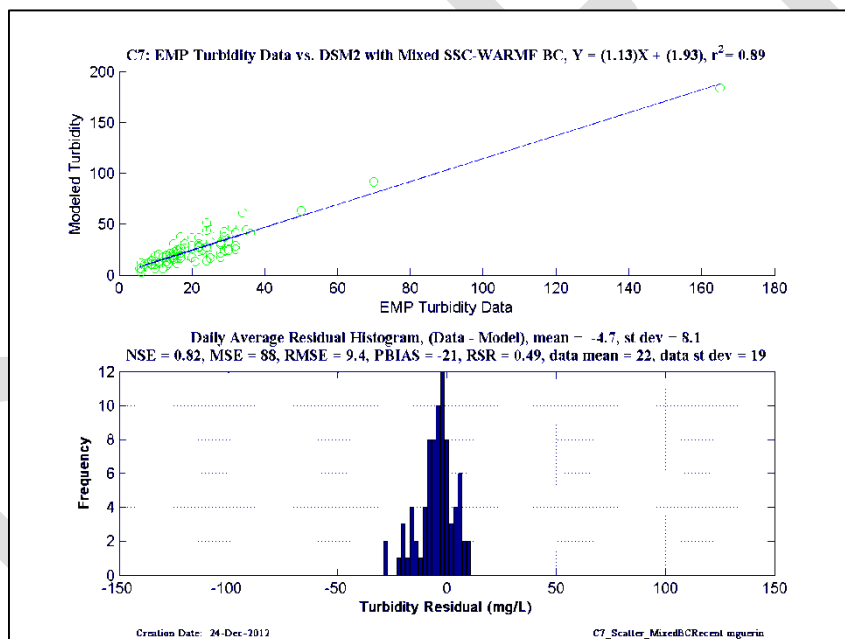
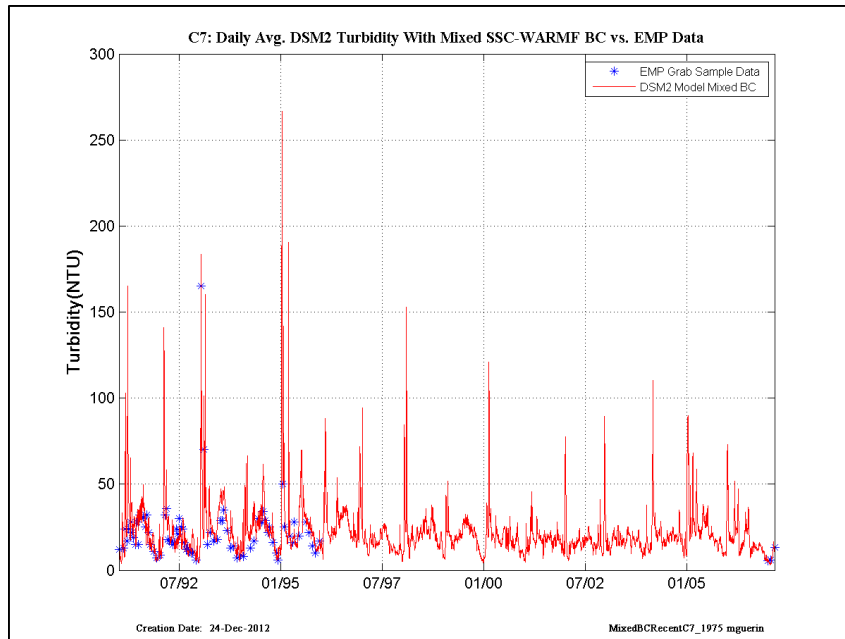


Figure 13-28 DSM2 daily-averaged turbidity model results using USGS-SSC at Freeport and Vernalis, and WARMF turbidity at other inflow boundaries compared to EMP grab-sample data, recent years– location is EMP C7.

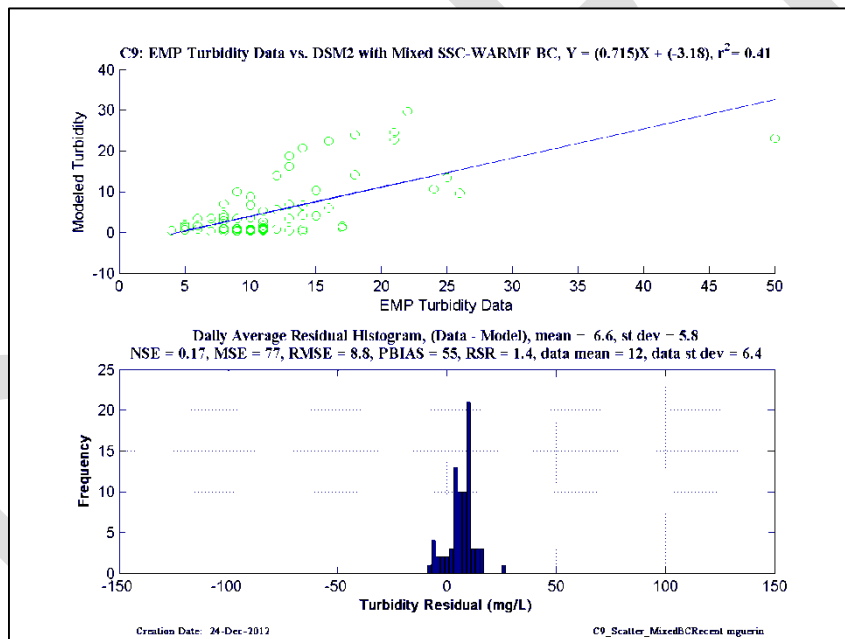
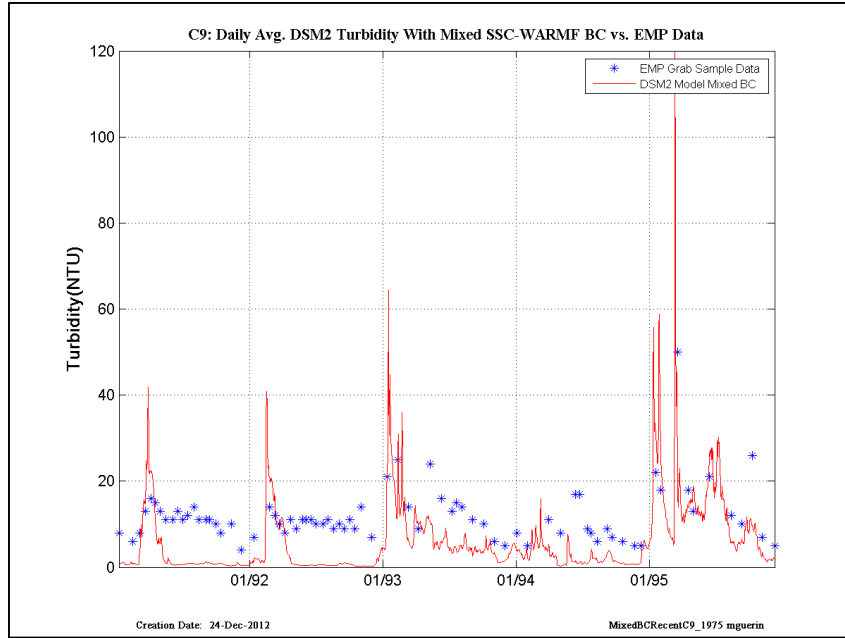


Figure 13-29 DSM2 daily-averaged turbidity model results using USGS-SSC at Freeport and Vernalis, and WARMF turbidity at other inflow boundaries compared to EMP grab-sample data, recent years— location is EMP C9.

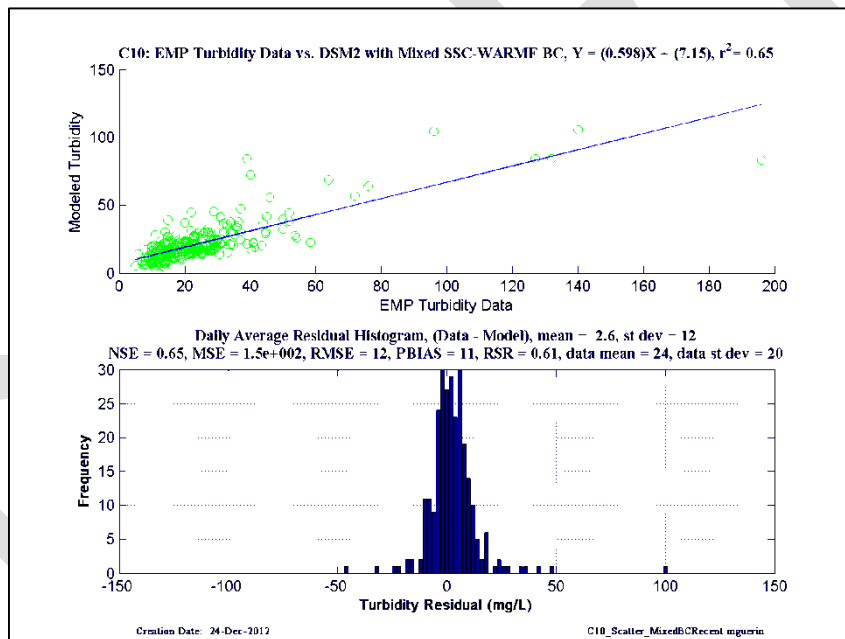
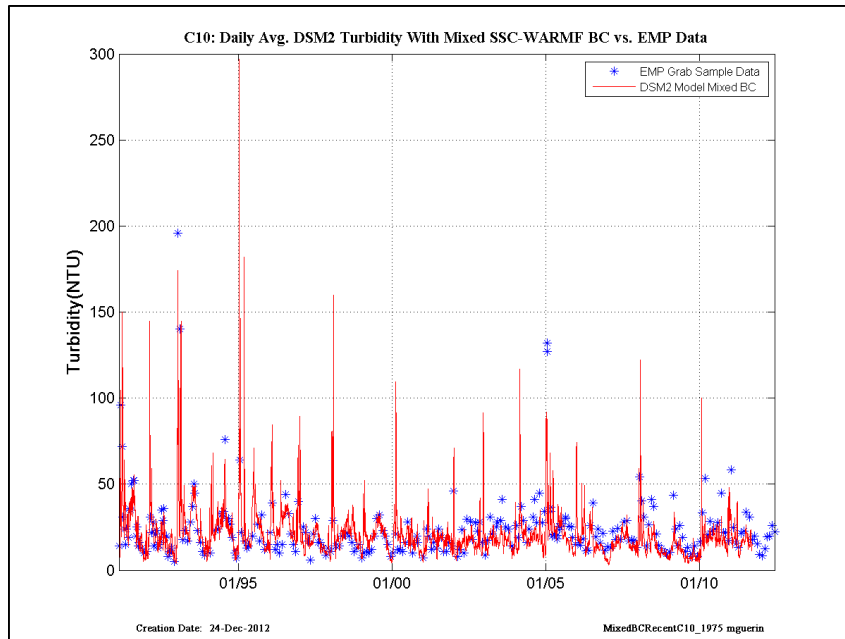


Figure 13-30 DSM2 daily-averaged turbidity model results using USGS-SSC at Freeport and Vernalis, and WARMF turbidity at other inflow boundaries compared to EMP grab-sample data, recent years– location is EMP C10.

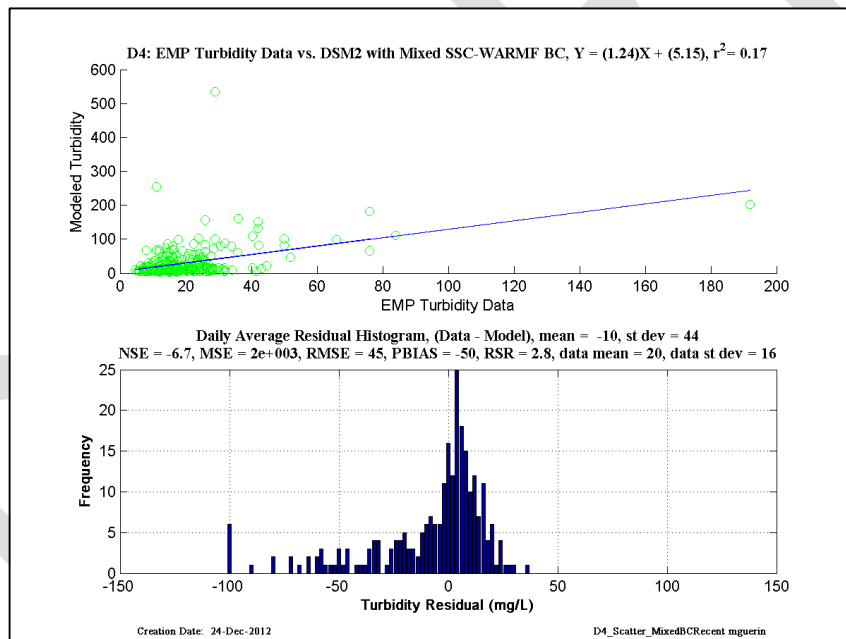
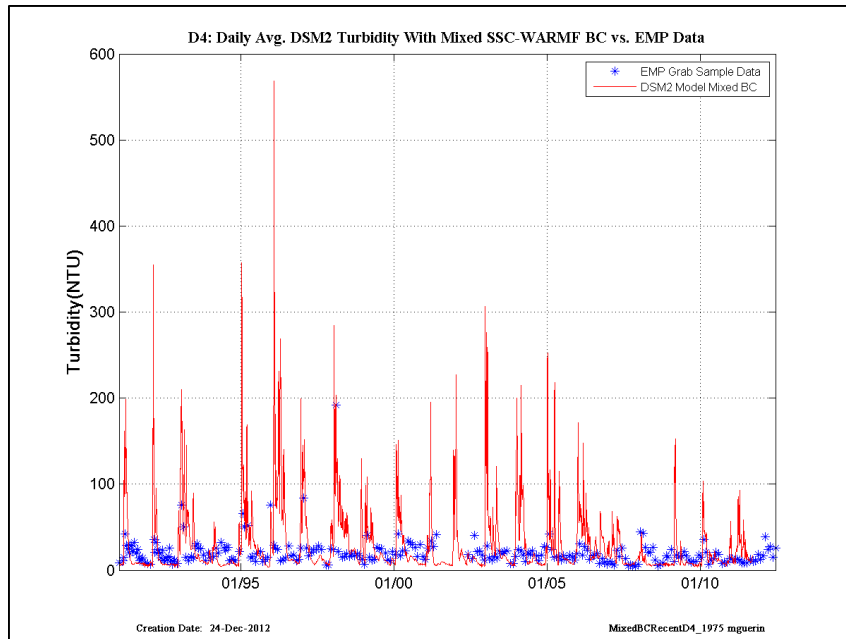


Figure 13-31 DSM2 daily-averaged turbidity model results using USGS-SSC at Freeport and Vernalis, and WARMF turbidity at other inflow boundaries compared to EMP grab-sample data, recent years– location is EMP D4.

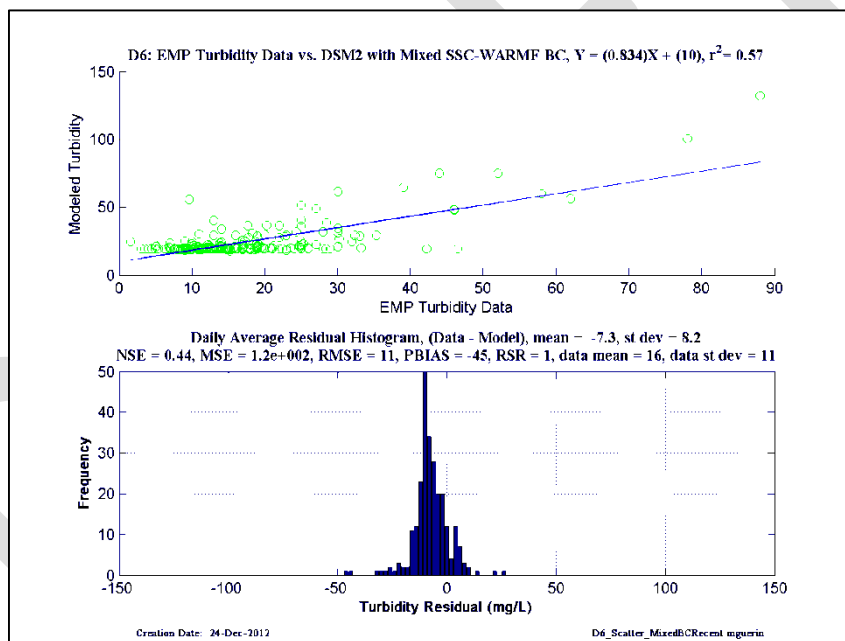
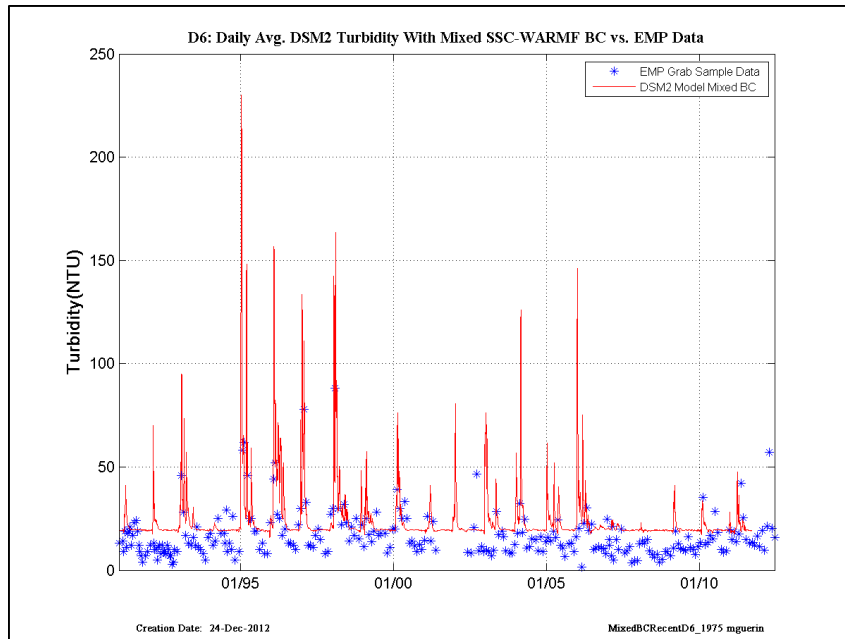


Figure 13-32 DSM2 daily-averaged turbidity model results using USGS-SSC at Freeport and Vernalis, and WARMF turbidity at other inflow boundaries compared to EMP grab-sample data, recent years– location is EMP D6.

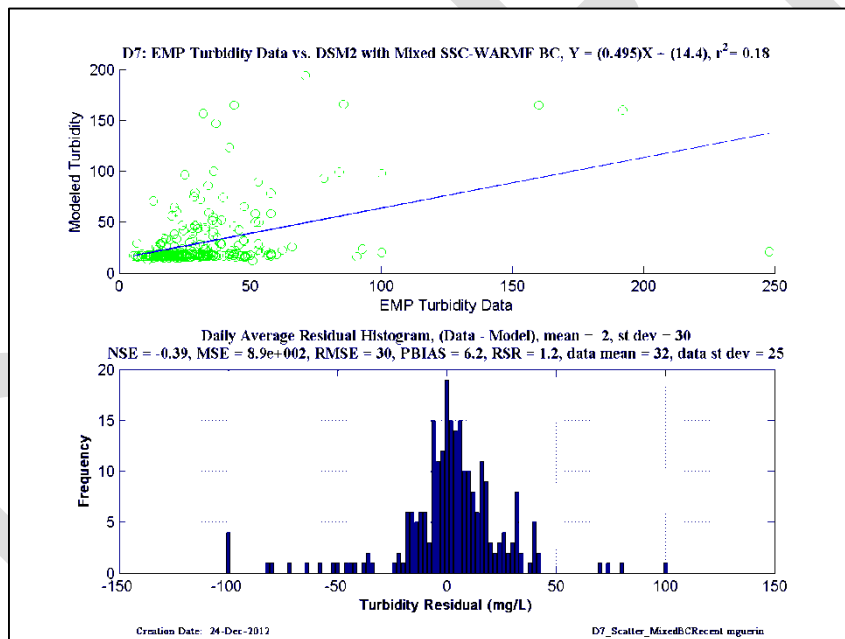
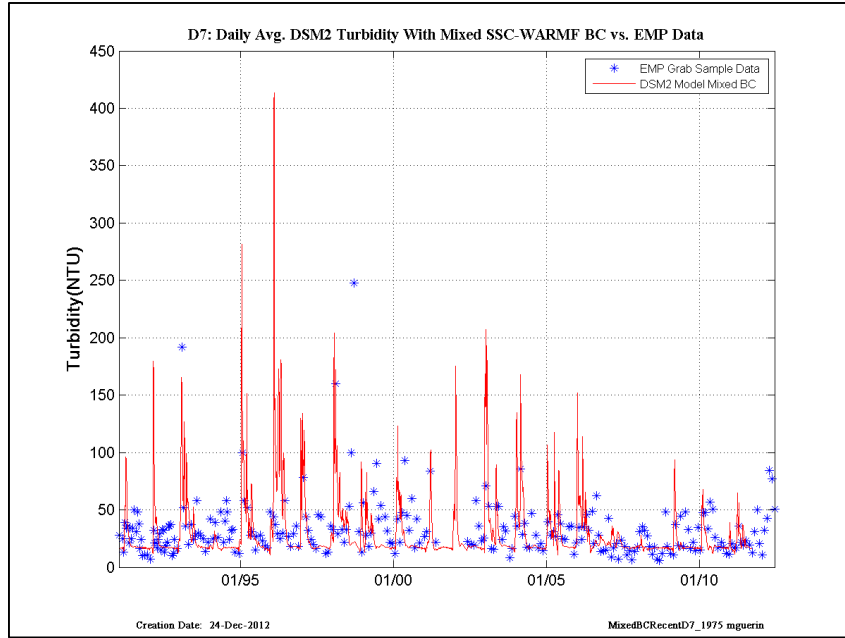


Figure 13-33 DSM2 daily-averaged turbidity model results using USGS-SSC at Freeport and Vernalis, and WARMF turbidity at other inflow boundaries compared to EMP grab-sample data, recent years– location is EMP D7.

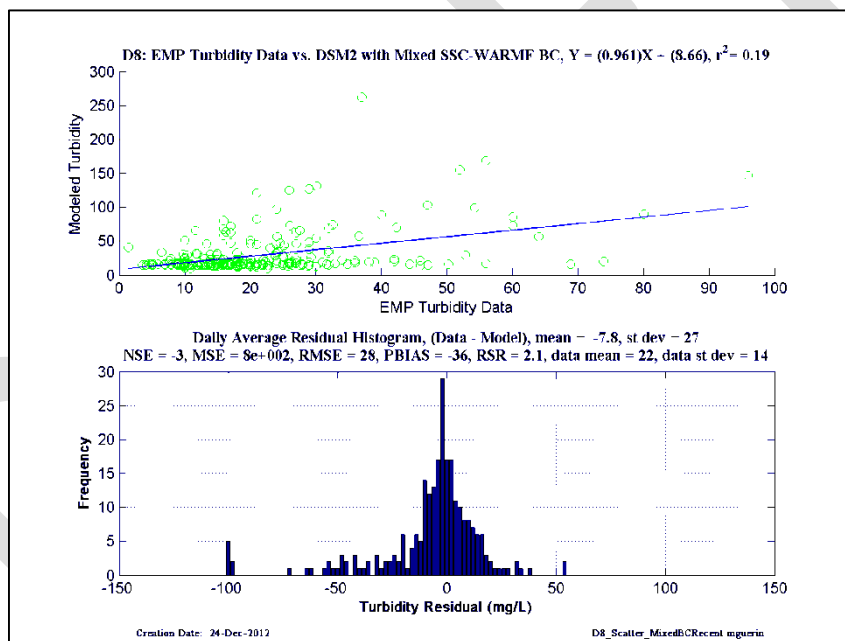
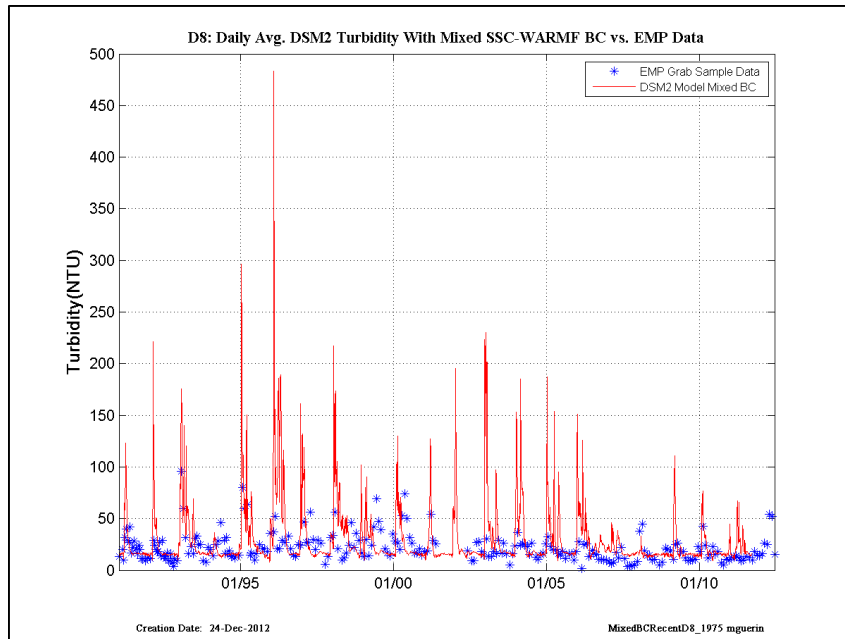


Figure 13-34 DSM2 daily-averaged turbidity model results using USGS-SSC at Freeport and Vernalis, and WARMF turbidity at other inflow boundaries compared to EMP grab-sample data, recent years– location is EMP D8.

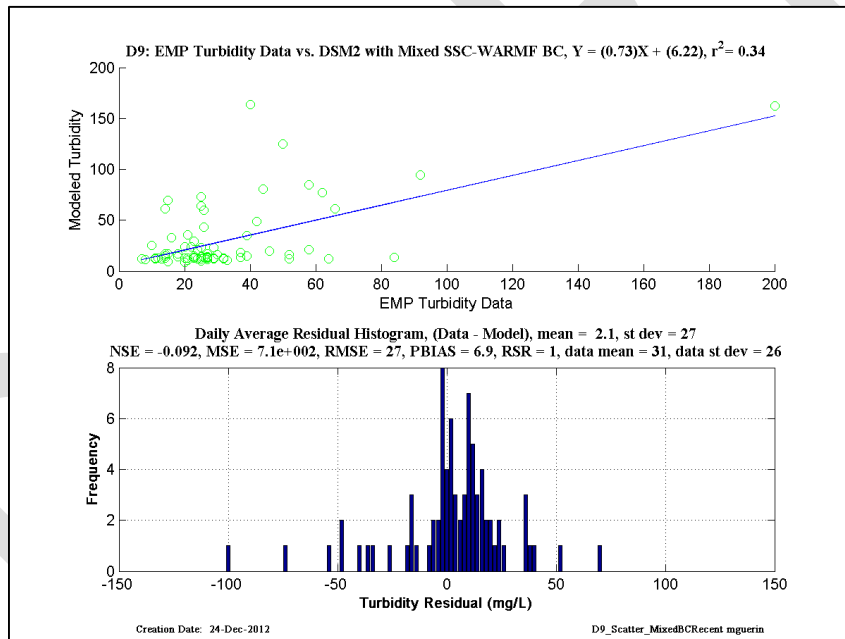
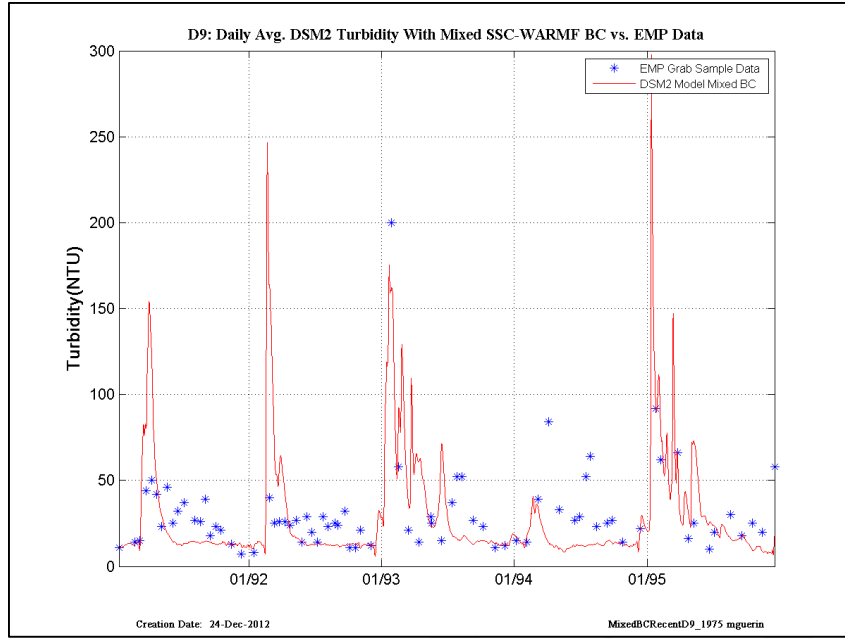


Figure 13-35 DSM2 daily-averaged turbidity model results using USGS-SSC at Freeport and Vernalis, and WARMF turbidity at other inflow boundaries compared to EMP grab-sample data, recent years– location is EMP D9.

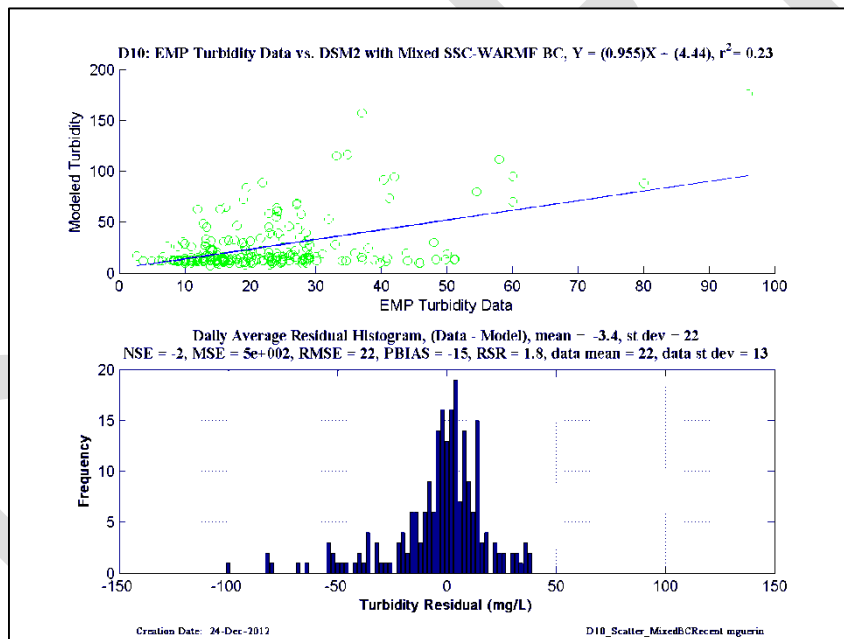
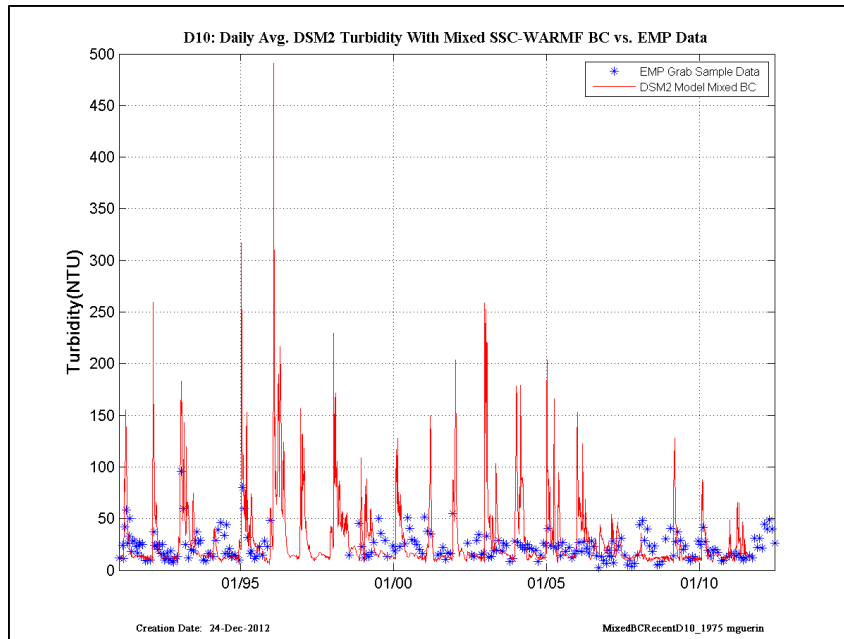


Figure 13-36 DSM2 daily-averaged turbidity model results using USGS-SSC at Freeport and Vernalis, and WARMF turbidity at other inflow boundaries compared to EMP grab-sample data, recent years— location is EMP D10.

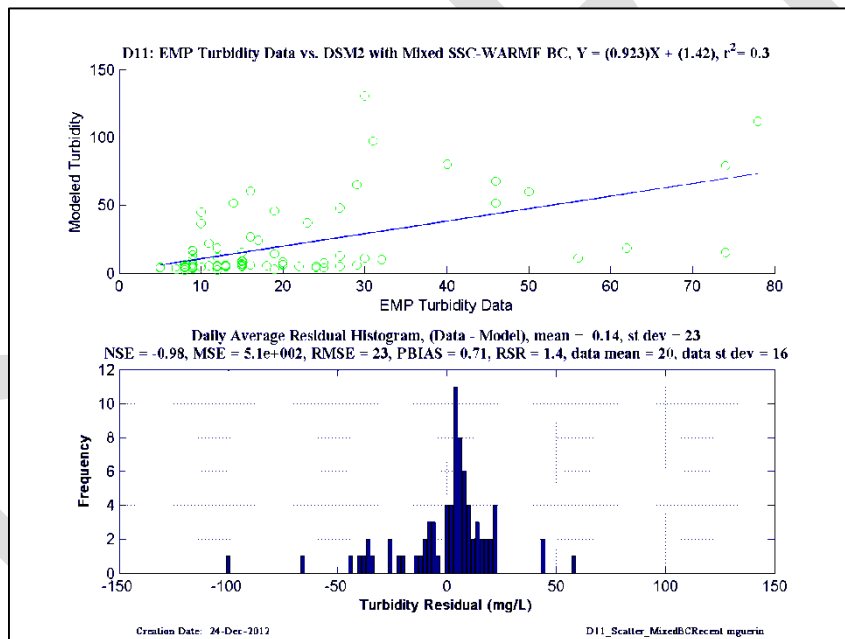
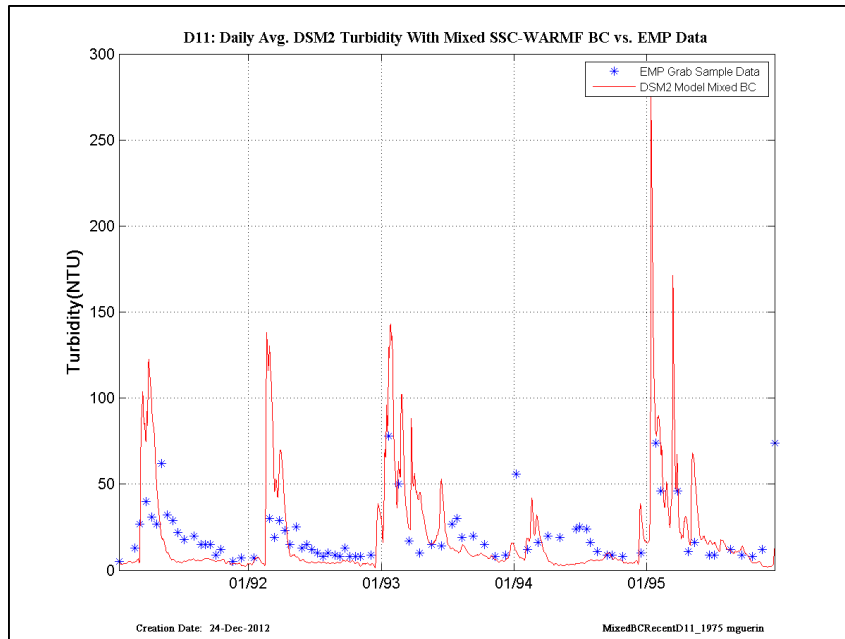


Figure 13-37 DSM2 daily-averaged turbidity model results using USGS-SSC at Freeport and Vernalis, and WARMF turbidity at other inflow boundaries compared to EMP grab-sample data, recent years– location is EMP D11.

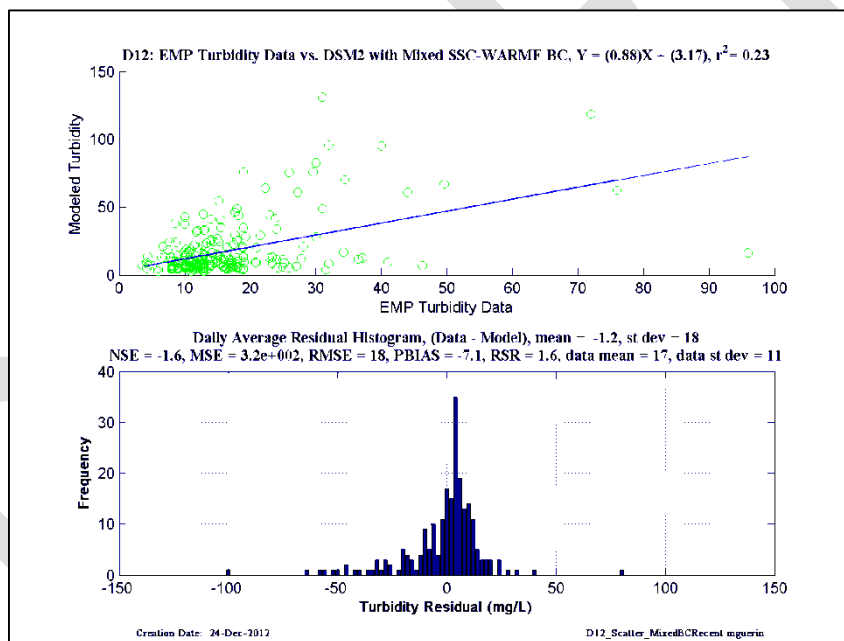
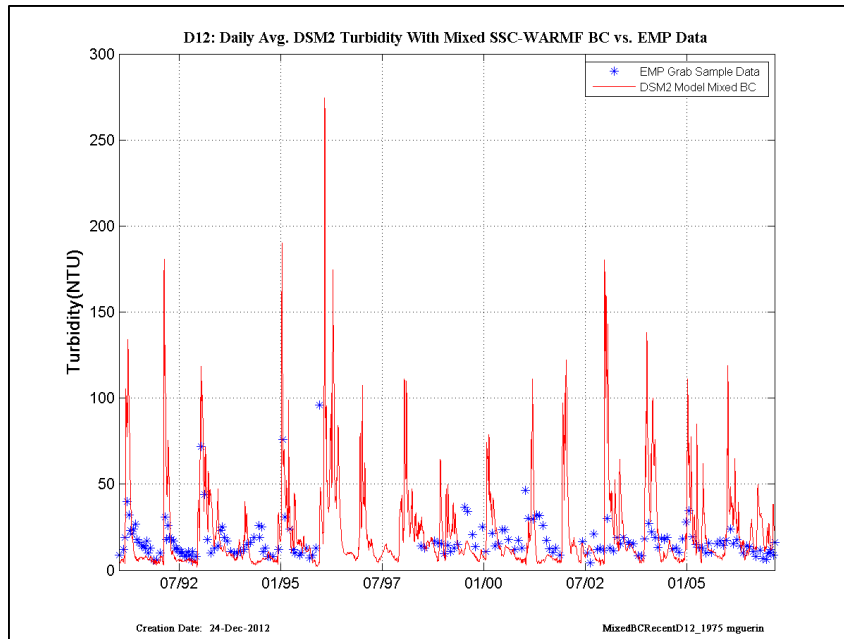


Figure 13-38 DSM2 daily-averaged turbidity model results using USGS-SSC at Freeport and Vernalis, and WARMF turbidity at other inflow boundaries compared to EMP grab-sample data, recent years– location is EMP D12.

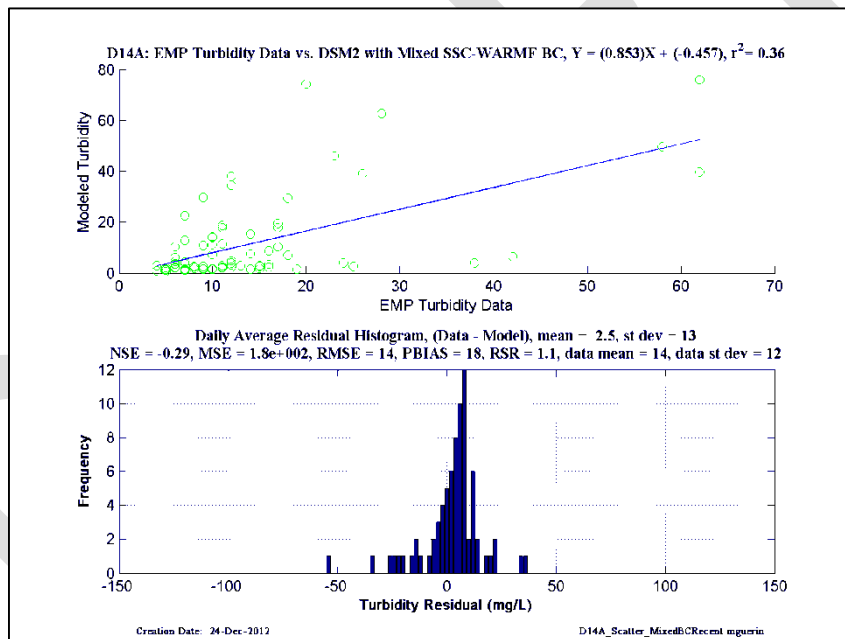
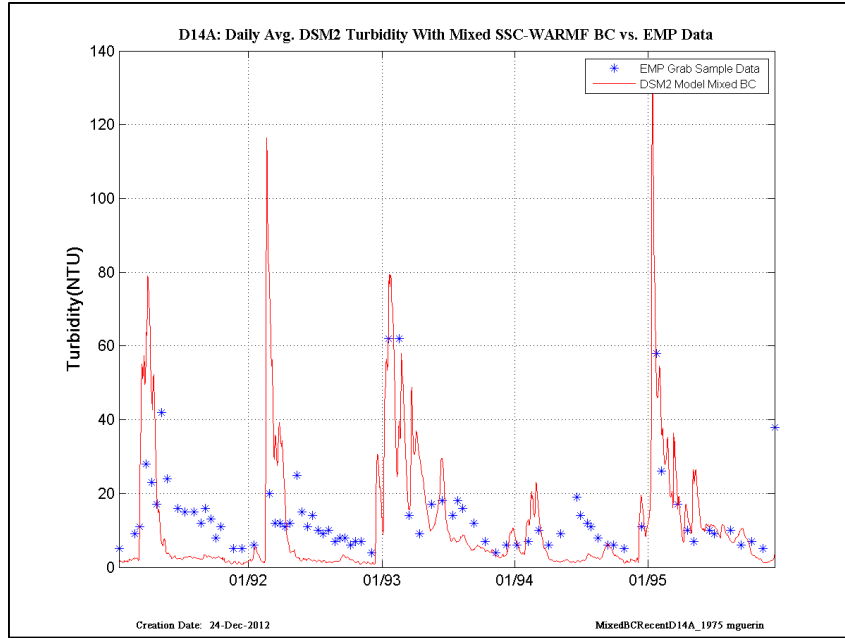


Figure 13-39 DSM2 daily-averaged turbidity model results using USGS-SSC at Freeport and Vernalis, and WARMF turbidity at other inflow boundaries compared to EMP grab-sample data, recent years– location is EMP D14A.

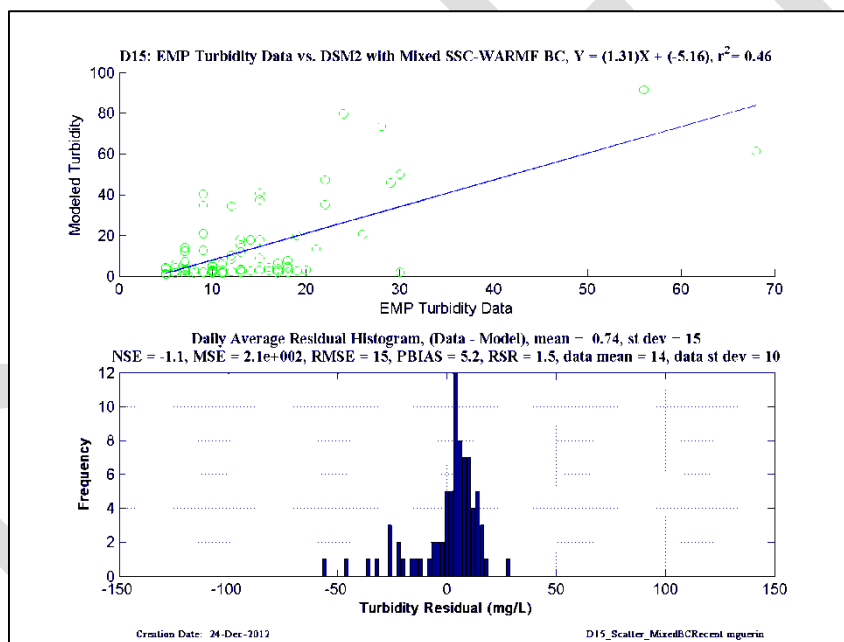
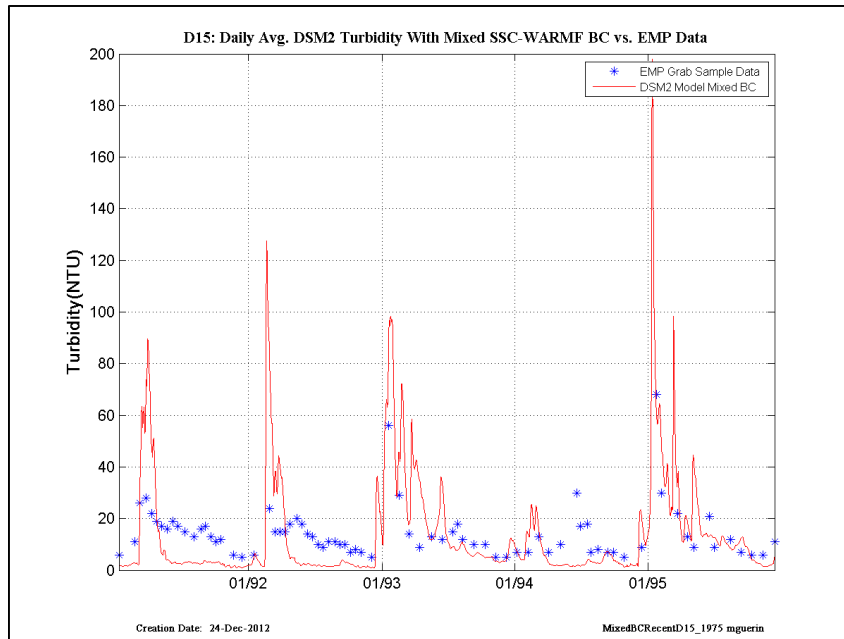


Figure 13-40 DSM2 daily-averaged turbidity model results using USGS-SSC at Freeport and Vernalis, and WARMF turbidity at other inflow boundaries compared to EMP grab-sample data, recent years– location is EMP D15.

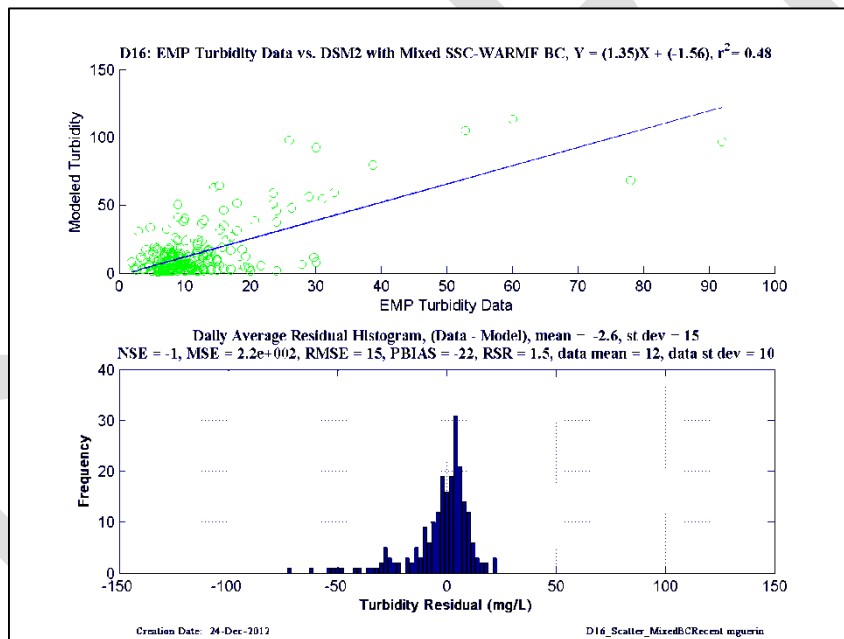
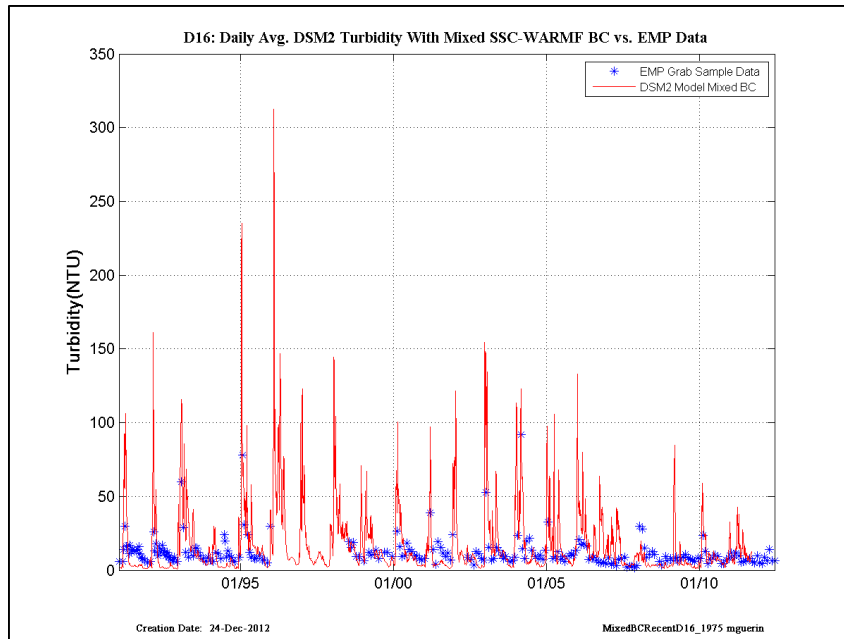


Figure 13-41 DSM2 daily-averaged turbidity model results using USGS-SSC at Freeport and Vernalis, and WARMF turbidity at other inflow boundaries compared to EMP grab-sample data, recent years– location is EMP D16.

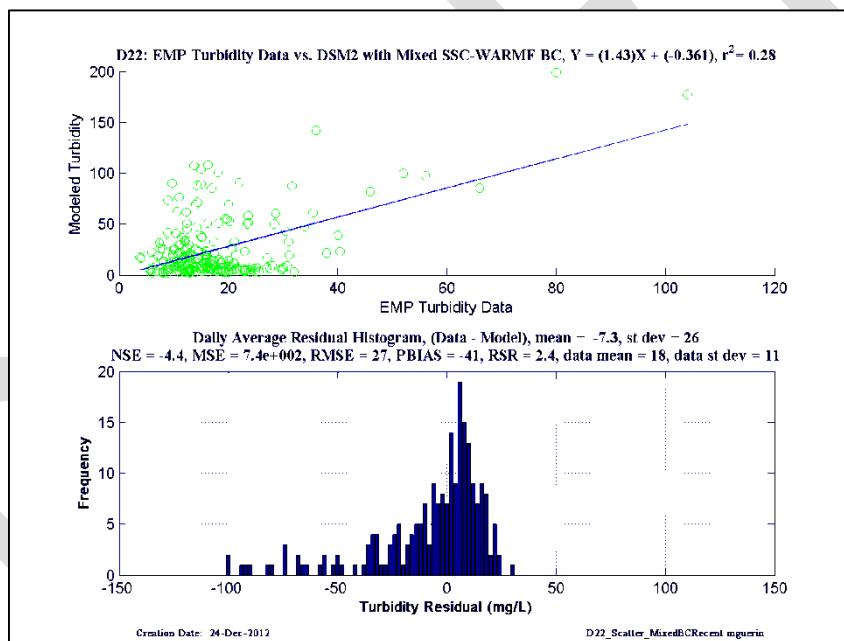
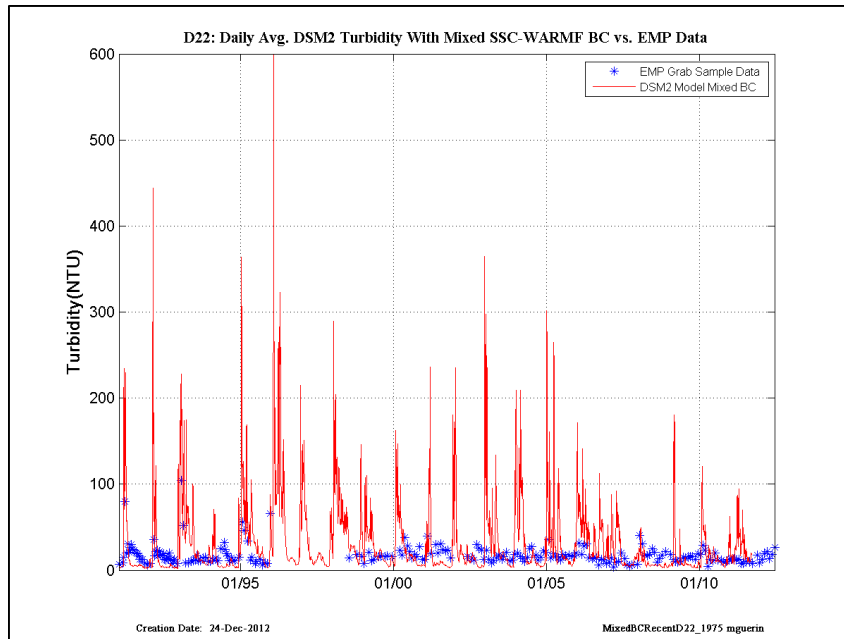


Figure 13-42 DSM2 daily-averaged turbidity model results using USGS-SSC at Freeport and Vernalis, and WARMF turbidity at other inflow boundaries compared to EMP grab-sample data, recent years– location is EMP D22.

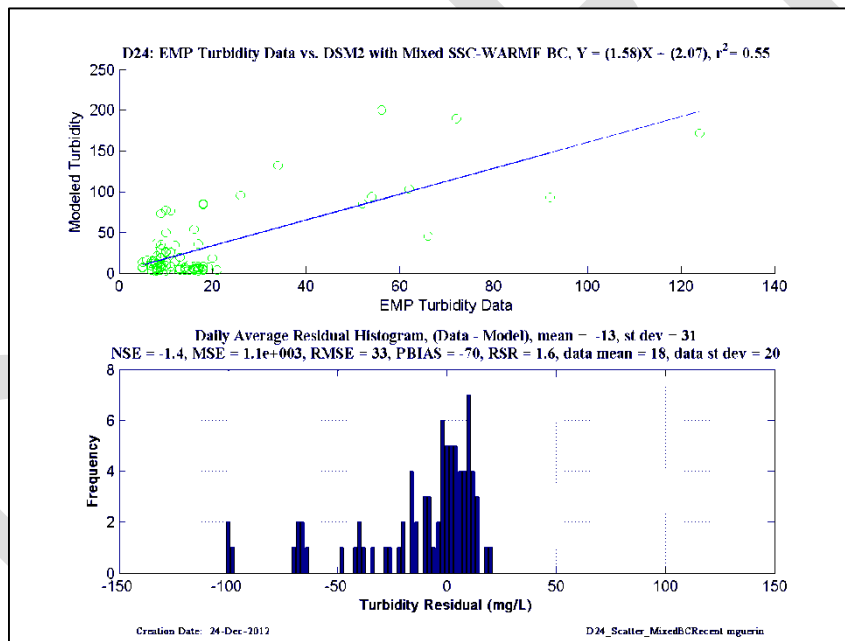
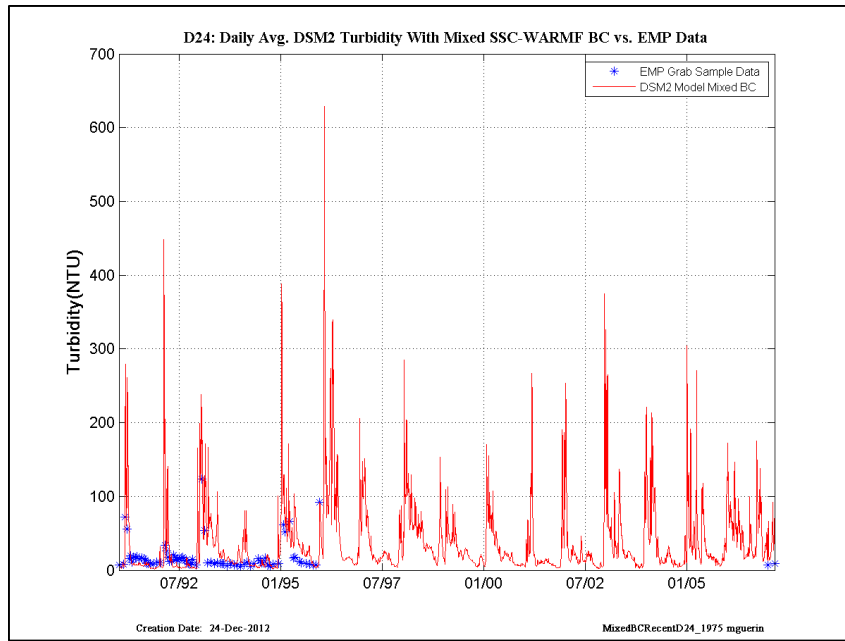


Figure 13-43 DSM2 daily-averaged turbidity model results using USGS-SSC at Freeport and Vernalis, and WARMF turbidity at other inflow boundaries compared to EMP grab-sample data, recent years– location is EMP D24.

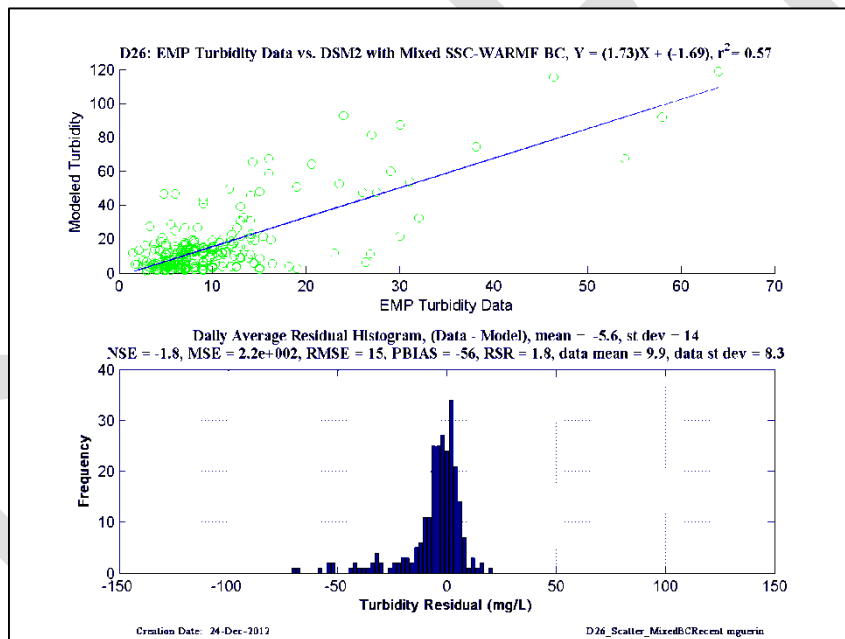
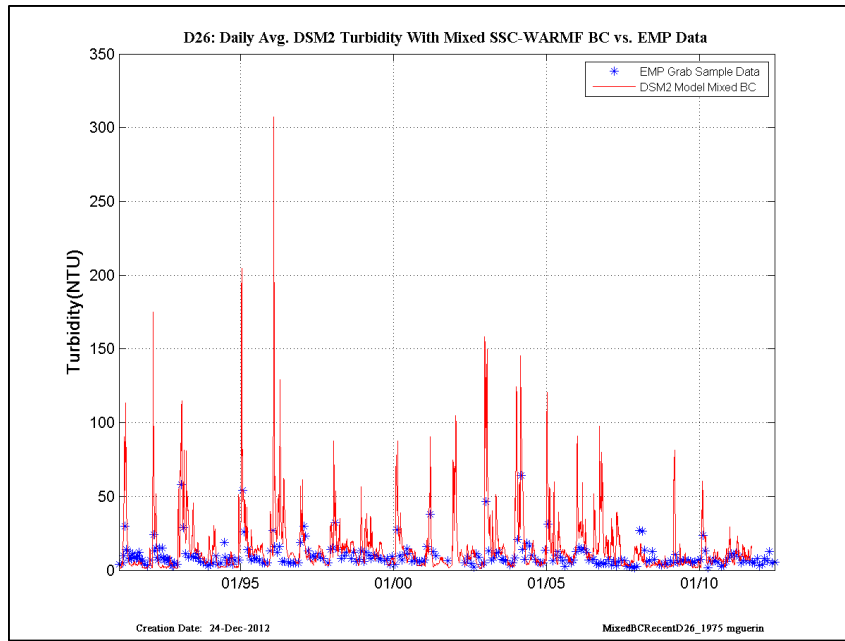


Figure 13-44 DSM2 daily-averaged turbidity model results using USGS-SSC at Freeport and Vernalis, and WARMF turbidity at other inflow boundaries compared to EMP grab-sample data, recent years—location is EMP D26.

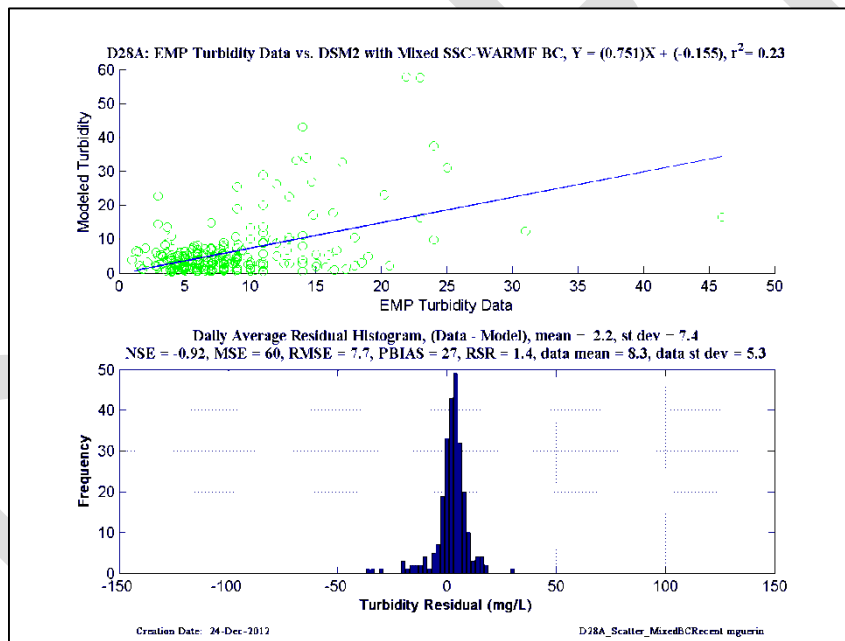
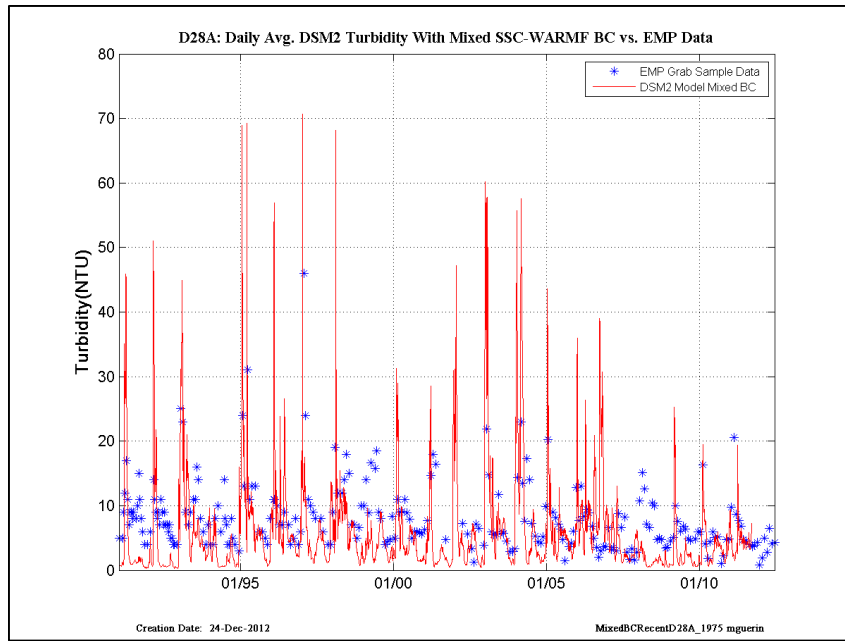


Figure 13-45 DSM2 daily-averaged turbidity model results using USGS-SSC at Freeport and Vernalis, and WARMF turbidity at other inflow boundaries compared to EMP grab-sample data, recent years– location is EMP D28A.

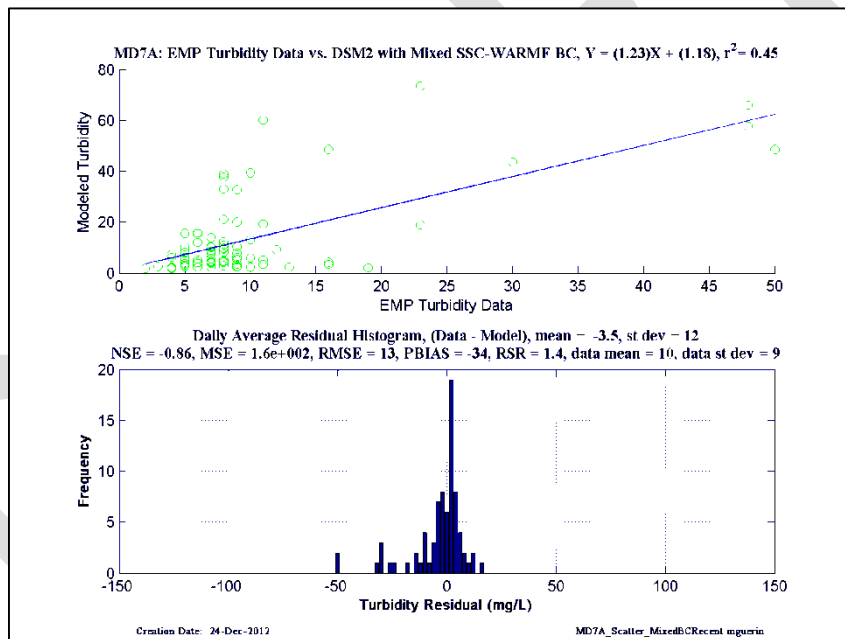
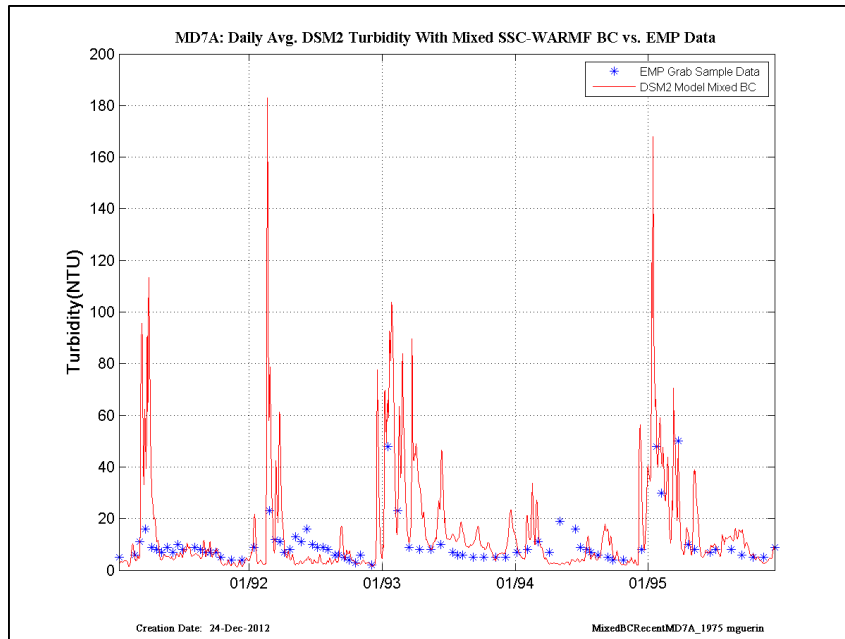


Figure 13-46 DSM2 daily-averaged turbidity model results using USGS-SSC at Freeport and Vernalis, and WARMF turbidity at other inflow boundaries compared to EMP grab-sample data, recent years— location is EMP MD7A.

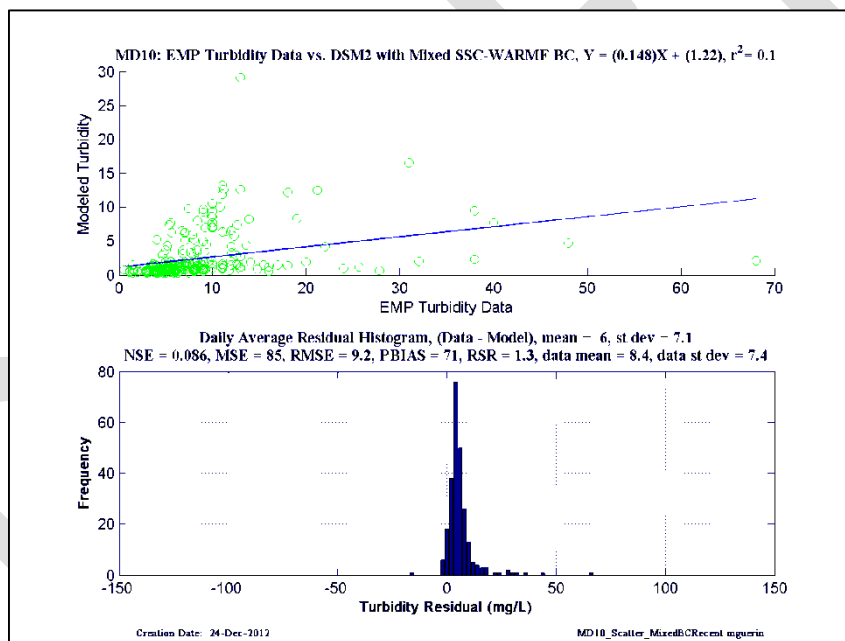
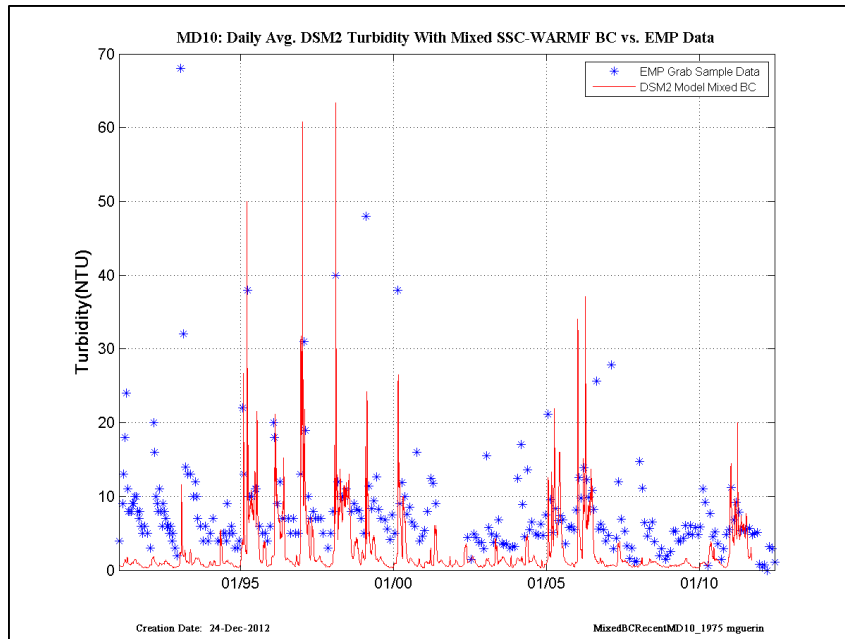


Figure 13-47 DSM2 daily-averaged turbidity model results using USGS-SSC at Freeport and Vernalis, and WARMF turbidity at other inflow boundaries compared to EMP grab-sample data, recent years— location is EMP MD10.

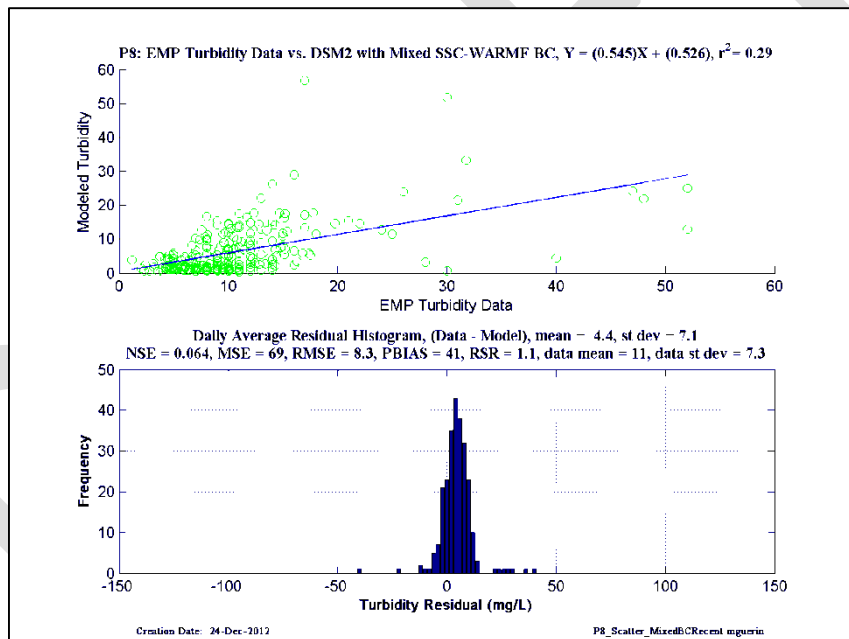
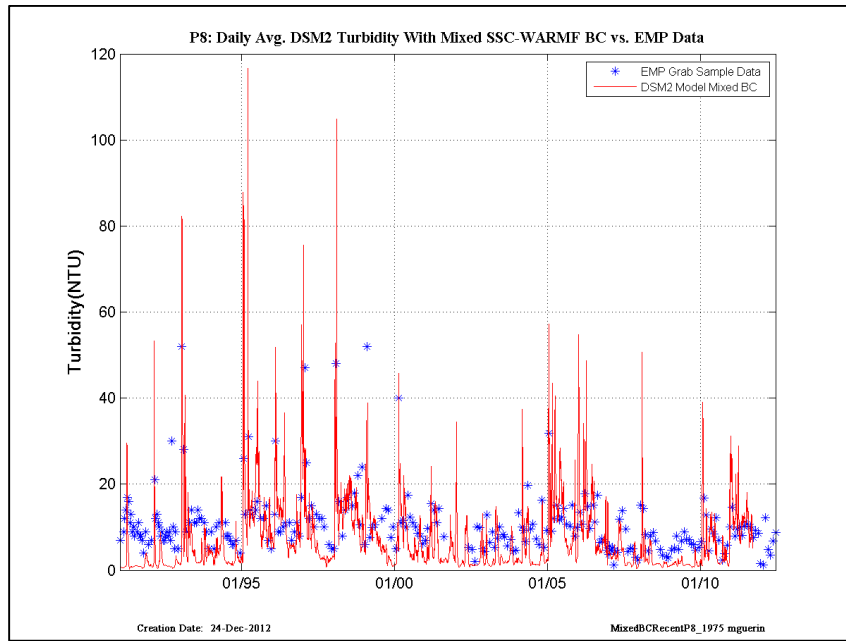


Figure 13-48 DSM2 daily-averaged turbidity model results using USGS-SSC at Freeport and Vernalis, and WARMF turbidity at other inflow boundaries compared to EMP grab-sample data, recent years– location is EMP P8.

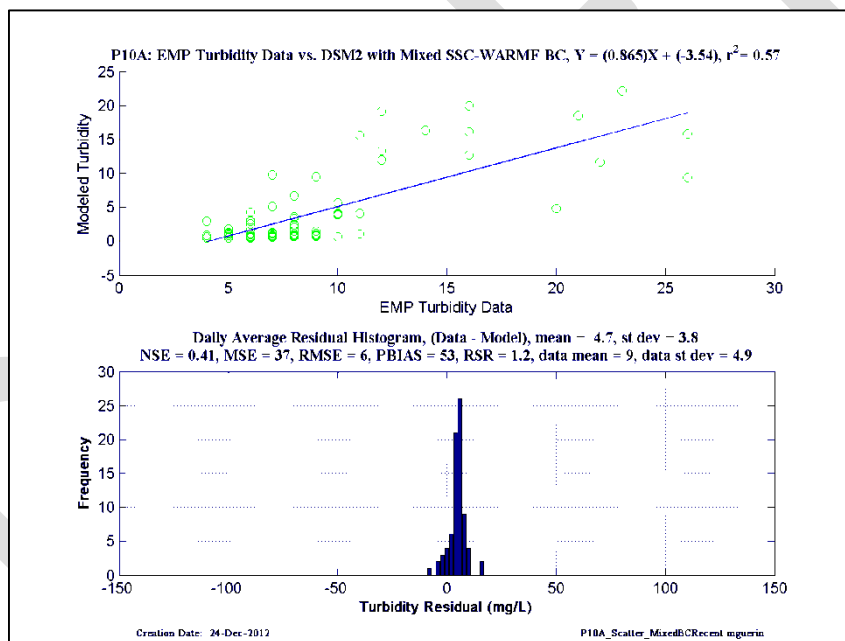
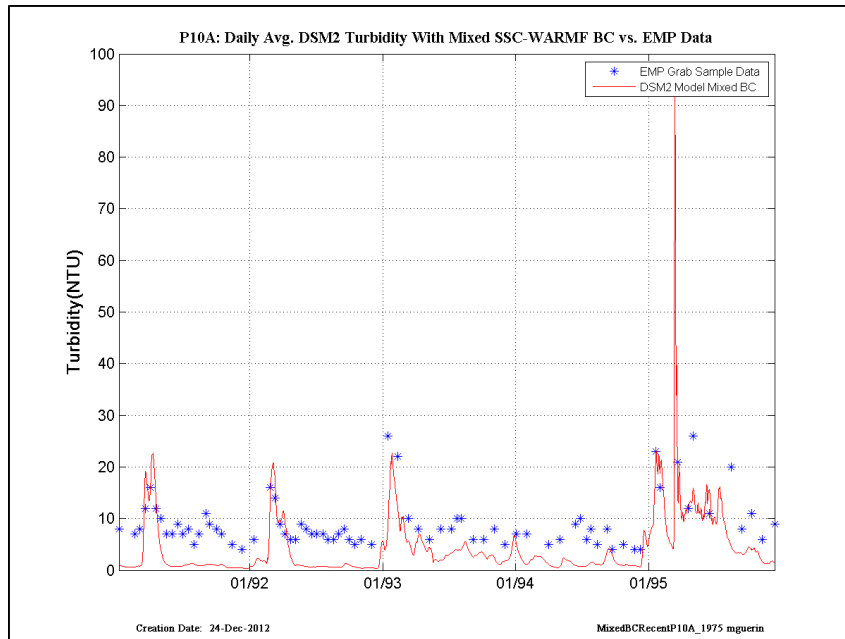


Figure 13-49 DSM2 daily-averaged turbidity model results using USGS-SSC at Freeport and Vernalis, and WARMF turbidity at other inflow boundaries compared to EMP grab-sample data, recent years– location is EMP P10A.

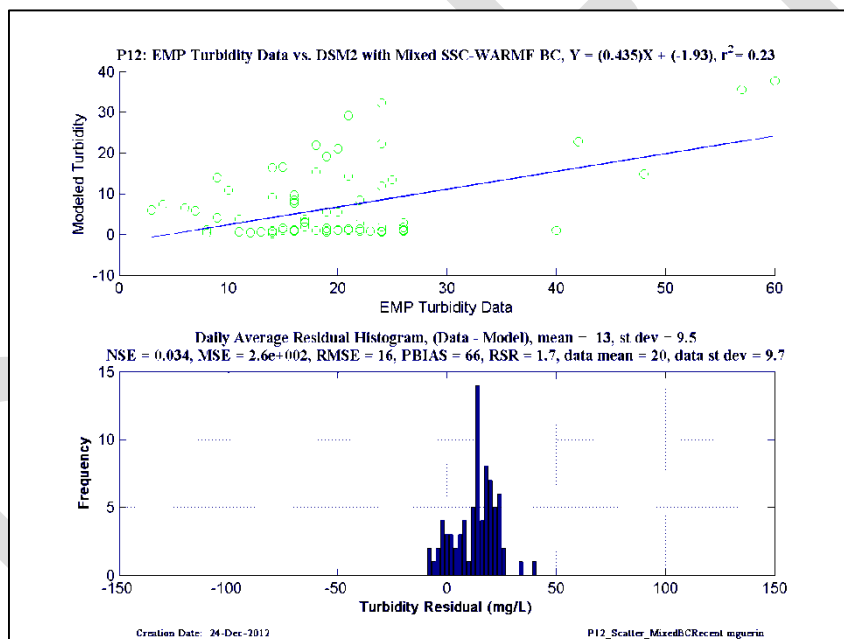
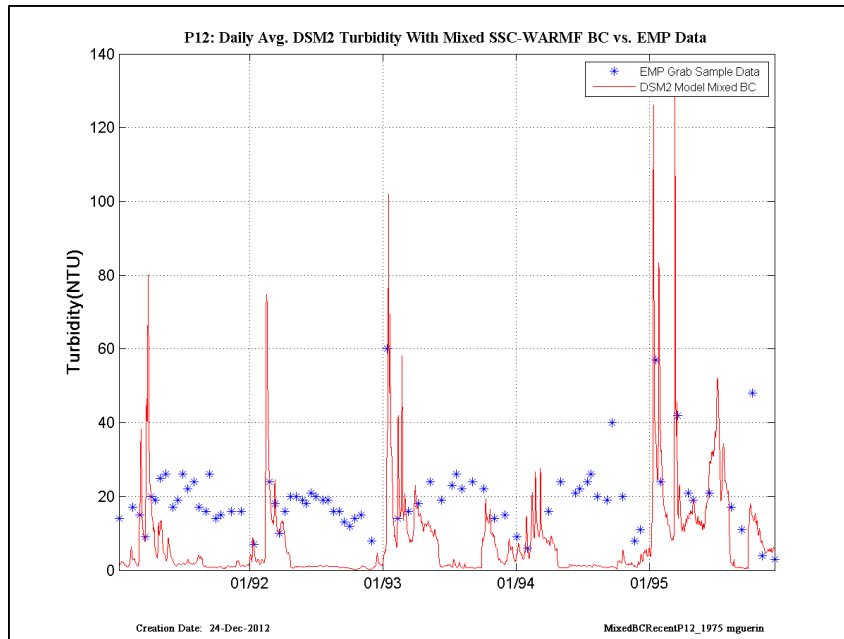


Figure 13-50 DSM2 daily-averaged turbidity model results using USGS-SSC at Freeport and Vernalis, and WARMF turbidity at other inflow boundaries compared to EMP grab-sample data, recent years– location is EMP P12.